Acta Neurochirurgica Supplement 127

Robert D. Martin
Warren Boling
Gang Chen
John H. Zhang *Editors*

Subarachnoid Hemorrhage

Neurological Care and Protection

Springer

Acta Neurochirurgica Supplement 127

Series Editor
H.-J. Steiger

For further volumes:
http://www.springer.com/series/4

Robert D. Martin • Warren Boling
Gang Chen • John H. Zhang
Editors

Subarachnoid Hemorrhage

Neurological Care and Protection

Springer

Editors
Robert D. Martin
Department of Anethesiology
Loma Linda University Medical Center
Loma Linda, CA
USA

Gang Chen
Department of Neurosurgery
First Affiliated Hospital of Soochow University
Suzhou
China

Warren Boling
Department of Neurosurgery
Loma Linda University Medical Center
Loma Linda, CA
USA

John H. Zhang
Department of Anesthesiology and Physiology
Loma Linda University Medical Center
Loma Linda, CA
USA

ISSN 0065-1419 ISSN 2197-8395 (electronic)
Acta Neurochirurgica Supplement
ISBN 978-3-030-04614-9 ISBN 978-3-030-04615-6 (eBook)
https://doi.org/10.1007/978-3-030-04615-6

This Springer imprint is published by the registered company Springer Nature Switzerland AG
The registered company address is: Gewerbestrasse 11, 6330 Cham, Switzerland

Preface

It has been a long, winding, and mysterious way to get here.

The former, current, and future leaders have met at the 14th International Conference on Neurovascular Events after Subarachnoid Hemorrhage or Vasospasm 2017 at the beautiful Pacific Ocean Huntington Beach invited here by Prof. John Zhang to his neck of the woods (Loma Linda University Health) to discuss "Subarachnoid Hemorrhage: Neurological Care and Protection."

It has been a long time since the first meeting in Jackson, Mississippi, in 1972 and even longer from not always civilized public arguments among neurology and neurosurgery giants about the existence and the role of delayed vasospasm on the outcome of an aneurismal rupture. Fortunately, those altercations were "peacefully" settled by Bryce Weir's (this meeting Honorary Guest) seminal paper published in 1978, which through linking the presence of delayed vasospasm with poor outcome had opened the door to the intensive all-over-the-world research and led to organizing the international meetings, which since then have been taking place on three continents at the different time intervals and which have been devoted to the still-evolving ideas on pathomechanism, prevention, and treatment of vasospasm after aneurismal SAH.

A little bit nostalgic, at the 14th International Conference on Neurovascular Events after Subarachnoid Hemorrhage or Vasospasm 2017 at the Huntington Beach Resort, CA, 176 registrants from 14 countries (with an encouraging and importantly an increasing number of women participants (29; 17%)) gathered to present and discuss their past, current, and future research and share the experiences and anecdotes about the late and current leaders in the field and their thoughts and opinions about past mistakes and successes while dealing with an aneurismal subarachnoid hemorrhage and its effects on patients.

This book consists of 31 excellent papers selected from 167 oral and poster presentations exploring "known knowns, known unknowns," as well as some "unknown unknowns" in many fields integrated into preclinical and clinical research of events leading to and evoked by an aneurismal subarachnoid hemorrhage. Put together, they provide in-depth inside view of the current state of our knowledge and understanding of events before and after intracranial subarachnoid hemorrhage and indicate the new directions in our long pursuit of prevention and treatment of a devastating, despite being treatable, intracranial aneurism rupture. We strongly believe that those proceedings not only will help the young basic and clinical researchers to accrue good foundations for understanding pathomechanism(s) of subarachnoid hemorrhage and vasospasm(s?) to proceed and/or develop their own ideas and projects but also will facilitate opening of multipronged venues for further research.

We thank Dr. John Lenart, Ms. Shirley Jones, Ms. Sheila Risley, and Ms. Kathrine McAllister from the Department of Anesthesiology and Ms. Olivia Portugal and Ms. Xiomara Pineda from the Department of Neurosurgery for putting in an immense amount of time to set up all

aspects of the meeting. The foundation they laid made this symposium possible. The last but not by any means the least, our gratitude is extended to all members of the Organizing Committee; Dr. Robert D. Martin, Chair of the Department of Anesthesiology, and Dr. Warren Boling, Chair of the Department of Neurosurgery of Loma Linda University Health; medical companies; and *above all the participants*!

Thank you and see you at the 15th Symposium at the Netherlands in 2019!

From the Organizing Committee
Ryszard M. Pluta
John H. Zhang

Loma Linda, CA, USA

Contents

Vasospasm: A Personal Odyssey

Bryce Weir

History of Vasospasm

1951 A Ecker, PA Riemenschneider (1951) Arteriographic demonstration of spasm of the intracranial arteries: With special reference to saccular arterial aneurysms. J Neurosurg 8: 660–667. [**1982** The discovery of human cerebral arterial spasm in angiograms: an autobiographical note (Arthur Ecker) (1982). Neurosurgery 10(1), 90].

1958 JL Pool (1958) Cerebral Vasospasm. New Engl J Med 259(26), 1259–1264.

1980 FA Echlin (1980) Some historical remarks Ch. 1, 1–7. Cerebral Arterial Spasm. Proceedings of the Second International Workshop. 1979.

1990 B Weir (1990) The history of cerebral vasospasm. Neurosurg Clin North America 1: 265–276.

1999 R Aaslid (1999) Hemodynamics of cerebrovascular spasm. Acta Neurochir, Suppl 72: 47–57.

2009 RM Pluta, J Hanssen-Schwartz, J Dreier, P Vajkoczy, RL Macdonald, S Nishiwaza, H Kasuya, G Wellman E Keller, A Zauner, N Dorsch, J Clark, S Ono, T Kiris, P Leroux, JH Zhang et al. (2009) Cerebral vasospasm following subarachnoid hemorrhage: time for a new world of thought. Neurol Res 31(2), 151–158.

2013 RL Macdonald (2013) History and definition of delayed cerebral ischemia. pp. 3–7 in M Zuccarello et al., eds. Cerebral Vasospasm. Neurovascular Events after Subarachnoid Hemorrhage.

2016 RL Macdonald (2016) Origins of the concept of vasospasm. Stroke 47: e11-e15.

B. Weir (✉)
Neurosurgery, The University of Alberta, Edmonton, AB, Canada

The University of Chicago, Chicago, IL, USA

B.K.A. Weir; Selected Bibliography: Aneurysms and Vasospasm

Clinical Studies

Prognostic Factors and Outcome

Grade and Vasospasm

1975 B Weir, C Rothberg, M Grace, F Davis (1975) Relative prognostic significance of vasospasm following subarachnoid hemorrhage. Can J Neurol Sci 2(2), 109–114.

1980 Weir BKA (1980) The incidence and onset of vasospasm after subarachnoid hemorrhage. Ch 43. In Cerebral Arterial Spasm, RH Wilkins (ed), Williams & Wilkins, Baltimore.

Cigarette Addiction

1998 BKA Weir, GL Kongable, NF Kassell, et al. (1998) Cigarette smoking as a cause of aneurysmal subarachnoid hemorrhage and risk for vasospasm: a report of the Cooperative Aneurysm Study. J Neurosurg 89(3), 405–411.

Outcome

1980 BKA Weir (1980) The effect of vasospasm on morbidity and mortality after subarachnoid hemorrhage from ruptured aneurysm. Ch. 58. RH Wilkins (ed), Williams & Wilkins, Baltimore.

1987 RA Bornstein, BKA Weir, KC Petruk, LB Disney (1987) Neuropsychological function in patients after subarachnoid hemorrhage. Neurosurgery 21(5), 651–654.

1988 L Disney, B Weir, M Grace, Canadian Nimodipine Study Group (1988) Factors influencing the outcome of aneurysm rupture in poor grade patients: A prospective series. Neurosurgery 23(1), 1–9.

R. D. Martin et al. (eds.), *Subarachnoid Hemorrhage*, Acta Neurochirurgica Supplement 127,
https://doi.org/10.1007/978-3-030-04615-6_1,

2000 M Foroohar, RL Macdonald, S Roth, M Stoodley, B Weir (2000) Intraoperative variables and early outcome after aneurysm surgery. Surgical Neurology 54(4), 304–315.

Time Course of Vasospasm

1978 B Weir, M Grace, J Hansen, C Rothberg (1978) Time course of vasospasm in man. J Neurosurg 48 (2). 173–178.

Management Mortality and Timing of Surgery

1981 B Weir, K Aronyk (1981) Management mortality and the timing of surgery for intracranial aneurysms. J Neurosurg 54(2), 146–150.

1982 B Weir, K Aronyk (1982) Management and postoperative mortality related to time of clipping for supratentorial aneurysms: a personal series. Acta Neurochirurgica 63(1–4), 135–139.

1987 L Disney, B Weir, K Petruk (1987) Effect on management mortality of a deliberate policy of early operation on supratentorial aneurysms. Neurosurgery 20(5), 695–701.

Perioperative Care

1979 B Weir (1979) Medical aspects of the preoperative management of aneurysms. Can J Neurol Sci 6, 441–450.

1980 WL Ritchie, B Weir, T Overton (1980) Experimental subarachnoid hemorrhage in the cynomolgus monkey: evaluation of treatment with hypertension, volume expansion and ventilation. Neurosurgery 6(1), 57–62.

1981 B Weir (1981) Value of immediate postoperative angiography following aneurysm surgery: Report of two cases. J Neurosurg 54(3), 396–398.

1987 B Weir (1987) Antifibrinolytics in subarachnoid hemorrhage: do they have a role? No. Archives of Neurology 44(1), 116–118.

1995 B Weir (1995) Protection of the brain after aneurysm rupture. Can J Neurol Sci 22: 177–186.

Blood Flow and Angiographic Studies

1978 B Weir D Menon T Overton (1978) Regional cerebral blood flow in patients with aneurysms: estimation by Xenon 133 inhalation. Canad J Neurol Sci 5(3), 301–305.

1981 D Menon, B Weir, T Overton (1981) Ventricular size and cerebral blood flow following subarachnoid hemorrhage. J Computer Assisted Tomography 5(3), 328–333.

1986 SL Norris, EG King, M Grace, B Weir (1986) Thermodilution cardiac output – an in vitro model of low-flow states. Critical Care Medicine 14(1), 57–59.

1989 K Hutchison, B Weir (1989) Trans-cranial Doppler studies in aneurysm patients. Can J Neurol Sci 16(4), 411–416.

1996 TD Alexander, RL Macdonald, B Weir, A Kowalczuk (1996) Intraoperative angiography in cerebral aneurysm surgery: a prospective study of 100 craniotomies. Neurosurgery 39(1), 10–18.

Sequelae of Hemorrhage

Edema

1978 BK Weir (1978) Pulmonary edema following fatal aneurysm rupture. J Neurosurg 49(4)502–507.

1994 B Weir (1994) Headaches from aneurysms. Caphalalgia 14(20), 79–87.

Cerebral Infarction

2004 B Weir (2004) Cerebral Infarction: Surgical Treatment. p. 1447–1458 In JP Mohr, et al. Stroke. Pathophysiology, Diagnosis, and Management. 4th ed. Churchill Livingstone.

Hematologic and Metabolic

1989 B Weir, L Disney, M Grace, P Roberts (1989) Daily trends in white blood cell count and temperature after subarachnoid hemorrhage from aneurysm. Neurosurgery 25(2), 161–165.

1989 L Disney, B Weir, M Grace, P Roberts (1989) Trends in blood pressure, osmolality and electrolytes after subarachnoid hemorrhage from aneurysms. Can J Neurol Sci 16(3). 299–304.

1991 B Weir, C Drake (1991) Rapid growth of residual aneurysmal neck during pregnancy: case report. J Neurosurg 75(5), 780–782.

1999 RL Macdonald, C Amidei, G Lin, I Munshi, B Weir, F Brown, RB Erickson, J Hekmatpanah (1999) Safety of perioperative subcutaneous heparin for prophylaxis of venous thromboembolism for patients undergoing craniotomy. Neurosurgery 45, 245–252.

Hydrocephalus

1987 D Steinke, B Weir, L Disney (1987) Hydrocephalus following aneurysmal subarachnoid hemorrhage. Neurological Research 9(1), 3–9.

Types of Hemorrhage

Subarachnoid

1998 B Weir (1998) **SUBARACHNOID HEMORRHAGE: CAUSES AND CURES**, Oxford University Press, New York, pp. 391.

Intracerebral

1983 B Wheelock, B Weir, R Watts, G Mohr, M Khan, M Hunter, D Fewer, et al. (1983) Timing of surgery for intracerebral hematomas due to aneurysm rupture. J Neurosurg 58(4), 476–481.

1982 BG Benoit, DD Cochrane, F Durity, GG Ferguson, D Fewer, KM Hunter, MI Khan, G Mohr, AR Watts, Weir BKA, WB Wheelock (1982) Clinical-radiological correlates in intracerebral hematomas due to aneurysmal rupture. Can J Neurol Sci 9, 409–414.

1993 B Weir (1993) The clinical problem of intracerebral hematoma. Stroke 24 (suppl 12), 193.

Intraventricular

1983 G Mohr, G Ferguson, M Khan, D Malloy, R Watts, B Benoit, B Weir (1983) Intraventricular hemorrhage from ruptured aneurysm: Retrospective analysis of 91 cases J Neurosurg 58(4), 482–487.

1991 JM Findlay, BKA Weir, DE Stollery (1991) Lysis of intraventricular hematoma with tissue plasminogen activator: case report. J Neurosurg 74(5), 803–807.

Subdural

1971 B Weir (1971) The osmolality of subdural hematoma fluid. J Neurosurg 34(4), 528–533.

1980 B Weir (1980) Oncotic pressure of subdural fluids. J Neurosurg 53(4), 512–515.

1983 B Weir, P Gordon (1983) Factors affecting coagulation, fibrinolysis in chronic subdural fluid collections. J Neurosurg 58(2), 242–245.

1984 B Weir, T Myles, M Khan, F Maroun, et al. (1984) Management of acute subdural hematomas from aneurysmal rupture. Can J Neurol Sci 11: 371–376.

2000 M Stoodley, B Weir (2000) Contents of chronic subdural hematoma. Neurosurg Clin North America 11(3), 425.

Prospective Human Drug Trials

Nimodipine

1983 GS Allen, HS Ahn, TJ Preziosi, R Battye, SC Boone, SN Chou, DL Kelly, BK Weir, RA Crabbe, PJ Lavik, SB Rosenbloom, FC Dorsey, CR Ingram, DE Melilts, LA Bertsch, DP Boisvert, MB Huntley, RK Johnson, JA Strom, CR Transou (1983) Cerebral arterial spasm – a controlled trial of nimodipine in patients with subarachnoid hemorrhage. New Engl J Med 308 (11), 619–624.

1988 KC Petruk, M West, G Mohr, B Weir, B Benoit, F Gentili, LB Disney, M Khan, M Grace, RO Holness, MS Karwon, RF Ford, GS Cameron, WS Tucker, GB Purves, JDR Miller, KM Hunter, MT Richard, FA Durity, R Chan, LJ Clein, FB Maroun, A Godon (1988) Nimodipine treatment in poor-grade aneurysm patients: results of a multicenter double-blind placebo-controlled trial. J Neurosurg 68(4), 505–517.

Nicardipine

Participant in trials.

Tirilazad

Participant in trials.

Tissue Plasminogen Activator

1991 JM Findlay, BKA Weir, NF Kassell, LB Disney, MGA Grace (1991) Intracisternal recombinant tissue plasminogen activator after aneurysmal subarachnoid hemorrhage. J Neurosurg 75(2), 181–188.

1993 JM Findlay, MGA Grace, BKA Weir (1993) Treatment of intraventricular hemorrhage with tissue plasminogen activator. Neurosurgery 32(6), 941–947.

1995 JM Findlay, NF Kassell, BKA Weir, EC Haley, G Kongable, T Germanson, L Truskowski, WM Alves, RO Holness, NW Knuckey (1995) A randomized trial of intraoperative intracisternal tissue plasminogen activator for the prevention of vasospasm. Neurosurgery 37(1), 168–178.

Unruptured Aneurysms

1998 D Wiebers, J Whisnant, G Forbes … B Weir, et al. (1998) Unruptured intracranial aneurysms – risk of rupture and risks of surgical intervention. New Engl J Med 339(24), 1725–1733.

2002 B Weir (2002) Unruptured intracranial aneurysms: a review. J Neurosurg 96 (1), 3–42.

2002 B Weir, L Disney, Karrison T (2002) Sizes of ruptured and unruptured aneurysms in relation to their sites and the ages of patients. J Neurosurg 96(1), 64–70.

2003 B Weir, C Amidei, G Kongable, JM Findlay, NF Kassell, et al. (2003) The aspect ratio (dome/neck) of ruptured and unruptured aneurysms. J Neurosurg 99(3), 447–451.

2005 B Weir (2005) Patients with small, asymptomatic, unruptured intracranial aneurysms and no history of subarachnoid hemorrhage should be treated conservatively – against. Stroke 36(2), 410–411.

Experimental Studies

In Vitro Pharmacological and Genetic Studies

1978 DA Cook, BK Weir, FK Okwuasaba, CA Krueger (1978) Effects of hemoglobin on smooth muscle. Proc Wester Pharmacological Soc 22, 429–434.

1981 FK Okwuasaba, BKA Weir, DA Cook, CA Krueger (1981) Effect of various intracranial fluids on smooth muscle. Neurosurgery 9(4), 402–406.

1981 F Okwuasaba, D Cook, B Weir (1981) Changes in vasoactive properties of blood products with time and

attempted identification on the spasmogens. Stroke 12(6), 775–780.

1986 M Nosko, CA Krueger, BKA Weir, DA Cook (1986) Effects of nimodipine on in vitro contractility of cerebral arteries of dog, monkey and man J Neurosurg 65(3), 376–381.

1988 M Nosko, R Schultz, B Weir, DA Cook, M Grace (1988) Effects of vasospasm on levels of prostacyclin and thromboxane A2 in cerebral arteries of the monkey. Neurosurgery 22(1), 45–50.

1989 K Kanamaru, BKA Weir, JM Findlay, CA Krueger, DA Cook (1989) Pharmacological studies on relaxation of spastic primate cerebral arteries J Neurosurg 71(6), 909–915.

1989 T Tsuji, BKA Weir, DA Cook (1989) Time-dependent effects of extra-luminally applied oxyhemoglobin and endothelial removal of vasodilator responses in isolated perfused canine basilar arteries. Pharmacology 38(2), 101–112.

1990 B Vollrath, BKA Weir, DA Cook (1990) Hemoglobin causes release of inositol trisphosphate from vascular smooth muscle cells. Biochem & Biophysical Res Communications 171(1), 506–511.

1992 H Zhang, N Stockbridge, B Weir, C Krueger, D Cook (1992) Glibencamide relaxes vascular smooth muscle constriction produced by prostaglandin F 2α. European J Pharmacol 195(1), 27–35.

1992 RL Macdonald, BKA Weir, TD Runzer, MGA Grace, MJ Poznansky (1992) Effect of intrathecal superoxide dismutase and catalase on oxyhemoglobin – induced vasospasm in monkeys. Neurosurgery 30(4), 529–539.

1992 RL Macdonald, BK Weir MG Grace, MH Chen, TP Martin JD Young (1992) Mechanism of cerebral vasospasm following subarachnoid hemorrhage in monkeys. Can J Neurol Sci 19(4), 419–427.

1993 H Kasuya, BKA Weir, DM White, K Stefansson (1993) Mechanism of oxyhemoglobin-induced release of endothelin-1 from cultured vascular endothelial cells and smooth muscle cells. J Neurosurg 79(6), 892–898.

1993 H Kasuya, B Weir, Y Shen, G Hariton, B Vollrath, A Gahary (1993) Procollagen types 1 and 111 and transforming growth factor-beta gene expression in the arterial wall after exposure to periarterial blood. Neurosurgery 33(4), 716–722.

1994 BAM Vollrath, BKA Weir, RL Macdonald, DA Cook (1994) Intracellular mechanisms involved in the responses of cerebrovascular smooth-muscle cells to hemoglobin. J Neurosurg 80(2), 261–268.

1994 H Kasuya, BKA Weir, YJ Shen, EE Tredget, A Ghahary (1994) Insulin like growth factor-1 in the arterial wall after exposure to periarterial blood. Neurosurgery 35(1), 99–105.

1996 T Tsuji, DA Cook, BKA Weir, Y Handa (1996) Effect of clot removal on cerebrovascular contraction after subarachnoid hemorrhage in the monkey: pharmacological study. Heart & Vessels 11(2), 69–79.

1996 A Hino, Y Tokuyama, M Kobayashi, M Yano, B Weir et al. (1996) Increased expression of endothelin B receptor mRNA following subarachnoid hemorrhage in monkeys. J Cereb Blood Flow & Metab 16(4), 688–697.

1996 LS Marton, BK Weir, H Zhang (1996) Tyrosine phosphorylation and [Ca2+] i elevation induced by hemolysate in bovine endothelial cells: implications for cerebral vasospasm Neurological Res 18(4) 349–353.

1996 CJ Kim, B Weir, RL Macdonald, LS Marton, H Zhang (1996) Hemolysate inhibits L-type Ca2+ channels in rat basilar smooth muscle cells. J Vascular Research 33(3), 258–264.

1997 B Sima, BKA Weir, RL Macdonald, H Zhang (1997) Extracellular nucleotide- induced [Ca2+] i elevation in rat basilar smooth muscle cells. Stroke 28(10), 2053–2059.

1997 M Doi, H Kasuya, B Weir, DA Cook, A Ogawa (1997) Reduced expression of calponin in canine basilar artery after subarachnoid haemorrhage. Acta Neurochirurgica 139(1), 77–81.

1998 RL Macdonald, J Zhang, B Weir, LS Marton, R Wollman (1998) Adenosine triphosphate causes vasospasm in rat femoral artery. Neurosurgery 42(4), 825–832.

1998 CJ Kim, BK Weir, RL Macdonald, H Zhang (1998) Erythrocyte lysate releases Ca2+ from IP3 sensitive stores and activates Ca2+-dependent K+ channels in rat basilar smooth muscle cells. Neurological Research 20(1), 2–30.

1999 X Wang, LS Marton, BKA Weir, RL Macdonald (1999) Immediate early gene expression in vascular smooth-muscle cells synergistically induced by hemolysate components. J Neurosurg 90(6), 1083–1090.

1999 RL Macdonald, BK Weir, LS Marton, E Windmeyer, L Johns, A Kowalczuk, G Lin (1999) Heme oxygenase-1 and ferritin proteins are increased in cerebral arteries after subarachnoid hemorrhage in monkeys. Surg Forum 49, 501–503.

1999 RL Macdonald, J Zhang, LS Marton, B Weir (1999) Effect of cell-permeant calcium chelators, on contractility in monkey basilar artery. J Neurotrauma 16(1) 37–47.

2001 G Lin, RL Macdonald, LS Marton, A Kowalczukuk, NJ Solenski, BK Weir (2001) Hemoglobin increases endothelin-

1 in endothelial cells by decreasing nitric oxide. Biochem & Biophys Res Communications 280 (3), 824–830.

2001 RL Macdonald, S Ono, L Johns, LS Marton, B Weir, Z-D Zhang, B Yamini, T Komuro, I Ahmed, M Stoodley (2001) Molecular weight interactions in experimental vasospasm. Acta Neurochir (Suppl 77): 115–117.

In Vitro Physiological Studies

1991 JA Steele, N Stockbridge, G Malkovitch, B Weir (1991) Free radicals mediate actions of oxyhemoglobin on cerebrovascular smooth muscle cells. Circulation Research 68(2), 416–423.

1992 N Stockbridge, H Zhang, B Weir (1992) Potassium currents of rat basilar artery smooth muscle cells. Pflügers Archiv 421(1), 37–42.

1992 N Stockbridge, G Malkovitch, BK Weir (1992) No effect of bilirubin on electrical properties of isolated cerebrovascular smooth muscle cells. Cerebrovascular Diseases 2(3), 158–162.

1992 N Stockbridge, H Zhang, B Weir (1992) Effects of K+ channel agonists cromakilim and pinacidil on rat basilar artery smooth muscle cells are mediated by Ca++ activated K+ channels. Biochem & Biophys Res Communications 181(1), 172–178.

1992 H Zhang, N Stockbridge, B Weir, B Vollrath, D Cook (1992) Vasodilatation of canine cerebral arteries by nicorandil, pinacidil, and lemkalim. Gen Pharmacol: The Vascular System 23(2), 197–201.

1992 Y Takanashi, BKA Weir, B Vollrath, H Kasuya, RL Macdonald, D Cook (1992) Time course of changes in concentration of intracellular free calcium in cultured cerebrovascular smooth muscle cells exposed to oxyhemoglobin Neurosurgery 30(3), 376–381.

1994 H Zhang, M Inazu, B Weir, E Daniel (1994) Endothelin-1 inhibits inward rectifier potassium channels and activates nonspecific cation channels in cultured endothelial cells. Pharmacology 49(1), 11–22.

1994 H Zhang, M Inazu, B Weir, M Buchanan, E Daniel (1994) Cyclopiazonic acid stimulates Ca2+ influx through non-specific cation channels in endothelial cells. European J Pharmacology.

1995 H Kasua, BKA Weir, M Nakane, JS Pollock, L Johns, L Marton, K Stefansson (1995) Nitric oxide synthase and guanylate cyclase levels in canine basilar artery after subarachnoid hemorrhage. J Neurosurg 82(2), 250–255.

1995 H Zhang, B Weir, EE Daniel (1995) Activation of protein kinase C inhibits potassium currents in cultured cells. Pharmacology 50(4), 247–256.

1995 H Zhang, B Weir, LS Marton, RL Macdonald, V Bindokas, RJ Miller, JR Brorson (1995) Mechanisms of hemolysate-induced [Ca2+] elevation in cerebral smooth muscle cells. American Journal of Physiology – Heart and Circulatory Physiology 269(6), H1874–1890.

1996 H Zhang, BK Weir, RL Macdonald, LS Marton, NJ Solenski, AL Kwan et al. (1996) Mechanisms of [Ca++] i elevation induced by erythrocyte components in endothelial cells. J Pharm Exptl Therapeut 277(3), 1501–1509.

1996 B Sima, RL Macdonald, LS Marton, B Weir, J Zhang (1996) Effect of P2-purinoceptor antagonists on hemolysate-induced and adenosine 5′-triphosphate-induced contractions of dog basilar artery in vitro. Neurosurgery 39(4) 815–822.

1997 H Zhang, BKA Weir, LS Marton, KS Lee, RL Macdonald (1997) P2 purinoceptors in cultured bovine middle cerebral artery endothelial cells. J Cardiovascular Pharmacol 30(6), 767–774.

1998 YY Guan, BKA Weir, LS Marton, RL Macdonald, H Zhang (1998) Effect of erythrocyte lysate of different incubation times on intracellular free calcium in rat basilar artery smooth muscle cells. J Neurosurg 89(6), 1007–1014.

1998 R Macdonald, M Bassiounny, L Johns, M Sajdak, LS Marton, BK Weir et al. (1998) U74389G prevents vaospasm after subarachnoid hemorrhage in dogs. Neurosurgery 42(6), 1339–1345.

2000 MK Borsody, GM DeGiovanni, LS Marton, RL Macdonald, B Weir (2000) Thrombin reduces cerebral arterial contractions caused by cerebrospinal fluid from patients with subarachnoid hemorrhage. Stroke 31(9), 2149–2156.

2001 T Komuro, MK Borsody, S Ono, LS Marton, BK Weir, ZD Zhang, E Paik, RL Macdonald (2001) The vasorelaxation of cerebral arteries by carbon monoxide. Experimental Biology and Medicine 226(9), 860–865.

2001 RL Macdonald, BKA Weir, LS Marton, ZD Zhang, M Sajdak, LM Johns et al. (2001) Role of adenosine 5′-triphosphate in vasospasm after subarachnoid hemorrhage: human investigations. Neurosurgery 48(4), 854–863.

Animal Models

Liquid Blood Injections

1969 JWR McIntyre, JDR Miller, BKA Weir (1969) Anaesthesia for cerebral angiography: cardiovascular and cerebrospinal fluid pressure observations in the monkey under pentobarbital-halothane anesthesia. Can Anaesthetists' Soc J 16(4), 309–315.

1970 B Weir, R Erasmo, J Miller, J McIntyre, D Secord, B Mielke (1970) Vasospasm in response to repeated subarachnoid hemorrhages in the monkey. J Neurosurg 33(4), 395–406.

1972 KC Petruk, GR West, MR Marriot, JW Mcintyre, TR Overton, BKA Weir (1972) Cerebral blood flow following induced subarachnoid hemorrhage in the monkey. J Neurosurg 37(3), 316–324.

1973 KC Petruk, BKA Weir, MR Marriott, TR Overton (1973) Clinical grade, regional cerebral blood flow and angioraphical spasm in the monkey after subarachnoid and subdural hemorrhage. Stroke 4(3), 431–445.

1974 KC Petruk, BK Weir, TR Overton, MR Marriott, MG Grace (1974) The effect of graded hypocapnia and hypercapnia on regional cerebral blood flow and cerebral vessel caliber in the rhesus monkey: study of cerebral hemodynamics following subarachnoid hemorrhage and traumatic internal carotid spasm. Stroke 5(2), 230–246.

1976 DP Boisvert, TR Overton, B Weir. MG Grace (1976) Cerebral arterial responses to induced hypertension following subarachnoid hemorrhage in the monkey. J Neurosurg 49(1) 75–83.

1977 DP Boisvert, BK Weir, TR Overton, R Reiffenstein, MG Grace (1977) Cerebrovascular responses to subarachnoid blood and serotonin in the monkey. Acta Neurologica Scandinavica. Suppl 64: 322.

1977 D Boisvert, B Weir, T Overton, R Reiffenstein, M Grace (1977) Effect of subarachnoid injection of blood, serotonin and mock spinal fluid in monkeys. Stroke (8), 10–11.

1979 DPJ Boisvert, BKA Weir, TR Overton, RJ Reiffenstein, MGA Grace (1979) Cerebrovascular responses to subarachnoid blood and serotonin in the monkey. J Neurosurg 50(4), 441–448.

1979 CS Rothberg, B Weir, TR Overton (1979) Treatment of subarachnoid hemorrhage with sodium nitroprusside and phenylephrine: an experimental study. Neurosurgery 5(5), 588–595.

1980 C Rothberg, B Weir, T Overton, M Grace (1980) Responses to experimental subarachnoid hemorrhage in the spontaneously breathing primate. J Neurosurg 52(3), 302–308.

1982 F Espinosa, B Weir, D Boisvert, T Overton, W Castor (1982) Chronic cerebral vasospasm after large subarachnoid hemorrhage in monkeys. J Neurosurg 57(2), 224–232.

1984 F Espinosa, B Weir, T Noseworthy (1984) Rupture of an experimentally induced aneurysm in a primate. Can J Neurol Sci 11(1), 64–68.

1984 TW Noseworthy, B Weir, D Boisvert, F Espinosa, T Overton, ML Marshal (1984) Effect of reserpine-kanamycin treatment on chronic vasospasm after platelet-enriched subarachnoid hemorrhage in primates. Neurosurgery 14(2), 193–197.

Chronic Clot Application to Arteries

1984 F Espinosa, B Weir, T Overton, W Castor, M Grace, D Boisvert (1984) A randomized, placebo-controlled double-blind trial of nimodipine after SAH in monkeys. Part 1: Clinical and radiological findings. J Neurosurg 60(6), 1167–1175.

1984 F Espinosa, B Weir, T Schnitka, T Overton, D Boisvert (1984) A randomized, placebo-controlled, double-blind trial of nimodipine after subarachnoid hemorrhage in monkeys. Part 11. Pathological findings. J Neurosurg 60(6), 1176–1185.

1985 M Nosko, B Weir, C Kreuger, D Cook, S Norris, T Overton, D Boisvert (1985) Nimodipine and chronic vasospasm in monkeys. Part 1. Clinical and radiological findings. Neurosurgery 16(2), 129–136.

1985 C Krueger, B Weir, M Nosko, D Cook, S Norris (1985) Nimodipine and chronic vasospasm in monkeys: Part 2 Pharmacologic studies of vessels in spasm. Neurosurgery 16(2), 137–140.

1986 M Nosko, SL Norris, B Weir, GE King, M Grace (1986) Nimodipine and chronic vasospasm in Monkey: Part 3 Cardiopulmonary Effects. Neurosurgery 18(3), 261–265.

1987 M Nosko, BKA Weir, A Lunt, M Grace, P Allen, B Mielke (1987) Effect of clot removal at 24 hours on chronic vasospasm after SAH in the monkey J Neurosurg 66(3), 416–422.

1987 Y Handa, BKA Weir, M Nosko, R Mosewich, T Tsuji, M Grace (1987) The effect of timing of clot removal on chronic vasospasm in a primate model. J Neurosurg 67(40), 558–564.

1988 JP Lewis, BKA Weir, MG Nosko, T Tanabe, MG Grace (1988) Intrathecal nimodipine therapy in a primate model of chronic cerebral vasospasm. Neurosurgery 22(3), 492–500.

1988 JM Findlay, BKA Weir, D Steinke, T Tanabe, P Gordon, M Grace (1988) Effect of intrathecal thrombolytic therapy on subarachnoid clot and chronic vasospasm in a primate model of SAH. J Neurosurg 69(5), 723–735.

1990 JM Findlay, BKA Weir, K Kanamaru, M Grace, R Baughman (1990) The effect of timing of intrathecal fibrinolytic therapy on cerebral vasospasm in a primate model of subarachnoid hemorrhage. Neurosurgery 26(2), 201–206.

1990 B Weir (1990) The effect of clot removal on cerebral vasospasm. Neurosurg Clin North America 1(2), 377–385.

1991 JM Findlay, RL Macdonald, BKA Weir, MGA Grace (1991) Surgical Manipulation of primate cerebral arteries in established vasospasm. J Neurosurg 75(3), 425–432.

1991 RL Macdonald, BKA Weir, TD Runzer, MGA Grace, JM Findlay, K Saito, et al. (1991) Etiology of cerebral vasospasm in primates. J Neurosurg 75(3), 415–424.

1992 RL Macdonald, BK Weir, TD Runzer, MG Grace (1992) Malondialdehyde, glutathione peroxidase, and superoxide dismutase in cerebrospinal fluid during cerebral vasospasm in monkeys. Can J Neurol Sci 19(3), 326–332.

1996 A Hino, Y Tokuyama, B Weir, J Takeda, H Yano, GI Bell, RL Macdonald (1996) Changes in endothelial nitric oxide synthase mRNA during vasospasm after subarachnoid hemorrhage in monkeys. Neurosurgery 39(3), 562–568.

Drug Trials in Animals

1989 DE Steinke, BKA Weir, JM Findlay, T Tanabe, M Grace, BW Krushelnicky (1989) A trial of 21-aminosteroid U74006F [Tirilazad] in a primate model of chronic cerebral vasospasm. Neurosurgery 24(2), 179–186.

1989 JM Findlay, BKA Weir, P Gordon, M Grace, R Baughman (1989) Safety and efficacy of intrathecal thrombolytic therapy in a primate model of cerebral vasospasm. Neurosurgery 24(4), 491–498.

1989 JM Findlay, BK Weir, K Kanamaru, M Grace, P Gordon, R Baughman, A Howarth (1989) Intrathecal fibrinolytic therapy after subarachnoid hemorrhage: dosage study in a primate model and review of the literature. Can J Neurol Sci 16(1), 28–40.

1990 K Kanamaru, BKA Weir, JM Findlay, M Grace, LR Macdonald (1990) A dosage study of the effect of the 21-aminosteroid U74006F on chronic cerebral vasospasm in the primate model. Neurosurgery 27(1), 29–38.

1991 K Kanamaru, BKA Weir, I Simpson, T Witbeck, M Grace (1991) Effect of 21-aminosteroid U-74006F on lipid peroxidation in subarachnoid clot. J Neurosurg 74(3), 454–459.

1993 GB Hariton, JM Findlay, BKA Weir, H Kasuaya, MGA Grace, BW Mielke (1993) Comparison of intrathecal administration of urokinase and tissue plasminogen activator on subarachnoid clot and chronic vasospasm in a primate model. Neurosurgery 33(4), 691–697.

1995 A Hino, BKA Weir, RL Macdonald, RA Thisted, CJ Kim, LM Johns (1995) Prospective, randomized, double-blind trial of BQ-123 [endothelin A receptor antagonist] and bosentan [dual endothelin receptor antagonist] for prevention of vasospasm following subarachnoid hemorrhage in monkeys. J Neurosurg 83(3), 503–509.

1996 CJ Kim, M Bassiounny, RL Macdonald, B Weir, LM Johns (1996) Effect of BQ-123 and tissue plasminogen activator on vasospasm after subarachnoid hemorrhage in monkeys. Stroke 27(9), 1629–1633.

Anatomical Observations

1977 RM Henderson, DP Boisvert, BK Weir (1977) Intercellular contacts in primate cerebral arteries: acute effects of subarachnoid injection of artificial cerebrospinal fluids, serotonin and blood. Advances in Neurology 20, 25–34.

1979 DPJ Boisvert, RM Henderson, BK Weir (1979) The ultrastructure of inter-cellular contacts in cerebral arteries and arterioles. Acta Neurol Scand (Suppl 72); X-16, 1979.

1986 H Hara, M Nosko, B Weir (1986) Cerebral perivascular nerves in subarachnoid hemorrhage: A histochemical and imunohistochemical study. J Neurosurg. 65(4), 531–539.

1986 H Hara, B Weir (1986) Pathway of acetylcholinesterase containing nerves to the major cerebral arteries in the rat. J Comp Neurology 250(2), 245–252.

1986 H Hara, B Weir (1986) Different distributions of substance P and vasoactive intestinal polypeptide in the cerebral arterial distribution in rat and guinea pig. Anatomische Anzeiger 163(1), 19–23.

1986 F Espinosa, B Weir, T Schnitka (1986) Electron microscopy of simian cerebral arteries after subarachnoid hemorrhage and after the injection of horseradish peroxidase. Neurosurgery 19(6), 935–945.

1988 F Espinosa, B Weir, T Schnitka (1988) Treatment of chronic cerebral vasospasm in monkeys and electron microscopic anatomy of normal and subarachnoid hemorrhage arteries Cerebral Vasospasm. 195–210 in Cerebral Vasospasm. RH Wilkins (ed), Raven Press, New York.

1988 RH Lehman, NF Kassell, GB Nazar, BK Weir, H Johshita, M Nosko, et al. (1988) Morphometric methods in the study of vasospasm. Cerebral Vasospasm 113–117 RH Wilkins (ed) Raven Press, New York.

1988 H Hara, B Weir (1988) Pathway of nerves with vasoactive intestinal polypeptide-like immunoreactivity to the major cerebral arteries of the rat. Cell & Tissue Research 251(2), 275–280.

1989 JM Findlay, BKA Weir, K Kanamaru, F Espinosa (1989) Arterial wall changes in cerebral vasospasm. Neurosurgery 25(5), 736–746.

1991 RL Macdonald, BKA Weir, MG Grace, TP Martin, DA Cook (1991) Morphometric analysis of monkey cerebral arteries exposed in vivo to whole blood oxyhemoglobin, methemoglobin and bilirubin. J Vascular Research 28(6). 860–865.

1991 RL Macdonald, BKA Weir, MH Chen, MGA Grace (1991) Scanning electron microscopy of normal and vasospastic monkey cerebrovascular smooth muscle cells. Neurosurgery 29(4), 5440550.

1992 RL Macdonald, BKA Weir, JD Young, MGA Grace (1992) Cytoskeletal and extracellular matrix proteins in cerebral arteries following subarachnoid hemorrhage in monkeys. J Neurosurg 76(1), 81–90.

2000 M Stoodley, RL Macdonald, B Weir, LS Marton, L Johns, Z Du Zhang, et al. (2000) Subarachnoid hemorrhage as a cause of adaptive response in cerebral arteries. J Neurosurg 93(3), 463–470.

2001 ZD Zhang, B Yamini, T Komuro, S Ono, L Johns, LS Marton, B Weir, RL Macdonald (2001) Vasospasm in monkeys resolves because of loss of and encasement of subarachnoid blood clot. Stroke 32(8), 1868–1874.

General

1977 B Weir, J Miller, D Russel (1977) Intracranial aneurysms: a clinical, angiographic and computerized tomographic study. Can J Neurol Sci 4(2), 99–105.

1984 B Weir (1984) Intracranial aneurysms. An overview In *Neurosurgery – A Comprehensive Textbook*. R Wilkins (ed), McGraw Hill.

1987 B Weir (1987) The management of intracranial aneurysms: prospects for improvement. Clinical Neurosurgery 34: 154–160.

1987 B Weir (1987) **ANEURYSMS AFFECTING THE NERVOUS SYSTEM**, Williams & Wilkins. Baltimore, pp. 687.

1990 JM Findlay, RL Macdonald, BK Weir (1990) Current concepts of pathophysiology and management of cerebral vasospasm following aneurysmal subarachnoid hemorrhage. Cerebrovascular and Brain Metabolism Reviews. 3(4) 336–361.

1990 BKA Weir (1990) Intracranial aneurysms. Current Opinion in Neurology 3(1), 55–62.

1990 F Espinosa, B Weir, T Noseworthy (1990) Non-operative treatment of subarachnoid hemorrhage. Ch 54, 1661–1688, in *Neurological Surgery. 3rd edition* J Youmans (ed).

1991 RL Macdonald, BK Weir (1991) A review of hemoglobin and the pathogenesis of cerebral vasospasm. Stroke 22(8), 971–982.

1991 BK Weir (1991) Vasospasme cérébrale. Étude expérimentale. Neuro-Chirurgie 38(3), 129–133.

1992 L Macdonald, B Weir (1992) Cerebral Vasospasm. Clinical Neurosurgery 40: 40–55.

1994 RL Macdonald, BK Weir (1994) Cerebral Vasospasm and free radicals. Free Radicals in Biology and Medicine 16(5), 633–643.

1994 B Weir, JM Findlay (1994) Subarachnoid hemorrhage. Ch 9, 557–582 in *Neurovascular Surgery*. LP Carter, RF Spetzler. McGraw-Hill.

1995 B Weir (1995) The pathophysiology of cerebral vasospasm. Brit J Neurosurgery 9(3), 375–390.

1996 B Weir, RL Macdonald (1996) Intracranial aneurysms and subarachnoid hemorrhage: An overview. Ch 214, in *Neurosurgery,* Wilkins RH, Rengachary SS (eds) McGraw-Hill, New York.

1996 RL Macdonald, B Weir (1996) Cerebral vasospasm and delayed cerebral ischemia. Ch 129 in *Practice of Neurosurgery.* GT Tindall, PR Cooper, DI Barrow (eds) Williams& Wilkins, Baltimore.

1997 KMA Welch, LR Caplan, DJ Reis, BK Seisjo, B Weir (ed) (1997) **PRIMER ON CEREBROVASCULAR DISEASES** pp. 823, Academic Press, San Diego.

1998 MA Stoodley, RL Macdonald, BK Weir (1998) Pregnancy and intracranial aneurysms. Neurosurgery Clinics North America 9(3), 549–556.

1998 MA Stoodley, RL Macdonald, BK Weir (1998) Surgical treatment of middle cerebral aneurysms. Neurosurg Clin North America 9(4), 823–834.

1999 B Weir, RL Macdonald, M Stoodley (1999) Etiology of cerebral vasospasm. Acta Neurochir (Suppl) 72: 27–46.

2001 RL Macdonald, B Weir **CEREBRAL VASOSPASM**, Academic Press, San Diego, pp. 518.

2001 RL Macdonald, M Stoodley, B Weir (2001) Intracranial aneurysms. Neurosurgical Quarterly 11(3) 181–198.

2003 F Maroun, K Squarey, J Jacob, G Murray, B Cramer, J Barron, B Weir (2003) Rupture of middle cerebral artery aneurysm in a neonate: case report and review of the literature. Surgical Neurology 59(2), 114–119.

2004 JP Mohr, D Choi, PA Wolf, JC Grotta, B Weir (ed) (2004) **STROKE – PATHOPHYSIOLOGY, DIAGNOSIS, AND MANAGEMENT**. 4th Ed. pp. 1591. Churchill Livingstone.

2010 B Weir (2010) Multiple sclerosis – a vascular etiology? Can J Neurol Sci 37(6), 745–757.

2011 J Spears, RL Macdonald, B Weir (2011) Perioperative management of subarachnoid hemorrhage. Ch 363, 3772–3790. In *Youmans Neurological Surgery*, HR Winn (ed), Elsevier-Saunders.

Musings from an Old World of Thought

Like many new concepts in medicine, the idea that radiologically observable vasospasm after aneurysmal rupture might be causally related to subsequent infarction and poor patient outcome was initially greeted with skepticism but eventually accepted with uncritical enthusiasm. It is rewriting history to suggest that early neurosurgeons considered it to be the sole cause of morbidity and mortality, although most agreed that it was a major one. Some clinical practices actually magnified the adverse consequences of vasospasm: performance of operation in the time of evolving and maximum vasospasm, deliberate hypotension, dehydration, deep hypothermia, the use of antifibrinolytic agents, avoidance of ventricular drainage, rigid retractor systems with prolonged brain compression, sacrifice of draining veins and perforating arteries, and failure to compensate for electrolyte abnormalities occurring spontaneously or as a result of diuretics.

In the first instants of aneurysmal rupture, the die is cast for most patients depending on the height of the intracranial pressure. If the pressure remains sufficiently elevated, the patient dies. There is a continuum in which the brain sustains massive or trivial damage. Fluid can shift into the brain and lungs. Infarcts can develop very early and may be clinically and radiologically undetected for some time depending on the assiduousness of the examiner and the sophistication of the radiological equipment. Blood that is life-sustaining within the brain's vessels on the abluminal side becomes life-threatening. All neural and vascular tissue is adversely affected.

A key insight was that the time interval from aneurysmal rupture to medical treatment and the "grade" at the time of admission were important determinants of outcome. The "grade" was shorthand for the cumulative damage sustained by the brain to a certain point in time as evidenced in the neurological examination.

The introduction of computed tomography added to our knowledge of vasospasm. Larger clots in the subarachnoid spaces result in a greater degree of radiologically observable vessel narrowing. There was some confusion in the first decades resulting from the use of the term vasospasm to describe both the angiographically observed vessel narrowing and the clinical syndrome of delayed ischemic neurological deficit. It has always been obvious that there are many causes of delayed deficits and that delayed ischemic neurological deficits from vasospasm alone was only one (although an important one) of the etiologies.

Decrease in conducting large vessel diameter must be of a sufficient degree to become hemodynamically significant as critical closing pressures are reached, in the absence of adequate compensatory collateral flow, in order to cause infarction. Vasospasm must be "severe" to cause sufficient reduction in distal flow as evidenced by prolongation of cerebral circulation time and time-to-peak times and measureable falls in regional cerebral blood flow. The measurement of time-to-peak and mean transit times in focal vascular territories by noninvasive technologies will provide valuable insights into the relative importance of intracerebral versus extracerebral resistance to flow. Measurement of tissue oxygen and glucose will be of importance when done atraumatically.

Some degree of angiographic vasospasm is more common than delayed deficits from all causes that in turn are more frequent than delayed ischemic deficits from vasospasm alone that usually outnumber radiologically demonstrable distal territorial ischemic infarcts. It has been known for a long time that infarcts could also result from brain shifts, venous obstruction, intravascular coagulation, emboli, sulcal clots, hypoxia, hypotension, and hypoglycemia as well as vasospasm.

It became possible to duplicate clinical and radiological events in animals by the placement of large clots directly on surgically exposed arteries, timely removal of these clots by surgical means or pharmacological dissolution could abort the subsequent development of vasospasm. Vasospasm is apparently independent of vessel rupture or an episode of greatly raised intracranial pressure. Clot placed on brain can apparently cause small vessel spasm and cortical infarction.

Oscillating aortic pressure is the driving force for the cerebral circulation. This is influenced by systemic blood pressure and ventricular function. Friction and kinetic pressure losses mount as the vessels become smaller. Most of the pressure loss is probably in the precapillary small arterioles and capillaries. The reduction in flow during "vasospasm" will be influenced by factors in addition to the predominant one—reduction in diameter of radiologically observable arteries—such as length of the narrowed segment, density, and viscosity of the blood, hematocrit, anatomy of vessels leaving the involved segment, vasoconstriction of other vessels providing resistance in series (distal) or in parallel (collaterals), and possible occluding pressures on bridging draining veins. The efficiency of cerebral autoregulation by intrinsic vasodilatation will counter proximal vasospasm and will vary with the health and age of the brain. The oxygen content of the reduced volume of circulating blood may be increasingly drawn down as a compensatory mechanism. However, at a certain point of critical vasospasm, it is inevitable that if flow falls sufficiently the survival of the cells and neuropil served by the spastic vessel will be threatened. How long the spasm lasts will play a role. The circle of Willis is probably a more efficient source of alternate blood supply than leptomeningeal collaterals.

Nimodipine was introduced because it was thought it would prevent angiographic vasospasm. We showed this does not occur. It was accepted as safe and efficacious never-

theless and became standard of care in the early 1990s when barriers to acceptance of new therapies were not what they are today. Its concurrent use was generally permitted in subsequent large drug trials with unknown interactions.

There are several possible explanations of why the clazosentan study failed to demonstrate improved outcome despite a significant reduction in vasospasm: too few cases; too short a follow-up; errors in classification; very late MRI was not employed; late neuropsychological assessment was not done; the overwhelming importance of other unknown factors such as deleterious side effects, efficacy of rescue therapy, and inclusion of "moderate" vasospasm in which the reduction in flow may not have been hemodynamically critical; or even a statistical fluke.

The mortality and serious morbidity from vasospasm has fortunately fallen progressively since it was first described. It is now at such a low rate that huge numbers of patients would be required to definitively demonstrate efficacy of putative treatments to prevent delayed ischemic deficits and infarcts due to vessel narrowing. It is also apparent that the optimal outcome assessment requires a long-term assessment both psychologically and radiologically—not feasible in most studies. Other sources of brain damage, particularly early, are rightly being explored as are other means of delivery of vasodilators. However, in my opinion it is premature to dismiss severe angiographic vasospasm as an independent cause of cerebral infarction or to downplay it as an epiphenomenon resulting from cortical spreading depression, inflammation, thromboembolism, or some unknown process. The "new world of thought" advocates should be careful they do not throw out the baby with the bathwater.

Conflict of Interest The author declares that he has no conflict of interest.

History of Vasospasm Research in Japan: Commemoration of Professor Tomio Ohta

Kenji Kanamaru

Dawn

In the 1960s Professor Setsuro Ebashi, a physiologist from the University of Tokyo, discovered calcium ion plays a pivotal role in muscle contraction for the first time. However, he was confounded by icy neglect of the society of physiologists. The International Conference on Physiology was held in Boston in 1962, and Dr. Ebashi and his coworker Dr. Anne Mary Weber gave a talk about calcium signal which is a key mechanism for regulating muscle contraction. Every single attendant stood against their theory and even laughed at them.

In the 1970s Dr. Koichi Yagi, a biochemist from Hokkaido University, and Dr. Shiro Kakiuchi, a biochemist from Osaka University, introduced calmodulin as an intracellular calcium receptor which plays an important role in smooth muscle cell contraction via activating myosin light chain kinase. In 1969 a pioneer neurosurgeon, Jirō Suzuki, Professor of Tohoku University coined moyamoya disease that is caused by obstruction of internal carotid artery bifurcation. Moyamoya means a puff of cigarette smoke in Japanese. He was a distinguished expert on aneurysm clipping and underwent several thousands of cases. Dr. Suzuki was also a former officer of Japanese Navy and had an extraordinary visual acuity good enough to clip aneurysms without microscope. In the 1970s Keiji Sano, a professor of the University of Tokyo, introduced early surgery of ruptured aneurysms and promoted researches for the prevention of vasospasm after subarachnoid hemorrhage (SAH). His group demonstrated that the earlier the surgery is started within 3 days of SAH, the less incidence of vasospasm was shown. Dr. Sano as a mentor had inspired many neurosurgeons in Japan.

Sunrise and Sunset

Professor Tomio Ohta, a composer of Vasospasm Research, from Osaka Medical College founded Spasm Symposium in 1985. The organizing committee included Keiji Sano, Hajime Handa from the University of Kyoto, Jiro Suzuki, Shozo Ishii from Juntendo University, Haruhiko Kikuchi from the University of Kyoto, and Kintomo Takakura from the University of Tokyo. In the first symposium, Dr. Hiroki Ohkuma presented "Changes of endothelial cells after vasoconstriction in feline basilar artery," Dr. Kenji Kanamaru "Pharmacological evaluation of endothelium-dependent relaxation (EDR) of canine basilar artery," Dr. Tomio Sasaki "SAH impairs endothelium-dependent vasodilating mechanism," and Dr. Hidetoshi Kasuya "Eicosanoids of CSF in patients with SAH." In 1986 the second Spasm Symposium moved to Kyoto City from Osaka City. Ordinarily Spasm Symposium was held in July, in which under a hottest summer season, the discussion heated up. In addition attendees enjoyed the Gion festival in July 17 to get rid of bad luck collected by 33 floats. In the second symposium, Professor Jiro Suzuki's group advocated cervical sympathectomy to dilate spastic cerebral arteries in SAH patients; however, the morbidity and mortality of such procedure were unacceptably high. Thus Professor Shozo Ishii criticized it as a dangerous procedure and did not recommend it universally. We enjoyed discussions made by famous professors who shouted and yelled occasionally. In the third symposium in 1987, case reports of vasospasm with uncertain causes were presented. The question was if a bunch of case reports without statistical analysis was anecdotal. Dr. Ohta remarked: "statistics look like young lady in bikini, it is attractive but a truth is hided." In the fourth symposium held in 1988, topics were angioplasty, clot removal, irrigation drainage with urokinase and vitamin C, and intracisternal calcium antagonists. Clinical trials with small numbers of patients are undergone in each institute sporadically. In the fifth symposium held in 1989, endothelin was the focus of discussion. Endothelin was discovered by Professor Tomoo Masaki's group from Tsukuba University. It was an attractive idea for us that endothelin antag-

K. Kanamaru (✉)
Kanamaru Neurosurgical Clinic, Iga, Japan
e-mail: kanamaru@h6.dion.ne.jp

R. D. Martin et al. (eds.), *Subarachnoid Hemorrhage*, Acta Neurochirurgica Supplement 127,
https://doi.org/10.1007/978-3-030-04615-6_2, © Springer Nature Switzerland AG 2020

onists could ameliorate vasospasm. Indeed, endothelin antagonist such as clazosentan prevented vasospasm in animal model of SAH. Unfortunately its clinical trial was prematurely aborted due to serious lung complications. In the sixth symposium held in 1990, two special lectures were given: one was EDR factor (EDRF) inhibition in vasospasm after SAH presented by Dr. Pyo Kim from the University of Tokyo and the other was cerebrovascular disorder and lipid peroxidation presented by myself from Mie University School of Medicine. In the seventh symposium held in 1991, Professor Bryce Weir from the University of Alberta came and presented with extensive study for aneurysm pathology and related diseases. Trends in vasospasm research were protein kinase C, endothelin, irrigation and drainage of clots after SAH, and intracisternal urokinase and/or nicardipine. Professor Namio Kodama from Fukushima University School of Medicine was a pioneer of intracisternal thrombolysis by using urokinase. Prevalence of vasospasm in his study was as low as below 1%. In the eighth symposium held in 1992, Professor Neal F. Kassell from the University of Virginia came and presented with pharmacological approaches for the treatment of vasospasm. In the 11th symposium held in 1995, Professor Max Findlay from the University of Alberta presented with randomized trial of intraoperative, intracisternal TPA for the prevention of vasospasm. However, there was no significant difference in occurrence of vasospasm between placebo and TPA groups. In the 12th symposium held in 1996, Professor Joseph M. Eskridge from the University of Washington presented with balloon angioplasty for symptomatic vasospasm. From this symposium some intra-arterial vasodilators, papaverine, AT877 (Eril®), and PGE1, were introduced for the prevention of vasospasm. Head shaking method was also introduced during irrigation and drainage after SAH. The retrospective study demonstrated that head shaking was effective in improving vasospasm, infarction, and neurological outcome of patients with SAH. In the 16th symposium held in 2000, the highlight of discussion was a Rho kinase inhibitor, fasudil hydrochloride (Eril®), that had been used in clinical trial for 5 years. The results were published in the *Journal of Neurosurgery* by Drs. Masato Shibuya, Yoshio Suzuki, Masakazu Takayasu, and Hiroyoshi Hidaka from the University of Nagoya. Dr. Hidetoshi Kasuya presented with intracisternal nicardipine pellets placed during surgery for the prevention of vasospasm. 17th symposium joined up with Japan Stroke Conference and Surgery for Cerebral Stroke Conference. The organizing committee of Spasm Symposium worried about shrinkage of prestige of Spasm Symposium. In the 18th symposium held in 2002, the president was Professor Shigeharu Suzuki from Hirosaki University School of Medicine. Professor Bryce Weir came again and presented with cerebral vasospasm—what is known, what is not. In the 20th symposium held in 2004, the president was Dr. Yoshio Suzuki, a disciple of Professor Kenichiro Sugita famous for his Sugita clip. He devoted himself to education of neurosurgical practice in India for years succeeding Dr. Sugita. It was with great sadness that we learned of his sudden death from renal cancer in 2008. In the 24th symposium held in 2008, the president was Professor Isao Date from Okayama University. His group has published extensive studies for vasospasm in basic science and clinical trials. He is now the secretary of Spasm Symposium. In the 13th symposium held in 2014, the president was Professor Hiroki Ohkuma from Hirosaki University School of Medicine. He and his colleague, Dr. Norihito Shimamura, published extensive works for vasospasm in basic science and clinical trials. Remarkably, they published in the *Journal of Neurosurgery* that the local product of apple extracts (procyanidins) prevents vasospasm. In the 31st symposium held in 2015, I served as the president of the symposium. The place was of peace memorial as the only city attacked by atomic bomb. The honored guest was Professor R. Loch Macdonald from the University of Toronto. My longtime colleague, Dr. Hidenori Suzuki, who became the chairman of the Department of Neurosurgery, Mie University School of Medicine, in 2014 supported my presidency. He was also a member of research associates as a disciple of Professor John Zhang in Loma Linda. Thirteenth International Conference on Neurovascular events after subarachnoid hemorrhage held in Karuizawa in 2015, president was Tomio Sasaki professor emeritus University of Kyushu. The honored guest was Tomio Ohta who gave an impressive talk about vasospasm research (Fig. 1). In the last days of his life, he was so enthusiastic to

Fig. 1 Professor Tomio Ohta presented at Karuizawa

develop limited hypothermia machine for cooling the brain. Professor Tomio Ohta, born in 1931 and founder of Spasm Symposium and chairman of the Department of Neurosurgery, Osaka Medical College, died of pancreatic cancer on November 21, 2016. He was not only a founder of Spasm Symposium but also the chief editor of *Textbook of Neurosurgery* from its 1st edition up to its 12th edition. Professor Tomio Ohta was courageous, humble, and extremely gracious as he interacted with his coworkers and followers throughout his life but especially in his final year. And his legacy will live on forever within us.

Conflict of Interest We declare that we have no conflict of interest.

Heparin Treatment in Aneurysmal Subarachnoid Hemorrhage: A Review of Human Studies

Nicolas K. Khattar, Esther Bak, Andrew C. White, and Robert F. James

Abstract Aneurysmal subarachnoid hemorrhage (aSAH) remains a significant cause of stroke disability despite gradual reductions in physical morbidity and mortality. Heparin is an effective anti-inflammatory agent and may potentially prevent delayed neurological injury in the days to weeks after the hemorrhage. Various human studies have shown the safety of a continuous infusion of low-dose unfractionated heparin in the setting of subarachnoid hemorrhage as well as its efficacy in minimizing delayed neurological deficits including symptomatic cerebral vasospasm, vasospasm-related infarction, and cognitive dysfunction. Studies have also shown mixed results with low-molecular-weight heparin usage in this patient population. Heparin treatment is not associated with significant hemorrhagic complications; however, vigilance is essential for early detection of heparin-induced thrombocytopenia in order to prevent devastating sequelae. Multicenter randomized controlled trials are necessary for objective characterization of the effects of heparin.

Keywords Low-dose IV heparin · Enoxaparin · Subarachnoid hemorrhage

Introduction

Aneurysmal subarachnoid hemorrhage (aSAH) remains a significant cause of stroke fatality and physical disability, despite some reductions in morbidity and mortality over the past few decades. The risk of life-altering complications in the form of debilitating psychosocial and cognitive impairments remains significant in up to 70% of patients who survive the initial bleed [1, 11]. Verbal and visual memory, language, and executive function are the most commonly impaired cognitive domains [9]. These impairments surface in the days to weeks following aneurysmal repair and have been postulated to be due to cerebral vasospasm, neuroinflammation, non-obstructive hydrocephalus, cerebral microthrombi, cortical spreading depolarization, oxidative damage, neuronal cell death, and white matter loss [3, 12–14, 19, 20, 25]. A reported 59% of surviving patients never return to their previous occupation, with an even larger majority experiencing deficits in activities of daily living [1, 7]. No treatment strategies have yet proven the ability to prevent neurocognitive impairments after aSAH.

Unfractionated heparin has been shown to be a promising agent in preventing symptomatic cerebral vasospasm and vasospasm-related infarction in the setting of aneurysmal subarachnoid hemorrhage [16, 17]. In addition to its primary clinical usage as an anticoagulant, heparin binding has been shown to interfere with a significant number of other biological pathways [16]. As a negatively charged glycosaminoglycan, heparin has been shown to be involved in the prevention of neuroinflammation, myelin preservation, and inhibition of apoptosis [18, 23]. Such effects can be attributed to heparin's high negative charge density and strong affinity to bind positively charged molecules such as plasma proteins, proteins released from platelets, cytokines, chemokines, other small biologically active molecules, as well as endothelial cells themselves [18, 23]. In this manuscript, we briefly review the human studies that demonstrate the effect of heparin on aSAH survivors.

Heparin and Subarachnoid Hemorrhage

Initial human studies investigated the role of enoxaparin (low-molecular-weight fractionated heparin) in aneurysmal SAH with mixed results. Citing cerebral vasospasm as the

N. K. Khattar · E. Bak · R. F. James (✉)
Department of Neurological Surgery, School of Medicine, University of Louisville, Louisville, KY, USA
e-mail: robert.james@louisville.edu

A. C. White
Department of Radiology, School of Medicine, University of Louisville, Louisville, KY, USA

R. D. Martin et al. (eds.), *Subarachnoid Hemorrhage*, Acta Neurochirurgica Supplement 127, https://doi.org/10.1007/978-3-030-04615-6_3, © Springer Nature Switzerland AG 2020

leading cause of fatalities and physical impairment after subarachnoid hemorrhage, Wurm et al. sought to compare exnoaparin's abilities to reduce risk of vasospasm compared to placebo [22]. One hundred twenty consecutive patients with aSAH (Hunt-Hess I–III) were included after aneurysm repair and were randomly allocated to either one subcutaneous injection of 20 mg enoxaparin or placebo per day for 21 days following SAH [22], Results of the study revealed marked reduction in vasospasm-related infarction (3.5% vs. 28.3%; $p < 0.001$), shunt-dependent hydrocephalus (1.8% vs. 16.7% placebo; $p = 0.019$), and delayed ischemic deficits (DID) (8.8% vs. 66.7% placebo; $p < 0.001$). At 1-year follow-up, patients in the enoxaparin group had significantly better outcomes than the placebo group, supporting the neuroprotective properties of low-molecular-weight heparin [22].

This trial is in stark contrast to a previously conducted double-blind randomized trial showing no effect of enoxaparin on the outcomes of patients following subarachnoid hemorrhage [15]. One hundred seventy patients with aSAH (WFNS grades I–V) were enrolled within 48 h of aneurysm repair. The main endpoint of the trial was neurological outcome at 3 months and did not show any difference between the placebo group and the enoxaparin group [15]. In addition, there was a slight increase in intracranial hemorrhagic complications with no concomitant improvement in neurological outcome [15].

The conflicting data decreased the overall enthusiasm generated by enoxaparin in the treatment of subarachnoid hemorrhage.

Recently, a retrospective cohort study showed significant benefits of unfractionated heparin (UFH) in Fisher grade 3 aneurysmal subarachnoid hemorrhage patients. Eighty-six consecutive patients post aSAH were included in the study evaluating the effects of a continuous infusion of low-dose intravenous unfractionated heparin (LDIVH) on symptomatic cerebral vasospasm and delayed infarct [16]. All patients were treated with craniotomy and surgical clipping of the ruptured aneurysm at least 12 h prior to administration of LDIVH. Forty-seven percent of patients in the control group had symptomatic cerebral vasospasm as compared to 9% in the heparin group ($p = 0.0002$). Patients in the heparin group had significantly decreased vasospasm-related CT infarctions as compared to the patients in the control group (0% vs. 21%, $p = 0.003$; Fig. 1). The study demonstrated the safety and potential significant benefit of LDIVH in patients presenting Fisher grade 3 aSAH.

In another retrospective review of 118 patients with Fisher grade 2–4 aSAH, nimodipine compliance was evaluated as a predictor of discharge to home. The patients were divided into three groups: full dosing compliance, one or more doses split to prevent nimodipine-induced hypotension, and missed dosing. Full dosing compliance in patients co-treated with low-dose heparin infusion was found to be associated with the highest odds of discharge to home (75% who received all doses, 67% who received ≥1 split doses,

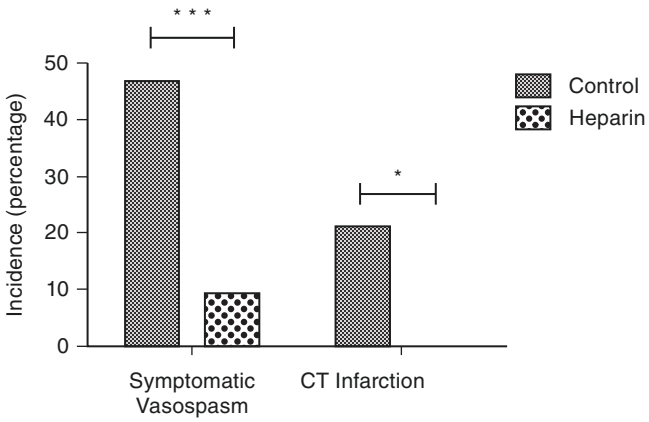

Fig. 1 Adapted from Simard et al. [16]. Vasospasm-related outcomes. Incidence of clinical vasospasm and CT infarctions in the control (CTR) and heparin (HEP) groups. *** $p = 0.0002$; * $p = 0.03$

and 37% with ≥1 missed doses ($p = 0.003$)). This study reinforces the importance of full dosing nimodipine compliance and the potential association with improved disposition outcomes [21].

Bruder et al. conducted a retrospective review of 718 patients receiving treatment for aSAH from 1999 to 2014 to evaluate the neuroprotective functions of intravenous unfractionated heparin. One hundred ninety-seven patients in this cohort were treated with a continuous infusion of unfractionated heparin following endovascular coiling of the aneurysm. The rate of cerebral vasospasm was significantly reduced in the heparin group compared with the control group (14.2% vs. 25.4%; $p = 0.05$) [2]. Duration of treatment was included as an independent variable in heparin treatment. The neuroprotective effect of heparin was enhanced when the treatment was continued for 7 days, but was not significant. About 66.8% of patients who received therapeutic dosage of heparin post aSAH achieved good modified Rankin scores (0–2) at 6 months [2]. In combination with the findings from Simard et al., heparin was proven once again to be safe and potentially efficacious in the treatment of aSAH with a secured aneurysm.

Furthermore, James et al. evaluated a retrospective cohort of 47 aSAH patients for cognitive outcomes based on standard of care therapy versus LDIVH. The Montreal Cognitive Assessment (MoCA) test was used to evaluate the cognitive changes in aSAH patients treated with the LDIVH protocol vs. controls. Patients in the heparin-treated group had a mean MoCA score of 26.4, while those in the control group scored 22.7 ($p = 0.013$, Fig. 2). Serious cognitive impairment did not occur in the heparin-treated cohort as opposed to the control group (0% vs. 32%; $p = 0.008$). In their analysis, the authors showed that LDIVH was associated with a positive influence on MoCA score, while fevers and anterior communicating artery aneurysms were associated with negative influences on MoCA scores [8].

Table 1 is a summary of the main findings in all the human studies of heparin in aSAH.

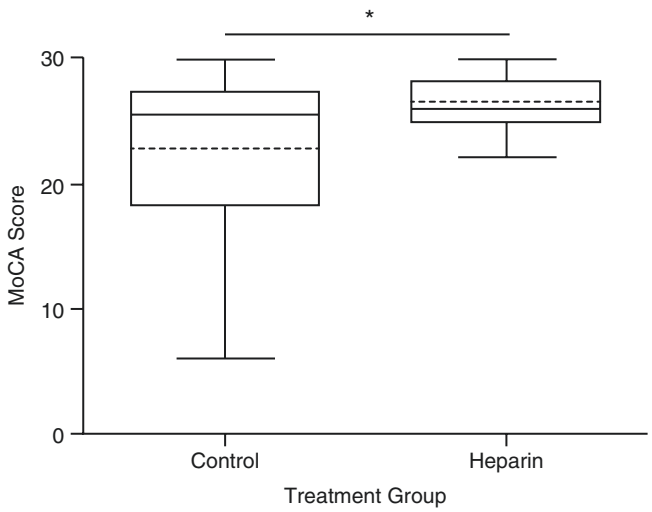

Fig. 2 Used with permission from the *Journal of Neurosurgery* [8]. Box and whiskers plot showing the distribution of MoCA scores for each treatment group. Solid horizontal line, median; dashed horizontal line, mean. Note the tight packing and decreased variance of MoCA scores in the LDIVH treatment group. Asterisk denotes significance between the two groups ($p = 0.013$)

Complications of Heparin

Hydrocephalus is often considered a delayed neurological deficit associated with aneurysmal subarachnoid hemorrhage. A ventriculostomy drain and a shunt for CSF diversion are the two commonly accepted treatment modalities for hydrocephalus. Ventriculostomy-related hemorrhages have always been a concern in patients placed on IV heparin following aSAH. A retrospective review including 241 patients over a 13-year period was conducted to study the risk of hemorrhage and DVT for ventriculostomy patients on heparin prophylaxis [24]. Hemorrhages were labeled as major or minor depending on the size and mass effect, while DVT incidences were also noted. Among the 53 patients on prophylactic IV heparin, three experienced minor hemorrhages with no incidence of major hemorrhage. This study provided more conclusive evidence that hemorrhages related to IV heparin are rare and minor [24]. This was corroborated by the study by Manoel et al., which showed that DVT chemoprophylaxis does not increase the risk of intracranial hemor-

Table 1 Review of studies available regarding the use of heparin in aneurysmal subarachnoid hemorrhage

Author, year	Study design	Number of patients (treatment, control)	Drug, dose, and route	Primary outcome results (treatment vs. control)
Sironen et al., 2003 [15]	Single-center, prospective, double-blind, RCT	170 (85, 85)	Enoxaparin 40 mg SQ QD *Control*: Saline	No significant difference in outcomes between the control and the treatment group
Wurm et al., 2004 [22]	Single-center, prospective, double-blind, RCT	117 (57, 60)	Enoxaparin 20 mg SQ QD *Control*: Saline	Cerebral vasospasm: Delayed ischemic deficit (8.8% vs. 66.7%; $p = 0.001$) Cerebral infarction (3.5% vs. 28.3%; $p = 0.001$) Shunt-dependent hydrocephalus (1.8% vs. 16.7%; $p = 0.019$) Overall outcome (GOS) at 1 year following SAH (4.39 vs. 4.02; $p = 0.017$)
Simard et al., 2013 [16]	Single-center, retrospective analysis	86 (43, 43)	LDIVH (started at 8 U/kgh and increased to 9, and 10–12 U/kg/h at 12, 24, and 36 h after craniotomy, respectively) maintained for 12–16 days after ictus *Control*: UFH 5000U SQ BID	Clinical vasospasm (9% vs. 47%; $p = 0.0002$) Vasospasm-related CT infarct (0% vs. 21%; $p = 0.003$) Discharge home (62.8% vs. 40.5%; $p = 0.05$)
Wessel et al., 2017 [21]	Single-center, retrospective analysis	118 (20, 6, 92)	LDIVH infusion protocol, and Nimodipine 60 mg PO Q4H beginning within 96 h of ictus continued until discharge or up to 21 days (if SBP < 90 mmHg, change in dosing to 30 mg Q2H)	Discharge home (75% vs. 67% vs. 37%; $p = 0.003$)
Bruder et al., 2017 [2]	Single-center, retrospective analysis (matched pair analysis)	394 (197, 197)	LDIVH infusion (goal PTT 60 s) for 1–7 days following endovascular treatment *Control*: LMWH 40 mg SQ QD	Severe vasospasm (14.2% vs. 25.4%; $p = 0.005$)
James et al., 2018 [8]	Single-center, retrospective analysis	47 (25, 22)	Maryland LDIVH infusion protocol [16]	Cognitive outcome (MoCA) at ≥3 months after treatment (26.4 vs. 22.7 $p = 0.013$) MoCA < 20 (0% vs. 31.8%; $p = 0.008$)

RCT randomized control trial, *GOS* Glasgow Outcome Score, *SAH* subarachnoid hemorrhage, *mRS* Modified Rankin Scale, *LDIVH* low-dose intravenous heparin, *UFH* unfractionated heparin, *CT* computed tomography, *LMWH* low molecular weight heparin, *MoCA* Montreal Cognitive Assessment

rhage in the setting of aSAH [10]. However, the authors cautioned against the usage of IV heparin with dual antiplatelet therapy due to significant concerns of an induced bleeding diathesis [10].

In addition to hemorrhagic complications, heparin-induced thrombocytopenia is a potentially fatal complication associated with a significant decrease in platelet count following multiple day exposure to intravenous heparin [5]. The incidence of heparin-induced thrombocytopenia type II (HIT II) ranges between 0.2 and 3% and has been reported to raise the risk of thrombotic events in patients with this autoimmune disorder [4]. HIT II is characterized by antibodies directed against complexes that form between heparin or other anionic mucopolysaccharides and platelet factor 4, a heparin-binding protein released by activated platelets [6]. Despite a higher incidence of HIT in patients with cerebrovascular neurologic disease, careful daily monitoring of platelet count allows early detection and treatment of HIT with cessation of the heparin infusion [6].

Conclusion

Intravenous unfractionated heparin is a neuroprotective agent in aSAH with proven safety and effectiveness in humans. Multicenter randomized controlled trials are needed to definitively demonstrate the various neuroprotective effects of heparin in patients with aSAH. The Aneurysmal Subarachnoid Hemorrhage Trial Randomizing Heparin (ASTROH) is a phase 2 randomized multicenter trial with blinded adjudication of outcomes and is currently enrolling subjects to evaluate LDIVH in aSAH patients (NCT02501434). Additional evidence supporting the safety and effectiveness of LDIVH in aSAH may help direct future phase 3 studies that could potentially prove heparin is beneficial allowing its acceptance as a standard treatment for aneurysmal subarachnoid hemorrhage survivors.

Conflict of Interest RFJ is the study chair for ASTROH, a phase 2 clinical trial evaluating heparin treatment in aneurysmal subarachnoid hemorrhage. We delare that we have no other conflicts of interest with the contents of this manuscript.

Source of Funding: **None.**

References

1. Al-Khindi T, Macdonald RL, Schweizer TA. Cognitive and functional outcome after aneurysmal subarachnoid hemorrhage. Stroke. 2010;41:e519–36.
2. Bruder M, Won S-YY, Kashefiolasl S, Wagner M, Brawanski N, Dinc N, Seifert V, Konczalla J. Effect of heparin on secondary brain injury in patients with subarachnoid hemorrhage: an additional 'H' therapy in vasospasm treatment. J Neurointerv Surg. 2017;9:659–63.
3. Crowley MG, Liska MG, Borlongan CV. Stem cell therapy for sequestering neuroinflammation in traumatic brain injury: an update on exosome-targeting to the spleen. J Neurosurg Sci. 2017;61:291–302.
4. Girolami B, Prandoni P, Stefani PM, Tanduo C, Sabbion P, Eichler P, Ramon R, Baggio G, Fabris F, Girolami A. The incidence of heparin-induced thrombocytopenia in hospitalized medical patients treated with subcutaneous unfractionated heparin: a prospective cohort study. Blood. 2003;101:2955–9.
5. Hacker RI, Ritter G, Nelson C, Knobel D, Gupta R, Hopkins K, Marini CP, Barrera R. Subcutaneous heparin does not increase postoperative complications in neurosurgical patients: an institutional experience. J Crit Care. 2012;27:250–4.
6. Harbrecht U, Bastians B, Kredteck A, Hanfland P, Klockgether T, Pohl C. Heparin-induced thrombocytopenia in neurologic disease treated with unfractionated heparin. Neurology. 2004;62:657–9.
7. Hellawell DJ, Taylor R, Pentland B. Persisting symptoms and carers' views of outcome after subarachnoid haemorrhage. Clin Rehabil. 1999;13:333–40.
8. James RF, Khattar NK, Aljuboori ZS, Page P, Shao EY, Carter LM, Meyer KS, Daniels MJ, Craycroft J, Gaughen JR Jr, Chaudry MI, Rai SN, Everhart DE, Simard JM. Continuous infusion of low-dose unfractionated heparin after aneurysmal subarachnoid hemorrhage: a preliminary study of cognitive outcomes. J Neurosurg. 2018;11:1–8. https://doi.org/10.317.1/2017.11.JNS17894 [Epub ahead of print].
9. Kreiter KT, Copeland D, Bernardini GL, Bates JE, Peery S, Claassen J, Du YE, Stern Y, Connolly ES, Mayer SA. Predictors of cognitive dysfunction after subarachnoid hemorrhage. Stroke. 2002;33:200–8.
10. Manoel AL, Turkel-Parrella D, Germans M, Kouzmina E, Almendra Pda S, Marotta T, Spears J, Abrahamson S. Safety of early pharmacological thromboprophylaxis after subarachnoid hemorrhage. Can J Neurol Sci. 2014;41:554–61.
11. Mavaddat N, Sahakian BJ, Hutchinson PJ, Kirkpatrick PJ. Cognition following subarachnoid hemorrhage from anterior communicating artery aneurysm: relation to timing of surgery. J Neurosurg. 1999;91:402–7.
12. Parra A, Kreiter KT, Williams S, Sciacca R, Mack WJ, Naidech AM, Commichau CS, Fitzsimmons BF, Janjua N, Mayer SA, Connolly ES Jr. Effect of prior statin use on functional outcome and delayed vasospasm after acute aneurysmal subarachnoid hemorrhage: a matched controlled cohort study. Neurosurgery. 2005;56:476–84; discussion 476–84.
13. Provencio JJ, Vora N. Subarachnoid hemorrhage and inflammation: bench to bedside and back. Semin Neurol. 2005;25:435–44.
14. Pyne-Geithman GJ, Caudell DN, Prakash P, Clark JF. Glutathione peroxidase and subarachnoid hemorrhage: implications for the role of oxidative stress in cerebral vasospasm. Neurol Res. 2009;31:195–9.
15. Siironen J, Juvela S, Varis J, Porras M, Poussa K, Ilveskero S, Hernesniemi J, Lassila R. No effect of enoxaparin on outcome of aneurysmal subarachnoid hemorrhage: a randomized, double-blind, placebo-controlled clinical trial. J Neurosurg. 2003;99:953–9.
16. Simard JM, Aldrich EF, Schreibman D, James RF, Polifka A, Beaty N. Low-dose intravenous heparin infusion in patients with aneurysmal subarachnoid hemorrhage: a preliminary assessment. J Neurosurg. 2013;119:1611–9.
17. Simard JM, Schreibman D, Aldrich EF, Stallmeyer B, Le B, James RF, Beaty N. Unfractionated heparin: multitargeted therapy for delayed neurological deficits induced by subarachnoid hemorrhage. Neurocrit Care. 2010;13:439–49.

18. Simard JM, Tosun C, Ivanova S, Kurland DB, Hong C, Radecki L, Gisriel C, Mehta R, Schreibman D, Gerzanich V. Heparin reduces neuroinflammation and transsynaptic neuronal apoptosis in a model of subarachnoid hemorrhage. Transl Stroke Res. 2012;3:155–65.
19. Stein SC, Levine JM, Nagpal S, LeRoux PD. Vasospasm as the sole cause of cerebral ischemia: how strong is the evidence? Neurosurg Focus. 2006;21:E2.
20. Vergouwen MD, Vermeulen M, Coert BA, Stroes ES, Roos YB. Microthrombosis after aneurysmal subarachnoid hemorrhage: an additional explanation for delayed cerebral ischemia. J Cereb Blood Flow Metab. 2008;28:1761–70.
21. Wessell A, Kole MJ, Badjatia N, Parikh G, Albrecht JS, Schreibman DL, Simard JM. High compliance with scheduled nimodipine is associated with better outcome in aneurysmal subarachnoid hemorrhage patients cotreated with heparin infusion. Front Neurol. 2017;8:268.
22. Wurm G, Tomancok B, Nussbaumer K, Adelwohrer C, Holl K. Reduction of ischemic sequelae following spontaneous subarachnoid hemorrhage: a double-blind, randomized comparison of enoxaparin versus placebo. Clin Neurol Neurosurg. 2004;106:97–103.
23. Young E. The anti-inflammatory effects of heparin and related compounds. Thromb Res. 2008;122:743–52.
24. Zachariah J, Snyder KA, Graffeo CS, Khanal DR, Lanzino G, Wijdicks EF, Rabinstein AA. Risk of ventriculostomy-associated hemorrhage in patients with aneurysmal subarachnoid hemorrhage treated with anticoagulant thromboprophylaxis. Neurocrit Care. 2016;25:224–9.
25. Zhang ZD, Macdonald RL. Contribution of the remodeling response to cerebral vasospasm. Neurol Res. 2006;28:713–20.

Subarachnoid Hemorrhage-Related Epilepsy

Warren Boling and Lydia Kore

Abstract Epilepsy is a significant worldwide public health problem that leads to reduced quality of life and negative psychosocial consequences and significantly increases mortality rates in those who are affected. The development of epilepsy from subarachnoid hemorrhage (SAH) has an important negative impact on long-term survival, functional status, and cognitive recovery in patients following aneurysmal rupture. Anticonvulsant medication (AED) administration to prevent the development of epilepsy following SAH is controversial, and studies to date have not shown effectiveness of AED use as prophylaxis. This paper reviews the pathophysiology of SAH in the development of epilepsy, the scope of the problem of epilepsy related to SAH, and the studies that have evaluated AED administration as prophylaxis for seizures and epilepsy.

Introduction

Epilepsy affects many people worldwide representing 0.6% of the global burden of disease as measured by disability-adjusted life years [18]. In North America the prevalence rate is estimated to be 10/1000 [9]. However, in the severely underresourced regions of the world such as sub-Saharan Africa, epilepsy prevalence is much higher. For example, epilepsy prevalence in East Africa has been estimated to be as high as 13% [13]. Worldwide including North America, poverty has been strongly linked with elevated epilepsy prevalence [4].

Most people with epilepsy (PWE) will have their seizures controlled with medication. However, a surprisingly large population (about 30%) of PWE will be refractory to medication, so-called medically intractable epilepsy (MIE). MIE is defined by the International League Against Epilepsy as the failure of two or more antiepileptic medications (AEDs) to control the seizures [16]. Despite the currently approximately 20 medications available in the United States and Europe for epilepsy, only 2 need to be tried and failed to meet the definition of intractability. If two or more AEDs have failed to stop the epilepsy, the opportunity of any new medication or combination of medications to stop the epilepsy is less than 5% [15].

Individuals with MIE are found to have reduced health-related quality of life, and MIE is associated with significant negative psychological and social consequences including lower education levels, lower rates of employment, social isolation, and stigma [2, 5, 7].

MIE results over time in morbidity of cognitive decline due to recurrent seizures and significantly increases the mortality rate of individuals with epilepsy. The cognitive consequence of MIE is most commonly seen in patients with temporal lobe epilepsy that particularly negatively impacts memory function. A decline in declarative memory is thought to result from excitotoxic injury to the mesial temporal lobe structures, which often manifests neuroanatomically as an atrophic hippocampus [8]. Epilepsy is a dangerous disease that has a mortality rate 2.3 times that of age-matched controls in the general population. Most striking however are individuals with MIE who are exposed to a risk of death 4.69 times the general population [26]. The excess mortality is mostly due to sudden unexpected death in epilepsy (SUDEP), trauma, and other injuries.

The Epileptic Focus

A seizure results from paroxysmal depolarization, which is an exaggeration of the normal neuronal depolarization. This occurs when a predominance of glutaminergic excitation

W. Boling (✉)
Department of Neurosurgery, Loma Linda University, Loma Linda, CA, USA
e-mail: wboling@LLU.edu

L. Kore
Loma Linda University, School of Medicine, Loma Linda, CA, USA

R. D. Martin et al. (eds.), *Subarachnoid Hemorrhage*, Acta Neurochirurgica Supplement 127, https://doi.org/10.1007/978-3-030-04615-6_4,

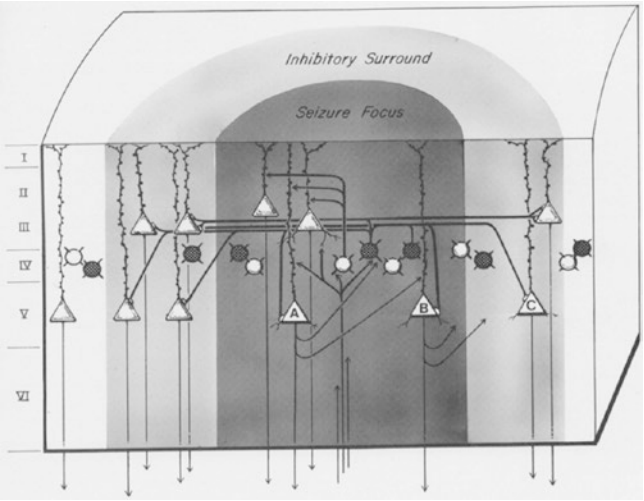

Fig. 1 The figure illustrates a conceptual framework for the initiation and propagation of a seizure. Cell A represents an epileptic pyramidal neuron; discharges will capture cell B via excitatory recurrent collateral connections. When many cells like A and B fire synchronously, an epileptic spike appears on EEG. Inhibitory interneurons (dark round cells) become activated and turn off cells A and B as well prevent spread of the seizure discharge to neurons in the surrounding cortex (cell C). Reprinted by permission of Oxford University Press, USA. From Lothman EW, Collins RC. Seizures and Epilepsy. In: Neurobiology of Disease: Seizures and Epilepsy edited by Pearlman and Collins (1990) Fig. 1 pp. 276–298

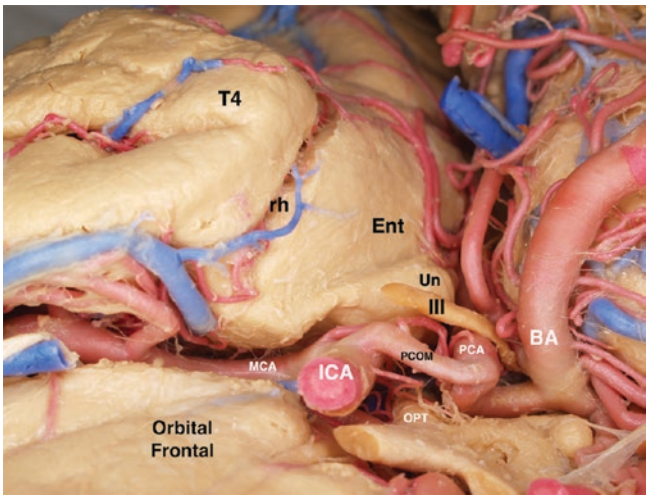

Fig. 2 View of a fixed and injected brain from the orbital frontal surface looking posteriorly. The normal relationship of internal carotid artery and circle of Willis vascular structures that lie adjacent to the highly epileptogenic limbic brain structures of the mesial temporal and orbital frontal regions is visualized. *T4* fusiform gyrus of the temporal lobe, *rh* rhinal sulcus, *Ent* entorhinal sulcus (most anterior extent of the parahippocampus), *Un* uncus, *III* oculomotor cranial nerve, *ICA* internal carotid artery, *PCA* posterior cerebral artery, *PCOM* posterior communicating artery, *OPT* optic chiasm, *BA* basilar artery

overcomes the surrounding GABAergic inhibition (Fig. 1). The limbic structures including basal forebrain and mesial temporal lobes are the most susceptible brain regions to epileptogenesis, and these supratentorial bases of the brain regions are most likely to be involved by an anterior circulation aneurysmal subarachnoid hemorrhage due to the close proximity to the circle of Willis (Fig. 2).

Different factors related to SAH can induce the changes required in the cortex that will lead to cortical hyperexcitability. One of the most important contributors to injury and neuronal hyper-excitability is the breakdown products of subarachnoid hemorrhage, predominantly Fe compounds derived from hemoglobin. Free iron is a potent oxidizer that damages cell membranes due to creation of reactive oxygen species, peroxidation damage to cell membrane lipids, production of free radicals, and injury to oxidant-sensitive cellular enzymes such as Na, K-ATPase [25]. Yip and Sastry studied the effects of hemoglobin and its degradation products (hemin and iron) on synaptic transmission in a rat model [31]. While hemoglobin did not appear to produce significant effects on synaptic transmission, both hemin and iron were shown to have significant effect on neuronal function by depressing the excitatory postsynaptic potential. In hemorrhagic stroke or intracerebral hemorrhage, iron released from the hemoglobin that has leaked out of the neurovascular space is a potent oxidative metabolite that produces free radicals which ultimately leads to neuronal cell death [23]. Additionally, iron compounds, such as FeCl3, have been commonly used in animal models of epilepsy due to their highly epileptogenic effect when injected into the animal hippocampus and cortex [27, 30].

Brain injury of any type leads to an increase in permeability of the blood-brain barrier and neuroinflammatory responses [1]. Subarachnoid hemorrhage and blood breakdown products result in oxidative stress due to overproduction of reactive oxygen species, which in turn incite a neuroinflammatory reaction. Neuroinflammation results from a myriad of mediators released from the injured blood vessels and immune cells of the body that responds to injury. The resulting inflammatory process is a powerful epilepsy inducer that contributes to not only epileptogenesis but drug resistance as well in animal models [29]. And a number of anti-inflammatory drugs have been found to reduce experimental model epilepsy seizure frequency and/or seizure duration as well as mitigate experimental epileptogenesis [28]. Many human epilepsy syndromes are being recognized to be mediated by neuroinflammation resulting in an increase in immune-modulating therapies benefitting human epilepsy as well [14].

Subarachnoid Hemorrhage-Related Epilepsy

The risk of developing epilepsy after SAH has been analyzed in two large population-based studies. The cumulative incidence of epilepsy in a Finnish population served by one ter-

tiary hospital was found to be 8% at 1 year after hemorrhage and increased to 12% after 5 years [11]. Olafsson et al. in an Iceland population-based study identified that 25% of individuals with ruptured aneurysmal SAH developed epilepsy [20]. The actuarial risk of epilepsy was 18% by the first year, 23% by the second year, and 25% by the fifth year in survivors of SAH. Aneurysm location most associated with the development of SAH-related chronic epilepsy is middle cerebral artery at the M1 branch and artery bifurcation [11]. Severe Hunt and Hess scores as well as intraventricular hemorrhage elevate the risk of having a seizure after SAH [21]. Also, the degree of neurological impairment and presence of an acute seizure soon after the time of SAH have been identified as factors increasing the risk of chronic epilepsy [20].

The development of epilepsy from subarachnoid hemorrhage has an important impact on the cognitive recovery and long-term survival of the patient after aneurysm rupture. In one population study of individuals admitted to an Eastern Finland hospital and alive at least 12 months after subarachnoid hemorrhage, Jukka Huttunen et al. analyzed epilepsy-related long-term mortality [12]. Using cox regression analysis of risk factors of mortality from ruptured intracranial aneurysms, the authors identified that acute seizures occurring within 1 week after admission had no significant relationship with death. However, death at over 12 months after subarachnoid hemorrhage was highly correlated with SAH-related chronic epilepsy.

Seizures following SAH more commonly occur acutely during hospitalization and may be identified in as many as 10–20% of patients who suffer from SAH and are mostly nonconvulsive [10]. Barret Rush et al. queried a nationwide inpatient database to evaluate the association between seizures and mortality in patients with aneurysmal subarachnoid hemorrhage [24]. The presence of seizures during the hospital stay among several other variables was identified to be a factor significantly associated with mortality, and in those patients who survived hospitalization, having a seizure increased the patients' hospital length of stay. The overall burden of number of seizures experienced in SAH-related nonconvulsive epilepsy was found by De Marchis et al. to be highly associated with functional and cognitive decline [6]. The authors identified in SAH patients who underwent continuous EEG monitoring during the hospital stay, the detection of any seizure on EEG was associated with more than threefold elevated odds of unfavorable outcome at 3 months in functional status and cognitive abilities.

AED Prophylaxis

AED prophylaxis is a topic of both interest and controversy. Due to the high seizure risk observed following SAH and the unfavorable outcome associated with seizures, prevention should be an important part of treatment to reduce disability and death. However, prophylactic anticonvulsant medications have performed poorly and not substantially reduced the incidence of early or late seizures and epilepsy after SAH [22].

Raper et al., after reviewing seizures following aneurysmal SAH, determined there was no significant difference in the incidence of early or late seizures in individuals who received AEDs compared to those who received no AEDs [22]. Similarly, Panczykowski et al. analyzed the use of prophylactic AED administration following spontaneous subarachnoid hemorrhage [21]. This study identified the risk of clinical or electrographic seizures was significantly associated with severe Hunt-Hess score and intraventricular hemorrhage. However, the incidence of seizures did not vary significantly based on the use of AED prophylaxis, and a propensity score-matched analysis suggested patients who received prophylactic AED had a similar likelihood of suffering seizures as those who did not. After adjustment for Hunt-Hess score, cisternal SAH burden, and intraventricular hemorrhage, the multivariable regression analysis did not reveal prophylactic AED therapy to be a significant predictor of seizure risk; likewise, timing of prophylactic AED administration and duration of treatment did not impact seizure risk.

Despite a lack of evidence of efficacy, anticonvulsants are often prescribed to patients as seizure prophylaxis. Of the anticonvulsant therapies available, phenytoin has historically been administered for seizure prophylaxis after SAH, though current practice is trending toward the use of levetiracetam. However, adverse effects of AEDs may outweigh benefit in preventing seizures. Naidech et al. studied the use of phenytoin in SAH patients [19]. The use of phenytoin was associated with poor functional and cognitive outcome in a dose-dependent manner following subarachnoid hemorrhage at 14 days. The higher phenytoin dose burden increased the odds of poor functional outcome at 14 days. The higher quartile of phenytoin dosage was also associated with worse cognitive status scores both at discharge and at 3 months.

The newer anticonvulsants have also been implicated in worse functional outcome when prescribed as seizure prophylaxis in SAH. Human et al. identified in a randomized open-label trial of levetiracetam use as prophylaxis in SAH patients that administration of medication during the entire hospitalization resulted in significantly reduced functional status compared to patients that stopped medication after 3 days from admission [10]. In an animal model of neuroinflammation type of epilepsy, exposure to levetiracetam increased the number of seizures and seizure burden of the epileptic mice that was cumulative over time [3].

Conclusion

Epilepsy is a worldwide burden that results in reduced quality of life, is associated with negative psychosocial consequences, and significantly elevates mortality rates in those who are affected. The development of epilepsy from SAH plays an important role in the impact of long-term survival, functional status, and cognitive recovery in patients following aneurysmal rupture. Utilization of AEDs to prevent the development of epilepsy following SAH continues to remain a controversy, and studies to date have not shown effectiveness of AED use as prophylaxis. In fact, the weight of the evidence suggests harm from the administration of AEDs as prophylaxis. Despite clear guidelines existing for the use of AED to prevent early seizures in traumatic brain injury, evidence is lacking in SAH. The Epilepsy Group of the Cochrane Collaboration identified a lack of evidence to support or refute the use of AEDs for the prevention of SAH-related seizures and concluded that "well-designed randomized controlled trials are urgently needed to guide clinical practice [17]."

Conflict of Interest The authors affirm that they have no conflicts of interest related to this manuscript.

References

1. Abdul-Muneer PM, Chandra N, Haorah J. Interactions of oxidative stress and neurovascular inflammation in the pathogenesis of traumatic brain injury. Mol Neurobiol. 2015;51:966–79.
2. Baker GA. The psychosocial burden of epilepsy. Epilepsia. 2002;43(Suppl 6):26–30.
3. Barker-Haliski ML, Löscher W, White HS, Galanopoulou AS. Neuroinflammation in epileptogenesis. Epilepsia. 2017;58(Suppl 3):39–47.
4. Baumann RJ, Marx BM, Leonidakis MG. An estimate of the prevalence of epilepsy in a rural Appalachian population. Am J Epidemiol. 1977;106:42–52.
5. Birbeck G, Chomba E, Atadzhanov M, Mbewe E, Haworth A. The social and economic impact of epilepsy in Zambia: a cross-sectional study. Lancet Neurol. 2007;6:39–44.
6. De Marchis GM, Pugin D, Meyers E, Velasquez A, Suwatcharangkoon S, Park S, Falo MC, Agarwal S, Mayer S, Schmidt JM, Connolly ES, Claassen J. Seizure burden in subarachnoid hemorrhage associated with functional and cognitive outcome. Neurology. 2016;86:253–60.
7. Fletcher A, Sims-Williams H, Wabulya A, Boling W. Stigma and quality of life at long-term follow-up after surgery for epilepsy in Uganda. Epilepsy Behav. 2015;52:128–31.
8. Helmstaedter C, Elger CE. Chronic temporal lobe epilepsy: a neurodevelopmental or progressively dementing disease? Brain. 2009;132:2822–30.
9. Hesdorffer DC, Beck V, Begley CE, Bishop ML, Cushner-Weinstein S, Holmes GL, Shafer PO, Sirven JI, Austin JK. Research implications of the Institute of Medicine Report, Epilepsy Across the Spectrum: Promoting Health and Understanding. Epilepsia. 2013;54:207–16.
10. Human T, Diringer MN, Allen M, Zipfel GJ, Chicoine M, Dacey R, Dhar R. A randomized trial of brief versus extended seizure prophylaxis after aneurysmal subarachnoid hemorrhage. Neurocrit Care. 2018;28(2):169–74. https://doi.org/10.1007/s12028-017-0440-5.
11. Huttunen J, Kurki MI, von Und Zu Fraunberg M, Koivisto T, Ronkainen A, Rinne J, Jääskeläinen JE, Kälviäinen R, Immonen A. Epilepsy after aneurysmal subarachnoid hemorrhage: a population-based, long-term follow-up study. Neurology. 2015;84:2229–37.
12. Huttunen J, Lindgren A, Kurki MI, Huttunen T, Frösen J, Koivisto T, von Und Zu Fraunberg M, Immonen A, Jääskeläinen JE, Kälviäinen R. Epilepsy-associated long-term mortality after aneurysmal subarachnoid hemorrhage. Neurology. 2017;89:263–8.
13. Kaddumukasa M, Mugeny L, Kaddumukasa MN, Ddumba E, Devereaux M, Furlan A, Sajatovic M, Katabira E. Prevalence and incidence of neurological disorders among adult Ugandans in rural and urban Mukono district; a cross-sectional study. BMC Neurol. 2016;16:227.
14. Korff CM, Dale RC. The immune system in pediatric seizures and epilepsies. Pediatrics. 2017. https://doi.org/10.1542/peds.2016-3534.
15. Kwan P, Brodie MJ. Early identification of refractory epilepsy. N Engl J Med. 2000;342:314–9.
16. Kwan P, Arzimanoglou A, Berg AT, Brodie MJ, Allen Hauser W, Mathern G, Moshé SL, Perucca E, Wiebe S, French J. Definition of drug resistant epilepsy: consensus proposal by the ad hoc Task Force of the ILAE Commission on Therapeutic Strategies. Epilepsia. 2010;51:1069–77.
17. Marigold R, Günther A, Tiwari D, Kwan J. Antiepileptic drugs for the primary and secondary prevention of seizures after subarachnoid haemorrhage. 2013. http://www.cochrane.org/CD008710/EPILEPSY_antiepileptic-drugs-for-the-primary-and-secondary-prevention-of-seizures-after-subarachnoid-haemorrhage. Accessed 1 Mar 2018.
18. Murray CJ, Vos T, Lozano R, Naghavi M, Flaxman AD, Michaud C, Ezzati M, et al. Disability-adjusted life years (DALYs) for 291 diseases and injuries in 21 regions, 1990–2010: a systematic analysis for the Global Burden of Disease Study. Lancet. 2012;380:2197–223.
19. Naidech AM, Kreiter KT, Janjua N, Ostapkovich N, Parra A, Commichau C, Connolly ES, Mayer SA, Fitzsimmons BF. Phenytoin exposure is associated with functional and cognitive disability after subarachnoid hemorrhage. Stroke. 2005;36:583–7.
20. Olafsson E, Gudmundsson G, Hauser WA. Risk of epilepsy in long-term survivors of surgery for aneurysmal subarachnoid hemorrhage: a population-based study in Iceland. Epilepsia. 2000;41:1201–5.
21. Panczykowski D, Pease M, Zhao Y, Weiner G, Ares W, Crago E, Jankowitz B, Ducruet AF. Prophylactic antiepileptics and seizure incidence following subarachnoid hemorrhage: a propensity score-matched analysis. Stroke. 2016;47:1754–60.
22. Raper DM, Starke RM, Komotar RJ, Allan R, Connolly ES Jr. Seizures after aneurysmal subarachnoid hemorrhage: a systematic review of outcomes. World Neurosurg. 2013;79:682–90.
23. Regan RF, Panter SS. Neurotoxicity of hemoglobin in cortical cell culture. Neurosci Lett. 1993;153:219–22.
24. Rush B, Wiskar K, Fruhstorfer C, Hertz P. Association between seizures and mortality in patients with aneurysmal subarachnoid hemorrhage: a nationwide retrospective cohort analysis. Seizure. 2016;41:66–9.
25. Sadrzadeh SMH, Eaton JW. Hemoglobin-mediated oxidant damage to the central nervous system requires endogenous ascorbate. J Clin Invest. 1988;82:1510–5.

26. Sperling MR, Feldman H, Kinman J, Liporace JD, O'Connor MJ. Seizure control and mortality in epilepsy. Ann Neurol. 1999;46:45–50.
27. Ueda Y, Willmore LJ, Triggs WJ. Amygdalar injection of FeCl3 causes spontaneous recurrent seizures. Exp Neurol. 1998;153:123–7.
28. van Vliet EA, Aronica E, Vezzani A, Ravizza T. Review: neuroinflammatory pathways as treatment targets and biomarker candidates in epilepsy: emerging evidence from preclinical and clinical studies. Neuropathol Appl Neurobiol. 2018;44:91–111.
29. Vezzani A, French J, Bartfai T, Baram TZ. The role of inflammation in epilepsy. Nat Rev Neurol. 2011;7:31–40.
30. Willmore LJ, Sypert GW, Munson JB, Hurd RW. Chronic focal epileptiform discharges induced by injection of iron into rat and cat cortex. Science. 1978;200:1501–3.
31. Yip S, Sastry B. Effects of hemoglobin and its breakdown products on synaptic transmission in rat hippocampal CA1 neurons. Brain Res. 2000;864:1–12.

Part I

Basic Science Section

Cell Culture Model to Study Cerebral Aneurysm Biology

Alejandra N. Martinez, Crissey L. Pascale, Peter S. Amenta, Rachel Israilevich, and Aaron S. Dumont

Abstract Mechanisms governing cerebral aneurysm (CA) formation, progression, and rupture remain incompletely understood. However, understanding such mechanisms is critical to improving treatment for patients harboring CA. In vitro studies facilitate dissecting molecular mechanisms underlying vascular pathology and allow screening of therapies that can be subsequently explored in vivo. Cerebral vascular smooth muscle cells (VSMC) are an important constituent of the vessel wall, and phenotypic modulation of these cells to a pro-inflammatory, pro-matrix remodeling phenotype appears to be important in CA pathology. We have taken a reductionist approach using cultured cerebral VSMC to further explore CA biology. We describe techniques for culturing cerebral VSMC and outline experimental approaches incorporating these cells to study CA biology.

Keywords Vascular smooth muscle cells · Cell culture · Cerebral aneurysm · Phenotypic modulation · Inflammation

Introduction

Cerebral aneurysms (CA) remain a devastating disease despite intense research interest and clinical focus. Approximately 2–3% of the population harbors unruptured CA [7]. Rupture of CA produces subarachnoid hemorrhage (SAH) which unfortunately continues to be associated with a poor outcome. More than 10% of patients with ruptured CA die before receiving medical attention, and up to 40% die in the hospital. Furthermore, only 25% of those surviving for more than 1 month recover completely [6, 19]. There are approximately 30,000 ruptures per year in the United States (6–9 per 100,000) although this may be fivefold higher in certain populations [18]. Although SAH accounts for 3–11% of all strokes, this devastating disease accounts for more than one-quarter of potential life years lost through stroke [10, 26].

There is much that is unknown about the basic biology of CA. For example, consider the following case illustration. A 47-year-old female presents with sudden severe headache. A non-contrast head computed tomography (CT) demonstrates subarachnoid hemorrhage predominantly in the right sylvian fissure and carotid cistern (Fig. 1a). The patient undergoes uncomplicated coil embolization of a right posterior communicating artery aneurysm (posttreatment angiogram shown Fig. 1b). At this time, two other unruptured aneurysms were found on the left internal carotid artery angiogram including a left anterior choroidal artery aneurysm and left middle cerebral artery aneurysm (Fig. 1c). The patient is lost to follow-up. Five years later she presents with another SAH (Fig. 1d). A new angiogram demonstrates that the rupture source is a right carotid bifurcation aneurysm (Fig. 1e). In retrospect, there was a tiny bump at this location 5 years earlier. However, according to our current understanding, the larger previously documented left-sided aneurysms should have ruptured. Hence, despite the technological advances in this field, research efforts are still needed to precisely predict the risk of rupture and to better understand the mechanisms of origin and growth of aneurysms. Such understanding will facilitate selecting which patients to treat when an unruptured CA is found and also allow the development of noninvasive or minimally invasive therapies for CA. Currently, there is no known medical therapy for CA.

Vascular Smooth Muscle Cells

Vascular smooth muscle cells (VSMC) are highly specialized in mature animals whose principal function is to regulate the attributes of blood vessels in the body, thus having a vasoregulatory role. However, VSMC, unlike other smooth

A. N. Martinez · C. L. Pascale · P. S. Amenta · R. Israilevich
A. S. Dumont (✉)
Department of Neurosurgery, Tulane Center for Clinical Neurosciences, Tulane University School of Medicine, New Orleans, LA, USA
e-mail: adumont2@tulane.edu

R. D. Martin et al. (eds.), *Subarachnoid Hemorrhage*, Acta Neurochirurgica Supplement 127, https://doi.org/10.1007/978-3-030-04615-6_5,

muscle cells (SMC), retain remarkable plasticity and can undergo profound, reversible changes in phenotype in response to environmental cues. During development, VSMC undergo a phenotypic switch, changing into a differentiated state where its primary function is contraction to regulate vascular tone and blood pressure. This state is characterized by expression of SMC marker genes, including smooth muscle myosin heavy chain (SM-MHC), SM-22α, and SM α-actin. Environmental factors such as cigarette smoke [22, 25] can induce phenotypic modulation in producing VSMC characterized by a pro-inflammatory, pro-matrix remodeling phenotype with reduced expression of VSMC marker genes and concomitant induction of pro-inflammatory and pro-matrix remodeling genes.

We and others [3, 20, 21, 23, 24] have demonstrated that SMC marker gene expression is subject to complex combinatorial controls. CArG elements are found in the promoter and/or intronic regions of SMC marker genes and are critical in the regulation of SMC marker gene expression [16, 17, 29]. Compelling evidence has demonstrated that SMC

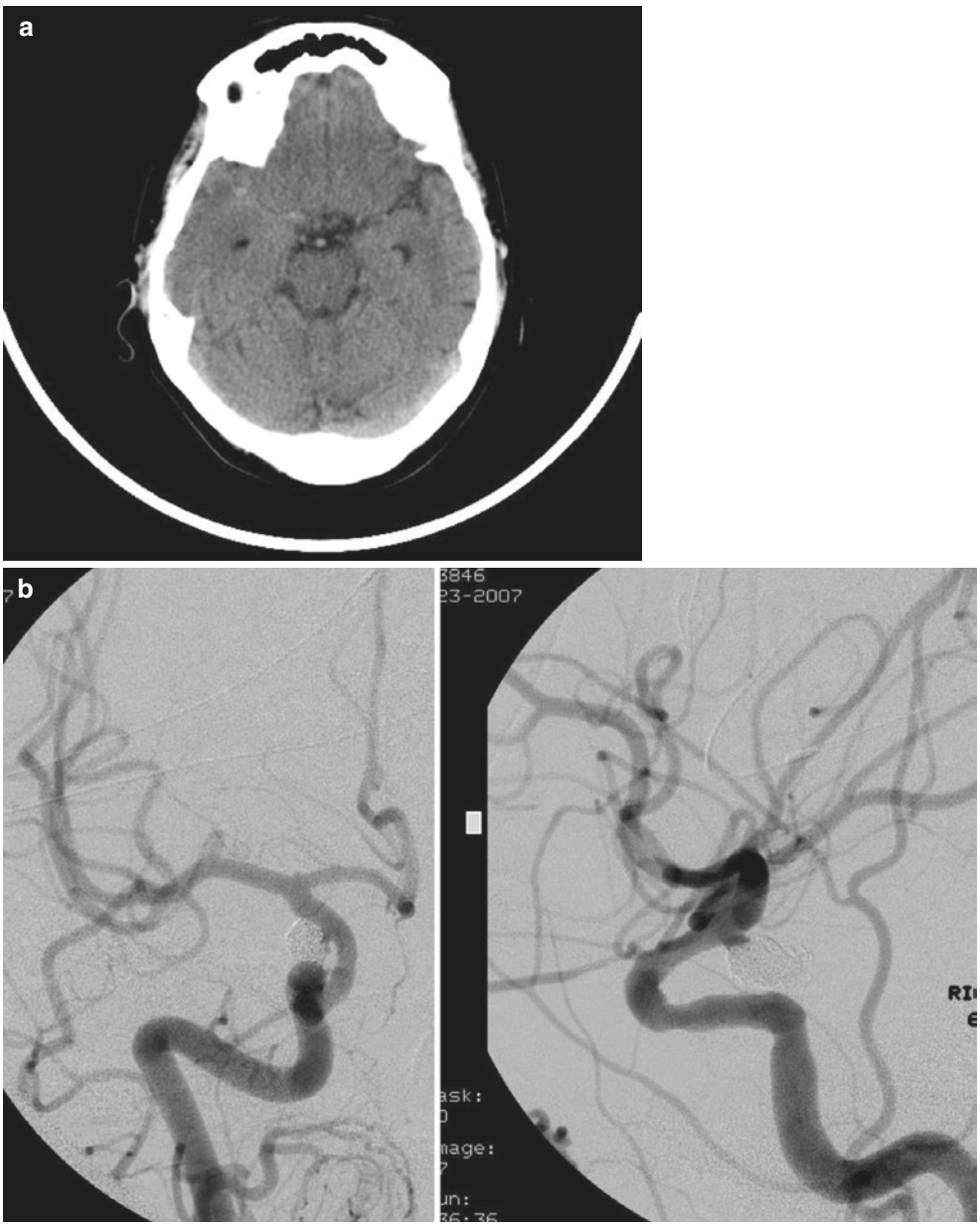

Fig. 1 (**a**) Non-contrast head CT of a 47-year-old female demonstrates subarachnoid hemorrhage, predominantly in the right sylvian fissure and carotid cistern. (**b**) Posttreatment angiogram of uncomplicated coil embolization of a right posterior communicating artery aneurysm. (**c**) Two other unruptured aneurysms on the left internal carotid artery angiogram, including a left anterior choroidal artery aneurysm and left middle cerebral artery aneurysm, were found at the time of ICA aneurysm coiling. (**d**) Another SAH presented in patient 5 years later. (**e**) New angiogram demonstrating right carotid bifurcation aneurysm as rupture source

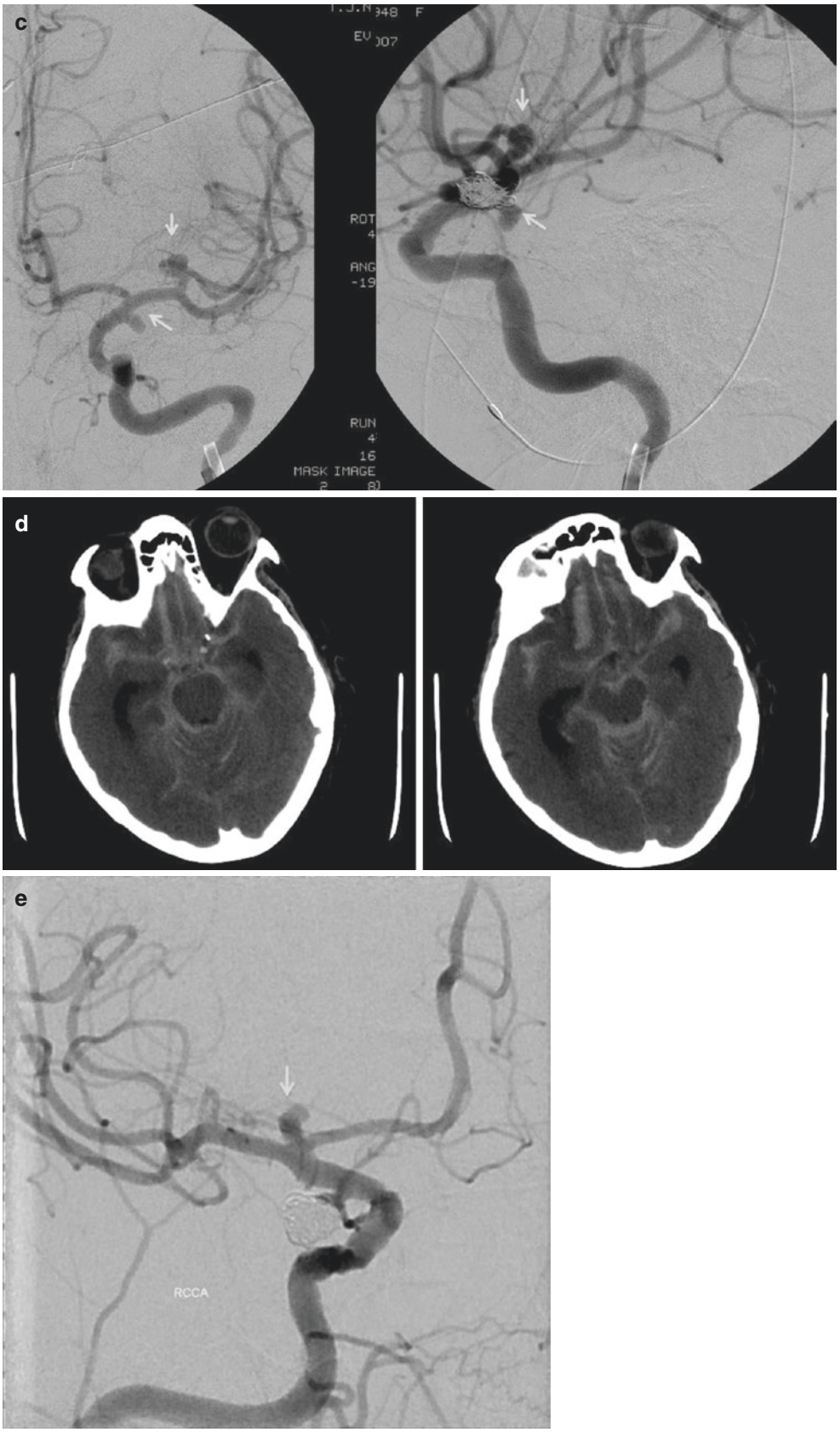

Fig. 1 (continued)

marker genes are activated through CArG-dependent mechanisms and that myocardin plays a key role as a transcriptional coactivator of the CArG element [15, 27]. Atherosclerotic lesions are found in all cerebral aneurysms [5, 8, 11], and the role of SMCs in the pathogenesis of atherosclerosis has been well stablished [3]. Genetic lineage tracing has shown that VSMC phenotypic switching results in less-differentiated forms that lack VSMC markers including macrophage-like cells, and this switching directly promotes atherosclerosis [1]. In addition, VSMC proliferation may be beneficial throughout atherogenesis, not only in advanced lesions, whereas VSMC apoptosis, cell senescence, and VSMC-derived macrophage-like cells promote inflammation [3].

Based upon the above, we have hypothesized that VSMC phenotypic modulation plays a critical role in CA pathogenesis. The differentiated cerebral VSMC, in response to environmental cues, undergoes phenotypic modulation to a pro-inflammatory state that ultimately degrades the vessel wall, leading to CA formation and rupture. In addition, a terminal fate for certain VSMC may be apoptosis which further weakens the vessel and/or aneurysm wall. This has been the subject of numerous studies from our group [2, 4, 20, 24].

In Vitro VSMC Culture Model to Study CA Biology

Given the unique plasticity of VSMC and the established importance of VSMC phenotypic modulation in vascular disease, we have incorporated VSMC culture in our studies of CA pathogenesis. This reductionist approach allows us to efficiently investigate molecular mechanisms that may be important in CA pathogenesis in vivo and also facilitates screening of candidate therapeutic agents or approaches that may translate to in vivo models.

We have established cerebral VSMC primary cultures from rodents (mice and rats) and have more recently utilized human VSMC (Fig. 2). For primary rodent cultures, cerebral blood vessels are harvested from the circle of Willis of three 7-week-old Sprague-Dawley rats. The vessels are placed in cold Hank's balanced salt solution (HBSS), and the connective and arachnoid tissues are removed. The processed vessel segments are then placed in culture dishes containing enzyme solution (collagenase II 1 mg/mL, soybean trypsin inhibitor 1 mg/mL, and elastase 0.744 U/mL in HBSS) for 2 h. Next, vessels are washed in media to inactivate the enzymes and then plated in 60 mm collagen I-coated culture dishes containing growth medium [Dulbecco's Modified Eagle Medium/F12 media (20% FBS and 1% anti-anti)]. Cells are allowed to grow in a humidified atmosphere of 95% air and 5% CO_2 and passaged at 70–80% confluence. Cells are

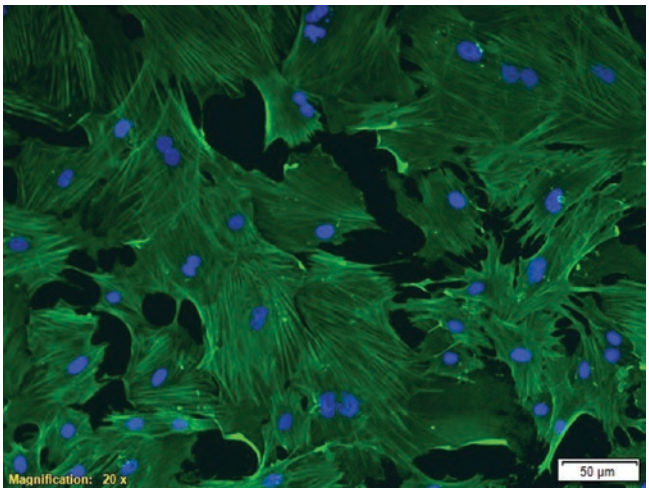

Fig. 2 Differentiated cerebral VSMC cultured from cerebral blood vessels and harvested from the circle of Willis from 7-week-old Sprague-Dawley rats. Image was collected using an Olympus IX73 inverted microscope

weaned to 10% FBS after passages 3–5. For experiments, cells are starved for 2 h in serum-free media with supplement [DMEM/F12 L-ascorbic acid (200 µM), apotransferrin (5 µg/mL), and selenium selenite (6.25 ng/mL)]. They are subsequently treated with the desired stimulus or stimuli (e.g., TNF-α).

We have previously shown that TNF-α plays a role in the mechanism of aneurysm formation and rupture. It increases the permeability of the aneurysm wall via cytokine cascades and induces the migration of macrophages and/or neutrophils to inflamed endothelial cells. Furthermore, it contributes to phenotypic modulation of VSMC characterized by downregulation of contractile proteins (SM-MHC, SM-α-actin, SM-22α) and upregulation of matrix metalloproteinases (MMPs) and other inflammatory mediators [2]. Dimethyl fumarate (DMF) (BG-12, Tecfidera) is an oral fumaric acid ester (FAE) that exhibits immunomodulatory properties and has been shown to reduce brain damage after experimental stroke, subarachnoid and intracerebral hemorrhage, and traumatic brain injury [9, 12–14, 28]. Hence, to explore the prospective effects of DMF on VSMC, we cultured primary cells as described above, stimulated them with a previously determined concentration of TNF-α (50 ng/mL), and treated them with DMF (75 µM) for 24 h. Control cells were also treated with the same dose of DMF. Gene expression analysis confirmed that TNF-α induces cell dysfunction by upregulating the inflammatory markers (CCL-2, MMP2, VCAM) (Fig. 3a–c) and downregulating the expression of the SMC markers (SM-α-actin, SM-MHC) (Fig. 3d, e). This effect was significantly improved by DMF in a dose-dependent manner. These data suggest that DMF regulates the phenotypic modulation of VSMC involved in the pathogenesis of IAs and can potentially improve vascular function after vascular injury.

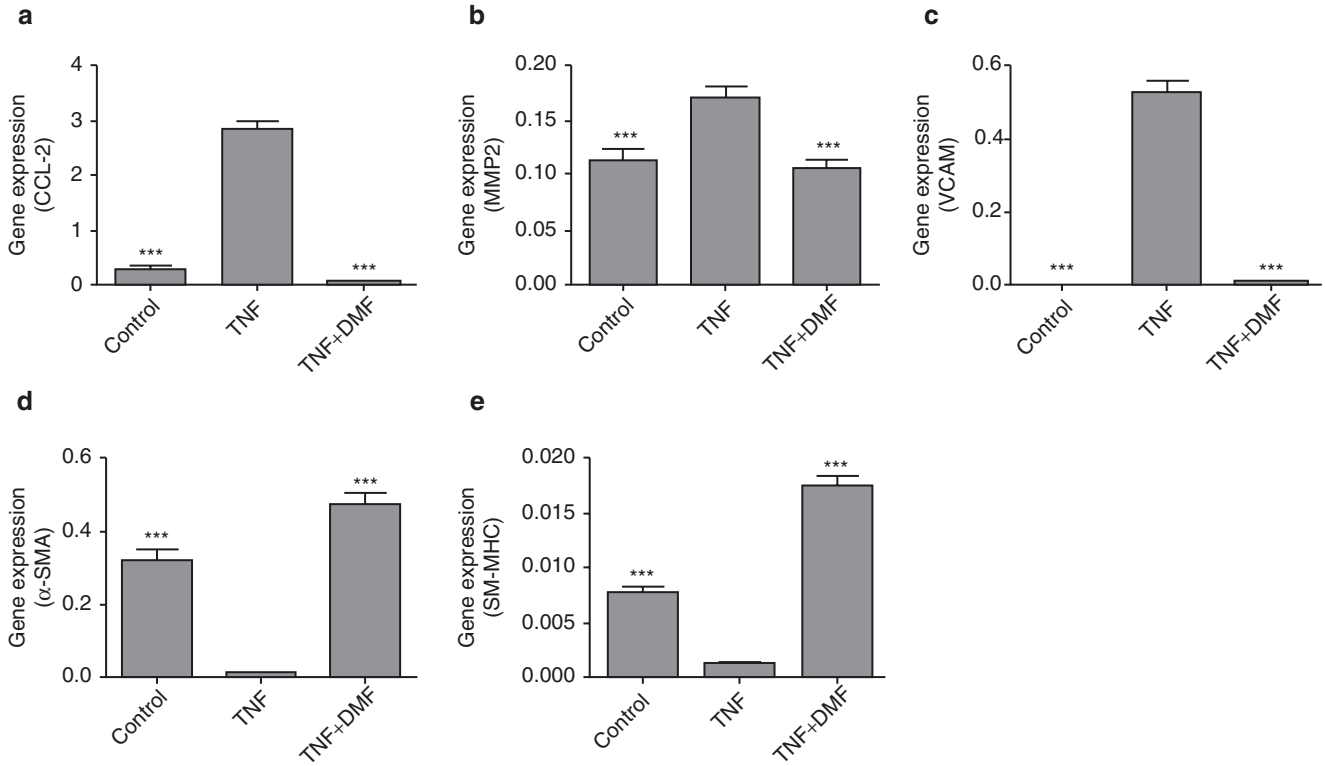

Fig. 3 Gene expression from VSMCs treated with TNFα at 50 ng/mL and DMF (75 μM) for 24 h. Control cells were also treated with DMF. (**a**) MCP1, (**b**) MMP2, (**c**) VCAM-1, (**d**) SM-α-actin, and (**e**) SM-MHC. Statistical analyses were performed using one-way ANOVA followed by Bonferroni's post hoc test (Graph Prism Version 5.0). TNF-α-treated cells were used as the control group, ***$p < 0.001$

Conclusions

Cerebral aneurysms linger as a devastating and common clinical problem. Improvements in clinical treatment have been hindered by a deficient understanding of the basic biology and pathogenesis of CA. Delineation of CA pathogenesis and biology will allow better patient selection and the implementation of medical therapy or novel minimally invasive treatment for patients harboring CA. Cerebral VSMC phenotypic modulation appears to be critical in the pathogenesis of CA. Cultured cerebral VSMC allow in vitro investigation of potential mechanisms contributing to CA pathogenesis as well as screening of candidate therapeutics that can subsequently be investigated in vivo and ultimately translated to the care of patients harboring CA.

Conflict of Interest The authors declare that they have no conflict of interest.

References

1. Albarrán-Juárez J, Kaur H, Grimm M, Offermanns S, Wettschureck N. Lineage tracing of cells involved in atherosclerosis. Atherosclerosis. 2016;251:445–53. https://doi.org/10.1016/j.atherosclerosis.2016.06.012.
2. Ali MS, Starke RM, Jabbour PM, Tjoumakaris SI, Gonzalez LF, Rosenwasser RH, Owens GK, Koch WJ, Greig NH, Dumont AS. TNF-alpha induces phenotypic modulation in cerebral vascular smooth muscle cells: implications for cerebral aneurysm pathology. J Cereb Blood Flow Metab. 2013;33:1564–73. https://doi.org/10.1038/jcbfm.2013.109.
3. Bennett MR, Sinha S, Owens GK. Vascular smooth muscle cells in atherosclerosis. Circ Res. 2016;118:692–702. https://doi.org/10.1161/circresaha.115.306361.
4. Chalouhi N, Ali MS, Jabbour PM, Tjoumakaris SI, Gonzalez LF, Rosenwasser RH, Koch WJ, Dumont AS. Biology of intracranial aneurysms: role of inflammation. J Cereb Blood Flow Metab. 2012;32:1659–76. https://doi.org/10.1038/jcbfm.2012.84.
5. Coen M, Burkhardt K, Bijlenga P, Gabbiani G, Schaller K, Kövari E, Rüfenacht DA, Ruíz DSM, Pizzolato G, Bochaton-Piallat M-L. Smooth muscle cells of human intracranial aneurysms assume phenotypic features similar to those of the atherosclerotic plaque. Cardiovasc Pathol. 2013;22:339–44. https://doi.org/10.1016/j.carpath.2013.01.083.
6. Eskesen V, Rosenorn J, Schmidt K, Espersen JO, Haase J, Harmsen A, Hein O, Knudsen V, Marcussen E, Midholm S, et al. Clinical features and outcome in 48 patients with unruptured intracranial saccular aneurysms: a prospective consecutive study. Br J Neurosurg. 1987;1:47–52.
7. Etminan N, Rinkel GJ. Unruptured intracranial aneurysms: development, rupture and preventive management. Nat Rev Neurol. 2016;12:699–713. https://doi.org/10.1038/nrneurol.2016.150.
8. Hokari M, Isobe M, Imai T, Chiba Y, Iwamoto N, Isu T. The impact of atherosclerotic factors on cerebral aneurysm is location dependent: aneurysms in stroke patients and healthy controls. J Stroke Cerebrovasc Dis. 2014;23:2301–7. https://doi.org/10.1016/j.jstrokecerebrovasdis.2014.04.019.

9. Iniaghe LO, Krafft PR, Klebe DW, Omogbai EKI, Zhang JH, Tang J. Dimethyl fumarate confers neuroprotection by casein kinase 2 phosphorylation of Nrf2 in murine intracerebral hemorrhage. Neurobiol Dis. 2015;82:349–58. https://doi.org/10.1016/j.nbd.2015.07.001.
10. Johnston SC, Selvin S, Gress DR. The burden, trends, and demographics of mortality from subarachnoid hemorrhage. Neurology. 1998;50:1413–8.
11. Kosierkiewicz TA, Factor SM, Dickson DW. Immunocytochemical studies of atherosclerotic lesions of cerebral berry aneurysms. J Neuropathol Exp Neurol. 1994;53:399–406.
12. Kramer T, Grob T, Menzel L, Hirnet T, Griemert E, Radyushkin K, Thal SC, Methner A, Schaefer MKE. Dimethyl fumarate treatment after traumatic brain injury prevents depletion of antioxidative brain glutathione and confers neuroprotection. J Neurochem. 2017;143(5):523–33. https://doi.org/10.1111/jnc.14220.
13. Lin SX, Lisi L, Dello Russo C, Polak PE, Sharp A, Weinberg G, Kalinin S, Feinstein DL. The anti-inflammatory effects of dimethyl fumarate in astrocytes involve glutathione and haem oxygenase-1. ASN Neuro. 2011;3. https://doi.org/10.1042/AN20100033.
14. Liu Y, Qiu J, Wang Z, You W, Wu L, Ji C, Chen G. Dimethyl fumarate alleviates early brain injury and secondary cognitive deficits after experimental subarachnoid hemorrhage via activation of Keap1-Nrf2-ARE system. J Neurosurg. 2015;123:915–23. https://doi.org/10.3171/2014.11.JNS132348.
15. Long X, Bell RD, Gerthoffer WT, Zlokovic BV, Miano JM. Myocardin is sufficient for a smooth muscle-like contractile phenotype. Arterioscler Thromb Vasc Biol. 2008;28:1505–10. https://doi.org/10.1161/atvbaha.108.166066.
16. Mack CP, Thompson MM, Lawrenz-Smith S, Owens GK. Smooth muscle alpha-actin CArG elements coordinate formation of a smooth muscle cell-selective, serum response factor-containing activation complex. Circ Res. 2000;86:221–32.
17. Manabe I, Owens GK. CArG elements control smooth muscle subtype-specific expression of smooth muscle myosin in vivo. J Clin Invest. 2001;107:823–34. https://doi.org/10.1172/jci11385.
18. Rincon F, Rossenwasser RH, Dumont A. The epidemiology of admissions of nontraumatic subarachnoid hemorrhage in the United States. Neurosurgery. 2013;73:217–22. ; discussion 212–3. https://doi.org/10.1227/01.neu.0000430290.93304.33.
19. Saveland H, Sonesson B, Ljunggren B, Brandt L, Uski T, Zygmunt S, Hindfelt B. Outcome evaluation following subarachnoid hemorrhage. J Neurosurg. 1986;64:191–6. https://doi.org/10.3171/jns.1986.64.2.0191.
20. Sawyer DM, Amenta PS, Medel R, Dumont AS. Inflammatory mediators in vascular disease: identifying promising targets for intracranial aneurysm research. Mediat Inflamm. 2015;2015:896283. https://doi.org/10.1155/2015/896283.
21. Shankman LS, Gomez D, Cherepanova OA, Salmon M, Alencar GF, Haskins RM, Swiatlowska P, Newman AA, Greene ES, Straub AC, Isakson B, Randolph GJ, Owens GK. Corrigendum: KLF4-dependent phenotypic modulation of smooth muscle cells has a key role in atherosclerotic plaque pathogenesis. Nat Med. 2016;22:217. https://doi.org/10.1038/nm0216-217a.
22. Starke RM, Ali MS, Jabbour PM, Tjoumakaris SI, Gonzalez F, Hasan DM, Rosenwasser RH, Owens GK, Koch WJ, Dumont AS. Cigarette smoke modulates vascular smooth muscle phenotype: implications for carotid and cerebrovascular disease. PLoS One. 2013;8:e71954. https://doi.org/10.1371/journal.pone.0071954.
23. Starke RM, Chalouhi N, Ali MS, Jabbour PM, Tjoumakaris SI, Gonzalez LF, Rosenwasser RH, Koch WJ, Dumont AS. The role of oxidative stress in cerebral aneurysm formation and rupture. Curr Neurovasc Res. 2013;10:247–55.
24. Starke RM, Chalouhi N, Jabbour PM, Tjoumakaris SI, Gonzalez LF, Rosenwasser RH, Wada K, Shimada K, Hasan DM, Greig NH, Owens GK, Dumont AS. Critical role of TNF-alpha in cerebral aneurysm formation and progression to rupture. J Neuroinflammation. 2014;11:77. https://doi.org/10.1186/1742-2094-11-77.
25. Starke RM, Thompson JW, Ali MS, Pascale CL, Martinez Lege A, Ding D, Chalouhi N, Hasan DM, Jabbour P, Owens GK, Toborek M, Hare JM, Dumont AS. Cigarette smoke initiates oxidative stress-induced cellular phenotypic modulation leading to cerebral aneurysm pathogenesis. Arterioscler Thromb Vasc Biol. 2018;38(3):610–21. https://doi.org/10.1161/atvbaha.117.310478.
26. Sudlow CL, Warlow CP. Comparable studies of the incidence of stroke and its pathological types: results from an international collaboration. International Stroke Incidence Collaboration. Stroke. 1997;28:491–9.
27. Sun Q, Taurin S, Sethakorn N, Long X, Imamura M, Wang DZ, Zimmer WE, Dulin NO, Miano JM. Myocardin-dependent activation of the CArG box-rich smooth muscle gamma-actin gene: preferential utilization of a single CArG element through functional association with the NKX3.1 homeodomain protein. J Biol Chem. 2009;284:32582–90. https://doi.org/10.1074/jbc.M109.033910.
28. Yao Y, Miao W, Liu Z, Han W, Shi K, Shen Y, Li H, Liu Q, Fu Y, Huang D, Shi FD. Dimethyl fumarate and monomethyl fumarate promote post-ischemic recovery in mice. Transl Stroke Res. 2016;7:535–47. https://doi.org/10.1007/s12975-016-0496-0.
29. Yoshida T, Sinha S, Dandre F, Wamhoff BR, Hoofnagle MH, Kremer BE, Wang DZ, Olson EN, Owens GK. Myocardin is a key regulator of CArG-dependent transcription of multiple smooth muscle marker genes. Circ Res. 2003;92:856–64. https://doi.org/10.1161/01.res.0000068405.49081.09.

Rat Model of Intracranial Aneurysm: Variations, Usefulness, and Limitations of the Hashimoto Model

Tomohiro Aoki, Haruka Miyata, Yu Abekura, Hirokazu Koseki, and Kampei Shimizu

Abstract Given the poor outcome of subarachnoid hemorrhage due to rupture of intracranial aneurysms (IAs) and high prevalence of IAs in general public, elucidation of mechanisms underlying the pathogenesis of the disease and development of effective treatment are mandatory for social health. Recent experimental findings have revealed the crucial contribution of macrophage-mediated chronic inflammation to and greatly promoted our understanding of the pathogenesis. Also a series of studies have proposed the potential of anti-inflammatory drugs as therapeutic ones. In this process, a rodent model of IAs plays an indispensable role. Basic concept of IA induction in such kind of models is that IA formation is triggered by hemodynamic stress loaded on damaged arterial walls. To be more precise, although detailed procedures are different among researchers, animals are subjected to a ligation of a unilateral carotid artery and systemic hypertension achieved by a salt overloading, and IAs are induced at the contralateral bifurcation site. Importantly, trigger of IA formation in the model mimics human one, and IA lesions induced share similarity in histology with human ones such as degenerative changes of media. For further elucidating the pathogenesis, we need to well understand variations, usefulness, and also limits of this model.

Keywords Intracranial aneurysm · Subarachnoid hemorrhage · Hemodynamic stress · Chronic inflammation Macrophage · Animal model

T. Aoki (✉) · H. Miyata · Y. Abekura · H. Koseki · K. Shimizu
Department of Molecular Pharmacology, Research Institute, National Cerebral and Cardiovascular Center, Suita City, Osaka, Japan
e-mail: tomoaoki@ncvc.go.jp

Introduction

Given the poor outcome of subarachnoid hemorrhage due to rupture of intracranial aneurysm (IA) once after the onset and high prevalence of IAs in general public [10, 15], development of preemptive medical treatment for IAs, incidentally found through a brain check or so, is mandatory for social health [4]. To achieve this goal, mechanisms underlying the pathogenesis of IAs should be well understood. In this process, rodent models of IAs have greatly contributed to the conceptualization of IAs as a macrophage-mediated chronic inflammatory disease affecting cerebral arteries and also to the identification of therapeutic targets for IAs.

Animal Model of IAs

To clarify the pathogenesis of IAs, an animal model in which IA lesion is induced by biological processes well-mimicking human pathology is essential. Dr. Nobuo Hashimoto established the IA model in rats in accordance with such a requirement first at 1978 [8], and this kind of model has been used for about 40 years as a major one in the field. The basic concept to induce IAs in this model (the Hashimoto model) is "loading hemodynamic stress to damaged arterial walls" via referencing the putative trigger, hemodynamic stress, and histological characteristics, i.e., degenerative changes of media and disruption of internal elastic lamina, of human IAs. To achieve this concept, β-aminopropionitrile (BAPN) [14], a selective inhibitor of lysyl oxidase which mediates cross-linking of collagen and elastin, is administered to rats to fragile arterial walls, and the ligation of a unilateral common carotid artery (Figs. 1 and 2) and the uninephrectomy and administration of sodium chloride and deoxycorticosterone acetate were applied to alternate and increase hemodynamic stress to bifurcation sites of cerebral arteries [8]. After reported in 1978 [8], this model has underwent modifications

R. D. Martin et al. (eds.), *Subarachnoid Hemorrhage*, Acta Neurochirurgica Supplement 127, https://doi.org/10.1007/978-3-030-04615-6_6,

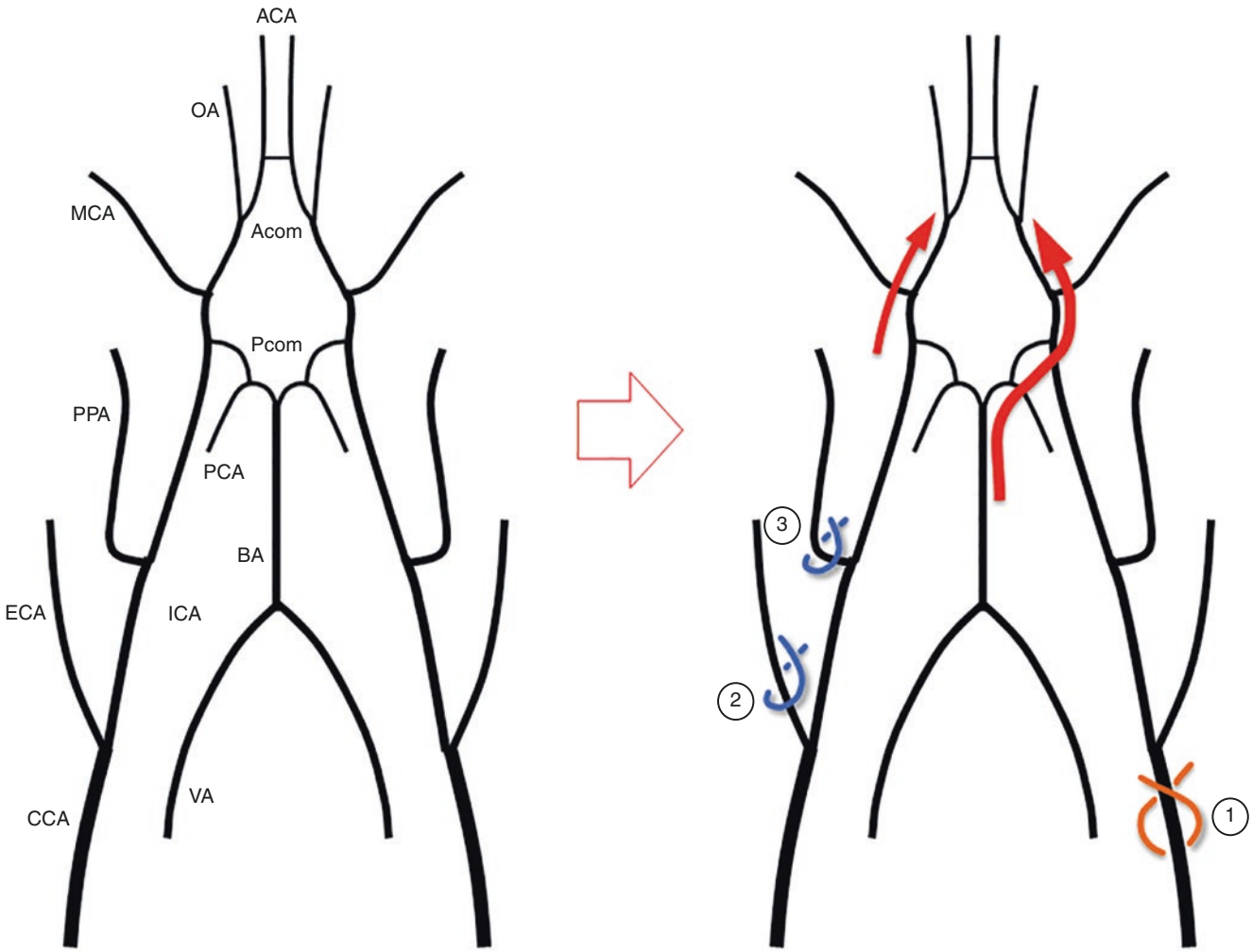

Fig. 1 Schematic drawing of the vasculature from carotid artery to the circle of Willis. Points of an arterial ligation to alternate circulatory dynamics in the circle of Willis are indicated as 1 (common carotid artery), 2 (external carotid artery) or 3 (pterygopalatine artery). Red arrows indicate alternation or increase of blood flow. *CCA* common carotid artery, *ICA* internal carotid artery, *ECA* external carotid artery, *PPA* pterygopalatine artery, *MCA* middle cerebral artery, *ACA* anterior cerebral artery, *OA* olfactory artery, *PCA* posterior cerebral artery, *Acom* anterior communicating artery, *Pcom* posterior communicating artery, *BA* basilar artery, *VA* vertebral artery

[1, 3, 11, 13] (Table 1) and also applied to other experimental animal species like mouse [12] and monkey [9].

This kind of IA model shares common pathological features with human ones such as disruption of internal elastic lamina and degenerative changes of media (Fig. 3a). Importantly, IA lesions are spontaneously induced due to increase of hemodynamic stress loaded on bifurcation sites without direct handling of cerebral arteries, making lesions mimicking human pathology more precisely and analysis and interpretation much easier. Furthermore, incidence of IAs in rat model is high, almost 100% at the anterior cerebral—olfactory artery bifurcation in our current model [1] (Table 1), enough to examine mechanisms underlying formation and progression of IAs. Indeed, this model has greatly contributed to conceptualization of IAs as a macrophage-mediated chronic inflammatory disease and successfully identified some therapeutic targets [1, 2, 18] (Table 2). In addition to high incidence, IA is gradually enlarged and degeneration of media such as a loss of medial smooth muscle cells is also gradually exacerbated within a small deviation after the induction. Thereby, IAs with a specific stage can be selectively analyzed, i.e., effect of interventional drugs on initiation, degeneration of media, or size of IAs. In some derivative models from the original Hashimoto model, subarachnoid hemorrhage occurs at a relatively high rate, at around 50%, during experimental period [11] (Table 1, Fig. 3b). Thus, effect of interventional drugs or genetic modification on rupture of IAs may be assessable. Also, mechanisms triggering rupture of IAs which still remain elusive can be addressed.

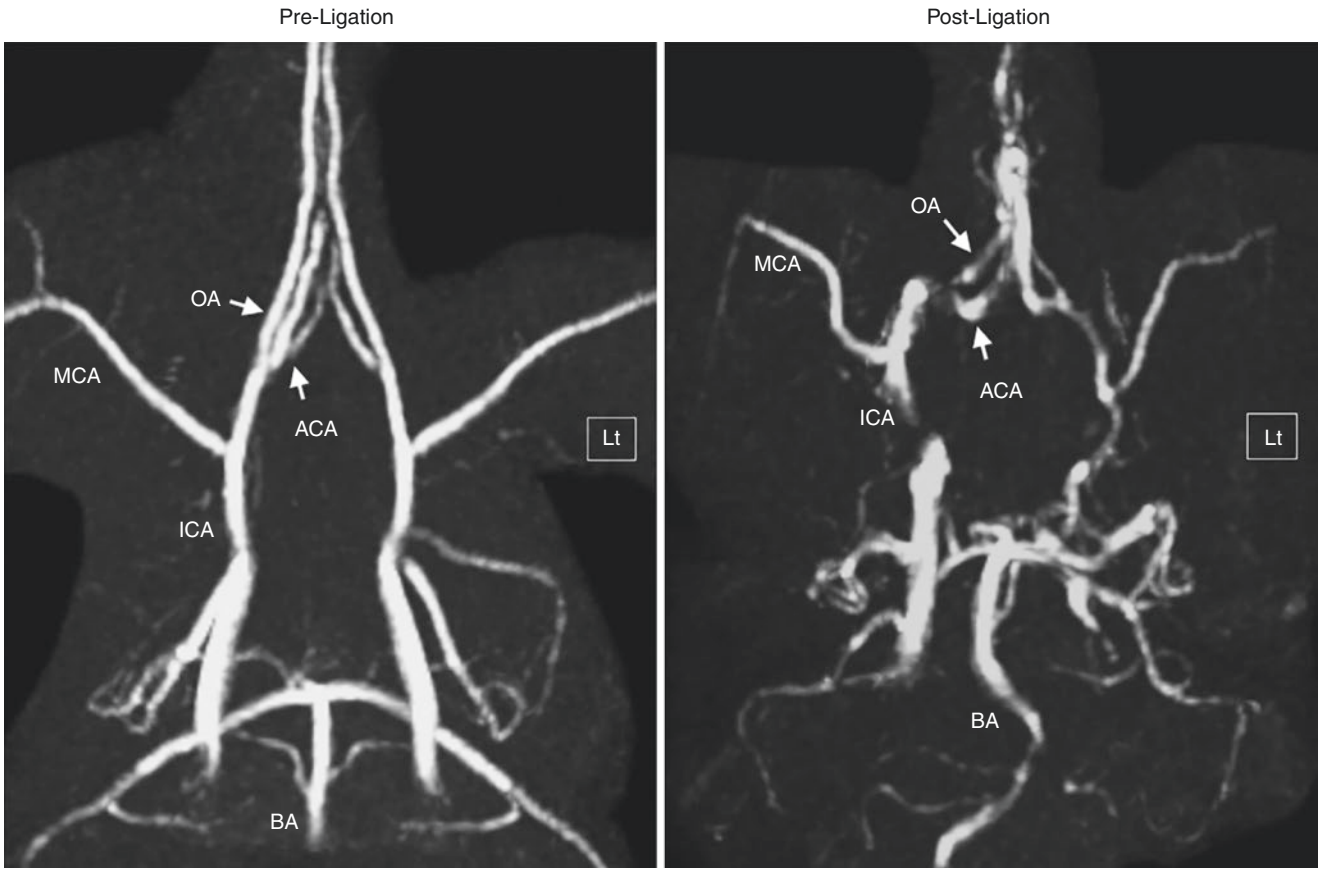

Fig. 2 Magnetic resonance angiography (MRA) imaging of the circle of Willis before and after a ligation of a unilateral common carotid artery. Representative MRA images from a sham-treated (Pre-Ligation, the left panel) or surgically manipulated rat (Post-Ligation, the right panel) are shown. Noted the remarkable change of signal intensity and the tortuous change in the anterior circulation in response to a ligation of a left common carotid artery. *Lt* left side, *ICA* internal carotid artery, *MCA* middle cerebral artery, *ACA* anterior cerebral artery, *OA* olfactory artery, *BA* basilar artery

Special Insight in Some Modifiable Factors

BAPN

As BAPN inhibits cross-linking of collagens and elastin through irreversibly inhibiting enzymatic activity of lysyl oxidase [14], this compound induces fragility of arterial walls and thus facilitates degenerative changes and resultant IA progression. Thereby, addition of BAPN to chow or drinking water greatly contributes to reduction of experimental period and may be helpful to make animal experiments like an evaluation of suppressive effect of drugs on progression of IAs easier and less expensive. However, as BAPN interferes a turnover of extracellular matrix which presumably occurs during IA progression to counteract to excessive degeneration of media, careful considerations to the usage of BAPN and if used cautious interpretations should be paid especially when researchers aim to examine something related with extracellular matrix.

Strains

Incidence of subarachnoid hemorrhage has the great difference in races, i.e., over three times higher in Japanese and Finnish although incidence of IAs is similar [7, 10, 15, 17]. In rats, the similar difference of incidence and progression of IAs among strains such as Sprague-Dawley (SD) rat, Lewis (Lew) rat, and Long-Evans rat is observed. SD rats, presumably the most popular rat strain used for creating the Hashimoto model (Table 1), develop larger IAs with more degenerative changes. Careful examination of differences in IA progression among each rat strain may reveal some important insights regarding mechanisms regulating progression or rupture of IAs.

Table 1 Variation of a rat model of intracranial aneurysm (the Hashimoto model)

Author	Reference	Strain	Age	Sex	Cervical artery ligation	Renal hypertension	Oophorectomy	NaCl	BAPN	DOCA	Follow-up period	Incidence of aneurysm	Incidence of SAH
Hashimoto et al.			3 w									5% (1/20)	
			4 w									10% (2/20)	
			6 w									10% (1/10)	
	Surg Neurol 1978;10:3	SD	6 m	M/F	L/CCA	R/nephrectomy	(−)	1% in water	0.12%	2.5 mg/100 g	2 m	40% (2/5)	
Hashimoto et al.	Surg Neurol 1979;11:243	SD	4 m	M/F	L/CCA	R/nephrectomy	(−)	1% in water	0.12%	2.5 mg/100 g	21 w	37% (11/30, Acom)	3% (1/30)
Hashimoto et al.	Surg Neurol 1980;13:41	SD	6 m	M	None	R/nephrectomy		1% in water	0.12%	2.5 mg/100 g	21 w	0% (0/23)	
					L/CCA							41% (9/22, Acom), 18% (4/22, Pcom)	
					Bil/CCA							35% (8/23, Pcom)	
Nagata et al.	Surg Neurol 1980;14:477	SD	6 m	M	L/CCA	Bil/post. renal artery		(−)	(−)	2.5 mg/100 g	12 w	29% (2/17)	0% (0/17)
								(−)	0.12%		12 w	61% (11/18)	22% (4/18)
								1% in water	(−)		16 w	61% (11/18)	17% (3/18)
								1% in water	0.12%		16 w	100% (18/18)	33% (6/18)
Jamous et al.	J Neurosurg 2005;103:1046	SD	7 w	F	R/CCA	Bil/post. renal artery	(−)	1% in water	(−)	(−)	3 m	60% (9/15)	
							Bilateral					100% (15/15)	
Aoki et al.	Stroke 2007;38:2237	SD	7 w	M	L/CCA	Bil/post. renal artery		8% in chow	0.12%	(−)	1 m	53% (10/19, ACA-OA)	
											3 m	91% (19/21, ACA-OA)	
Aoki et al.	Br J Pharmacol2011;163:1237	SD	7 w	M	L/CCA	L/renal artery		8% in chow	0.12%	(−)	3 m	100% (21/21, ACA-OA)	
Korai et al.	J Neuroinflammation2016;13:165	SD	13 w	F	R/CCA	Bil/post. renal artery(2 weeks later)	Bilateral	8% in chow	(−)	(−)	12 w		20–30%[a]
Miyamoto et al.	J Cereb Blood Flow Metab2017;37:2795	SD	10 w	F	L/CCA	Bil/post. renal artery(2 weeks later)	Bilateral	8% in chow	(−)	(−)	90 d	22% (6/27, Acom/Pcom)	11% (3/27)
					L/CCA, R/ECA + PPA							58% (15/26, Acom/Pcom)	50% (13/26)

d day, *w* week, *m* month, *M* male, *F* female, *CCA* common carotid artery, *ECA* external carotid artery, *PPA* pterygopalatine artery, *Acom* anterior communicating artery, *Pcom* posterior communicating artery, *post* posterior, *R* right, *L* left, *BAPN* β-aminopropionitrile, *DOCA* deoxycorticosterone

[a]Accurate incidence is not shown in the manuscript

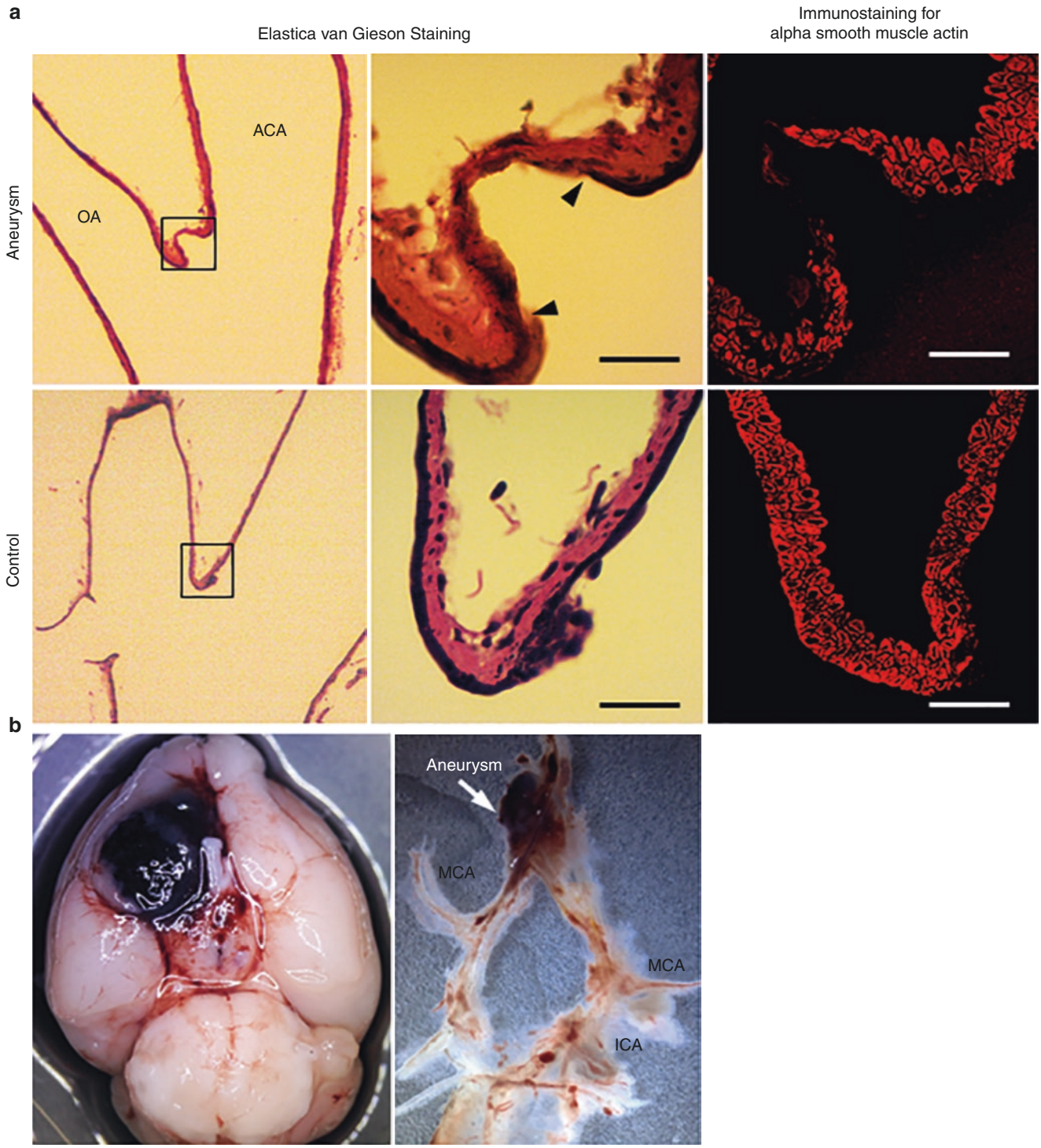

Fig. 3 Histopathological examination of intracranial aneurysm lesions induced in rats and onset of subarachnoid hemorrhage in a rat model. (**a**) Disruption of internal elastic lamina and thinning of medial smooth muscle cell layer in the intracranial lesion induced in a rat model. Images after Elastica van Gieson staining (left and middle panels) to visualize internal elastic lamina and of immunostaining for alpha-smooth muscle actin to visualize medial smooth muscle cells (right panels) from control arterial walls (lower panels) or aneurysm lesions at an anterior cerebral (ACA)—olfactory (OA) bifurcation site of a rat model (upper panels) are shown. Magnified images corresponding to the square in left panels are shown in middle panels. Arrow heads indicate disrupted portion of internal elastic lamina. Bar, 10 μm. (**b**) Macroscopic view of brain surface and the circle of Willis from autopsy after onset of subarachnoid hemorrhage in rats. *ICA* internal carotid artery, *MCA* middle cerebral artery

Table 2 Potential therapeutic targets and candidates of drugs to treat an intracranial aneurysm revealed by experiments using a rodent model

		Aneurysm				
Therapeutic target and cell	Compounds	Formation	Growth	Rupture	Author	Reference
NF-κB	Simvastatin		↓		Aoki et al.	Stroke 2008;39:1276
	Pitavastatin		↓		Aoki et al.	Neurosurgery 2009;64:357
	Pravastatin		↓		Kimura et al.	Brain Res 2010;1322:144
	Nifedipine		↓		Aoki et al.	Curr Neurovasc Res 2008;5:37
Cyclooxygenase (COX)	Aspirin		↓		Li et al.	Neurochem Res 2015;40:1537
				↓	Chalouhi et al.	Hypertension 2016;68:411
COX-2	Celecoxib		↓		Aoki et al.	Br J Pharmacol 2011;163:1237
	NS-398			↓	Chalouhi et al.	Hypertension 2016;68:411
Prostaglandin E receptor subtype 2 (EP2)	PF-04418948		↓		Aoki et al.	Sci Signal 2017;10
Sphingosine-1-phosphate receptor type 1 ($S1P_1$)	ASP4058		↓		Yamamoto et al.	Br J Pharmacol 2017;174:2085
TNF-α	Etanercept		↓		Yokoi et al.	J Neurosurg 2014;120:1193
	3,6′ dithiothalidomide	↓		↓	Starke et al.	J Neuroinflammation 2014;11:77
Matrix metalloproteinases	Minocycline			↓	Makino et al.	Stroke 2012;43:2450
	Doxycycline			↓	Makino et al.	Stroke 2012;43:2450
	Tolylsam		↓		Aoki et al.	Stroke 2007;38:162
Inducible nitric oxide synthase (iNOS)	Amnoguanidine	↓			Fukuda et al.	Circulation 2000;101:2532
Endothelin receptor	K-8794		↓		Sadamasa et al.	J Neurosurg 2007;106:330
Cathepsins	NC-2300		↓		Aoki et al.	Stroke 2008;39:2603
Reactive oxygen species	Edaravone		↓		Aoki et al.	Lab Invest 2009;89:730
Phosphodiesterase 4	Ibudilast		↓		Yagi et al.	Neurosurgery 2010;66:551
Rho-kinase	Fasudil hydrochloride	↓			Eldawoody et al.	Neurosci Lett 2010;470:76
Peroxisome proliferator-activated receptor-γ (PPAR-γ)	Pioglitazone			↓	Shimada et al.	Stroke 2015;46:1664
Dipeptidyl peptidase-4 (DPP-4)	Anagliptin		↓		Ikedo et al.	J Am Heart Assoc 2017;6
Angiotensin II type 2 receptor	Angiotensin-(1-7)			↓	Shimada et al.	J Cereb Blood Flow Metab 2015;35:1163
Estrogen receptor	17β-estradiol			↓	Tada et al.	Hypertension 2014;63:1339
	Diarylpropionitrile			↓	Tada et al.	Hypertension 2014;63:1339
		↓			Tada et al.	Neurosurgery 2014;75:690
Mast cell	Emedastine difumarate		↓		Ishibashi et al.	Curr Neurovasc Res 2010;7:113
	Tranilast		↓		Ishibashi et al.	Curr Neurovasc Res 2010;7:113
Macrophage	Clodronate liposome	↓			Kanematsu et al.	Stroke 2011;42:173

Ligation of Pterygopalatine Artery

In the Hashimoto model, IAs are induced by an increase of hemodynamic stress loaded on bifurcation sites of cerebral arteries. In this process, a unilateral ligation of a common carotid artery is applied to increase blood flow in a contralateral carotid artery (Figs. 1 and 2). In addition of a ligation of common carotid artery, a ligation of a contralateral external carotid artery of course further increases a blood flow in an internal carotid artery. Intriguingly, as recently reported, in rodents unlike primates, a pterygopalatine artery is branched as a most proximal branch of an internal carotid artery, and thus a ligation of this artery moreover increases a hemodynamic stress presumably resulting in the exacerbation of IA progression [5, 11] (Fig. 1).

Limitations

As described above, the Hashimoto model has greatly contributed to our understanding of the pathogenesis underlying IA formation and progression, and thus its establishment is really a breakthrough in the field. However, there are of course some limitations in the Hashimoto model we should well recognize. First, size of IAs induced in this model is small, usually within 0.1 mm in diameter. As a natural consequence, imaging of a lesion is quite challenging given the resolution of imaging modalities used for analysis such as MRA (Fig. 2) and CTA, making the sequential following up of a same lesion quite difficult. Second, IAs induced in the Hashimoto model usually have a broad neck unlike many human ones (Fig. 3a). Thence, hemodynamic status of IA lesions seems to be considerable different from human ones. Taken together with the small size for imaging, the Hashimoto model may not be suitable for computational flow dynamic (CFD) analysis to evaluate hemodynamic status regulating IA progression.

Although there are certainly some limitations about the Hashimoto model, this model has revealed many important insights regarding the pathogenesis of IAs [2, 6, 16].

Acknowledgment The authors express their sincere gratitude to all the researchers, assistants, secretaries, and grants supporting their research works.

Conflict of Interest: **The authors declare that they have no conflict of interest.**

References

1. Aoki T, Frosen J, Fukuda M, Bando K, Shioi G, Tsuji K, Ollikainen E, Nozaki K, Laakkonen J, Narumiya S. Prostaglandin E2-EP2-NF-kappaB signaling in macrophages as a potential therapeutic target for intracranial aneurysms. Sci Signal. 2017;10.
2. Aoki T, Nishimura M. Targeting chronic inflammation in cerebral aneurysms: focusing on NF-kappaB as a putative target of medical therapy. Expert Opin Ther Targets. 2010;14:265–73.
3. Aoki T, Nishimura M. The development and the use of experimental animal models to study the underlying mechanisms of CA formation. J Biomed Biotechnol. 2011;2011:535921.
4. Aoki T, Nozaki K. Preemptive medicine for cerebral aneurysms. Neurol Med Chir. 2016;56:552–68.
5. Cai J, He C, Yuan F, Chen L, Ling F. A novel haemodynamic cerebral aneurysm model of rats with normal blood pressure. J Clin Neurosci. 2012;19:135–8.
6. Fukuda M, Aoki T. Molecular basis for intracranial aneurysm formation. Acta Neurochir Suppl. 2015;120:13–5.
7. Greving JP, Wermer MJ, Brown RD Jr, Morita A, Juvela S, Yonekura M, Ishibashi T, Torner JC, Nakayama T, Rinkel GJ, Algra A. Development of the PHASES score for prediction of risk of rupture of intracranial aneurysms: a pooled analysis of six prospective cohort studies. Lancet Neurol. 2014;13:59–66.
8. Hashimoto N, Handa H, Hazama F. Experimentally induced cerebral aneurysms in rats. Surg Neurol. 1978;10:3–8.
9. Hashimoto N, Kim C, Kikuchi H, Kojima M, Kang Y, Hazama F. Experimental induction of cerebral aneurysms in monkeys. J Neurosurg. 1987;67:903–5.
10. Iwamoto H, Kiyohara Y, Fujishima M, Kato I, Nakayama K, Sueishi K, Tsuneyoshi M. Prevalence of intracranial saccular aneurysms in a Japanese community based on a consecutive autopsy series during a 30-year observation period. The Hisayama study. Stroke. 1999;30:1390–5.
11. Miyamoto T, Kung DK, Kitazato KT, Yagi K, Shimada K, Tada Y, Korai M, Kurashiki Y, Kinouchi T, Kanematsu Y, Satomi J, Hashimoto T, Nagahiro S. Site-specific elevation of interleukin-1beta and matrix metalloproteinase-9 in the Willis circle by hemodynamic changes is associated with rupture in a novel rat cerebral aneurysm model. J Cereb Blood Flow Metab. 2017;37:2795–805.
12. Morimoto M, Miyamoto S, Mizoguchi A, Kume N, Kita T, Hashimoto N. Mouse model of cerebral aneurysm: experimental induction by renal hypertension and local hemodynamic changes. Stroke. 2002;33:1911–5.
13. Nagata I, Handa H, Hashimoto N, Hazama F. Experimentally induced cerebral aneurysms in rats: part VI. Hypertension. Surg Neurol. 1980;14:477–9.
14. Narayanan AS, Siegel RC, Martin GR. On the inhibition of lysyl oxidase by-aminopropionitrile. Biochem Biophys Res Commun. 1972;46:745–51.
15. Rinkel GJ, Djibuti M, Algra A, van Gijn J. Prevalence and risk of rupture of intracranial aneurysms: a systematic review. Stroke. 1998;29:251–6.
16. Turjman AS, Turjman F, Edelman ER. Role of fluid dynamics and inflammation in intracranial aneurysm formation. Circulation. 2014;129:373–82.
17. Wermer MJ, van der Schaaf IC, Algra A, Rinkel GJ. Risk of rupture of unruptured intracranial aneurysms in relation to patient and aneurysm characteristics: an updated meta-analysis. Stroke. 2007;38:1404–10.
18. Yamamoto R, Aoki T, Koseki H, Fukuda M, Hirose J, Tsuji K, Takizawa K, Nakamura S, Miyata H, Hamakawa N, Kasuya H, Nozaki K, Hirayama Y, Aramori I, Narumiya S. A sphingosine-1-phosphate receptor type 1 agonist, ASP4058, suppresses intracranial aneurysm through promoting endothelial integrity and blocking macrophage transmigration. Br J Pharmacol. 2017;174:2085–101.

Possible Involvement of Caspase-Independent Pathway in Neuronal Death After Subarachnoid Hemorrhage in Mice

Fumi Nakano, Lei Liu, Fumihiro Kawakita, Yoshinari Nakatsuka, Hirofumi Nishikawa, Takeshi Okada, Masato Shiba, and Hidenori Suzuki

Abstract Early brain injury is now considered as an important cause of delayed neurological deterioration after aneurysmal subarachnoid hemorrhage (SAH), and neuronal apoptosis is one of the constituents of early brain injury. Caspase family is popular proteases in apoptotic pathways, but there also exist caspase-independent cell death pathways in many pathologic states. In this study, we investigated the ratio of caspase-related and caspase-unrelated neuronal deaths in a mice endovascular perforation SAH model. At 24 h after SAH, about half of neurons in the perforation-side cortex showed increased cleaved caspase-3 immunoreactivity. On the other hand, about half of cleaved caspase-3-immunonegative neurons showed abnormal morphology, suggesting that they were in the process of some sort of cell death in the absence of caspase-3 activity. These findings suggest that both caspase-dependent and caspase-independent signaling pathways may cause neuronal death after SAH.

Keywords Cell death · Early brain injury · Neuronal apoptosis · Subarachnoid hemorrhage

Introduction

Delayed neurological deterioration after aneurysmal subarachnoid hemorrhage (SAH) has been a main concern among neurosurgeons for many years, and today it is supposed to be mainly caused by vasospasm and early brain injury (EBI) [1]. Neuronal apoptosis is one of constituents of EBI [1]. Caspase family forms major population among apoptosis-related proteases and works in several apoptotic signaling pathways [5]. Its role in experimental SAH models has already been studied and clarified [4, 7]. However, pan-caspase inhibitors showed great preventive effects against neuronal apoptosis after SAH, but there remained some neurons to be destined to die [7]. Considering that there are some caspase-independent cell death pathways reported in other pathologic states [2, 9], it is supposed that both caspase-dependent and caspase-independent pathways may work in neuronal death after SAH. However, studies of the latter are limited. In this study, thus, we investigated the ratio of immunopositive and immunonegative neurons for cleaved caspase-3, which is an essential protein through apoptotic pathways, and showed the possible involvement of caspase-independent pathways in neuronal death in SAH mice cortex.

Materials and Methods

All procedures were approved by the Animal Ethics Review Committee of Mie University and were carried out in accordance with the institution's Guidelines for Animal Experiments.

SAH Modeling and Study Protocol

C57BL/6 mice (25–30 g, male) were used for SAH modeling or sham operation as previously described [8] (Fig. 1). Briefly, mice were anesthetized, positioned supinely, and skin incision was made at the midline of the neck to expose the left carotid artery. A 4-0 monofilament with a sharpen tip was inserted from the left external carotid artery (ECA) into the left internal carotid artery and push further to perforate the bifurcation of anterior cerebral artery and middle cerebral artery. Then the filament was withdrawn, and the stump

F. Nakano (✉) · L. Liu · F. Kawakita · Y. Nakatsuka · H. Nishikawa
T. Okada · M. Shiba · H. Suzuki
Department of Neurosurgery, Mie University Graduate School of Medicine, Tsu, Mie, Japan
e-mail: fumi-n21@mva.biglobe.ne.jp

R. D. Martin et al. (eds.), *Subarachnoid Hemorrhage*, Acta Neurochirurgica Supplement 127,
https://doi.org/10.1007/978-3-030-04615-6_7,

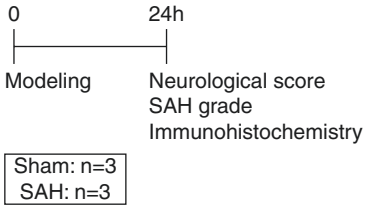

Fig. 1 Experimental designs. Experiment was designed to examine presence or absence of cleaved caspase-3 immunoreactivities among individual neurons in mice cortex after experimental subarachnoid hemorrhage (SAH)

of ECA was coagulated. The wound was sutured. The sham group underwent the same procedure as described above except for perforating the artery. After evaluating neurological scores, mice were sacrificed at 24 h after modeling, and then assessments of SAH grade and immunohistochemistry were performed (Fig. 1). Mice were assigned to SAH ($n = 3$) and sham groups ($n = 3$).

SAH Grade

SAH grade was evaluated as previously described [8]. The basal cistern was divided into six segments, and each segment was allotted a grade from 0 to 3 depending on the amount of SAH. A total score ranging from 0 to 18 was determined by summing the scores. Mice with moderate SAH grade (8–12) were used for experiments as the SAH group.

Neurological Score

Neurological impairments were blindly evaluated as previously described [8]. Neurological scores (3–18) were determined by summing up six test scores (spontaneous activity, spontaneous movement of four limbs, forepaw outstretching, climbing, body proprioception, and response to whisker stimulation).

Histology

Mice's brains were used for making paraffin-embedded coronal sections at bregma +1 mm as previously described [8]. At 24 h after modeling, mice were deeply anesthetized with Avertin® (2,2,2-tribromoethanol) solution and perfused with cold phosphate-buffered saline followed by 4% paraformaldehyde for brain fixation. The brains were removed, embedded in paraffin and cut into 4 μm sections. Sections were dewaxed, underwent heat-induced antigen retrieval in 10 mM citrate butter (pH 6.0), and were incubated with rabbit anti-cleaved caspase-3 primary antibody (1:25; Cell Signaling Technology; cat #9661) in SignalStain® antibody diluent (Cell Signaling Technology; cat#8112) at 4 °C for overnight. Then sections underwent reaction with SignalStain® boost immunohistochemistry detection reagent (Cell Signaling Technology; cat#8114) for 30 min at room temperature, visualized by diaminobenzidine (brown color) and counterstained with hematoxylin. Sections were dehydrated, cleared in xylene, and mounted for observation under light microscope.

Cell Counting

Left (perforation-side) temporal base cortex was used for observation of neurons. Neurons were counted in five sequential fields at ×400 magnification. Neurons were determined morphologically as cells having bright, large, and oval nuclei with some prominent nucleoli [6, 10]. Cells with small nuclei were not counted because the possibility of glia was not excluded. Irregular cell outlines, cell shrinkage or pyknosis was defined as abnormal morphology [3].

Statistics

The number of neuron was expressed as means ±standard error of the mean, and unpaired *t*-tests were used for the comparison between the two groups. $P < 0.05$ was considered significant.

Results

Cleaved Caspase-3-Positive Neurons Appeared 24 h After SAH

No mice in the sham group died before sacrifice. Mice in the sham group showed full scores on neurological assessments, while mice in the SAH group showed neurological deterioration at 24 h after operation (data not shown). At 24 h after modeling, there were few neurons being immunoreactive for cleaved caspase-3 in the sham group. On the other hand, about half of neurons showed immunoreactivities for cleaved caspase-3 in the SAH group (Fig. 2). There were significant differences in the number of immunopositive neurons with

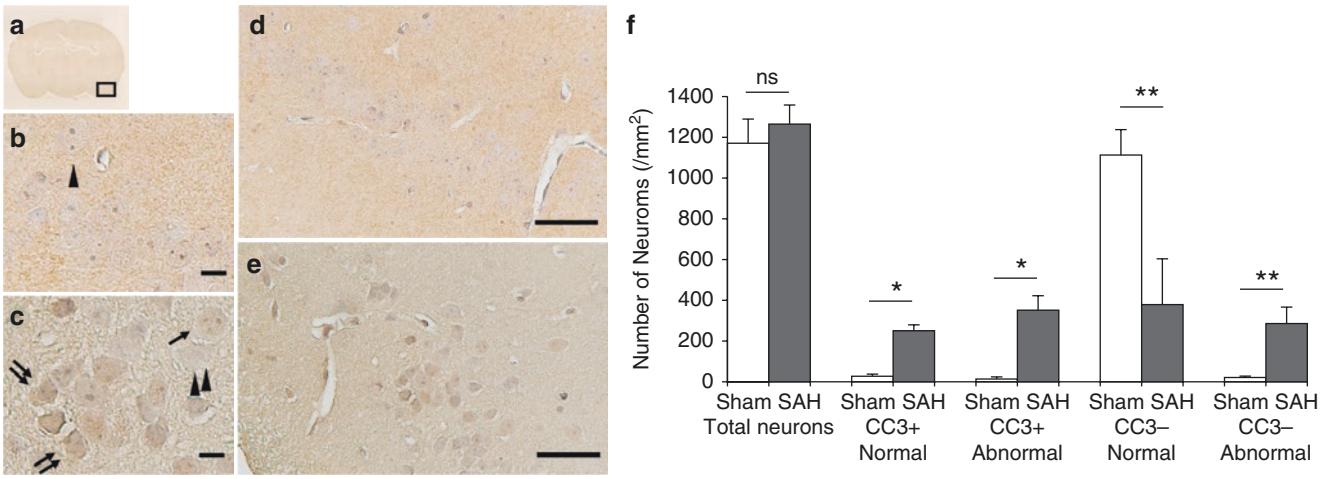

Fig. 2 Cleaved caspase-3 (CC3) immunoreactivity and morphological abnormality in neurons in the ipsilateral (perforation-side) temporal base cortex at 24 h after subarachnoid hemorrhage (SAH) in mice. (**a**) Representative brain coronal section at bregma +1 mm; (**b**–**e**) CC3 immunostaining; (**f**) comparison between the sham and SAH groups. Most neurons are negative for CC3 in the sham group (**b**, **d**), but positive (moderate immunoreactivity) in the SAH group (**c**, **e**). Scale bars: 10 μm (**b**, **c**) and 50 μm (**d**, **e**). Unpaired *t*-test: *ns* no significance; $*P < 0.01$, $**P < 0.05$. Single or double arrows, CC3-positive (CC3+) neurons with normal or abnormal morphology, respectively; single or double arrowheads, CC3-negative (CC3−) neurons with normal or abnormal morphology, respectively. Normal, morphologically normal neurons; abnormal, morphologically abnormal neurons

normal or abnormal morphology between the sham and the SAH groups ($P < 0.01$, respectively, unpaired *t*-test; Fig. 2). There was no significant difference about the total number of neurons between the two groups at 24 h after modeling (unpaired *t*-test, Fig. 2).

Both Caspase-3-Related and Caspase-3-Unrelated Dying Neurons Were Observed After SAH

As to neurons in the SAH group, both positive and negative immunoreactivities for cleaved caspase-3 were observed (Fig. 2). In immunonegative neurons for cleaved caspase-3, normal morphology (i.e., intact neurons) was more frequently observed in the sham group ($P < 0.05$ vs. SAH group, unpaired *t*-test), while abnormal morphology was more frequently observed in the SAH group ($P < 0.05$ vs. sham group, unpaired *t*-test; Fig. 2). About half of immunonegative neurons for cleaved caspae-3 in the SAH group showed morphologically abnormal appearance, which was suggested to be dying.

Discussion

This study showed that almost half of cortical neurons expressed cleaved caspase-3 and that one fourth of cortical neurons had both characteristics of no immunoreactivities for cleaved caspase-3 and morphologically abnormal appearance in the perforation-side temporal base cortex at 24 h after SAH (Fig. 2).

Apoptosis is a well-recognized mechanism under physiological conditions such as developmental or mature stages to form normal organs or eliminate abnormal cells, and also inappropriate triggers make cells inclined to apoptosis under many pathologic states [3]. Caspase family forms major population among apoptosis and inflammation-related proteins [3, 5]. Under physiological conditions, inhibiting caspases sometimes causes cells to undergo necrosis. It is suggested that whether cells are destined to undergo apoptosis or necrosis depends on the extent of adenosine triphosphate depletion and availability of caspases [2]. Nevertheless, under pathologic conditions, caspase inhibitors are commonly considered to have therapeutic effects and direct cells to survive [5]. Among caspase family, caspase-3 works in both extrinsic and intrinsic pathways and is in an essential position in apoptosis signaling [3, 5]. Caspase-3 exists as an inactive precursor and then becomes an active form after cleavage by other proteases [3, 5]. Therefore cleaved (active) caspase-3 could be an indicator of ongoing apoptotic status as used in our study.

Previous studies showed that the rate of active caspase-3-positive cell was higher in SAH mice cortex compared to that in the sham group [4]. In addition, a pan-caspase inhibitor suppressed neuronal apoptosis after experimental SAH [7]. In this study, we compared the number of cleaved caspase-3-positive and caspase-3-negative neurons directly in the temporal base cortex in SAH mice. We defined cell shrinkage, pyknosis, and unusual cell outlines as morphological abnormalities during apoptosis according to previous studies [3, 6, 10]. As a result,

one fourth of neurons had both characteristics of morphological abnormalities and no immunoreactivities for cleaved caspase-3 in mice cortex after SAH. Although there exists the possibility that cells in progressive or terminal stages of caspase-dependent apoptosis had already lost the immunoreactivity for cleaved caspase-3, at least some of them presumably underwent caspase-independent neuronal death.

Apoptosis-inducing factor (AIF) is a molecule released from mitochondrial membrane and known to induce apoptosis directly [2, 9]. In terms of mitochondrial pathways, cytochrome *c*, which is also released from mitochondrial membrane, is thought to have an important role in caspase-dependent pathways through activating caspase-9 [1]. On the other hand, some studies showed that AIF causes apoptosis in a caspase-independent manner [2, 9]. However, its role in SAH models has not been fully investigated. Previous studies suggested that during development, at least partly, caspase-independent pathway can compensate for the lack of caspase activity [9]. Thus, caspase-independent pathways after SAH would be worth investigating in the following two points: (1) finding a new neuronal death pathway in SAH and (2) possible activation of caspase-independent pathways after administrating caspase inhibitors as a potential therapeutic target.

In conclusion, we showed that a considerable number of neuronal deaths were caspase-dependent, but caspase-independent cell death pathways also might be involved in neuronal death after experimental SAH.

Acknowledgment This work was supported in part by a grant-in-aid for Scientific Research from Japan Society for the Promotion of Science to Drs. Shiba and Suzuki. We thank Chiduru Yamamoto (Department of Neurosurgery, Mie University Graduate School of Medicine) for her assistance.

Conflicts of Interest: **We declare that we have no conflict of interest.**

References

1. Cahill J, Calvert JW, Zhang JH. Mechanisms of early brain injury after subarachnoid hemorrhage. J Cereb Blood Flow Metab. 2006;26:1341–53.
2. Cregan SP, Fortin A, MacLaurin JG, Callaghan SM, Cecconi F, Yu SW, Dawson TM, Dawson VL, Park DS, Kroemer G, Slack RS. Apoptosis-inducing factor is involved in the regulation of caspase-independent neuronal cell death. J Cell Biol. 2002;158:507–17.
3. Elmore S. Apoptosis: a review of programmed cell death. Toxicol Pathol. 2007;35:495–516.
4. Li M, Wang W, Mai H, Zhang X, Wang J, Gao Y, Wang Y, Deng G, Gao L, Zhou S, Chen Q, Wang X. Methazolamide improves neurological behavior by inhibition of neuron apoptosis in subarachnoid hemorrhage in mice. Sci Rep. 2016;6:35055.
5. Mcllwain DR, Berger T, Mak TW. Caspase functions in cell death and disease. Cold Spring Harb Perspect Biol. 2013;5:a008656.
6. Northington FJ, Zelaya ME, O'Riordan DP, Blomgren K, Flock DL, Hagberg H, Ferriero DM, Martin LJ. Failure to complete apoptosis following neonatal hypoxia-ischemia manifests as "continuum" phenotype of cell death and occurs with multiple manifestations of mitochondrial dysfunction in rodent forebrain. Neuroscience. 2007;149:822–33.
7. Park S, Yamaguchi M, Zhou C, Calvert JW, Tang J, Zhang JH. Neurovascular protection reduces early brain injury after subarachnoid hemorrhage. Stroke. 2004;35:2412–7.
8. Shiba M, Fujimoto M, Imanaka-Yoshida K, Yoshida T, Taki W, Suzuki H. Tenascin-C causes neuronal apoptosis after subarachnoid hemorrhage in rats. Transl Stroke Res. 2014;5:238–47.
9. Tait SW, Green DR. Caspase-independent cell death: leaving the set without the final cut. Oncogene. 2008;27:6452–61.
10. Wang B, Armstrong JS, Lee JH, Bhalala U, Kulikowicz E, Zhang H, Reyes M, Moy N, Spicer D, Zhu J, Yang ZJ, Koehler RC, Martin LJ, Lee JK. Rewarming from therapeutic hypothermia induces cortical neuron apoptosis in a swine model of neonatal hypoxic-ischemic encephalopathy. J Cereb Blood Flow Metab. 2015;35:781–93.

Nox2 and Nox4 Participate in ROS-Induced Neuronal Apoptosis and Brain Injury During Ischemia-Reperfusion in Rats

Jinjin Wang,[$] Yin Liu,[$] Haitao Shen, Haiying Li, Zhong Wang, and Gang Chen

Abstract *Background*: Previously studies have shown that Nox2 and Nox4, as members of nicotinamide adenine dinucleotide phosphate oxidase (NADPH oxidase, Nox), participate in brain damage caused by ischemia-reperfusion (I/R). The aim of this study is to investigate the effects of specific chemical inhibitors of Nox2 and Nox4 on cerebral I/R--induced brain injury in rats.

Methods: At 0.5 h before MCAO surgery, the rats were pretreated with vehicle, Nox2 inhibitor (gp91ds-tat), and Nox4 inhibitor (GKT137831), respectively. After reperfusion for 24 h, the infarct sizes of brain tissues in rats in various groups are determined. The penumbra (ischemic) tissues are collected to measure ROS levels, neuronal apoptosis, and degeneration, as well as the integrity of the blood-brain barrier (BBB) in brain tissues of rats.

Results: gp91ds-tat and GKT137831 pretreatment significantly reduced the infarct sizes in brain tissues of rats, effectively suppressed I/R-induced increase in ROS levels, neuronal apoptosis and degeneration, and obviously alleviated BBB damage.

Conclusion: Under cerebral I/R conditions, Nox2 inhibitor (gp91ds-tat) and Nox4 inhibitor (GKT137831) can effectively play a protective role in the brain tissues of rats.

Keywords Cerebral ischemia-reperfusion · Nox2 · Nox4 · Middle cerebral artery occlusion · Reactive oxygen species

Introduction

Stroke and its related complications are one of the leading causes of morbidity and mortality worldwide [4, 24, 30]. Among them, the ischemic stroke patients account for 87% of stroke-related mortality [13, 21, 22, 27]. Neurons quickly die at 5 min after hypoxia; therefore, the effective time frame for treatment of the ischemic stroke is very narrow [28]. Early intravenous thrombolytic therapy is the only method of treatment in ischemic stroke patients and is currently approved [19]. Although the blood flow was restored after early intravenous thrombolytic therapy, the ischemia-reperfusion (I/R) injury caused by increased reactive oxygen species (ROS) in the reperfusion phase is particularly serious and may lead to a poor outcome in patients [11, 25].

Ischemic penumbra is a transitional area between the infarction and normal brain tissues after ischemic stroke [3]. The mechanisms underlying cerebral ischemia and potential clinical therapies have attracted more and more attention in various studies. Although there are many enzymes playing important roles in oxidative stress in various tissues and cells in many diseases, the family of nicotinamide adenine dinucleotide phosphate oxidase (NADPH oxidase, Nox) is considered as major source of ROS [13]. In mammals, Nox family includes Nox1, Nox2, Nox3, Nox4, dual oxidase (Duox)-1, and Duox-2 [14]. Previous studies have shown that some members of Nox family, particularly Nox2 and Nox4, are important sources of ROS in cerebral I/R [7].

[$]Jinjin Wang and Yin Liu contributed equally to this work.

J. Wang
Department of Neurosurgery and Brain and Nerve Research Laboratory, The First Affiliated Hospital of Soochow University, Suzhou, China

Department of Neurosurgery, Jiangsu Shengze Hospital, Suzhou, China

Y. Liu
Department of Neurosurgery and Brain and Nerve Research Laboratory, The First Affiliated Hospital of Soochow University, Suzhou, China

Department of Neurosurgery, Suzhou Municipal Hospital, Suzhou, China

H. Shen · H. Li · Z. Wang (✉) · G. Chen
Department of Neurosurgery and Brain and Nerve Research Laboratory, The First Affiliated Hospital of Soochow University, Suzhou, China

R. D. Martin et al. (eds.), *Subarachnoid Hemorrhage*, Acta Neurochirurgica Supplement 127,
https://doi.org/10.1007/978-3-030-04615-6_8,

Previously, radical scavengers or natural antioxidants, such as vitamin C and vitamin E, were mostly used to inhibit oxidative stress with limited efficacy [6]. Nox family play important roles in cerebral I/R injury through oxidative stress, nitration stress, blood-brain barrier (BBB) damage, and cell apoptosis. Therefore, Nox has become a new target for the treatment of ischemic stroke [26]. Recently, it has been reported that genetic knockout and/or specific chemical inhibitor of Nox treatment can significantly reduce oxidative stress-induced brain damage ischemic stroke [23, 29]. However, the exact mechanisms of the activation of Nox are not clear, and there is lack of effective drugs that can significantly inhibit Nox in clinical practice [17]. gp91ds-tat is a specific inhibitor of Nox2 and GKT137831 is a Nox4-specific inhibitor. To our knowledge, these two Nox-specific inhibitors in the treatment of ischemic stroke have not been reported.

In this study, we hypothesized that the specific inhibitors of Nox2 and Nox4 can attenuate cerebral I/R injury in a rat model of middle cerebral artery occlusion (MCAO) through reducing ROS levels, inhibiting neuronal apoptosis and degeneration, and alleviating BBB damage.

Materials and Methods

Ethical Approval

All experiments are approved by the Ethics Committee of the First Affiliated Hospital of Soochow University and are in accordance with the guidelines of the National Institutes of Health on the care and use of animals. Adult male Sprague-Dawley (SD) rats (250–300 g) are purchased from Animal Center of Chinese Academy of Sciences (Shanghai, China). The rats are housed in temperature- and humidity-controlled animal quarters with a 12-h light/dark cycle.

Establishing the MCAO Model in Rats

Following the intraperitoneal anesthesia with chloral hydrate (36 mg/100 g body weight), under an operating microscope, focal cerebral ischemia in rats is achieved by right-sided endovascular MCAO. In brief, the right common, external, and internal carotid arteries (CCA, ECA, and ICA) are revealed via a midline cervical incision. Then, a piece of 4.0-monofilament nylon suture with the tip rounded by heating before coating with polylysine is inserted through the right CCA and advanced it along the ICA until the tip occluded the proximal stem of the middle cerebral artery (MCA). Rectal temperature is maintained between 36.5 and 37.5 °C with a heating pad. After 2 h of ischemia, the filament is withdrawn to allow reperfusion. At 24 h after reperfusion, the brain tissue samples of rats in various groups are obtained for further analyses.

Experimental Group and Drug Administration

The sample sizes in each group were determined by power analysis during the animal ethics dossier application. Thirty-two adult male SD rats are randomly divided into two experimental groups: sham operation group (Sham group, $n = 8$) and middle cerebral artery occlusion group (MCAO group, $n = 24$). MCAO group is then subdivided into three groups: At 0.5 h before MCAO surgery, the rats are, respectively, pretreated with vehicle ($n = 8$), gp91ds-tat ($n = 8$), and GKT137831 ($n = 8$). According to our previous study [32], the gp91ds-tat (AnaSpec., USA) is dissolved in normal saline. 20 μL gp91ds-tat solution is infused into the ventricle using a Hamilton microsyringe, and the final concentration of gp91ds-tat is 100 ng/kg. Meanwhile, the GKT137831 (MedChem Express, USA) is given by oral gavage at 60 mg/kg as the previous research [9]. At 24 h after reperfusion, eight rats in one group were randomly divided into three parts. For four rats, the total brain sections were collected for TTC staining; two rats were killed for TUNEL and FJB staining; the other two rats were used for BBB permeability and ROS assay. For TUNEL and FJB staining, representative images from at least three independent experiments using six different brain sections were shown. For Western blot analysis and ROS assay showing quantitative results, each n represents data collected from one independent experiment; combined data from six independent experiments using two different rats are shown. The "n" is always defined as number of independent experiments in every figure legend.

Assay of ROS

The levels of ROS are measured by the Reactive Oxygen Species Assay Kit (Nanjing Jiancheng Biotechnology Institute, China). Briefly, after the brain tissues are collected, the samples are homogenized and centrifuged at 12,000 g for 10 min in 4 °C. The supernatants are then collected for ROS assay. ROS concentrations are assessed using the oxidant-sensitive probe 2,7-dichlorofluorescein diacetate (DCF-DA) according to the manufacturer's proto-

col. The fluorescence intensity is tested by a fluorimetric microplate reader (FilterMax F5; Molecular Devices, USA) with excitation and emission at 485 and 530 nm, respectively. The ROS concentration is expressed as the fluorescence intensity/mg protein and then normalized to the mean value of sham group.

TTC Staining

At 24 h after reperfusion, rats are deeply anesthetized by chloral hydrate (36 mg/100 g body weight) and decapitated. The brain tissues are quickly removed and frozen in stainless steel brain matrices (−20 °C) for 10 min. The brain tissues are subsequently sectioned into 2 mm thick slices starting from the frontal pole. The cerebellum and olfactory bulb are discarded. Slices are then immersed in 10 mL of 2% TTC (Sigma, USA) for 30 min at 37 °C. After staining, the slices are washed three times with saline, fixed in 10% formalin, and then captured with a digital camera. Then, the infarct volume in brain slices of rats are calculated as described previously [21]. Briefly, the total mean infarct area of each section is calculated as the average of the area on the rostral and the caudal side. The total area is calculated by adding the average area from each section. Multiplication of the total area by 2 mm (thickness of the sections) is calculated as infarct volume. The infarct volume is expressed as a percentage of the ipsilateral hemispheric volume.

Ischemic Penumbra Dissection

After indicated treatment, the rats are deeply anesthetized by chloral hydrate (36 mg/100 g body weight) and transcardially perfused with ice-cold PBS. Then, in each rat, the cerebellum and olfactory bulb are discarded, and the brain tissues are quickly removed and frozen in stainless steel brain matrices (−20 °C) for 10 min. The ischemic penumbra is determined according to the method described by Ashwal et al. [2]. Briefly, the brain tissues are subsequently sectioned into three slices beginning 3 mm from the anterior tip of the frontal lobe. The front and back slices are 3 mm in thickness. The middle slice is 4 mm in thickness, which is cut longitudinally in the ischemic hemisphere 2 mm from the midline. A transverse diagonal cut is made at the 2 o'clock position to separate the core from the penumbra. The cerebral cortical penumbra and analogous contralateral region are harvested for Western blot analysis and immunofluorescence assay.

Terminal Deoxynucleotidyl Transferase dUTP Nick End-Labeling (TUNEL) Staining and Fluoro-Jade B Staining

TUNEL staining is used to detect cell apoptosis in brain tissues and performed according to the manufacturer's protocol (Dead End Flurometric kit, Promega, USA). The sections are visualized using a fluorescence microscope (Olympus BX50/BXFLA/DP70; Olympus Co., Japan). The TUNEL-positive cells are counted by an observer who is blind to the experimental groups. To evaluate the extent of cell apoptosis, the apoptotic index is defined as the average number of TUNEL-positive cells in each section counted in six microscopic fields.

Fluoro-Jade B (FJB, Histo-Chem Inc., USA) staining is served as a marker of neuronal degeneration. Brain sections are deparaffinized and rehydrated. After incubation with deionized water for 1 min, the slides are incubated in 0.06% K permanganate (Sigma, USA) for 15 min. Slides are then rinsed in deionized water and immersed in 0.001% Fluoro-Jade working solution (0.1% acetic acid) for 30 min. Then they are washed and dried in an incubator (50–60 °C) for 10 min. Sections are cleared in xylene and coverslipped with a nonaqueous, low-fluorescence, styrene-based mounting medium (DPX, Sigma, USA). Microscopy of the stained brain sections are performed by an experienced pathologist blind to the experimental condition.

Western Blot Analysis

After brain tissues of each rat are collected, the brain samples are separately homogenized and lysed in ice-cold RIPA lysis buffer (Beyotime, China). After centrifuge at 12,000 g for 10 min at 4 °C, the supernatants are collected. The protein concentration is determined by using the bicinchoninic acid (BCA) kit (Beyotime, China). Then, protein samples (20 μg/lane) are loaded on a 15% SDS polyacrylamide gel, separated, and electrophoretically transferred to a polyvinylidene difluoride membrane (PVDF, Millipore, USA). The membrane is blocked with PBST (PBS + 0.1% Tween-20) containing 5% skim milk for 1 h at 37 °C. Subsequently, the membrane is incubated with the primary antibodies against albumin and GAPDH (abcam, USA) overnight at 4 °C. Next, the membrane is incubated with the horseradish peroxidase (HRP)-linked secondary antibody (abcam, USA) for 2 h at 37 °C and then washed with PBST for three times. Then, the membrane is revealed with use of an enhanced chemiluminescence detection kit. The relative quantity of proteins is

analyzed by using Image J program (NIH, USA), and the data are normalized to that of loading controls.

Statistical Analysis

All data are expressed as mean ± SEM and GraphPad Prism 6.0 (GraphPad, USA) is adopted for all statistical analyses. Data sets are tested for normality of distribution with Kolmogorov-Smirnov test. Data groups (two groups) with normal distribution are compared using two-sided unpaired Student's t-test, and the Mann-Whitney U test is used for nonparametric data. $P < 0.05$ is considered as statistically significant difference.

Results

General Observation

No significant differences in mortality rate, body weight, mean arterial blood pressure, heart rate, temperature, or blood gas data are detected in any experimental groups (data not shown).

Nox2 Inhibitor (gp91ds-tat) and Nox4 Inhibitor (GKT137831) Treatments Reduce ROS Levels in Brain Tissues of Rats After MCAO

Compared to the sham group, the level of ROS is significantly increased in penumbra of brain tissues at 24 h after reperfusion in rats in the MCAO group ($P < 0.01$, Fig. 1). However, treatment with Nox2 inhibitor (gp91ds-tat) or Nox4 inhibitor (GKT137831) significantly decreased the ROS levels in penumbra of brain tissues of rats compared with that in the MCAO group (both $P < 0.01$, Fig. 1).

gp91ds-tat and GKT137831 Treatments Reduce Cerebral Infarction Area at 24 h After Reperfusion in MCAO Rats

As shown in Fig. 2, there is a significant infarct area in the brain tissues of rats in the MCAO group compared to the sham group ($P < 0.01$, Fig. 2). However, the cerebral infarct area is significantly reduced after treatment with gp91ds-tat or GKT137831 when compared with that in the MCAO group (both $P < 0.01$, Fig. 2).

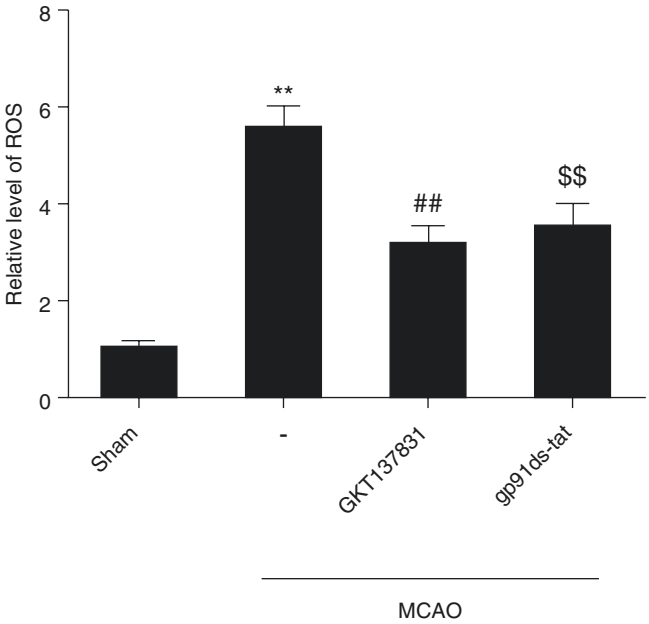

Fig. 1 ROS levels in the penumbra are significantly higher in the MCAO group than that in the sham group; Nox2 inhibitor (gp91ds-tat) or Nox4 inhibitor (GKT137831) treatment significantly reduced the ROS levels in brain tissues compared with the MCAO group. All data are expressed as mean ± SD, $^{**}P < 0.01$, vs. Sham group; $^{\#\#}P < 0.01$, vs. MCAO group; $^{\$\$}P < 0.01$, vs. MCAO group; $n = 6$

gp91ds-tat and GKT137831 Treatments Decrease the Rate of Neuronal Apoptosis in Penumbra of Brain Tissues in Rats at 24 h After Reperfusion After MCAO

Compared with the sham group, the TUNEL-positive neurons are obviously increased in the penumbra of brain tissues at 24 h after reperfusion in rats after MCAO ($P < 0.01$, Fig. 3). However, the gp91ds-tat or GKT137831 treatment significantly reduced the numbers of TUNEL-positive cells in brain tissues of rats after MCAO compared with that in the MCAO group, (both $P < 0.01$, Fig. 3).

gp91ds-tat and GKT137831 Treatments Reduce Neurodegeneration in Penumbra of Brain Tissues in Rats After MCAO

We also assessed neuronal degeneration in the penumbra of brain tissues at 24 h after reperfusion by FJB staining. In the

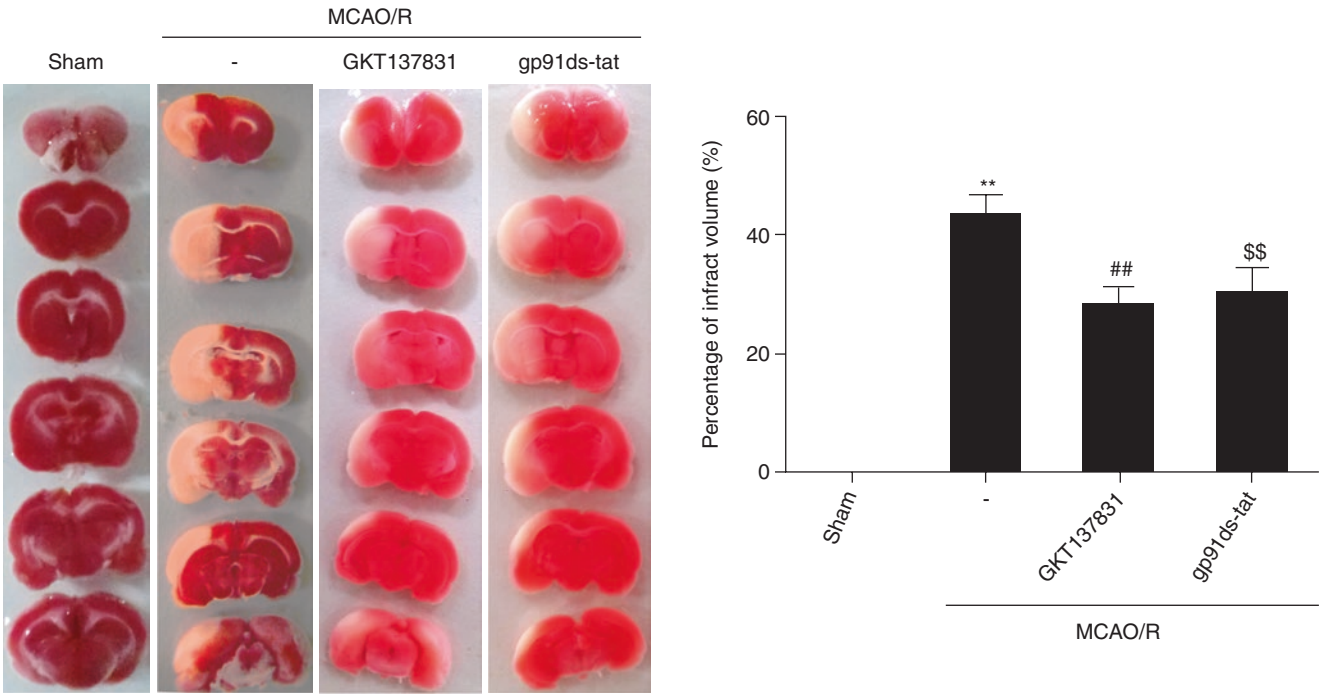

Fig. 2 It is shown that there is a significant infarct area in the brain tissues of rats in the MCAO group compared with the sham group, gp91ds-tat or GKT137831 treatment significantly reduced the percentages of the infarct volume compared with the MCAO group. All data are expressed as mean ± SD, $^{**}P < 0.01$, vs. Sham group; $^{\#\#}P < 0.01$, vs. MCAO group; $^{\$\$}P < 0.01$, vs. MCAO group; $n = 4$

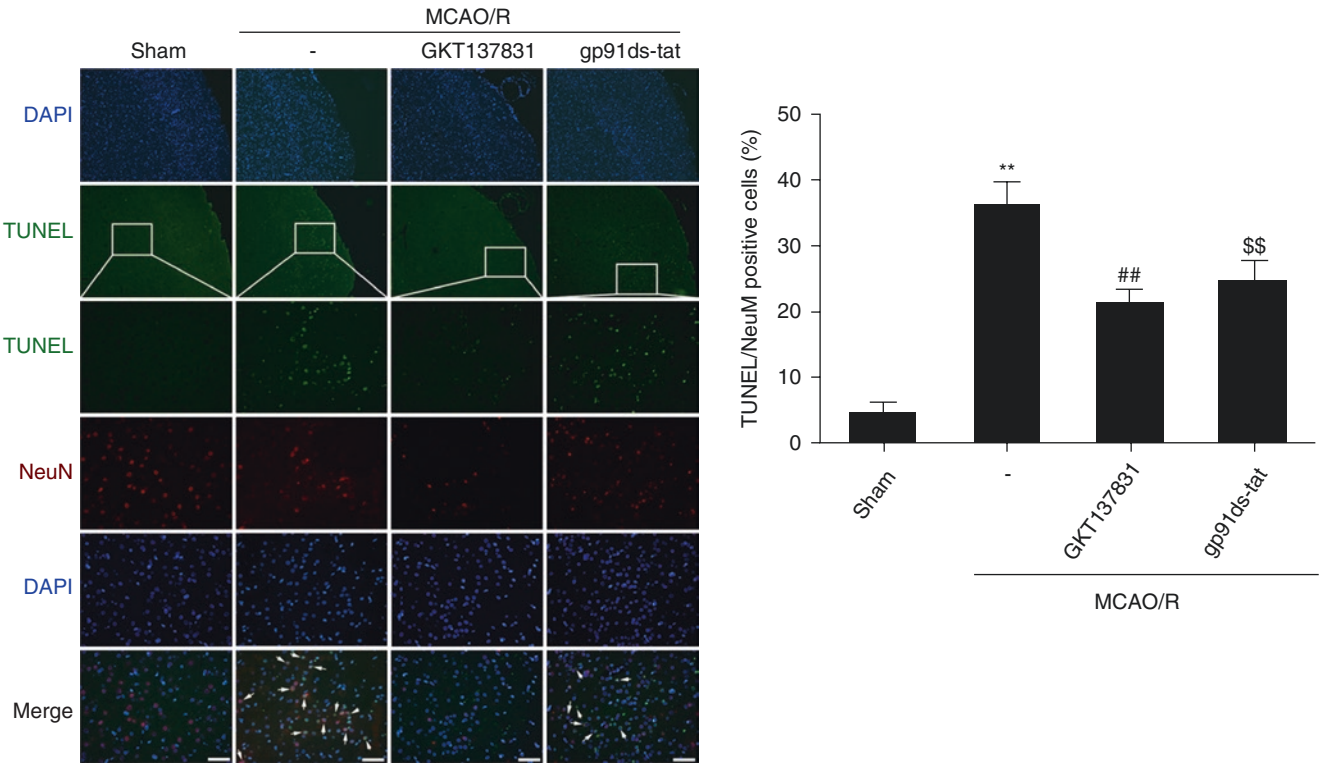

Fig. 3 The TUNEL-positive neurons are significantly increased in brain tissues of rats in the MCAO group relative to the sham group; while gp91ds-tat or GKT137831 treatment significantly reduced the numbers of apoptosis neurons compared with that in the MCAO group. All data are expressed as mean ± SD, $^{**}P < 0.01$, vs. Sham group; $^{\#\#}P < 0.01$, vs. MCAO group; $^{\$\$}P < 0.01$, vs. MCAO group; scale bar = 100 μm; $n = 6$

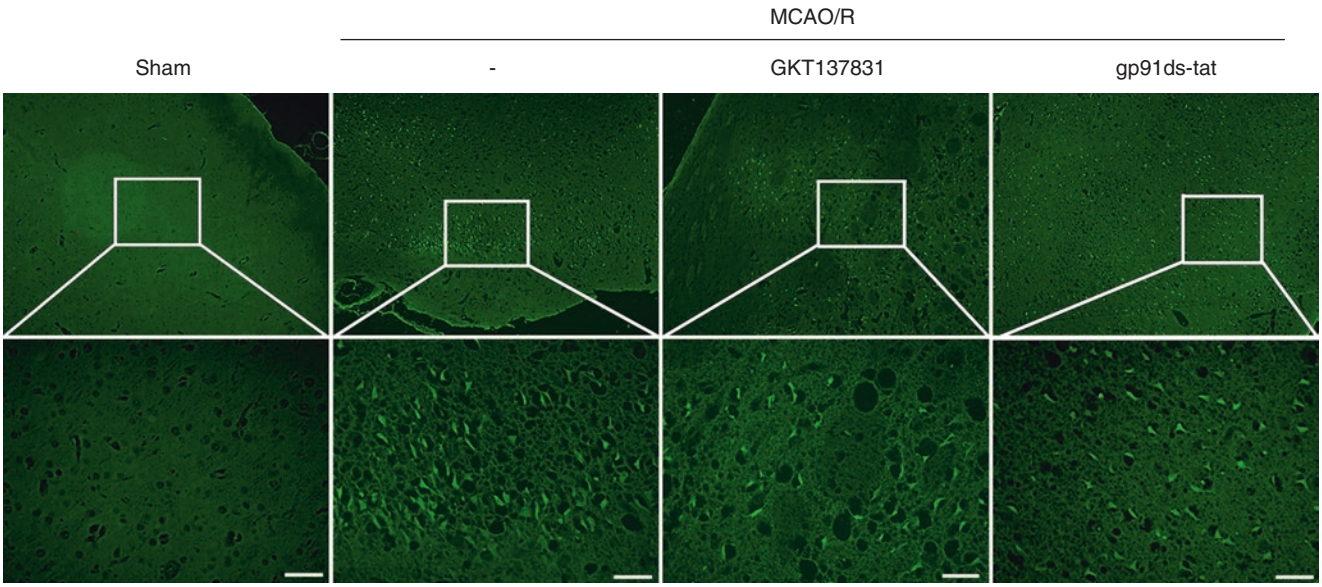

Fig. 4 The FJB-positive cells are significantly increased in brain tissues of rats in the MCAO group relative to the sham group; while gp91ds-tat or GKT137831 administration significantly reduced the numbers of neurodegenerative cells compared with that in the MCAO group; scale bar = 100 μm

MCAO group, FJB-positive cells are significantly increased compared with that in the sham group (Fig. 4). However, treatments with gp91ds-tat or GKT137831 significantly reduce the numbers of FJB-positive cells in brain tissues of rats compared with that in the MCAO group (Fig. 4).

gp91ds-tat and GKT137831 Treatments Protect the BBB Integrity at 24 h After Reperfusion in Rats After MCAO

In order to determine the integrity of BBB in rats, we assess the levels of albumin in brain tissues by Western blot analysis. Compared with the sham group, the level of albumin is significantly increased in brain tissues of the rats in the MCAO group ($P < 0.01$, Fig. 5), which suggests that there is albumin leakage in brain tissues of rats after MCAO, resulting in BBB injury. However, compared with the MCAO group, gp91ds-tat or GKT137831 treatment significantly reduced the levels of albumin in brain tissues in rats after MCAO (both $P < 0.01$, Fig. 5).

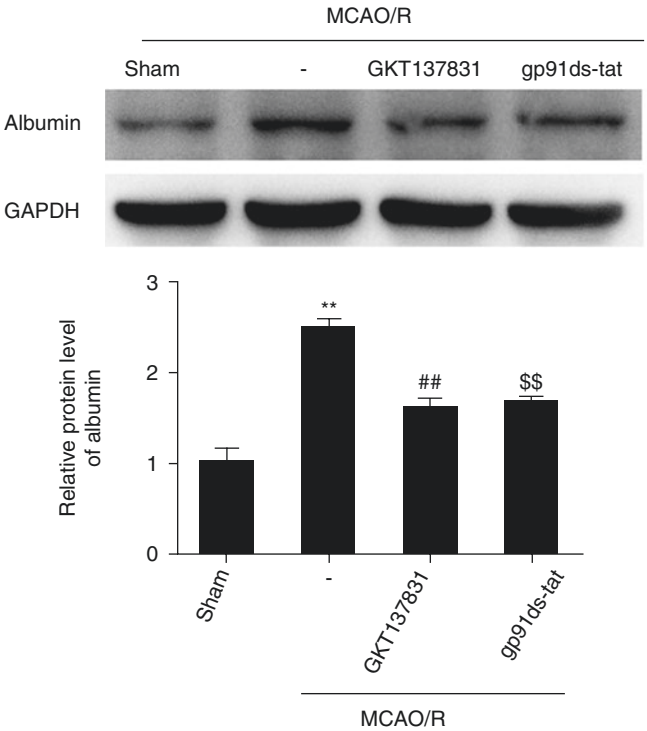

Fig. 5 The protein levels of albumin are significantly increased in brain tissues of rats in the MCAO group relative to the sham group; however, gp91ds-tat or GKT137831 administration significantly reduced the protein levels of Albumin in brain tissues of rats compared with that in the MCAO group. All data are expressed as mean ± SD, $^{**}P < 0.01$, vs. Sham group; $^{\#\#}P < 0.01$, vs. MCAO group; $^{\$\$}P < 0.01$, vs. MCAO group; $n = 6$

Discussion

Previous studies have shown that the increasing expression and activation of Nox induced the massive production of ROS in cerebral I/R injury [16]. Excessive ROS may cause the peroxidation of lipid, protein, and nucleic acids [1, 8], destruction of the blood-cerebrospinal fluid structure and further increase 3 cysteine-aspartic acid proteases, decrease Bcl-2/Bax ratios, and finally result in cell apoptosis [12]. In addition, oxidative stress and inflammation can influence and interact with each other in a synergistic manner in cerebral I/R-induced brain injury [5]. Another previous research also found that Nox acti-

vation and ROS production may lead to activation of microglia and production of inflammatory mediators, such as IL-1β and TNF-α in a mice model with focal cerebral I/R injury [15].

As our previous report, Nox2 and Nox4 may play greater roles than other members of Nox family in cerebral I/R--induced brain injury [22]. It is reported that Nox2 increases from 24 to 72 h after reperfusion in endothelial cells and microglia of the penumbra in a mice model of MCAO. Nox4 is also been conformed that it was increased in the brain tissues after ischemic stroke. In a mice model of MCAO, Nox4 mRNA levels in neurons increase within the 24 h, peak between days 7 and 15, and slowly decline until day 30 [10, 31]. In analysis of whole brain tissues, the mRNA and protein levels of Nox2 and $p22^{phox}$ increase in the ischemic hemisphere in a rat model of MCAO [20], and Nox4 increases in the ischemic cortex and basal ganglia after ischemic stroke in mice [18]. In this study, our results show that Nox2-specific inhibitor (gp91ds-tat) and Nox4-specific inhibitor (GKT137831) have significant protective effects in brain injury induced by cerebral I/R in a rat model of MCAO. It is expected that Nox2 and Nox4 specific inhibitors may have superior effects than omni-spectrum inhibitors of the Nox family.

The present study also has the following limitations. Firstly, we use healthy adult rats in this study, which do not maximally mimic human high-risk populations, such as the elderly, women, and patients with cardiovascular diseases. Additionally, the mechanisms underlying the effects of treatment with Nox2 and Nox4 inhibitors on cerebral I/R induced brain injury are also not fully investigated. Of course, these limitations involved in Nox2-specific inhibitor (gp91ds-tat) and Nox4-specific inhibitor (GKT137831)-induced neuroprotective effects showed in this study would be explored in our future work.

In conclusion, this study suggests that Nox2 inhibitor (gp91ds-tat) and Nox4 inhibitor (GKT137831) treatment could, respectively, inhibit I/R-induced excessive increasing of ROS in the penumbra of brain tissues, reduce cerebral infarction area, mitigate neuronal apoptosis and degeneration, and alleviate BBB damage. Meanwhile, our study provides a theoretical basis for the clinical use of Nox2-specific inhibitor (gp91ds-tat) and Nox4-specific inhibitor (GKT137831) for stroke therapy.

Acknowledgments None.

Conflict of Interest: **The authors declare that they have no conflict of interest.**

References

1. Andreadou I, Iliodromitis EK, Farmakis D, Kremastinos DT. To prevent, protect and save the ischemic heart: antioxidants revisited. Expert Opin Ther Targets. 2009;13:945–56. https://doi.org/10.1517/14728220903039698.
2. Ashwal S, Tone B, Tian HR, Cole DJ, Liwnicz BH, Pearce WJ. Core and penumbral nitric oxide synthase activity during cerebral ischemia and reperfusion in the rat pup. Pediatr Res. 1999;46:390–400. https://doi.org/10.1203/00006450-199910000-00006.
3. Astrup J, Siesjo BK, Symon L. Thresholds in cerebral ischemia—the ischemic penumbra. Stroke. 1981;12:723–5.
4. Cao G, Ye X, Xu Y, Yin M, Chen H, Kou J, Yu B. YiQiFuMai powder injection ameliorates blood-brain barrier dysfunction and brain edema after focal cerebral ischemia-reperfusion injury in mice. Drug Des Devel Ther. 2016;10:315–25. https://doi.org/10.2147/DDDT.S96818.
5. Chen H, Kim GS, Okami N, Narasimhan P, Chan PH. NADPH oxidase is involved in post-ischemic brain inflammation. Neurobiol Dis. 2011;42:341–8. https://doi.org/10.1016/j.nbd.2011.01.027.
6. Chen YH, Du GH, Zhang JT. Salvianolic acid B protects brain against injuries caused by ischemia-reperfusion in rats. Acta Pharmacol Sin. 2000;21:463–6.
7. De Silva TM, Brait VH, Drummond GR, Sobey CG, Miller AA. Nox2 oxidase activity accounts for the oxidative stress and vasomotor dysfunction in mouse cerebral arteries following ischemic stroke. PLoS One. 2011;6:e28393. https://doi.org/10.1371/journal.pone.0028393.
8. Djordjevic VB, Zvezdanovic L, Cosic V. [Oxidative stress in human diseases]. Srp Arh Celok Lek. 2008;136(Suppl 2):158–65.
9. Green DE, Murphy TC, Kang BY, Kleinhenz JM, Szyndralewiez C, Page P, Sutliff RL, Hart CM. The Nox4 inhibitor GKT137831 attenuates hypoxia-induced pulmonary vascular cell proliferation. Am J Respir Cell Mol Biol. 2012;47:718–26. https://doi.org/10.1165/rcmb.2011-0418OC.
10. Green SP, Cairns B, Rae J, Errett-Baroncini C, Hongo JA, Erickson RW, Curnutte JT. Induction of gp91-phox, a component of the phagocyte NADPH oxidase, in microglial cells during central nervous system inflammation. J Cereb Blood Flow Metab. 2001;21:374–84. https://doi.org/10.1097/00004647-200104000-00006.
11. Hafez S, Hoda MN, Guo X, Johnson MH, Fagan SC, Ergul A. Comparative analysis of different methods of ischemia/reperfusion in hyperglycemic stroke outcomes: interaction with tPA. Transl Stroke Res. 2015;6:171–80. https://doi.org/10.1007/s12975-015-0391-0.
12. Huttemann M, Lee I, Grossman LI, Doan JW, Sanderson TH. Phosphorylation of mammalian cytochrome c and cytochrome c oxidase in the regulation of cell destiny: respiration, apoptosis, and human disease. Adv Exp Med Biol. 2012;748:237–64. https://doi.org/10.1007/978-1-4614-3573-0_10.
13. Kahles T, Brandes RP. NADPH oxidases as therapeutic targets in ischemic stroke. Cell Mol Life Sci. 2012;69:2345–63. https://doi.org/10.1007/s00018-012-1011-8.
14. Kahles T, Brandes RP. Which NADPH oxidase isoform is relevant for ischemic stroke? The case for nox 2. Antioxid Redox Signal. 2013;18:1400–17. https://doi.org/10.1089/ars.2012.4721.
15. Kahles T, et al. NADPH oxidase Nox1 contributes to ischemic injury in experimental stroke in mice. Neurobiol Dis. 2010;40:185–92. https://doi.org/10.1016/j.nbd.2010.05.023.
16. Kalogeris T, Bao Y, Korthuis RJ. Mitochondrial reactive oxygen species: a double edged sword in ischemia/reperfusion vs preconditioning. Redox Biol. 2014;2:702–14. https://doi.org/10.1016/j.redox.2014.05.006.
17. Kleikers PW, et al. NADPH oxidases as a source of oxidative stress and molecular target in ischemia/reperfusion injury. J Mol Med. 2012;90:1391–406. https://doi.org/10.1007/s00109-012-0963-3.
18. Kleinschnitz C, Grund H, Wingler K, Armitage ME, Jones E, Mittal M, Barit D, Schwarz T, Geis C, Kraft P, Barthel K, Schuhmann MK, Herrmann AM, Meuth SG, Stoll G, Meurer S, Schrewe A, Becker L, Gailus-Durner V, Fuchs H, Klopstock T, de Angelis MH, Jandeleit-Dahm K, Shah AM, Weissmann N, Schmidt HH. Post-stroke inhibition of induced NADPH oxidase type 4 prevents oxidative stress and neurodegeneration. PLoS Biol. 2010;8(9). https://doi.org/10.1371/journal.pbio.1000479.

19. Kochanski R, Peng C, Higashida T, Geng X, Huttemann M, Guthikonda M, Ding Y. Neuroprotection conferred by post-ischemia ethanol therapy in experimental stroke: an inhibitory effect on hyperglycolysis and NADPH oxidase activation. J Neurochem. 2013;126:113–21. https://doi.org/10.1111/jnc.12169.
20. Kusaka I, Kusaka G, Zhou C, Ishikawa M, Nanda A, Granger DN, Zhang JH, Tang J. Role of AT1 receptors and NAD(P)H oxidase in diabetes-aggravated ischemic brain injury. Am J Physiol Heart Circ Physiol. 2004;286(6):H2442–51. https://doi.org/10.1152/ajpheart.01169.2003.
21. Li H, Gao A, Feng D, Wang Y, Zhang L, Cui Y, Li B, Wang Z, Chen G. Evaluation of the protective potential of brain microvascular endothelial cell autophagy on blood-brain barrier integrity during experimental cerebral ischemia-reperfusion injury. Transl Stroke Res. 2014;5(5):618–26. https://doi.org/10.1007/s12975-014-0354-x.
22. Li H, Wang Y, Feng D, Liu Y, Xu M, Gao A, Tian F, Zhang L, Cui Y, Wang Z, Chen G. Alterations in the time course of expression of the Nox family in the brain in a rat experimental cerebral ischemia and reperfusion model: effects of melatonin. J Pineal Res. 2014;57(1):110–9. https://doi.org/10.1111/jpi.12148.
23. Liu W, Chen Q, Liu J, Liu KJ. Normobaric hyperoxia protects the blood brain barrier through inhibiting Nox2 containing NADPH oxidase in ischemic stroke. Med Gas Res. 2011;1:22. https://doi.org/10.1186/2045-9912-1-22.
24. Liu X, et al. Remote ischemic postconditioning alleviates cerebral ischemic injury by attenuating endoplasmic reticulum stress-mediated apoptosis. Transl Stroke Res. 2014;5:692–700. https://doi.org/10.1007/s12975-014-0359-5.
25. Molina CA. Reperfusion therapies for acute ischemic stroke: current pharmacological and mechanical approaches. Stroke. 2011;42:S16–9. https://doi.org/10.1161/STROKEAHA.110.598763.
26. Pang T, Wang J, Benicky J, Sanchez-Lemus E, Saavedra JM. Telmisartan directly ameliorates the neuronal inflammatory response to IL-1beta partly through the JNK/c-Jun and NADPH oxidase pathways. J Neuroinflammation. 2012;9:102. https://doi.org/10.1186/1742-2094-9-102.
27. Qi Z, et al. Bcl-2 phosphorylation triggers autophagy switch and reduces mitochondrial damage in limb remote ischemic conditioned rats after ischemic stroke. Transl Stroke Res. 2015;6:198–206. https://doi.org/10.1007/s12975-015-0393-y.
28. Radermacher KA, Wingler K, Kleikers P, Altenhofer S, JR Hermans J, Kleinschnitz C, Hhw Schmidt H. The 1027th target candidate in stroke: will NADPH oxidase hold up? Exp Transl Stroke Med. 2012;4:11. https://doi.org/10.1186/2040-7378-4-11.
29. Shen J, et al. Interrupted reperfusion reduces the activation of NADPH oxidase after cerebral I/R injury. Free Radic Biol Med. 2011;50:1780–6. https://doi.org/10.1016/j.freeradbiomed.2011.03.028.
30. Taylor TN, Davis PH, Torner JC, Holmes J, Meyer JW, Jacobson MF. Lifetime cost of stroke in the United States. Stroke. 1996;27:1459–66.
31. Yoshioka H, Niizuma K, Katsu M, Okami N, Sakata H, Kim GS, Narasimhan P, Chan PH. NADPH oxidase mediates striatal neuronal injury after transient global cerebral ischemia. J Cereb Blood Flow Metab. 2011;31(3):868–80. https://doi.org/10.1038/jcbfm.2010.166.
32. Zhang L, Li Z, Feng D, Shen H, Tian X, Li H, Wang Z, Chen G. Involvement of Nox2 and Nox4 NADPH oxidases in early brain injury after subarachnoid hemorrhage. Free Radic Res. 2017;51(3):316–28. https://doi.org/10.1080/10715762.2017.1311015.

Link Between Receptors That Engage in Developing Vasospasm After Subarachnoid Hemorrhage in Mice

Fumi Nakano, Fumihiro Kawakita, Lei Liu, Yoshinari Nakatsuka, Hirofumi Nishikawa, Takeshi Okada, Masato Shiba, and Hidenori Suzuki

Abstract Vasospasm after subarachnoid hemorrhage (SAH) has been studied, but the mechanisms remain to be unveiled. Tenascin-C (TNC), which is a matricellular protein and reported to increase in spastic cerebral artery wall after SAH, is a ligand for both Toll-like receptor 4 (TLR4) and epidermal growth factor receptor (EGFR). Our previous studies suggested the involvement of TNC and these receptors in vasoconstriction or vasospasm after SAH. In this study, we investigated whether upregulation of TNC and TLR4 is observed and if an EGFR inhibitor has suppressive effects against them in a mice endovascular perforation SAH model. At 24 h after SAH, TNC and TLR4 expressions were widely observed in spastic cerebral arteries, and these expressions were suppressed by the administration of an EGFR inhibitor. From these results, EGFR inhibitors possibly suppress the expression of not only EGFR but also TLR4 at least partly through regulating TNC upregulation. More studies are needed to clarify the precise mechanisms linking these receptors.

Keywords Epidermal growth factor receptor · Toll-like receptor 4 · Tenascin-C · Cerebral vasospasm

Introduction

Cerebral vasospasm remains an important prognostic factor after aneurysmal subarachnoid hemorrhage (SAH), but the mechanisms are still not well unveiled [1]. Tenascin-C (TNC) is a matricellular protein and one of ligands for epidermal growth factor receptor (EGFR) and Toll-like receptor 4 (TLR4) [2]. Our previous studies showed that TNC was suggested to be involved in vasospasm development in both patients [3] and an experimental animal model [4]. TLR4 activation was also suggested to be involved in vasoconstriction or vasospasm development [1, 5, 6]. Another our previous study showed that administration of recombinant TNC, which consisted of epidermal growth factor (EGF)-like repeats only and did not contain TLR4-binding sites, brought cerebral vasoconstriction in healthy rats [5]. Surprisingly, an anti-TLR4 agent had the most therapeutic effects against this vasoconstriction, and therefore TNC upregulation and subsequent TLR4 activation were suggested [7]. In this study, we investigated whether an EGFR inhibitor has suppressive effects against TNC and TLR4 expression in in vivo SAH models.

Materials and Methods

All procedures were approved by the Animal Ethics Review Committee of Mie University and were carried out in accordance with the institution's guidelines for animal experiments.

SAH Modeling and Study Protocol

Mice (C57BL/6 N, 25–30 g, male) underwent endovascular perforation SAH or sham modeling as previously described [1]. Briefly, mice were anesthetized, positioned supinely, and skin incision was made at the midline of the neck to expose the left carotid artery. A 4–0 monofilament with a sharpen tip was inserted from the left external carotid artery (ECA) into the left internal carotid artery and push further to perforate the bifurcation of anterior cerebral artery and middle cerebral artery. Then the filament was withdrawn and the stump of ECA was coagulated. The wound was sutured. The sham

F. Nakano (✉) · F. Kawakita · L. Liu · Y. Nakatsuka · H. Nishikawa
T. Okada · M. Shiba · H. Suzuki
Department of Neurosurgery, Mie University Graduate School of Medicine, Tsu, Mie, Japan
e-mail: fumi-n21@mva.biglobe.ne.jp

R. D. Martin et al. (eds.), *Subarachnoid Hemorrhage*, Acta Neurochirurgica Supplement 127,
https://doi.org/10.1007/978-3-030-04615-6_9,

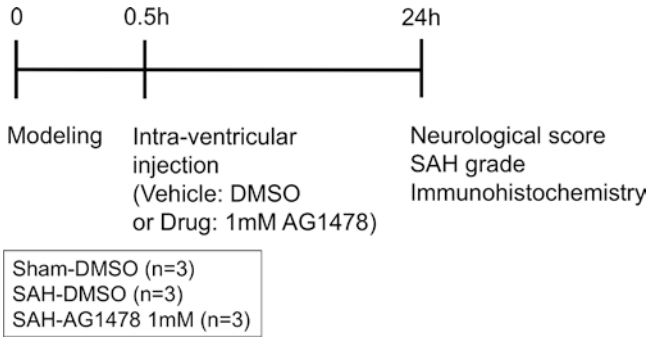

Fig. 1 Experimental designs. Experiment was designed to examine the effects of epidermal growth factor receptor inhibitor (AG1478) on tenascin-C upregulation and subsequent Toll-like receptor 4 upregulation after subarachnoid hemorrhage (SAH). *DMSO* dimethyl sulfoxide

group underwent the same procedure as described above except for perforating the artery. At 30 min after surgery, vehicle or drug was administrated intraventricularly. After evaluating neurological scores, mice were sacrificed at 24 h after modeling, and then assessment of SAH grade and immunohistochemistry were performed (Fig. 1). Mice were assigned to SAH-vehicle, SAH-drug, and sham groups (n = 3/group).

Intraventricular Injection

Intraventricular injection of vehicle or drug was performed as previously described [1]. Mouse was set on the stereotactic head holder, and using a surgical microscope (Zeiss, Germany), a midline frontoparietal skin incision was performed. A burr hole was perforated at 0.2 mm caudal and 1.0 mm lateral (left) to the bregma. The needle of Hamilton syringe was inserted 2.2 mm below the horizontal plane of the bregma, and 2 μL of vehicle (dimethyl sulfoxide, DMSO) or drug diluent (AG1478; 1 mM diluted in DMSO; Cayman; cat#10010244) was injected intraventricularly, and the wound was sutured.

SAH Grade

SAH grading was performed as previously described [1]. The basal cistern was divided into six segments, and each segment was allotted a grade from 0 to 3 depending on the amount of SAH. A total score ranging from 0 to 18 was determined by summing the scores. Mice with moderate SAH grade (8–12) were used for experiments as the SAH groups.

Neurological Score

Neurological impairments were blindly evaluated as previously described [1]. Neurological scores (3–18) were determined by summing up six test scores (spontaneous activity, spontaneous movement of four limbs, forepaw outstretching, climbing, body proprioception, and response to whisker stimulation).

Histology

Mice's brains were used for making paraffin-embedded coronal sections at bregma +1 mm as previously described [1]. Briefly, at 24 h after modeling, mice were deeply anesthetized with Avertin® (2,2,2-tribromoethanol) solution and perfused with cold phosphate-buffered saline followed by 4% paraformaldehyde for brain fixation. The brains were removed, embedded in paraffin, and cut into 4 μm sections. Sections were first deparaffinized followed by rehydration and heat-induced antigen retrieval in 10 mM citrate butter (pH 6.0). Sections were incubated with rabbit anti-TNC primary antibody (1:50; Santacruz Biotechnology; cat #20932) or rabbit anti-TLR4 primary antibody (1:1000; Abcam; cat#13556) at 4 °C for overnight. Then, sections were incubated with anti-rabbit secondary antibody (Vector; cat#BA-1000) at room temperature for 30 min, incubated with avidin-biotin complex solution (Vector; cat#PK-6100) at room temperature for 30 min, visualized by diaminobenzidine (brown color), and counterstained with hematoxylin. Sections were dehydrated, cleared in xylene, and mounted for observation under light microscope.

Results

Increased Expressions of TNC and TLR4 Were Observed in Spastic Cerebral Arteries After SAH

No mice died before sacrifice in the sham group. Mice in the sham group showed full scores at neurological assessment, while mice in the SAH-vehicle group showed neurological deterioration (data not shown). TNC and TLR4 were almost undetected in cerebral arteries in the sham group (Fig. 2a). In contrast, expressions of these molecules were widely observed in the vascular endothelial cells and smooth muscle cells of spastic cerebral arteries after SAH (Fig. 2a).

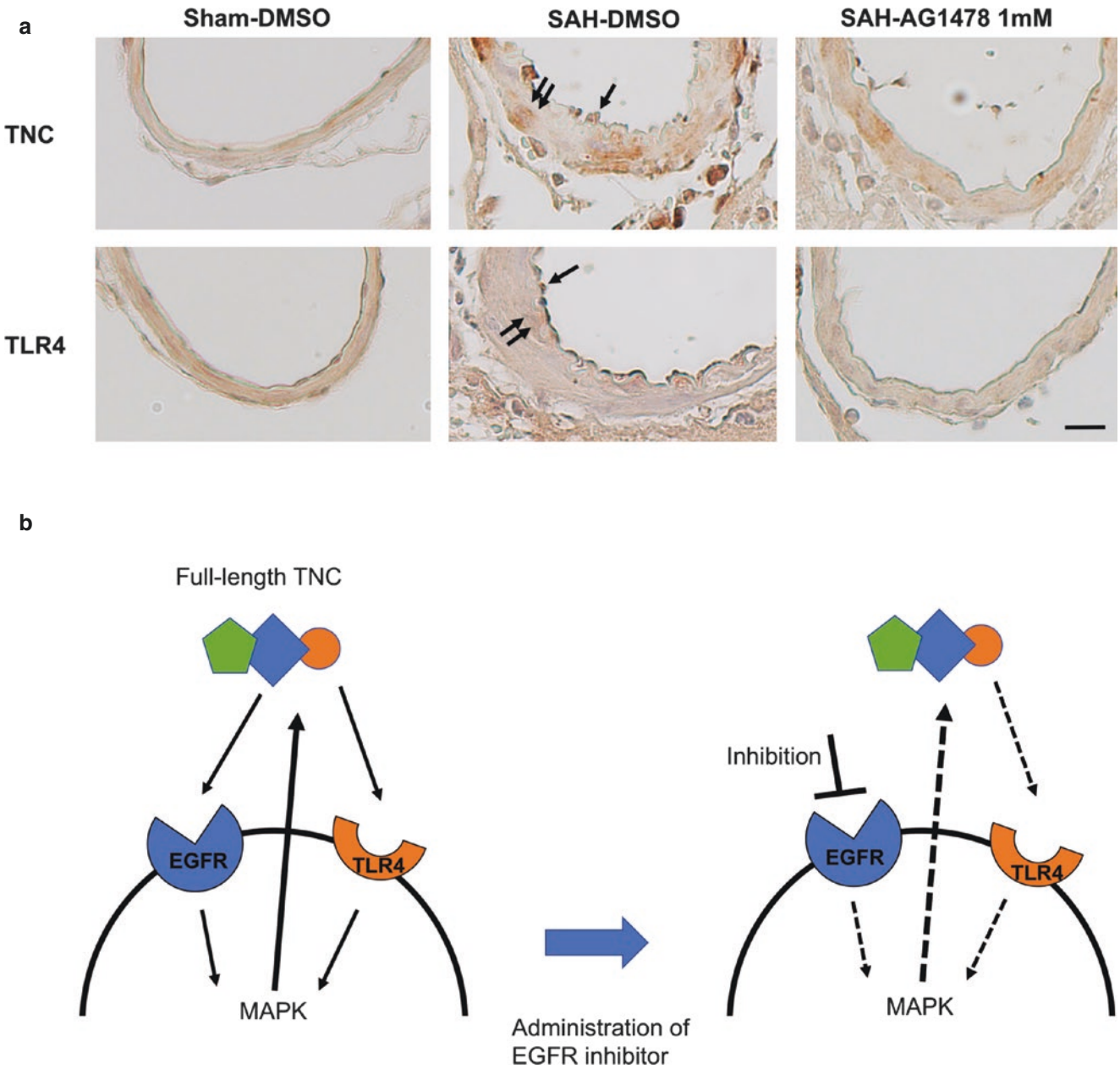

Fig. 2 Effects of an epidermal growth factor receptor (EGFR) inhibitor (AG1478) on expressions of tenascin-C (TNC) and Toll-like receptor 4 (TLR4) after subarachnoid hemorrhage (SAH). (**a**) Representative pictures of coronal sections of internal carotid artery. Single arrow, immunoreactive endothelial cells; double arrow, immunoreactive vascular smooth muscle cells. DMSO, dimethyl sulfoxide; bar, 50 μm. (**b**) Possible links among molecules, which engage in vasospasm development after SAH. *MAPK* mitogen-activated protein kinase

Administration of EGFR Inhibitor Suppressed Expression of TNC and TLR4 in Cerebral Arteries

Neurological behavior of the SAH-drug group showed improvement compared with that of the SAH-vehicle group (data not shown). In the SAH-drug group, immunoreactivities for TNC and TLR4 on cerebral arteries with improved vasospasm were suppressed mainly in the vascular smooth muscle cells (Fig. 2a).

Discussion

This study showed that after administration of EGFR inhibitor, expressions of TNC and TLR4 were suppressed in cerebral arteries in an experimental SAH model (Fig. 2a).

TNC is a matricellular protein, which is rarely detected in the normal adult tissues [2]. Under pathological conditions, TNC appears and is suggested to be involved in the pathogenesis of various diseases such as lung fibrosis [8], rheuma-

toid arthritis [2], and cerebral vasospasm [3, 4]. TNC is also known as a ligand for EGFR and TLR4 [2].

Our previous studies suggested that TNC was upregulated [4] and that TLR4 was one of the receptors activated in major cerebral arteries after SAH [1, 6]. Positive feedback of TNC was observed in spastic cerebral arterial wall after SAH [4]. Jones et al. suggested that exogenous TNC caused EGFR activation in vascular smooth muscle cells [9]. TNC is thought to be involved in its own protein synthesis at least partly through mitogen-activated protein kinase pathway [3]. Furthermore, another of our previous study showed that EGFR stimulation using recombinant TNC, which had only EGF-like repeats, caused cerebral vasoconstriction in healthy rats [5] and that unexpectedly a TLR4 antagonist had therapeutic effects against this vasoconstriction [7]. Taking these findings into consideration, after activating EGFR, TNC positive feedback and subsequent TLR4 activation were suggested. In this study, diminished expressions of TNC and TLR4 on cerebral artery were observed under the presence of an EGFR inhibitor (Fig. 2a), suggesting the similar reactions occurred in in vivo SAH models (Fig. 2b).

Inflammation is suggested to cause upregulation of matricellular proteins such as TNC to manage tissue injury [2]. Besides our previous study [4], TNC positive feedback was reported in experimental animal models of arthritis [2] and epilepsy [10]. Overexpression of TNC could progress diseases in each condition [6]. Therefore, TNC has been suggested to be a therapeutic target to prevent cerebral vasospasm [3, 4]. Our results in this study added a new potential feature of TNC that TNC could exert signaling pathways to upregulate a specific receptor: thus, several working points of inhibitors can be used to block the signaling.

As mentioned in our previous reports [3, 7], there are many studies suggesting crosstalk signaling between receptors. Interaction between EGFR and TLR4 was also reported [11]. In this study, we could not investigate such crosstalk signalings, but they are possibly involved in vasospasm development after SAH. More studies are needed to unveil the mechanisms.

In conclusion, we showed the possibility that an EGFR inhibitor may have suppressive effects against TLR4 upregulation at least partly via reducing TNC upregulation after SAH.

Acknowledgments This work was supported in part by a grant-in-aid for Scientific Research from Japan Society for the Promotion of Science to Drs. Shiba and Suzuki. We thank Chiduru Yamamoto (Department of Neurosurgery, Mie University Graduate School of Medicine) for her assistance.

Conflict of Interest: **The authors declare that they have no conflict of interest.**

References

1. Kawakita F, Fujimoto M, Liu L, Nakano F, Nakatsuka Y, Suzuki H. Effects of Toll-like receptor 4 antagonists against cerebral vasospasm after experimental subarachnoid hemorrhage in mice. Mol Neurobiol. 2017;54:6624–33.
2. Midwood K, Sacre S, Piccinini AM, Inglis J, Trebaul A, Chan E, Drexler S, Sofat N, Kashiwagi M, Orend G, Brennan F, Foxwell B. Tenascin-C is an endogenous activator of Toll-like receptor 4 that is essential for maintaining inflammation in arthritic joint disease. Nat Med. 2009;15:774–80.
3. Suzuki H, Kanamaru K, Shiba M, Fujimoto M, Imanaka-Yoshida K, Yoshida T, Taki W. Cerebrospinal fluid tenascin-C in cerebral vasospasm after aneurysmal subarachnoid hemorrhage. J Neurosurg Anesthesiol. 2011;23:310–7.
4. Shiba M, Suzuki H, Fujimoto M, Shimojo N, Imanaka-Yoshida K, Yoshida T, Kanamaru K, Matsushima S, Taki W. Imatinib mesylate prevents cerebral vasospasm after subarachnoid hemorrhage via inhibiting tenascin-C expression in rats. Neurobiol Dis. 2012;46:172–9.
5. Fujimoto M, Shiba M, Kawakita F, Liu L, Nakasaki A, Shimojo N, Imanaka-Yoshida K, Yoshida T, Suzuki H. Epidermal growth factor-like repeats of tenascin-C-induced constriction of cerebral arteries via activation of epidermal growth factor receptors in rats. Brain Res. 2016;1642:436–44.
6. Okada T, Suzuki H. Toll-like receptor 4 as a possible therapeutic target for delayed brain injuries after aneurysmal subarachnoid hemorrhage. Neural Regen Res. 2017;12:193–6.
7. Nakano F, Fujimoto M, Kawakita F, Nakazaki A, Liu L, Nakatsuka Y, Imanaka-Yoshida K, Yoshida T, Suzuki H. Receptors that mediate tenascin-C-induced constriction of cerebral arteries in rats. In: Sasaki T, Ohkuma H, Kanamaru K, Suzuki M, editors. Neurovascular events after subarachnoid hemorrhage. Tokyo: Narunia; 2017. p. 151–6.
8. Estany S, Vicens-Zygmunt V, Llatjós R, Montes A, Penín R, Escobar I, Xaubet A, Santos S, Manresa F, Dorca J, Molina-Molina M. Lung fibrotic tenascin-C upregulation is associated with other extracellular matrix proteins and induced by TGFβ1. BMC Pulm Med. 2014;14:120.
9. Jones PL, Crack J, Rabinovitch M. Regulation of tenascin-C, a vascular smooth muscle cell survival factor that interacts with the alpha v beta 3 integrin to promote epidermal growth factor receptor phosphorylation and growth. J Cell Biol. 1997;139:279–93.
10. Mercado-Gómez O, Landgrave-Gómez J, Arriaga-Avila V, Nebreda-Corona A, Guevara-Guzmán R. Role of TGFβ signaling pathway on Tenascin C protein upregulation in a pilocarpine seizure model. Epilepsy Res. 2014;108:1694–704.
11. De S, Zhou H, DeSantis D, Croniger CM, Li X, Stark GR. Erlotinib protects against LPS-induced endotoxicity because TLR4 needs EGFR to signal. Proc Natl Acad Sci U S A. 2015;112:9680–5.
12. Fujimoto M, Suzuki H, Shiba M, Shimojo N, Imanaka-Yoshida K, Yoshida T, Kanamaru K, Matsushima S, Taki W. Tenascin-C induces prolonged constriction of cerebral arteries in rats. Neurobiol Dis. 2013;55:104–9.

Aquaporin4 Knockout Aggravates Early Brain Injury Following Subarachnoid Hemorrhage Through Impairment of the Glymphatic System in Rat Brain

E. Liu,[$] Linlin Sun,[$] Yixuan Zhang, Aibo Wang, and Junhao Yan

Abstract *Background*: It is reported that the expression of aquaporin4 (AQP4) in the brain is increased and leads to the brain edema after subarachnoid hemorrhage (SAH). In this study, by using AQP4 knockout rat model, the opposite role of AQP4 in early brain injury following SAH through modulation of interstitial fluid (ISF) transportation in the brain glymphatic system had been explored.

Methods: The SAH model was established using endovascular perforation method, the AQP4 knockout rat model was generated using TALENs (transcription activator-like (TAL) effector nucleases) technique. The animals were randomly divided into four groups: sham (n = 16), AQP4$^{-/-}$sham (n = 16), SAH (n = 24), and AQP4$^{-/-}$SAH groups (n = 27). The roles of AQP4 in the brain water content and neurological function were detected. In addition, immunohistochemistry and Nissl staining were applied to observe the effects of AQP4 on the blood–brain barrier (BBB) integrity and the loss of neurons in the hippocampus. To explore the potential mechanism of these effects, the distribution of Gd-DTPA (interstitial fluid indicator) injected from cisterna magna was evaluated with MRI.

Results: Following SAH, AQP4 knockout could significantly increase the water content in the whole brain and aggravate the neurological deficits. Furthermore, the loss of neuron and BBB disruption in hippocampus were also exacerbated. The MRI results indicated that the ISF transportation in the glymphatic system of AQP4 deficit rat was significantly injured.

Conclusion: AQP4 facilitates the ISF transportation in the brain to eliminate the toxic factors; AQP4 knockout will aggravate the early brain injury following SAH through impairment of the glymphatic system.

Keywords Aquaporin4 · Early brain injury · Subarachnoid hemorrhage · Glymphatic system · Rat

Introduction

Subarachnoid hemorrhage (SAH) is a life-threatening disease and accounts for about 6–8% of all human strokes [1]. Early brain injury (EBI) is one of the key mechanisms which plays a critical role in high mortality and disability after SAH [2]. After SAH, numerous inflammatory factors (e.g., TNF-α) and apoptosis factors (e.g., p53) are produced and released into the extracellular space (ECS), which are harmful to the microvasculature and neurons, and lead to blood–brain barrier (BBB) disruption and loss of neurons. Physiologically, the interstitial fluid (ISF) in the ECS is largely originated from cerebrospinal fluid (CSF). ISF flows into the brain from para-arterial space and drains out from the para-venous space and takes the metabolite and toxicant factors out of the brain [3], that is, glymphatic system in the brain [4]. Obviously, the glymphatic system damage will result in accumulation of poisonous substance in ECS and consequent brain injury.

Aquaporin4 (AQP4) is mainly expressed on the end feet of astrocyte, which facilitates the ISF circulation within the glymphatic system. It was reported that the expression of AQP4 after SAH was increased, which was commonly considered to develop brain edema [5]. However, in this

[$]E. Liu and Linlin Sun contributed equally to this study.

E. Liu · L. Sun · Y. Zhang
Department of Anatomy and Histology, School of Basic Medical Sciences, Peking University, Beijing, China

A. Wang
Beijing Key Lab of Magnetic Resonance Imaging Technology, Beijing, China

J. Yan (✉)
Department of Anatomy and Histology, School of Basic Medical Sciences, Peking University, Beijing, China

Beijing Key Lab of Magnetic Resonance Imaging Technology, Beijing, China
e-mail: yjh@bjmu.edu.cn

R. D. Martin et al. (eds.), *Subarachnoid Hemorrhage*, Acta Neurochirurgica Supplement 127,
https://doi.org/10.1007/978-3-030-04615-6_10,

study, using AQP4 knockout rat model, we found that total AQP4 knockout could not attenuate the EBI after SAH. The results indicated that AQP4 might maintain the ISF flow and preserve the homeostasis through modulation of glymphatic system function in the brain.

Methods

The methods in this study were approved by the Animal Care and Use Committee at Peking University Health Sciences Center and with the Guidelines for the Use of Animals in Neuroscience Research by the Society for Neuroscience (Beijing, Certificate No. SCXK 2002–0001).

SAH Model

The male Sprague–Dawley rats (300–350 g) were randomly divided into four groups: sham (n = 16), AQP4$^{-/-}$sham (n = 16), SAH (n = 24), and AQP4$^{-/-}$SAH groups (n = 27).

The SAH model was established using endovascular perforation method [6, 7]. The rat was anesthetized with 4% isoflurane in a mixture of 60% medical air and 40% oxygen and maintained anesthesia with 2% isoflurane. A 4–0 monofilament nylon suture was inserted through the right internal carotid artery to perforate the junction of the middle and anterior cerebral arteries. The sham rat underwent the same process except the suture was withdrawn, while the resistance was felt at the junction.

AQP4 knockout rats were generated using transcription activator-like effector nuclease (TALENs) method [8, 9]. Highly active TALENs were synthesized against the sequence (5′-CACAGCAGAGTTCCTGG-3′) for the sense strand, and TALEN right was designed against the sequence (5′-GGATCCCACGCTGAGCA-3′) for the antisense strand. The TALEN mRNAs were injected into the cytoplasm of rat pronuclear stage embryos to produce mutant founders (F0). The F0 which were lack of three base pairs were crossed with the wild-type rat to generate F1 generation. The heterozygous offspring of F1 were crossed to produce the F2 generation (AQP4$^{-/-}$ rats). The effects of TALEN-induced mutation were confirmed by western blot and immunohistology method (data not shown).

Brain Water Content

The water content of the whole brain was measured as reported by the others [10]. The brain was harvested and weighed immediately (wet weight) and weighed again after being dried in an oven at 105 °C for 24 h (dry weight). The water content was calculated as [(wet weight − dry weight)/wet weight] × 100%, n = 6 each group.

Neurological Functions

The neurological functions were blindly assessed at 24 h after SAH. It is an 18-point sensory–motor assessment system and consists of six items with scores of 0–3 (or 1–3) for each item. These tests include spontaneous activity, symmetry of the limb movement, forepaw outstretching, climbing, body proprioception, and whisker stimulation response [6, 11], n = 6 each group.

Magnetic Resonance Imaging (MRI) Examination

Gd-DTPA is a common contrast used for MRI imaging. It is also a good tracer for observing the flow and drainage of ISF in the brain due to its impermeability to the cellular membrane [12]. A 3.0 T MRI system (Magnetom Trio, Siemens Medical Solutions, Erlangen, Germany) with an eight-channel wrist coil was applied by using a T1-weighted magnetization-prepared rapid acquisition with gradient echo (MP-RAGE) sequence. The acquisition parameters were as follows: echo time, 3.7 ms; repetition time, 1500 ms; flip angle, 12°; inversion time, 900 ms; field of view, 267 mm; voxel, 0.5 mm^3; matrix, 512 × 512; number of averages, 2; and phase-encoding steps, 96. The acquisition time for each rat was 290 s. The scanning was performed before and after the introduction of Gd-DTPA. The scan time points were set at 0, 0.5 h, 1 h, 2 h, and 3 h following Gd-DTPA injection, n = 6 each group.

Immunohistochemistry Staining

The immunohistochemistry staining was performed at 24 h following SAH. The anesthetic animals were perfused using 250 mL ice-cold 0.1 mol/L PBS followed by 400 mL 4% paraformaldehyde (pH 7.4) through the left ventricles, n = 4 each group. The brain was postfixed in 4% paraformaldehyde overnight. The brain sample was embedded in paraffin, and the coronal sections (10 μm thickness) were prepared.

The sections including bilateral hippocampi each group were stained by Nissl dye and then observed under the BX51 microscope (Olympus, Japan).

To observe the BBB leakage in the brain, IgG immunohistochemistry staining was performed. The section was incubated with rabbit anti-rat IgG antibody (1:100, ab6735, Abcam, MA) at 4 °C overnight and then treated with the corresponding staining kit. The control serum was applied instead of the antibody as a negative control [13].

Statistical Evaluation

In the present study, multiple comparisons were analyzed by one-way analysis of variance (ANOVA) followed by Tukey multiple comparison post hoc analysis. The neurological scores were analyzed using the Kruskal–Wallis one-way ANOVA and then followed by Steel–Dwass multiple comparisons. The SigmaPlot software (13.0 version) was used to create the figures. A *P*-value<0.05 was considered statistically significant.

Results

The whole brain water contents in sham and AQP4$^{-/-}$sham were 78.5% ± 0.3% and 78.7% ± 0.2%, respectively; there was no significantly difference between them. After SAH, the brain water content was markedly increased (79.8% ± 0.6% in the SAH rat and 80.1% ± 0.7% in the AQP4$^{-/-}$ SAH rat) (Fig. 1a).

The neurological scores of the animals in SAH, AQP4$^{-/-}$ SAH groups were markedly decreased following SAH compared with those of sham and AQP4$^{-/-}$sham ($p < 0.05$); the neurological deficits in AQP4$^{-/-}$ SAH group were more severe than that of SAH group ($p < 0.05$) (Fig. 1b).

The Nissl staining results indicated that the neurons in the CA1 region of hippocampus in the sham and AQP4$^{-/-}$sham rats were round and distributed with a layer mode (Fig. 2A1, A2, a1, a2). However, after SAH, the shape of neuron was irregular (such as triangle or polygon) due to ischemic injury, and the spatial conformation of neurons was disordered, especially in the AQP4$^{-/-}$SAH group (Fig. 2A3, A4, a3, a4).

In the sham and AQP4$^{-/-}$sham rats, there was rare positive IgG staining around the microvasculature in the hippocampus (Fig. 2B1 and B2). However, numerous IgG positive products were detected around the microvessels in SAH and AQP4$^{-/-}$SAH groups, which were localized on the capillary wall and perivascular parenchyma (Fig. 2B3 and B4). A large number of glial cells were also activated in the AQP4$^{-/-}$ SAH group (Fig. 2B4).

In sham group, the Gd-DTPA injected into the cisterna magna was widely diffused in subarachnoid space and ventricle system, and gradually distributed throughout the brain parenchyma, and concentrated in the olfactory bulb at 1 h and totally cleared from the brain at 3 h following injection (Fig. 3a1–a5). However, the diffusion of Gd-DTPA into the brain was markedly blocked in Aqp4$^{-/-}$sham group (Fig. 3b1–b5). After SAH, Gd-DTPA was concentrated in the cisterna magna and basilar cisterna, and only a small amount of Gd-DTPA was drained to the olfactory bulb at 2 h after injection, especially in the AQP4$^{-/-}$SAH rats (Fig. 3c1–d5).

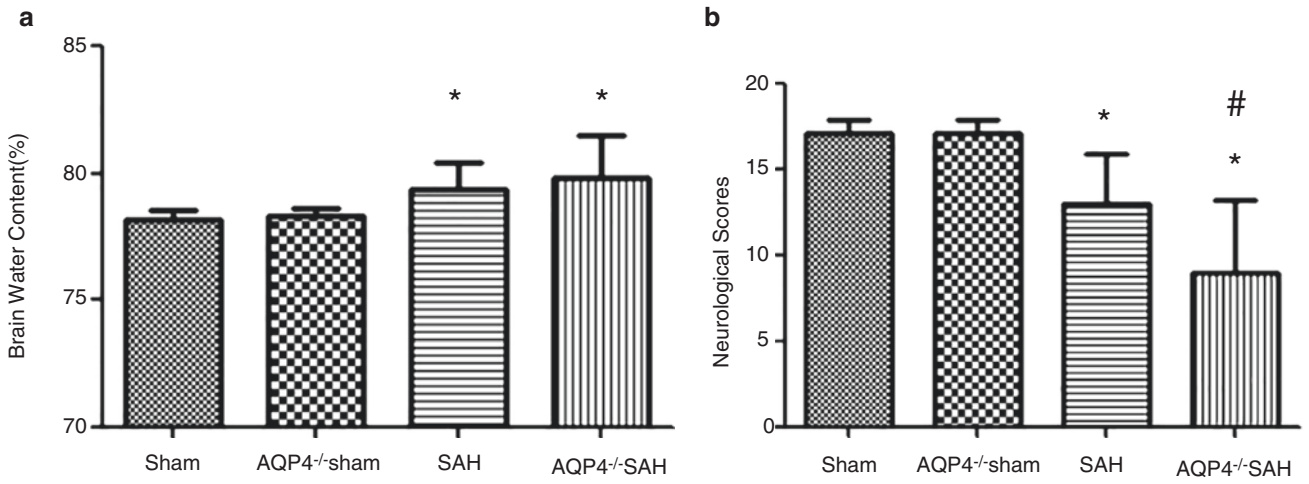

Fig. 1 The brain water content and neurological deficits following SAH. After SAH, the brain water content was significantly increased in both SAH and AQP4$^{-/-}$ SAH groups (**a**). Additionally, the neurological scores of the animals in SAH and AQP4$^{-/-}$ SAH groups were markedly decreased compared with those of sham and AQP4$^{-/-}$sham ($p < 0.05$), especially in AQP4$^{-/-}$ SAH group (**b**). "*"$p < 0.05$ compared with those of sham and AQP4$^{-/-}$sham groups; "#"$p < 0.05$ compared with that of SAH group

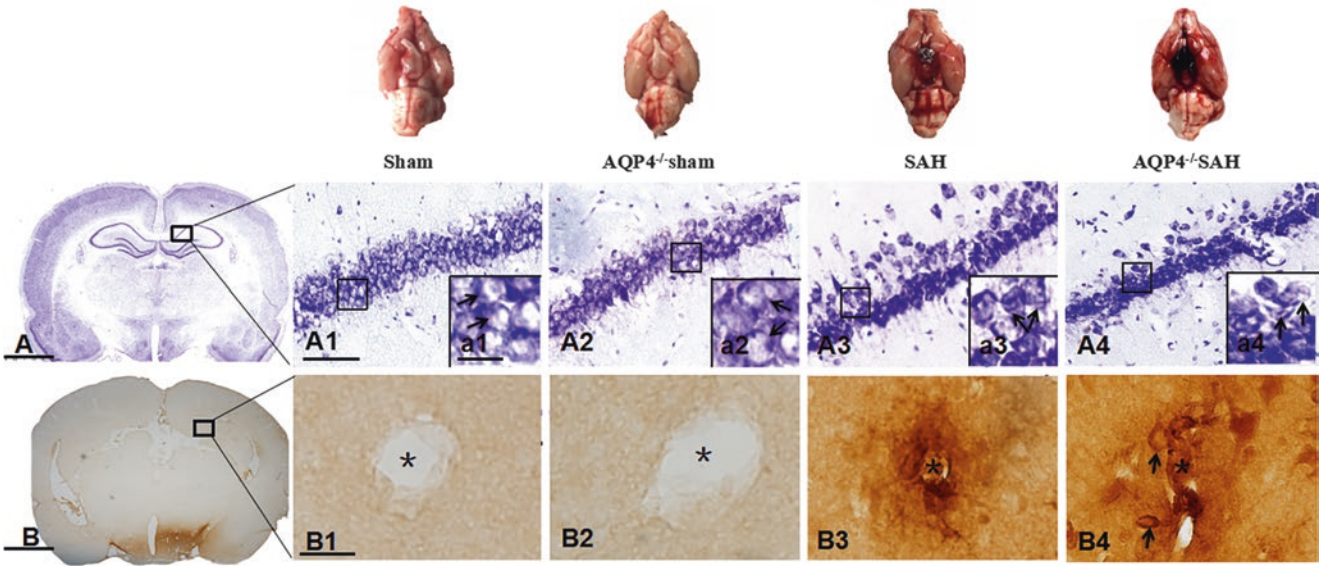

Fig. 2 The neuron damage and BBB disruption following SAH. At 24 h after SAH, the Nissl staining results indicated that the neurons in the CA1 region of hippocampus in the sham and AQP4$^{-/-}$sham rats were round and distributed with a layer mode (A1, A2, a1, a2). However, after SAH, the shape of neuron was irregular (triangle or polygon), and the layer mode was damaged, especially in the AQP4$^{-/-}$ SAH group (A3, A4, a3, a4). In the sham and AQP4$^{-/-}$sham rats, there was rare positive IgG in the hippocampus (B1 and B2). However, numerous IgG positive products were observed around the microvessels in the hippocampus in SAH and AQP4$^{-/-}$SAH groups; furthermore, the glial cells adjacent to the microvessels were also activated in the AQP4$^{-/-}$SAH groups (B3 and B4). The figures A and B were, respectively, the Nissl staining and IgG staining of sham group for showing the whole brain and bilateral hippocampi. Figures a1–a4 were the magnification for the square boxes in figures A1–A4, respectively. The arrows in figures a1–a4 indicated the neurons in the CA1 region of hippocampus; the arrows in figure B4 indicated the activated glial cells. The "*" in figures B1–B4 indicated the lumen of microvessel. In figures A and B, scale bar = 2.5 mm; in figures A1–A4, scale bar = 100 μm; in figures a1–a4 and B1–B4, scale bar = 25 μm

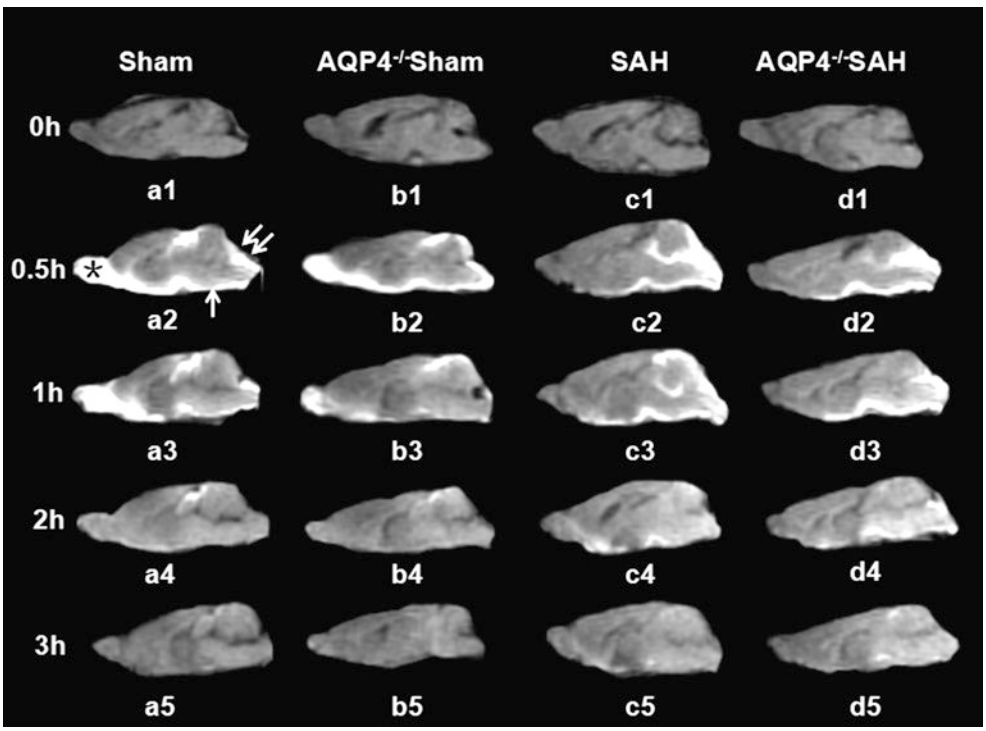

Fig. 3 The distribution and clearance of Gd-DTPA following SAH. In sham group, at 0.5 and 1 h after injection, the Gd-DTPA injected into the cisterna magna was widely diffused in subarachnoid space and ventricle system, gradually distributed throughout the whole brain parenchyma, and cleared from the brain at 2 h (a1–a5). However, the diffusion of Gd-DTPA in AQP4 deficit animals was markedly decreased compared with sham group (b1–b5). After SAH, Gd-DTPA was concentrated in the cisterna magna and basilar cisterna; only a small amount of Gd-DTPA was diffused to the olfactory bulb and brain parenchyma at 2 h after injection, especially in the AQP4$^{-/-}$SAH rats (c1–d5). In figure a2, the arrow showed basilar cistern, the double arrows indicated cisterna magna, and "*" indicated olfactory bulb

Discussion

In this study, we explored the roles of AQP4 in EBI following SAH. The results indicated that AQP4 might facilitate the ISF drainage in the glymphatic system of the brain. Furthermore, the damage of this system owing to AQP4 knockout could aggravate the EBI after SAH.

Early brain injury (EBI) after SAH is the immediate brain damage within 72 h. After SAH, the increased intracranial pressure, decreased cerebral blood flow, and global cerebral ischemia due to ruptured aneurysm will lead to BBB disruption, inflammation, and oxidative stress [14, 15]. After SAH, the ECS is filled with numerous toxic materials, such as hemoglobin metabolite and thrombin, which will lead to neuron death [12, 16] and microvascular injury [17]. How to eliminate these toxins might be a promising therapeutic strategy to alleviate the injury of neuron and microvasculature following SAH.

The ECS in central nervous system is the microenvironment of the neural cells. The average ECS volume is 15 ± 25% of the total adult brain volume as shown by using some techniques, such as electron microscopy, radiotracers, and ion diffusion methods [16, 18, 19]. The ISF drainage system in the brain is critical for clearance of metabolite and toxin in the ECS. It is reported that the CSF can flow into ECS from the para-arterial space and out from the para-venous space [20], that is, glymphatic system in the brain [4]. The impairment of this drainage system has been verified to be related to some brain diseases, such as Alzheimer disease (AD) [21] and brain ischemia injury [22].

The water channel protein AQP4 plays pivotal roles in regulation of the glymphatic system in the brain. AQP4 is mainly expressed on the astrocyte end feet [23], which is the boundary of para-arterial/para-venous space. AQP4 can facilitate the inflow and outflow of ISF drainage and promote indirectly the circulation between the CSF and ISF in the brain [24, 25]. Therefore, AQP4 can accelerate the clearance of metabolite released from the neural cells, even the blood components in CSF following SAH.

In this study, we found that, compared with sham animals, AQP4 knockout rats had no effects on the brain water content and neurological function. However, after SAH, AQP4 knockout rats showed more severe brain edema and neurological deficits. These results implied that AQP4 played important roles in EBI following SAH. These results were in accordance with the outcomes from other reports. At 7d after SAH, Luo and colleagues found that AQP4$^{-/-}$ mice showed no improvements in neurological deficits and neuroinflammation compared with wild-type control mice [17].

In this study, we used the Gd-DTPA under MRI (T1WI) method to observe the ISF drainage in the glymphatic system. Gd-DTPA is a common contrast for MRI imaging and has been proved to be a good indicator for detecting ISF flow owing to its impermeability to the cellular membrane [26]. Previously, there were some methods to measure the physiological characteristics of ECS in the brain, such as TMA$^+$ method and IOI method [27–29]. Compared with TMA$^+$ and IOI methods, the MRI method in this study can detect the ISF drainage in the deep brain (such as in hippocampus and caudate nucleus) with a three-dimensional mode. This method has been used to explore the potential mechanism of some central nervous system diseases, such as AD and aging [30]. Using this MRI method, we found that the ISF drainage in glymphatic system was significantly blocked after SAH, especially in AQP4$^{-/-}$ rats, which revealed that AQP4 was critical for CSF–ISF circulation and ISF clearance. Combined with the effects of AQP4 knockout on the brain edema and neurological function in this study, we speculated that, after SAH, AQP4 had multiple effects, not only leading to the brain edema [31] but facilitating the ISF drainage in the glymphatic system to eliminate the toxic factors in the brain and attenuating the neuron death and BBB disruption. AQP4 knockout destroyed the glymphatic system homeostasis, which resulted in accumulation of poisonous substance and more injury to the neural cells and BBB, finally exacerbated EBI following SAH.

Conclusion

Our results demonstrated that AQP4 deficits will aggravate the EBI following SAH, and AQP4 played important roles in facilitating the transportation of ISF flow to eliminate the toxicant in the brain after SAH. Furthermore, the MRI-Gd-DTPA method used in this study will open an avenue to detecting the unknown ECS structure in the brain and potential mechanism for some brain diseases.

Acknowledgments This work was supported by the National Natural Science Foundation of China (Grant No. 31471028) and the interdisciplinary medicine Seed Fund of Peking University (Grant No. BMU2018MC001).

Conflict of Interest: The authors declare that they have no conflict of interest.

References

1. Li J, Chen J, Mo H, Chen J, Qian C, Yan F, Gu C, Hu Q, Wang L, Chen G. Minocycline protects against NLRP3 inflammasome-induced inflammation and P53-associated apoptosis in early brain injury after subarachnoid hemorrhage. Mol Neurobiol. 2016;53:2668–78.

2. Yuan J, Liu W, Zhu H, Zhang X, Feng Y, Chen Y, Feng H, Lin J. Curcumin attenuates blood-brain barrier disruption after subarachnoid hemorrhage in mice. J Surg Res. 2017;207:85–91.
3. Plog BA, Nedergaard M. The glymphatic system in central nervous system health and disease: past, present, and future. Annu Rev Pathol. 2018;13:379–94.
4. Jessen NA, Munk AS, Lundgaard I, Nedergaard M. The glymphatic system: a beginner's guide. Neurochem Res. 2015;40:2583–99.
5. Badaut J, Brunet JF, Grollimund L, Hamou MF, Magistretti PJ, Villemure JG, Regli L. Aquaporin 1 and aquaporin 4 expression in human brain after subarachnoid hemorrhage and in peritumoral tissue. Acta Neurochir Suppl. 2003;86:495–8.
6. Yang X, Chen C, Hu Q, Yan J, Zhou C. Gamma-secretase inhibitor (GSI1) attenuates morphological cerebral vasospasm in 24h after experimental subarachnoid hemorrhage in rats. Neurosci Lett. 2010;469:385–90.
7. Yan JH, Khatibi NH, Han HB, Hu Q, Chen CH, Li L, Yang XM, Zhou CM. p53-induced uncoupling expression of aquaporin-4 and inwardly rectifying K+ 4.1 channels in cytotoxic edema after subarachnoid hemorrhage. CNS Neurosci Ther. 2012;18: 334–42.
8. Tesson L, Usal C, Menoret S, Leung E, Niles BJ, Remy S, Santiago Y, Vincent AI, Meng X, Zhang L, Gregory PD, Anegon I, Cost GJ. Knockout rats generated by embryo microinjection of TALENs. Nat Biotechnol. 2011;29:695–6.
9. Sung YH, Jin Y, Kim S, Lee HW. Generation of knockout mice using engineered nucleases. Methods. 2014;69:85–93.
10. Duris K, Manaenko A, Suzuki H, Rolland W, Tang J, Zhang JH. Sampling of CSF via the cisterna magna and blood collection via the heart affects brain water content in a rat SAH model. Transl Stroke Res. 2011;2:232–7.
11. Garcia JH, Wagner S, Liu KF, Hu XJ. Neurological deficit and extent of neuronal necrosis attributable to middle cerebral artery occlusion in rats. Statistical validation. Stroke. 1995;26:627–34. discussion 635.
12. Gaberel T, Gakuba C, Goulay R, Martinez De Lizarrondo S, Hanouz JL, Emery E, Touze E, Vivien D, Gauberti M. Impaired glymphatic perfusion after strokes revealed by contrast-enhanced MRI: a new target for fibrinolysis? Stroke. 2014;45:3092–6.
13. Zhou C, Yamaguchi M, Colohan AR, Zhang JH. Role of p53 and apoptosis in cerebral vasospasm after experimental subarachnoid hemorrhage. J Cereb Blood Flow Metab. 2005;25:572–82.
14. Sehba FA, Hou J, Pluta RM, Zhang JH. The importance of early brain injury after subarachnoid hemorrhage. Prog Neurobiol. 2012;97:14–37.
15. Fujii M, Yan J, Rolland WB, Soejima Y, Caner B, Zhang JH. Early brain injury, an evolving frontier in subarachnoid hemorrhage research. Transl Stroke Res. 2013;4:432–46.
16. Goulay R, Flament J, Gauberti M, Naveau M, Pasquet N, Gakuba C, Emery E, Hantraye P, Vivien D, Aron-Badin R, Gaberel T. Subarachnoid hemorrhage severely impairs brain parenchymal cerebrospinal fluid circulation in nonhuman primate. Stroke. 2017;48:2301–5.
17. Luo C, Yao X, Li J, He B, Liu Q, Ren H, Liang F, Li M, Lin H, Peng J, Yuan TF, Pei Z, Su H. Paravascular pathways contribute to vasculitis and neuroinflammation after subarachnoid hemorrhage independently of glymphatic control. Cell Death Dis. 2016;7:e2160.
18. Morris AW, Sharp MM, Albargothy NJ, Fernandes R, Hawkes CA, Verma A, Weller RO, Carare RO. Vascular basement membranes as pathways for the passage of fluid into and out of the brain. Acta Neuropathol. 2016;131:725–36.
19. Aspelund A, Antila S, Proulx ST, Karlsen TV, Karaman S, Detmar M, Wiig H, Alitalo K. A dural lymphatic vascular system that drains brain interstitial fluid and macromolecules. J Exp Med. 2015;212:991–9.
20. Mestre H, Kostrikov S, Mehta RI, Nedergaard M. Perivascular spaces, glymphatic dysfunction, and small vessel disease. Clin Sci (Lond). 2017;131:2257–74.
21. Peng W, Achariyar TM, Li B, Liao Y, Mestre H, Hitomi E, Regan S, Kasper T, Peng S, Ding F, Benveniste H, Nedergaard M, Deane R. Suppression of glymphatic fluid transport in a mouse model of Alzheimer's disease. Neurobiol Dis. 2016;93:215–25.
22. Arbel-Ornath M, Hudry E, Eikermann-Haerter K, Hou S, Gregory JL, Zhao L, Betensky RA, Frosch MP, Greenberg SM, Bacskai BJ. Interstitial fluid drainage is impaired in ischemic stroke and Alzheimer's disease mouse models. Acta Neuropathol. 2013;126:353–64.
23. Papadopoulos MC, Verkman AS. Aquaporin water channels in the nervous system. Nat Rev Neurosci. 2013;14:265–77.
24. Vindedal GF, Thoren AE, Jensen V, Klungland A, Zhang Y, Holtzman MJ, Ottersen OP, Nagelhus EA. Removal of aquaporin-4 from glial and ependymal membranes causes brain water accumulation. Mol Cell Neurosci. 2016;77:47–52.
25. Li X, Liu H, Yang Y. Magnesium sulfate attenuates brain edema by lowering AQP4 expression and inhibits glia-mediated neuroinflammation in a rodent model of eclampsia. Behav Brain Res. 2017;364:403–12.
26. Han H, Shi C, Fu Y, Zuo L, Lee K, He Q, Han H. A novel MRI tracer-based method for measuring water diffusion in the extracellular space of the rat brain. IEEE J Biomed Health Inform. 2014;18:978–83.
27. Nicholson C, Phillips JM. Ion diffusion modified by tortuosity and volume fraction in the extracellular microenvironment of the rat cerebellum. J Physiol. 1981;321:225–57.
28. Nicholson C. Quantitative analysis of extracellular space using the method of TMA+ iontophoresis and the issue of TMA+ uptake. Can J Physiol Pharmacol. 1992;70(Suppl):S314–22.
29. Xiao F, Nicholson C, Hrabe J, Hrabetova S. Diffusion of flexible random-coil dextran polymers measured in anisotropic brain extracellular space by integrative optical imaging. Biophys J. 2008;95:1382–92.
30. Ten Kate M, Visser PJ, Bakardjian H, Barkhof F, Sikkes SAM, van der Flier WM, Scheltens P, Hampel H, Habert MO, Dubois B, Tijms BM. Gray matter network disruptions and regional amyloid beta in cognitively normal adults. Front Aging Neurosci. 2018;10:67.
31. Blixt J, Gunnarson E, Wanecek M. Erythropoietin attenuates the brain edema response after experimental traumatic brain injury. J Neurotrauma. 2018;35:671–80.

The Role of Galectin-3 in Subarachnoid Hemorrhage: A Preliminary Study

Hirofumi Nishikawa, Fumi Nakano, Lei Liu, Yoshinari Nakatsuka, Takeshi Okada, Masato Shiba, and Hidenori Suzuki

Abstract Despite advances in diagnosis and treatment of subarachnoid hemorrhage (SAH), combined morbidity and mortality rate in SAH patients accounted for greater than 50%. Many prognostic factors have been reported including delayed cerebral ischemia, cerebral vasospasm-induced infarction, and shunt-dependent hydrocephalus as potentially preventable or treatable causes. Recent experimental studies emphasize that early brain injury, a concept to explain acute pathophysiological events that occur in brain before onset of cerebral vasospasm within the first 72 h of SAH, may be more important than cerebral vasospasm, a classically important determinant of poor outcome, in post-SAH outcome. Galectin-3 is known for one of matricellular proteins and a mediator of inflammation in the central nervous system. Galectin-3 was also reported to contribute to poor outcomes in SAH patients, but the role of galectin-3 after SAH has not been determined. We produced experimental SAH mice, of which the top of the internal carotid artery was perforated by 4-0 monofilament, and evaluated effects of a galectin-3 inhibitor. We assessed neurological scores and brain water content at 24 h. The administration of a galectin-3 inhibitor significantly ameliorated brain edema and neuronal score in experimental SAH mice.

Keywords Galectin-3 · Subarachnoid hemorrhage · Early brain injury

Introduction

Early brain injury (EBI) is thought to be a pivotal determinant for poor outcome after subarachnoid hemorrhage (SAH). EBI is defined as acute pathophysiological events that occur in the brain before onset of cerebral vasospasm within 72 h of SAH and consists of any pathophysiological mechanisms except for iatrogenic brain injury [1]. We previously reported the possible mechanisms of EBI, focusing on inflammation and microcirculatory disturbance [2–4]. SAH not only induces transient global brain ischemia secondary to elevated intracranial pressure and mechanical stress but also produces various substances including heme, fibrinogen, intracellular components, and inflammation-related proteins. These substances stimulate cell surface receptors including toll-like receptor 4 and induce several inflammatory pathways [5]. Mitogen-activated protein kinase (MAPK) pathway seems to be a major inflammatory pathway related with early brain injury [2–4]. Finally, proinflammatory substances such as matrix metalloproteinase-9 (MMP-9) and tenascin-C (TNC) cause and exacerbate cerebral vasospasm, neuronal apoptosis, and blood-brain barrier disruption [2–4, 6].

Galectin-3 belongs to galectin family, which consists of β-galactoside-binding lectins participating in a wide range of biological processes including immune responses, cell–cell/extracellular matrix interaction, and apoptosis. Galectin-3 is the only chimera-type galectin and reported to be involved in brain inflammatory responses [7]. We previously reported that plasma galectin-3 levels in non-severe SAH patients were significantly correlated with the occurrence of delayed cerebral ischemia (DCI) and delayed cerebral infarction [8]. In this study, first, we elucidated whether a high concentration of plasma galectin-3 in SAH patients, including those with severe World Federation of Neurological Surgeons (WFNS) grade, was associated with poor outcome. Then, we evaluated whether inhibition of galectin-3 reduced brain edema in experimental SAH models.

Materials and Methods

Clinical Measurements of Plasma Galectin-3 Levels in SAH Patients

We collected blood samples from patients who participated in the Prospective Registry for Searching Mediators of

H. Nishikawa (✉) · F. Nakano · L. Liu · Y. Nakatsuka · T. Okada
M. Shiba · H. Suzuki
Department of Neurosurgery, Mie University Graduate School of Medicine, Tsu, Mie, Japan

R. D. Martin et al. (eds.), *Subarachnoid Hemorrhage*, Acta Neurochirurgica Supplement 127,
https://doi.org/10.1007/978-3-030-04615-6_11,

Neurovascular Events After Aneurysmal SAH [pSEED] performed at eight tertiary referral centers in Mie prefecture in Japan between September 2013 and December 2015 [8]. Inclusion criteria were as follows: ≥20 years of age at onset, SAH on computed tomography (CT) scans or lumbar puncture, saccular aneurysm as the cause of SAH confirmed on three-dimensional CT angiography, magnetic resonance (MR) angiography, digital subtraction angiography, aneurysmal obliteration by clipping or endovascular coiling within 48 h of onset, and post-clipping or post-coiling blood sampling on days 1–3 after onset [8]. SAH that was not due to a ruptured saccular aneurysm, patients who underwent parental artery occlusion, patients who had angiographic or treatment-related complications, patients with pre-onset modified Rankin scale (mRS) 3–5, patients who could not receive enough anti-DCI therapy due to severe medical complications, and patients who had past medical history of concomitant inflammatory diseases that are known to upregulate galectin-3 were excluded [8]. All blood samples were centrifuged for 5 min at 3000 × *g*, and the supernatant fluid was stored at −78 °C until assayed. Plasma galectin-3 levels were blindly determined by enzyme-linked immunosorbent assay kit for human galectin-3 (code no. 27755; Immuno-Biological Laboratories, Fujioka, Japan) [8] . We defined poor outcome as mRS 3–6 at 3 months of post-SAH.

Experimental Study as to the Role of Galectin-3 in SAH

All procedures were approved by the Animal Ethics Review Committee of Mie University and followed the institution's Guidelines for Animal Experiments. C57BL/6 wild-type (WT) male adult mice (weight, 25–30 g) were used for this study. To make SAH, endovascular filament perforation was performed as previously described [9]. Briefly, after midline skin incision of neck, the left external carotid artery (ECA) was exposed, and ECA was cut to insert 4-0 nylon monofilament, perforating the bifurcation of internal carotid artery. At 30 min after modeling, an intraventricular injection of 4 μg modified citrus pectin (MCP), which is known to be a galectin-3 inhibitor [10, 11], or vehicle (sterile phosphate-buffered saline [PBS]), was performed as previously described [9].

To assess the effect of MCP on EBI, 26 WT mice were randomly divided into 3 groups: sham + vehicle (n = 7), SAH + vehicle (n = 10), and SAH + MCP (n = 9) groups. Neurological score, SAH severity, and brain water content were evaluated at 24 h after modeling. Neurological score was blindly evaluated by modified Garcia's scale as previously described [4]. Animals were given a total score of 2 to 18 in 1-number steps, and higher scores indicated better function. SAH severity was blindly evaluated using high-resolution pictures of the base of the brain taken at each sacrifice as previously reported [4], and mice with moderate severity of SAH were enrolled in this study. Brain water content was measured by the wet/dry method for assessing brain edema. In brief, the brain of sacrificed mice under deep anesthesia was quickly removed and separated into the left and right hemispheres, cerebellum, and brain stem. Each part of the brain was weighed as wet weight, and then they were dried for 24 h at 105 °C and weighed again as dry weight. The percentage of water content was calculated according to the following formula: [(wet weight − dry weight)/wet weight] × 100%.

Statistical Analysis

Categorical variables were reported as the number and percentage, and continuous variables were reported as the mean ± standard deviation (SD) and compared between two groups using the unpaired t-test or among three groups using one-way analysis of variance with Tukey-Kramer post hoc tests. A P value ≤0.05 was considered significant.

Results

High Concentrations of Plasma Galectin-3 Associated with Poor Outcome in SAH Patients

249 patients were registered in pSEED between September 2013 and December 2015, and 149 patients were eligible for inclusion criteria. Mean age was 63.9 ± 13.5, and there were 107 females. Fifty-four patients developed poor outcome defined as mRS 3–6. Plasma concentrations of galectin-3 on days 1–3 were significantly higher in patients with poor outcomes than those with good outcomes (5.43 ± 3.39 vs. 3.77 ± 2.24 ng/mL, P < 0.001; Fig. 1).

Inhibition of Galectin-3 Ameliorates Brain Edema in Experimental SAH Mice

No sham-operated mice died, and the mortality rate was not significantly different between the SAH + vehicle group (30%) and SAH + MCP group (22%). SAH grade was similar between the SAH + vehicle group and SAH + MCP group (Fig. 2a). The SAH-MCP group showed significant improvement of neurological score and brain water content in the left hemisphere compared with the SAH-vehicle group (P < 0.001, P = 0.020, respectively, Fig. 2b, c).

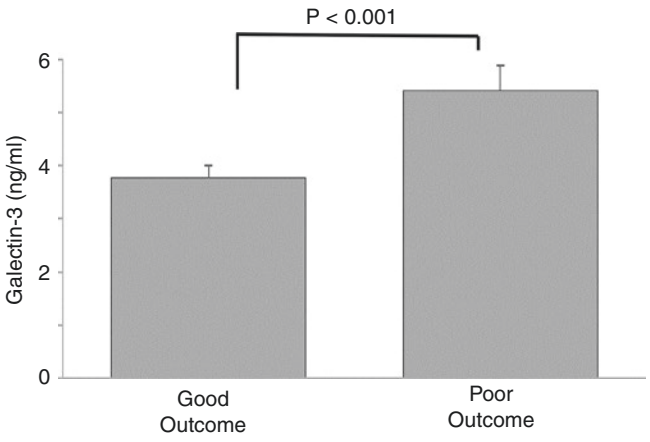

Fig. 1 Relationships between acute-stage plasma galectin-3 levels and outcomes. The patients with poor outcome show significantly higher levels of plasma galectin-3 compared with good outcome. Data, mean ± SD; *P* value, unpaired *t*-tests

Discussion

Clinically, elevated plasma galectin-3 levels were reported to be correlated with the severity and poor outcome in spontaneous brain hemorrhage and traumatic brain injury [12, 13], and these results suggested the possibility of the linkage between galectin-3 and inflammation [12, 13]. Our previous study elucidated that elevated plasma galectin-3 levels in non-severe SAH patients were significantly correlated with the incidence of DCI and delayed cerebral infarction without cerebral vasospasm and consequently might contribute to poor outcome [8]. However, the former study did not include severe SAH patients defined as WFNS grade 4–5 because of the difficulty in detecting neurological worsening due to its severe state [8]. Therefore, in this preliminary study, we first demonstrated that higher con-

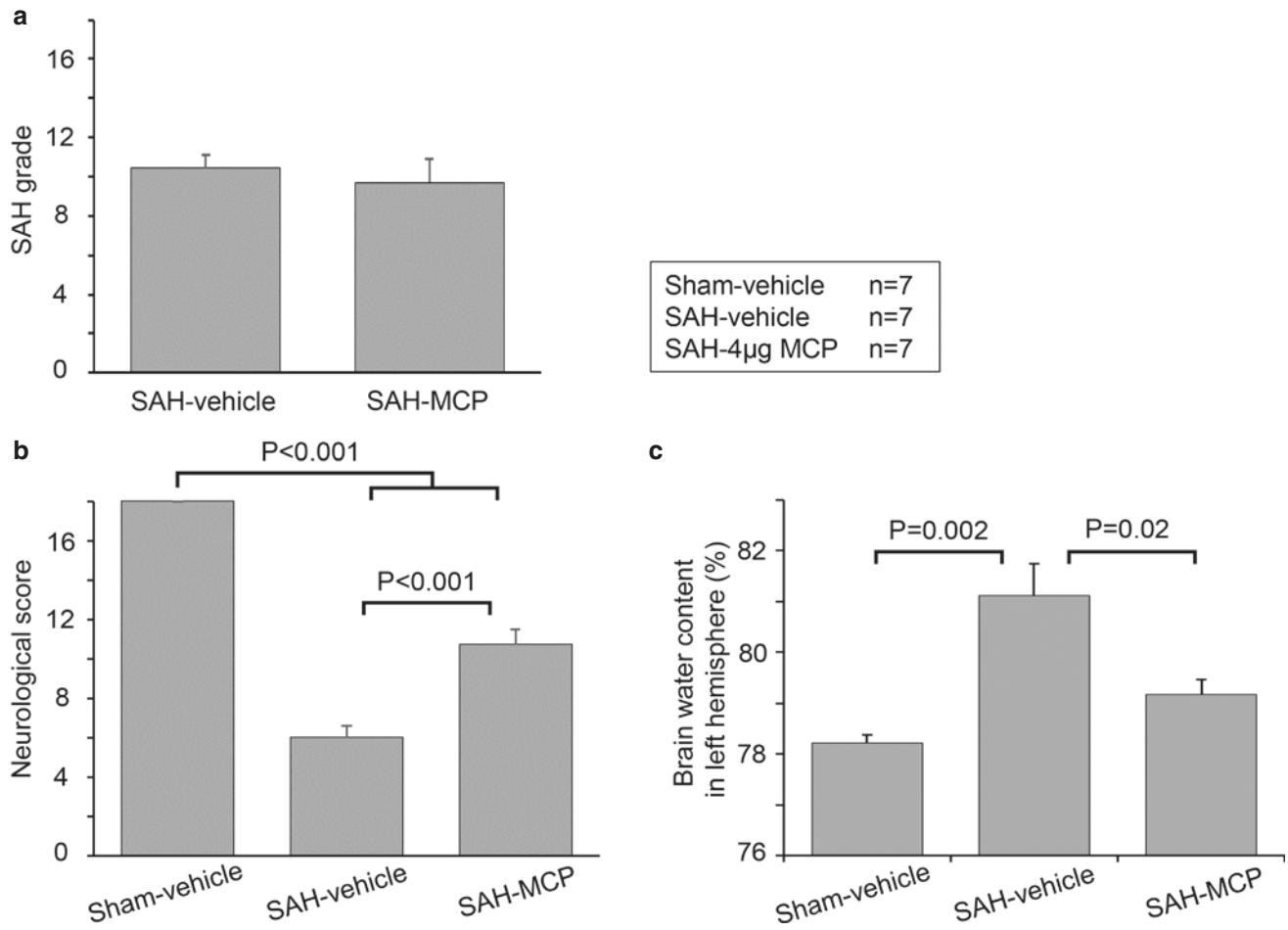

Fig. 2 Effects of modified citrus pectin (MCP) treatment on the severity of subarachnoid hemorrhage (**a**), neurological scores (**b**), and brain water content in the left hemisphere (**c**). Data, mean ± SD; *P* value, one-way analysis of variance with Tukey-Kramer post hoc tests

centrations of plasma galectin-3 were significantly associated with poor outcome in SAH patients, including those with worse WFNS grades.

Our preliminary experimental study showed that administration of MCP ameliorated both neuronal score and brain edema in experimental SAH mice. In the process of development of the central nervous system, galectin-3 is expressed in various glial cells and induces migration of neural stem cell and myelination of oligodendrocyte [14]. However, in rodent brain-resident immune cells, correlating with Janus kinase/signal transducers and activator of transcription (JAK-STAT) pathway, galectin-3 acts as an inflammatory mediator [15]. Buruguillos et al. reported that galectin-3 induces sustained microglial activation and prolonged inflammatory response through binding to toll-like receptor 4 (TLR4) [7, 16]. Yip et al. demonstrated that galectin-3, binding to TLR4, promotes inflammation and neuronal death in traumatic brain injury models of mice [17]. On the other hand, neuroinflammation after SAH, which is included in the mechanisms of EBI, induces brain permeability and neuronal apoptosis [1]. Therefore, galectin-3 might induce the brain permeability as an inflammatory mediator.

The limitations of this study are as follows: the number of rodent models was too small, and the mechanism how galectin-3 caused brain edema was undetermined. Therefore, further studies are needed to elucidate the role of galectin-3 after SAH.

Acknowledgments We thank Ms. Chiduru Yamamoto, Department of Neurosurgery, Mie University Graduate School of Medicine, for providing technical assistance.

Conflict of interest: **The authors declare that they have no conflict of interest.**

References

1. Suzuki H. What is early brain injury? Transl Stroke Res. 2015;6:1–3.
2. Fujimoto M, Shiba M, Kawakita F, Liu L, Shimojo N, Imanaka-Yoshida K, Yoshida T, Suzuki H. Deficiency of tenascin-C and attenuation of blood-brain barrier disruption following experimental subarachnoid hemorrhage in mice. J Neurosurg. 2016;124:1693–702.
3. Liu L, Fujimoto M, Kawakita F, Nakano F, Imanaka-Yoshida K, Yoshida T, Suzuki H. Anti-vascular endothelial growth factor treatment suppresses early brain injury after subarachnoid hemorrhage in mice. Mol Neurobiol. 2016;53:4529–38.
4. Liu L, Kawakita F, Fujimoto M, Nakano F, Imanaka-Yoshida K, Yoshida T, Suzuki H. Role of periostin in early brain injury after subarachnoid hemorrhage in mice. Stroke. 2017;48:1108–11.
5. Okada T, Suzuki H. Toll-like receptor 4 as a possible therapeutic target for delayed brain injuries after aneurysmal subarachnoid hemorrhage. Neural Regen Res. 2017;12:193–6.
6. Fujimoto M, Shiba M, Kawakita F, Liu L, Shimojo N, Imanaka-Yoshida K, Yoshida T, Suzuki H. Effects of Tenascin-C knockout on cerebral vasospasm after experimental subarachnoid hemorrhage in mice. Mol Neurobiol. 2018;55(3):1951–8. https://doi.org/10.1007/s12035-017-0466-x.
7. Burguillos Miguel A, Svensson M, Schulte T, Boza-Serrano A, Garcia-Quintanilla A, Kavanagh E, Santiago M, Viceconte N, Oliva-Martin Maria J, Osman Ahmed M, Salomonsson E, Amar L, Persson A, Blomgren K, Achour A, Englund E, Leffler H, Venero Jose L, Joseph B, Deierborg T. Microglia-secreted Galectin-3 acts as a Toll-like receptor 4 ligand and contributes to microglial activation. Cell Rep. 2015;10:1626–38.
8. Nishikawa H, Nakatsuka Y, Shiba M, Kawakita F, Fujimoto M, Suzuki H. Increased plasma Galectin-3 preceding the development of delayed cerebral infarction and eventual poor outcome in non-severe aneurysmal subarachnoid hemorrhage. Transl Stroke Res. 2018;9(2):110–9. https://doi.org/10.1007/s12975-017-0564-0.
9. Altay O, Suzuki H, Hasegawa Y, Caner B, Krafft PR, Fujii M, Tang J, Zhang JH. Isoflurane attenuates blood-brain barrier disruption in ipsilateral hemisphere after subarachnoid hemorrhage in mice. Stroke. 2012;43:2513–6.
10. Ma Z, Han Q, Wang X, Ai Z, Zheng Y. Galectin-3 inhibition is associated with neuropathic pain attenuation after peripheral nerve injury. PLoS One. 2016;11:e0148792. https://doi.org/10.1371/journal.pone.0148792.
11. Vergaro G, Prud'homme M, Fazal L, Merval R, Passino C, Emdin M, Samuel JL, Cohen Solal A, Delcayre C. Inhibition of Galectin-3 pathway prevents isoproterenol-induced left ventricular dysfunction and fibrosis in mice. Hypertension. 2016;67:606–12.
12. Shen YF, Yu WH, Dong XQ, Du Q, Yang DB, Wu GQ, Zhang ZY, Wang H, Jiang L. The change of plasma galectin-3 concentrations after traumatic brain injury. Clin Chim Acta. 2016;456:75–80.
13. Yan XJ, Yu GF, Jie YQ, Fan XF, Huang Q, Dai WM. Role of galectin-3 in plasma as a predictive biomarker of outcome after acute intracerebral hemorrhage. J Neurol Sci. 2016;368:121–7.
14. Shin T. The pleiotropic effects of galectin-3 in neuroinflammation: a review. Acta Histochem. 2013;115:407–11.
15. Jeon SB, Yoon HJ, Chang CY, Koh HS, Jeon SH, Park EJ. Galectin-3 exerts cytokine-like regulatory actions through the JAK-STAT pathway. J Immunol. 2010;185:7037–46.
16. Kawakita F, Fujimoto M, Liu L, Nakano F, Nakatsuka Y, Suzuki H. Effects of Toll-like receptor 4 antagonists against cerebral vasospasm after experimental subarachnoid hemorrhage in mice. Mol Neurobiol. 2017;54(8):6624–33. https://doi.org/10.1007/s12035-016-0178-7.
17. Yip PK, Carrillo-Jimenez A, King P, Vilalta A, Nomura K, Chau CC, Egerton AM, Liu ZH, Shetty AJ, Tremoleda JL, Davies M, Deierborg T, Priestley JV, Brown GC, Michael-Titus AT, Venero JL, Burguillos MA. Galectin-3 released in response to traumatic brain injury acts as an alarmin orchestrating brain immune response and promoting neurodegeneration. Sci Rep. 2017;7:41689. https://doi.org/10.1038/srep41689.

17-Allylamino-Demethoxygeldanamycin Ameliorate Microthrombosis Via HSP90/RIP3/NLRP3 Pathway After Subarachnoid Hemorrhage in Rats

Yuchun Zuo, Tibiao He, Peiqiang Liao, Kai Zhuang, Xiaoxin Yan, and Fei Liu

Abstract *Background*: Subarachnoid hemorrhage (SAH) is a severe and emergent cerebrovascular disease, the prognosis of which usually very poor. Microthrombi formation highlighted with inflammation occurs early after SAH. As the main cause of DCI, microthrombosis associated with the prognosis of SAH. The aim of this study was to show HSP90 inhibitor 17-AAG effect on microthrombosis after SAH in rats.

Methods: Ninety-five SD rats were used for the experiment. For time course study, the rats were randomly divided into five groups: sham group and SAH group with different time point (1d, 2d, 3d, 5d). Endovascular perforation method was conducted for SAH model. Neurological score, SAH grade, and mortality were measured after SAH. The samples of the left hemisphere brain were collected. The expression of HSP90 was detected by Western blot. The microthrombosis after SAH in rats' brain was detected by immunohistochemistry. For mechanism study, rats were randomly divided into three groups: sham, SAH + vehicle, and SAH +17-AAG (n = 6/group). 17-AAG was given by intraperitoneal injection (80 mg/kg) 1 h after SAH. Neurological function were measured at 24 h after SAH. The expression of RIP3, NLRP3, ASC, and IL-1β was measured by Western blot. Microthrombosis was detected by immunohistochemistry.

Results: Our results showed that the HSP90 protein level increased and peaked at 2 days after SAH. Microthrombosis caused by SAH was increased in 1 day and peaked at 2 days after SAH. Administration HSP90 specific inhibitor 17-AAG reduced expression of RIP3, NLRP3, ASC, and IL-1β, reduced microthrombosis after SAH, and improved neurobehavior when compared to vehicle group.

Conclusions: 17-AAG can ameliorate microthrombosis via HSP90/RIP3/NLRP3 pathway and improve neurobehavior after SAH.

Keywords SAH · 17-AAG · Microthrombosis · HSP90

Introduction

Subarachnoid hemorrhage (SAH) is a severe and emergent cerebrovascular disease with high morbidity and mortality and always leads to poor outcome. SAH mainly affects middle-aged patients and counts a highest fatality in all stroke subtypes, which brings about a huge burden on economy and society [1]. Inflammation has been extensively studied in early brain injury (EBI) after SAH, which is considered to be the main cause of mortality and lead to poor outcome [2, 3]. NLRP3 inflammasome, as a part of pro-inflammation, has been well established to take part in the pathophysiology of EBI after SAH [4–6].The inflammatory response and its effect on the occurrence of microthrombosis are frequently discussed as potential protagonists.

Microthrombosis, usually found to be dissociation between cerebral vasospasm (CVS) and delayed cerebral ischemia (DCI), regarded as the major cause of neurologic deterioration and consequent poor outcome [7]. Microthrombi were firstly described in patients who were thought to have died of DCI. The autopsy study showed significantly high amounts of microthrombi were found in ischemic regions [8]. Recently, the occurrence of microthrombi was verified after SAH in animal models [9–11]. Furthermore, endothelial cell apoptosis and coagulation induced by inflammation have been well established [7, 12],which were considered the main cause of microthrombosis [10].

17-Allylamino-demethoxygeldanamycin (17-AAG), a specific inhibitor of HSP90, has been proved to show its effect on preventing cell death especially necroptosis [11, 13, 14]. Moreover, necroptosis plays a potential role in

Y. Zuo · T. He · P. Liao · K. Zhuang · F. Liu (✉)
Department of Neurosurgery, The Third Xiangya Hospital, Central South University, Changsha, China

X. Yan
Department of Anatomy, The XiangYa Medical School, Central South University, Changsha, China

R. D. Martin et al. (eds.), *Subarachnoid Hemorrhage*, Acta Neurochirurgica Supplement 127,
https://doi.org/10.1007/978-3-030-04615-6_12,

inflammation [15]. Furthermore, HSP90 inhibition shows its protection effect by attenuating inflammation response [16] and maintaining blood-brain barrier after ischemia stroke [17]. RIP3 has been described as a key protein in NLRP3 inflammasome previously [4, 18]. More recently, HSP90 has been proven to be an upstream regulator of RIP3 in necroptosis [19, 20].More recently, the HSP90 inhibitor can reduce cell death induced by oxygen-glucose deprivation model [19]. Therefore, we hypothesize that 17-AAG reduces microthrombosis via HSP90/RIP3/NLRP3 pathway after SAH.

Methods and Materials

Animals and SAH Model

Adult male Sprague-Dawley rats (250–280 g) were purchased from the Animal Center of Central South University (Changsha, China). Rats were housed in a room with constant temperature (25 °C), humidity control and with a 12/12 h light/dark cycle. Standard animal chow and water were freely available. All the experimental procedures were approved by the Institutional Animal Care and Use Committee of Central South University.

SAH model was conducted by modified endovascular perforation method as previously described. Briefly, rats were anesthetized with chloral hydrate (400 mg/kg, intraperitoneally). The left common carotid artery and external and internal carotid arteries were exposed, and a 4–0 monofilament nylon suture was inserted into the left internal carotid artery through the external carotid artery stump until feeling resistance and then advanced 3 mm to perforate the bifurcation of the anterior and middle cerebral artery. Sham rats underwent identical procedures except the perforation.

Experiment Design

Experiment 1: For the time course experiment, 70 animals were divided randomly into 5 groups (n = 12/group): sham and SAH (1, 2, 3, 5 days (d)) groups. The neurological function was measured by modified Gracia score, and beam balance test was measured. Rats in the sham group underwent a procedure similar to that of the SAH group except perforation; rats in the SAH group underwent perforation and then euthanized in different time point after SAH. At the same time, SAH grade was measured. Then every group was divided into two groups used for Western blot and immunohistochemistry, respectively (n = 6/group).

Experiment 2: For 17-AAG treatment, 36 rats were divided randomly into three groups: sham (n = 6), SAH + vehicle (n = 12), and SAH + 17-AAG (n = 12). Modified Gracia score and beam balance test were measured. Then every group was divided into two groups used for Western blot and immunohistochemistry, respectively. Brain samples were collected after perfusion by 4% PFA for immunostaining.

Measurement of SAH Grade

As a parameter to evaluate the severity of SAH, SAH grade was obtained according to a grading system that was described previously. Briefly, the system was based on the amount of subarachnoid blood clots distributed in the six segments of basal cistern: grade 1, no subarachnoid blood (score = 0); grade 2, minimal subarachnoid clots (score = 1); grade 3, moderate subarachnoid clots with recognizable arteries (score = 2); and grade 4, blood clots covering all arteries (score = 3). A total score ranging from 0 to 18 was obtained by adding the scores from all six segments. The grading of SAH was performed by a partner who was blinded to the experiment. Rats with the SAH grade lower than 9 were excluded from this study.

Assessment of Neurological Function

The neurological status of all rats was evaluated at 24 h after SAH induction using the previously described modified Garcia scoring system and beam balance test [21].

The assessment of neurological score was performed by a partner who was blind to the experiment.

Western Blot Analysis

Western blot was performed as previously described [22]. Briefly, tissues were extracted by RIPA buffer. The protein concentrations were detected by using a bicinchoninic acid (BCA) assay (Beyotime, Shanghai, China). The protein samples were separated by 10% SDS-polyacrylamide gel electrophoresis (PAGE) and transferred to polyvinylidene fluoride membranes (Millipore, USA). After blocked, the membranes were incubated overnight at 4 °C with the following primary antibodies: anti-HSP90 (1:1000, Proteintech), anti-RIP3 (1:1000, Abcam, USA), anti-NLRP3 (1:500, Abcam, USA), anti-ASC (1:300, Santa Cruz, USA), anti-IL-1β (1:1000, Proteintech), and anti-GAPDH (1:1000,

Proteintech). After incubation with a secondary antibody, the immunocomplexes were visualized by enhanced chemiluminescence (SuperSignal Pierce Biotechnology).

Immunohistochemistry

Immunohistochemistry was performed as previously described [23]. Thirty micrometer coronal brain sections were cut as previously described in a cryostat (Leica CM3050S, Buffalo Grove, IL). Sections from each animal were divided into several subsets for immunohistochemistry. Microthrombi were visualized by immunohistochemistry with fibrinogen staining. After antigen retrieval, the slides were incubated in anti-fibrinogen antibody (1:500) (LifeSpan, Seattle, WA, USA) for 2 h and then incubated by biotinylated secondary antibody (1:400, Abcam, Cambridge, UK) for 1 h and ABC reagents (1:400; Vector Laboratories, Burlingame, CA, USA) for 1 h, with the immunoreactivity visualized in 0.003% H_2O_2 and 0.05% 3, 3′-diaminobenzidine(DAB), and counterstaining was performed with hematoxylin.

Immunofluorescence

Double immunofluorescence staining was performed as previously described [24]. The primary antibodies were biotinylated lectin (1:500, B-1175, Vector), followed by incubation with appropriate fluorescence-conjugated secondary antibody AMCA streptavidin (1:200, SA-5008, Vector). TUNEL staining (In Situ Cell Death Detection Kit, Roche) was performed following the manufacturer's instruction. The sections were visualized under a fluorescence microscope Leica DMi8.

Quantification and Statistical Analysis

Microthrombi counts were performed as previously described [23]. Predefined regions of interest (ROIs) were photographed at ×200 magnification. The cumulative number of microthrombi was counted in a blinded fashion. The data were expressed as means ± SD. One-way analysis of variance (ANOVA) was used in this study to compare means of different groups followed by a Tukey's multiple comparison test. The statistical analysis was carried out using SPSS 16.0 software (SPSS Inc., Chicago, Illinois, USA). Statistically significance was accepted with $p < 0.05$.

Results

General Observation and SAH Severity and Localization of SAH

A total of 107 rats were used. Eighteen rats were sham group and 87 rats underwent SAH. Two rats were excluded from the study due to mild SAH. At 24 h after SAH induction, blood clots were mainly observed around the Willis circle and ventral brainstem (Fig. 1a). No statistical differences in the average of SAH grades were observed between SAH groups (Fig. 1b). About 17.2% rats (15 of 87) under SAH condition died within 24 h after SAH induction. No animals died in the sham group (0 of 18 rats). No statistical significance was observed for mortality between operated groups.

Time Course of HSP90 Detected in the Left Hemisphere and Microthrombosis in the Cerebellum Following SAH

Western blot was performed to determine the HSP90 expression in the left hemisphere at the 1, 2, 3, and 5 days after SAH. Results showed that HSP90 level increased as early as 1 day after SAH and peaked 2 days and then decreased (Fig. 2a). Quantitative analyses of HSP90 time course show nearly 2.8 times higher at 2 days when compared with sham group (Fig. 2a). Immunohistochemistry was performed to detect the microthrombosis at same time point (Fig. 2b). Results showed that microthrombi counts increased as early as 1 day after SAH and peaked 2 days and then decreased (Fig. 2c).

HSP90 Inhibitor 17-AAG Treatment Reduces RIP3 and NLRP3 Inflammasome, Ameliorates Microthrombosis, and Improves Short-Term Neurobehavior

The modified Garcia and beam balance scores were significantly lower in the SAH + vehicle group than those in the sham group, and administration of 17-AAG improved the neurological scores in SAH + 17-AAG group significantly compared with SAH + vehicle group ($P < 0.05$; Fig. 1c, d). At 2 days after SAH, the expression of HSP90 was remarkably increased, and RIP3, NLRP3, ASC, and IL-1β were dramatically increased in SAH + vehicle group compared with the sham group. However, 17-AAG treatment reduced the level of HSP90 and inhibited the expression of RIP3, NLRP3,

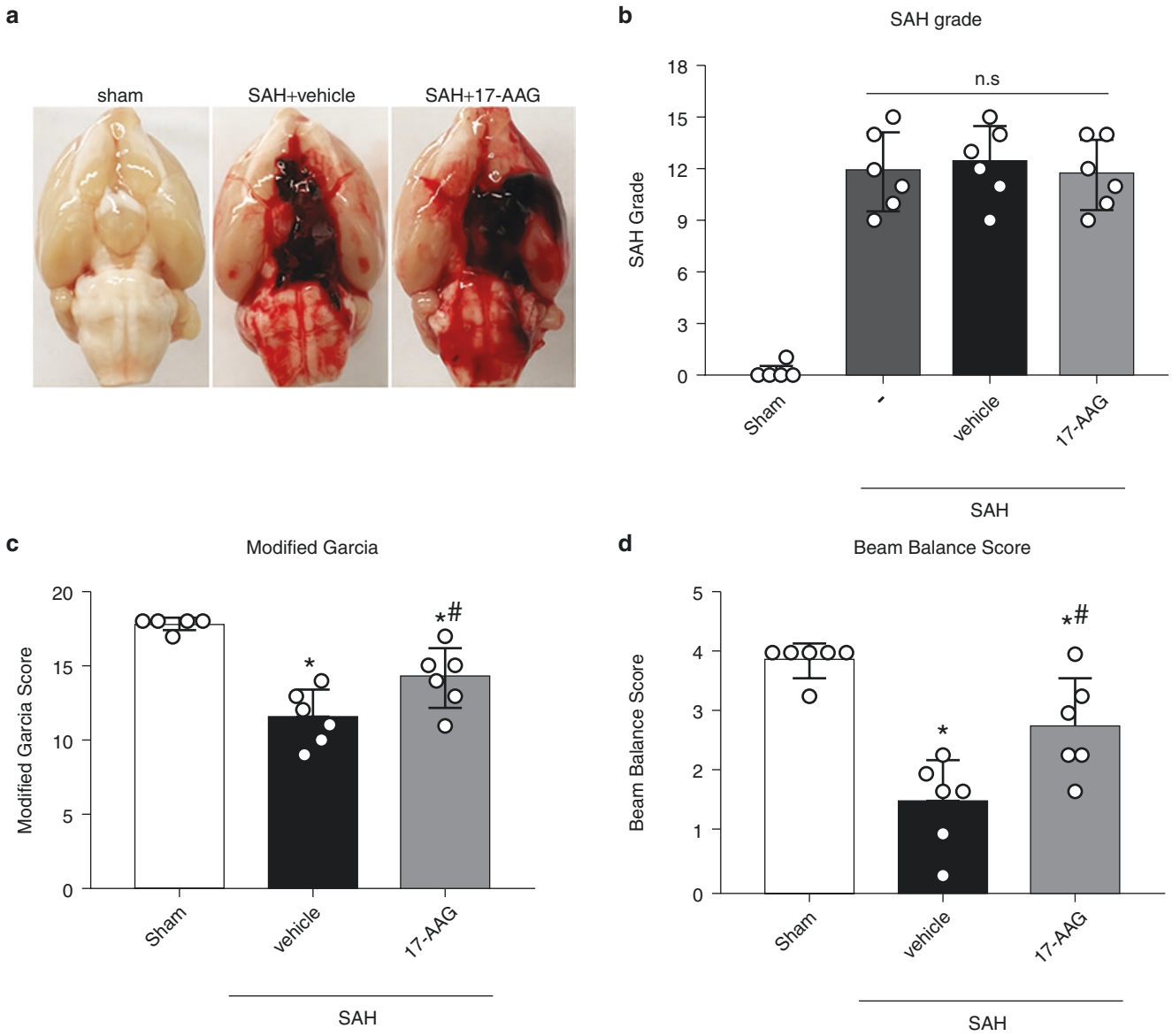

Fig. 1 General observation and SAH grade and neurological score. (**a**) Representative images of the brains from each group at 24 h after operation. Subarachnoid blood clots were mainly around the Willis circle and ventral brainstem. No blood present in the sham group. (**b**) There were no significant difference of SAH grade between the SAH groups ($p < 0.05$). Similar SAH bleeding severity was observed in all SAH groups. (**c**) Modified Garcia score and (**d**) beam balance test between sham, SAH + vehicle, and SAH + 17-AAG group. $n = 6$ per group. $^{*}p < 0.05$ vs. sham, $\#p < 0.05$ vs. SAH + vehicle

ASC, and IL-1β in SAH + 17-AAG group when compared with SAH + vehicle group ($P < 0.05$; Fig. 3a). When co-labeling with TUNEL and vessel marker lectin, the results show the endothelial cells on the inner surface vessels under apoptosis in SAH + vehicle when compared to sham; however the 17-AAG treatment can reverse this change (Fig. 3b, c). The microthrombosis was remarkably increased at 2 days in SAH + vehicle group compared with the sham group. However, 17-AAG treatment reduced microthrombosis when compared with SAH + vehicle group ($P < 0.05$; Fig. 3d, e).

Discussion

In the present study, we found that both microthrombosis and the expression of HSP90 increased in the brain after SAH in rats. In addition, the 17-AAG treatment improved neurofunction after SAH, which were accompanied by a decrease in RIP3 and NLRP3 inflammasome expression. Furthermore, 17-AAG showed the neuroprotective effects after SAH, which were associated with the decreased microthrombosis 2 days after SAH.

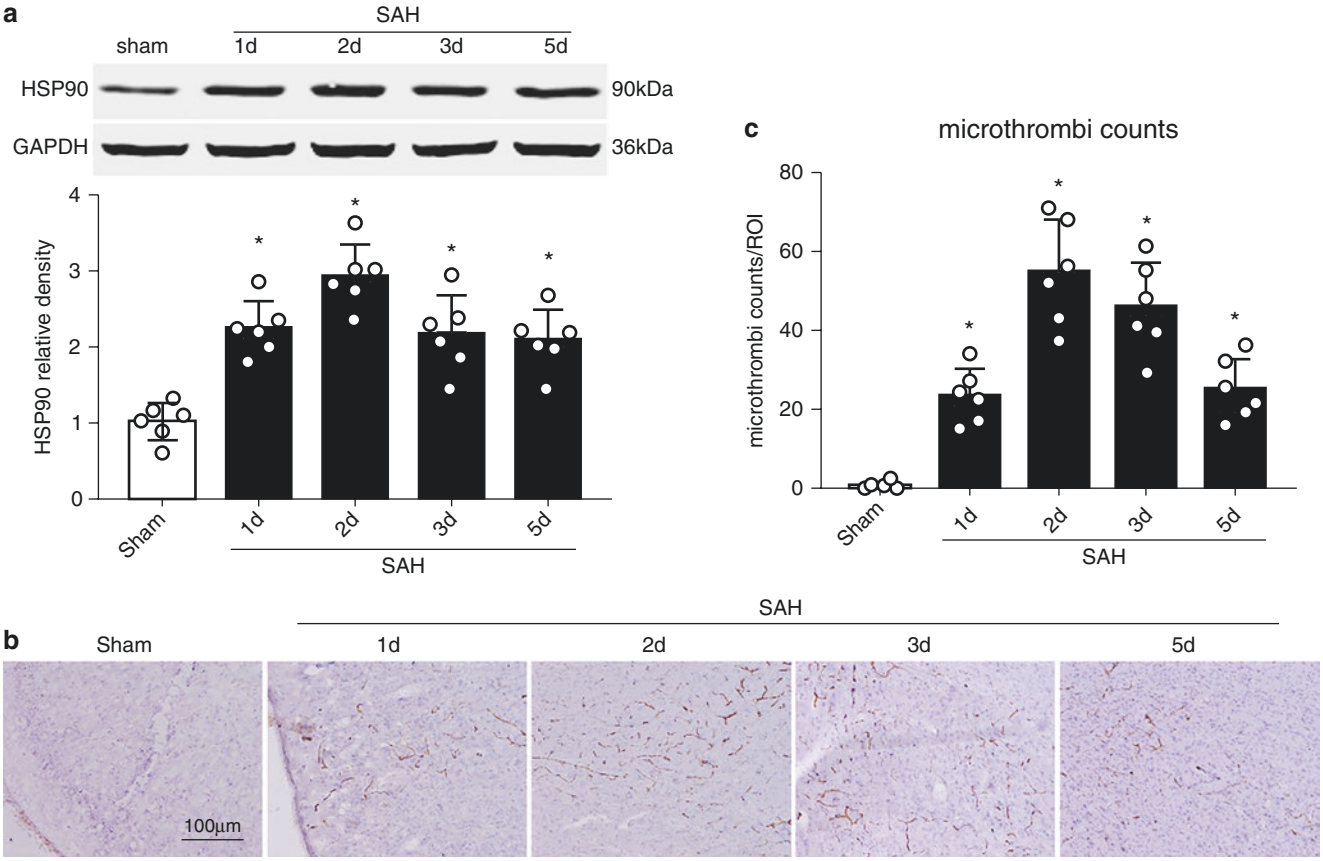

Fig. 2 Microthrombosis in cerebellum and expression HSP90 in left hemisphere after SAH. (**a**) Representative Western blot images and quantitative analyses of HSP90 time course from the left hemisphere after SAH. (**b**) Representative image and (**c**) quantitative analyses of microthrombosis in sham and SAH group with different time point. $n = 6$ per group. $^*p < 0.05$ vs. sham

The role of NLRP3 inflammasome in the pathophysiology of EBI after SAH has been proved previously [12]. The NLRP3 form a complex with ASC and pro-caspase-1 when activated and then maturate IL-1β and IL-18 by cleaved caspase-1 contributes to inflammation after SAH [12]. ROS generation, K+ efflux, and Cl− efflux were proved be three common upstream of NLRP3 activation [25]. Recently, RIP3 has been elucidated to have regulated NLRP3 inflammasome after SAH [4]. HSP90, as a chaperone protein, has been proven to show its effect on ischemia stroke. HSP90 inhibitors such as 17-AAG show its protective effects in ischemia stroke by attenuating inflammatory responses, ameliorating neuronal autophagic death, and protecting neural progenitor cell death and blood-brain barrier from disruption [16, 17, 26, 27]. More recently, HSP90 as a direct upstream regulator of RIP3 has been proved in neuronal oxygen-glucose deprivation model, and inhibition of HSP90 protected neurons from necroptosis [20]. Interestingly, a clinical study show that the antibody level of heat shock proteins increased in stroke patients [28]. However, the HSP90 regulate the NLRP3 activation after SAH have not been elucidated. In our present study, we found that HSP90 increased 1 day and peaked 2 days after SAH, and administration of HSP90 inhibitor 17-AAG reduced inflammation via HSP90/RIP3/NLRP3 signaling pathway as well as improve neurofunction.

Microthrombosis, as well as pro-inflammatory cascades and blood-brain barrier disruption, consist the main cascade events of secondary injury after SAH. One of the main causes of microthrombi formation after SAH was endothelial cell injury [10]. What's more, endothelial apoptosis after SAH has been shown to be associated with inflammatory mediators such as interleukin-1β (IL-1β) [7, 29]. In the present study, our results show that 17-AAG can reduce IL-1β by inhibiting NLRP3 inflammasome formation and then reduce microthrombosis after SAH. Thus, reduce NLRP3 inflammasome mediated inflammatory response by administration of 17-AAG may be a pential target to therapy microthrombosis after SAH.

These findings suggested that the administration of 17-AAG could attenuate NLRP3 inflammasome activation, inhibit microthrombosis, and improve neurofunction after SAH, at least, in part, through the HSP90/RIP3/NLRP3 signaling pathway.

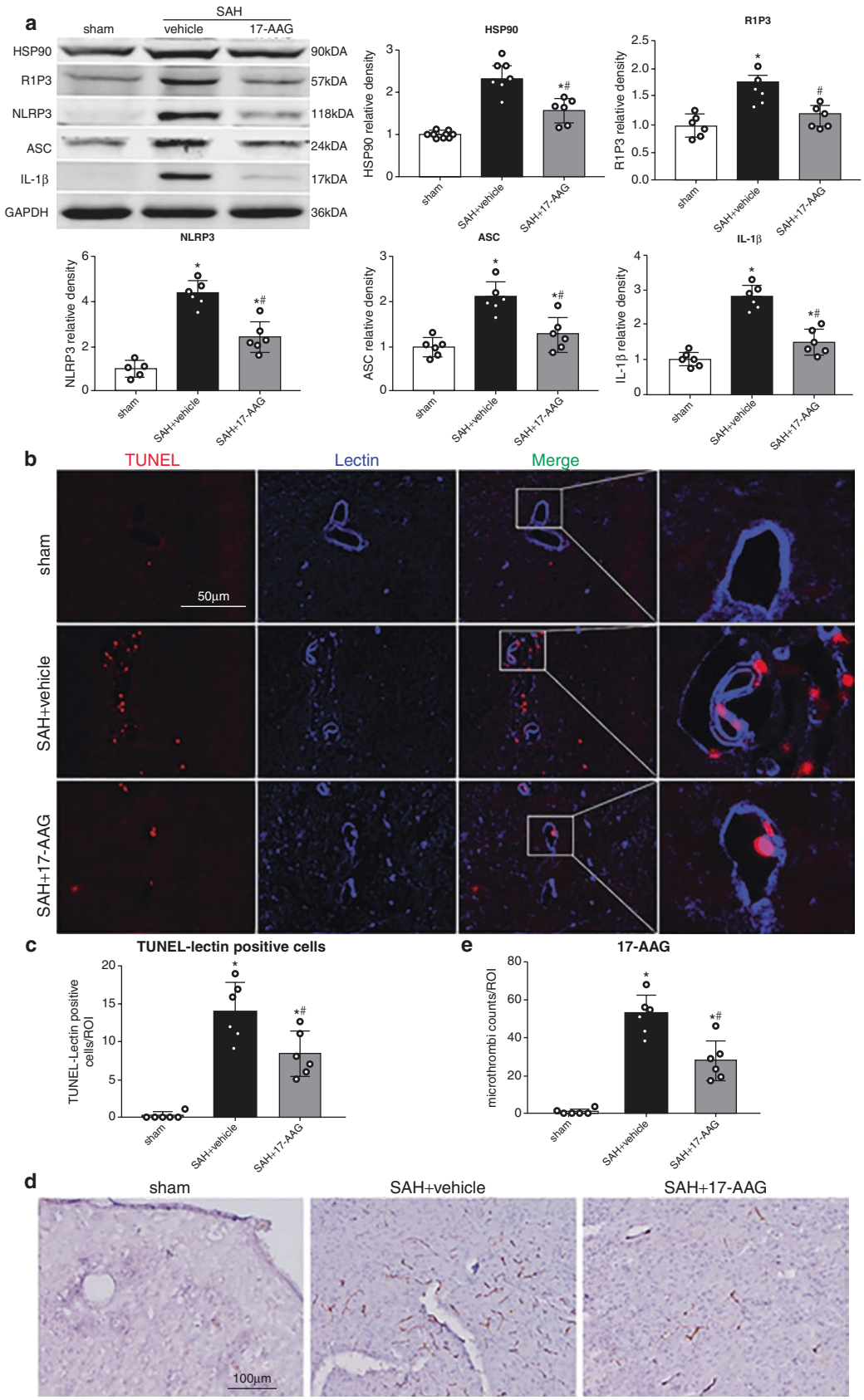

Fig. 3 The effects of 17-AAG in the protein expression of RIP3, NLRP3, ASC, IL-1β, and microthrombosis. (**a**) Representative Western blot images and quantitative analyses of HSP90, RIP3, NLRP3, ASC, and IL-1β. $n = 6$ per group. *$P < 0.05$ vs. sham group; #$P < 0.05$, vs. SAH + vehicle group. Bars represent mean ± SD. (**b**) Representative image and (**c**) quantitative analyses of double staining of TUNEL and lectin. (**d**) Immunostaining of fibrinogen and (**e**) quantitative analyses of microthrombi. $n = 6$ per group. *$P < 0.05$ vs. sham group; #$P < 0.05$, vs. SAH + vehicle group

Conclusion

Our study showed that 17-AAG can improve neurofunction and alleviate inflammation through the HSP90/RIP3/NLRP3 pathway as well as reduce microthrombosis after SAH. It may provide an optical method to treatment of SAH.

Acknowledgments This project was funded by Grant 81571150 from National Natural Science Foundation of China.

Conflict of Interest: **The authors declare that they have no conflict of interest.**

References

1. Lapchak PA, Zhang JH. The high cost of stroke and stroke cytoprotection research. Transl Stroke Res. 2017;8:307–17.
2. Caner B, Hou J, Altay O, Fujii M, Zhang JH. Transition of research focus from vasospasm to early brain injury after subarachnoid hemorrhage. J Neurochem. 2012;123(Suppl 2):12–21.
3. Fujii M, Yan J, Rolland WB, Soejima Y, Caner B, Zhang JH. Early brain injury, an evolving frontier in subarachnoid hemorrhage research. Transl Stroke Res. 2013;4:432–46.
4. Zhou K, Shi L, Wang Z, Zhou J, Manaenko A, Reis C, Chen S, Zhang J. RIP1-RIP3-DRP1 pathway regulates NLRP3 inflammasome activation following subarachnoid hemorrhage. Exp Neurol. 2017;295:116–24.
5. Khalafalla MG, Woods LT, Camden JM, Khan AA, Limesand KH, Petris MJ, Erb L, Weisman GA. P2X7 receptor antagonism prevents IL-1beta release from salivary epithelial cells and reduces inflammation in a mouse model of autoimmune exocrinopathy. J Biol Chem. 2017;292:16626–37.
6. Chen S, Ma Q, Krafft PR, Hu Q, Rolland W II, Sherchan P, Zhang J, Tang J, Zhang JH. P2X7R/cryopyrin inflammasome axis inhibition reduces neuroinflammation after SAH. Neurobiol Dis. 2013;58:296–307.
7. Vergouwen MD, Vermeulen M, Coert BA, Stroes ES, Roos YB. Microthrombosis after aneurysmal subarachnoid hemorrhage: an additional explanation for delayed cerebral ischemia. J Cereb Blood Flow Metab. 2008;28:1761–70.
8. Suzuki S, Kimura M, Souma M, Ohkima H, Shimizu T, Iwabuchi T. Cerebral microthrombosis in symptomatic cerebral vasospasm--a quantitative histological study in autopsy cases. Neurol Med Chir (Tokyo). 1990;30:309–16.
9. Andereggen L, Neuschmelting V, von Gunten M, Widmer HR, Fandino J, Marbacher S. The role of microclot formation in an acute subarachnoid hemorrhage model in the rabbit. Biomed Res Int. 2014;2014:161702.
10. Sabri M, Ai J, Lakovic K, D'Abbondanza J, Ilodigwe D, Macdonald RL. Mechanisms of microthrombi formation after experimental subarachnoid hemorrhage. Neuroscience. 2012;224:26–37.
11. Pisapia JM, Xu X, Kelly J, Yeung J, Carrion G, Tong H, Meghan S, El-Falaky OM, Grady MS, Smith DH, Zaitsev S, Muzykantov VR, Stiefel MF, Stein SC. Microthrombosis after experimental subarachnoid hemorrhage: time course and effect of red blood cell-bound thrombin-activated pro-urokinase and clazosentan. Exp Neurol. 2012;233:357–63.
12. Dong YS, Fan CX, Hu W, Jiang S, Ma ZQ, Yan XL, Deng C, Di SY, Xin ZL, Wu GL, Yang Y, Reiter RJ, Liang GB. Melatonin attenuated early brain injury induced by subarachnoid hemorrhage via regulating NLRP3 inflammasome and apoptosis signaling. J Pineal Res. 2016;60:253–62.
13. Li D, Li C, Li L, Chen S, Wang L, Li Q, Wang X, Lei X, Shen Z. Natural product Kongensin A is a non-canonical HSP90 inhibitor that blocks RIP3-dependent necroptosis. Cell Chem Biol. 2016;23:257–66.
14. Zhao XM, Chen Z, Zhao JB, Zhang PP, Pu YF, Jiang SH, Hou JJ, Cui YM, Jia XL, Zhang SQ. Hsp90 modulates the stability of MLKL and is required for TNF-induced necroptosis. Cell Death Dis. 2016;7:e2089.
15. Pasparakis M, Vandenabeele P. Necroptosis and its role in inflammation. Nature. 2015;517:311–20.
16. Qi J, Han X, Liu HT, Chen T, Zhang JL, Yang P, Bo SH, Lu XT, Zhang J. 17-Dimethylaminoethylamino-17-demethoxygeldanamycin attenuates inflammatory responses in experimental stroke. Biol Pharm Bull. 2014;37:1713–8.
17. Qi J, Liu Y, Yang P, Chen T, Liu XZ, Yin Y, Zhang J, Wang F. Heat shock protein 90 inhibition by 17-Dimethylaminoethylamino-17-demethoxygeldanamycin protects blood-brain barrier integrity in cerebral ischemic stroke. Am J Transl Res. 2015;7:1826–37.
18. Wang X, Jiang W, Yan Y, Gong T, Han J, Tian Z, Zhou R. RNA viruses promote activation of the NLRP3 inflammasome through a RIP1-RIP3-DRP1 signaling pathway. Nat Immunol. 2014;15:1126–33.
19. Park SY, Shim JH, Chae JI, Cho YS. Heat shock protein 90 inhibitor regulates necroptotic cell death via down-regulation of receptor interacting proteins. Pharmazie. 2015;70:193–8.
20. Wang Z, Guo LM, Wang Y, Zhou HK, Wang SC, Chen D, Huang JF, Xiong K. Inhibition of HSP90alpha protects cultured neurons from oxygen-glucose deprivation induced necroptosis by decreasing RIP3 expression. J Cell Physiol. 2018;233:4864–84.
21. Liao F, Li G, Yuan W, Chen Y, Zuo Y, Rashid K, Zhang JH, Feng H, Liu F. LSKL peptide alleviates subarachnoid fibrosis and hydrocephalus by inhibiting TSP1-mediated TGF-β1 signaling activity following subarachnoid hemorrhage in rats. Exp Ther Med. 2018;12:2537–43.
22. Liu F, Chen Y, Hu Q, Li B, Tang J, He Y, Guo Z, Feng H, Tang J, Zhang JH. MFGE8/integrin beta3 pathway alleviates apoptosis and inflammation in early brain injury after subarachnoid hemorrhage in rats. Exp Neurol. 2015;272:120–7.
23. Muroi C, Fujioka M, Mishima K, Irie K, Fujimura Y, Nakano T, Fandino J, Keller E, Iwasaki K, Fujiwara M. Effect of ADAMTS-13 on cerebrovascular microthrombosis and neuronal injury after experimental subarachnoid hemorrhage. J Thromb Haemost. 2014;12:505–14.
24. Xiao Y, Li G, Chen Y, Zuo Y, Rashid K, He T, Feng H, Zhang JH, Liu F. Milk fat globule-epidermal growth factor-8 pretreatment attenuates apoptosis and inflammation via the integrin-β3 pathway after surgical brain injury in rats. Front Neurol. 2018;9:96.
25. Tang T, Lang X, Xu C, Wang X, Gong T, Yang Y, Cui J, Bai L, Wang J, Jiang W, Zhou R. CLICs-dependent chloride efflux is an essential and proximal upstream event for NLRP3 inflammasome activation. Nat Commun. 2017;8:202.
26. Li J, Yang F, Guo J, Zhang R, Xing X, Qin X. 17-AAG post-treatment ameliorates memory impairment and hippocampal CA1 neuronal autophagic death induced by transient global cerebral ischemia. Brain Res. 2015;1610:80–8.
27. Bradley E, Zhao X, Wang R, Brann D, Bieberich E, Wang G. Low dose Hsp90 inhibitor 17AAG protects neural progenitor cells from ischemia induced death. J Cell Commun Signal. 2014;8:353–62.
28. Banecka-Majkutewicz Z, Grabowski M, Kadzinski L, Papkov A, Wegrzyn A, Banecki B. Increased levels of antibodies against heat shock proteins in stroke patients. Acta Biochim Pol. 2014;61:379–83.
29. Zhou C, Yamaguchi M, Kusaka G, Schonholz C, Nanda A, Zhang JH. Caspase inhibitors prevent endothelial apoptosis and cerebral vasospasm in dog model of experimental subarachnoid hemorrhage. J Cereb Blood Flow Metab. 2004;24:419–31.

TAK-242, Toll-Like Receptor 4 Antagonist, Attenuates Brain Edema in Subarachnoid Hemorrhage Mice

Takeshi Okada, Liu Lei, Hirofumi Nishikawa, Fumi Nakano, Yoshinari Nakatsuka, and Hidenori Suzuki

Abstract *Background*: Brain edema is a common and critical pathology following subarachnoid hemorrhage (SAH). Toll-like receptor 4 (TLR4) activation may exacerbate brain edema. The purpose of this study was to clarify if TAK-242, a TLR4 antagonist, suppresses brain edema formation and neurological impairments after SAH in mice.

Methods: A total of 46 mice underwent endovascular perforation to induce SAH or sham operation and were classified as Sham+TAK-242, SAH+ phosphate-buffered saline (PBS), and SAH + TAK-242 groups. The PBS or TAK-242 was administered intracerebroventricularly to mice at 30 min from the operation. Neurobehavioral tests, SAH severity, and brain water content were evaluated at 24 h from the operation.

Results: The SAH + PBS group was significantly worse in neurological tests ($P < 0.001$) and brain water content of the cerebral hemisphere in the bleeding side ($p = 0.005$) compared with the Sham+PBS group, while there were no differences between the SAH + TAK-242 and Sham+PBS groups. SAH severity in the SAH + PBS group was similar to that in the SAH + TAK-242 group.

Conclusions: Intracerebroventricular administration of TAK-242 possibly prevents neurological impairments at least via suppression of brain edema.

Keywords Brain edema · Neuroinflammation · Subarachnoid hemorrhage · Toll-like receptor 4

Introduction

Subarachnoid hemorrhage (SAH) is a cerebrovascular disease with devastating consequences. Brain edema is a common and critical pathology following SAH, and it is an independent risk factor for mortality and poor outcome after SAH [1]. A number of different mechanisms possibly lead to global edema formation after SAH such as progression of abnormalities related to ictal circulatory arrest, diffuse microvascular spasm resulting in ischemia, autoregulatory breakthrough in the setting of hypertension, shifting of water into the intracellular compartment due to hyponatremia, and cerebral inflammation induced by blood products [1, 2] . However, the underlying mechanisms are obscure. Therefore, treatment options of brain edema following SAH are limited. Recent evidences implicated that Toll-like receptor 4 (TLR4) known as a receptor of immune response is activated in the central nervous system by damage-associated molecular patterns following SAH [3]. TLR4 activation leads to the production of proinflammatory substances via mitogen-activated protein kinase (MAPK) pathway and nuclear factor-kappa B (NF-κB) pathway and caused cerebral vasospasm and neuronal apoptosis [4–6]. However, it has not been determined if there are some relationships between TLR4 activation and brain edema following SAH. An exogenous TLR4 antagonist, TAK-242, binds selectively to TLR4 and inhibits its downstream signaling events [7]. Thus, the aim of this study was to investigate if TAK-242 is effective against post-SAH neurological impairments and brain edema aggravation.

Materials and Methods

The Animal Ethics Review Committee of Mie University approved the study protocol, and all experiments were conducted in accordance with the institution's Guidelines for Animal Experiments.

T. Okada (✉) · L. Lei · H. Nishikawa · F. Nakano · Y. Nakatsuka
H. Suzuki
Department of Neurosurgery, Mie University Graduate School of Medicine, Tsu, Mie, Japan
e-mail: t-okada@clin.medic.mie-u.ac.jp

R. D. Martin et al. (eds.), *Subarachnoid Hemorrhage*, Acta Neurochirurgica Supplement 127,
https://doi.org/10.1007/978-3-030-04615-6_13,

Figure 1 shows the study protocol. We used C57BL/six mice (male; weight, 25–30 g) to establish the SAH model. The SAH was induced by endovascular perforation of left internal carotid artery (ICA) bifurcation with a sharpened 4-0 nylon monofilament suture as previously described [8]. Sham group underwent the same operative procedures, except for not puncturing the left ICA. At 30 min after operative procedures for SAH or Sham, 46 surviving mice were divided randomly into 3 groups as follows: Sham+TAK-242 ($n = 8$), SAH + phosphate-buffered saline (PBS; $n = 21$), and SAH + TAK-242 ($n = 7$). The PBS or TAK-242 (0.072 μg in 2 μL PBS; EMD Millipore Corp, Billerica, MA) was administered intracerebroventricularly with the needle of a 2-μL Hamilton syringe (Hamilton Company, Reno, Nev) by a modification of the method previously described [8] . The needle was removed at 10 min after an infusion, and the wound was quickly sutured. Neurological impairments, SAH severity, and brain water content of these groups were assessed at 24 h after modeling.

Neurological impairments were blindly evaluated using two methods. Neurological score was assessed using modified Garcia's neurological score system as previously described [4]. In six categories, we marked a grade from 0 to 3 points depending on the degree of response, respectively. Thus the final neurological score was determined by adding the value from all 6 categories, with 2 being the worst and 18 the best. A beam balance test investigated the animal's ability to walk on a narrow wooden beam for 60 s. The mice received a score ranging from 0 to 4 points as previously described [9]. The median score of 3 consecutive trials in a 5-min period was calculated. The SAH grading system was used to determine the SAH severity as previously described [10]. The mice received a total score ranging from 0 to 18, depending on the amount of SAH. We excluded the models with SAH grade less than 8 points. Brain edema was determined using the wet/dry method as previously described [8] . Brain water content was calculated according to the following formula: [(wet weight − dry weight)/wet weight] × 100%.

Discrete variables were expressed as count (percentage) and continuous variables as mean (standard deviation [SD]) or median (interquartile range [IQR]), as appropriate. Neurological and beam balance scores and SAH grade were compared with Mann-Whitney *U* tests or Kruskal-Wallis tests for data analysis between the groups, while brain water content was compared with unpaired Student's *t*-test. SPSS for Windows, version 21.0 (SPSS Japan Inc., IBM, Tokyo, Japan), was used to perform statistical analyses. Two-side *P* value of less than 0.05 was considered as a statistically significant difference.

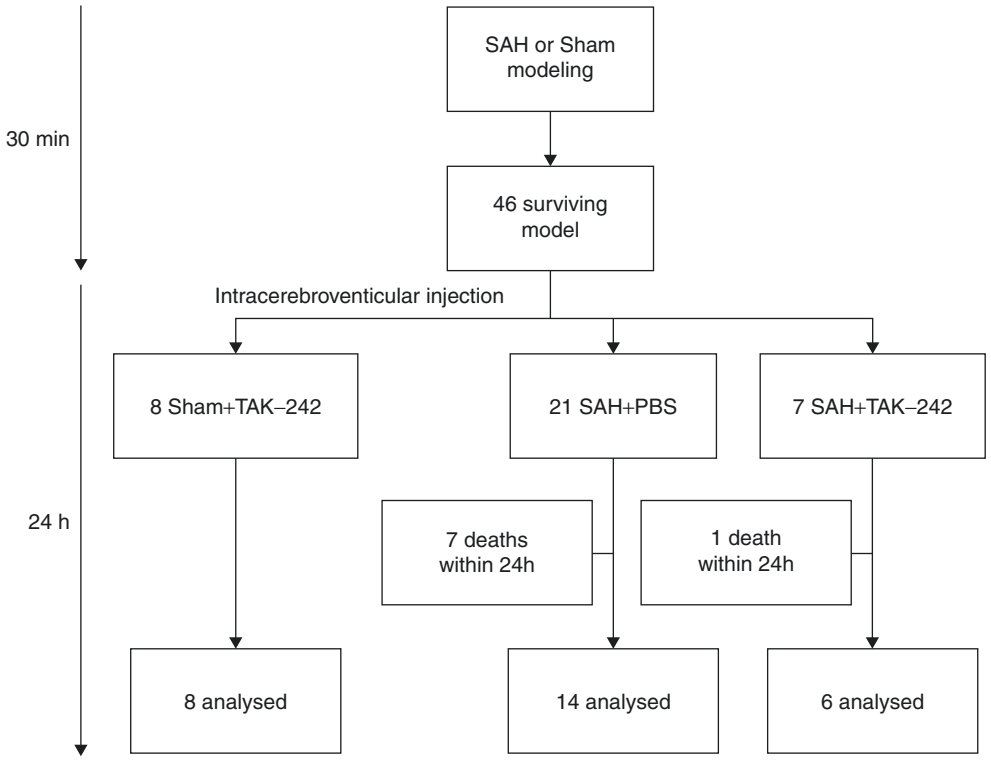

Fig. 1 Flow diagram of the study design. *SAH* subarachnoid hemorrhage; *PBS* phosphate-buffered saline

Results

At 24 h from modeling, the mortality rate was higher in the SAH + PBS group, accounting for 0 (0%) of 8 Sham+TAK-242 mice, 7 (33%) of 21 SAH + PBS mice, and 1 (14%) of 7 SAH + TAK-242 mice (Fig. 1). Neurological score except for mortality models was significantly worse in the SAH + PBS group (median, 6; IQR, 3–12) compared with the Sham+TAK-242 group (median, 18; IQR, 18–18), while there was no significant difference between the SAH + TAK-242 (median, 16; IQR, 14–18) and Sham+TAK-242 groups (Fig. 2a). Beam balance score except for mortality models was also significantly impaired in the SAH + PBS group (median, 1; IQR, 0–1) compared with the Sham+TAK-242 group (median, 4; IQR, 4–4), while there was no significant difference between the SAH + TAK-242 (median, 2; IQR, 0–4) and Sham+TAK-242 groups (Fig. 2b). The SAH grading score was similar between the SAH + PBS (median, 8; IQR, 8–10) and SAH + TAK-242 groups (median, 11; IQR, 9–12; Fig. 2c). Brain water content in the left hemisphere was significantly higher in the SAH + PBS group (mean, 79.7; SD, 1.8) compared with the SAH + TAK-242 group (mean, 78.1; SD, 0.9; Fig. 3a). In contrast, brain water contents in the right hemisphere, cerebellum, and brain stem were similar between the two groups (Fig. 3b–d).

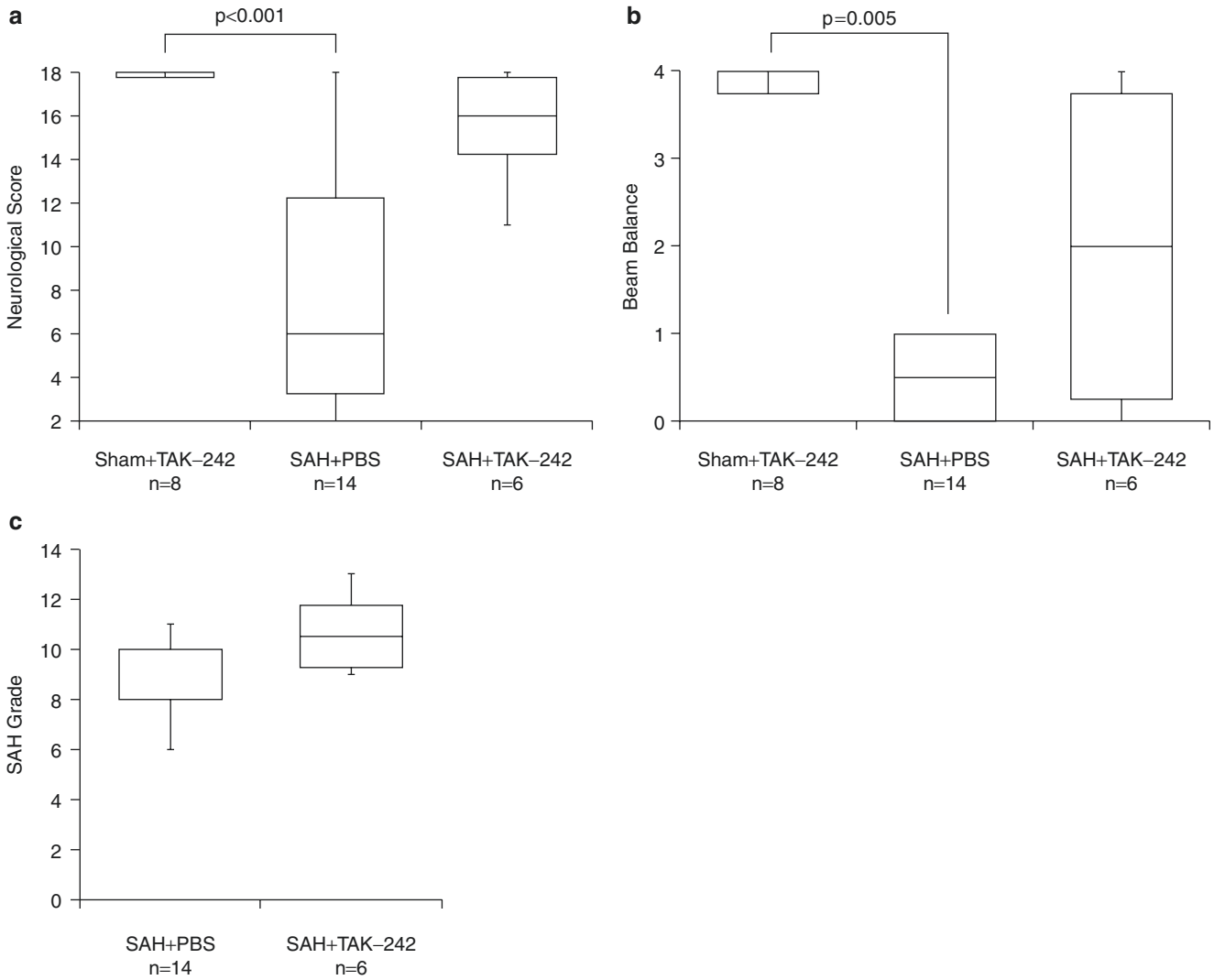

Fig. 2 Box-and-whisker plots showing neurological score (**a**), beam balance score (**b**), and the amount of subarachnoid hemorrhage (SAH; **c**) at 24 h except for mortality models. Data are expressed as median ± 25th-75th percentile. *SAH* subarachnoid hemorrhage; *PBS* phosphate-buffered saline

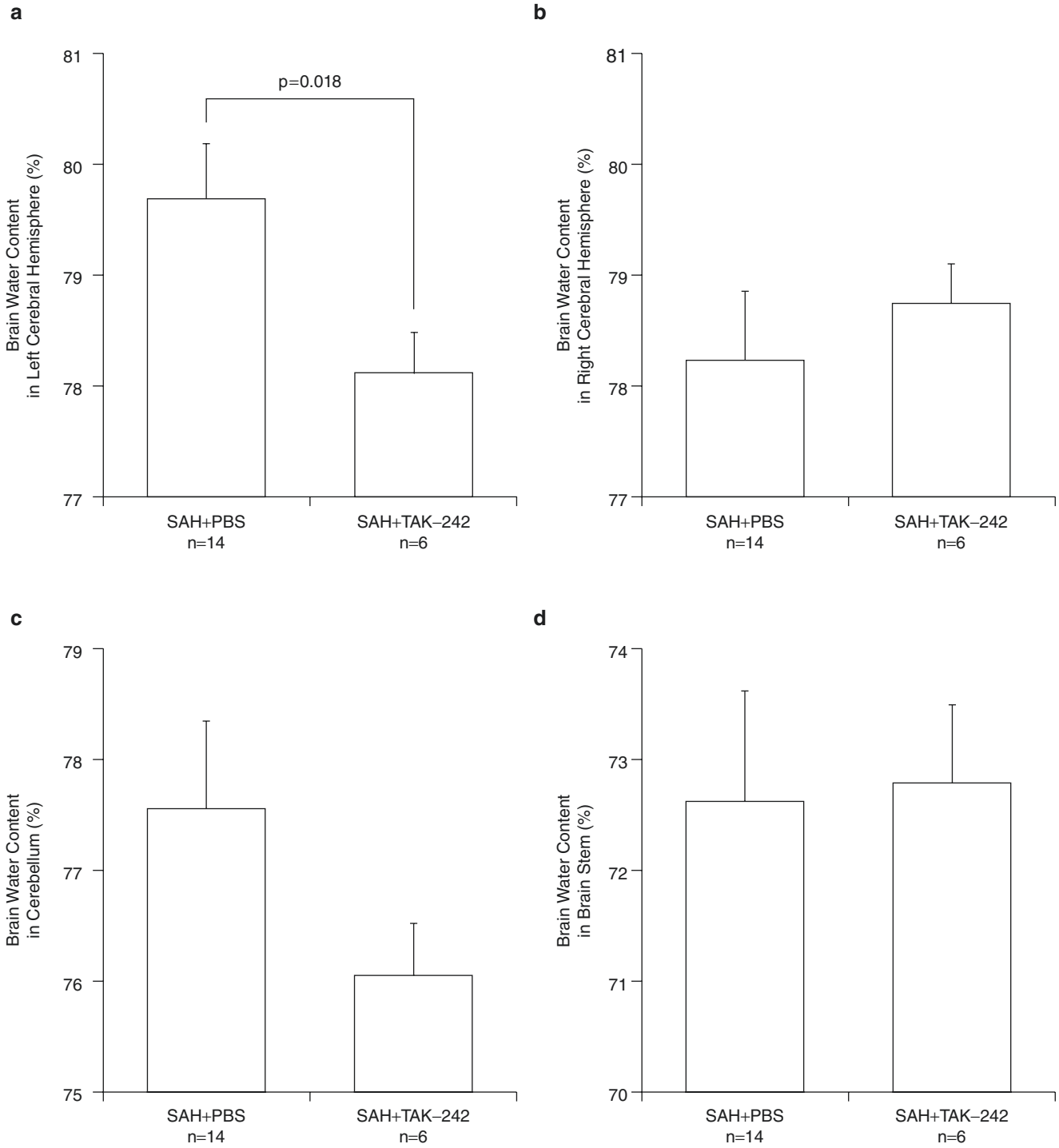

Fig. 3 Bar graphs showing brain water content in the left cerebral hemisphere (**a**), right cerebral hemisphere (**b**), cerebellum (**c**), and brain stem (**d**) between subarachnoid hemorrhage (SAH)-operated mice except for mortality models. Data are expressed as mean ± standard deviation. *PBS* phosphate-buffered saline

Discussion

TAK-242 selectively inhibits TLR4 signal by covalently binding to Cys747 in the intracellular domain of TLR4 [7]. The present study demonstrated that brain water content in the bleeding side and neurological score improved in mouse SAH models by injecting TAK-242 intracerebroventricularly without expediting SAH clearance. This finding suggests that TLR4 antagonists suppressed brain edema formation caused by a mechanism different from mechanical injury with elevation of intracranial pressure resulting from the bleeding spreading into the subarachnoid space after occurrence of SAH. Klatzo [11] classified brain edema as vasogenic edema arising from a breakdown of the tight interendothelial junction forming blood-brain barrier (BBB) and cytotoxic edema arising from a disruption in cellular metabolism. TLR4 stimulation leads to the radiation of NF-κB and activator protein (AP)-1 via the myeloid differentiation primary response gene-dependent pathway [3]. NF-κB produces proinflammatory substances, such as tumor necrosis factor-α, interleukins (ILs), intercellular adhesion molecule-1, monocyte chemoattractant protein-1, matrix metalloproteinase (MMP)-9, cyclooxygenases, and reactive oxygen species, while AP-1 mainly mediated by MAPKs also produces many proinflammatory mediators, such as MMPs, protease, IL-1, and interferon [3]. Among the proinflammatory mediators, MMP-9 possibly plays critical roles in BBB disruption leading to vasogenic brain edema by devastating tight junction proteins and basal membrane proteins, such as fibronectin, laminin, and collagen [2, 12] . MMP-9 knockout mice significantly suppressed the BBB disruption leading to the prevention of brain edema formation after transient focal ischemia [13]. Thus, TLR4 activation possibly implicates BBB disruption by inducing MMP-9. This study cannot show that the exact mechanism leading to reduction of brain edema via TLR4 inactivation. However, the present study is potentially important in showing that TLR4 may be a novel treatment option targeting SAH by suppressing brain edema. Immunohistochemical analysis and protein quantification assay will reveal the pathological mechanism of brain edema leading to neurological impairment. Another limitation of this study is the possibility that TAK-242 inactivates other TLRs and neuroreceptor known to be involved in brain edema and neurological impairments rather than TLR4. Further studies are needed to reinforce the findings.

In conclusion, an intracerebroventricular administration of TAK-242 possibly prevents neurological impairments and brain edema in mouse SAH models.

Acknowledgments This work was funded by a Grant-in-Aid for Scientific Research from Japan Society for the Promotion of Science to Drs. Fujimoto and Suzuki.

Conflict of Interest: **The authors report no conflict of interest concerning the materials or methods used in this study or the findings specified in this paper.**

References

1. Claassen J, Carhuapoma JR, Kreiter KT, Du EY, Connolly ES, Mayer SA. Global cerebral edema after subarachnoid hemorrhage: frequency, predictors, and impact on outcome. Stroke. 2002;33:1225–32.
2. Lee CZ, Xue Z, Zhu Y, Yang G-Y, Young WL. Matrix Metalloproteinase-9 inhibition attenuates vascular endothelial growth factor-induced intracerebral hemorrhage. Stroke. 2007;38:2563–8.
3. Okada T, Suzuki H. Toll-like receptor 4 as a possible therapeutic target for delayed brain injuries after aneurysmal subarachnoid hemorrhage. Neural Regen Res. 2017;12:193–6.
4. Garcia JH, Wagner S, Liu KF, Hu XJ. Neurological deficit and extent of neuronal necrosis attributable to middle cerebral artery occlusion in rats. Statistical validation. Stroke. 1995;26:627–34. discussion 635.
5. Hanafy KA. The role of microglia and the TLR4 pathway in neuronal apoptosis and vasospasm after subarachnoid hemorrhage. J Neuroinflammation. 2013;10:83.
6. Lu P, Gonzales C, Chen Y, Adedoyin A, Hummel M, Kennedy JD, Whiteside GT. CNS penetration of small molecules following local inflammation, widespread systemic inflammation or direct injury to the nervous system. Life Sci. 2009;85:450–6.
7. Peri F, Calabrese V. Toll-like receptor 4 (TLR4) modulation by synthetic and natural compounds: an update. J Med Chem. 2014;57:3612–22.
8. Altay O, Suzuki H, Hasegawa Y, Caner B, Krafft PR, Fujii M, Tang J, Zhang JH. Isoflurane attenuates blood-brain barrier disruption in ipsilateral hemisphere after subarachnoid hemorrhage in mice. Stroke. 2012;43:2513–6.
9. Fujimoto M, Shiba M, Kawakita F, Liu L, Shimojo N, Imanaka-Yoshida K, Yoshida T, Suzuki H. Deficiency of tenascin-C and attenuation of blood-brain barrier disruption following experimental subarachnoid hemorrhage in mice. J Neurosurg. 2015;124:1–10.
10. Sugawara T, Ayer R, Jadhav V, Zhang JH. A new grading system evaluating bleeding scale in filament perforation subarachnoid hemorrhage rat model. J Neurosci Methods. 2008;167:327–34.
11. Klatzo I. Pathophysiological aspects of brain edema. Acta Neuropathol. 1987;72:236–9.
12. Yang Y, Estrada EY, Thompson JF, Liu W, Rosenberg GA. Matrix metalloproteinase-mediated disruption of tight junction proteins in cerebral vessels is reversed by synthetic matrix metalloproteinase inhibitor in focal ischemia in rat. J Cereb Blood Flow Metab. 2007;27:697–709.
13. Asahi M, Wang X, Mori T, Sumii T, Jung JC, Moskowitz MA, Fini ME, Lo EH. Effects of matrix metalloproteinase-9 gene knock-out on the proteolysis of blood-brain barrier and white matter components after cerebral ischemia. J Neurosci. 2001;21:7724–32.

Subarachnoid Hemorrhage Pattern Predicts Acute Cerebral Blood Flow Response in the Rat

Jesse J. Liu, Jeffrey S. Raskin, Robin McFarlane, Ravi Samatham, and Justin S. Cetas

Abstract There is considerable variability in the presentation of patients with acute subarachnoid hemorrhage (aSAH). Evidence suggests that a thick, diffuse clot better predicts the development of delayed cerebral ischemia and poor outcomes. In a rodent model of acute SAH, we directly measured the effects of the volume of blood injected versus the pattern of distribution of hemorrhage in the subarachnoid space on markers of early brain injury, namely, cerebral blood flow (CBF), cerebrospinal fluid (CSF) concentrations of P450 eicosanoids and catecholamines, and cortical spreading depolarizations (CSDs). There is a significant decrease in CBF, an increase in CSF biomarkers, and a trend toward increasing frequency and severity of CSDs when grouped by severity of hemorrhage but not by volume of blood injected. In severe hemorrhage grade animals, there was a progressive decrease in CBF after successive CSD events. These results suggest that the pattern of SAH (thick diffuse clots) correlates with the "clinical" severity of SAH.

Keywords Subarachnoid hemorrhage · P450 eicosanoids · 20-HETE · 14,15-EET · Cortical spreading depolarization · Early brain injury · Stroke glymphatic

J. J. Liu · J. S. Raskin · R. Samatham
Department of Neurological Surgery, Oregon Health & Science University, Portland, OR, USA

R. McFarlane
Portland VA Medical Center, Portland, OR, USA

J. S. Cetas (✉)
Department of Neurological Surgery, Oregon Health & Science University, Portland, OR, USA

Portland VA Medical Center, Portland, OR, USA
e-mail: cetasj@ohsu.edu

Introduction

Aneurysmal subarachnoid hemorrhage (aSAH) is a devastating form of stroke with an incidence of approximately 9 in 100,000 person-years [1]. This condition results in immediate mortality of approximately 22%. There is a nearly 50% mortality rate in the first month, and of those patients surviving at least 1 year, 46–60% remain dependent [2]. One major hallmark of aSAH is the marked variability in clinical presentation, radiographic appearance, and long-term outcomes across patients. Furthermore, many patients, but not all, develop delayed cerebral ischemia (DCI) that, in the past, has been attributed to large vessel vasospasm due to numerous vasoactive compounds in the subarachnoid space. Progressive iterations of radiographic grading scales have improved the prediction of DCI by accounting for diffuse thick hemorrhage [3–5]. In addition, several recent reports have shown that the *pattern* of SAH and not the *volume* of blood per se, in patients with *non*-aneurysmal SAH is correlated with the development of angiographic vasospasm and delayed infarcts [6–8].

Early brain injury (EBI), damage sustained within the first 72 h after ictus, leads to delayed pathological changes such as brain tissue hypoxia, cerebral inflammation, and blood-brain barrier disruption [9, 10]. EBI plays a primary role in the initial clinical presentation of patients with SAH and contributes to secondary injuries, including DCI and subsequent poor prognosis [10]. Consequently, multiple groups have been studying the effects of various biomarkers after aSAH. The P450 eicosanoids are vasoactive and inflammatory products of arachidonic acid metabolism that have been shown to be present in the spinal fluid of aSAH patients. These metabolites play numerous and often opposing roles. Some have been shown to be vasoconstrictive and contribute to DCI [11, 12], and others have been shown to be neuroprotective in cerebral ischemia/reperfusion injury and can reduce cerebral edema [13, 14].

R. D. Martin et al. (eds.), *Subarachnoid Hemorrhage*, Acta Neurochirurgica Supplement 127,
https://doi.org/10.1007/978-3-030-04615-6_14,

Epoxyeicosatrienoic acids (EETs) are vasodilatory, anti-inflammatory, and antithrombotic [15]. 14,15-EET may protect against the development of DCI in both human and animal studies [16, 17], whereas 20-hydroxyeicosatetraenoic acid (20-HETE) and 5-hydroxytryptamine (5-HT) are associated with early and delayed vasospasm [11, 12]. Another hallmark brain injury after SAH is the presence of cortical spreading depolarizations (CSDs) that may contribute to the development of DCI [18]. These are self-propagating waves of neuronal and glial depolarization that trigger a vascular response through neurovascular coupling. The vascular response can range from a spreading hyperemia to a pronounced oligemia and can lead to significant ischemia and cell death [19]. Under normal conditions, CSDs lead to increased cerebral metabolic demand and trigger a hemodynamic response composed of multiple opposing vasomotor influences at various stages of the CSD wave [20]. In the pathologic state after SAH CSDs lead to paradoxical hypoperfusion during the period of elevated metabolic demand which leads to tissue damage [21]. CSDs have been well-documented in animal models and human patients with severe SAH [19, 21]. We propose that a thick diffuse pattern of hemorrhage is the driver of the cascade of events that occurs after hemorrhage rather than a dose response to the spasmogens in the extravasated blood.

In this study, we directly compare the *pattern* of blood in experimental SAH [22, 23] to the *volume* of blood on cerebral blood flow, the CSF expression of P450 eicosanoids, and the development of CSDs. We find that a thick diffuse hemorrhage most closely correlates with the severity of injury after SAH.

Materials and Methods

Animals and Surgical Preparation

This study protocol was approved by the Institutional Animal Care and Use Committee at Oregon Health & Science University, which is in accordance with the NIH Guide for the Care and Use of Laboratory Animals. All institutional and national guidelines for the care and use of laboratory animals were followed. As previously published [22], rats were anesthetized with isoflurane, catheterized (central venous and arterial), placed in a stereotactic frame, and maintained in a "lightly anesthetized state" with i.v. Brevital. The skull was thinned for laser Doppler flowmetry and optical intrinsic signaling (OIS) and a craniotomy performed for placement of a spinal needle in the prechiasmatic cistern for injection of autologous blood into the subarachnoid space.

Experimental Subarachnoid Hemorrhage and Recording

Freshly drawn autologous blood of varying volumes (50 μL, 100 μL, 200 μL, and 250 μL) was infused over 1 min through the spinal needle to minimize changes in intracranial pressure (ICP) [24, 25]. Control animals received an injection of 200 μL of artificial cerebral spinal fluid (aCSF). CBF, mean arterial pressure (MAP), flick latency, and temperature were monitored during a 10-min baseline to ensure a stable anesthetic plane and for an additional 30 min after induction of SAH. OIS was recorded using a multispectral imaging system using QiOptiq Optem FUSION (QiOptiq, NY) modular lens system. A broadband light from a fiber-optic illuminator filtered through a liquid crystal tunable filter (VariSpec VIS, Perkin-Elmer, MA) was used to illuminate the thin skull preparation 3 mm right lateral to the sagittal suture and 2 mm posterior to the coronal suture, at 30° angle with respect to the optical axis of the imaging system. The reflectance from the sample was acquired by monochrome camera (Model: Flea2 IEEEb, Point Grey Research, Inc., Canada) controlled by custom software written using LabVIEW (National Instruments, Austin, TX).

Cerebrospinal Fluid Collection

The rat was given a bolus of 0.5 mL sodium Brevital (20 mg/mL), and the head angled ventrally 30°. A 27-gauge needle was percutaneously inserted into the cisterna magna and 100–200 μL of CSF aspirated. CSF was centrifuged for 10 s at 10,000 RPM and then at −80 °C. Control CSF was obtained from anesthetized naïve rats in a similar fashion. All samples were analyzed for P450 eicosanoids and catecholamines by the lipidomics core on a mass spectrometer. Following CSF collection, the animals were euthanized by sodium Brevital overdose and perfusion fixed with 100 mL saline followed by 100 mL 10% formalin. The whole brain was removed carefully and images of the ventral and dorsal surfaces obtained. The hemorrhage grade was assigned as previously described [22]. Briefly, the ventral surface of the brain was partitioned into six sections. Each section was allotted a number from 0 to 3 depending on the amount of subarachnoid blood in the section: 0 no blood, 1 minimal blood, 2 moderate blood clot with recognizable arteries, and 3 blood clot obliterating all arteries. Scores were summed from all six sections. Scores were categorized as follows: 0–7 mild, 8–12 moderate, and 13–18 severe.

Analysis

CBF was normalized to the baseline. The mean percent change, in 5-min epochs, was calculated for each group and

compared using the one-way ANOVA and post hoc Tukey test. Differences in the mean concentrations of metabolite markers in the CSF were compared using the one-way ANOVA and post hoc Tukey test. The number of cortical spreading depressions was compared with the nonparametric Kruskal-Wallis test. Statistics were performed with MATLAB and IBM SPSS v24 software.

Results

There were a total of 31 experimental animals. Five (5) animals were given a 250 μL injection, eight (8) animals were given a 200 μL injection, four (4) animals were given a 100 μL injection, and four (4) animals were given a 50 μL injection. Ten (10) animals were given an aCSF injection. This resulted in fourteen (14) mild hemorrhages, eight (8) moderate hemorrhages, and nine (9) severe hemorrhages. There were no severe hemorrhages in the 50 μL group (2/4 mild and 2/4 moderate). Of the other three injection groups, there were 25% (1/4), 62.5% (5/8), and 60% (3/5) severe hemorrhages in the 100 μL, 200 μL, and 250 μL injection groups, respectively.

Cerebral Blood Flow

CBF was reduced immediately after experimental SAH in all animals; however, there was a large amount of variability in the severity of the reduction. CBF categorized according to the volume of blood injected was only significantly reduced from aCSF injection in the 250 μL group (the largest volume injected) due to the large variability in responses across groups (Fig. 1a). By contrast, there is a significant difference in relative CBF depending on the hemorrhage grade of the animal (Fig. 1b) consistent with previous reports [22]**.** There is a substantial decrease in CBF in the early phase after SAH injection compared to the baseline in the moderate and severe groups. The differences between mild, moderate, and severe hemorrhages are significant for the first minutes after injection ($P < 0.05$), after which differences between mild and severe hemorrhages persist for 20 min post-injection ($P < 0.05$).

Cerebrospinal Fluid

The concentration of 14,15-EET was significantly elevated in all hemorrhage grades compared to naïve controls ($P < 0.01$). When grouped by injected blood volume, only the largest blood volume group was statistically different ($P < 0.05$) likely due to the large variability. Similarly, the mean concentrations of 20-HETE are significantly different when grouped by hemorrhage severity but not by volume injected. The mean concentration of 5-HT is significantly different in severe hemorrhage compared to control ($P < 0.01$) and moderate hemorrhage ($P < 0.05$), whereas there is no significance when grouped by volume injected. There was no significant difference in the CSF concentration of norepinephrine (NE) independent of grouping (Fig. 2 and Table 1).

Cortical Spreading Depolarization

The number of CSD events were compared between hemorrhage grades as well as volume of blood injected. Of the 14 animals with mild hemorrhages, 3 experienced CSD events; of the 8 moderate hemorrhage animals, 3 experienced CSD events; and of the 9 severe hemorrhage animals, 5 experienced CSD events. There was a trend toward increased frequency of CSD events in severe hemorrhages, but it did not quite reach significance ($P = 0.064$). In animals with multiple CSD events, subsequent CSD events appeared different between mild and severe hemorrhage grades (Fig. 3). In the mild hemorrhage animal, the initial CSD event was a brief period of oligemia followed by hyperemia. In subsequent CSD events, oligemia diminished or was absent and the hyperemic response increased. In the moderate hemorrhage animal, there is a more gradual shift from oligemia to hyperemia. In the severe hemorrhage animal, successive CSD events lead to progressively worsening oligemia and a loss of the hyperemic component (Fig. 3).

Discussion

In this study we examined the correlation between the volume of blood injected in the subarachnoid space and the distribution or pattern of SAH on markers of early brain injury: cerebral perfusion, CSF levels of the P450 eicosanoids and catecholamines (14,15-EET, 20-HETE, 5-HT, and NE), as well as the development of CSDs and their effects on CBF. We found that an acute decrease in cerebral perfusion was quite variable across animals if grouped by the volume of blood injected. By contrast, Sugawara grade correlated closely with the severity of cerebral perfusion deficits and levels of the vasoactive metabolites 20-HETE, 5-HT, and 14–15-EET. There was a trend toward increasing frequency of CSD events in high-grade hemorrhages, and these CSD profiles demonstrated worsening oligemia compared to those associated with low-grade hemorrhages. These changes

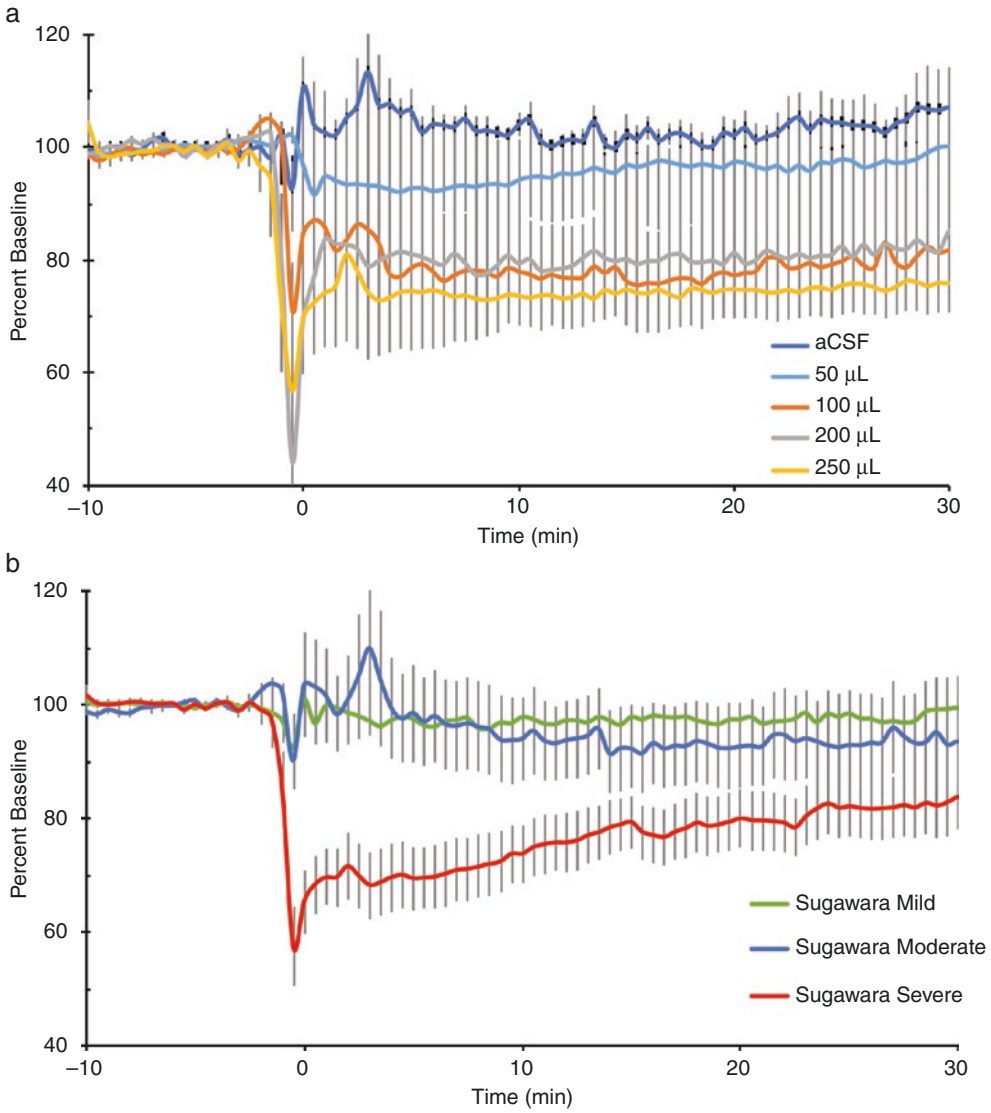

Fig. 1 rCBF after induced SAH (**a**) When grouped by volume of blood injected, only the 250 µL group demonstrated a significant difference from controls (aCSF injection) and was not different from other injected blood volume groups. (**b**) When grouped by pattern of clot in subarachnoid space (Sugawara grade), there is a substantial decrease in rCBF immediately after blood injection in the moderate and severe groups compared to the baseline. Mild, moderate, and severe hemorrhages are significantly different from each other until 5 min after injection ($P < 0.05$), after which mild and severe hemorrhages remain significantly different until 20 min after the injection ($P < 0.05$)

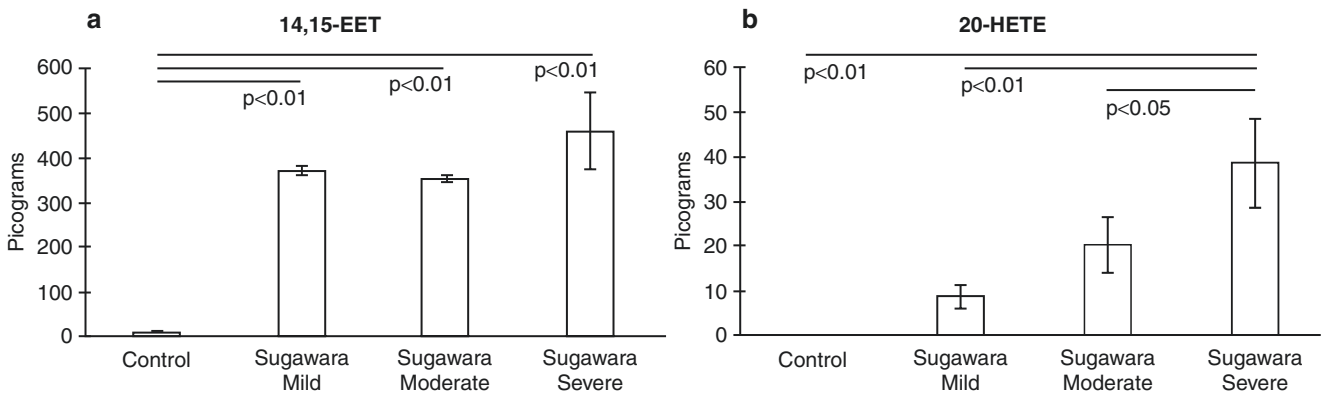

Fig. 2 (**a**) CSF concentrations of 14,15-EET increased in all hemorrhage grades after experimental hemorrhage. (**b**) CSF concentrations of 20-HETE increased proportionally with increasing severity of hemorrhage grade

Table 1 Eicosanoid concentrations by hemorrhage grade and volume injected blood

	Hemorrhage Grade				Injection Volume		
Metabolite	Control	Sugawara Mild	Sugawara Moderate	Sugawara Severe	aCSF	50&100 μL	200&250 μL
14,15-EET	6.75 ± 3.94	371.5 ± 11.44*	354.4 ± 6.66*	460.8 ± 87.5*	396.1 ± 45.77	440.7 ± 97.80	458.3 ± 121.65°
20-HETE	0	8.7 ± 2.52	20.2 ± 6.31	38.6 ± 10.20*#‡	1.5 ± 1.45	19.9 ± 7.55	22.1 ± 9.10
5-HT	0.09 ± 0.02	18 ± 5.70	11.6 ± 5.23	44.4 ± 10.91*#	13.1 ± 4.78	19.6 ± 8.34	28.0 ± 8.86
NE	0.58 ± 0.03	1.80 ± 1.27	3.43 ± 2.63	0.97 ± 0.21	3.24 ± 1.99	0.46 ± 0.23	0.53 ± 0.20

Units are pg/100 μL for the eicosanoids (EETs, HETEs, and DHETs) and units are ng/mL for NE
*$P < 0.01$ when compared to Control; °$P < 0.05$ when compared to Control; # $P < 0.05$ when compared to Moderate; ‡ $P < 0.01$ when compared to Mild

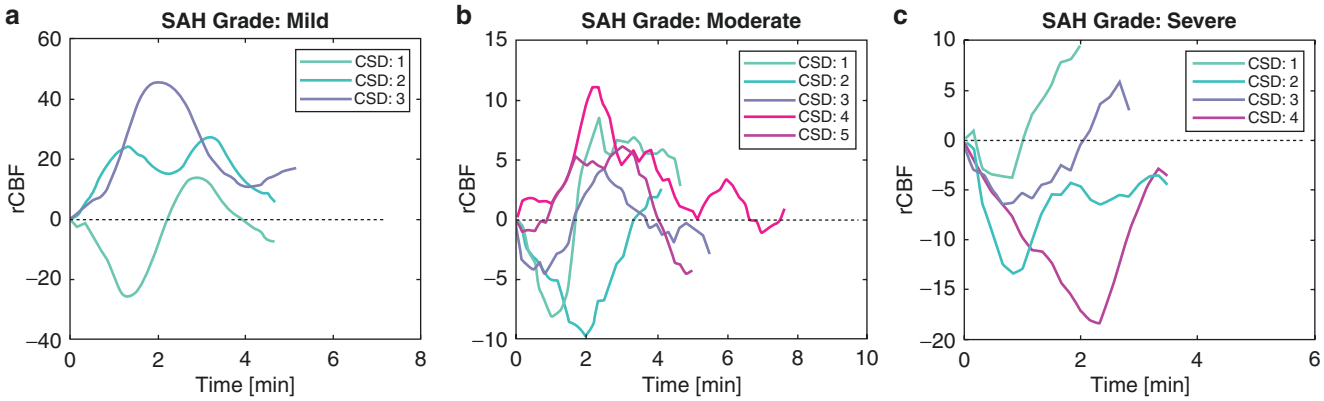

Fig. 3 rCBF changes in successive CSD events. (**a**) An animal with mild-grade hemorrhage and three spontaneous CSD events. Initial oligemia of the first CSD is absent in subsequent CSD events. (**b**) An animal with moderate-grade hemorrhage and five spontaneous CSD events. Initial oligemia persists for four CSD events but begins to diminish after the second event and is absent in the fifth event. The late hyperemic phase increases in magnitude with each successive wave. In high-grade hemorrhage, there is an initial oligemia with a mild compensatory hyperemia that progresses to severe, uncompensated oligemia. (**c**) An animal with severe-grade hemorrhage and four CSD events. Initial oligemia increases with each successive event, while the compensatory hyperemia diminishes and is eventually absent in the third and fourth waves

likely contribute to early brain injury and prime the brain for DCI [26] .

Acute global ischemia is well-known to accompany high clinical grade hemorrhages. Patients have poor neurological function, cerebral edema, and at times early infarcts [27, 28]. In our study, animals with large perfusion deficits had significant increases in the CSF concentration of 20-HETE, 14,15-EET, and 5-HT. Previous work has shown that an increase in 5-HT stimulates the synthesis and/or release of 20-HETE, which is a powerful vasoconstrictor [11] that contributes to vasospasm and poor outcomes in animal models and human studies [17, 29, 30]. 14,15-EET, on the other hand, is a potent vasodilator [17] and has been shown to be neuroprotective in ischemic stroke [31, 32], reduce perivascular inflammation [14], and decrease DCI [17, 33] after SAH. Different genetic polymorphisms of soluble epoxide hydrolase (sEH), an enzyme that metabolizes EETs into inactive secondary products, have been shown to correlate with neurologic outcomes after SAH [14, 16, 33]. Human polymorphisms with decreased sEH activity or animal models of knockout sEH demonstrated improved neurologic outcomes. Both 14,15-EET and 20-HETE are elevated in the CSF of patients with poor clinical grade [17, 30, 33]. Consistent with these clinical studies, we demonstrate elevated 20-HETE and 14,15-EET with severe hemorrhage grades. Interestingly, 14,15-EET is also elevated in low-grade hemorrhages suggesting that an increase in 14,15-EET is a compensatory response to SAH to maintain cerebral blood flow and that it is overwhelmed by the increased vasoconstrictive tone secondary to 20-HETE and 5-HT release in high-grade hemorrhages [17, 34].

Though previous work has reported elevated CSF epinephrine levels in human subjects at a higher risk for early death or disability [34], the CSF concentration of NE was not significantly different regardless of animals grouped by hemorrhage grade or volume of blood injected. The predictive value of elevated NE and epinephrine was weak with low sensitivity and specificity in the human study, and our finding is consistent given the small sample size. It has also been shown that plasma concentrations of catecholamines can be increased after SAH [35]. Our data did not demonstrate con-

sistently elevated catecholamines in the CSF in high-grade hemorrhages, which suggests that catecholamine release associated with SAH is peripheral rather than central. Interestingly, we did not see a close relationship between CSF marker and volume of blood injected which would have been expected if CSF levels of metabolites were due to their presence in the peripheral blood used for SAH. In our model, ICP is controlled which may impact the degree of plasma catecholamines in the CSF sample due to a diminished Cushing's response.

Consistent with the findings of reduced CBF and increased CSF levels of 20-HETE, there is a trend toward increasing frequency of CSD events with increasing hemorrhage grade. Increased 20-HETE reduces CBF through vasoconstriction and has also been shown to be released at the level of the capillaries after CSD events [36] potentially exacerbating underlying ischemia. Interestingly, the CSD events in an animal with severe hemorrhage and multiple CSD events demonstrated increasing oligemia with each successive event (Fig. 3). By contrast, in animals with mild and moderate hemorrhages, the successive CSD events demonstrated hyperemic responses suggesting intact compensatory systems. Without these systems, animals with severe hemorrhages are at an increased risk of global ischemia and potential infarction due to decoupling of the neurovascular unit and an inability to compensate for the elevated metabolic demand [37].

The risk of DCI is also likely related to the diffuse distribution of blood through the subarachnoid space. Previous work has demonstrated the importance of a paravascular, glymphatic, waste clearance mechanism in the brain which is disrupted by blood in the subarachnoid space [38–40]. Tissue plasminogen activator (tPA) injected into the intraventricular space improves glymphatic perfusion and restores CSF flow [41–43] and cortical perfusion [43] after experimental SAH. In addition, parenchymal CSF flow is severely impaired secondary to perivascular blood clots which supports a localized effect of blood and its contribution to DCI [39]. Our model and data support the idea that the diffuse, thick distribution of subarachnoid blood impairs paravascular, glymphatic CSF flow and increases the incidence of EBI and DCI.

Conclusion

In conclusion, this study demonstrates no significant correlation between the volume of blood injected into the subarachnoid space and the severity of induced SAH as measured by the modified Sugawara grade. When grouped by hemorrhage grade, there is a significant decreased initial post SAH CBF; increased CSF concentrations of 20-HETE, 14,15-EET, and 5-HT; and a trend toward increased CSD events in high Sugawara grade experimental SAH. Our model confirms that the diffuse, thick pattern of SAH leads to increased early brain injury and therefore a likely increased risk of DCI.

Acknowledgments This work was supported by the Veterans Administration Merit # 5I01 BX001659-03 from the US Department of Veterans Affairs.

Conflict of Interest: **The authors declare that they have no conflict of interest.**

References

1. de Rooij NK, Linn FHH, van der Plas JA, Algra A, Rinkel GJE. Incidence of subarachnoid haemorrhage: a systematic review with emphasis on region, age, gender and time trends. J Neurol Neurosurg Psychiatry. 2007;78(12):1365–72.
2. Al-Shahi R. Subarachnoid haemorrhage. BMJ. 2006;333(7561):235–40.
3. Dengler NF, Diesing D, Sarrafzadeh A, Wolf S, Vajkoczy P. The Barrow neurological institute scale revisited: predictive capabilities for cerebral infarction and clinical outcome in patients with aneurysmal subarachnoid hemorrhage. Neurosurgery. 2017;81(2):341–9.
4. Fisher CM, Kistler JP, Davis JM. Relation of cerebral vasospasm to subarachnoid hemorrhage visualized by computerized tomographic scanning. Neurosurgery. 1980;6(1):1–9.
5. Frontera JA, Claassen J, Schmidt JM, Wartenberg KE, Temes R, Connolly ES, MacDonald RL, Mayer SA. Prediction of symptomatic vasospasm after subarachnoid hemorrhage: the modified fisher scale. Neurosurgery. 2006;59(1):21–7. discussion 21-27.
6. Konczalla J, Kashefiolasl S, Brawanski N, Bruder M, Gessler F, Senft C, Berkefeld J, Seifert V, Tritt S. Cerebral vasospasm–dependent and cerebral vasospasm–independent cerebral infarctions predict outcome after nonaneurysmal subarachnoid hemorrhage: a single-center series with 250 patients. World Neurosurg. 2017;106:861–869.e4.
7. Raya A, Zipfel GJ, Diringer MN, Dacey RG, Derdeyn CP, Rich KM, Chicoine MR, Dhar R. Pattern not volume of bleeding predicts angiographic vasospasm in nonaneurysmal subarachnoid hemorrhage. Stroke. 2014;45(1):265–7.
8. Walcott BP, Stapleton CJ, Koch MJ, Ogilvy CS. Diffuse patterns of nonaneurysmal subarachnoid hemorrhage originating from the Basal cisterns have predictable vasospasm rates similar to aneurysmal subarachnoid hemorrhage. J Stroke Cerebrovasc Dis. 2015;24(4):795–801.
9. Al-Mufti F, Amuluru K, Smith B, Damodara N, El-Ghanem M, Singh IP, Dangayach N, Gandhi CD. Emerging markers of early brain injury and delayed cerebral ischemia in aneurysmal subarachnoid hemorrhage. World Neurosurg. 2017;107:148–59.
10. Sehba FA, Hou J, Pluta RM, Zhang JH. The importance of early brain injury after subarachnoid hemorrhage. Prog Neurobiol. 2012;97(1):14–37.
11. Cambj-Sapunar L, Yu M, Harder DR, Roman RJ. Contribution of 5-hydroxytryptamine1b receptors and 20-hydroxyeiscosatetraenoic acid to fall in cerebral blood flow after subarachnoid hemorrhage. Stroke. 2003;34(5):1269–75.
12. Roman RJ, Renic M, Dunn KMJ, Takeuchi K, Hacein-Bey L. Evidence that 20-HETE contributes to the development of acute and delayed cerebral vasospasm. Neurol Res. 2006;28(7):738–49.
13. Qu Y-Y, Yuan M-Y, Liu Y, Xiao X-J, Zhu Y-L. The protective effect of epoxyeicosatrienoic acids on cerebral ischemia/reperfusion

injury is associated with PI3K/AKT pathway and ATP-sensitive potassium channels. Neurochem Res. 2015;40(1):1–14.
14. Siler DA, Berlow YA, Kukino A, Davis CM, Nelson JW, Grafe MR, Ono H, Cetas JS, Pike M, Alkayed NJ. Soluble epoxide hydrolase in hydrocephalus, cerebral edema, and vascular inflammation after subarachnoid hemorrhage. Stroke. 2015;46(7):1916–22.
15. Sudhahar V, Shaw S, Imig JD. Epoxyeicosatrienoic acid analogs and vascular function. Curr Med Chem. 2010;17(12): 1181–90.
16. Martini RP, Ward J, Siler D, Eastman JM, Nelson J, Borkar R, Alkayed N, Dogan A, Cetas J. Genetic variation in soluble epoxide hydrolase is associated with outcome after aneurysmal subarachnoid hemorrhage. J Neurosurg. 2014;121(6):1359–66.
17. Siler DA, Martini RP, Ward JP, et al. Protective role of P450 epoxyeicosanoids in subarachnoid hemorrhage. Neurocrit Care. 2015;22(2):306–19.
18. Sánchez-Porras R, Zheng Z, Santos E, Schöll M, Unterberg AW, Sakowitz OW. The role of spreading depolarization in subarachnoid hemorrhage. Eur J Neurol. 2013;20(8):1121–7.
19. Dreier JP, Drenckhahn C, Woitzik J, et al. Spreading ischemia after aneurysmal subarachnoid hemorrhage. Acta Neurochir Suppl. 2013;115:125–9.
20. Ayata C, Lauritzen M. Spreading depression, spreading depolarizations, and the cerebral vasculature. Physiol Rev. 2015;95(3):953–93.
21. Hamming AM, Wermer MJ, Umesh Rudrapatna S, et al. Spreading depolarizations increase delayed brain injury in a rat model of subarachnoid hemorrhage. J Cereb Blood Flow Metab. 2016;36(7):1224–31.
22. Cetas JS, McFarlane R, Kronfeld K, Smitasin P, Liu JJ, Raskin JS. Brainstem opioidergic system is involved in early response to experimental SAH. Transl Stroke Res. 2015;6(2):140–7.
23. Sugawara T, Ayer R, Jadhav V, Zhang JH. A new grading system evaluating bleeding scale in filament perforation subarachnoid hemorrhage rat model. J Neurosci Methods. 2008;167(2):327–34.
24. Prunell GF, Mathiesen T, Diemer NH, Svendgaard N-A. Experimental subarachnoid hemorrhage: subarachnoid blood volume, mortality rate, neuronal death, cerebral blood flow, and perfusion pressure in three different rat models. Neurosurgery. 2003;52(1):165–76.
25. Prunell GF, Mathiesen T, Svendgaard N-A. A new experimental model in rats for study of the pathophysiology of subarachnoid hemorrhage. Neuroreport. 2002;13(18):2553.
26. Fujii M, Yan J, Rolland WB, Soejima Y, Caner B, Zhang JH. Early brain injury, an evolving frontier in subarachnoid hemorrhage research. Transl Stroke Res. 2013;4(4):432–46.
27. Balbi M, Koide M, Wellman GC, Plesnila N. Inversion of neurovascular coupling after subarachnoid hemorrhage in vivo. J Cereb Blood Flow Metab. 2017;37(11):3625–34.
28. Wang J, Alotaibi NM, Akbar MA, Ayling OGS, Ibrahim GM, Macdonald RL. Loss of consciousness at onset of aneurysmal subarachnoid hemorrhage is associated with functional outcomes in good-grade patients. World Neurosurg. 2017;98:308–13.
29. Crago EA, Thampatty BP, Sherwood PR, Kuo C-WJ, Bender C, Balzer J, Horowitz M, Poloyac SM. CSF 20-HETE is associated with delayed cerebral ischemia and poor outcomes after aneurysmal subarachnoid hemorrhage. Stroke J Cereb Circ. 2011;42(7):1872–7.
30. Donnelly MK, Crago EA, Conley YP, Balzer JR, Ren D, Ducruet AF, Kochanek PM, Sherwood PR, Poloyac SM. 20-HETE is associated with unfavorable outcomes in subarachnoid hemorrhage patients. J Cereb Blood Flow Metab. 2015;35(9):1515–22.
31. Geng H-X, Li R-P, Li Y-G, Wang X-Q, Zhang L, Deng J-B, Wang L, Deng J-X. 14,15-EET suppresses neuronal apoptosis in ischemia–reperfusion through the mitochondrial pathway. Neurochem Res. 2017;42(10):2841–9.
32. Yuan L, Liu J, Dong R, Zhu J, Tao C, Zheng R, Zhu S. 14,15-epoxyeicosatrienoic acid promotes production of brain derived neurotrophic factor from astrocytes and exerts neuroprotective effects during ischaemic injury. Neuropathol Appl Neurobiol. 2016;42(7):607–20.
33. Donnelly MK, Conley YP, Crago EA, Ren D, Sherwood PR, Balzer JR, Poloyac SM. Genetic markers in the EET metabolic pathway are associated with outcomes in patients with aneurysmal subarachnoid hemorrhage. J Cereb Blood Flow Metab. 2015;35(2):267–76.
34. Moussouttas M, Huynh TT, Khoury J, Lai EW, Dombrowski K, Pello S, Pacak K. Cerebrospinal fluid catecholamine levels as predictors of outcome in subarachnoid hemorrhage. Cerebrovasc Dis. 2012;33(2):173–81.
35. Ogura T, Satoh A, Ooigawa H, et al. Characteristics and prognostic value of acute catecholamine surge in patients with aneurysmal subarachnoid hemorrhage. Neurol Res. 2012;34(5):484–90.
36. Hall CN, Reynell C, Gesslein B, Hamilton NB, Mishra A, Sutherland BA, O'Farrell FM, Buchan AM, Lauritzen M, Attwell D. Capillary pericytes regulate cerebral blood flow in health and disease. Nature. 2014;508(7494):55–60.
37. Piilgaard H, Lauritzen M. Persistent increase in oxygen consumption and impaired neurovascular coupling after spreading depression in rat neocortex. J Cereb Blood Flow Metab. 2009;29(9):1517–27.
38. Bacyinski A, Xu M, Wang W, Hu J. The paravascular pathway for brain waste clearance: current understanding, significance and controversy. Front Neuroanat. 2017;11:101. https://doi.org/10.3389/fnana.2017.00101.
39. Goulay R, Flament J, Gauberti M, et al. Subarachnoid hemorrhage severely impairs brain parenchymal cerebrospinal fluid circulation in nonhuman primate. Stroke. 2017;48(8):2301–5.
40. Iliff JJ, Nedergaard M. Is there a cerebral lymphatic system? Stroke. 2013;44(6 suppl 1):S93–5.
41. Gaberel T, Gakuba C, Goulay R, De Lizarrondo SM, Hanouz J-L, Emery E, Touze E, Vivien D, Gauberti M. Impaired glymphatic perfusion after strokes revealed by contrast-enhanced MRI. Stroke. 2014;45(10):3092–6.
42. Luo C, Yao X, Li J, et al. Paravascular pathways contribute to vasculitis and neuroinflammation after subarachnoid hemorrhage independently of glymphatic control. Cell Death Dis. 2016;7(3):e2160.
43. Siler DA, Gonzalez JA, Wang RK, Cetas JS, Alkayed NJ. Intracisternal administration of tissue plasminogen activator improves cerebrospinal fluid flow and cortical perfusion after subarachnoid hemorrhage in mice. Transl Stroke Res. 2014;5(2):227–37.

Toll-Like Receptor 4 and Tenascin-C Signaling in Cerebral Vasospasm and Brain Injuries After Subarachnoid Hemorrhage

Hidenori Suzuki, Masashi Fujimoto, Fumihiro Kawakita, Lei Liu, Fumi Nakano, Hirofumi Nishikawa, Takeshi Okada, Kyoko Imanaka-Yoshida, Toshimichi Yoshida, and Masato Shiba

Abstract Toll-like receptor 4 (TLR4) is expressed in various cell types in the central nervous system and exerts maximal inflammatory responses among the TLR family members. TLR4 can be activated by many endogenous ligands having damage-associated molecular patterns including heme and fibrinogen at the rupture of a cerebral aneurysm, and therefore its activation is reasonable as an initial step of cascades to brain injuries after aneurysmal subarachnoid hemorrhage (SAH). TLR4 activation induces tenascin-C (TNC), a representative of matricellular proteins that are a class of inducible, nonstructural, secreted, and multifunctional extracellular matrix glycoproteins. TNC is also an endogenous activator and inducer of TLR4, forming positive feedback mechanisms leading to more activation of the signaling transduction. Our studies have demonstrated that TLR4 as well as TNC are involved in inflammatory reactions, blood-brain barrier disruption, neuronal apoptosis, and cerebral vasospasm after experimental SAH. This article reviews recent understanding of TLR4 and TNC in SAH to suggest that the TLR4-TNC signaling may be an important therapeutic target for post-SAH brain injuries.

Keywords Cerebral vasospasm · Early brain injury Inflammation · Subarachnoid hemorrhage · Toll-like receptor

Introduction

The rupture of a cerebral aneurysm suddenly elevates intracranial pressure, followed by transient global cerebral ischemia. Global cerebral ischemia as well as breakdown products of red blood cells derived from subarachnoid hemorrhage (SAH) trigger a number of cascades including inflammatory reactions, causing early brain injury (EBI), cerebral vasospasm, and delayed cerebral ischemia (DCI) [21]. DCI remains a major preventable cause of morbidity and mortality after aneurysmal SAH, and many pathophysiologies may be involved in the development of DCI including EBI and cerebral vasospasm [21, 29]. Toll-like receptors (TLRs) belong to a large family of pattern recognition receptors that recognize damage-associated molecular patterns (DAMPs) and mediate host inflammatory responses to injury [19]. TLR4 is unique in that it can activate two parallel signaling pathways, the myeloid differentiation primary-response protein 88 (MyD88)-dependent and the toll-receptor-associated activator of interferon (TRIF)-dependent cascades, because all TLRs except TLR3 and TLR4 rely on the MyD88-dependant cascade and TLR3 signals solely through the TRIF adaptor [19]. Thus, TLR4 exerts maximal inflammatory responses among the TLR family members. In addition, TLR4 is activated by many endogenous ligands having DAMPs such as heme, fibrinogen, heat shock proteins, matricellular protein (MCP) tenascin-C (TNC), intracellular components of ruptured cells, and products of genes that are activated by inflammation, all of which are produced after SAH [10, 26]. Moreover, TLR4 is expressed in various cell types in the central nervous system, including neurons, astrocytes, microglia, and capillary endothelial cells in the brain, endothelial, smooth muscle, and adventitial (fibroblasts and macrophages) cells of cerebral arteries, as well as in peripheral blood cells, such as leukocytes, macrophages, and platelets [10, 19]. Thus, activation of TLR4 is reasonable as an initial step of cascades to neuroinflammation, EBI, cerebral vasospasm, and DCI after aneurysmal SAH.

H. Suzuki (✉) · M. Fujimoto · F. Kawakita · L. Liu · F. Nakano · H. Nishikawa · T. Okada · M. Shiba
Department of Neurosurgery, Mie University Graduate School of Medicine, Tsu, Mie, Japan
e-mail: suzuki02@clin.medic.mie-u.ac.jp

K. Imanaka-Yoshida · T. Yoshida
Department of Pathology and Matrix Biology, Mie University Graduate School of Medicine, Tsu, Mie, Japan

R. D. Martin et al. (eds.), *Subarachnoid Hemorrhage*, Acta Neurochirurgica Supplement 127,
https://doi.org/10.1007/978-3-030-04615-6_15,

Possible TLR4-TNC Signaling After SAH (Fig. 1)

As described above, TLR4 is widely expressed in the brain and can be activated by the extravasated blood and damaged brain at the onset of SAH, and the resultant inflammatory reaction and thereby tissue damages may furthermore activate TLR4, causing EBI [19]. At an early phase, the MyD88-dependent pathway activates transcriptional factors nuclear factor (NF)-κB and activator protein (AP)-1, the latter of which is mainly mediated by mitogen-activated protein kinases (MAPKs) [19]. Both transcription factors produce proinflammatory cytokines or mediators such as tumor necrosis factor (TNF)-α, interleukins (ILs: IL-1β, IL-6, IL-8, and IL-12), intercellular adhesion molecule-1, monocyte chemoattractant protein-1, matrix metalloproteinase (MMP)-9, cyclooxygenases, and reactive oxygen species (nitric oxide, hydrogen peroxide, and superoxide) [19]. Proinflammatory cytokines coordinate other immune cells, attract them to the site of invasion or damage, and amplify it until the insult is eliminated or dampened by immune-suppressing feedback mechanisms [19]. NF-κB and MAPKs also upregulate a MCP TNC [1, 18], which is a ligand of TLR4 and may have the positive feedback mechanisms on upregulation of TNC itself and TLR4, leading to more activation of the TLR4-TNC signaling transduction [19, 26]. TLR4 upregulation may be mediated by both NF-κB and MAPKs [19, 30]. In addition, cytokines and reactive oxygen species may induce TNC production by NF-κB and MAPK-dependent or MAPK-independent pathways [14] . TNC may modulate activation, adhesion, rolling and infiltration of inflammatory cells via various signaling pathways, resulting in promotion of inflammatory reaction in SAH, although TNC may inhibit inflammatory reaction depending on the pathological conditions [14].

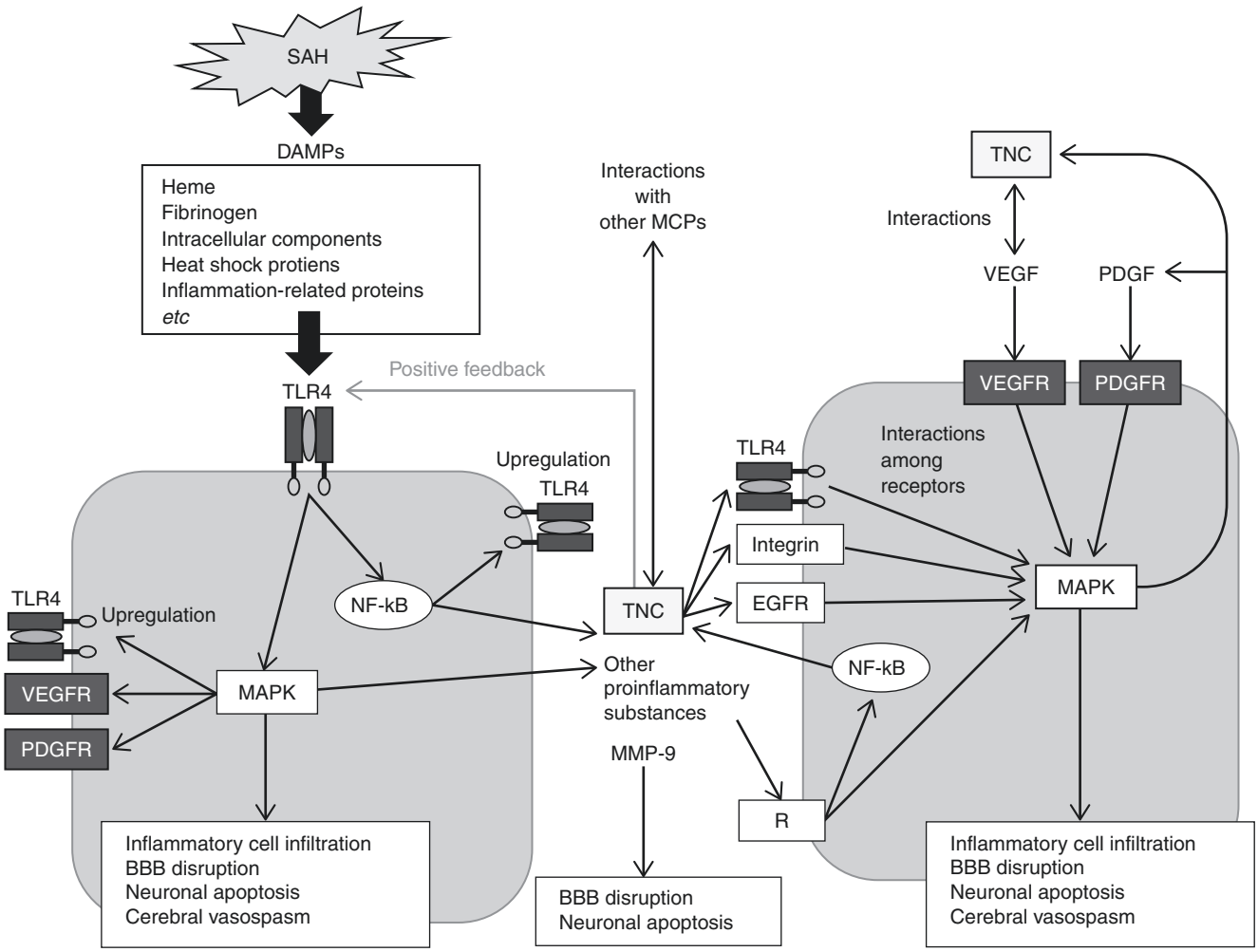

Fig. 1 Possible toll-like receptor 4 (TLR4) and tenascin-C (TNC) signaling in cerebral vasospasm and brain injuries after subarachnoid hemorrhage (SAH). *BBB* blood-brain barrier, *DAMP* damage-associated molecular pattern, *EGFR* epidermal growth factor receptor, *MAPK* mitogen-activated protein kinase, *MCP* matricellular protein, *MMP* matrix metalloproteinase, *NF-κB* nuclear factor-κB, *PDGF* platelet-derived growth factor, *PDGFR* PDGF receptor, *R* receptor, *VEGF* vascular endothelial growth factor, *VEGFR* VEGF receptor

On the other hand, the TRIF-dependent pathway induces "late phase"activation of NF-κB and AP-1, and the subsequent reaction is basically similar to the MyD88-dependent pathway [19]. The TRIF-dependent pathway also induces interferon-β synthesis through the "late phase" NF-κB, which exerts both anti-inflammatory and anti-apoptotic effects, counteracting inflammation [19]. However, when and why the proinflammatory pathway is switched to the anti-inflammatory pathway is not well understood [19].

Possible Role of TLR4 Signaling in EBI, Cerebral Vasospasm, and DCI After SAH

A clinical study reported that patients with aneurysmal SAH had higher TLR4 levels on peripheral blood mononuclear cells, which were associated with more massive SAH, occurrence of cerebral vasospasm, delayed cerebral infarction, and worse outcome [19]. An experimental study showed that TLR4 knockout suppressed neuronal apoptosis in the dentate gyrus in a prechiasmatic cisternal blood injection model in mice: the early phase was largely dependent on the TLR4-MyD88-dependent and microglial-dependent pathways, while the late phase was dependent on the TLR4-TRIF-dependent and microglial-independent pathways [8]. TLR4 knockout also inhibited cerebral vasospasm in the same model via the suppression of the MyD88-dependent pathway in the early phase and the TRIF-dependent pathway in the late phase: microglial TLR4 was necessary for vasospasm development in both the early and late phases of vasospasm possibly via TNF-α induction [8]. Some experimental studies also reported that non-specific TLR4 antagonists suppressed EBI and cerebral vasospasm by the inhibition of NF-κB signaling [19]. Our recent studies demonstrated that specific TLR4 antagonists prevented EBI by MAPK inactivation and TNC downregulation (unpublished data) and cerebral vasospasm by downregulation of cyclooxygenase-1 [10].

Possible Role of TNC Signaling in EBI, Cerebral Vasospasm, and DCI After SAH

TNC, an MCP, belongs to inducible and secreted extracellular matrix (ECM) glycoproteins that do not contribute directly to the formation of structural elements but serve diverse functions as biological mediators of cell function by direct binding to cell surface receptors, other matrix proteins, and soluble factors [13, 26]. TNC is composed of an assembly domain, 14 epidermal growth factor (EGF)-like repeats, a series of fibronectin type III repeats, and a C-terminal fibrinogen-like globular domain and forms a typical disulfide-linked hexamer emanating from a central globular particle [26]. In addition, due to alternative splicing of the fibronectin type III-like repeats, posttranslational modifications, and proteolytic processing, TNC exists as a number of isoforms with varying functions and sizes, although this has not been clearly defined [13, 14]. TNC levels are low in steady-state condition, and the distribution of TNC is typically limited in adult tissues, but TNC is readily and transiently upregulated in pathological conditions, apparently regardless of the location or type of causative insult, by various pro- and anti-inflammatory cytokines, hypoxia, reactive oxygen species, and mechanical stress [14]. In a clinical setting, cerebrospinal fluid (CSF) TNC levels peaked immediately after SAH, and the highest levels in CSF occurred in the first 3 days followed by a decrease over time [27]. It was suggested that more severe SAH or EBI induces more TNC in CSF, causing angiographic vasospasm and DCI separately or simultaneously; that is, DCI may occur by severe angiographic vasospasm with more TNC induction and/or by vasospasm-unrelated causes with TNC induction that are supposed to be EBI [26]. TNC in the peripheral blood also transiently increased a few days before the onset of DCI in patients with aneurysmal SAH [25].

Experimental studies demonstrated that TNC is induced in both cerebral arterial wall (smooth muscle cell layers, adventitia, and periarterial inflammatory cells) and brain parenchyma (possibly astrocytes, neurons, and capillary endothelial cells) in an endovascular puncture model of SAH in rats or mice [7, 26]. Exogenous TNC activated MAPKs in the smooth muscle cells of the major cerebral artery, causing prolonged cerebral arterial contraction in both healthy and SAH rats, while effects of exogenous TNC on brain may be different between healthy and SAH rats possibly because of cleavage of TNC by SAH-induced MMPs and serine proteases [4, 19, 26]. Hexameric, monomeric, and protease-cleaved TNC exhibit distinct functions through binding to different receptors, although the full extent of these functions is not currently clear [14]. In recent studies using a filament perforation SAH model in mice, however, TNC knockout (TNKO) prevented EBI, that is, suppressed neurological impairments, brain edema, and blood-brain barrier (BBB) disruption associated with inactivation of three major MAPKs (c-Jun N-terminal kinase [JNK], p38, and extracellular signal-regulated kinase [ERK] 1/2) in the brain capillary endothelial cells leading to an inhibition of MMP-9 induction and the consequent preservation of the tight junction protein zona occludens-1 [6]. TNKO also inhibited post-SAH activation of ERK1/2 and JNK possibly in neurons in the cerebral cortex [5]. Although a previous study suggested that post-SAH neuronal apoptosis occurred via TNC-induced activation of ERK1/2 and p38 [20], differences in expression of MAPKs in post-SAH brain may be explained by limited injury with an irregular pattern in the cerebral cortex or by differences in animal species or models. Apoptosis may be

induced through EGF-like repeats of TNC [13]. Furthermore, TNKO suppressed post-SAH neuronal apoptosis in the cerebral cortex associated with inactivation of NF-κB and downregulation of IL-1β and IL-6 (unpublished data). Exogenous TNC treatment re-aggravated EBI in TNKO SAH mice [6]. In contrast, exogenous TNC treatment had no effects on neuroscore, brain edema formation, and BBB disruption in TNKO sham mice [6]. Post-SAH TNC induction upregulates MMP-9, and MMP-9 in turn cleaves TNC, which may activate different pathways causing brain injuries. TNKO SAH mice also showed less severe cerebral vasospasm as well as fewer inflammatory cell infiltration in the periarterial space associated with inactivation of MAPKs in the smooth muscle cell layers of the cerebral artery, compared with wild-type SAH mice [7]. Thus, TNC may be a key mediator of EBI in terms of neuroinflammation, BBB disruption, and neuronal apoptosis, as well as cerebral vasospasm after SAH.

Receptors that Mediate TNC's Effect

TNC is cleaved by some proteases and interacts with several cell surface receptors including EGF receptors, TLR4, and integrins [14]. Intracisternally administered intact (full-length) TNC was reported to cause prolonged cerebral vasoconstriction, which was reversed by a TLR4 antagonist in healthy rats [19]. On the other hand, recombinant TNC (r-TNC) consisting of the EGF-like repeats that theoretically can activate only EGF receptors also constricted cerebral artery in healthy rats, which was significantly inhibited by not only an EGF receptor antagonist [4] but also TLR4 and L-arginyl-glycyl-L-aspartate-dependent integrin receptor antagonists [15]. One plausible explanation for this phenomenon is that the r-TNC induces full-length TNC through EGF receptor activation, as we previously reported that r-TNC upregulated TNC itself [26]. Other possible explanations are that cross signaling exists between EGF receptor and TLR4 and that TLR4 may be downstream of EGF receptor activation. De et al. [2] reported that an EGF receptor inhibitor prevented EGF-stimulated phosphorylation of TLR4. The crosstalk of EGF receptors and integrins is also reported [3]. Thus, there may be many approaches existing for blocking TNC's effects.

Interactions with Other Molecules and Receptors

TNC directly binds to ECM molecules such as fibronectin, perlecan, aggrecan, versican, brevican, and presumably many other ECM molecules that remain to be identified, modulating their functions [14]. For example, periostin, another MCP and mediator of post-SAH BBB disruption, is induced in brain capillary endothelial cells and neurons after SAH, and interacts with TNC through its fasciclin I domains, forming a positive feedback mechanism to aggravate BBB disruption by regulating the expression each other and altering downstream signaling pathways including NF-κB and MAPK [12]. Osteopontin (OPN), another MCP, may antagonize TNC's effect by inactivating NF-κB [22, 26], activating an endogenous MAPK inhibitor MAPK phosphatase-1 [23, 24], and inhibiting TNC's binding to its receptor competitively, because they share some receptors [14].

TNC also may be involved in post-SAH upregulation of platelet-derived growth factor (PDGF) receptor in spastic cerebral arteries and vascular endothelial growth factor (VEGF) receptor-2 in the brain [11, 26]. In addition, TNC may enhance activation of PDGF receptor by PDGF via crosstalk signaling through Src between TNC and PDGF receptors [9, 26]. Although both PDGF and VEGF are inducers of TNC and may cause EBI and cerebral vasospasm, induced TNC may be an important mediator that in turn activates the cell itself through a paracrine and autocrine mechanism, leading to more upregulation or activation of PDGF, VEGF, TNC, the receptors, and signaling and therefore internally augmenting EBI and cerebral vasospasm after SAH [11, 20, 26]. In addition, TNC interacts with growth factors including VEGF via binding sites located in fibronectin type III repeats 3–5, prolonging their half-life, increasing their local concentrations, and/or affecting their conformation, all of which will affect their ability to signal to the cell [13]. Furthermore, TNC can modulate phospholipase C, protein kinase C, calcium/calmodulin kinase, and RhoA and upregulate endothelin receptor type A in addition to proinflammatory cytokines and some growth factors [14]. These TNC's effects have not been investigated in the context of SAH but may contribute to the development of EBI, vasospasm, and DCI.

Perspective

Increasing evidence has shown that TLR4-TNC signaling plays an important role in SAH-induced brain injuries. TNC may be efficient modulators of post-SAH brain injuries at several different levels. As TLR4 and TNC may have the positive feedback mechanisms on upregulation of TLR4 and TNC themselves in an acute phase of SAH, the vicious cycle may lead to more activation of the signaling transduction and the development or aggravation of cerebral vasospasm and brain injuries after SAH. Cells can interact with TNC via other cell surface receptors that are not described in this article including syndecans 1 and 4 and annexin II [14]. It is also

interesting to investigate a possibility of the interaction between TNC and other MCPs or molecules in the extracellular space or inside the cells, which may provide TNC with crosslinking functions [13]. There are many other known MCPs that have never been investigated in the context of cerebral vasospasm and brain injuries after SAH [17]. Future studies are required to determine if other MCPs are involved in post-SAH pathophysiological process, how each MCP orchestrates various phases of vasospasm and brain injuries, and to define the therapeutic potential of MCPs in post-SAH vasospasm and brain injuries. Thus, TNC is equipped not only to modulate the cellular environment but also to influence the behavior of cells. However, the resulting cell responses and their potential in vivo relevance are still poorly understood at a mechanistic level [16]. In addition, the biological functions of TNC are highly variable, and often seemingly contradictory, depending on the biological scenario surrounding its induction. Although further meticulous studies are needed [28], novel treatment options targeting TLR4 and TNC are being to be proved efficacious in preclinical models as well as clinical studies for preventing EBI, vasospasm, and DCI .

Acknowledgments This work was supported in part by a grant-in-aid for Scientific Research from Japan Society for the Promotion of Science to Drs. Suzuki and Shiba.

Conflict of Interest Statement

The authors declare that they have no conflict of interest.

References

1. Chiquet M, Sarasa-Renedo A, Tunc-Civelek V. Induction of tenascin-C by cyclic tensile strain versus growth factors: distinct contributions by Rho/ROCK and MAPK signaling pathways. Biochim Biophys Acta. 2004;1693:193–204.
2. De S, Zhou H, DeSantis D, Croniger CM, Li X, Stark GR. Erlotinib protects against LPS-induced endotoxicity because TLR4 needs EGFR to signal. PNAS. 2015;112:9680–5.
3. Eberwein P, Laird D, Schulz S, Reinhard T, Steinberg T, Tomakidi P. Modulation of focal adhesion constituents and their down-stream events by EGF: on the cross-talk of integrins and growth factor receptors. Biochim Biophys Acta. 2015;1853: 2183–98.
4. Fujimoto M, Shiba M, Kawakita F, Liu L, Nakasaki A, Shimojo N, Imanaka-Yoshida K, Yoshida T, Suzuki H. Epidermal growth factor-like repeats of tenascin-C-induced constriction of cerebral arteries via activation of epidermal growth factor receptors in rats. Brain Res. 2016;1642:436–44.
5. Fujimoto M, Shiba M, Kawakita F, Liu L, Shimojo N, Imanaka-Yoshida K, Yoshida T, Kanamaru K, Suzuki H. Early brain injury and mitogen-activated protein kinase after subarachnoid hemorrhage: evaluation using tenascin-C knockout mice. In: Sasaki T, Ohkuma H, Kanamaru K, Suzuki M, editors. Neurovascular events after subarachnoid hemorrhage. Tokyo: Narunia; 2017. p. 131–6.
6. Fujimoto M, Shiba M, Kawakita F, Liu L, Shimojo N, Imanaka-Yoshida K, Yoshida T, Suzuki H. Deficiency of tenascin-C and attenuation of blood-brain barrier disruption following experimental subarachnoid hemorrhage in mice. J Neurosurg. 2016;124:1693–702.
7. Fujimoto M, Shiba M, Kawakita F, Liu L, Shimojo N, Imanaka-Yoshida K, Yoshida T, Suzuki H. Effects of tenascin-C knockout on cerebral vasospasm after experimental subarachnoid hemorrhage in mice. Mol Neurobiol. 2017; https://doi.org/10.1007/s12035-017-0466-x.
8. Hanafy KA. The role of microglia and the TLR4 pathway in neuronal apoptosis and vasospasm after subarachnoid hemorrhage. J Neuroinflammation. 2013; https://doi.org/10.1186/1742-2094-10-83.
9. Ishigaki T, Imanaka-Yoshida K, Shimojo N, Matsushima S, Taki W, Yoshida T. Tenascin-C enhances crosstalk signaling of integrin αvβ3/PDGFR-β complex by SRC recruitment promoting PDGF-induced proliferation and migration in smooth muscle cells. J Cell Physiol. 2011;226:2617–24.
10. Kawakita F, Fujimoto M, Liu L, Nakano F, Nakatsuka Y, Suzuki H. Effects of Toll-like receptor 4 antagonists against cerebral vasospasm after experimental subarachnoid hemorrhage in mice. Mol Neurobiol. 2017;54:6624–33.
11. Liu L, Fujimoto M, Kawakita F, Nakano F, Imanaka-Yoshida K, Yoshida T, Suzuki H. Anti-vascular endothelial growth factor treatment suppresses early brain injury after subarachnoid hemorrhage in mice. Mol Neurobiol. 2016;53:4529–38.
12. Liu L, Kawakita F, Fujimoto M, Nakano F, Imanaka-Yoshida K, Yoshida T, Suzuki H. Role of periostin in early brain injury after subarachnoid hemorrhage in mice. Stroke. 2017;48:1108–11.
13. Midwood KS, Chiquet M, Tucker RP, Orend G. Tenascin-C at a glance. J Cell Sci. 2016;129:4321–7.
14. Midwood KS, Orend G. The role of tenascin-C in tissue injury and tumorigenesis. J Cell Commun Signal. 2009;3:287–310.
15. Nakano F, Fujimoto M, Kawakita F, Nakazaki A, Liu L, Nakatsuka Y, Imanaka-Yoshida K, Yoshida T, Suzuki H. Receptors that mediate tenascin-C-induced constriction of cerebral arteries in rats. In: Sasaki T, Ohkuma H, Kanamaru K, Suzuki M, editors. Neurovascular events after subarachnoid hemorrhage. Tokyo: Narunia; 2017. p. 151–6.
16. Nakatsuka Y, Kawakita F, Yasuda R, Umeda Y, Toma N, Sakaida H, Suzuki H, pSEED group. Preventive effects of cilostazol against the development of shunt-dependent hydrocephalus after subarachnoid hemorrhage. J Neurosurg. 2017;127:319–26.
17. Nishikawa H, Nakatsuka Y, Shiba M, Kawakita F, Fujimoto M, Suzuki H, pSEED group. Increased plasma galectin-3 preceding the development of delayed cerebral infarction and eventual poor outcome in non-severe aneurysmal subarachnoid hemorrhage. Transl Stroke Res. 2017; https://doi.org/10.1007/s12975-017-0564-0.
18. Nong Y, Wu D, Lin Y, Zhang Y, Bai L, Tang H. Tenascin-C expression is associated with poor prognosis in hepatocellular carcinoma (HCC) patients and the inflammatory cytokine TNF-α-induced TNC expression promotes migration in HCC cells. Am J Cancer Res. 2015;5:782–91.
19. Okada T, Suzuki H. Toll-like receptor 4 as a possible therapeutic target for delayed brain injuries after aneurysmal subarachnoid hemorrhage. Neural Regen Res. 2017;12:193–6.
20. Shiba M, Fujimoto M, Imanaka-Yoshida K, Yoshida T, Taki W, Suzuki H. Tenascin-C causes neuronal apoptosis after subarachnoid hemorrhage in rats. Transl Stroke Res. 2014;5:238–47.
21. Suzuki H. What is early brain injury? Transl Stroke Res. 2015;6:1–3.
22. Suzuki H, Ayer R, Sugawara T, Chen W, Sozen T, Hasegawa Y, Kanamaru K, Zhang JH. Protective effects of recombinant osteopontin on early brain injury after subarachnoid hemorrhage in rats. Crit Care Med. 2010;38:612–8.

23. Suzuki H, Hasegawa Y, Chen W, Kanamaru K, Zhang JH. Recombinant osteopontin in cerebral vasospasm after subarachnoid hemorrhage. Ann Neurol. 2010;68:650–60.
24. Suzuki H, Hasegawa Y, Kanamaru K, Zhang JH. Mechanisms of osteopontin-induced stabilization of blood-brain barrier disruption after subarachnoid hemorrhage in rats. Stroke. 2010;41:1783–90.
25. Suzuki H, Kanamaru K, Suzuki Y, Aimi Y, Matsubara N, Araki T, Takayasu M, Kinoshita N, Imanaka-Yoshida K, Yoshida T, Taki W. Tenascin-C is induced in cerebral vasospasm after subarachnoid hemorrhage in rats and humans: a pilot study. Neurol Res. 2010;32:179–84.
26. Suzuki H, Kawakita F. Tenascin-C in aneurysmal subarachnoid hemorrhage: deleterious or protective? Neural Regen Res. 2016;11:230–1.
27. Suzuki H, Kinoshita N, Imanaka-Yoshida K, Yoshida T, Taki W. Cerebrospinal fluid tenascin-C increases preceding the development of chronic shunt-dependent hydrocephalus after subarachnoid hemorrhage. Stroke. 2008;39:1610–2.
28. Suzuki H, Nakano F. To improve translational research in subarachnoid hemorrhage. Transl Stroke Res. 2017; https://doi.org/10.1007/s12975-017-0546-2.
29. Suzuki H, Shiba M, Nakatsuka Y, Nakano F, Nishikawa H. Higher cerebrospinal fluid pH may contribute to the development of delayed cerebral ischemia after aneurysmal subarachnoid hemorrhage. Transl Stroke Res. 2017;8:165–73.
30. Wan J, Shan Y, Fan Y, Fan C, Chen S, Sun J, Zhu L, Qin L, Yu M, Lin Z. NF-κB inhibition attenuates LPS-induced TLR4 activation in monocyte cells. Mol Med Rep. 2016;14:4505–10.

Spreading Depolarization during the Acute Stage of Experimental Subarachnoid Hemorrhage in Mice

Zelong Zheng, Michael Schoell, Renan Sanchez-Porras, Christian Diehl, Andreas Unterberg, and Oliver W. Sakowitz

Abstract Spreading depolarization (SD) has been suggested as a pathomechanism for delayed cerebral ischemia after subarachnoid hemorrhage (SAH). However, the role of SD during the acute phase of SAH is still unclear. The objective of this study was to investigate (a) the occurrence of SD with intrinsic optical signal (IOS) imaging, (b) the effect of ketamine on SD, and (c) the resulting brain edema (brain water content (BWC)) during the acute stage of experimental SAH in mice. SAH was elicited by the endovascular filament perforation method. After SAH or sham operation, ketamine or saline, 30 mg/kg, was given every half hour. Changes in tissue light reflectance were recorded with IOS. BWC was measured during the acute stage. Overall, 199 SDs occurred in SAH groups and 33 SDs appeared in sham groups. These SDs displayed distinct originating and spreading patterns. Compared with saline, ketamine decreased SD spread and influenced the amplitude, duration, and speed of SD. However, the occurrence of SD was not prevented by ketamine. Moreover, ketamine did not reduce BWC after SAH. These results demonstrate that SD occurs with a high incidence during the acute stage of SAH. SDs are heterogeneous in incidence, origination, and propagation. It remains unclear whether ketamine effects on SD may be viewed as therapeutically beneficial after SAH.

Keywords Brain edema · Ketamine · Intrinsic optical signal imaging · Spreading depolarization · Subarachnoid hemorrhage

Introduction

Spreading depolarization (SD) is a near-complete depolarization wave of neuronal and glial cells in the gray matter of central nervous system, propagating at 2–5 mm/min [6, 14]. A main feature of these waves is a remarkable breakdown of ion gradients between extra- and intracellular spaces, which favors neuronal swelling and dendrite distortion due to an osmotic imbalance [14]. For the restoration of ion hemostasis, SD is accompanied by an increase of energy metabolism with a pronounced utilization of oxygen and an increase of the regional cerebral blood flow (rCBF). Under conditions of anoxia and ischemia, the hemodynamic response to SD is sometimes inverted to a marked, prolonged hypoperfusion initiated by the severe vasoconstriction [6]. This perfusion deficit is so severe that it markedly elevates metabolic stress and is capable of inducing brain damage.

Subarachnoid hemorrhage (SAH) resulting from intracranial aneurysmal rupture is associated with a high morbidity and mortality [22]. Early brain injury, activated at aneurysm rupture, evolves with time and has been considered as one of important factors determining the prognosis of SAH [21]. Currently, SD was reported to occur during the early phase of SAH in clinical and experimental studies. Hubschmann et al. [11] recorded cellular depolarization waves with ECoG and ion-specific microelectrodes in a cat SAH model and suggested that SAH generated a primary cellular dysfunction capable of inducing SD during the acute phase. In another study, Beaulieu et al. [4] detected SD in rat cortex after SAH using diffusion-weighted MRI. They concluded that the occurrence of SD was a consequence of the acute hemorrhage process during SAH. Moreover, Van Den Bergh et al. [24] found that prolonged depolarizations occur immediately after SAH in a rat

Z. Zheng (✉)
Department of Neurosurgery, Heidelberg University Hospital, Heidelberg, Germany

Department of Neurosurgery, Guangzhou First People's Hospital, School of Medicine, South China University of Technology, Guangzhou, China

M. Schoell
Institute for Medical Biometry and Informatics, Heidelberg University, Heidelberg, Germany

R. Sanchez-Porras · C. Diehl · A. Unterberg · O. W. Sakowitz
Department of Neurosurgery, Heidelberg University Hospital, Heidelberg, Germany

R. D. Martin et al. (eds.), *Subarachnoid Hemorrhage*, Acta Neurochirurgica Supplement 127, https://doi.org/10.1007/978-3-030-04615-6_16,

model and the duration of SD was associated with the extent of ischemic lesions. Additionally, multicenter, retrospective clinical studies have demonstrated that SD appeared during the early phase of SAH [7, 18]. However, until now, little information about SD during the acute phase of SAH is known.

Intrinsic optical signal (IOS) imaging is a functional neuroimaging technique that enables the visualization of optical reflectance changes at the brain surface [3]. IOS allows for fine temporal and spatial resolution (i.e., seconds and micrometer). It is particularly appropriate for the study of SD because a large region of cortex can be studied simultaneously and multiple time points can be collected over time as the depolarization spreads.

Here, we investigated SD incidence, the effect of ketamine on SD, and the dynamic of the spatial-temporal patterns of SD with IOS during the acute phase of SAH. Moreover, acutely developing brain edema was studied at 3 h after SAH. Meanwhile, intracranial pressure (ICP) was monitored.

Materials and Methods

Forty-eight male C57Bl6 mice (23–25 g body weight; Charles River Laboratory, Sulzfeld, Germany) (Fig. 1) were used for experiments approved by the authorities in animal research in Baden-Württemberg (Protocol Number 35-9185.81/G-203/12).

Experimental Animals and Monitoring

Animals had free access to food and water prior to surgery. Anesthesia was induced by intraperitoneal injection with a threefold combination of midazolam (5 mg/kg), fentanyl (0.05 mg/kg), and medetomidine (0.5 mg/kg) and maintained by hourly injections of one-third of the initial dose. Animals were intubated and mechanically ventilated with 50% oxygen and 50% nitrogen (Minvent Type 845, Hugo Sachs Elektronik Harvard Apparatus GmbH, March, Germany). The left femoral artery was cannulated for continuous blood pressure measurement, blood sample collection, and fluid administration. The body temperature was recorded by a rectal thermometer (LSI, Letica Scientific Instruments, Barcelona, Spain) and kept constantly at 37 °C by a servo-controlled heating pad.

ICP was continuously measured from 40 min before until 3 h after SAH in the parenchyma of the left hemisphere using a Codman ICP microsensor (Johnson & Johnson Medical Limited, Berkshire, UK).

Induction of Subarachnoid Hemorrhage

After the right carotid artery was exposed with careful conservation of the vagus nerve, a 5-0 nylon monofilament was advanced via the external carotid artery (ECA) into the internal carotid artery (ICA). Then the filament was pushed forward until a massive ICP increase was observed. This was the sign of perforation and SAH. After observing ICP increase, the filament was withdrawn immediately into the stump of ECA, and then the vessel was closed by means of ligature. Then the wound was sutured.

Assessment of Brain Water Content

Animals were sacrificed 3 h after induction of SAH. The olfactory bulb and the cerebellum were removed, and the wet weight (WW) of the brain was assessed. Thereafter, the brain was dried for 24 h at 110 °C and their dry weight (DW) was determined. Brain water content (%) was calculated using the following formula $[(WW - DW)/WW] \times 100$.

IOS Acquisition

The mouse's head was illuminated by two LED white-light sources. A CCD camera (Smartec GC1621M, 8 bit gray-

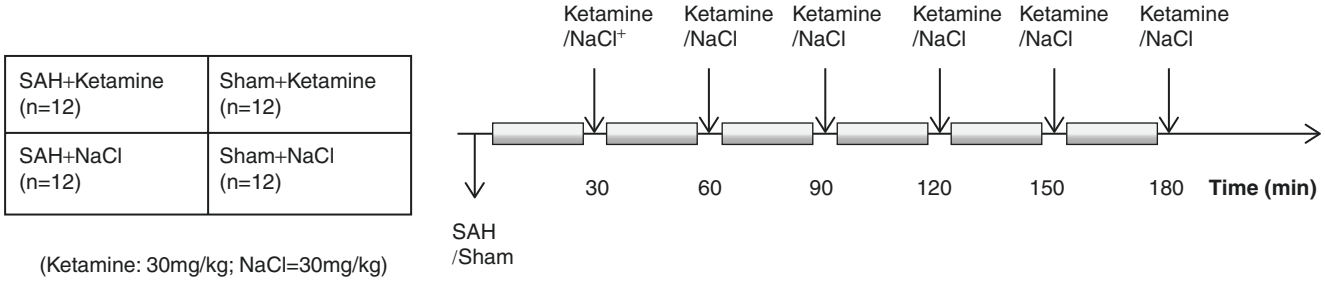

Fig. 1 Schematic design of the current study for IOS after SAH. Animals were randomly assigned into SAH and sham groups. After SAH or sham operation, they were given ketamine or saline every 30 min until 180 min later

scale, 1628 × 1236 pixels, Maxx Vision GmbH, Stuttgart, Germany) was mounted above the thinned skull and connected to a computer. An optical band-pass filter (564 nm, 10 nm FWHM) in front of the camera selected the desired wavelength. Image acquisition was performed until 3 h after induction of SAH at a rate of two images per second at 700 × 600 resolutions to fit the size of mouse's head. Images were saved onto a hard disk for later processing.

Data Analysis

IOS images were elastically registered to a manually chosen reference image. The registration procedure was to reduce movement artifacts of the cortex induced by breathing and heartbeat.

For each experiment, ten regions of interest (ROIs) with 5 × 5 pixels in size distributed along one hemisphere were selected. Similar locations for ROIs were chosen in all of the experiments by taking anatomical landmarks, such as skull sutures and large vessels, to identify similar locations. Custom-written software based on ImageJ was used to inspect the large amounts of images and to identify relevant ROIs. The intensity profiles extracted from the ROIs at identified time points were then analyzed in Labchart software. After obtaining a baseline intensity value, the amplitude was achieved. The duration of intensity changes and the speed and number of ROIs reached per SD were also measured. The cortex area touched per SD was also analyzed with our software. Aided by the parameter images of maximal and minimal intensity changes during SD, the manually selected expansion area gave the absolute visible area of expansion of SD. To compare the expansion areas between different animals, these areas were normalized by the whole visible cortex area, for each mouse. This resulted in the percentage of visible cortex covered by a specific SD.

Statistical Analysis

Descriptive statistics were calculated for all outcome variables of interest. All data are presented as means±standard error of the mean (SEM), if not indicated otherwise. To test differences in means and numbers of events, independent sample Student's t-test and Mann-Whitney tests were used. All statistical tests were performed two-sided, and the statistical significance was assumed as $p < 0.05$. For statistical analysis SPSS 20.0 for Windows (SPSS Inc., Chicago, Illinois, USA) was used.

Results

Physiological Parameters

The mean arterial pressure, rectal temperature, and arterial blood gases were in the normal range before induction of SAH (Table 1).

Observation of SD

A total of 199 SDs occurred in animals with SAH (8.3 SD per animal), while, interestingly, 33 SDs also occurred in sham groups (1.4 SD per animal) (Mann-Whitney U-test: $p < 0.01$ vs. sham). Most of SD appeared within 30–60 min (42.6%) after SAH, which means that SAH leads to immediate SD.

Spatiotemporal Patterns of SD

SD had different originating sites, propagation direction, and patterns (Fig. 2) in the cerebral cortex of mice after SAH.

Originating Sites

The originating sites of SD were classified into three types: the cerebral cortex adjacent to the ICP sensor, other area of the cerebral cortex, and the olfactory bulb. After SAH, 48 SDs initiated from the cerebral cortex next to the ICP sensor, 115 SDs came from other parts of the cerebral cortex, and 36 SDs originated from the olfactory bulb.

Initiation and Propagation Patterns

Radial wave: These waves originated from a single point, and their wave front diverged in all directions, assuming a

Table 1 The result of blood gas analysis before SAH induction or sham surgery

	pH	pO_2	pCO_2	HCO_3^-	Na^+	K^+	Cl^-	Ca^{2+}
SAH + ketamine	7.29 ± 0.01	92.2 ± 1.8	40.5 ± 0.8	19.0 ± 0.2	147.45 ± 0.50	4.6 ± 0.1	119.5 ± 0.7	0.94 ± 0.04
Sham+ketamine	7.32 ± 0.01	96.2 ± 1.0	40.3 ± 0.4	19.7 ± 0.2	147.00 ± 0.49	4.4 ± 0.1	116.8 ± 0.5	1.04 ± 0.02
SAH + NaCl	7.32 ± 0.01	92.2 ± 1.1	39.1 ± 0.9	19.3 ± 0.3	147.22 ± 0.58	4.4 ± 0.1	117.9 ± 0.7	1.00 ± 0.02
Sham+NaCl	7.31 ± 0.01	96.2 ± 0.7	40.3 ± 0.4	19.2 ± 0.2	146.68 ± 0.64	4.3 ± 0.1	116.7 ± 0.7	0.99 ± 0.01

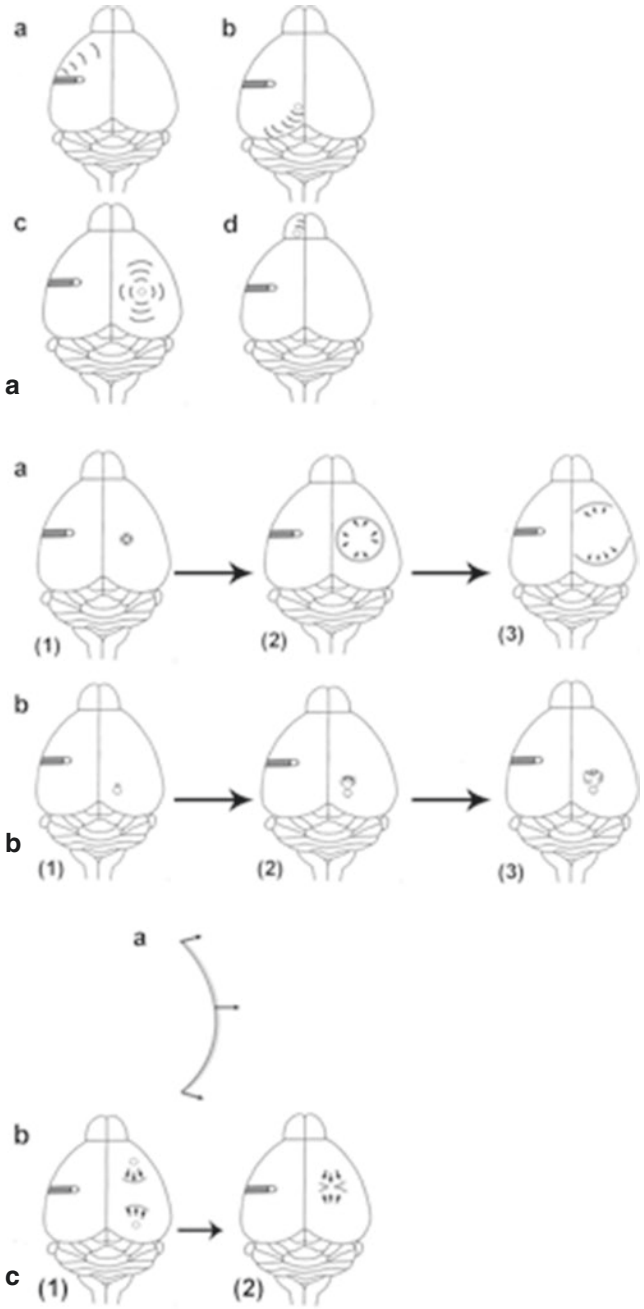

Fig. 2 Spatiotemporal patterns of SD after SAH. Origins of spontaneous SDs (**A**) distributed on different locations of the brain: the cerebral cortex adjacent to the ICP sensor (**A***a*), other cerebral cortex in the contralateral hemisphere (**A***b*) or the ipsilateral hemisphere (**A***c*), and the olfactory bulb (**A***d*). And SD initiates with radial (**B***a1*) or irregular radial pattern (**B***b1*). The most common initiation pattern in the current study is the irregular radial pattern. It expands and creates a solitary broken radial wave (*b2–3*). The radial wave of SD forms two semi-planar waves when it encounters vessels or fissures (a2–3). All SDs evolve into semi-planar waves (**C***a*). When two wave fronts collide, they interact and may annihilate (**C***b1–2*)

spherical shape. Waves may then "break" at some time points when hampered, forming two or more semi-planar waves.

Irregular radial wave: These waves began as a radial wave from the origination point expanding asymmetrically during the early spreading phase, breaking the integrated circle. Wave fronts could develop into a single semi-planar wave.

There were 186 SDs (93.5%) initiating as irregular radial waves and 13 SDs (6.5%) originating as radial waves after SAH.

Semi-planar wave: Waves with a flat-rounded front preserve some radial direction and have two open ends, traveling in one direction.

Collision: When two wave fronts collide, they can annihilate because of the resistance of the excitable medium.

One hundred and ninety-nine SDs quantified in all experiments spread in a semi-planar fashion. The morphology of SD waves was affected by the surface of the cerebral cortex, the presence of ICP sensors, and other SDs. When two SDs wave fronts encountered each other, they interacted and collided.

Effect of Ketamine on SD

After SAH, 91 SDs occurred in animals treated with ketamine, and 108 SDs appeared in saline-treated animals (Mann-Whitney U-test: $p = 0.775$). ROIs reached by SD was 3.2 ± 0.3 in ketamine-treated SAH animals and 3.8 ± 0.3 in saline-treated SAH group (Mann-Whitney U-test: $p < 0.05$). After SAH, the speed of SD between ketamine-treated and saline-treated groups significantly differed (2.7 ± 0.1 mm/min vs. 3.3 ± 0.1, independent sample Student's t-test, $p < 0.01$). The area covered by SD was 14.4 ± 1.5% in ketamine-treated mice with SAH and 19.0 ± 1.7% in saline-treated animals with SAH (Mann-Whitney U-test, $p < 0.01$). Moreover, the intensity change between these two groups was also significantly different (7.7 ± 0.6% vs. 9.9 ± 0.5%, Mann-Whitney U-test, $p < 0.001$). In addition, the interval time among SDs was 21.2 ± 3.1 min in the ketamine-treated SAH group, whereas, in the saline-treated mice with SAH, the interval was significantly lower at 11.9 ± 1.1 min.

Brain Water Content

After SAH, the brain water content at 3 h was 80.2 ± 0.6% vs. 79.6 ± 0.3% in sham-operated animals (independent sam-

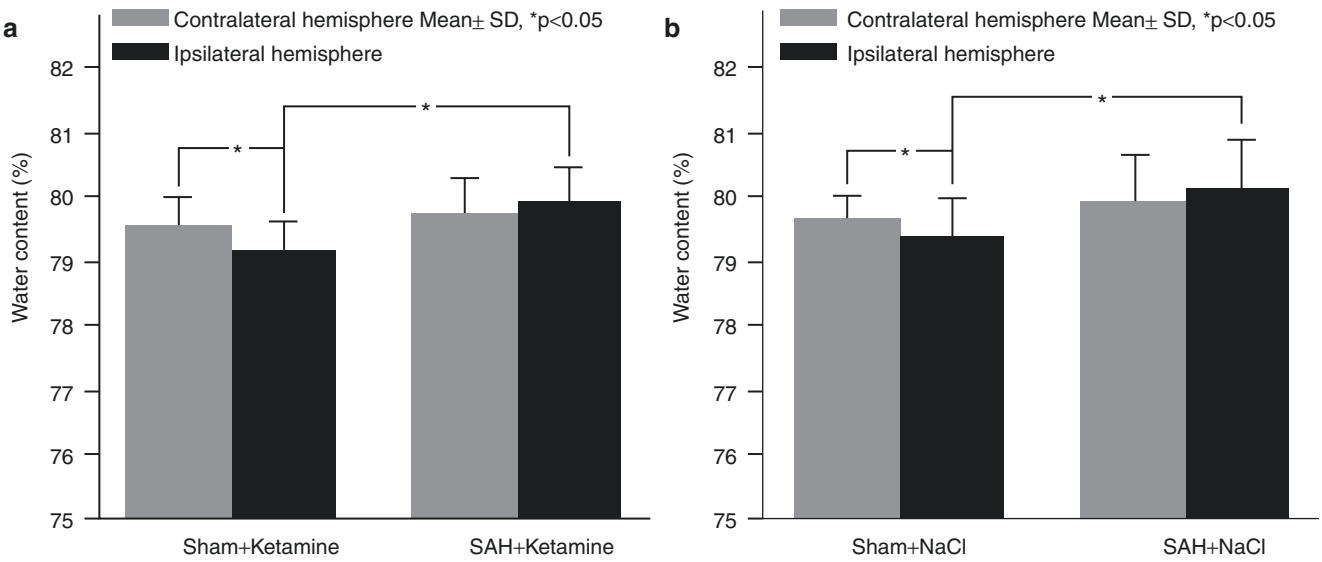

Fig. 3 Total brain water content (BWC) after SAH or sham surgery: the water content in ketamine-treated (**a**) and saline-treated (**b**) SAH or sham groups. BWC of SAH groups is higher than that of sham groups, and in sham groups, BWC of contralateral hemispheres significantly increases. The data is expressed as mean ± standard deviation

ple Student's t-test, $p < 0.05$). Although brain water content in ketamine-treated animals (79.8 ± 0.1%) was lower than in saline-treated groups (79.9 ± 0.1%) after SAH, there was no significant difference (independent sample Student's t-test, $p = 0.683$) (Fig. 3).

Discussion

Using IOS, the incidence of SD during the acute stage (3 h) of SAH was measured, as exemplified by a mouse model. It was found that SD occurred in almost 100% of mice after SAH, which is higher than had been reported following aneurysmal SAH (72%) in patients [7] and similar to that after malignant ischemic stroke (100%) in humans [5]. A possible reason for higher incidence of SD is the recording method: IOS can record SD in large area of cerebral cortex and has high spatiotemporal resolution. However, subdural electrode strips only capture SD that spread across it. In addition, SD during the first 3 hours after SAH cannot be investigated in patients. Furthermore, global brain ischemia exists during the first hour after SAH and coincides with the peak of SD activity at that time.

The results presented by this study also demonstrate that SD is heterogeneous in incidence, origination, and propagation after SAH in mice. SD may originate from the cerebral cortex adjacent to the ICP sensor, olfactory bulb, or other area of the cerebral cortex. As an exception, SD from the olfactory bulb did not spread out of this region. These phenomena would appear at least superficially consistent with the anatomical differences between cerebral cortex and the olfactory bulb. In the olfactory bulb, the susceptibility to SD is low because of GABAergic inhibition [2]. Moreover, the cytoarchitectural separation of the olfactory bulb might provide an explanation for restriction of SD propagation in this area. SDs originating from the cerebral cortex nearby the ICP sensor were most likely induced by the sensor, since it is known that relatively minor mechanical stimuli are able to evoke SD.

SD is regarded as a roughly isotropic and concentric phenomenon; however, we found that expansion patterns of SD after SAH in mice were different. As we know, the truly concentric and isotropic SD is observed in chicken retina, which has a uniform, avascular structure [15]. This implies that the heterogeneity of SD in cerebral cortex may be due to ununiformed cellular and vascular structures. In our study, most of SD with the radial pattern appear in the ipsilateral hemisphere. As we know, The origin sites of radial pattern SD are areas with apparent reduced perfusion because of accumulation of K^+ and ischemia after SAH [19]. The ipsilateral hemisphere suffers more serious ischemic damage than contralateral one after SAH [23], in which accumulation of $[K^+]_o$ and ischemia can appreciate the area with marked decreased perfusion, observed in SD with radial patterns.

Furthermore, the present study underscores that ketamine with the dosage of 30 mg/kg has the capacity to suppress SD propagation and reduce SD amplitude and duration in mouse

SAH model. However, SD induction is not prohibited. Moreover, ketamine does not reduce brain edema at 3 h after SAH. As a noncompetitive antagonist, ketamine can bind at the phencyclidine site and thus decrease the channel opening time and the amplification of the response to a repeated stimulation. In addition, ketamine is capable of binding in one site located in the hydrophobic domain of the NMDA receptor where it decreases the frequency of channel opening [20]. Therefore, ketamine is capable of modulating SD properties. Other experimental studies also report that SD is blocked by ketamine at significantly high doses in diverse lissencephalic animal models [1, 13]. In addition, ketamine at dosage used in human can prevent SD induced by KCl stimulation in the gyrencephalic swine brain [17]. However, those studies were carried out in physiological conditions, and the effect of ketamine on SD may be different in pathological situations. In the current study, SD induction after SAH was not blocked by ketamine, although it did suppress SD expansion and propagation. Petzold et al. suggested that in pathological conditions, the efficacy of NMDA receptor antagonists was reduced, and they were not able to block SD induced by high extracellular potassium concentration [16]. Conversely, after the MCAO model in rats, delayed (8 h after ischemia) application of an NMDA receptor antagonist reduced infarct volume and the frequency of SDs [8]. Furthermore, clinical studies demonstrated that ketamine decreased SD incidence in patients with brain injury [10, 18]. It may be implied that the occurrence of SD is related to both different intensities between conditions and usage of NMDA receptor antagonists; if the effect of the deleterious condition is stronger than the NMDA receptor antagonist, SD will occur despite the presence of the drug in the region exposed to the deleterious condition [9]. Additionally, the blocking effect of ketamine on SD is also dependent on used dosage and administration route. In the present study, a subanesthetic dosage of 30 mg/kg was used through intraperitoneal injection, but SDs were not blocked. Ketamine may be able to block SD completely through intravascular infusion or increasing the dosage. As shown by Sanchez-Porras et al., ketamine infusion at 2 mg/kg/h was not able to inhibit SD induction but prevented its expansion, whereas at 4 mg/kg/h, SDs were fully blocked [17]. Until now, there has been limited evidence available regarding clinical benefits after the administration of ketamine. The low dosage of ketamine and occult adverse effects may contribute to this failure in patients with brain injury [12]. However, ketamine still exhibits a neuroprotective potential, and it is necessary to carry on more experimental studies in proper animal models and prospective clinical trials in patients with deleterious conditions to clarify the effect of ketamine on SD in pathophysiological condition and to establish optimal dosages and administration routes.

Acknowledgments The author, Zelong Zheng, thanks the Chinese Scholarship Council for financial support.

Conflict of Interest
None.

References

1. Amemori T, Bures J. Ketamine blockade of spreading depression: rapid development of tolerance. Brain Res. 1990;519:351–4.
2. Amemori T, Gorelova NA, Bures J. Spreading depression in the olfactory bulb of rats: reliable initiation and boundaries of propagation. Neuroscience. 1987;22:29–36.
3. Ba AM, Guiou M, Pouratian N, Muthialu A, Rex DE, Cannestra AF, Chen JW, Toga AW. Multiwavelength optical intrinsic signal imaging of cortical spreading depression. J Neurophysiol. 2002;88:2726–35. https://doi.org/10.1152/jn.00729.2001.
4. Beaulieu C, Busch E, de Crespigny A, Moseley ME. Spreading waves of transient and prolonged decreases in water diffusion after subarachnoid hemorrhage in rats. Magn Reson Med. 2000;44:110–6.
5. Dohmen C, Sakowitz OW, Fabricius M, Bosche B, Reithmeier T, Ernestus RI, Brinker G, Dreier JP, Woitzik J, Strong AJ. Spreading depolarizations occur in human ischemic stroke with high incidence. Ann Neurol. 2008;63:720–8.
6. Dreier JP. The role of spreading depression, spreading depolarization and spreading ischemia in neurological disease. Nat Med. 2011;17:439–47. https://doi.org/10.1038/nm.2333.
7. Dreier JP, Woitzik J, Fabricius M, Bhatia R, Major S, Drenckhahn C, Lehmann T-N, Sarrafzadeh A, Willumsen L, Hartings JA. Delayed ischaemic neurological deficits after subarachnoid haemorrhage are associated with clusters of spreading depolarizations. Brain. 2006;129:3224–37.
8. Hartings JA, Rolli ML, X-CM L, Tortella FC. Delayed secondary phase of peri-infarct depolarizations after focal cerebral ischemia: relation to infarct growth and neuroprotection. J Neurosci. 2003;23:11602–10.
9. Hernández-Cáceres J, Macias-González R, Brožek G, Bureš J. Systemic ketamine blocks cortical spreading depression but does not delay the onset of terminal anoxic depolarization in rats. Brain Res. 1987;437:360–4.
10. Hertle DN, Dreier JP, Woitzik J, Hartings JA, Bullock R, Okonkwo DO, Shutter LA, Vidgeon S, Strong AJ, Kowoll C, Dohmen C, Diedler J, Veltkamp R, Bruckner T, Unterberg AW, Sakowitz OW. Effect of analgesics and sedatives on the occurrence of spreading depolarizations accompanying acute brain injury. Brain. 2012;135:2390–8. https://doi.org/10.1093/brain/aws152.
11. Hubschmann OR, Kornhauser D. Cortical cellular response in acute subarachnoid hemorrhage. J Neurosurg. 1980;52:456–62. https://doi.org/10.3171/jns.1980.52.4.0456.
12. Ikonomidou C, Turski L. Why did NMDA receptor antagonists fail clinical trials for stroke and traumatic brain injury? The Lancet Neurology. 2002;1:383–6.
13. Krüger H, Heinemann U, Luhmann HJ. Effects of ionotropic glutamate receptor blockade and 5-HT1A receptor activation on spreading depression in rat neocortical slices. Neuroreport. 1999;10:2651–6.
14. Lauritzen M, Dreier JP, Fabricius M, Hartings JA, Graf R, Strong AJ. Clinical relevance of cortical spreading depression in neurological disorders: migraine, malignant stroke, subarachnoid and intracranial hemorrhage, and traumatic brain injury. J Cereb

Blood Flow Metab. 2011;31:17–35. https://doi.org/10.1038/jcbfm.2010.191.
15. Martins-Ferreira H, Nedergaard M, Nicholson C. Perspectives on spreading depression. Brain Res Rev. 2000;32:215–34.
16. Petzold GC, Windmüller O, Haack S, Major S, Buchheim K, Megow D, Gabriel S, Lehmann T-N, Drenckhahn C, Peters O. Increased extracellular K+ concentration reduces the efficacy of N-methyl-D-aspartate receptor antagonists to block spreading depression-like depolarizations and spreading ischemia. Stroke. 2005;36:1270–7.
17. Sánchez-Porras R, Santos E, Schöll M, Stock C, Zheng Z, Schiebel P, Orakcioglu B, Unterberg AW, Sakowitz OW. The effect of ketamine on optical and electrical characteristics of spreading depolarizations in gyrencephalic swine cortex. Neuropharmacology. 2014;84:52–61.
18. Sakowitz OW, Kiening KL, Krajewski KL, Sarrafzadeh AS, Fabricius M, Strong AJ, Unterberg AW, Dreier JP. Preliminary evidence that ketamine inhibits spreading depolarizations in acute human brain injury. Stroke. 2009;40:e519–22. https://doi.org/10.1161/strokeaha.109.549303.
19. Santos E, Schöll M, Sánchez-Porras R, Dahlem MA, Silos H, Unterberg A, Dickhaus H, Sakowitz OW. Radial, spiral and reverberating waves of spreading depolarization occur in the gyrencephalic brain. NeuroImage. 2014;99:244–55.
20. Schmid RL, Sandler AN, Katz J. Use and efficacy of low-dose ketamine in the management of acute postoperative pain: a review of current techniques and outcomes. Pain. 1999;82:111–25.
21. Sehba FA, Hou J, Pluta RM, Zhang JH. The importance of early brain injury after subarachnoid hemorrhage. Prog Neurobiol. 2012;97:14–37. https://doi.org/10.1016/j.pneurobio.2012.02.003.
22. Serrone JC, Maekawa H, Tjahjadi M, Hernesniemi J. Aneurysmal subarachnoid hemorrhage: pathobiology, current treatment and future directions. Expert Rev Neurother. 2015;15:367–80. https://doi.org/10.1586/14737175.2015.1018892.
23. Thal SC, Sporer S, Klopotowski M, Thal SE, Woitzik J, Schmid-Elsaesser R, Plesnila N, Zausinger S. Brain edema formation and neurological impairment after subarachnoid hemorrhage in rats: laboratory investigation. J Neurosurg. 2009;111:988–94.
24. van den Bergh WM, Zuur JK, Kamerling NA, van Asseldonk JT, Rinkel GJ, Tulleken CA, Nicolay K. Role of magnesium in the reduction of ischemic depolarization and lesion volume after experimental subarachnoid hemorrhage. J Neurosurg. 2002;97:416–22. https://doi.org/10.3171/jns.2002.97.2.0416.

The PERK Pathway Plays a Neuroprotective Role During the Early Phase of Secondary Brain Injury Induced by Experimental Intracerebral Hemorrhage

Juyi Zhang[#], Peng Zhang[#], Chengjie Meng, Baoqi Dang, Haiying Li, Haitao Shen, Zhong Wang, Xiang Li, and Gang Chen

Abstract The protein kinase RNA-like endoplasmic reticulum kinase (PERK) pathway, which is a branch of the unfolded protein response, participates in a range of pathophysiological processes of neurological diseases. However, few studies have investigated the role of the PERK in intracerebral hemorrhage (ICH). The present study evaluated the role of the PERK pathway during the early phase of ICH-induced secondary brain injury (SBI) and its potential mechanisms. An autologous whole blood ICH model was established in rats, and cultured primary cortical neurons were treated with oxyhemoglobin to mimic ICH in vitro. We found that levels of phosphorylated alpha subunit of eukaryotic translation initiation factor 2 (p-eIF2α) and activating transcription factor 4 (ATF4) increased significantly and peaked at 12 h during the early phase of the ICH. To further elucidate the role of the PERK pathway, we assessed the effects of the PERK inhibitor, GSK2606414, and the eIF2α dephosphorylation antagonist, salubrinal, at 12 h after ICH both in vivo and in vitro. Inhibition of PERK with GSK2606414 suppressed the protein levels of p-eIF2α and ATF4, resulting in increase of transcriptional activator CCAAT/enhancer-binding protein homologous protein (CHOP) and caspase-12, which promoted apoptosis and reduced neuronal survival. Treatment with salubrinal yielded opposite results, which suggested that activation of the PERK pathway could promote neuronal survival and reduce apoptosis. In conclusion, the present study has demonstrated the neuroprotective effects of the PERK pathway during the early phase of ICH-induced SBI. These findings highlight the potential value of PERK pathway as a therapeutic target for ICH.

Keywords Intracerebral hemorrhage · Endoplasmic reticulum stress · Unfolded protein response · PERK pathway · Neuroprotection

Introduction

Stroke, also known as a cerebrovascular accident, is a morbid state produced by insufficient blood flow to meet the metabolic demands of the brain. Intracerebral hemorrhage (ICH) is the deadliest type of stroke with a 30-day mortality up to 40% and severe disability in the majority of survivors [1]. The mechanisms of ICH are extremely complex, including primary brain injury and secondary brain injury (SBI). At present, it is generally accepted that SBI plays a more critical role in the poor prognosis of hemorrhagic stroke. Unfortunately, we currently have no effective solutions to SBI, which involves oxidation, inflammation, apoptosis, and hematotoxicity [2]. SBI results in disruption of cellular metabolism and activation of a series of stress responses such as the unfolded protein response (UPR) in endoplasmic reticulum (ER) stress [3].

The ER is an important subcellular organelle in eukaryotic cells. It plays a vital role in many cellular processes that include folding of newly synthesized secretory and membrane proteins, posttranslational modifications, and regulation of intracellular Ca^{2+} homeostasis [4]. Normally, only properly folded proteins are transported from the ER to the Golgi apparatus; unfolded or misfolded proteins are degraded. ER stress occurs when unfolded or misfolded

[#]These authors contributed equally to this work.

J. Zhang · P. Zhang · H. Li · H. Shen · Z. Wang (✉) · X. Li (✉)
G. Chen
Department of Neurosurgery and Brain and Nerve Research Laboratory, The First Affiliated Hospital of Soochow University, Suzhou, China
e-mail: xiangli2017@suda.edu.cn

C. Meng
Department of Neurosurgery and Brain and Nerve Research Laboratory, The First Affiliated Hospital of Soochow University, Suzhou, China

Department of Neurosurgery, Yancheng First People's Hospital, Yancheng, China

B. Dang
Department of Rehabilitation Medicine, Zhangjiagang Hospital of Traditional Chinese Medicine, Suzhou, China

R. D. Martin et al. (eds.), *Subarachnoid Hemorrhage*, Acta Neurochirurgica Supplement 127,
https://doi.org/10.1007/978-3-030-04615-6_17,

proteins accumulate and the folding capacity of ER chaperones exceeds the capacity of the ER lumen to facilitate their disposal. As a consequence, a battery of adaptive processes, collectively known as the UPR, can be activated that transmit signals from the ER to the cytosol and nucleus to combat harmful effects of ER stress and restore normal cellular homeostasis [5]. The UPR can remove unfolded or misfolded proteins when ER stress occurs, and it might play a significant role in cell survival [6]. However, if stimuli are severe or prolonged, ER stress responses may be unable to compensate, and cell apoptosis may be induced [7].

The UPR is triggered by activation of three sensor proteins at the ER membrane: activating transcription factor-6 (ATF6), inositol-requiring enzyme-1 (IRE1), and protein kinase RNA-like ER kinase (PERK) [8]. Activated PERK phosphorylates the alpha subunit of eukaryotic translation initiation factor 2 (eIF2α), which can block the initiation stage of translation, thereby reducing protein synthesis and decreasing the ER load [9]. If ER stress is sustained, the ER-specific apoptosis pathway is activated by promoting expression of transcriptional activator CCAAT/enhancer-binding protein homologous protein (CHOP) and caspase-12 (CASP12) [10]. In recent years, several studies have reported that the UPR plays a vital role in the fate of neuronal cells following ischemic stroke. Although ICH only accounts for 10–20% of all cerebrovascular accidents worldwide [11], it is the most devastating type of stroke with a high morbidity and mortality; up to 50% of patients die within the first 24 h [12].

It is not clear whether ER stress and the UPR are involved in mechanisms that underlie ICH-induced SBI. The purpose of this study was to investigate the role of the PERK pathway during the early phase of ICH-induced SBI and its potential mechanisms. We monitored the time course of expression of the PERK pathway and utilized two experimental tools, PERK inhibitor GSK2606414 [13, 14] and eIF2α dephosphorylation inhibitor salubrinal [15, 16], which exert opposite effects both in vivo and in vitro.

Materials and Methods

Animals

Adult male Sprague-Dawley rats (250–300 g, Animal Center of the Chinese Academy of Sciences, Shanghai, China) were raised with free access to water and food and housed in temperature- and humidity-controlled animal quarters with a 12-h light/dark cycle. All animal experiments were approved by the Ethics Committee of the First Affiliated Hospital of Soochow University and in accordance with the National Institutes of Health Guide.

ICH Model

The ICH model was established in rats using stereotaxic injection of autologous whole blood according to a previous report [17] with some modifications. In brief, rats were anesthetized and then mounted on a stereotaxic frame (ZH-Lanxing B type, Anhui Zhenghua Biological Equipment Co. Ltd. Anhui, China). Then, a cranial burr hole was drilled 0.2 mm anterior to bregma and 3.5 mm lateral to the midline, which corresponded to the right basal ganglia. Autologous whole blood (100 μL) was collected by cardiac puncture and injected slowly (5.5 mm ventral to the cortical surface, 20 μL/min) with a microinjector (Hamilton Company, NV, USA). To prevent reflux, the needle was kept in place for an additional 5 min. The bone hole was sealed with bone wax, and the scalp was then disinfected and sutured. During the entire surgery, rats were placed on a heating pad in a supine position, and the pad was maintained at ~27–35 °C. Vital signs were monitored continuously. After establishment of the ICH model, the rats were returned to their cages with food and water. A representative brain coronal section was shown in Fig. 1a.

Experimental Design

There were two types of in vivo experiments. In experiment 1, we analyzed the time course of changes in levels of p-eIF2α and ATF4 after ICH. A total of 72 rats (80 rats were used, 72 rats survived after surgery) were randomly (used the randomization table) divided into six groups of 12 rats per group, which included a sham group and five experimental groups arranged by time after ICH: 4, 8, 12, 16, and 24 h. At the indicated time point after ICH, rats were killed, and the brain samples of six rats in each group were dissected and used for Western blot analysis. Double immunofluorescence staining of p-eIF2α and ATF4 with neuronal nuclei (NeuN) was performed in the sham group and 12 h after ICH (Fig. 1b).

In experiment 2, 108 rats (129 rats were used, 108 rats survived) were randomly (used the randomization table) divided into six groups of 18 rats per group: sham, ICH, ICH + vehicle (for GSK2606414), ICH + GSK2606414 (90 μg in 5 μL sterile saline), ICH + vehicle (for salubrinal), and ICH + salubrinal (1 mg/kg body weight). Neurological scoring and brain edema were assessed at 12 h after ICH. Expression levels of p-eIF2α, ATF4, CHOP, and CASP12 were determined by Western blot analysis at 12 h after ICH. Finally, terminal deoxynucleotidyl transferase-mediated dUTP nick end labeling (TUNEL) and fluoro-jade B (FJB) staining were also performed at 12 h after ICH in each group (Fig. 1c).

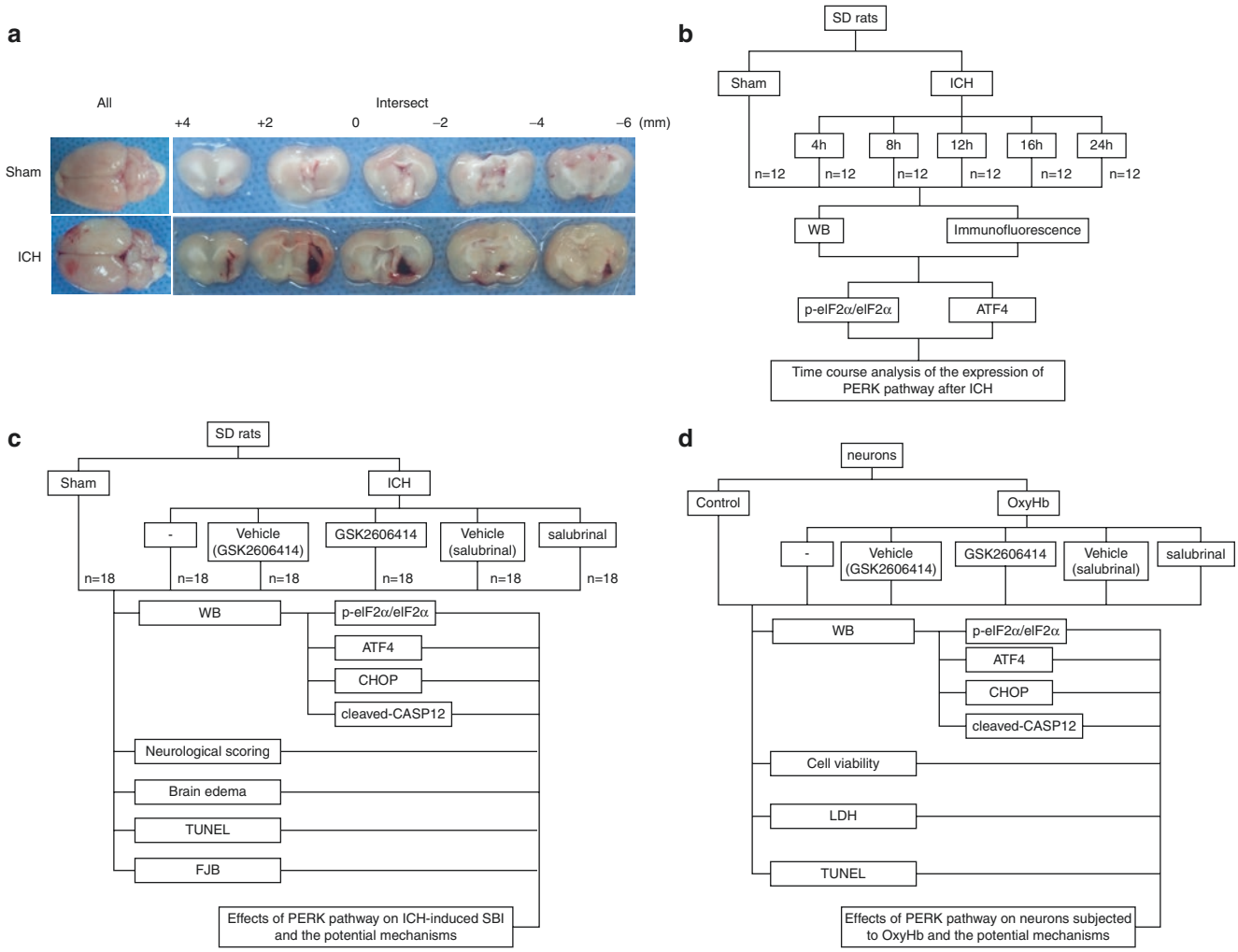

Fig. 1 Intracerebral hemorrhage model and experimental design. (**a**) Representative whole brains and brain slices from ICH model rats. (**b**) Experiment 1 was designed to evaluate expression of p-eIF2α and ATF4 at different time points. (**c**) Experiment 2 was designed to investigate effects of the PERK pathway on ICH-induced SBI and potential mechanisms. (**d**) Experiment 3 was designed to investigate the role of the PERK pathway in vitro

In experiment 3, primary rat cortical neurons were treated with oxyhemoglobin (OxyHb) (10 μmol/L) to mimic effects of ICH in vitro. The experimental groups were similar to those of experiment 2 in vivo, and we assessed changes in protein levels of p-eIF2α, ATF4, CHOP, and cleaved CASP12. At 12 h after OxyHb treatment, a sulforhodamine B (SRB) assay was used to test cell viability, and the cell culture supernatants were collected for lactate dehydrogenase (LDH) activity detection. Double immunofluorescence staining of TUNEL and NeuN was performed in all groups (Fig. 1d).

For neurological scoring and brain edema evaluation, the observers did not know group of rats, either the component of infusion. For Western blot analysis, the bands were collected from one independent experiment using one rat, and the statistical data were from at least six rats. For all the immunofluorescence analysis, the representative images were from at least three independent experiments using six rats.

Antibody Characterization and Drugs

Anti-p-eIF2α antibody (ab32157), anti-eIF2α antibody (ab169528), anti-CHOP antibody (ab11419), anti-CASP12 antibody (ab62484), mouse anti-NeuN monoclonal antibody (ab104224), and anti-β-tubulin antibody (ab179513) were purchased from Abcam (Cambridge, MA, USA). Anti-ATF4 antibody (sc-200) was purchased from Santa Cruz (Santa Cruz, CA, USA). Salubrinal and GSK2606414 were purchased from TargetMol (Boston, MA, USA).

Drug Administration

One hour after surgery, the PERK pathway inhibitor, GSK2606414, was dissolved in dimethyl sulfoxide (DMSO)

and further diluted in sterile saline to a final concentration of 0.5%. Five microliters of GSK2606414 (90 μg) was then administered intracerebroventricularly at a rate of 0.5 μL/min [18]. The microsyringe was left in situ for another 10 min before being removed slowly. The eIF2α dephosphorylation inhibitor, salubrinal, was infused intraperitoneally at a dose of 1 mg/kg in saline with 1.5% DMSO [19]. Equal volumes of DMSO solutions were respectively administered to vehicle control animals.

Intracerebroventricular Injection

Intracerebroventricular injection was conducted as reported previously [20]. Briefly, rats were placed in a stereotaxic frame after anesthetization as described above. Then, a small burr hole was drilled into the skull 1.0 mm lateral to and 1.5 mm posterior to bregma over the left hemisphere. The needle of a 10 μL Hamilton syringe was slowly inserted through the burr hole into the left lateral ventricle 4.0 mm below the dural surface. A reagent was infused into the left lateral ventricle at a rate of 0.5 μL/min.

Establishment of the In Vitro ICH Model and Cell Treatment

Isolation and culture of primary cortical neurons has been described previously [21, 22]. Briefly, whole brains of 17-day rat embryos were used to prepare primary neuron-enriched cultures. Every effort was made to minimize the number of embryos used and their suffering. First, we removed the blood vessels and the meninges. Then, the brain tissues were digested with 0.25% trypsin for 5 min at 37 °C. After termination of digestion, the suspension was centrifuged at 1500 rpm for 5 min, and the pellet was resuspended in plates and cultured in Neurobasal Medium (GIBCO, Carlsbad, CA, USA). Cultures were maintained in an atmospheric incubator at 37 °C with 5% CO_2. Neurons were cultured for 2 weeks, and half of the media was replaced every 2 days. To mimic ICH, neurons were treated with 10 μM OxyHb [23]. The cultures were divided into four groups as follows: control; OxyHb treatment for 12 h; OxyHb + vehicle (for GSK2606414), pretreatment with GSK2606414 (1 μM) for 1 h, thorough rinsing, and OxyHb treatment for 12 h [24]; OxyHb + vehicle (for salubrinal); and pretreatment with salubrinal (50 μM) for 1 h, thorough rinsing, and OxyHb treatment for 12 h [25].

Table 1 Behavior and activity scores

Category	Behavior	Score
Appetite	Finished meal	0
	Left meal unfinished	1
	Scarcely ate	2
Activity	Walk and reach at least three corners of the cage	0
	Walk with some stimulations	1
	Almost always lying down	2
Deficits	No deficits	0
	Unstable walk	1
	Impossible to walk	2

Neurological Scoring

At 12 h after ICH, rats in experiment 2 were assessed by neurological scoring before euthanasia. All rats were evaluated using a previously published scoring system that monitored appetite, activity, and neurological deficits [21] (Table 1).

Brain Edema

The index of brain edema was determined using the wet/dry method as described previously [26]. Briefly, the brain tissue was removed and collected, and the samples were weighed immediately (wet weight), followed by drying at 100 °C for 72 h. And then the tissues were reweighted to obtain the dry weight. The percentage of water content was calculated as follows: [(wet weight − dry weight)/wet weight] × 100%.

Cell Viability

Neuronal viability was evaluated by SRB assay. Following treatment incubation, the culture medium was removed, and neurons were fixed with 10% trichloroacetic acid (TCA) followed by staining with 0.4% SRB. Absorbances were measured at 540 nm with a Bio-Rad Microplate reader. Cell viability was measured in triplicate and repeated at least three independent times.

LDH Assay

The concentrations of LDH in the culture medium were measured using a LDH detecting kit (A020-2; Jiancheng Biotech, Nanjing, China) according to the instructions. The data were presented relative to standard curves.

Western Blot Analysis

After perihematomal tissues were collected, the brain samples of each animal were homogenized separately and then mechanically lysed in lysis buffer (Beyotime Institute of Biotechnology, Jiangsu, China). After centrifuging at 15000 × g for 10 min at 4 °C, the supernatants were collected immediately. Protein concentration was determined using an enhanced bicinchoninic acid (BCA) protein assay kit (Beyotime Institute of Biotechnology). Then, the protein (30 μg/lane) were loaded on a 10% SDS-PAGE gel, separated, and then electrophoretically transferred to a polyvinylidene difluoride (PVDF) membrane (Millipore Corporation, Billerica, MA, USA). The membrane was blocked with 5% bovine serum albumin (Biosharp, Hefei, AH, China) for 1 h at room temperature and then probed with the primary antibody overnight at 4 °C. Next, the membrane was incubated with the corresponding HRP-conjugated secondary antibody for 2 h at 37 °C and then washed with phosphate buffer saline (PBS)-Tween20 (PBST). Finally, bands were visualized by enhanced chemiluminescence (ECL) as reported previously [26] and analyzed using ImageJ software. Relative quantity of proteins was determined by normalizing to levels of loading controls.

Immunofluorescence Microscopy

Brain tissues were fixed in 4% paraformaldehyde and embedded in paraffin. The tissues were cut into 4 μm sections and dewaxed immediately before immunofluorescence staining. Double immunofluorescence was performed with primary antibodies for p-eIF2α or ATF4 and NeuN. After washing three times with PBS, the samples were stained with appropriate secondary antibodies. All primary antibodies were applied at a dilution of 1:100, and all secondary antibodies were diluted 1:500. Normal rabbit IgG was used as a negative control (data not shown). Sections were observed with a fluorescence microscope (BX50/BX-FLA/DP70, Olympus Co., Japan), and relative fluorescence intensity was analyzed as described previously [27].

TUNEL Staining

Quantitation of apoptotic cells was performed using TUNEL staining according to the manufacturer's protocol (DeadEnd Fluorometric Kit, Promega, WI, USA). Three sections per rat were examined and photographed in parallel for TUNEL-positive cell counting.

FJB Staining

FJB staining was used to reveal the neuronal degradation, which was sensitive and highly specific [28]. The procedures were performed as previously described [29]. In brief, the brain sections were deparaffinized and then dried in an oven. Then, sections were rehydrated using xylene and a series of graded ethanol solutions followed by water. Brain sections were permeabilized in 0.04% Triton X-100 and incubated with FJB dye solution. Then they were observed and photographed in parallel by a fluorescence microscope (BX50/BX-FLA/DP70, Olympus Co.). The FJB-positive cell numbers were counted after being observed and photographed in parallel for six microscopic fields in each tissue. Microscopy was performed by an observer blind to the experimental group.

Statistical Analysis

GraphPad Prism 7 was used for all statistical analysis. Neurobehavioral scoring is presented as the median with the interquartile range. All other data represent mean ± SEM. One-way ANOVA for multiple comparisons and the Student-Newman-Keuls post hoc test were used to assess differences among all groups. Differences were considered significant at $p < 0.05$.

Post hoc power analysis was performed according to a power analysis (PRISM, *t*-test comparison of the mean). Based on a two-sample *t*-test with a specified mean difference between the sham and ICH group, an estimated standard deviation was calculated, and alpha = 0.05, power > 0.75 for a sample size of $n = 6$ per groups. We assigned six rats in each groups because this number was close to the prediction.

Results

Elevation of p-eIF2α and ATF4 Levels in Brain Tissues After ICH

In experiment 1, the Western blot analysis showed that the ICH group expressed higher protein levels of p-eIF2α and ATF4 compared with the sham group. After induction of ICH, protein levels of p-eIF2α and ATF4 in brain tissues were significantly elevated at 4 h and peaked at 12 h, which were remarkably higher in the 12 h group compared with the 8 h and 16 h groups (Fig. 2a, b). Double immunofluores-

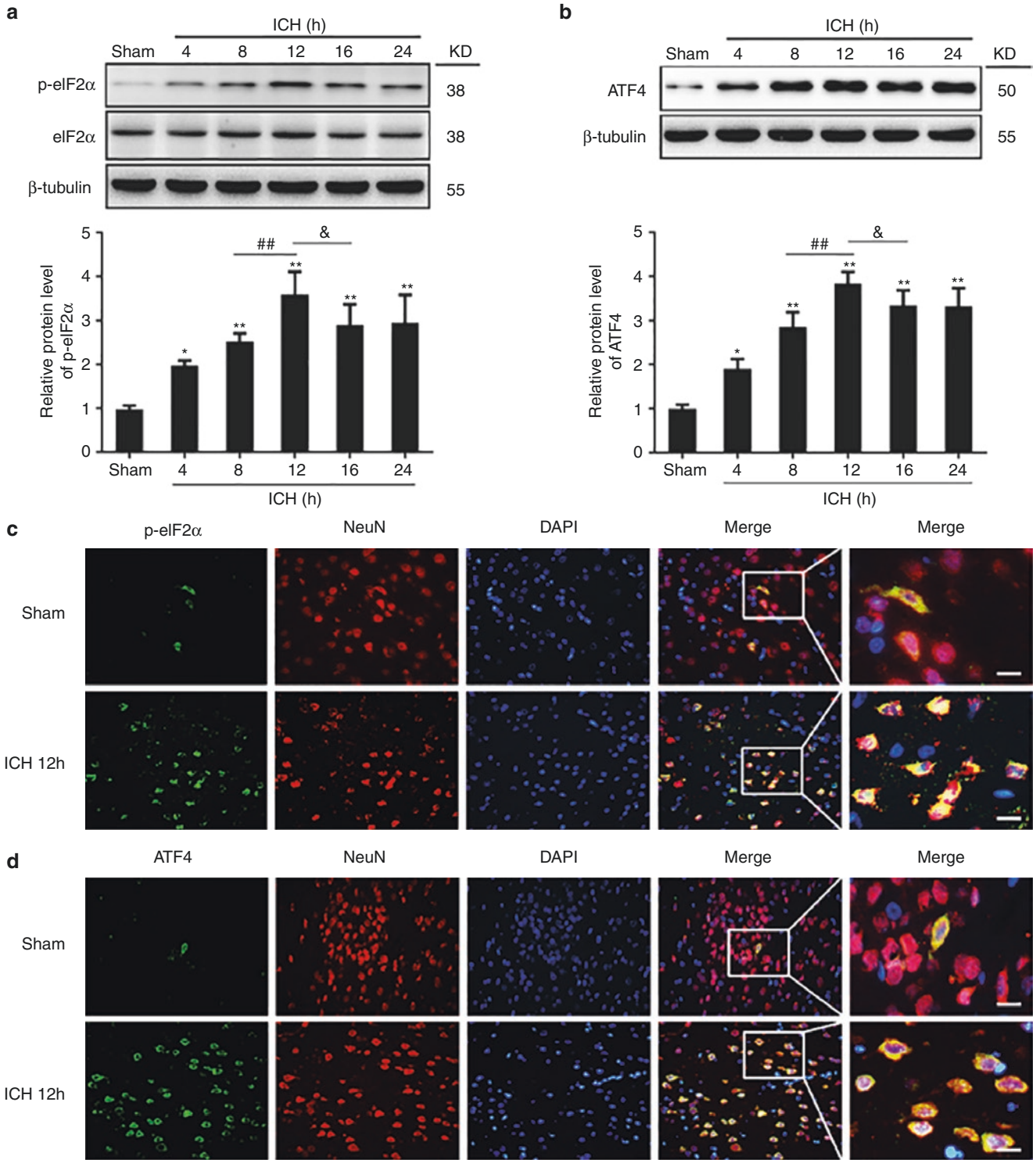

Fig. 2 Protein levels of p-eIF2α and ATF4 in brain tissues after ICH. (**a**) Western blot analysis and quantification of p-eIF2α and eIF2α protein levels at different time points following ICH in brain tissues. (**b**) Western blot analysis and quantification of ATF4 protein levels at different time points following ICH in vivo. (**c**) Immunofluorescence in brain tissues. Double immunofluorescence was performed with p-eIF2α antibodies (green) and a neuronal marker (NeuN, red). Nuclei were fluorescently labeled with DAPI (blue). Scale bar = 30 μm. (**d**) Immunofluorescence in brain tissues. Double immunofluorescence was performed with ATF4 antibodies (green) and a neuronal marker (NeuN, red). Nuclei were fluorescently labeled with DAPI (blue). Scale bar = 30 μm. In A and B, mean values for the sham group or control group were normalized to 1.0. One-way ANOVA followed by Student-Newman-Keuls post hoc tests were used. Data are mean ± SEM. $^{*}p < 0.05$, $^{**}p < 0.01$ vs. sham group; $^{\#\#}p < 0.01$ 12 h group vs. 8 h group; $^{\&}p < 0.05$ 12 h group vs. 16 h group, $n = 12$

cence staining in sham and ICH groups further verified that p-eIF2α and ATF4 were markedly expressed in neurons and increased at 12 h after ICH (Fig. 2c, d). Hence, we focused on the PERK pathway in neurons at 12 h after ICH in the following studies.

PERK Pathway Activation Ameliorated Neurological Behavior Impairment and Brain Edema in the Early Phase of ICH

The PERK inhibitor, GSK2606414, was injected intracerebroventricularly at 1 h after ICH, and the eIF2α dephosphorylation inhibitor, salubrinal, was injected intraperitoneally at 30 min before ICH. Then the protein levels of p-eIF2α and ATF4 were detected by Western blot. It was shown that administering GSK2606414 significantly suppressed the increases in protein levels of p-eIF2α and ATF4 after ICH. On the contrary, the inhibitor of eIF-2α dephosphorylation, salubrinal, could significantly increase protein levels of p-eIF2α and ATF4 (Fig. 3a–c). To assess the effects of manipulating the PERK pathway on neurological behavioral impairment after ICH, all rats were subjected to behavioral testing before being killed. Remarkable neurological behavioral impairment was observed in the ICH, ICH + vehicle (for GSK2606414), and ICH + vehicle (for salubrinal) groups compared with the sham group at 12 h after ICH. After intracerebroventricular GSK2606414 injection, neurological behavioral impairment was exacerbated. In contrast, after intraperitoneal injection of salubrinal, neurobehavioral deficits were significantly ameliorated (Fig. 3d). Furthermore, we evaluated brain water content in each group. In the ICH group, brain water content was significantly increased when compared with the sham group. Salubrinal treatment significantly reduced ICH-induced brain water content, whereas GSK2606414 treatment significantly increased brain edema (Fig. 3e).

PERK Pathway Activation Inhibited Neuronal Apoptosis and Necrosis Induced by ICH at 12 h In Vivo

It has been reported that PERK signaling pathway was involved in ER stress-induced apoptosis. The ER-specific apoptosis pathway is activated by promoting expression of CHOP and CASP12 [10]. Western blot was used to measure the protein levels of CHOP and the cleavage of CASP12. The protein levels of CHOP and cleaved CASP12 significantly increased at 12 h in the ICH, ICH + vehicle (for GSK2606414), and ICH + vehicle (for salubrinal) groups (Fig. 4a). With the administering of GSK2606414, the levels of CHOP and cleaved CASP12 were significantly increased. Otherwise, with the treatment of salubrinal, it showed an opposite effect, exhibiting that significantly suppressed the increase of CHOP and cleaved CASP12 induced by ICH (Fig. 4a). In addition, histological examination showed that the number of TUNEL-positive neurons and FJB-positive cells significantly increased at 12 h in the ICH, ICH + vehicle (for GSK2606414), and ICH + vehicle (for salubrinal) groups (Fig. 4b, c). Treatment with GSK2606414 significantly increased the total number of TUNEL and NeuN double-stained cells at 12 h after ICH, as well as the FJB-positive cells, compared with the ICH + vehicle (for GSK2606414) group at 12 h after ICH (Fig. 4b, c). Compared with the inhibition experiments, activation of the PERK pathway yielded opposite results. Treatment with salubrinal significantly lowered the total number of TUNEL and NeuN double-stained cells at 12 h after ICH (Fig. 4b). Similarly, the ICH + salubrinal group showed a significant reduction in the number of FJB-positive cells compared with the ICH + vehicle (for salubrinal) group at 12 h after ICH (Fig. 4c).

PERK Pathway Activation Promoted Neuronal Survival at 12 h After ICH In Vitro

In vitro, primary cortical neurons were subjected to OxyHb to mimic the ICH model. Similar trends were observed in expression of p-eIF2α and ATF4 with the in vivo experiment after the treatment of GSK2606414 and salubrinal. The results demonstrated that GSK2606414 treatment could significantly suppress the increases in protein levels of p-eIF2α and ATF4 induced by the OxyHb treatment. On the other hand, salubrinal significantly increased protein levels of p-eIF2α and ATF4 (Fig. 5a). Compared with the control group, a significant decrease in neuronal viability was observed in the OxyHb group, and this was exacerbated by inhibition of the PERK pathway (Fig. 5b). On the contrary, after the treatment of salubrinal, the cell viability was rescued in neurons under OxyHb stimulus (Fig. 5b). Similar to the results of cell viability, the LDH release was elevated after OxyHb stimulus. And with the treatment of GSK2606414 and salubrinal, the release of LDH was exacerbated rescued respectively compared to vehicle group (Fig. 5c).

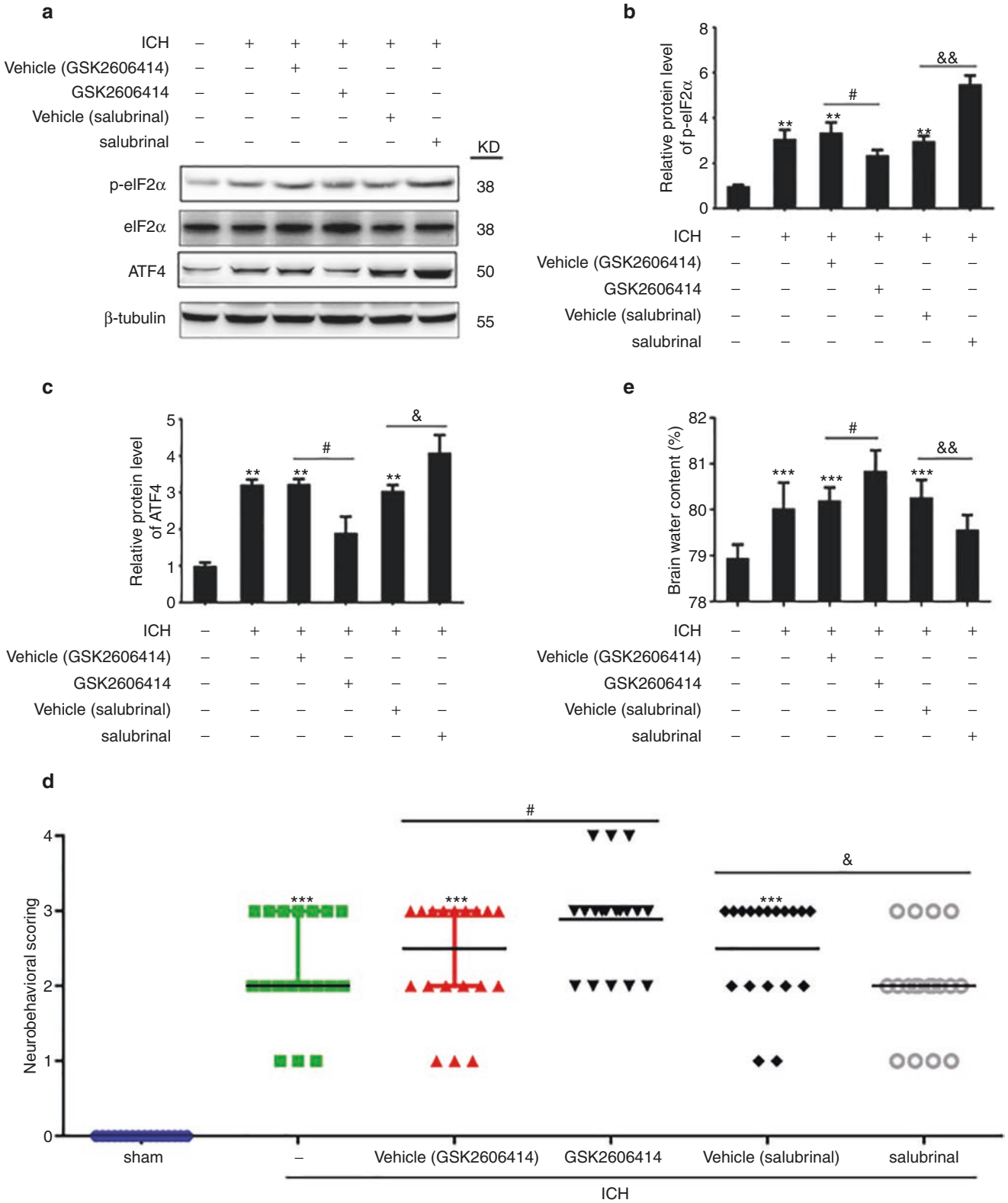

Fig. 3 Effects of PERK pathway on brain injury in vivo at 12 h after ICH. (**a**–**c**) Western blot analysis showing phosphorylation levels of eIF2α and expression of ATF4 in the sham, ICH, ICH + vehicle (for GSK2606414), ICH + GSK2606414, ICH + vehicle (for salubrinal), and ICH + salubrinal groups at 12 h after ICH onset. $^{*}p < 0.05$ vs. sham group, $^{**}p < 0.01$ vs. sham group; $^{\#}p < 0.05$, $^{\&}p < 0.05$, $^{\&\&}p < 0.01$, $n = 12$. (**d**) Neurological scoring. $^{***}p < 0.001$ vs. sham group; $^{\#}p < 0.05$, $^{\&}p < 0.05$, $n = 18$. (**e**) Brain water content at 12 h post-ICH. $^{***}p < 0.001$ vs. sham group; $^{\#}p < 0.05$, $^{\&\&}p < 0.01$, $n = 6$

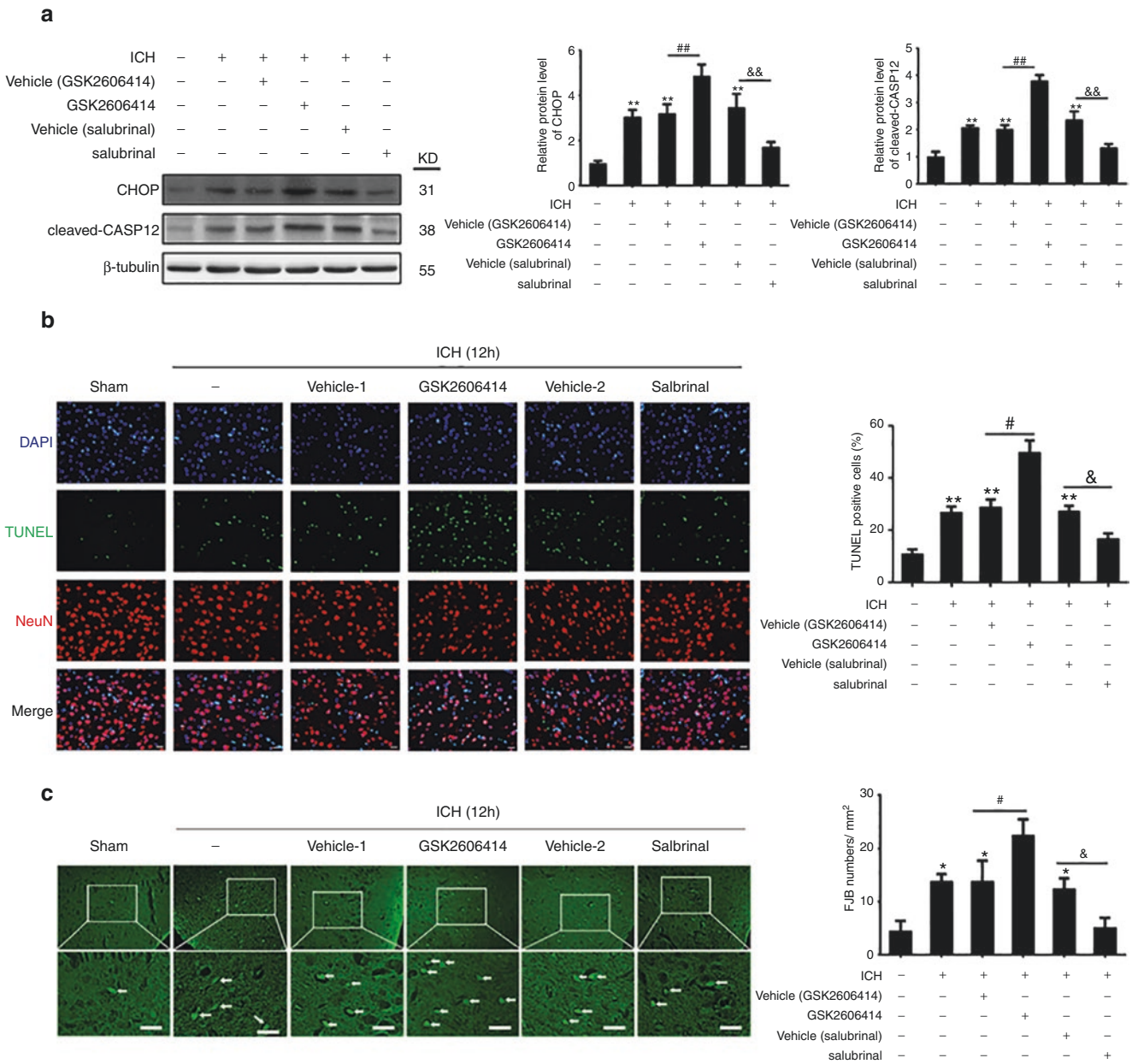

Fig. 4 PERK pathway was involved in ICH-induced neuronal apoptosis and necrosis in vivo at 12 h. (**a**) Western blot analysis showing expression of CHOP and cleaved CASP12 in the sham, ICH, ICH + vehicle (for GSK2606414), ICH + GSK2606414, ICH + vehicle (for salubrinal), and ICH + salubrinal groups at 12 h after ICH onset. $^{**}p < 0.01$ vs. sham group; $^{\#\#}p < 0.01$, $^{\&\&}p < 0.01$, $n = 6$. (**b**) TUNEL staining showing apoptotic cells in the sham, ICH, ICH + vehicle (for GSK2606414), ICH + GSK2606414, ICH + vehicle (for salubrinal), and ICH + salubrinal groups at 12 h after ICH onset. Double immunofluorescence was performed with TUNEL (green) and a neuronal marker (NeuN, red), and nuclei were fluorescently labeled with DAPI (blue). Scale bar = 30 μm. The percentage of TUNEL-positive neurons in each group. $^{**}p < 0.01$ vs. sham group; $^{\#}p < 0.05$, $^{\&}p < 0.05$, $n = 12$. (**c**) FJB staining (green) shows neuronal degradation in the cerebral cortex. Scale bar = 26 μm. Arrows indicate FJB-positive cells. FJB-positive cells/mm^2 was determined in the brain cortex at 12 h. $^{*}p < 0.05$ vs. sham group; $^{\#}p < 0.05$, $^{\&}p < 0.05$, $n = 12$

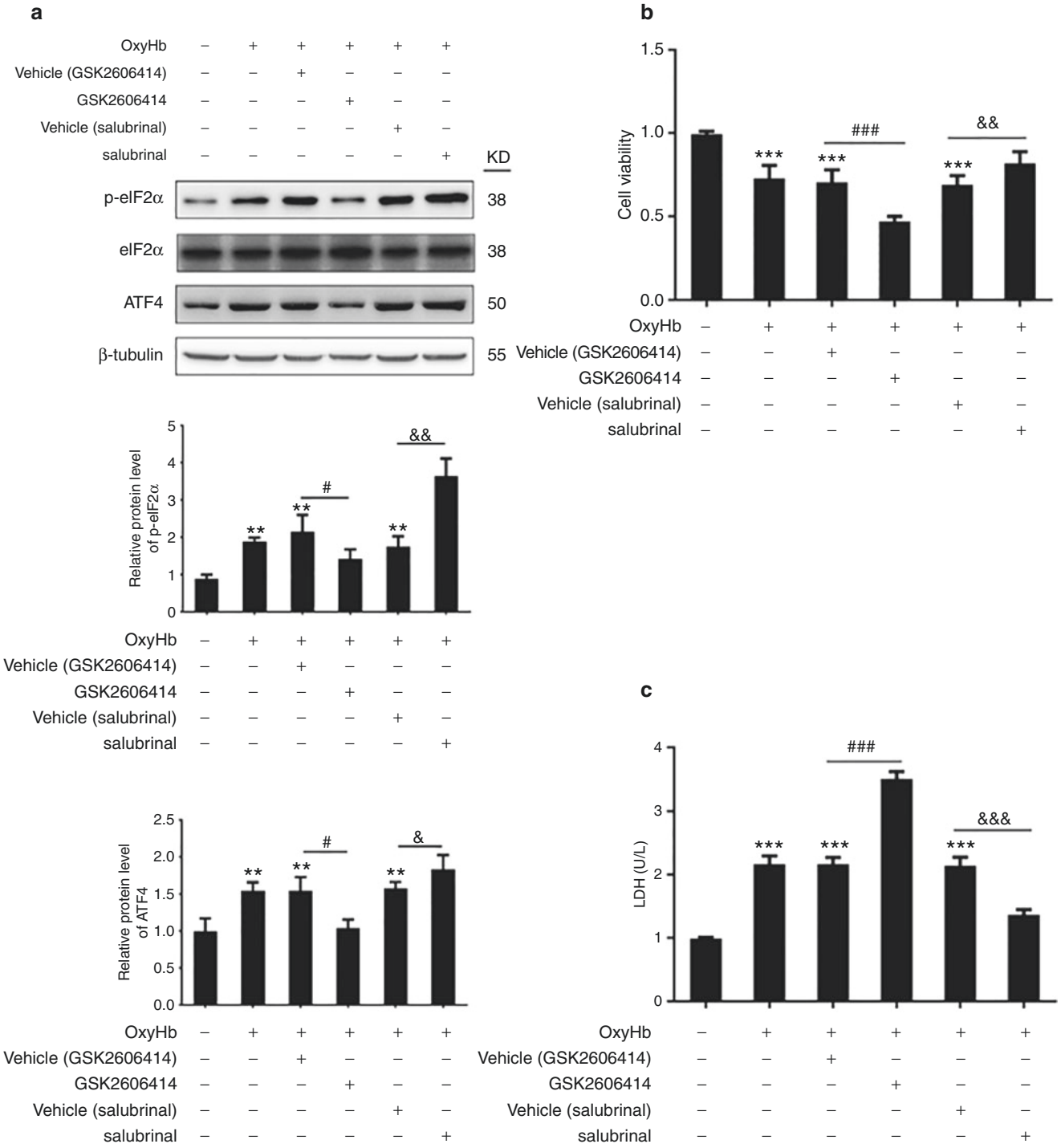

Fig. 5 Effects of PERK-eIF2-ATF4 pathway on in OxyHb-induced neuronal damage. (**a**) Western blot analysis showing phosphorylation levels of eIF2α and expression of ATF4 in the control, OxyHb, OxyHb + vehicle (for GSK2606414), OxyHb + GSK2606414, OxyHb + vehicle (for salubrinal), and OxyHb + salubrinal groups at 12 h. $^{**}p < 0.01$ vs. control group; $^{\#}p < 0.05$, $^{\&}p < 0.05$, $^{\&\&}p < 0.01$, $n = 6$. (**b**) Cell viability in neurons was measured by SRB assay. $^{***}p < 0.001$ vs. control group; $^{\#\#\#}p < 0.001$; $^{\&\&}p < 0.01$, $n = 6$. (**c**) LDH analysis. $^{***}p < 0.001$ vs. control group; $^{\#\#\#}p < 0.001$; $^{\&\&\&}p < 0.001$, $n = 6$

PERK Pathway Activation Reduced Neuronal Apoptosis at 12 h After ICH In Vitro

Experiments performed in vitro yielded similar results. With the treatment of GSK2606414, the protein levels of CHOP and cleaved CASP12 were significantly increased at 12 h in neurons after treatment with OxyHb (Fig. 6a), when compared with the OxyHb + vehicle (for GSK2606414) group. In addition, neurons subjected to OxyHb + GSK2606414 showed a significant increase in neuronal apoptosis compared with the OxyHb + vehicle (for GSK2606414) group measured by TUNEL staining (Fig. 6b). However, treatment with salubrinal could significantly suppress the expression of CHOP and cleaved CASP12 at 12 h in neurons after treatment with OxyHb (Fig. 6a) when compared with the OxyHb + vehicle (for salubrinal) group. Also, neurons subjected to OxyHb + salubrinal showed significant inhibition of neuronal apoptosis compared with the OxyHb + vehicle (for salubrinal) group (Fig. 6b).

Discussion

ER stress-induced cell death is one of the most significant causes of brain injury [30]. When ER stress occurs, cells restore ER function by initiating a series of adaptive processes through the UPR [31]. Previous reports have suggested that the PERK pathway, which is part of the UPR, may participate in a range of pathophysiological processes of neurological diseases [32, 33]. However, it is unclear whether the PERK pathway is involved in the occurrence and development of post-ICH brain injury. Here, for the first time, we explored a possible role of the PERK pathway during the early phase of ICH-induced SBI both in vivo and in vitro. As previously reported, when unfolded or misfolded protein accumulates, PERK is activated by oligomerization and trans-autophosphorylation [34]. Phosphorylated PERK specifically induces phosphorylation of eIF2α at ser51 (p-eIF2α), which then upregulates transcription factor ATF4 (Fig. 7) [35]. In experiment 1, we first investigated spatial-temporal expression of p-eIF2α and ATF4 protein after ICH. As shown in Fig. 2a, b, under ICH condition, p-eIF2α and downstream ATF4 showed the same trend, such that the ratio of p-eIF2α/eIF2α and protein levels of ATF4 were remarkably elevated at 4 h and peaked at 12 h. Furthermore, to investigate spatial expression of the PERK pathway in brain tissue, as shown in Fig. 2c, d, double immunofluorescence staining indicated that p-eIF2α and ATF4 were markedly expressed in neurons after ICH. This suggests that the PERK pathway was activated and that this pathway may play a vital role in ICH-induced SBI. Based on these findings, subsequent experiments focused on the PERK pathway in neurons at 12 h after ICH.

It is well known that levels of phosphorylated protein can be regulated by inhibiting both phosphorylation and dephosphorylation. Consistent with previous studies [36, 37], as shown in Fig. 3a, the potent p-eIF2α dephosphorylation inhibitor, salubrinal, significantly increased expression of p-eIF2α and ATF4 at 12 h after ICH, whereas levels of both proteins were decreased by the selective PERK inhibitor, GSK2606414. Previous research has demonstrated that p-eIF2α suppresses initiating translation of global protein synthesis, which promotes cell survival by preventing further accumulation of unfolded or misfolded proteins in the ER [38, 39]. In addition, it is important for recovery from various stresses that ATF4 triggers expression of genes involved in amino acid metabolism, antioxidant stress, protein folding, and autophagy [40]. To define the effects of the PERK pathway on ICH-induced neurological behavioral impairment and brain edema, we performed neurological scoring and measured brain water content.

As shown in Fig. 3d, e, rats showed severe neurological behavioral impairment and brain edema compared with the sham group at 12 h after ICH induction. ICH-induced neurological deficits and edema were ameliorated after activating the PERK pathway with salubrinal and aggravated by blocking the PERK pathway with GSK2606414. In addition, TUNEL and FJB staining were utilized to explore effects of the PERK pathway on apoptosis in brain tissues at 12 h post-ICH induction. As shown in Fig. 4b, c, the numbers of TUNEL-positive cells and FJB-positive cells in brain tissue around the hematomas were significantly increased in the ICH group compared with the sham group, and these cell numbers were augmented in the ICH + GSK2606414 group and reduced in the ICH + salubrinal group. These data clearly suggest that increasing expression of p-eIF2α and ATF4 promotes neuronal survival and suppresses apoptosis, and this process can be reversed by reducing these protein levels after ICH.

At least three branches participate in ER stress-induced apoptotic events. These include the CHOP pathway [41], the ER-associated CASP12 pathway [42], and the cJUN NH2-terminal kinase (JNK) pathway [43, 44]. Interestingly, as shown in Fig. 4a, GSK2606414 administration significantly increased CHOP expression at 12 h after ICH, while treatment with salubrinal remarkably suppressed expression of

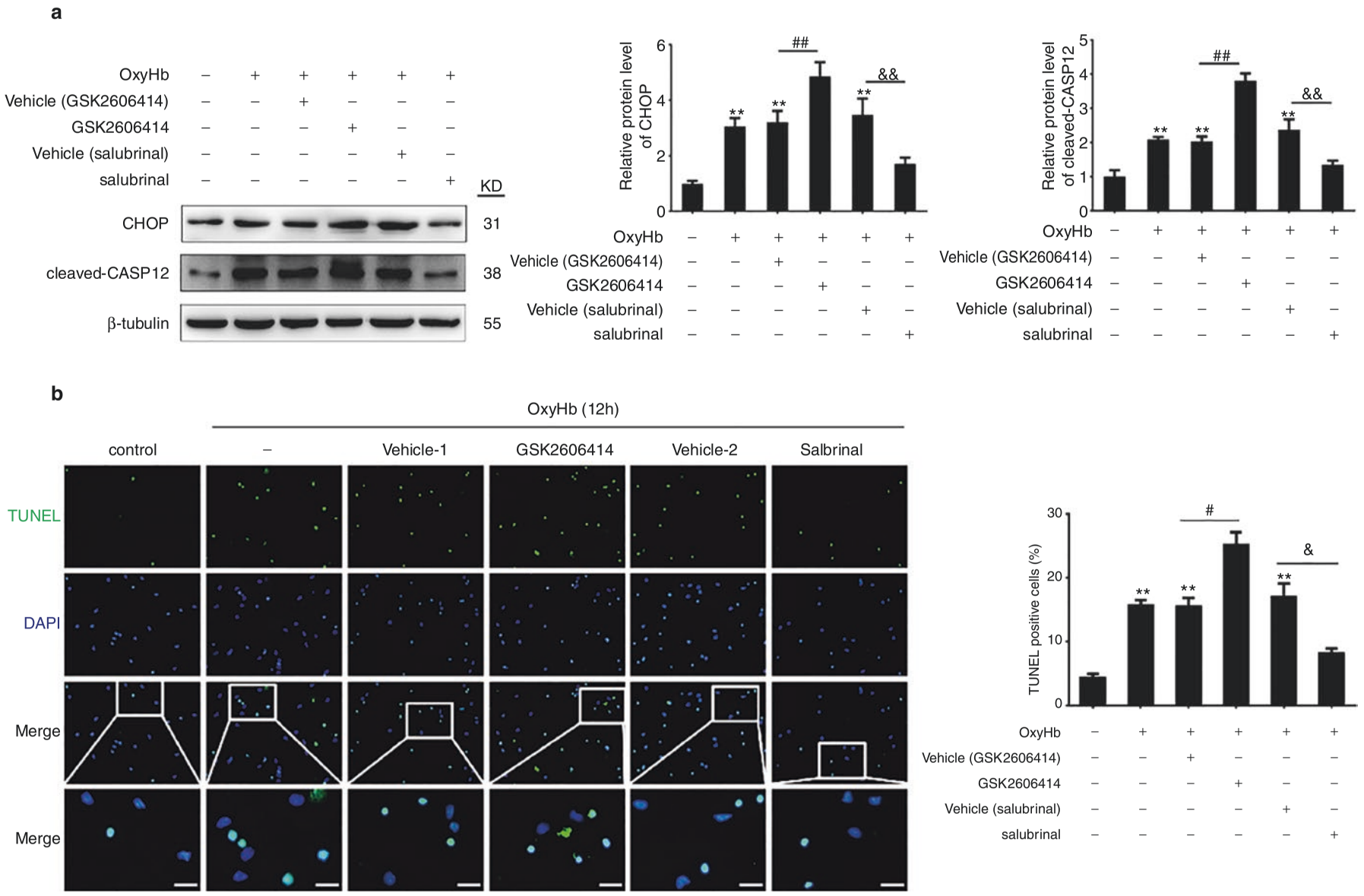

Fig. 6 PERK-eIF2-ATF4 pathway participated in OxyHb-induced neuronal apoptosis in vitro. (**a**) Western blot analysis showing expression of CHOP and CASP12 in the control, OxyHb, OxyHb + vehicle (for GSK2606414), OxyHb + GSK2606414, OxyHb + vehicle (for salubrinal), and OxyHb + salubrinal groups at 12 h. $^{**}p < 0.01$ vs. control group; $^{\#\#}p < 0.01$; $^{\&\&}p < 0.01$, $n = 6$. (**b**) TUNEL staining to elucidate the role of PERK in OxyHb-treated neurons in vitro at 12 h. Representative images from control, OxyHb, OxyHb + vehicle (for GSK2606414), OxyHb + GSK2606414, OxyHb + vehicle (for salubrinal), and OxyHb + salubrinal groups. Each group was subjected to OxyHb except for the control group. Scale bar = 20 μm. The percentage of TUNEL-positive cells. $^{**}p < 0.01$ vs. control group; $^{\#}p < 0.05$, $^{\&}p < 0.05$, $n = 6$

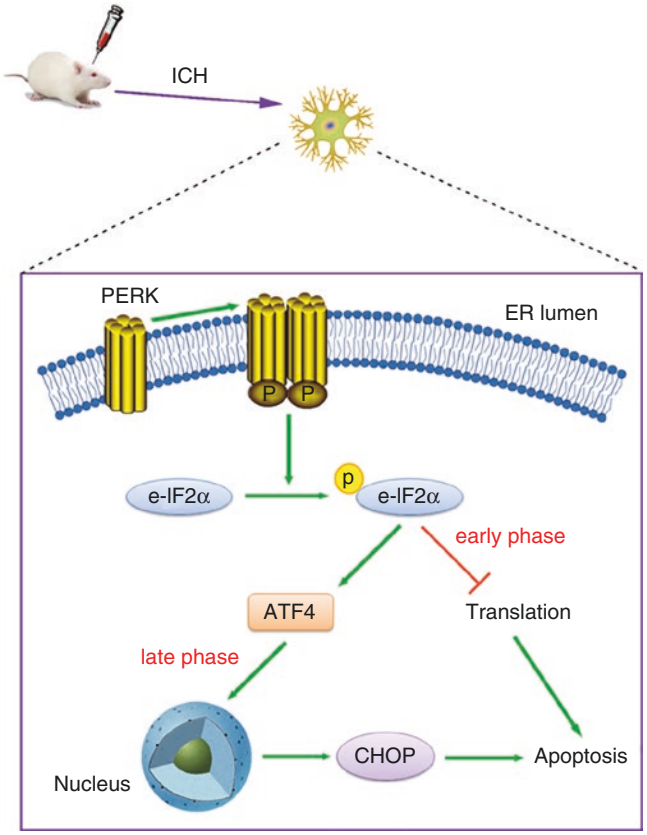

Fig. 7 Schematic representation of potential mechanisms of the PERK pathway in neuroprotection under ICH conditions. Following ICH, the activation of the ER stress response induces neuronal apoptosis. Consequently, activated PERK pathway increases the protein levels of p-eIF2α and ATF4. At the early phase of ICH-induced brain injury, the PERK pathway is triggered to block the initiation process of translation, thereby reducing protein synthesis and decreasing the ER load, which might play a significant role in neuroprotection

these pro-apoptotic proteins. CHOP, also known as growth arrest- and DNA damage-inducible gene 153 (GADD153), is an ER stress-specific transcription factor that consist of an N-terminal transcriptional activation domain and a C-terminal basic-leucine zipper [45]. Normally, CHOP is expressed at extremely low levels. However, once ER stress occurs, its expression significantly increases. CHOP can be activated via the PERK-eIF2α phosphorylation pathway, which triggers an increase in expression of ATF4. ATF4 then binds to the site of an amino acid reaction element of the CHOP promoter. In this study, we found that although the PERK-eIF2α-ATF4 axis is indispensable for CHOP expression, after treatment, there is an inverse relationship between protein levels of CHOP and expression of p-eIF2α and ATF4. This suggests that the PERK pathway primarily plays a neuroprotective rather than pro-apoptotic role at 12 h after ICH.

Another important pro-apoptosis protein is CASP12, which can induce apoptosis alone through ER stress rather than other apoptotic pathways. Under normal physiological conditions, CASP12 exists as an inactive zymogen similar to other cysteine proteases. Abnormal calcium can trigger specific activation of CASP12 in the ER, which coordinates with other ER stress molecules to activate CASP9 that transmits information to CASP3, causing cells to eventually undergo apoptosis [46]. In CASP12-deficient cells, apoptosis can be evoked by certain stimuli other than ER stress, which suggests that CASP12 is a specific apoptosis factor associated with ER stress [47]. Therefore, we selected CHOP and CASP12 as markers of ER stress and apoptosis. As shown in Fig. 3b, results support anti-apoptotic effects of the PERK pathway during the early phase of ICH-induced SBI. However, although CASP12 has been recognized as a marker of ER stress-induced apoptosis in rats and mice, humans lack a functional CASP12 homologue due to multiple stop codons [45]. This represents a major impediment in translation from basic experiments to clinical practice.

In many previous in vitro studies, ER stress could be induced by tunicamycin, which is a glycosylation inhibitor, or thapsigargin, which is a highly selective inhibitor of the ER Ca^{2+}-dependent ATPase [48, 49]. To define further the role of the PERK pathway, we established an in vitro model of ICH by treating primary cortical neurons with OxyHb. As shown in Figs. 5 and 6, neurons subjected to OxyHb yielded similar results regarding TUNEL staining and expression of p-eIF2α, ATF4, CHOP, and CASP12. Compared with the control group, a significant decrease in neuronal viability was observed in the OxyHb group, and viability was reduced by GSK2606414 treatment and enhanced by salubrinal administration. Consistent with these findings, as shown in Fig. 6b, the necrosis index showed a trend similar to that of the apoptotic index. Taken together, these data further confirm that the PERK pathway plays a neuroprotective role during the early phase of SBI induced by ICH. In addition, studies of ICH have increasingly recognized the significance of particular blood components in brain injury [50]. Thus, different responses may be induced by different blood components. Although that OxyHb mimics ICH induction has been well-accepted, which specific blood component is predominantly responsible for activation of the PERK pathway is unknown.

The current study has several limitations. The generally accepted view is that in a physiological state, the three transmembrane protein receptors, ATF6, IRE1, and PERK, are bound by glucose-regulated protein 78 (GRP78), which dissociates from these receptors and allows their activation under stress conditions [51]. This point of view has been challenged because it has been reported that unfolded or misfolded proteins can bind directly to ER stress sensor proteins to activate the UPR [52]. In this study, we only focused on effects of the PERK pathway, and initiation of the PERK pathway after ICH requires further study. In addition, current knowledge indicates that the UPR protects cells from ER

stress by reducing synthesis of new proteins and enhancing degradation of unfolded or misfolded proteins. However, failure of the UPR due to severe or prolonged ER stress eventually promotes apoptotic cell death, which is an effective measure of protecting an organism from rogue cells expressing dysfunctional signal molecules [53]. Unfortunately, it has not been clear how the UPR globally coordinates cytoprotective and pro-apoptotic outcomes between a survival or death fate [54].

Based on this, we have proposed a hypothesis that the PERK pathway predominantly plays a neuroprotective role in the early phase and a pro-apoptotic role in the late phase of ICH-induced SBI. In our recent study, it has been reported that PERK pathway activation promoted ICH-induced SBI by inducing neuronal apoptosis in the late phase [55]. And in this study, the neuroprotective role of the PERK pathway in the early phase has been confirmed.

Acknowledgments This work was supported by the Project of Jiangsu Provincial Medical Innovation Team (No. CXTDA2017003), Jiangsu Provincial Medical Youth Talent (No. QNRC2016728), Suzhou Key Medical Centre (No. Szzx201501), Scientific Department of Jiangsu Province (No. BE2017656), Suzhou Government (No. SYS201608 and LCZX201601), Jiangsu Province (No. 16KJB320008), and Zhangjiagang Science and Technology Pillar Program (ZKS1712).

Conflict of Interest: **We declare that we have no conflicts of interest.**

References

1. van Asch CJ, Luitse MJ, Rinkel GJ, van der Tweel I, Algra A, Klijn CJ. Incidence, case fatality, and functional outcome of intracerebral haemorrhage over time, according to age, sex, and ethnic origin: a systematic review and meta-analysis. Lancet Neurol. 2010;9(2):167–76.
2. Wilkinson DA, Pandey AS, Thompson BG, Keep RF, Hua Y, Xi G. Injury mechanisms in acute intracerebral hemorrhage. Neuropharmacology. 2017;
3. Niu M, Dai X, Zou W, Yu X, Teng W, Chen Q, Sun X, Yu W, Ma H, Liu P. Autophagy, endoplasmic reticulum stress and the unfolded protein response in intracerebral hemorrhage. Transl Neurosci. 2017;8(1)
4. Begum G, Harvey L, Dixon CE, Sun D. ER stress and effects of DHA as an ER stress inhibitor. Transl Stroke Res. 2013;4(6):635–42.
5. Nakka VP, Prakash-babu P, Vemuganti R. Crosstalk between endoplasmic reticulum stress, oxidative stress, and autophagy: potential therapeutic targets for acute CNS injuries. Mol Neurobiol. 2016;53(1):532–44.
6. Halliday M, Hughes D, Mallucci GR. Fine-tuning PERK signaling for neuroprotection. J Neurochem. 2017;
7. Wang Y, Mao L, Zhang L, Zhang L, Yang M, Zhang Z, Li D, Fan C, Sun B. Adoptive regulatory T-cell therapy attenuates subarachnoid hemorrhage-induced cerebral inflammation by suppressing TLR4/NF-B signaling pathway. Curr Neurovasc Res. 2016;13(2):121–6.
8. Choi SK, Lim M, Byeon SH, Lee YH. Inhibition of endoplasmic reticulum stress improves coronary artery function in the spontaneously hypertensive rats. Sci Rep. 2016;6:31925.
9. Zhang HY, Wang ZG, Lu XH, Kong XX, Wu FZ, Lin L, Tan X, Ye LB, Xiao J. Endoplasmic reticulum stress: relevance and therapeutics in central nervous system diseases. Mol Neurobiol. 2015;51(3):1343–52.
10. Shen H, Pan XD, Zhang J, Zeng YQ, Zhou M, Yang LM, Ye B, Dai XM, Zhu YG, Chen XC. Endoplasmic reticulum stress induces the early appearance of pro-apoptotic and anti-apoptotic proteins in neurons of five familial alzheimer's disease mice. Chin Med J. 2016;129(23):2845–52.
11. Ikram MA, Wieberdink RG, Koudstaal PJ. International epidemiology of intracerebral hemorrhage. Curr Atheroscler Rep. 2012;14(4):300–6.
12. Morotti A, Goldstein JN. Diagnosis and management of acute intracerebral hemorrhage. Emerg Med Clin North Am. 2016;34(4):883–99.
13. Axten JM, Medina JR, Feng Y, Shu A, Romeril SP, Grant SW, Li WH, Heerding DA, Minthorn E, Mencken T, Atkins C, Liu Q, Rabindran S, Kumar R, Hong X, Goetz A, Stanley T, Taylor JD, Sigethy SD, Tomberlin GH, Hassell AM, Kahler KM, Shewchuk LM, Gampe RT. Discovery of 7-methyl-5-(1-{[3-(trifluoromethyl) phenyl]acetyl}-2,3-dihydro-1H-indol-5-yl)-7H-p yrrolo[2,3-d] pyrimidin-4-amine (GSK2606414), a potent and selective first-in-class inhibitor of protein kinase R (PKR)-like endoplasmic reticulum kinase (PERK). J Med Chem. 2012;55(16):7193–207.
14. Scheper W, Hoozemans JJ. A new PERKspective on neurodegeneration. Sci Transl Med. 2013;5(206):206fs37.
15. Rubovitch V, Barak S, Rachmany L, Goldstein RB, Zilberstein Y, Pick CG. The neuroprotective effect of salubrinal in a mouse model of traumatic brain injury. NeuroMolecular Med. 2015;17(1):58–70.
16. Boyce M, Bryant KF, Jousse C, Long K, Harding HP, Scheuner D, Kaufman RJ, Ma D, Coen DM, Ron D, Yuan J. A selective inhibitor of eIF2alpha dephosphorylation protects cells from ER stress. Science. 2005;307(5711):935–9.
17. Deinsberger W, Vogel J, Kuschinsky W, Auer LM, Boker DK. Experimental intracerebral hemorrhage: description of a double injection model in rats. Neurol Res. 1996;18(5):475–7.
18. Hu M, Luo Q, Alitongbieke G, Chong S, Xu C, Xie L, Chen X, Zhang D, Zhou Y, Wang Z, Ye X, Cai L, Zhang F, Chen H, Jiang F, Fang H, Yang S, Liu J, Diaz-Meco MT, Su Y, Zhou H, Moscat J, Lin X, Zhang XK. Celastrol-induced Nur77 interaction with TRAF2 alleviates inflammation by promoting mitochondrial ubiquitination and autophagy. Mol Cell. 2017;66(1):141–153 e6.
19. Anuncibay-Soto B, Perez-Rodriguez D, Santos-Galdiano M, Font E, Regueiro-Purrinos M, Fernandez-Lopez A. Post-ischemic salubrinal treatment results in a neuroprotective role in global cerebral ischemia. J Neurochem. 2016;138(2):295–306.
20. Shen H, Chen Z, Wang Y, Gao A, Li H, Cui Y, Zhang L, Xu X, Wang Z, Chen G. Role of neurexin-1beta and neuroligin-1 in cognitive dysfunction after subarachnoid hemorrhage in rats. Stroke. 2015;46(9):2607–15.
21. Wang Z, Zhou F, Dou Y, Tian X, Liu C, Li H, Shen H, Chen G. Melatonin alleviates intracerebral hemorrhage-induced secondary brain injury in rats via suppressing apoptosis, inflammation, oxidative stress, DNA damage, and mitochondria injury. Transl Stroke Res. 2018;9(1):74–91.
22. Pacifici M, Peruzzi F. Isolation and culture of rat embryonic neural cells: a quick protocol. J Vis Exp. 2012;(63):e3965.
23. Wang Z, Chen Z, Yang J, Yang Z, Yin J, Zuo G, Duan X, Shen H, Li H, Chen G. Identification of two phosphorylation sites essential for annexin A1 in blood-brain barrier protection after experimental intracerebral hemorrhage in rats. J Cereb Blood Flow Metab. 2017;37(7):2509–25.
24. Jiang X, Wei Y, Zhang T, Zhang Z, Qiu S, Zhou X, Zhang S. Effects of GSK2606414 on cell proliferation and endoplasmic reticulum stress associated gene expression in retinal pigment epithelial cells. Mol Med Rep. 2017;15(5):3105–10.

25. Sokka AL, Putkonen N, Mudo G, Pryazhnikov E, Reijonen S, Khiroug L, Belluardo N, Lindholm D, Korhonen L. Endoplasmic reticulum stress inhibition protects against excitotoxic neuronal injury in the rat brain. J Neurosci. 2007;27(4): 901–8.
26. Zhai W, Chen D, Shen H, Chen Z, Li H, Yu Z, Chen G. A1 adenosine receptor attenuates intracerebral hemorrhage-induced secondary brain injury in rats by activating the P38-MAPKAP2-Hsp27 pathway. Mol Brain. 2016;9(1):66.
27. Cui Y, Duan X, Li H, Dang B, Yin J, Wang Y, Gao A, Yu Z, Chen G. Hydrogen sulfide ameliorates early brain injury following subarachnoid hemorrhage in rats. Mol Neurobiol. 2016;53(6): 3646–57.
28. Zhu HT, Bian C, Yuan JC, Chu WH, Xiang X, Chen F, Wang CS, Feng H, Lin JK. Curcumin attenuates acute inflammatory injury by inhibiting the TLR4/MyD88/NF-kappaB signaling pathway in experimental traumatic brain injury. J Neuroinflammation. 2014;11:59.
29. Lin S, Yin Q, Zhong Q, Lv FL, Zhou Y, Li JQ, Wang JZ, Su BY, Yang QW. Heme activates TLR4-mediated inflammatory injury via MyD88/TRIF signaling pathway in intracerebral hemorrhage. J Neuroinflammation. 2012;9:46.
30. Kaufman RJ. Stress signaling from the lumen of the endoplasmic reticulum: coordination of gene transcriptional and translational controls. Genes Dev. 1999;13(10):1211–33.
31. Harding HP, Calfon M, Urano F, Novoa I, Ron D. Transcriptional and translational control in the Mammalian unfolded protein response. Annu Rev Cell Dev Biol. 2002;18:575–99.
32. Roussel BD, Kruppa AJ, Miranda E, Crowther DC, Lomas DA, Marciniak SJ. Endoplasmic reticulum dysfunction in neurological disease. Lancet Neurol. 2013;12(1):105–18.
33. Saito A, Cai L, Matsuhisa K, Ohtake Y, Kaneko M, Kanemoto S, Asada R, Imaizumi K. Neuronal activity-dependent local activation of dendritic unfolded protein response promotes expression of brain-derived neurotrophic factor in cell soma. J Neurochem. 2018;144(1):35–49.
34. Wang P, Li J, Tao J, Sha B. The luminal domain of the ER stress sensor protein PERK binds misfolded proteins and thereby triggers PERK oligomerization. J Biol Chem. 2018;293(11):4110–21.
35. Lin JH, Li H, Zhang Y, Ron D, Walter P. Divergent effects of PERK and IRE1 signaling on cell viability. PLoS One. 2009;4(1):e4170.
36. Mercado G, Castillo V, Soto P, Lopez N, Axten JM, Sardi SP, Hoozemans JJM, Hetz C. Targeting PERK signaling with the small molecule GSK2606414 prevents neurodegeneration in a model of Parkinson's disease. Neurobiol Dis. 2018;112:136–48.
37. Wang R, Sun DZ, Song CQ, Xu YM, Liu W, Liu Z, Dong XS. Eukaryotic translation initiation factor 2 subunit alpha (eIF2alpha) inhibitor salubrinal attenuates paraquat-induced human lung epithelial-like A549 cell apoptosis by regulating the PERK-eIF2alpha signaling pathway. Toxicol In Vitro. 2018;46:58–65.
38. Xiang C, Wang Y, Zhang H, Han F. The role of endoplasmic reticulum stress in neurodegenerative disease. Apoptosis. 2017;22(1):1–26.
39. Penaranda Fajardo NM, Meijer C, Kruyt FA. The endoplasmic reticulum stress/unfolded protein response in gliomagenesis, tumor progression and as a therapeutic target in glioblastoma. Biochem Pharmacol. 2016;118:1–8.
40. Urra H, Dufey E, Lisbona F, Rojas-Rivera D, Hetz C. When ER stress reaches a dead end. Biochim Biophys Acta. 2013;1833(12):3507–17.
41. Han K, Hassanzadeh S, Singh K, Menazza S, Nguyen T T, Stevens M V, Nguyen A, San H, Anderson S A, Lin Y, Zou J, Murphy E, and Sack M N (2017) Parkin regulation of CHOP modulates susceptibility to cardiac endoplasmic reticulum stress. Sci Rep 7(1):2093.
42. Li XF, Zhang Z, Chen ZK, Cui ZW, Zhang HN. Piezo1 protein induces the apoptosis of human osteoarthritis-derived chondrocytes by activating caspase-12, the signaling marker of ER stress. Int J Mol Med. 2017;40(3):845–53.
43. Urano F, Wang X, Bertolotti A, Zhang Y, Chung P, Harding HP, Ron D. Coupling of stress in the ER to activation of JNK protein kinases by transmembrane protein kinase IRE1. Science. 2000;287(5453):664–6.
44. Nishitoh H, Matsuzawa A, Tobiume K, Saegusa K, Takeda K, Inoue K, Hori S, Kakizuka A, Ichijo H. ASK1 is essential for endoplasmic reticulum stress-induced neuronal cell death triggered by expanded polyglutamine repeats. Genes Dev. 2002;16(11):1345–55.
45. Oyadomari S, Mori M. Roles of CHOP/GADD153 in endoplasmic reticulum stress. Cell Death Differ. 2004;11(4):381–9.
46. Tan Y, Dourdin N, Wu C, De Veyra T, Elce JS, Greer PA. Ubiquitous calpains promote caspase-12 and JNK activation during endoplasmic reticulum stress-induced apoptosis. J Biol Chem. 2006;281(23):16016–24.
47. Nakagawa T, Yuan J. Cross-talk between two cysteine protease families. Activation of caspase-12 by calpain in apoptosis. J Cell Biol. 2000;150(4):887–94.
48. Serrano-Negron JE, Zhang Z, Rivera-Ruiz AP, Banerjee A, Romero-Nutz EC, Sanchez-Torres N, Baksi K, Banerjee DK. Tunicamycin-induced ER stress in breast cancer cells neither expresses GRP78 on the surface nor secretes it into the media. Glycobiology. 2018;28(2):61–8.
49. Schmeits PC, Katika MR, Peijnenburg AA, van Loveren H, Hendriksen PJ. DON shares a similar mode of action as the ribotoxic stress inducer anisomycin while TBTO shares ER stress patterns with the ER stress inducer thapsigargin based on comparative gene expression profiling in Jurkat T cells. Toxicol Lett. 2014;224(3):395–406.
50. Garton T, Keep RF, Wilkinson DA, Strahle JM, Hua Y, Garton HJ, Xi G. Intraventricular hemorrhage: the role of blood components in secondary injury and hydrocephalus. Transl Stroke Res. 2016;7(6):447–51.
51. Nakka VP, Gusain A, Raghubir R. Endoplasmic reticulum stress plays critical role in brain damage after cerebral ischemia/reperfusion in rats. Neurotox Res. 2010;17(2):189–202.
52. Yang W, Paschen W. Unfolded protein response in brain ischemia: A timely update. J Cereb Blood Flow Metab. 2016;36(12):2044–50.
53. Lin JH, Li H, Yasumura D, Cohen HR, Zhang C, Panning B, Shokat KM, Lavail MM, Walter P. IRE1 signaling affects cell fate during the unfolded protein response. Science. 2007;318(5852):944–9.
54. Valenzuela V, Onate M, Hetz C, Court FA. Injury to the nervous system: a look into the ER. Brain Res. 2016;1648(Pt B):617–25.
55. Meng C, Zhang J, Dang B, Li H, Shen H, Li X, Wang Z. PERK pathway activation promotes intracerebral hemorrhage induced secondary brain injury by inducing neuronal apoptosis both in vivo and in vitro. Front Neurosci. 2018;12:111.

The Time Course of Cognitive Deficits in Experimental Subarachnoid Hemorrhage

Zhiyuan Vera Zheng, Ping Kuen Lam, Wai Sang Poon, and Kwok Chu George Wong

Abstract Subarachnoid hemorrhage (SAH) is a devastating stroke type. Approximately 50% of survivors suffer from the permanent disability, caused by the cognitive deficits. To enrich the pre-clinical research on the neurological deficits after SAH, we investigate the temporal cognitive deficits and the longitudinal course of cognitive recovery in endovascular perforation SAH murine model. The SAH mice show reproducible body weakness and headache-symbolized moaning symptoms, which is closed to clinical patients. SAH mice exhibit significantly impaired cognitive function in domains of learning ability, short-term and long-term memory. The cognitive deficits occur mostly in the early phase and recover gradually till day 10 after SAH. The systematical assessments of cognitive function after experimental aneurysmal SAH elucidate the time course of cognitive deficits and provide the time window of potential interventions.

Keywords Subarachnoid hemorrhage · Animal model · Cognitive deficits

Introduction

Subarachnoid hemorrhage (SAH) is a devastating disease which accounts for the second mortality among stroke population. The most common cause of SAH is the ruptured aneurysm. Approximately 50% of survivors suffer from the permanent disability, caused by the cognitive deficit [3]. More than 20% of aneurysmal SAH (aSAH) patients experience one or more domain deficits, which commonly present in memory, executive function, and language [1, 16]. Early cognitive deficits exhibit more in the domains of visuospatial memory and language [17] . Delayed cerebral infarction is reported the potential risk factors for post-SAH cognitive impairments. Cognitive deficits correlate independently with poor functional outcome after aSAH [13, 16] . Since the mechanism underlying the cognitive impairments after aSAH is poorly understood, few effective therapeutic targets are proven to improve the cognitive outcome.

Rodent SAH models are highly developed since for its low costs and short experimental timeline. SAH models vary with different induction methods. The endovascular perforation model is considered the closest to human patients, which mimicked the ruptured aneurysm. Well-established SAH animal models contribute to reveal the pathogenesis and evaluate the intervention with therapeutic targets. So far, few studies systematically evaluate the impact of the cognitive domain in experimental aSAH model. Therefore, in this study, we aim to investigate the temporal cognitive deficits and the longitudinal course of cognitive recovery in the endovascular perforation SAH murine model.

Materials and Methods

Endovascular Perforated SAH Model

Male, wild-type C57BL/6, average weighing 25–30 g, were used in this study. SAH was induced by endovascular perforation under ketamine anesthesia. Briefly, a 20 mm-long blunted 5-0 monofilament nylon suture was inserted from external carotid artery (ECA) to the lumen of internal carotid artery (ICA). The artery was perforated at the bifurcation

Z. V. Zheng · W. S. Poon · K. C. G. Wong (✉)
Division of Neurosurgery, Department of Surgery, The Chinese University of Hong Kong, Prince of Wales Hospital, Hong Kong, China
e-mail: georgewong@surgery.cuhk.edu.hk

P. K. Lam
Department of Surgery, Chow Tai Fook-Cheng Yu Tung Surgical Stem cell Research Centre, The Chinese University of Hong Kong, Hong Kong, China

R. D. Martin et al. (eds.), *Subarachnoid Hemorrhage*, Acta Neurochirurgica Supplement 127, https://doi.org/10.1007/978-3-030-04615-6_18,

where the resistance was encountered. The filament was immediately withdrawn to introduce the blood into subarachnoid space. The sham model was operated in the same procedures without inserting the filament. Buprenorphine was injected twice a day for consecutive 3 days for the analgesic. The procedures involving animal and their care were conducted under the approval of the Ethics Committee of the Chinese University of Hong Kong.

Mouse Motor and Sensory Scale (mMSS)

Neurobehavioral assessments were performed on post-surgery day 1, day 3, day 5, and day 10. The Mouse Motor and Sensory Scale (mMSS) was employed to evaluate the sensorimotor functions as published previously. Neurologic function was graded on a scale of 5–27 (27 as normal score and 5 as maximal deficit score). The scale was a composite of the motor (0–12) (spontaneous activity, symmetry of limb movements, climbing, balance) and sensory (5–15) (proprioception, vibrissae, visual, olfactory, and tactile responses) [5].

Morris Water Maze Test

Morris water maze (MWM) was widely used to test learning ability and memory in rodents [15]. MWM testing was performed in a circular water tank, 114 cm in diameter and 71 cm in height. The tank was filled with opaque water made by white nontoxic baby powder. The water temperature was maintained at 25 ± 2 °C. Mice were given a 5-day training to learn to escape on hidden platform, depending on the spatial cues. The spatial learning ability was presented as the latency to escape platform.

To detect the long-term memory, a probe test was conducted 24 h after the last training trial. Mice were allowed a 60-s free swimming to explore in the water tank without escape platform. Memory was determined by the preference for the target quadrat where the platform was placed previously.

Object Recognition Test

Short-term memory was assessed by object recognition test [11]. Mice were allowed to get familiar with two same objects within an open-field chamber in the familiarization phase. After a 2-h interval, in the test phase, one object was replaced by a novel one to test the short-term discriminative memory. The discrimination index (DI) eliminated the variation of exploration time to define the short-term memory operationally. Discrimination Index (DI) = (Novel Object Exploration Time/Total Exploration Time)–(Familiar Object Exploration Time/Total Exploration Time) × 100] [2].

Statistic

All data were analyzed by SPSS 23 (IBM, Armonk, New York, USA) and Prism 7.0 (GraphPad Software, Inc., La Jolla, CA, USA). P value <0.05 was regarded significant. $***p < 0.001$, $**p < 0.01$, $*p < 0.05$. Repeated measures ANOVA was used for the statistical analyses of mMSS and MWM test. Two-way ANOVA was used in ORT. Single time-point behavioral measurements were compared with a Student's t-test. Data were presented as mean ± standard error of the mean (SEM).

Results

SAH Model Establishment

Mice were randomized to each group. The mortality of SAH group is 13.1%, and the most death occurred in the first 24 hours. There was no death in sham group. The endovascular perforation induced subarachnoid bleeding around the circle of Willis. The sham model presented the clean skull base (Fig. 1). The mice with unfavorable hemorrhage in epidural or ventricular space would be excluded for the subsequent studies. SAH mice presented body weakness and headache-symbolized moaning, while the sham group mice showed the normal activities.

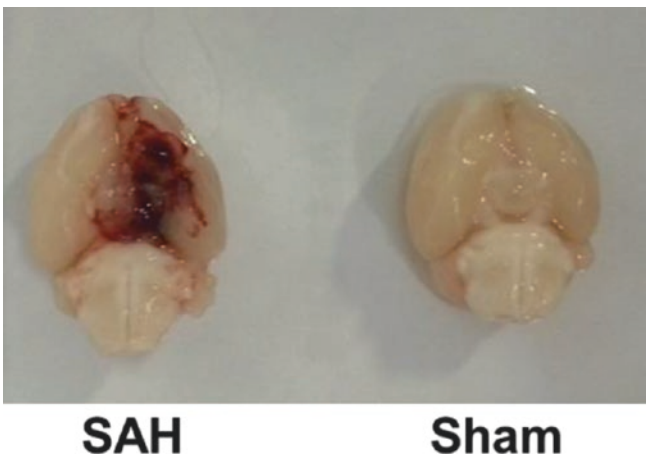

Fig. 1 The general appearance of the experimental SAH

The Time-Course of Neurological Deficits After SAH

Sensorimotor Deficits

Mice were scored according to mMSS on both motor and sensory domains. SAH mice had significantly lower scores compared with the sham-operated mice (group effect, $F[1,34] = 64.125$, $p < 0.001$; days effect, $F[2.252,76.558] = 101.059$, $p < 0.001$; interaction, $F[2.252,76.558] = 72.894$, $p < 0.001$). The significant sensorimotor deficits were observed from day 1 to day 5 after SAH and gradually recovered on delayed phase on day 10 (Fig. 2a).

Learning Disability and Long-Term Memory Dysfunction

In training phase of MWM test, SAH mice exhibited significantly impaired learning ability over time, with a flat learning curve at primary stage. However, the shamoperated mice displayed a relatively steep one. SAH mice spent longer latency to find the escape platform compared with the sham ones, which was significant from day 1 to day 4 (group effect, $F[1, 17] = 16.587$, $p = 0.001$; days effect, $F[2.903,49.343] = 75.840$, $p < 0.001$; interaction, $F[2.903,49.343] = 3.452$, $p = 0.025$; Fig. 2b). The swimming path showed the distance and pathway to reach the escape platform through training sessions. SAH mice obviously swam a longer distance than sham ones (Fig. 3A, B). All the mice were trained to successfully escape the water tank within 20 s during this phase.

In the probe trial, SAH mice showed the significant deterioration of long-term memory, presenting significantly less exploration in the target quadrant ($t[17] = -2.493$, $p = 0.023$; Figs. 2c and 3c, d). SAH mice failed to recall the memory of the position where the platform was previously placed after a long interval. SAH and sham mice showed the comparable swim speeds, suggesting equivalent swimming skills.

Short-Term Memory Dysfunction

In ORT, 2-hour interval was used for assessing the short-term memory. It was the intrinsic nature of normal mice to explore the novel things. SAH mice demonstrated the episodic short-term memory deficits, failing to discriminate the novel object from the familiar one in test phase. These deficits were characterized by a similar exploration duration on both novel and familiar object. The shamopereated mice showed preference for novel object, illustrated by the increased exploration time and frequency of the novel object compared to the familiar one (objects effect, $F[1,72] = 11.225$, $p = 0.001$; days effect, $F[3,72] = 3.441$, $p = 0.021$; interaction, $F[3,72] = 5.56$, $p = 0.002$; Figs. 2d, e and 3e, f). The short-term memory deficit occurred in the early phase from day 1 to day 3 and gradually recovered on delayed phase from day 5 to day 10. Consistently, the discrimination index eliminated the variation of exploration time, showing a significant decrease in SAH group compared to control one (Fig. 2f).

Discussion

SAH, even less common, accounts for nearly 30% of stroke-related life lost before age 65 and is responsible for the great burden for both individuals and society [9]. The development of effective treatment is of great urgency. The pre-clinical animal models are facilitated for the investigation of pathogenesis and potential therapy. Especially, recent studies suggest that prevention of vasospasm fails to generate the long-lasting benefits to SAH patients. Neither sufficient nor necessary conditions of vasospasm contribute to the delayed ischemic infarct after SAH [7, 18]. That is essential to explore the relevant mechanism by employing the pre-clinical SAH models. The endovascular perforated SAH model in this study mimics the ruptured aneurysm, which is similar to the clinical patient, presenting the SAH-like symptoms. The behavioral assays illustrate a stable and persistent neurological dysfunction after SAH. That should be an approach for developing the targeted therapeutics by defining the broader landscape of cognitive deficits. Given the cross-laboratory and experimental variability in model establishment, the evaluation of cognitive deficits on SAH model suffers discrepancy [6]. That may be a limitation we face when applying this approach widely.

Global cerebral edema and left-sided infarction are the evidenced risk factors for the cognitive dysfunction after SAH [10]. That is also reported that the frontal hematoma, intraventricular hemorrhage, and acute hydrocephalus contribute to the cognitive dysfunction compared with SAH patients without these findings [8]. Although several events are proved highly related to the cognitive dysfunction, the underlying mechanism largely remains to be clear. SAH mice, in this study, shows the neurological dysfunctions on sensory-motor, spatial learning, and short-term and long-term memory domains. The neurological deficits arise in early phase after SAH induction. The early brain injury (EBI) in human patients initiates within the first 72 h, during which the most deaths occur. The EBI is believed owing to the increased intracranial pressure (ICP), acute hydrocephalus, microvascular alterations, and transient global ischemia [14]. The early nature of neurobehavioral deficits might potentially relate to early brain injury. One-third of patients develop into the secondary injury, which contributes to the delayed cerebral deteriora-

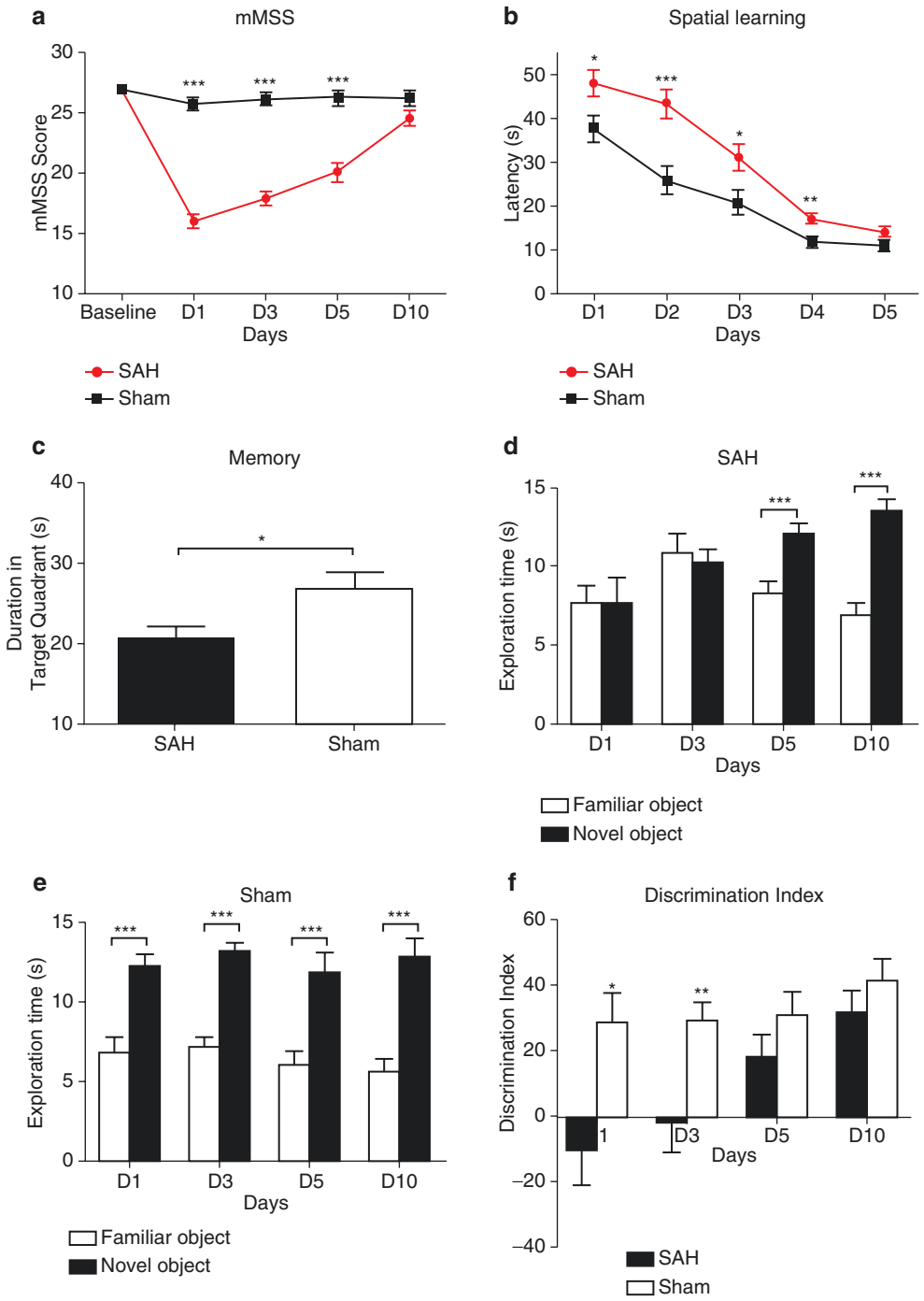

Fig. 2 Neurobehavioral assessments after SAH on murine model. (**a**) mMSS (5–27) score on pre-surgery and post-surgery day 1, day 3, day 5, and day 10. (**b**) Training trials in MWM test. The spatial learning ability was presented as the latency to escape platform. (**c**) Probe trial in MWM test. Long-term memory was present as the time mice spent in the target quadrant where the platform was placed previously. (**d**, **e**) The time-course performances in the test phase of ORT for SAH mice and sham mice. The short-term memory was present as the discrimination of the novel object from the familiar object. (**f**) Discrimination Index = [(Novel Object Exploration Time/Total Exploration Time) – (Familiar Object Exploration Time/Total Exploration Time)] × 100. Values were the mean ± SEM. $*p \leq 0.05$, $**p \leq 0.01$, $***p \leq 0.001$

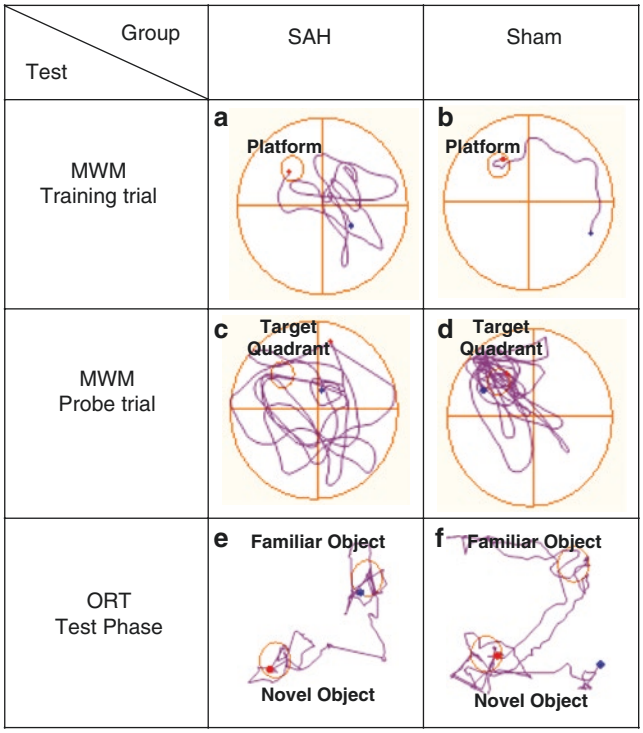

Fig. 3 Behavioral assessments on SAH/sham mice. (**a**, **b**) The typical swim path of SAH/sham mice in the training trials of MWM. SAH mice spent longer latency to reach the platform. (**c**, **d**) The typical swim path of SAH/sham in the probe trials of MWM. SAH mice spent less time exploring in target quadrant. (**e**, **f**) The typical exploration path in the test phase of ORT. SAH mice spent less time exploring the novel object

tion [4]. Events occurring in this phase include blood-brain barrier disruption, microvascular spasm, arteriolar constriction and thrombosis, and cortical spreading depolarization [12]. Delayed cerebral infarction is also an independent risk factor for two or more domains of cognitive deficit [16]. A better understanding of these issues is necessary to elucidate how the SAH affects cognitive function.

In conclusion, the systematical assessments of cognitive function after aneurysmal SAH elucidated the longitudinal course of cognitive recovery and provided the time window of potential interventions.

Acknowledgments The authors appreciate the help and support from the colleagues of the Department of Surgery, The Chinese University of Hong Kong.

Conflict of Interest Statement: **The authors declared no financial or intellectual conflict of interest.**

References

1. Al-Khindi T, MacDonald RL, Schweizer TA. Cognitive and functional outcome after aneurysmal subarachnoid hemorrhage. Stroke. 2010;41:e519–36.
2. Arqué G, Fotaki V, Fernández D, de Lagrán MM, Arbonés ML, Dierssen M. Impaired spatial learning strategies and novel object recognition in mice haploinsufficient for the dual specificity tyrosine-regulated kinase-1A (Dyrk1A). PLoS One. 2008;3:e2575.
3. Cahill J, Zhang JH. Subarachnoid hemorrhage: is it time for a new direction? Stroke. 2009;40:86–8.
4. Chen S, Hospital SA, Linda L, Linda L, Wu H, Hospital SA, Tang J, Zhang J, Hospital SA, Zhang JH. Neurovascular events after subarachnoid hemorrhage: focusing on subcellular organelles, vol. 120; 2015. p. 39–46.
5. Du GJ, Lu G, Zheng ZY, Poon WS, Chu K, Wong G. Endovascular perforation murine model of subarachnoid hemorrhage. Acta Neurochir Suppl. 2016;121:83–8.
6. Fanizzi C, Sauerbeck AD, Gangolli M, Zipfel GJ, Brody DL, Kummer TT. Minimal long-term neurobehavioral impairments after endovascular perforation subarachnoid hemorrhage in mice. Sci Rep. 2017;7:7569.
7. Hou J, Zhang JH. Does prevention of vasospasm in subarachnoid hemorrhage improve clinical outcome? No Stroke. 2013;44:29–30.
8. Hütter BO, Kreitschmann-Andermahr I, Gilsbach JM. Cognitive deficits in the acute stage after subarachnoid hemorrhage. Neurosurgery. 1998;43:1054–65.
9. Johnston SC, Selvin S, Gress DR. The burden, trends, and demographics of mortality from subarachnoid hemorrhage. Neurology. 1998;50:1413–8.
10. Kreiter KT, Copeland D, Bernardini GL, Bates JE, Peery S, Claassen J, Du E, Stern Y, Connolly ES, Mayer SA. Predictors of cognitive dysfunction after subarachnoid hemorrhage. Stroke. 2002;33:200–9.
11. Leger M, Quiedeville A, Bouet V, Haelewyn B, Boulouard M, Schumann-Bard P, Freret T. Object recognition test in mice. Nat Protoc. 2013;8:2531–7.
12. Macdonald RL. Delayed neurological deterioration after subarachnoid haemorrhage. Nat Rev Neurol. 2013;10:44–58.
13. Mayer S, Kreiter K, Copeland D, Bernardini G, Bates J, Peery S, Claassen J, Du Y, Connolly E. Global and domain-specific cognitive impairment and outcome after subarachnoid hemorrhage. Neurology. 2002;59:1750–8.
14. Sehba FA, Pluta RM, Zhang JH. Metamorphosis of subarachnoid hemorrhage research: from delayed vasospasm to early brain injury. Mol Neurobiol. 2011;43:27–40.
15. Vorhees CV, Williams MT. Morris water maze: procedures for assessing spatial and related forms of learning and memory. Nat Protoc. 2006;1:848–58.
16. Wong GKC, Lam SW, Ngai K, et al. Cognitive domain deficits in patients with aneurysmal subarachnoid haemorrhage at 1 year. J Neurol Neurosurg Psychiatry. 2013;84:1054–8.
17. Wong GKC, Lam SW, Wong A, Ngai K, Mok V, Poon WS. Early cognitive domain deficits in patients with aneurysmal subarachnoid hemorrhage correlate with functional status, vol. 114; 2012. p. 129–32.
18. Zheng VZ, Wong GKC. Neuroinflammation responses after subarachnoid hemorrhage: a review. J Clin Neurosci. 2017;42:7–11.

Endovascular Ultraviolet Laser-Facilitated Reversal of Vasospasm Induced by Subarachnoid Hemorrhage in Canines

Brant D. Watson, Chander Sadasivan, and Robert W. Hurst

Summary *Background*: Because treatments for cerebral arterial spasm—a delayed consequence of subarachnoid hemorrhage (SAH)—are clinically inconsistent, we describe here a new method for reversal of arterial spasm, possibly extensible to nitric oxide (NO)-sensitive microvasculature.

Methods: We subjected dogs to the intracisternal double-hemorrhage model of SAH (autologous blood injection on days 1 and 3) and began endovascular treatment of the spasmed basilar artery (BA) on Day 4. A conical-tip fused silica optical fiber was introduced via a microcatheter (inserted femorally) into the proximal vicinity of the spasmed BA. After local saline flushing of blood, an ultraviolet (UV) pulsed laser beam (355 nm Nd:YAG) was focused into the optical fiber and converted into a concentric ring beam, which facilitated endovascular irradiation for 30 s at intensities of 12–20 W/cm^2. BA diameters were measured angiographically using a semiautomated routine over the entire BA length as well as the proximal, medial, and distal segments.

Results: On Day 4 the BAs had constricted by 21 ± 11%. After UV laser irradiation on Day 4, the constricted BAs dilated to 93 ± 15% of their normal diameters within minutes, and the dilation (91 ± 12%) persisted on Day 5. Most BA segments recovered to their respective baselines after UV irradiation, even when the UV beam was located considerably proximal to the BA origin. At days 4 and 5, the percent BA dilation normalized to Day 4 pre-treatment decreased linearly (by scatter plot, $p < 0.02$) over a range of about 60 mm from the UV irradiation site.

Conclusions: We conjecture that the vasodilator nitric oxide, produced at high local concentration from its vascular storage forms (chiefly nitrites) by UV laser-induced photoscission, stimulates a wave of arterial dilation, possibly by longitudinal propagation of transnitrosation reactions in the arterial wall, which reverses cerebral vasospasm semi-locally and thus avoids the deleterious effects of systemic treatment.

Keywords Subarachnoid hemorrhage · Vasospasm · Nitric oxide · Angiography · Ultraviolet laser irradiation · Rapid vasodilation

Abbreviations

BA	Basilar artery
eNOS	Endothelial nitric oxide synthase
Nd:YAG	Neodymium yttrium aluminum garnet
NO	Nitric oxide
SAH	Subarachnoid hemorrhage
UV	Ultraviolet

Introduction

Cerebral vasospasm has long been thought to be a major contributor to morbidity and mortality following subarachnoid hemorrhage (SAH) caused by aneurysm rupture [1, 2, 28]. But interventional therapies (e.g., ballooning or stenting) [2, 12, 16, 20, 21, 24] to reverse post-SAH vasospasm lack consistency and clinical benefit, as they are often fraught with vascular complications [6, 7, 15]. Outcomes of drug-based therapies to reverse vasospasm and its sequelae have also been inconsistent and overall effectiveness compromised owing to systemic complications, chiefly hypotension [1, 4, 10, 18, 28, 34, 55]. This

B. D. Watson (✉)
Departments of Neurology and Biomedical Engineering, University of Miami Miller School of Medicine, Miami, FL, USA
e-mail: bwatson@med.miami.edu

C. Sadasivan
Department of Neurological Surgery, Stony Brook University Medical Center, Stony Brook, NY, USA
e-mail: csadasivan@sbumed.org

R. W. Hurst
Department of Radiology, University of Pennsylvania Perelman School of Medicine, Philadelphia, PA, USA
e-mail: Robert.Hurst@uphs.upenn.edu

R. D. Martin et al. (eds.), *Subarachnoid Hemorrhage*, Acta Neurochirurgica Supplement 127,
https://doi.org/10.1007/978-3-030-04615-6_19,

was recently exemplified by recent clinical trials of clazosentan, an endothelin-1 inhibitor, in which occasional reversal or inhibition of vasospasm was described but, owing to hypotension-induced enhanced morbidity, lacked overall clinical benefit at 3 months compared to placebo treatment [28–31, 47].

In the past decade, the clinical relevance of late-stage arterial spasm reversal has been challenged and maybe even subsumed by the concept of early brain injury (EBI), which postulates that microvascular effects such as arteriolar spasm and thrombosis occur at the *onset* of SAH, and thus are the progenitors of delayed ischemic neurological deficits (DINDS) arising from critical loss of tissue perfusion [7, 15, 39, 40, 45, 46]. Therefore, the optimal treatment must eventually include reversal of arteriolar spasm, which may be preceded by interventional reversal of arterial spasm. A new approach is evidently needed, perhaps based on known but underutilized physiological properties.

The possibility that SAH-induced vasospasm may be reversed reliably without concomitant loss of blood pressure has not been reported, however. Restoration of nitric oxide (NO)-mediated vascular tone to the spasmed artery would seem fundamental, inasmuch as degradation products such as oxyhemoglobin and bilirubin in the subarachnoid blood scavenge NO in the arterial wall, thus lowering smooth muscle cGMP and causing vasoconstriction [9, 11, 32, 39, 40, 58]. In the absence of exogenous donors, nitric oxide can be produced photophysically (independent of endothelium) from its vascular wall storage forms (e.g., nitrites and S-nitrosothiols) by means of ultraviolet light (UV) irradiation [3, 5, 25, 37]. To illustrate the utility of this application, severe vasospasm (to ca. 40% of baseline) in rat middle cerebral artery (MCA) was observed during platelet thrombus formation in a rat model of MCA-territory stroke [54]. This was reversed to 120% of baseline by *exo*vascular UV laser irradiation at 13 W/cm^2, concomitant with dissolution of the occluding platelet thrombus and recanalization of the MCA [51, 52, 54]. Subsequently, common carotid arteries (CCAs) in naïve rats were irradiated *endo*vascularly by a 351 nm argon laser beam delivered by a conical-tip optical fiber ensheathed within a microcatheter. The fiber transformed the input laser beam into an expanding ring pattern [51, 52] and facilitated circumferential endovascular irradiation at an intensity of 20 W/cm^2, with UV-absorbing blood displaced from the optical path by saline flushing. This resulted in dilation which was immediate (<1 s), persistent (>45 min), and long-range (>12 arterial diameters from the ring beam locus) [52].

Based on this work, we describe herein a pilot study of a clinically relevant demonstration of this technique in dogs subjected to the intracisternal double-hemorrhage model of SAH. The vertebrobasilar arterial system, constricted by post-SAH vasospasm, was exposed to endovascular illumination by a pulsed 355 nm ultraviolet Nd:YAG laser beam transported toward the affected territory. Our aims were to determine the capability of this treatment to quickly reverse post-SAH vasospasm in the proximal, medial, and distal segments of the basilar artery and to show that this method is semi-localized within the brain and cannot induce systemic consequences such as hypotension.

Materials and Methods

General Outline

A model of subarachnoid hemorrhage (administered in two stages, SAH1 and SAH 2; cf. [50]) was created in three mongrel dogs (22–29 kg), resulting in spasm of the vertebrobasilar arterial tree. Angiographic responses to SAH and its endovascular UV laser treatment were recorded and analyzed over a 5-day period on a Siemens Angiostar system (New York, NY) in the Large Animal Vascular and Interventional Radiology Research Suite at the University of Pennsylvania School of Medicine. All experimental protocols and procedures were approved by the Institutional Animal Care and Use Committee of the University of Pennsylvania in accord with the *Guide for Care and Use of Laboratory Animals*.

Endovascular Laser Irradiation via the Optical Fiber/Microcatheter System

The TEM_{00} beam of a acousto-optically Q-switched ultraviolet laser (New Micro frequency-tripled Nd:YAG, wavelength 355 nm, pulsewidth 100 ns, cycled at 7 Kz; Quanta System, Milan, Italy) was focused directly into a 100 μm core diameter fused silica optical fiber (Ocean Optics, Dunedin, FL) attached to the laser head. The fiber tip was ground and polished into a conical shape with an apex angle of 36° (Ultrapol Fiber Lensing System, Ultra Tec, Santa Ana, CA). Introduced into the vertebrobasilar arterial system via a microcatheter, the output ring beam facilitated annular irradiation of the inner circumference of a subject artery, in concert with continuous saline displacement of (the optically dense) blood. The beam power necessary to produce a preselected maximum ring beam intensity was deduced from a proprietary formula, but this intensity must not exceed 20 W/cm^2, a safety criterion determined from previous work [52].

Experimental Protocol

Dogs were fasted the night prior to procedures and i.v. catheters were placed into the cephalic veins. Subjects were sedated with intravenous injections of ketamine (10 mg/kg) and diazepam (0.2 mg/kg) and premedicated prior to intubation with intramuscular injections of atropine (0.05 mg/kg) and, for analgesia, maloxicam at 0.2 mg/kg. Once intubated, the dogs were placed

on inhaled isoflurane (1–5%) and oxygen for the remainder of the procedure. Temperature, heart rate, EKG, respiratory rate, blood pressure, and oxygen saturation were monitored and maintained within normal limits for the examination. Dogs received an intravenous infusion of normal saline (10 mL/kg per hour) to replace fluid losses. Dogs were then placed on a heating pad on the procedure table in dorsal recumbency.

Days 1 and 3 (SAH1 and SAH2)

The right groin was clipped, prepped, and draped in sterile fashion. Access to the femoral artery was obtained under ultrasound guidance with a Mini Access Kit (Infiniti Medical, Malibu, CA). A 0.018″ hydrophilic guide wire was advanced into the aorta, a 4 Fr introducer sheath was emplaced, and the vertebral artery with the larger diameter (or fewer anomalies) was selected with a 4 Fr Berenstein catheter followed by further insertion of the guide wire. A baseline cerebral arteriogram of the vertebrobasilar system in the anterior-posterior projection was performed by hand injection of Omnipaque 300 (GE Health Care, Waukesha, WI).

The base of the skull was clipped free of hair and then prepped and draped in sterile fashion. The dog was placed in lateral position with slight Trendelenburg. The cisterna magna was punctured with a 22-gauge spinal needle (Becton Dickinson, Franklin Lakes, NJ), and up to 3 mL of cerebral spinal fluid was removed. An equal volume of fresh, non-heparinized arterial blood was aspirated from the femoral sheath and injected into the cisterna magna via the indwelling needle; this procedure constituted SAH1. The dog was then placed in Trendelenburg position for 30 min. The dog was returned to dorsal recumbency and the vertebral artery was again selected and a cerebral arteriogram performed. The catheter and sheath were removed, hemostasis obtained with manual compression, and the animal recovered.

On Day 3 the identical procedure to Day 1 was performed and this second blood injection constituted SAH2.

Day 4

The right groin was prepped in sterile fashion and draped. Access to the femoral artery was obtained under ultrasound, and a 4 Fr sheath was placed. A cerebral arteriogram was performed in the anterior-posterior projection, utilizing the same technique as described previously. The dog was given a therapeutic dose of heparin (100 units/kg), and additional heparin was given as needed to maintain the activated clotting time between 200 and 400 s.

A 3 Fr Turbo-tracker 18 infusion microcatheter (Boston Scientific, Watertown, MA) was advanced through the 4 Fr guide catheter over a Synchro 2 guide wire (Boston Scientific, Watertown, MA) into the anterior spinal artery to a location either inside the proximal BA segment (Dog 1) or far proximal to it, owing to the presence of severe spasm (cf. Fig. 1). The guide wire was removed and a diagnostic arteriogram performed. A proprietary optical fiber (model Opus-14,

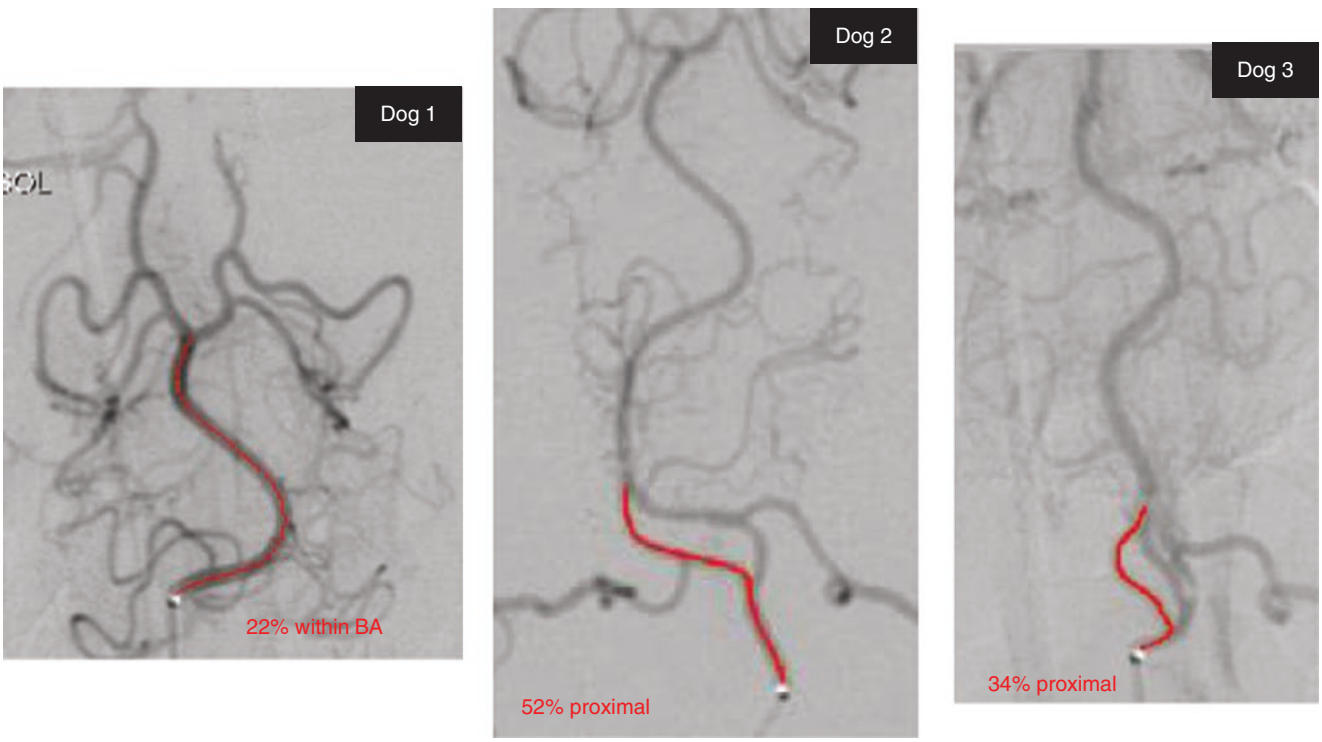

Fig. 1 Optical/fiber microcatheter emplacement in the three dogs. Note that in Dogs 2 and 3, spasm in the anterior spinal artery was sufficiently severe to prevent close approach to the BA origin. UV irradiation was nonetheless undertaken at these sites remote from the BA origin

OpusGen LLC, Doral, FL) was inserted and advanced through the catheter until its tip was marginally beyond the distal marker band of the microcatheter. A Touhy-Borst adapter was placed on the end of the microcatheter, and the side arm of the adapter was then connected to a three-way stopcock. A 60 mL syringe filled with normal saline and a 1 cm^3 polycarbonate syringe (Infiniti Medical, Malibu, CA) were connected to the three-way stopcock to allow rapid and continuous flushing of the microcatheter so as to provide an optically clear field for the UV irradiation. This saline flush of the microcatheter was performed manually at the maximal rate possible for the entire duration of the irradiation.

Dilution of the blood by >1000-fold was required to produce an optical field sufficiently clear (>91%) to allow endovascular transmission of UV laser light to the inner wall of the basilar artery [38], typically 1.5 mm in diameter. During saline flushing, the 355 nm UV laser beam was admitted into the optical fiber for 30 s, resulting in endovascular ring beam irradiation intensities of 12 W/cm^2 (for Dog 1) to 20 W/cm^2 (for Dogs 2 and 3) emitted from the optical fiber conical tip. The fiber was removed and cerebral arteriograms repeated by hand injection of contrast through the microcatheter and then, after the microcatheter was removed, through the 4 Fr diagnostic catheter. The anticoagulation was reversed with protamine (1 mg/kg per 100 units of heparin administered) and the sheath and catheters removed. A cutdown was performed, and the femoral artery was ligated above and below the puncture site. The incision was closed in two layers with Monosof nonabsorbable sutures (Syneture, Mansfield, MA).

Day 5

The right neck was clipped free of hair and the groin and right neck were prepped in sterile fashion and draped. Access to the femoral artery was obtained under ultrasound guidance and a 4 Fr sheath was placed. The same vertebral artery was selected, and a cerebral arteriogram was performed in the anterior-posterior projection using the technique previously described.

The 4 Fr sheath was exchanged for a 7 Fr sheath (Infiniti Medical, Malibu, CA). A 7 Fr compliant occlusion balloon (Infiniti Medical, Malibu, CA) was placed through the sheath and advanced to the descending thoracic aorta. A cutdown was performed on the right neck, and access to the right carotid artery was obtained with a needle and guide wire. An 8 Fr drainage catheter (Infiniti Medical, Malibu, CA) was placed into the ascending thoracic aorta. A jugular vein puncture was performed, and a 10 Fr drainage catheter (Infiniti Medical, Malibu, CA) was placed into the right atrium. The depth of anesthesia was increased. The occlusion balloon was inflated to isolate perfusion to the brain and forelimbs. The jugular catheter was attached to wall suction, and 4% paraformaldehyde at pH 7.4 was infused into the aorta using a pressure bag, and the dog was euthanized by an overdose of sodium pentobarbital. The brain, associated meninges, and cervical spinal cord were then explanted, trimmed, processed in paraffin, sectioned, and stained with hematoxylin and eosin.

Angiographic Diameter Measurements

The diameter of the basilar artery was determined with a semi-automated routine written in Matlab® (The Mathworks, Natick, MA). The angiographic image with maximal opacification of the basilar artery was selected and converted to a binary image by thresholding, and the centerline of the basilar was calculated. Grayscale profiles of the original angiographic image along lines perpendicular to the centerline were obtained. Vessel edges were determined as the full-width-at-half-maximum locations on the grayscale profiles. Gross errors in determining vessel edges (at side branch locations) were manually corrected. Diameters were calculated orthogonal to the centerline between the two edges. The calibration factor noted by the angiographic machine was used to scale the pixel values to millimeters. The extradural vertebral artery does not undergo spasm in this model, and thus its diameter can be expected to remain constant. If the extradural vertebral was adequately visualized in the angiogram, its diameter was measured to verify the accuracy of the machine calibration factor. On each angiogram, the diameter of the basilar artery was calculated at about 90 locations on average (range of 63–103 locations) over the entire length of the basilar artery. To evaluate the effect of dilation over distance, three segments approximately 3.5–4 mm in length were demarcated on the proximal, medial, and distal basilar segments (Fig. 2). The axial locations of these segments were identical on all angiograms for all animals. Diameters were calculated at about nine locations on average within each segment (range 7–11 locations). Changes in these basilar segment diameters were statistically compared using ANOVA. Further, the amplitude of dilation of these segments immediately post-treatment as well as at 24-h follow-up was normalized to Day 4 pre-treatment diameter and then correlated to the arc-length distance of these segments from the device tip. Statistics were conducted using GraphPad Instat (Instat, GraphPad Software, La Jolla, CA).

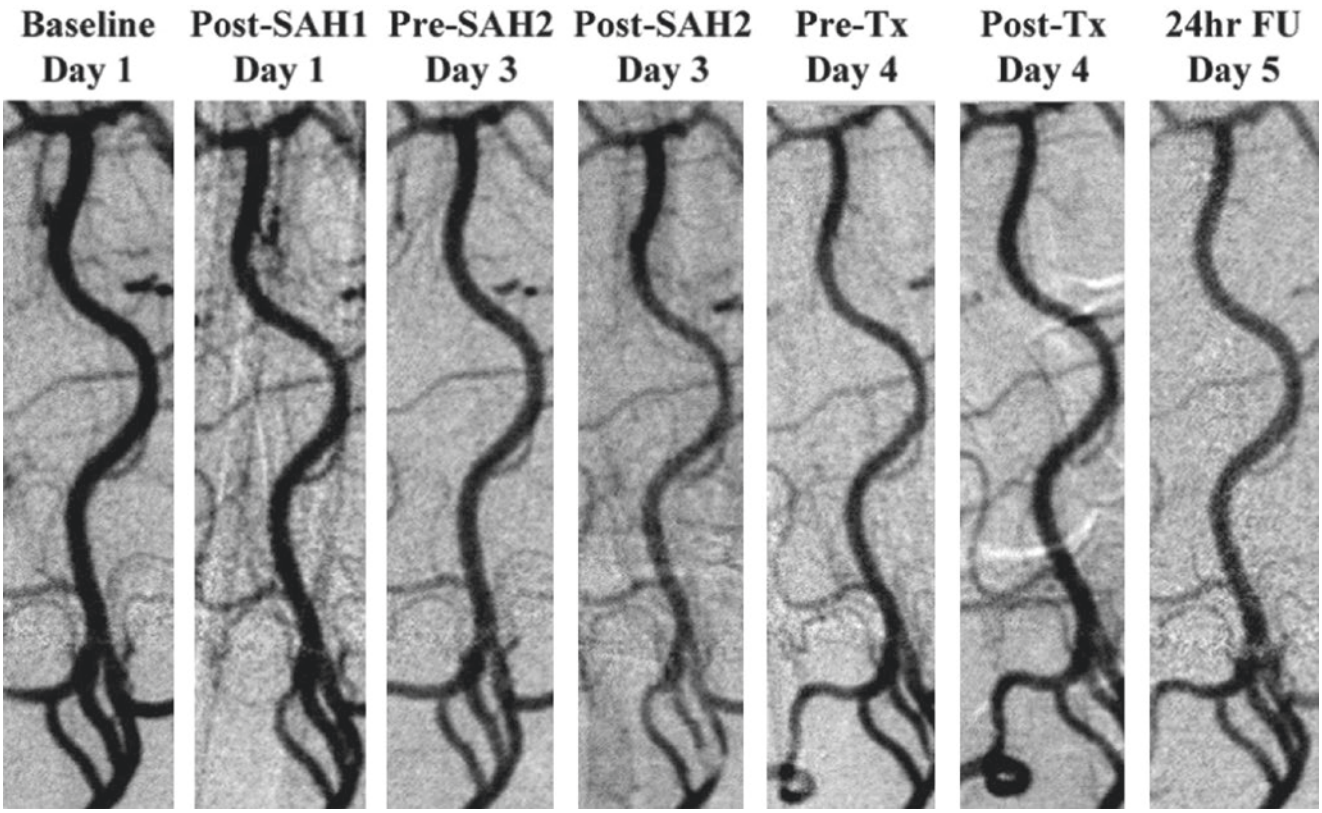

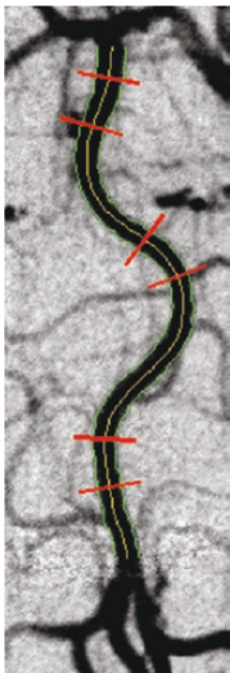

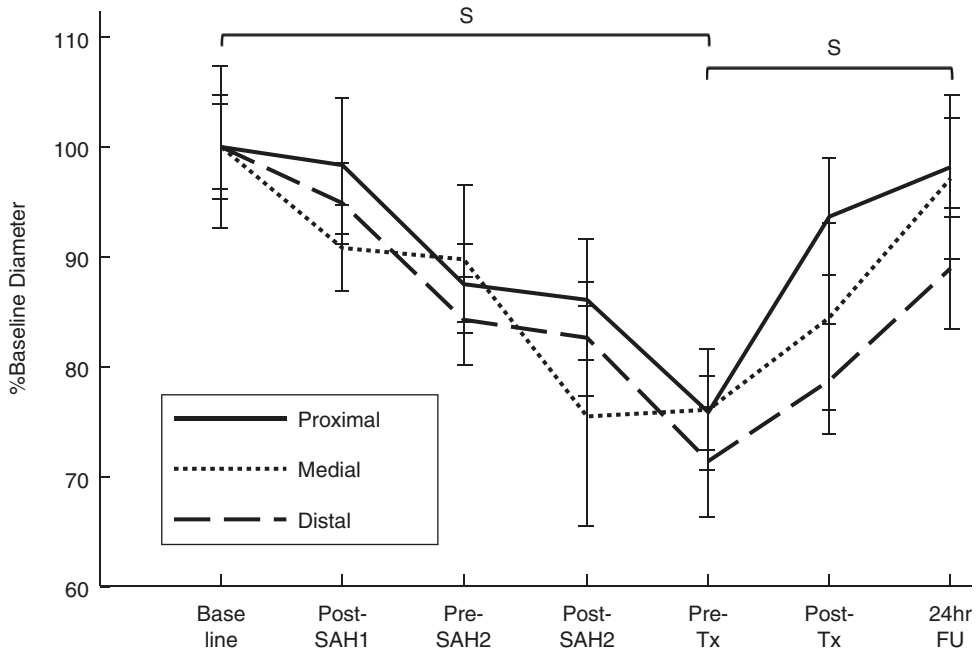

Fig. 2 Top: Angiograms of the basilar artery from Dog 3 at different stages of the study. Bottom left: proximal, medial, and distal segments marked (red lines) on the baseline angiogram. The location of these segments was kept constant for all cases. Bottom right: average diameters of the three segments at each stage for Dog 3; error bars represent standard deviation ($n \sim 9$ each segment); *S* statistically significant

Results

BA Spasm and Its Subsequent Reversal by Endovascular UV Laser Irradiation

The procedures were carried out successfully, although some individual variations were encountered. The fiber tip was positioned in the distal ventral spinal artery in Dogs 2 and 3 and in the proximal basilar artery in Dog 1 (Fig. 1); thus, the Dog 1 proximal segment could not be analyzed. However, this dog died after treatment on Day 4 owing to uncontrollable femoral artery hemorrhage at the access site; thus no Day 5 follow-up angiogram was acquired. The pre-treatment and post-treatment angiograms used for diameter quantification were acquired 112 ± 41 min apart (the post-treatment angiogram was acquired 2–3 min after irradiation), while the follow-up angiograms were acquired 21 ± 1 h after the post-treatment angiograms. In Fig. 2 the course of spasm development in Dog 3 and its post-treatment reversal is visually obvious (top); the locations of the analyzed BA segments are defined (lower left), and BA segment response over the 5-day study period is statistically analyzed (bottom). Figure 3 shows the average diameters taken over the entire basilar artery at the various time stages for all three animals. Figure 4 shows the proximal, medial, and distal segment diameters at baseline, pre-treatment, post-treatment, and follow-up for all three animals (except follow-up for Dog 1). Of the 20 angiograms acquired at the different stages in the 3 animals, the machine calibration factor was adjusted for 2 stages based on comparison with the extradural vertebral artery [27]: Dog 1 before the second SAH (pre-SAH2, changed from 0.13 mm/pixel to 0.12 mm/pixel) and Dog 3 post-treatment (post-Tx, changed from 0.09 mm/pixel to 0.1 mm/pixel).

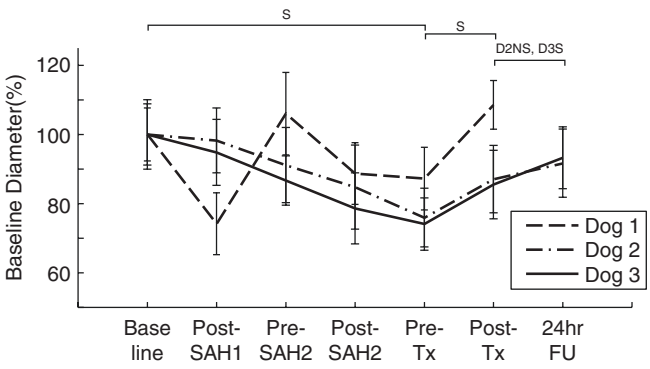

Fig. 3 Plots of the average diameter of the entire basilar artery at different study stages for the three animals; error bars represent standard deviation (*n* ranges from 63 to 103 for each point); *S* statistically significant, *NS* not significant, *D2* Dog 2, *D3* Dog 3, *Tx* treatment, *FU* follow-up

Over the entire basilar artery length, the vasospasm reduced the arterial diameter to 79 ± 11% of baseline before treatment ($p < 0.001$ as compared to baseline), and the irradiation dilated the vessel to 93 ± 15% of baseline immediately after treatment ($p < 0.001$ as compared to pre-treatment). The dilation was maintained until the 24-h follow-up time at 91 ± 12% of baseline ($p > 0.05$ as compared to post-treatment). Based on average diameters of the proximal, medial, and distal segments instead of the entire basilar artery, the corresponding values were 78 ± 10% at pre-treatment ($p < 0.001$ compared to baseline), 94 ± 14% at post-treatment ($p < 0.001$ compared to pre-treatment), and 93 ± 10% at 24-h follow-up ($p > 0.05$ compared to post-treatment). Figure 5 shows the progression of the overall average diameter superimposed on control (no treatment) literature data showing the natural progression of vasospasm in the canine dual hemorrhage model. The ability of the UV laser method to induce arterial dilation at locations distant from the irradiation site is shown in Fig. 6. The amplitude of dilation is negatively correlated with distance from the device tip and persists for about 6 cm.

Effect of UV Treatment on Blood Pressure

Blood pressure was monitored continuously for each dog during the procedures. For Dog 1, systolic pressure (SP, in mmHg) was unchanged (100–110) throughout, including the UV treatment interval. Diastolic pressure (DP, in mmHg) was 60 just before UV treatment, increased transiently, decreased to 50 within 45 min, and then increased in the next hour to 70. For Dog 2, SP ranged between 110 and 120 throughout, including during UV treatment. DP was 85 at the start of the UV irradiation, decreased to 75 an hour later, and resumed to baseline. For Dog 3, SP was 110 throughout, except for a transient increase to 120 just before UV treatment, which decreased to baseline within 15 min. DP was more variable, ranging from 40 to 70 but was stable at 70 during UV treatment and afterward. We thus observed no hypotension that could be correlated with UV laser irradiation.

Histology

Isolated focal ischemic areas with minimal to mild malacic changes were observed in the spinal cord and brainstem of two animals. Importantly, no vascular, meningeal, or parenchymal changes were observed that could be ascribed to the UV laser irradiation, but occasional slight mural laceration of the smooth muscle tissue was observed, likely from catheter manipulation during emplacement.

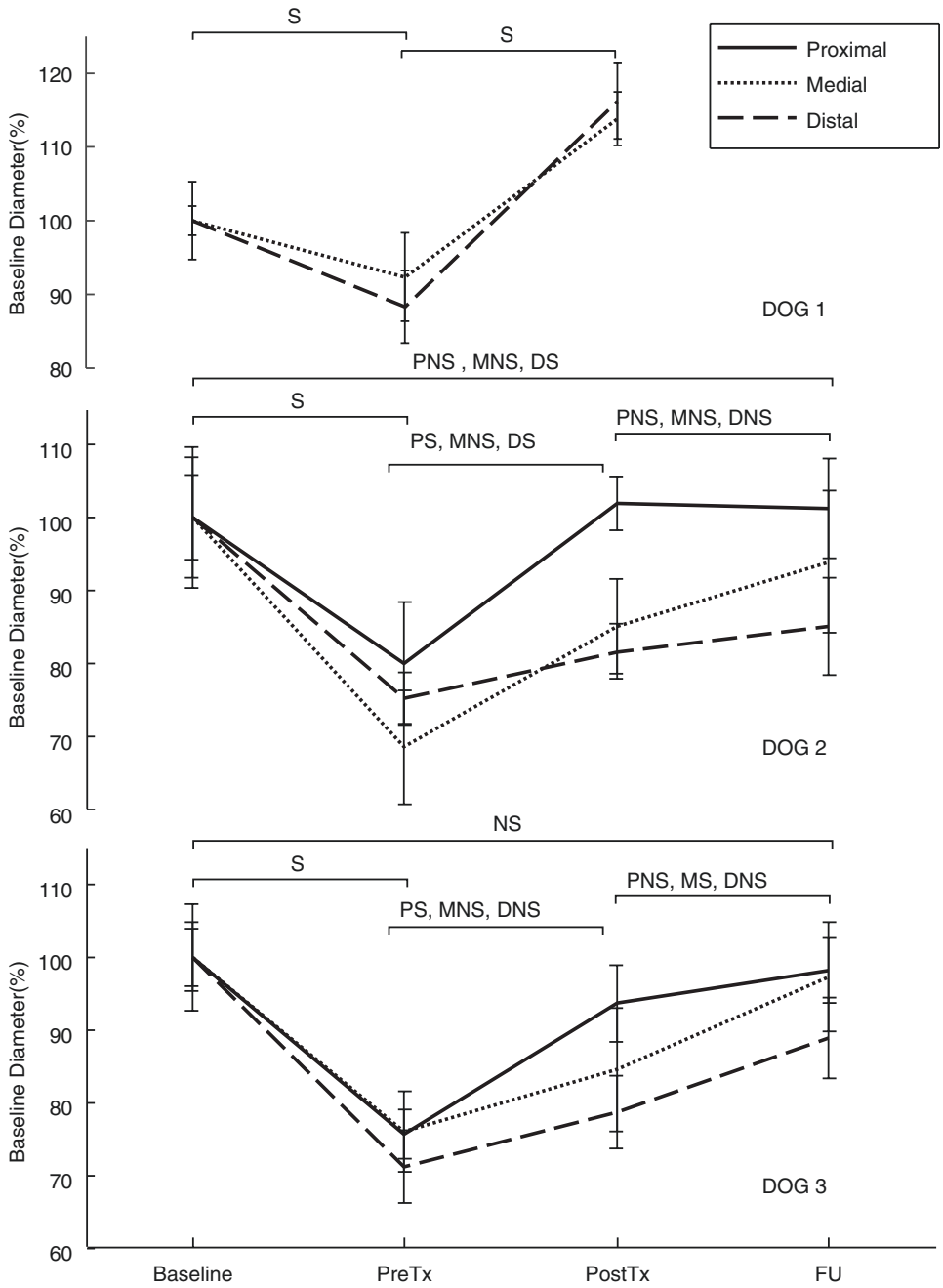

Fig. 4 Plots of the average diameter of the proximal, medial, and distal segments as shown in Fig. 2 at baseline, pre-treatment (Tx), post-treatment, and follow-up (FU) for the three animals; error bars represent standard deviation (n ranges from 7 to 11 for each point); *S* statistically significant, *NS* not significant, *P* proximal segment, *M* medial segment, *D* distal segment

Discussion

The double-hemorrhage model in dogs reproducibly facilitates post-SAH vasospasm in the intradural vertebral arteries and the basilar artery [19, 26, 33, 43, 50, 59]. In our hands, the BA in particular underwent statistically significant post-SAH vasospasm to a clinically relevant degree (22 ± 10%). We then demonstrated that these arterial segments could be dilated rapidly and sustainably (>18 h) by 10–30% over the minimum spastic basilar diameter, to their baseline or near-baseline diameters when irradiated by the UV laser system. The arterial diameter in the canine dual-hemorrhage model progressively reduces for 7 days after the first SAH and then begins to naturally resolve to the baseline diameter over the next 5 weeks [43]. We treated the artery 3 days after the first SAH (midway through the period of spasm, Fig. 5) in order to avoid conflation of treat-

ment-induced dilation with natural resolution. There was no evidence of vessel damage from laser treatment, such as intravascular thrombus formation, delay of flow, or thermal effects leading to barrier leakage.

UV light-induced relaxation of smooth muscle and its action spectrum (240–675 nm) were first determined by Furchgott et al. in preconstricted rabbit aortic rings [17]; such relaxation was later found to be independent of eNOS activity. The diffusibility of this effect was observed in a similar preparation, in which the entire aortic ring dilated after 351 nm UV irradiation was focused at one point [8]. Such relaxation is now ascribed to release of NO from vascular stores of UV-photolyzable metabolic by-products, such as nitrites and s-nitrosothiols, with subsequent activation of smooth muscle guanylate cyclase [3, 5, 25, 37, 48]. Scavenging of NO by hemoglobin or its degradation products has been implicated in large artery vasoconstriction and other deleterious consequences of SAH [46, 58]. The endovascular UV laser dilation system thus appears to replace the NO putatively scavenged during SAH, despite continuing confinement of the spasmed and then UV-irradiated arterial segments by extravasated blood.

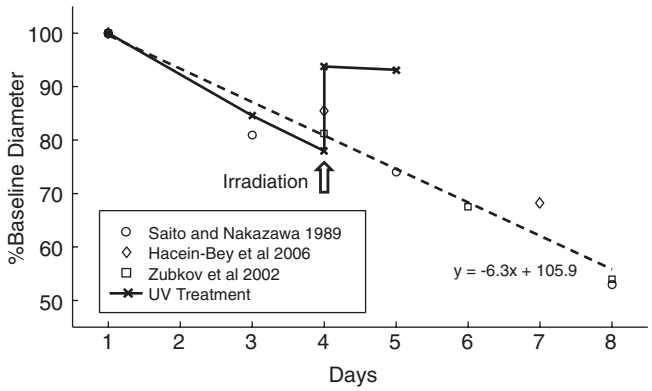

Fig. 5 The average (over all segments for all animals) basilar artery diameter from the study (UV treatment) plotted along with comparative literature data points [19, 43, 59] and dashed linear fit showing the decrease in basilar artery diameter in the native canine dual-hemorrhage model. The untreated control average diameter at Day 4 is about 78% of baseline before treatment, while the UV-treated diameter on the same day has dilated to about 94% of baseline. Note that the Day 5 follow-up average is over two animals

The rate of NO production by UV photolysis can be calculated from previously determined absorption cross sections (from formula 4 in [42]). A UV laser intensity of 5 W/cm^2 at 355 nm is predicted to convert nearly all of these adducts to NO within 45 s (demonstrated in [51, 52, 54]). Most of the initial NO is produced from nitrite photolysis, with less than 1% derived from S- and N-nitrosothiols. At saturation under UV laser irradiation, the intra-arterial NO concentration of 10 μM (in rat aorta) [42] is far higher than can be obtained from systemic NO donor drugs used safely [13]. Accordingly, we attribute the near-immediate arterial dilation and its acute propagation to a spreading chain of transnitrosation reactions in the arterial wall, initiated by a large initial bolus of NO and mediated by N_2O_3 [36], in

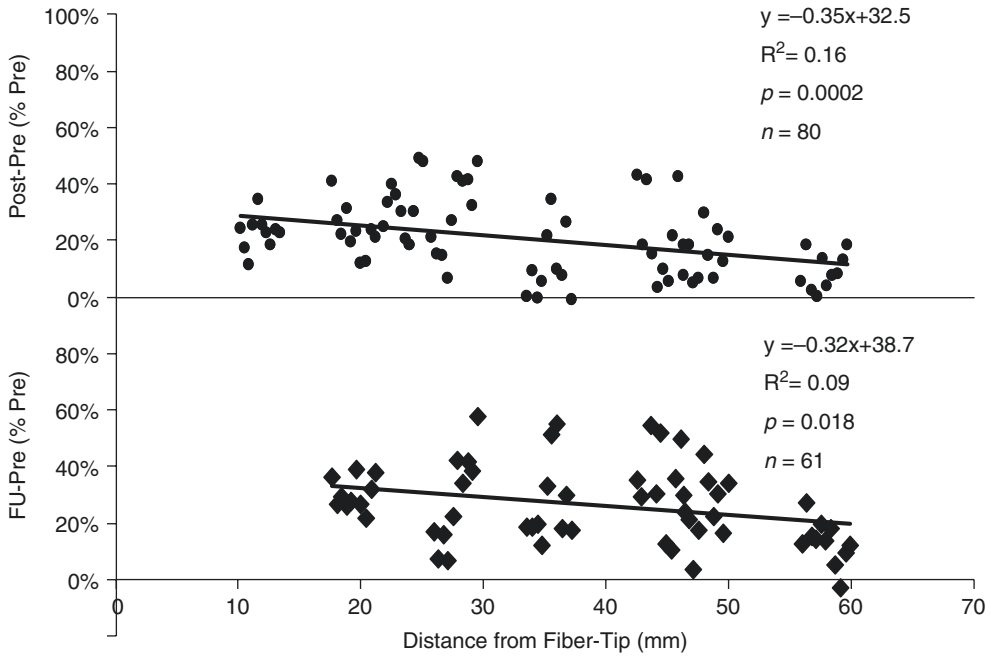

Fig. 6 Scatter plots of the amplitude of UV-induced arterial dilation normalized to the Day 4 pre-treatment diameter are negatively correlated with the distance of the measured segment from the irradiation site. Top: immediately post-treatment (post-pre). Bottom: at 24-h follow-up (FU-pre). Values are plotted as percentage increase over the Day 4 pre-treatment diameter (% Pre). Note: the follow-up data is for two animals. These plots show that the UV dilation effect is long range but semi-localized and thus incapable of inducing systemic hypotension, an assertion consistent with the blood pressure measurements

which the nitrosated product molecules act as vasorelaxants in sequence. However, a chain process in which new NO molecules are produced cyclically has not been reported.

"Spreading vasodilatation" over much smaller distances after acetylcholine application to resistance arteries was attributed to waves of hyperpolarization via gap junctions independent of NO signaling, but this requires *intact* endothelium [14]. We have previously seen that UV laser-facilitated dilation, however, can propagate in the presence of photochemically destroyed endothelium [51, 52, 54], in which mRNA for eNOS was undetectable [53]. In other works, distal transport of arterial dilation in a similar canine double-hemorrhage model was reported to reverse spasm transiently after stimulation of the sphenopalatine ganglion, but the posterior vertebrobasilar system is not accessible by this route [56].

In the present work, propagation of dilation during vasospasm has evidently contributed to angiographic reversal of vasospasm at long range. Serious mechanical damage such as rupture seems unlikely, so long as the UV irradiation safety criterion of 20 W/cm^2 [52] is obeyed, because the mechanism of dilation involves stimulation of an entirely natural pathway. This was demonstrated previously, in which quite severe (ca. 40% of baseline) vasospasm was observed during occlusion of rat MCA by a pure platelet thrombus following singlet oxygen-mediated photochemical injury to endothelium [51, 52, 54]. This was reversed to 20% beyond baseline following exovascular irradiation with 355 nm laser light at 5 W/cm^2 [54]. In fact, the principal result was complete MCA recanalization by means of a new process, designated UV laser-facilitated dethrombosis, in which destabilization of intraplatelet fibrinogen/GPIIb–IIIa cross links leads to continuous formation and branching of microchannels throughout the platelet matrix until disappearance of the occlusive platelet thrombus, indicating that a significant portion of NO escapes into the intravascular space [41]. We therefore propose that, to the extent that accumulation of platelets contributes additional diminution or obstruction of flow during hemorrhage-induced vasospasm, mural obstructions should also be cleared readily and flow anomalies resolved.

Limitations

Although we used a semiautomated routine to mitigate manual measurement errors, it was difficult with our Siemens Angiostar system to measure 10–30% changes in basilar arteries of approximately 1.5 mm in diameter. These changes amount to 1–3 pixel changes in an artery about 12 pixels wide in a 1024 × 1024 pixel image. We compensated for this imprecision by taking many measurements and extensively analyzing them statistically. We also adjusted the calibration factor at the Dog 3 post-treatment point, which has relevance to the results. If this adjustment had not been made, the average post-treatment diameter would have been 90 ± 15% instead of 94 ± 14%, with statistical significance being maintained ($p < 0.001$) over the pre-treatment diameter. Overall, therefore (and especially considering the natural progressive decrease in diameter in this model as shown in Fig. 5), the results clearly indicate that UV laser irradiation quickly (within minutes) induced sustainable dilation, which was visually evident by comparison of the pre- and post-treatment angiograms (cf. Fig. 2). As seen in Figs. 3 and 4, this dilation increased the diameter in Dog 1 to a statistically higher value than baseline (108 ± 7%, $p < 0.001$ in Fig. 4). Given that the pre-treatment diameter was higher (87 ± 9% of baseline) and that the irradiation site was within the proximal basilar segment as opposed to Dogs 2 and 3, this "supra-dilation" is entirely plausible (as noted previously in rats [51, 52, 54]).

Future Research

Whether UV laser-induced reversal of arterial spasm can mitigate reversal of DINDs remains to be ascertained, given that spasm is not apparent until 3–5 days from the onset of hemorrhage [5, 6, 22, 24, 35, 56]. The concept of "early brain injury (EBI)" has been invoked to explain the general refractoriness of SAH to treatment, where microvascular compromise mediated by barrier leakage, platelet activation, and embolic occlusion is believed to be a main acute consequence of SAH and, owing to its persistence, will contribute significantly to morbidity and lethality [7, 15, 39, 40, 45, 46]. The ultimate therapy for SAH and its complications is likely complicated beyond effective reversal of arterial spasm. But, the UV method has several unique properties: (1) arterial dilation at semi-local but still long range can be achieved independent of endothelial integrity, (2) adjacent mural and occlusive platelet thrombi can be dissolved by dethrombosis [51, 52, 54], (3) the maximum duration of spastic dilation in a milieu of exovascular blood is unknown but is at least 1 day, (4) there is no discernible negative systemic consequence of the dilation, (5) the dilation counteracts the propagation of spasm caused by extravasated blood in the perivascular space [23, 44, 57], and (6) platelet-occluded arteriolar-side microvasculature is likely responsive to nitric oxide-induced reversal of spasm and recanalization [49, 52, 54], thus posing the possibility of restoring tissue perfusion in addition to reversing parent artery spasm.

Conclusions

Post-subarachnoid hemorrhage basilar artery vasospasm in canines can be reversed, rapidly and sustainably by endovascular UV irradiation, even if considerably proximal to the

desired point, at laser intensities which apparently do not disrupt vascular structure and function. UV irradiation of NO storage forms in the arterial wall is believed to photophysically replace the arterial NO scavenged by hemorrhagic by-products, and the NO so produced continues to replicate the dilation effect, possibly via transnitrosation, far beyond the initial point of irradiation—but not systemically (Fig. 6). We conjecture that UV laser reversal of vasospasm might be extensible to recovery of NO-sensitive arteriolar function and mitigation of DINDs. For now, this method appears to treat the spastic consequences of hemorrhagic stroke in unique fashion and, owing to its concomitant potential for distal dethrombosis [51, 52, 54], may also be applicable to treatment of microfocal ischemic stroke as a sequela of SAH. We propose that this new approach has the potential to convey significant benefit to patients not responsive to currently available therapies.

Acknowledgments The optical fiber/microcatheter system was provided by OpusGen LLC of Doral, FL, under the name Opus-14 which, upon testing in rats and dogs (described above), led to a Phase I clinical trial on ischemic stroke in Italy in 2010, but OpusGen LLC ceased operations in 2013 when stentrievers became the accepted intervention. We thank Dr. Martin Feelisch for helpful comments regarding the propagating wave mechanism of dilation and Dr. Kunjan Dave for assistance with EndNote. Dr. Watson thanks Dr. John Zhang for suggesting that a canine model be used in what evolved into the present study.

Funding: Initial work on UV laser vasodilation was supported by grant R01 NS23244 (to Dr. Watson) from the National Institute of Neurological Diseases and Stroke. Subsequently, the same agency funded a collaboration via translational grant R21 NS48297 (to Dr. Watson) with VasCon LLC of Doral, FL, to develop the endovascular UV laser delivery system (then known as the Opus-14). To conduct the canine study, Dr. Hurst received research funds from VasCon LLC's successor OpusGen LLC of Doral, FL, and the University of Pennsylvania SRA. Since March 2013, further commercialization has been the responsibility of Photothrombotics, Inc., Miami Beach, FL.

Conflict of Interest: **US patent 6,593,944B1 entitled "Dethrombosis by Vasodilation" was awarded to Dr. Watson in 2003 and provided the conceptual backing for the dog study described herein; in 2013 the patent was assigned to Photothrombotics, Inc.**

Drs. Sadasivan and Hurst report no conflicts.

References

1. Adamczyk P, He S, Amar AP, Mack WJ. Medical management of cerebral vasospasm following aneurysmal subarachnoid hemorrhage: a review of current and emerging therapeutic interventions. Neurol Res Int. 2013;2013:462491. https://doi.org/10.1155/2013/462491.
2. Andaluz N, Tomsick TA, Tew JM Jr, van Loveren HR, Yeh HS, Zuccarello M. Indications for endovascular therapy for refractory vasospasm after aneurysmal subarachnoid hemorrhage: experience at the University of Cincinnati. Surg Neurol. 2002;58:131–8.
3. Andrews KL, McGuire JJ, Triggle CR. A photosensitive vascular smooth muscle store of nitric oxide in mouse aorta: no dependence on expression of endothelial nitric oxide synthase. Br J Pharmacol. 2003;138:932–40. https://doi.org/10.1038/sj.bjp.0705115.
4. Badjatia N, Topcuoglu MA, Pryor JC, Rabinov JD, Ogilvy CS, Carter BS, Rordorf GA. Preliminary experience with intra-arterial nicardipine as a treatment for cerebral vasospasm. AJNR Am J Neuroradiol. 2004;25:819–26.
5. Bauer AM, Rasmussen PA. Treatment of intracranial vasospasm following subarachnoid hemorrhage. Front Neurol. 2014;5:72. https://doi.org/10.3389/fneur.2014.00072.
6. Bederson JB, Connolly ES Jr, Batjer HH, Dacey RG, Dion JE, Diringer MN, Duldner JE Jr, Harbaugh RE, Patel AB, Rosenwasser RH, American Heart A. Guidelines for the management of aneurysmal subarachnoid hemorrhage: a statement for healthcare professionals from a special writing group of the Stroke Council, American Heart Association. Stroke. 2009;40:994–1025. https://doi.org/10.1161/STROKEAHA.108.191395.
7. Caner B, Hou J, Altay O, Fujii M, Zhang JH. Transition of research focus from vasospasm to early brain injury after subarachnoid hemorrhage. J Neurochem. 2012;123(Suppl 2):12–21. https://doi.org/10.1111/j.1471-4159.2012.07939.x.
8. Chaudhry H, Lynch M, Schomacker K, Birngruber R, Gregory K, Kochevar I. Relaxation of vascular smooth muscle induced by low-power laser radiation. Photochem Photobiol. 1993;58:661–9.
9. Clark JF, Sharp FR. Bilirubin oxidation products (BOXes) and their role in cerebral vasospasm after subarachnoid hemorrhage. J Cereb Blood Flow Metab. 2006;26:1223–33. https://doi.org/10.1038/sj.jcbfm.9600280.
10. Clouston JE, Numaguchi Y, Zoarski GH, Aldrich EF, Simard JM, Zitnay KM. Intraarterial papaverine infusion for cerebral vasospasm after subarachnoid hemorrhage. AJNR Am J Neuroradiol. 1995;16:27–38.
11. Dietrich HH, Dacey RG Jr. Molecular keys to the problems of cerebral vasospasm. Neurosurgery. 2000;46:517–30.
12. Eskridge JM, McAuliffe W, Song JK, Deliganis AV, Newell DW, Lewis DH, Mayberg MR, Winn HR. Balloon angioplasty for the treatment of vasospasm: results of first 50 cases. Neurosurgery. 1998;42:510–6.
13. Fathi AR, Bakhtian KD, Pluta RM. The role of nitric oxide donors in treating cerebral vasospasm after subarachnoid hemorrhage. Acta Neurochir Suppl. 2011;110:93–7. https://doi.org/10.1007/978-3-7091-0353-1_17.
14. Feletou M, Vanhoutte PM. Endothelium-derived hyperpolarizing factor: where are we now? Arterioscler Thromb Vasc Biol. 2006;26:1215–25. https://doi.org/10.1161/01.ATV.0000217611.81085.c5.
15. Fujii M, Yan J, Rolland WB, Soejima Y, Caner B, Zhang JH. Early brain injury, an evolving frontier in subarachnoid hemorrhage research. Transl Stroke Res. 2013;4:432–46. https://doi.org/10.1007/s12975-013-0257-2.
16. Fujii Y, Takahashi A, Yoshimoto T. Percutaneous transluminal angioplasty in a canine model of cerebral vasospasm: angiographic, histologic, and pharmacologic evaluation. Surg Neurol. 1995;44:163–70.
17. Furchgott RF, Ehrreich SJ, Greenblatt E. The photoactivated relaxation of smooth muscle of rabbit aorta. J Gen Physiol. 1961;44:499–519.
18. Grasso G. An overview of new pharmacological treatments for cerebrovascular dysfunction after experimental subarachnoid hemorrhage. Brain Res Brain Res Rev. 2004;44:49–63.
19. Hacein-Bey L, Harder DR, Meier HT, Varelas PN, Miyata N, Lauer KK, Cusick JF, Roman RJ. Reversal of delayed vasospasm

by TS-011 in the dual hemorrhage dog model of subarachnoid hemorrhage. AJNR Am J Neuroradiol. 2006;27:1350–4.
20. Hansen-Schwartz J, Vajkoczy P, Macdonald RL, Pluta RM, Zhang JH. Cerebral vasospasm: looking beyond vasoconstriction. Trends Pharmacol Sci. 2007;28:252–6. https://doi.org/10.1016/j.tips.2007.04.002.
21. Hoh BL, Ogilvy CS. Endovascular treatment of cerebral vasospasm: transluminal balloon angioplasty, intra-arterial papaverine, and intra-arterial nicardipine. Neurosurg Clin N Am. 2005;16:501–16. https://doi.org/10.1016/j.nec.2005.04.004.
22. Horikoshi T, Akiyama I, Yamagata Z, Nukui H. Retrospective analysis of the prevalence of asymptomatic cerebral aneurysm in 4518 patients undergoing magnetic resonance angiography—when does cerebral aneurysm develop? Neurol Med Chir. 2002;42:105–12.
23. Iliff JJ, Thrane AS, Nedergaard M. The glymphatic system and brain interstitial fluid homeostasis. Primer on cerebrovascular diseases, 2nd edn; 2017. Elsevier Inc.
24. Komotar RJ, Schmidt JM, Starke RM, Claassen J, Wartenberg KE, Lee K, Badjatia N, Connolly ES Jr, Mayer SA. Resuscitation and critical care of poor-grade subarachnoid hemorrhage. Neurosurgery. 2009;64:397–410. https://doi.org/10.1227/01.NEU.0000338946.42939.C7.
25. Kubaszewski E, Peters A, McClain S, Bohr D, Malinski T. Light-activated release of nitric oxide from vascular smooth muscle of normotensive and hypertensive rats. Biochem Biophys Res Commun. 1994;200:213–8. https://doi.org/10.1006/bbrc.1994.1436.
26. Kuwayama A, Zervas NT, Belson R, Shintani A, Pickren K. A model for experimental cerebral arterial spasm. Stroke. 1972;3:49–56.
27. Linfante I, Delgado-Mederos R, Andreone V, Gounis M, Hendricks L, Wakhloo AK. Angiographic and hemodynamic effect of high concentration of intra-arterial nicardipine in cerebral vasospasm. Neurosurgery. 2008;63:1080–6. https://doi.org/10.1227/01.NEU.0000327698.66596.35.
28. Macdonald RL. Vasospasm: my first 25 years—what worked? What didn't? what next? In: Fandino J, Marbacher S, Fathi AR, Muroi C, Keller E, editors. Neurovascular events after subarachnoid hemorrhage. Acta Neurochir Suppl, vol. 120; 2015. p. 1–10.
29. Macdonald RL, Higashida RT, Keller E, Mayer SA, Molyneux A, Raabe A, Vajkoczy P, Wanke I, Bach D, Frey A, Marr A, Roux S, Kassell N. Clazosentan, an endothelin receptor antagonist, in patients with aneurysmal subarachnoid haemorrhage undergoing surgical clipping: a randomised, double-blind, placebo-controlled phase 3 trial (CONSCIOUS-2). Lancet Neurol. 2011;10:618–25. https://doi.org/10.1016/S1474-4422(11)70108-9.
30. Macdonald RL, Higashida RT, Keller E, Mayer SA, Molyneux A, Raabe A, Vajkoczy P, Wanke I, Bach D, Frey A, Nowbakht P, Roux S, Kassell N. Randomized trial of clazosentan in patients with aneurysmal subarachnoid hemorrhage undergoing endovascular coiling. Stroke. 2012;43:1463–9. https://doi.org/10.1161/STROKEAHA.111.648980.
31. Macdonald RL, Kassell NF, Mayer S, Ruefenacht D, Schmiedek P, Weidauer S, Frey A, Roux S, Pasqualin A, CONSCIOUS-1 Investigators. Clazosentan to overcome neurological ischemia and infarction occurring after subarachnoid hemorrhage (CONSCIOUS-1): randomized, double-blind, placebo-controlled phase 2 dose-finding trial. Stroke. 2008;39:3015–21. https://doi.org/10.1161/STROKEAHA.108.519942.
32. Maxwell AJ. Mechanisms of dysfunction of the nitric oxide pathway in vascular diseases. Nitric Oxide. 2002;6:101–24. https://doi.org/10.1006/niox.2001.0394.
33. Megyesi JF, Vollrath B, Cook DA, Findlay JM. In vivo animal models of cerebral vasospasm: a review. Neurosurgery. 2000;46:448–60.
34. Miller BA, Turan N, Chau M, Pradilla G. Inflammation, vasospasm, and brain injury after subarachnoid hemorrhage. Biomed Res Int. 2014;2014:384342. https://doi.org/10.1155/2014/384342.
35. Morgenstern LB, Hemphill JC III, Anderson C, Becker K, Broderick JP, Connolly ES Jr, Greenberg SM, Huang JN, MacDonald RL, Messe SR, Mitchell PH, Selim M, Tamargo RJ, American Heart Association Stroke Council, Council on Cardiovascular and Stroke Nursing, Council on Clinical Cardiology. Guidelines for the management of spontaneous intracerebral hemorrhage: a guideline for healthcare professionals from the American Heart Association/American Stroke Association. Stroke. 2010;41:2108–29. https://doi.org/10.1161/STR.0b013e3181ec611b.
36. Nedospasov A, Rafikov R, Beda N, Nudler E. An autocatalytic mechanism of protein nitrosylation. Proc Natl Acad Sci U S A. 2000;97:13543–8. https://doi.org/10.1073/pnas.250398197.
37. Ng ES, Cheng ZJ, Ellis A, Ding H, Jiang Y, Li Y, Hollenberg MD, Triggle CR. Nitrosothiol stores in vascular tissue: modulation by ultraviolet light, acetylcholine and ionomycin. Eur J Pharmacol. 2007;560:183–92. https://doi.org/10.1016/j.ejphar.2007.01.016.
38. Nonoyama A. Using multiwavelength UV-visible spectroscopy for the characterization of red blood cells: an investigation of hypochromism. University of South Florida; 2004.
39. Pluta RM. Delayed cerebral vasospasm and nitric oxide: review, new hypothesis, and proposed treatment. Pharmacol Ther. 2005;105:23–56. https://doi.org/10.1016/j.pharmthera.2004.10.002.
40. Pluta RM, Hansen-Schwartz J, Dreier J, Vajkoczy P, Macdonald RL, Nishizawa S, Kasuya H, Wellman G, Keller E, Zauner A, Dorsch N, Clark J, Ono S, Kiris T, Leroux P, Zhang JH. Cerebral vasospasm following subarachnoid hemorrhage: time for a new world of thought. Neurol Res. 2009;31:151–8. https://doi.org/10.1179/174313209X393564.
41. Rassaf T, Preik M, Kleinbongard P, Lauer T, Heiss C, Strauer BE, Feelisch M, Kelm M. Evidence for in vivo transport of bioactive nitric oxide in human plasma. J Clin Invest. 2002;109:1241–8. https://doi.org/10.1172/JCI14995.
42. Rodriguez J, Maloney RE, Rassaf T, Bryan NS, Feelisch M. Chemical nature of nitric oxide storage forms in rat vascular tissue. Proc Natl Acad Sci U S A. 2003;100:336–41. https://doi.org/10.1073/pnas.0234600100.
43. Saito A, Nakazawa T. Cerebral vasospasm model produced by subarachnoid blood injection in dogs. Jpn J Pharmacol. 1989;50:250–2.
44. Saylisoy S, Simsek S, Adapinar B. Is there a connection between perivascular space and subarachnoid space? J Comput Assist Tomogr. 2014;38:33–5. https://doi.org/10.1097/RCT.0b013e3182a9a45a.
45. Sehba FA, Bederson JB. Mechanisms of acute brain injury after subarachnoid hemorrhage. Neurol Res. 2006;28:381–98. https://doi.org/10.1179/016164106X114991.
46. Sehba FA, Pluta RM, Zhang JH. Metamorphosis of subarachnoid hemorrhage research: from delayed vasospasm to early brain injury. Mol Neurobiol. 2011;43:27–40. https://doi.org/10.1007/s12035-010-8155-z.
47. Shen J, Pan JW, Fan ZX, Xiong XX, Zhan RY. Dissociation of vasospasm-related morbidity and outcomes in patients with aneurysmal subarachnoid hemorrhage treated with clazosentan: a meta-analysis of randomized controlled trials. J Neurosurg. 2013;119:180–9. https://doi.org/10.3171/2013.3.JNS121436.
48. Suschek CV, Schroeder P, Aust O, Sies H, Mahotka C, Horstjann M, Ganser H, Murtz M, Hering P, Schnorr O, Kroncke KD, Kolb-Bachofen V. The presence of nitrite during UVA irradiation protects from apoptosis. FASEB J. 2003;17:2342–4. https://doi.org/10.1096/fj.03-0359fje.
49. Terpolilli NA, Feiler S, Dienel A, Muller F, Heumos N, Friedrich B, Stover J, Thal S, Scholler K, Plesnila N. Nitric oxide inhalation

reduces brain damage, prevents mortality, and improves neurological outcome after subarachnoid hemorrhage by resolving early pial microvasospasms. J Cereb Blood Flow Metab. 2015;36(12):2096–107. https://doi.org/10.1177/0271678X15605848.
50. Varsos VG, Liszczak TM, Han DH, Kistler JP, Vielma J, Black PM, Heros RC, Zervas NT. Delayed cerebral vasospasm is not reversible by aminophylline, nifedipine, or papaverine in a "two-hemorrhage" canine model. J Neurosurg. 1983;57:11–7. https://doi.org/10.3171/jns.1983.58.1.0011.
51. Watson BD. Dethrombosis facilitated by vasodilation. USA Patent U.S. Patent No. 6,539,944 B1; 2003.
52. Watson BD, Prado R. Photochemically-based models of focal experimental thrombotic stroke in rodents. Manual of surgical stroke models on rodents. Boca Raton, FL: CRC Press; 2008.
53. Watson BD, Prado R, Truettner J, Dietrich WD. Common carotid artery photothrombosis alters eNOS gene expression in distal cerebral arteries. Soc Neurosci Abstr. 2000;26(Part 2):1811.
54. Watson BD, Prado R, Veloso A, Brunschwig JP, Dietrich WD. Cerebral blood flow restoration and reperfusion injury after ultraviolet laser-facilitated middle cerebral artery recanalization in rat thrombotic stroke. Stroke. 2002;33:428–34.
55. Wolf EW, Banerjee A, Soble-Smith J, Dohan FC Jr, White RP, Robertson JT. Reversal of cerebral vasospasm using an intrathecally administered nitric oxide donor. J Neurosurg. 1998;89:279–88. https://doi.org/10.3171/jns.1998.89.2.0279.
56. Yarnitsky D, Lorian A, Shalev A, Zhang ZD, Takahashi M, Agbaje-Williams M, Macdonald RL. Reversal of cerebral vasospasm by sphenopalatine ganglion stimulation in a dog model of subarachnoid hemorrhage. Surg Neurol. 2005;64:5–11; discussion 11. https://doi.org/10.1016/j.surneu.2004.09.029.
57. Yin J, Lu TM, Qiu G, Huang RY, Fang M, Wang YY, Xiao D, Liu XJ. Intracerebral hematoma extends via perivascular spaces and perineurium. Tohoku J Exp Med. 2013;230:133–9.
58. Zemke D, Farooq MU, Mohammed Yahia A, Majid A. Delayed ischemia after subarachnoid hemorrhage: result of vasospasm alone or a broader vasculopathy? Vasc Med. 2007;12:243–9. https://doi.org/10.1177/1358863X07081316.
59. Zubkov AY, Tibbs RE, Clower B, Ogihara K, Aoki K, Zhang JH. Morphological changes of cerebral arteries in a canine double hemorrhage model. Neurosci Lett. 2002;326:137–41.

Part II

Clinical Science Section

Role of Bedside Multimodality Monitoring in the Detection of Cerebral Vasospasm Following Subarachnoid Hemorrhage

Kasra Khatibi, Viktor Szeder, Manuel Buitrago Blanco, Satoshi Tateshima, Reza Jahan, Gary Duckwiler, and Paul Vespa

Abstract *Background.* Detection of delayed cerebral ischemia (DCI) after aneurysmal subarachnoid hemorrhage (aSAH) in patients with a poor clinical exam is challenging. Brain tissue oxygen tension monitoring ($PbtO_2$) and cerebral microdialysis (CMD) can detect ischemia and metabolic derangements. Our aim was to evaluate efficacy of these modalities in real-time detection of DCI.

Methods. All patients with aSAH who underwent with multimodality monitoring (MMM) with $PbtO_2$ and/or CMD between the years of 2013 and 2015 at our institution were retrospectively studied. Mean $PbTO_2$, lactate to pyruvate ratio (LPR), and glucose over the 24-h period prior to each angiogram for evaluation and treatment of vasospasm were correlated to the extent of vasospasm observed in the hemisphere with the monitors. The average measurements were also compared in the setting of presence and absence of angiographically significant vasospasm.

Results. A total of ten patients with aSAH who underwent MMM were identified. $PbtO_2$ decline correlates with severity of proximal vasospasm ($r = -0.66$). $PbtO_2$ was significantly lower in the setting of vasospasm (17.6 vs. 25.8, $p = 0.003$), but LPR (34.5 vs. 26.8, $p = 0.1$) and glucose (0.8 vs. 1.1, $p = 0.6$) were not significantly different.

Conclusion. Proximal vasospasm after aSAH is associated with MMM indicator of tissue ischemia and/or metabolic derangement. $PbtO_2$ and CMD help in real-time detection and management of DCI.

Keywords Delayed cerebral ischemia · Cerebral vasospasm Multimodality monitoring · Brain tissue oxygen tension Cerebral microdialysis

K. Khatibi (✉) · M. B. Blanco · P. Vespa
Division of Neurocritical Care, Department of Neurosurgery, University of California Los Angeles, Los Angeles, CA, USA
e-mail: kkhatibi@mednet.ucla.edu

V. Szeder · S. Tateshima · R. Jahan · G. Duckwiler
Department of Radiology, University of California Los Angeles, Los Angeles, CA, USA

Introduction

Delayed cerebral ischemia (DCI) is a major cause of death and disability after aneurysmal subarachnoid hemorrhage (aSAH). The clinical detection of DCI is challenging, particularly in the setting of a comatose patient. Up to 30% of ischemic lesions are clinically silent [1, 2]. Transcranial Doppler ultrasound (TCD) is routinely done at many institutions but has limited sensitivity and specificity in diagnosing DCI [3]. CT and MR angiography and perfusion imaging may provide detection of tissue ischemia during cerebral vasospasm but are limited by restrictions in temporal resolution and repeatability in the clinical setting [1].

Intraparenchymal tissue multimodality monitors (MMM), such as brain tissue oxygen tension monitor ($PbtO_2$) and cerebral microdialysis (CMD), are easily implanted at the bedside and provide real-time data points on the perfusion, metabolic state, and neuronal damage. Data from multimodality monitors have demonstrated prognostic value in patients with subarachnoid hemorrhage [1, 2, 4, 5]. However, there is a paucity of data about the reliability, impact, and usefulness of MMM to guide diagnosis and treatment of DCI after subarachnoid hemorrhage [6, 7]. Our objective was to study changes in brain tissue oxygen tension and cerebral microdialysis in the setting of confirmed angiographic cerebral vasospasm. Our hypothesis is that MMM would provide a reliable indicator of DCI after SAH in comatose patients. We selected to study the reliability of PbtO2 and CMD separately and in aggregate in this study.

Methods

This is retrospective observational, IRB-approved study of a consecutive series of comatose aSAH patients who underwent $PbtO_2$ and CMD monitoring between 2013 and 2015 at our institution. TCD was performed on a daily basis to screen for vasospasm. Indications for MMM were (1) coma and (2)

R. D. Martin et al. (eds.), *Subarachnoid Hemorrhage*, Acta Neurochirurgica Supplement 127, https://doi.org/10.1007/978-3-030-04615-6_20,

presumed DCI due to vasospasm, and MMM was used as standard of care. The probes for the $PbtO_2$ and CMD monitoring were placed at bedside at Kocher point 2–3 cm deep into the unaffected white matter. This location corresponds to anterior cerebral artery (ACA)-middle cerebral artery (MCA) watershed territory [8]. Hourly values of CMD and $PtbO_2$ were used for this study. Using CMD metabolic variables, glucose and lactate to pyruvate ratio (LPR) were sampled and monitored on an hourly basis. Licox® monitors were used to continuously monitor $PbtO_2$ [9]. The patients subsequently received routine clinical care in the intensive care unit (ICU) and underwent digital subtraction angiography (DSA) when there was concern for vasospasm that remained refractory to medical management.

Blinded assessment of data points was carried out retrospectively. MMM measures were averaged during the 24-h epoch prior to DSA. The angiographic vasospasm for each vessel was graded by the interventionalist performing the procedure and retrospectively quantified from 0, indicating there was no vasospasm, to 6 representing severe proximal vasospasm [10] (Fig. 1). The extent of vasospasm for each DSA was estimated by the weighted average of the internal carotid artery (ICA), MCA, and ACA: (3 × ICA + 2 × MCA + 1 × ACA)/6. Based on the proposed calculation, the epochs were dichotomized to one of two groups: vasospasm present, when the calculated value was equal or greater than one, and vasospasm absent.

Based on the limited number of observations, the simplifying assumption was made that the noted observations from all epochs were statistically independent. A two-tailed unpaired student T-test was used to compare the observations in the groups with and without vasospasm. We then looked at the relation of extent of vasospasm to $PbtO_2$ and LPR and the relationship between $PbtO_2$ and LPR in this population using the Spearman correlation coefficient. We subsequently fit receiver operating characteristic (ROC) curves for both $PbtO_2$ and LPR predicting presence of vasospasm.

Results

Ten subjects were identified with aSAH who had undergone $PbtO_2$ and CMD monitoring, out of which six had epochs with evidence of radiographic vasospasm. The patients' characteristics are depicted in Table 1.

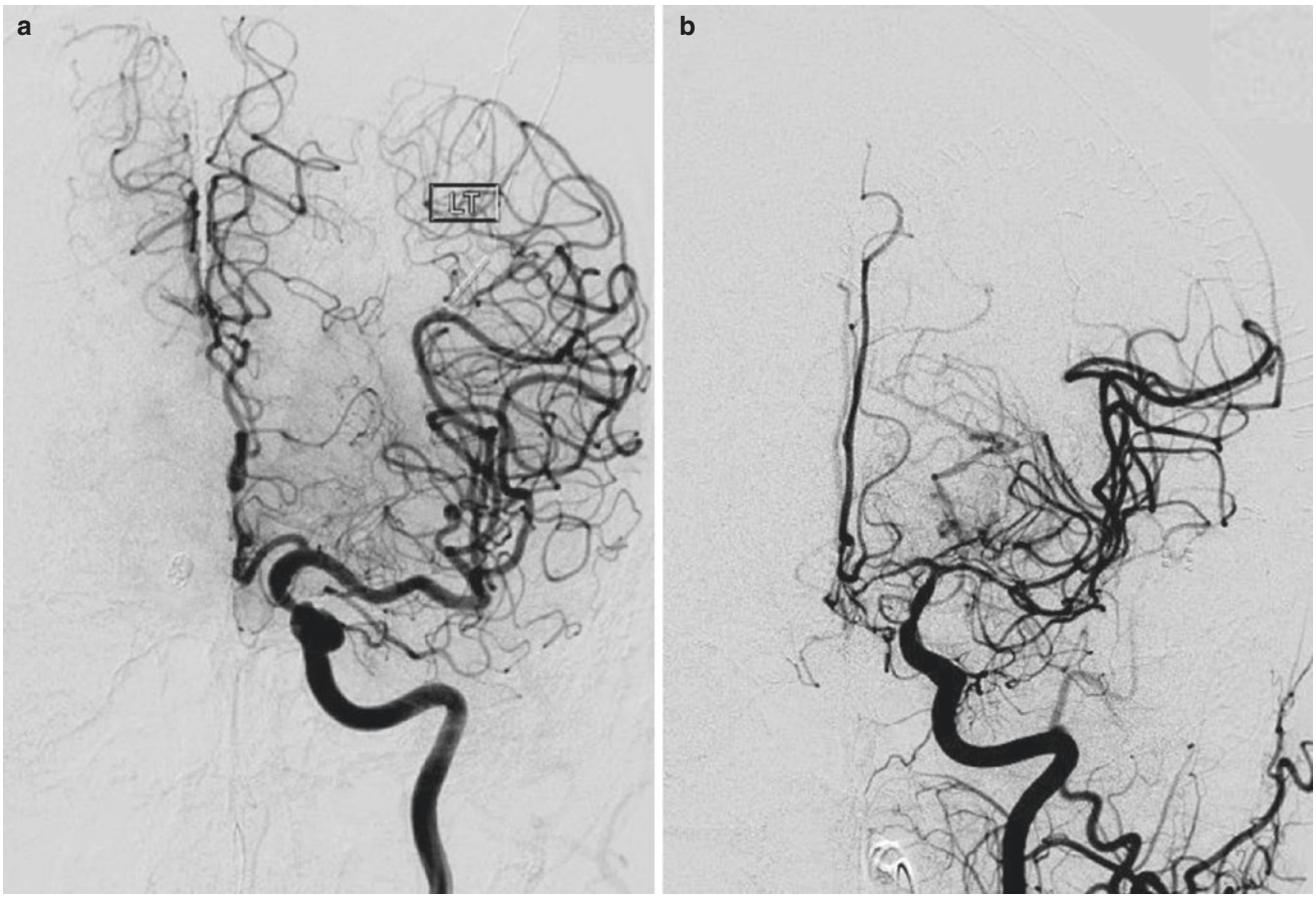

Fig. 1 A representative example of the left ICA without spasm (grade 0) B. A representative example of the left ICA in moderate spasm (grade 4)

Sixteen time intervals were evaluated for $PbtO_2$ and 18 intervals were utilized for glucose and LPR. The average $PbtO_2$ during spasm was significantly lower (17.6 ± 5.5 vs. 25.8 ± 3.73, $p = 0.003$). LPR was not different in spasm versus non-spasm (34.5 vs. 26.8, $p = 0.1$). Glucose was comparable in both groups: (0.8 vs. 1.1, $p = 0.6$) (Fig. 2). The correlation coefficients for the extent of spasm with $PbtO_2$, LPR, and $PbtO_2$ and LPR, respectively, were −0.66, 0.38, and −0.55 (Fig. 3).

The area under the curve (AUC) for fitted ROC curve for $PbtO_2$ was 0.9. When choosing the threshold for $PbtO_2$ to be less than 20 mmHg, it was 71% sensitive and 89% specific in prediction of vasospasm. AUC for fitter ROC curve for LPR was 0.75. When choosing threshold for LPR to be more than 25, it was 80% sensitive and 43% specific in prediction of vasospasm.

Table 1 Patient characteristics

Number of patients	10
Age: mean ± SD (years)	62 ± 10
Gender	
Women	60%
Aneurysm location	
Anterior circulation	90%
Hunt-Hess grade	
4	60%
3	20%
2	20%
Modified Fisher grade	
4	80%
3	20%
Intervention	
Coil embolization	90%
Duration of monitoring: mean ± SD (days)	7 ± 5

Discussion

Our study results indicate a severity-dependent reduction in pre-angiographic $PbtO_2$ values in patients with cerebral vasospasm. In contrast, CMD LPR was abnormal >25 in all severities of vasospasm and across a wide spectrum of $PtbO_2$ values. This indicates divergence of MMM indicators across the spectrum of vasospasm severity. These results occurred despite having clinical goals of desired cerebral perfusion pressure (CPP), intracranial pressure (ICP), oxygen saturation (SpO_2), and hemoglobin (Hgb) in both groups (Table 2). The ability to validate tissue-level ischemia in the setting of mild to moderate severity of large artery vasospasm is demonstrated by these data. Such validation may become important in making treatment decisions, especially when treatments may carry risk of iatrogenic injury [11–13].

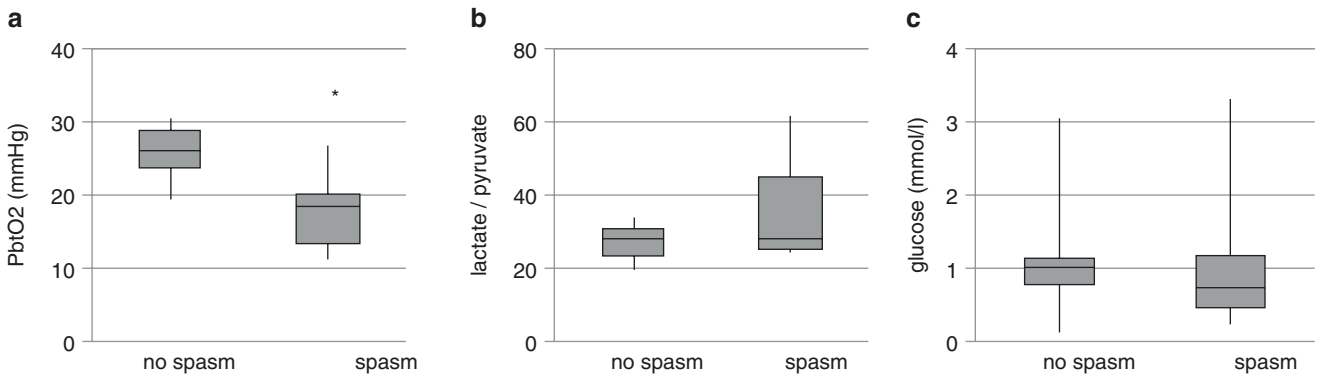

Fig. 2 (**a**) $PbtO_2$ significantly decreased in the setting of vasospasm, (**b**) LPR and (**c**) glucose were not significantly different during spasm

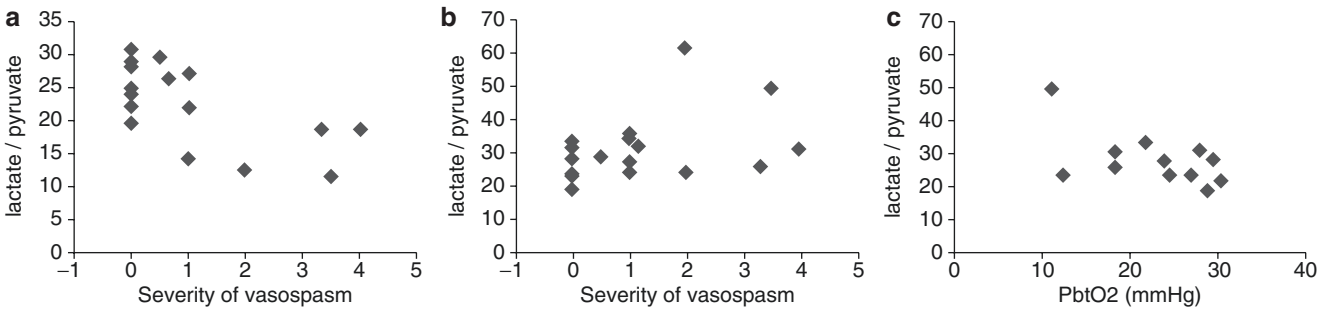

Fig. 3 (**a**) Scatter plot of $PbtO_2$ changes as a function of the extent of vasospasm. Spearman correlation coefficient was −0.66. (**b**) Scatter plot of LPR changes as a function of the extent of vasospasm. Spearman correlation coefficient was 0.38. (**c**). Scatter plot of LPR changes with $PbtO_2$. Spearman correlation coefficient was −0.55

Table 2 Level of other cofactors affecting cerebral oxygen delivery in epochs with and without vasospasm

	No spasm (mean ± SD)	Spasm (mean ± SD)	p-value
CPP (mmHg)	104 ± 9	115 ± 22	0.25
ICP (mmHg)	9.1 ± 3	10.2 ± 3	0.45
SpO2 (%)	99.6 ± 0.3	99.8 ± 0.2	0.1
Hgb (g/dL)	11.0 ± 0.6	10.7 ± 0.6	0.27

For reproducible and meaningful real-time clinical use of MMM, clear diagnostic thresholds need to be determined. To quantify such thresholds, quantitative angiographic measures of vasospasm need to be established. The optimum time window for comparison also remains poorly defined. A myriad of different intervals, a few hours for up to 24 h, have been used in other studies, with no established rationale to support such decisions [7].

Notable strengths of our study include diversity of population making the study generalizable. The patients included also have severe initial presentation with guarded clinical examination for whom clinical detection of vasospasm is challenging making them the best population for application such monitoring techniques.

There are several limitations to our study, including the study design as a retrospective observational study. This design subjects the study to recall bias and does not allow for controlling for confounding variables. However, the relevant clinical co-variables affecting cerebral perfusion are accounted for and are comparable in the two groups. Given the limited number of observations, the recorded intervals within and in-between subjects were presumed to be statistically independent.

In our study the extent of each subject's angiographic vasospasm was determined on a previously established grading scale based on caliber changes to large and medium cerebral vessels [10]. However, more dynamic measures of cerebral blood flow such as perfusion imaging would be more accurate in detection of hypoperfusion [14], such as MMM, which we propose.

Conclusion

Proximal vasospasm after aSAH is associated with MMM indicator of tissue ischemia and/or metabolic derangement. Brain tissue oxygen tension monitoring and cerebral microdialysis can assist in clinical decision-making for the real-time detection of vasospasm and guide perfusion optimization at the bedside.

Conflict of Interest We declare that we have no conflict of interest.

References

1. Schmidt JM, Ko SB, Helbok R, Kurtz P, Stuart RM, Presciutti M, et al. Cerebral perfusion pressure thresholds for brain tissue hypoxia and metabolic crisis after poor-grade subarachnoid hemorrhage. Stroke. 2011;42:1351–6.
2. Helbok R, Madineni RC, Schmidt MJ, Kurtz P, Fernandez L, Ko SB, et al. Intracerebral monitoring of silent infarcts after subarachnoid hemorrhage. Neurocrit Care. 2011;14:162–7.
3. Carrera E, Schmidt JM, Oddo M, Fernandez L, Claassen J, Seder D, et al. Transcranial doppler for predicting delayed cerebral ischemia after subarachnoid hemorrhage. Neurosurgery. 2009;65:316–23; discussion 323-314
4. Kett-White R, Hutchinson PJ, Al-Rawi PG, Gupta AK, Pickard JD, Kirkpatrick PJ. Adverse cerebral events detected after subarachnoid hemorrhage using brain oxygen and microdialysis probes. Neurosurgery. 2002;50:1213–21; discussion 1221-1212
5. Schulz MK, Wang LP, Tange M, Bjerre P. Cerebral microdialysis monitoring: Determination of normal and ischemic cerebral metabolisms in patients with aneurysmal subarachnoid hemorrhage. J Neurosurg. 2000;93:808–14.
6. Sarrafzadeh AS, Haux D, Ludemann L, Amthauer H, Plotkin M, Kuchler I, et al. Cerebral ischemia in aneurysmal subarachnoid hemorrhage: A correlative microdialysis-pet study. Stroke. 2004;35:638–43.
7. Unterberg AW, Sakowitz OW, Sarrafzadeh AS, Benndorf G, Lanksch WR. Role of bedside microdialysis in the diagnosis of cerebral vasospasm following aneurysmal subarachnoid hemorrhage. J Neurosurg. 2001;94:740–9.
8. Deshaies EM, Jacobsen W, Singla A, Li F, Gorji R. Brain tissue oxygen monitoring to assess reperfusion after intra-arterial treatment of aneurysmal subarachnoid hemorrhage-induced cerebral vasospasm: A retrospective study. AJNR Am J Neuroradiol. 2012;33:1411–5.
9. De Georgia MA. Brain tissue oxygen monitoring in neurocritical care. J Intensive Care Med. 2015;30:473–83.
10. Kassell NF, Helm G, Simmons N, Phillips CD, Cail WS. Treatment of cerebral vasospasm with intra-arterial papaverine. J Neurosurg. 1992;77:848–52.
11. Firlik AD, Kaufmann AM, Jungreis CA, Yonas H. Effect of transluminal angioplasty on cerebral blood flow in the management of symptomatic vasospasm following aneurysmal subarachnoid hemorrhage. J Neurosurg. 1997;86:830–9.
12. Hoelper BM, Hofmann E, Sporleder R, Soldner F, Behr R. Transluminal balloon angioplasty improves brain tissue oxygenation and metabolism in severe vasospasm after aneurysmal subarachnoid hemorrhage: Case report. Neurosurgery. 2003;52:970–4; discussion 974-976
13. Vajkoczy P, Horn P, Bauhuf C, Munch E, Hubner U, Ing D, et al. Effect of intra-arterial papaverine on regional cerebral blood flow in hemodynamically relevant cerebral vasospasm. Stroke. 2001;32:498–505.
14. Scalzo F, Liebeskind DS. Perfusion angiography in acute ischemic stroke. Comput Math Methods Med. 2016;2016:2478324.

Development of a Delayed Cerebral Infarction Load Scoring System (DCI Score)

George Kwok Chu Wong, Ryan Chi Hang Nung, Jacqueline Ching Man Sitt, Vincent Chung Tong Mok, Adrian Wong, Wai Sang Poon, Defeng Wang, Jill Abrigo, and Deyond Yun Woon Siu

Abstract Delayed cerebral infarction (DCI) is related to unfavorable outcome after aneurysmal subarachnoid hemorrhage (SAH). There lacks a clear understanding how the DCI load affects cognitive function after SAH. We conducted a literature review on the clinical classification systems on brain hemorrhages and cerebral infarction and devised a Delayed Cerebral Infarction Load Scoring System (DCI Score). DCI Score significantly correlated with Symbol Digit Modalities Test (−0.334, p = 0.032), Color Trail Test (−0.310, p = 0.032), Hong Kong List Learning Test (−0.318, p = 0.036), Verbal Digit Span Forward (−0.382, p = 0.017), and Visual Digit Span Backward (−0.425, p = 0.012). In conclusion, higher DCI load impacted significantly on memory and executive function. DCI Score is a useful system for clinical quantification of DCI load and clinical research.

Keywords Cognitive function · Delayed cerebral infarction Stroke · Subarachnoid hemorrhage

Introduction

Aneurysmal subarachnoid hemorrhage (SAH) is a highly morbid disease resulting in cognitive dysfunction and activity limitation despite reduction in mortality [1, 3, 4, 10–12]. Cognitive dysfunction is an important determinant for functional outcome and is associated with delayed cerebral infarction (DCI) [6]. However, few studies reported on the quantitative impact of DCI, and there is no commonly used quantification method for DCI. Although volume measurement seems to be the most accurate, it does not take into account the dispersal of DCI, and it is not practical to do volume measurement in routine clinical setting. We have reported recently that using a semiquantitative method to measure DCI load, after adjustment for age, admission World Federation of Neurosurgical Societies Grade and mode of aneurysm treatment, both middle cerebral artery cortical infarct load and perforator infarct load were independently associated with poor cognitive outcomes (Montreal Cognitive Assessment and Mini-Mental State Examination) and modified Rankin Scale [9]. We postulated that this DCI scoring system could predict neuropsychological test scores at 3 months post-SAH.

Materials and Methods

We prospectively recruited SAH patients in a regional neurosurgical center in Hong Kong over a 2-year period. The study was approved by the Joint NTEC-CUHK (New Territories East Cluster-Chinese University of Hong Kong) Clinical Research Ethics Committee. The study conformed to the Declaration of Helsinki, and written informed consent was obtained from all of the participants or their next of kin.

The patient inclusion criteria were (1) spontaneous SAH with angiography-confirmed intracranial aneurysms, (2) hospital admission within 96 h after ictus, (3) between 21 and 75 years of age, (4) a speaker of Chinese (Cantonese), (5) a CT of brain done at 4–6 weeks, and (6) informed consent from the patients or their next of kin. The patient exclusion criteria were (1) a history of previous cerebrovascular or neurological disease other than unruptured intracranial aneurysm or (2) a history of neurosurgery before ictus.

G. K. C. Wong (✉) · W. S. Poon
Division of Neurosurgery, Prince of Wales Hospital, the Chinese University of Hong Kong, Hong Kong, China
e-mail: georgewong@surgery.cuhk.edu.hk

R. C. H. Nung · J. C. M. Sitt · D. Wang · J. Abrigo · D. Y. W. Siu
Department of Imaging and Interventional Radiology, Prince of Wales Hospital, the Chinese University of Hong Kong, Hong Kong, China

V. C. T. Mok · A. Wong
Division of Neurology, Prince of Wales Hospital, the Chinese University of Hong Kong, Hong Kong, China

R. D. Martin et al. (eds.), *Subarachnoid Hemorrhage*, Acta Neurochirurgica Supplement 127,
https://doi.org/10.1007/978-3-030-04615-6_21,

All CT scans were performed on a 64-slice CT (Lightspeed VCT; GE Healthcare), with axial images acquired in 5-mm thick sections, which were reviewed for image analysis. Delayed CT was defined as posttreatment 4–6 weeks. DCI was defined as new parenchymal hypoattenuation on delayed CT, which was not present in early and posttreatment (after 24–48 h) CT and cannot be accounted by hydrocephalus.

DCI load was measured by DCI Score as described previously [9]. In brief, the affected territories of the anterior circulation were graded by a systematic quantitative scoring system modified from Alberta Stroke Program Early CT Score (ASPECTS) as m-ASPECTS [2]. The m-ASPECTS value was calculated from two standard axial CT cuts, at the level of the thalamus and basal ganglia, and just rostral to the ganglionic structures. The territory of the middle cerebral artery (MCA) is allocated 10 points. We modified by adding 1 point for each anterior cerebral artery territory for each cut. One point is subtracted for an area of parenchymal hypoattenuation, for each of the defined regions. The m-ASPECTS thus allocated the anterior circulation 24 points (Fig. 1). For posterior circulation infarct, posterior circulation Acute Stroke Prognosis Early CT Score (pc-ASPECTS) is used [5]. pc-ASPECTS allocated the posterior circulation 10 points (Fig. 2). DCI Score was the sum scores of the m-ASPECTS and pc-ASPECTS. The sum scores ranged from 0 to 34 (no parenchymal hypoattenuation).

Cognitive outcomes were assessed by a comprehensive neuropsychological battery at 3 months post-SAH. The battery of cognitive assessments used in this study was previously applied in a local Chinese population [7]. Its selection was based on (a) its efficacy in previous cognitive studies in local Chinese patients and standard cognitive tests validated in a Cantonese-speaking population and (b) its balanced range of tests covering verbal and visuospatial memory, attention and working memory, executive functions, psychomotor speed, and language. This battery included the following.

Verbal Memory Domain

1. Hong Kong List Learning Test (HKLLT).

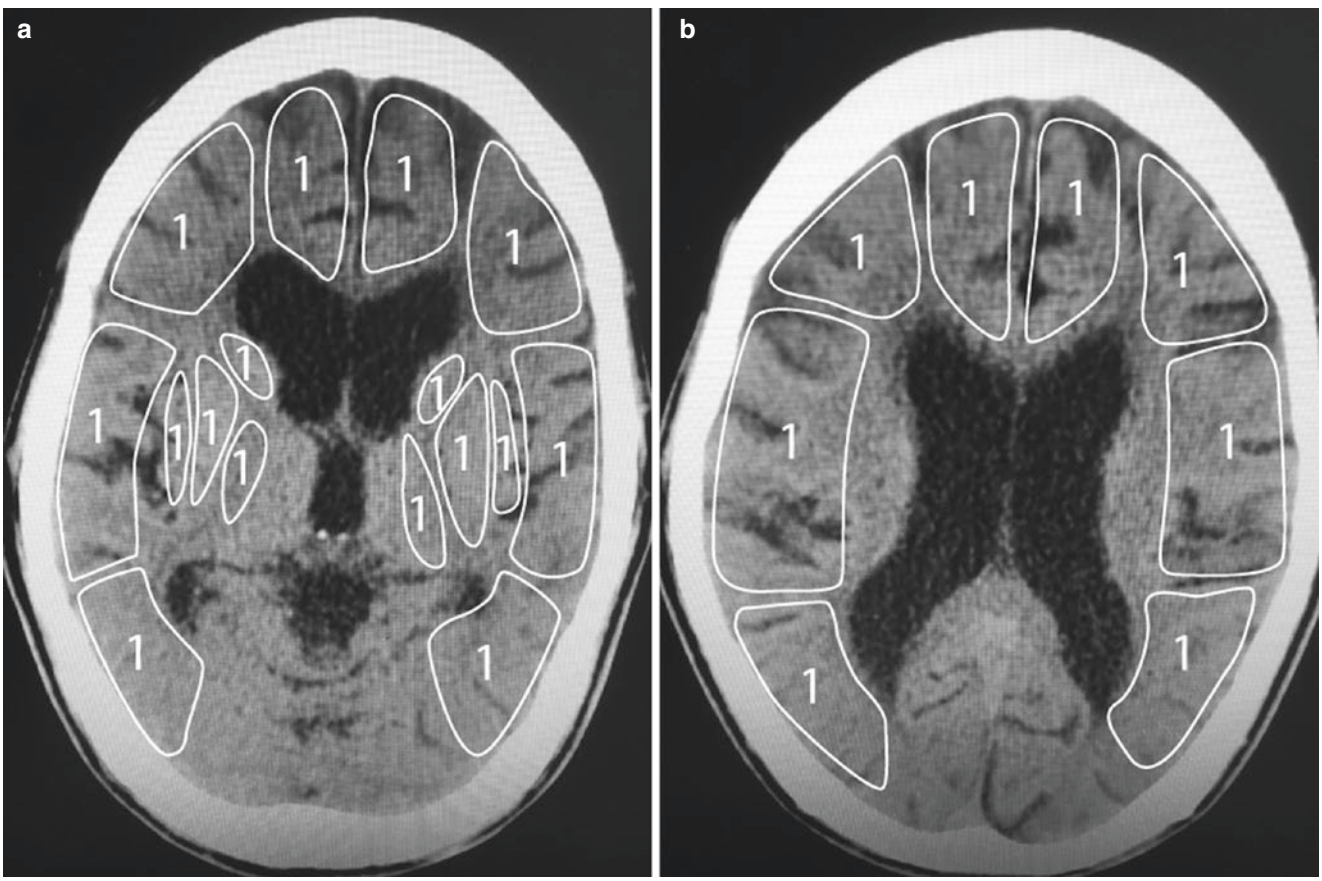

Fig. 1 m-ASPECTS. The m-ASPECTS value was calculated from two standard axial CT cuts, (**a**) at the level of the thalamus and basal ganglia and (**b**) just rostral to the ganglionic structures. The territory of the middle cerebral artery (MCA) is allocated 10 points. We modified by adding 1 point for each anterior cerebral artery territory for each cut. One point is subtracted for an area of parenchymal hypoattenuation, for each of the defined regions. The m-ASPECTS thus allocated the anterior circulation 24 points

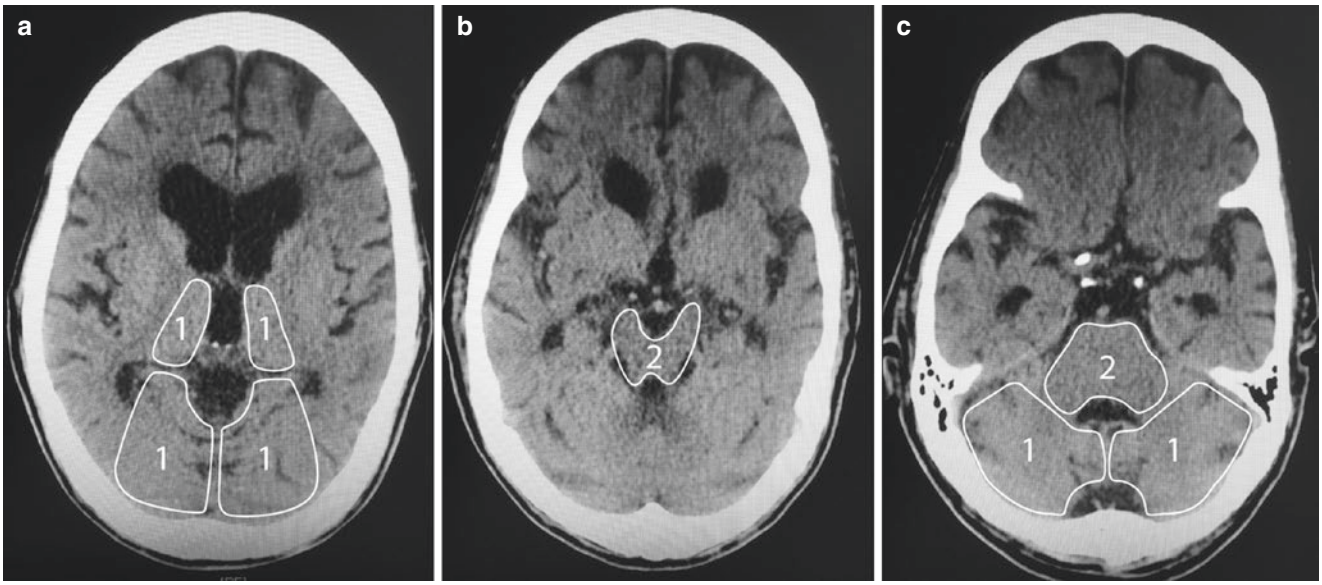

Fig. 2 pc-ASPECTS. The pc-ASPECTS allocated the posterior circulation 10 points. (**a**) Thalamus and occipital lobe, (**b**) midbrain, (**c**) pons and cerebellum

Visuospatial Skill and Memory Domain

1. The Rey Osterrieth Complex Figure Test.

Attention and Working Memory Domain

1. The verbal and visual digit span forward and backward tests from the Chinese Wechsler Memory Scale-Third Edition.

Executive Function and Psychomotor Speed Domain

1. Symbol-Digit Modalities Test.
2. Color Trails Test (CTT).
3. Animal fluency.

Language Domain

1. Modified Boston Naming Test (mBNT).

Cognitive test scores were converted into z scores of the respective test measures derived from established age- and education-matched norms.

Statistical Analyses

Data were analyzed using SPSS for Windows, version 20.0 (SPSS Inc.). Correlations were assessed by Kendall's tau b coefficients. Statistical significance was taken as a 2-tailed p value of 0.05 or less.

Results

Out of 126 SAH patients recruited into an earlier DCI study, 35 SAH patients consented for and completed the 3-month neuropsychology battery assessments. Twenty-four (69%) were female and age (mean ± SD) was 52 ± 10 years.

On admission, World Federation of Neurosurgical Societies (WFNS) grade was I in 20 (57%), II in 11 (37%), III in 2 (6%), and IV in 2 (6%). Thirteen (37%) had known preexisting hypertension. Sixteen (46%) had intraventricular hemorrhage, two (6%) had intracerebral hemorrhage, and one (3%) had subdural hematoma. Ten (29%) had hydrocephalus upon admission. Ruptured cerebral aneurysms were located in anterior circulation in 27 (77%) and in posterior circulation in 8 (23%). Twenty-one (60%) aneurysms were coiled and 14 (40%) aneurysms were clipped.

Median Mini-Mental State Examination score was 28 (IQR 24.75–29). Median Montreal Cognitive Assessment score was 22 (IQR 20–25). DCI Score significantly correlated with Symbol Digit Modalities Test (−0.334, $p = 0.032$), Color Trail Test (−0.310, $p = 0.032$), Hong Kong List

Learning Test (−0.318, p = 0.036), Verbal Digit Span Forward (−0.382, p = 0.017), and Visual Digit Span Backward (−0.425, p = 0.012).

Discussion

In this study, we found that DCI Score was associated with executive function, verbal and visual memory neuropsychological test scores. Cognitive function plays an important role in instrumental activity of daily living [7]. In our earlier analyses, domains of instrumental activity of daily living [use of telephone (OR 1.5; 95% CI 1.3–1.7; $p < 0.001$), transportation (OR 1.3; 95% CI 1.2–1.4; $p < 0.001$), shopping (OR 1.3; 95% CI 1.2–1.3; $p < 0.001$), meal preparation (OR 1.3; 95% CI 1.2–1.4; $p < 0.001$), housework (OR 1.2; 95% CI 1.1–1.3; $p < 0.001$), handyman work (OR 1.2; 95% CI 1.1–1.3; $p < 0.001$), laundry (OR 1.2; 95% CI 1.1–1.3; $p < 0.001$), medication management (OR 1.3; 95% CI 1.2–1.4; $p < 0.001$), and money management (OR 1.4; 95% CI 1.2–1.5; $p < 0.001$)] were significantly correlated with MoCA score after adjustment for age [8].

There were several limitations in our current study. Firstly, the study did not examine how cognitive dysfunction interfered with different tasks of activity of daily living. Secondly, quality of life and neuropsychiatric assessments were not included. Thirdly, the sample size did not allow meaningful evaluation of predictive values of DCI Score. Fourthly, we did not had serial assessments in these patients to see the pattern of cognitive dysfunction at different time points and how these dysfunction evoluted over time.

Our work is important as to provide an understanding of the DCI Score and cognitive dysfunction after SAH. These data suggests that DCI load as reflected by DCI Score predicts cognitive function 3 months after SAH. A multicenter study to further investigate the impact of DCI load should be pursued.

Conclusions

Higher DCI Scores impacted significantly on memory and executive function. DCI Score is a useful system for clinical quantification of DCI load and clinical research. Treatment strategy should be developed to minimize them.

Funding

This work was supported by Research and Training Fund of the Division of Neurosurgery of the Chinese University of Hong Kong.

Conflict of Interest Statement: All authors declared no conflict of interest.

References

1. Al-Khindi T, Macdonald RL, Schweizer TA. Cognitive and functional outcome after aneurysmal subarachnoid hemorrhage. Stroke. 2010;41:e519–36. https://doi.org/10.1161/STROKEAHA.110.581975.
2. Barber PA, Demchuk AM, Zhang J, Buchan AM. Validity and reliability of a quantitative computed tomography score in predicting outcome of hyperacute stroke before thrombolytic therapy. ASPECTS Study Group Alberta Stroke Programme Early CT Score. Lancet. 2000;355:1670–4.
3. Macdonald RL, Jaja B, Cusimano MD, Etminan N, Hanggi D, Hasan D, Ilodigwe D, Lantigua H, Le Roux P, Lo B, Louffat-Olivares A, Mayer S, Molyneux A, Quinn A, Schweizer TA, Schenk T, Spears J, Todd M, Torner J, Vergouwen MD, Wong GK, Singh J, SAHIT Collaboration. SAHIT Investigators—on the outcome of some subarachnoid hemorrhage clinical trials. Transl Stroke Res. 2013;4:286–96. https://doi.org/10.1007/s12975-012-0242-1.
4. Nieuwkamp DJ, Setz LE, Algra A, Linn FHH, de Rooij NK, Rinkel GJ. Changes in case fatality of aneurysmal subarachnoid haemorrhage over time, according to age, sex, and region: a meta-analysis. Lancet Neurol. 2009;8:635–42. https://doi.org/10.1016/S1474-4422(09)70126-7.
5. Puetz V, Sylaja PN, Coutts SB, Hill MD, Dzialowski I, Mueller P, Becker U, Urban G, O'Reilly C, Barber PA, Sharma P, Goyal M, Gahn G, von Kummer R, Demchuk AM. Extent of hypoattenuation on CT angiography source images predicts functional outcome in patients with basilar artery occlusion. Stroke. 2008;39:2485–90. https://doi.org/10.1161/STROKEAHA.107.511162.
6. Wong GK, Lam S, Ngai K, Wong A, Mok V, Poon WS, Cognitive Dysfunction after Aneurysmal Subarachnoid Haemorrhage Investigators. Evaluation of cognitive impairment by the Montreal cognitive assessment in patients with aneurysmal subarachnoid haemorrhage: prevalence, risk factors, and correlations with 3 month outcome. J Neurol Neurosurg Psychiatry. 2012;83:1112–7. https://doi.org/10.1136/jnnp-2012-302217.
7. Wong GK, Lam SW, Ngai K, Wong A, Siu D, Poon WS, Mok V, Cognitive Dysfunction after Aneurysmal Subarachnoid Hemorrhage Investigators. Cognitive domain deficits in patients with aneurysmal subarachnoid haemorrhage at 1 year. J Neurol Neurosurg Psychiatry. 2013;84:1054–8. https://doi.org/10.1136/jnnp-2012-304517.
8. Wong GK, Lam SW, Wong A, Lai M, Siu D, Poon WS, Mok V. MoCA-assessed cognitive function and excellent outcome after aneurysmal subarachnoid hemorrhage at 1 year. Eur J Neurol. 2014;21:725–30. https://doi.org/10.1111/ene.12363.
9. Wong GK, Nung RC, Sitt JC, Mok VC, Wong A, Ho FL, Poon WS, Wang D, Abrigo J, Siu DY. Location, infarct load, and 3-month outcomes of delayed cerebral infarction after aneurysmal subarachnoid hemorrhage. Stroke. 2015;46:3099–104. https://doi.org/10.1161/STROKEAHA.115.010844.
10. Wong GK, Poon WS, Boet R, Chan MT, Gin T, Ng SC, Zee BC. Health-related quality of life after aneurysmal subarachnoid hemorrhage: profile and clinical factors. Neurosurgery. 2011;68:1556–61. https://doi.org/10.1227/NEU.0b013e31820cd40d.
11. Wong GK, Poon WS, Chan MT, Boet R, Gin T, Ng SC, Zee BC, IMASH Investigators. Intravenous magnesium sulphate for aneurysmal subarachnoid hemorrhage (IMASH): a randomized, double-blinded, placebo-controlled, multicenter phase III trial. Stroke. 2010;41:921–6. https://doi.org/10.1161/STROKEAHA.109.571125.
12. Wong GK, Tam YY, Zhu XL, Poon WS. Incidence and mortality of spontaneous subarachnoid hemorrhage in Hong Kong from 2002 to 2010: a Hong Kong hospital authority clinical management system database analysis. World Neurosurg. 2014;81:552–6. https://doi.org/10.1016/j.wneu.2013.07.128.

Changes on Dynamic Cerebral Autoregulation Are Associated with Delayed Cerebral Ischemia in Patients with Aneurysmal Subarachnoid Hemorrhage

S. Ortega-Gutierrez, E. A. Samaniego, A. Reccius, A. Huang, B. Zheng-Lin, A. Masukar, R. S. Marshall, and N. H. Petersen

Abstract *Background*: Early identification of vasospasm prior to symptom onset would allow prevention of delayed cerebral ischemia (DCI) in aneurysmal subarachnoid hemorrhage (aSAH). Dynamic cerebral autoregulation (DCA) is a noninvasive means of assessing cerebral blood flow regulation by determining independence of low-frequency temporal oscillations of systemic blood pressure (BP) and cerebral blood flow velocities (CBFV).

Methods: Eight SAH patients underwent prospectively a median of 7 DCA assessments consisting of continuous measurements of BCFV and BP. Transfer function analysis was applied to calculate average phase shift (PS) in low (0.07–0.2 Hz) frequency range for each hemisphere as continuous measure of DCA. Lower PS indicated poorer regulatory response. DCI was defined as a 2-point decrease in Glasgow Coma Score and/or infarction on CT.

Results: Three subjects developed symptomatic vasospasm with median time-to-DCI of 9 days. DCI was significantly associated with lower PS over the entire recording period (Wald = 4.28; $p = 0.039$). Additionally, there was a significant change in PS over different recording periods after adjusting for DCI (Wald = 15.66; $p = 0.001$); particularly, a significantly lower mean PS day 3–5 after bleed (14.22 vs 27.51; $p = 0.05$).

Conclusions: DCA might be useful for early detection of symptomatic vasospasm. A larger cohort study of SAH patients is currently underway.

Keywords Vasospasm · Delay cerebral ischemia · Dynamic cerebral autoregulation

Abbreviations

ABP	Arterial blood pressure
aSAH	Aneurysmal subarachnoid hemorrhage
CBF	Cerebral blood flow
CBFV	Cerebral blood flow velocity
CPP	Cerebral perfusion pressure
CT	Computerized tomography
CTA	Computerized tomography angiogram
DCA	Dynamic cerebral autoregulation
DCI	Delayed cerebral ischemia
EBI	Early brain injury
FFT	Fast Fourier transformed
GCS	Glasgow Coma Scale
GEE	Generalized estimating equations
MAP	Mean arterial pressure
MCA	Middle cerebral artery
TCD	Transcranial Doppler

Introduction

Aneurysmal subarachnoid hemorrhage (aSAH) affects 21,000–30,000 people/year in the United States [20] and remains the most common cause of cerebral vasospasm.

Presentation at a conference: 14th International Conference on Neurovascular Events after Subarachnoid Hemorrhage or Vasospasm 2017.

S. Ortega-Gutierrez (✉) · E. A. Samaniego · B. Zheng-Lin
Stroke Division, Neurointerventional Surgery Section, Departments of Neurology, Neurosurgery and Radiology, University of Iowa Hospitals and Clinics, Iowa, IA, USA
e-mail: santy-ortega@uiowa.edu

A. Reccius
Department of Critical Care, Clinica Alemana, Universidad del Desarrollo, Santiago, Chile

A. Huang · A. Masukar · R. S. Marshall
Department of Neurology, Columbia University, New York, NY, USA

N. H. Petersen
Division of Neurocritical Care and Emergency Neurology, Department of Neurology, Yale University School of Medicine, New Haven, CT, USA

R. D. Martin et al. (eds.), *Subarachnoid Hemorrhage*, Acta Neurochirurgica Supplement 127,
https://doi.org/10.1007/978-3-030-04615-6_22,

Delayed cerebral ischemia (DCI) attributed to vasospasm is defined as clinical deterioration and/or the presence of new infarct not previously seen on admission or after the immediate postoperative period [8]. DCI may develop between days 4 and 14, with a peak incidence between days 7 and 10 [8, 9]. Despite medical and surgical advances, DCI remains a major cause for morbidity and mortality in aSAH survivors: it is responsible for 25–50% of permanent disability and 10–23% of death in aSAH [19].

DCI develops symptomatically in 20–30% among the initial aSAH survivors [8]. However, vasospasm can be detected invasively in up to 70% of aSAH with angiography [7, 11]. This dissociation between the angiographic appearance of vasospasm and the clinical symptomatology suggests the need of an optimal noninvasive screening tool for DCI.

The capability of brain vasculature of auto-adjusting CBF in response to variations of cerebral perfusion pressure (CPP) and systemic mean arterial pressure (MAP) is called dynamic cerebral autoregulation (DCA) [21]. DCA can be measured by determining the independence of low-frequency temporal oscillations of systemic blood pressure and cerebral flow velocities [13, 21]. The pathophysiologic mechanism of vasospasm and DCI is not yet fully disclosed, although alterations in inflammatory response, vascular biomechanics and cerebral blood flow (CBF) dysregulation are involved [2]. The aim of this study is to examine the presence of disturbed DCA in SAH and its potential value in the early detection of vasospasm prior to symptom onset.

Materials and Methods

In this prospective observational study, we included eight patients with aSAH admitted to the neurologic intensive care unit. Inclusion criteria were age greater than 18, subjects with SAH bleeding occurring in less than 48 h prior to admission, and Fisher score ≥3. Diagnosis was confirmed by computerized tomography (CT) of head and/or CT angiogram (CTA). Exclusion criteria were undetermined time of onset, subarachnoid hemorrhage of etiologies other than aneurysmal rupture, use of vasopressors within the first 48 h of onset, patients with inadequate transtemporal windows for insonation, and death or withdrawal of care within 72 h of admission. Consent was obtained from the patient or surrogate decision-maker prior to enrollment. All patients were provided detailed written information regarding the intent and methods of the study. Approval for the study was obtained from the Institutional Review Board at Columbia University Medical Center.

Dynamic autoregulation was assessed by calculating the relationship between changes in arterial blood pressure (ABP) and cerebral blood flow velocity (CBFV) using the transfer function analysis, which quantifies the spatial relation between slow fluctuations in ABP and CBFV in the frequency domain. DCA assessments occurred at day days 0–3, 4–6, and >7 after bleed.

Briefly, cerebral blood flow velocities were assessed using transcranial Doppler (TCD) (DWL-Multidop-X, Sipplingen, Germany). The proximal middle cerebral artery (MCA) was insonated through the temporal window with a 2 MHz probe attached to a head frame, insonation depth = 45–60 mm. Blood pressure was recorded simultaneously using intra-arterial catheter or servo-controlled finger plethysmography in the right or left middle finger (Finometer Pro, Amsterdam, Netherlands) [15]. After establishing a stable recording and calibration, measurements were recorded for 10 min. All analog signals sampled at 100 Hz were digitized and stored for editing and offline analysis. Temporal synchronization of the blood pressure and blood flow velocity wave forms using ICU pilot software (Dipylon Medical, Solna, Sweden) was followed by visual inspection and removal of all major artifacts. The data were then analyzed using Matlab (MathWorks, Natick, USA) with an in-house written program. The transfer function $H(f)$ relating each CBFV to ABP was approximated by assuming linearity and time invariance. Estimation of spectra and transfer function was based on the method described by Welch [7], details of which are described elsewhere [8]. In brief, arterial blood pressure ABP and CBFV from the left and right middle cerebral arteries were normalized and fast Fourier transformed (FFT) to calculate the auto-spectra and the cross spectrum of the two signals (ABP and CBFV). The coherence, gain $|H(f)|$, and phase $\Phi(f)$ of the system were calculated. Coherence significance criterion (γ_{min}), above which coherence differs significantly from 0, was derived from the degrees of freedom ν of the spectral estimate at a significance level α of 0.05 [9]. Phase shift was calculated by averaging the values of all valid bins in the low-frequency range (0.06–0.12 Hz; each bin is a frequency value at 0.01 Hz increments) where coherence was >0.53. The resulting phase shift describes the extent to which oscillations in CBFV lead those in ABP and can be interpreted as active early counterregulation. Less phase shift reflects increased latency in cerebral vasomotion and thus poorer autoregulation.

Daily Glasgow Coma Scale (GCS) evaluation was performed to evaluate clinical deterioration. CT head/CTA and/or angiography were used to determine the presence of DCI. If no symptoms occurred, a CT was performed to evaluate new silent infarcts before the patients left the ICU. DCI was used as the primary outcome and defined as a decrease of 2 points or more on GCS and/or new infarction on CT/CTA or angiogram.

Continuous variables were tested for normality using the Kolmogorov-Smirnov test. Data were reported as means and

standard deviation or median, 25th and 75th percentile. Univariate comparisons at single time points were performed using paired t-tests for normally distributed data and Wilcoxon signed-rank test for median comparison. Generalized estimating equations (GEE) with an exchangeable correlation matrix were used to examine the change in PS over time. A *p*-value of less than 0.05 was considered statistically significant.

Results

Among patients median age = 41 (IQR = 45–55), 100% women, median Hunt and Hess scale on admission was 3, median modified Fisher score was 3 (Table 1). Three of the subjects developed symptomatic vasospasm with median time-to-DCI of 9 days. Five underwent surgical clipping.

Presence of DCI was significantly associated with lower PS over the entire recording period (Wald = 4.28; $p = 0.039$). In addition, there was a significant change in phase shift over different recording periods after adjusting for DCI (Wald = 15.66; $p = 0.001$), in particular, a significantly lower mean PS on day 4–6 after bleed (14.22 vs 27.51; $p = 0.05$) (Fig. 1).

Discussion

aSAH is a devastating disease: about 10% of patients die prior to hospital admission, 25% die in the first 24 h after bleeding, and 45% in the following 30 days [1, 3, 10]. Despite therapeutic advances, DCI remains one of the most common complications and accounts for 25–50% of permanent disability and 10–23% of death in aSAH [19].

TCD performed within 48 h of bleeding onset to detect DCI has limited sensitivity and specificity and is only able to detect 38% of patients with impaired cerebral blood flow compared to 70% with angiography [5, 7]. Consequently, the

Table 1 Demographic data

Age	Gender	NIHSS on admission	Hunt and Hess scale	Fisher Scale	Aneurysm location	Aneurysm secure method	DCI
49	Female	18	4	3	ICA	Clipping	Yes
55	Female	3	2	4	ACom	Clipping	No
44	Female	0	1	3	PCom	Clipping	Yes
34	Female	11	4	1	ICA	Coiling	No
62	Female	0	3	3	ACA	Coiling	No
53	Female	25	5	3	PICA	Clipping	No
65	Female	2	2	3	MCA	Coiling	yes
45	Female	0	2	3	ICA	Clipping	No

NIHSS score, Hunt and Hess scale, and Fisher Scale were obtained on patient admission. *DCI* delayed cerebral ischemia, *NIHSS*, National Institute of Health Stroke Scale, *ACA* anterior cerebral artery, *ACom* anterior communicating artery, *ICA* internal carotid artery, *PCom* posterior communicating artery, *PICA* posterior inferior cerebellar artery, *MCA* middle cerebral aneurysm

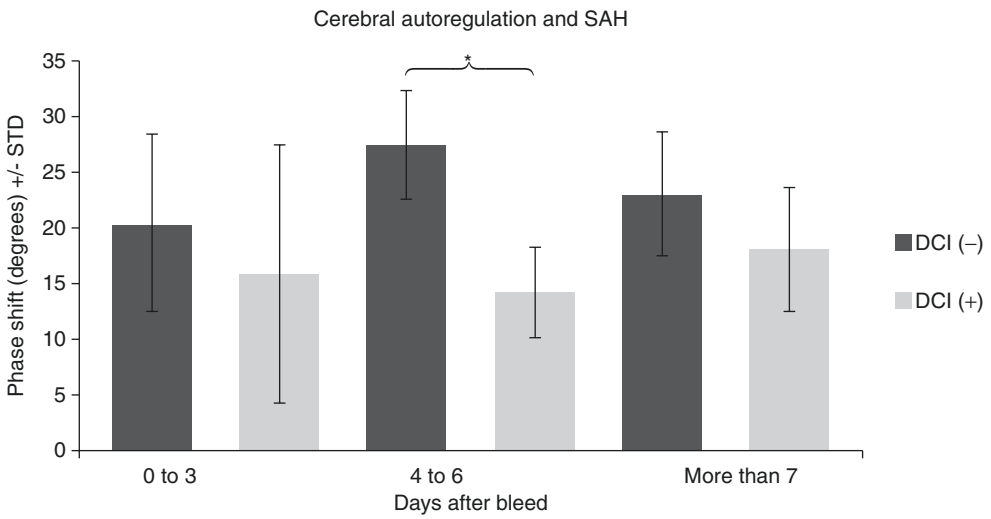

Fig. 1 The average values for phase shift over the three phases of study separated by patients with delayed cerebral ischemia developing. Phase 1, post-bleed day PBD 0–3; phase 2, PBD 4–6; phase 3, PBD >7. * $p = 0.05$

development of an optimal noninvasive screening tool to predict DCA before irreversible damage occurs is warranted.

In our study, the median time-to-DCI was 9 days, which was significantly associated with an impaired DCA indicated by lower mean PS on day 3–5 after initial bleed. We also observed that those patients might have an absolute lower PS during the entire recording period. These data suggest early impairment of DCA may predict a later occurrence of DCI in patients with aSAH. In addition, early decrease DCA without subsequent recovery might represent a novel biomarker of early brain injury (EBI).

The role of cerebral autoregulation in vasospasm is complex and remains poorly understood. Cerebral blood flow is under intricate continuous regulation controlled by several mechanisms. Brain vasculature dilates or constricts in response to (1) variations of blood gases, (2) activity of autonomic nervous system, and (3) to continuous and rapid fluctuation of blood pressure, in a homeostatic mechanism termed DCA [21]. Disturbance of DCA around the periischemic area is believed to be caused by tissue lactic acidosis and the subsequent local vasoparalysis, inhibiting the autoregulatory function of the blood vessel [6].

With advances in neuroimaging and operational informatics, cerebral autoregulation can be monitored using different time-domain and frequency-domain methodologies, and its measurement has been reported to be useful in a variety of neurological diseases including traumatic brain injury, intracranial hemorrhage, and stroke [12, 17, 18]. Otite et al. used daily measurements of TCD, heart rate, and blood pressure, and calculated the relationship between beat-to-beat fluctuations in the mean flow velocity and mean arterial pressure across low- and high-frequency ranges using transfer function analysis. They observed a higher transfer function gain was predictive of angiographic vasospasm and DCI [14]. Budohoski et al. suggested in their study that elevation in two autoregulatory indices, Sxa and TOxa, during the first 5 days within initial bleeding was independently predictive of DCI in SAH. Sxa was derived from the linear correlation coefficient between arterial blood pressure and systolic cerebral flow velocity measured with TCD, whereas TOxa was a linear coefficient that correlates arterial blood pressure with values of tissue oxygen index measured with near-infrared spectroscopy [4]. In our study, we applied a frequency-domain method using phase shift in low-frequency range as a continuous measurement for DCA, which was obtained using transfer function analysis and based on blood pressure and CBF velocities measured with TCD.

We previously studied measured DCA using PS in patients with ischemic stroke in the middle cerebral artery territory [16]. They observed a significant difference between the average PS in the infarcted cerebral hemisphere versus unaffected hemisphere, with a 29.6° ± 10.5° versus 42.5° ± 13°, respectively (p = 0.004). When comparing the infarcted hemisphere of patients with those of healthy control subjects (mean PS = 47.9 ± 16.8), the difference remained statistically significant (p = 0.001). More importantly, they reported DCA remained impaired 1 week after stroke [16]. To our knowledge this monitoring methodology has never been utilized in detection of DCI in aSAH, and this work represents the first experience using this noninvasive methodology as a predictive tool of DCI and potentially a marker of EBI. Our study is not without limitations. It is a single-center experience with a limited cohort. Additionally, TCD is an operator-dependent technology, and its use may be limited in some patients due to unfavorable temporal windows.

Conclusions

Our study suggests disturbance in DCA takes place after aSAH and may be predictive of vasospasm before clinical symptoms emerge. In summary, DCA monitoring may be a useful noninvasive bedside tool for early screening of DCI and biomarker of EBI. Future investigations with larger cohort should be conducted to further determine its impact on the acute management of patients with aSAH.

Funding
No funding was received for this research.

***Conflict of Interest*:** All authors certify that they have no affiliations with or involvement in any organization or entity with any financial interest or nonfinancial interest in the subject matter or materials discussed in this manuscript.

References

1. Al-Shahi R, White PM, Davenport RJ, Lindsay KW. Subarachnoid haemorrhage. BMJ. 2006;333:235–40. https://doi.org/10.1136/bmj.333.7561.235.
2. Baggott CD, Aagaard-Kienitz B. Cerebral vasospasm. Neurosurg Clin N Am. 2014;25:497–528. https://doi.org/10.1016/j.nec.2014.04.008.
3. Bederson JB, Connolly ES Jr, Batjer HH, Dacey RG, Dion JE, Diringer MN, Duldner JE Jr, Harbaugh RE, Patel AB, Rosenwasser RH, American Heart Association. Guidelines for the management of aneurysmal subarachnoid hemorrhage: a statement for healthcare professionals from a special writing group of the Stroke Council, American Heart Association. Stroke. 2009;40:994–1025. https://doi.org/10.1161/STROKEAHA.108.191395.
4. Budohoski KP, Czosnyka M, Smielewski P, Kasprowicz M, Helmy A, Bulters D, Pickard JD, Kirkpatrick PJ. Impairment of cerebral autoregulation predicts delayed cerebral ischemia after subarachnoid hemorrhage: a prospective observational study. Stroke. 2012;43:3230–7. https://doi.org/10.1161/STROKEAHA.112.669788.
5. Carrera E, Schmidt JM, Oddo M, Ostapkovich N, Claassen J, Rincon F, Seder D, Gordon E, Kurtz P, Lee K, Connolly ES, Badjatia N, Mayer SA. Transcranial Doppler ultrasound in the acute phase of aneurysmal subarachnoid hemorrhage. Cerebrovasc Dis. 2009;27:579–84. https://doi.org/10.1159/000214222.

6. Dohmen C, Bosche B, Graf R, Reithmeier T, Ernestus RI, Brinker G, Sobesky J, Heiss WD. Identification and clinical impact of impaired cerebrovascular autoregulation in patients with malignant middle cerebral artery infarction. Stroke. 2007;38:56–61. https://doi.org/10.1161/01.STR.0000251642.18522.b6.
7. Dorsch NW, King MT. A review of cerebral vasospasm in aneurysmal subarachnoid haemorrhage part I: incidence and effects. J Clin Neurosci. 1994;1:19–26.
8. Frontera JA, Fernandez A, Schmidt JM, Claassen J, Wartenberg KE, Badjatia N, Connolly ES, Mayer SA. Defining vasospasm after subarachnoid hemorrhage: what is the most clinically relevant definition? Stroke. 2009;40:1963–8. https://doi.org/10.1161/STROKEAHA.108.544700.
9. Hijdra A, Van Gijn J, Stefanko S, Van Dongen KJ, Vermeulen M, Van Crevel H. Delayed cerebral ischemia after aneurysmal subarachnoid hemorrhage: clinicoanatomic correlations. Neurology. 1986;36:329–33.
10. Hop JW, Rinkel GJ, Algra A, van Gijn J. Case-fatality rates and functional outcome after subarachnoid hemorrhage: a systematic review. Stroke. 1997;28:660–4.
11. Kassell NF, Torner JC, Haley EC Jr, Jane JA, Adams HP, Kongable GL. The international cooperative study on the timing of aneurysm surgery. Part 1: overall management results. J Neurosurg. 1990;73:18–36. https://doi.org/10.3171/jns.1990.73.1.0018.
12. Nakagawa K, Serrador JM, LaRose SL, Sorond FA. Dynamic cerebral autoregulation after intracerebral hemorrhage: a case-control study. BMC Neurol. 2011;11:108. https://doi.org/10.1186/1471-2377-11-108.
13. Ortega-Gutierrez S, Petersen N, Masurkar A, Reccius A, Huang A, Li M, Choi JH, Marshall RS. Reliability, asymmetry, and age influence on dynamic cerebral autoregulation measured by spontaneous fluctuations of blood pressure and cerebral blood flow velocities in healthy individuals. J Neuroimaging. 2014;24:379–86. https://doi.org/10.1111/jon.12019.
14. Otite F, Mink S, Tan CO, Puri A, Zamani AA, Mehregan A, Chou S, Orzell S, Purkayastha S, Du R, Sorond FA. Impaired cerebral autoregulation is associated with vasospasm and delayed cerebral ischemia in subarachnoid hemorrhage. Stroke. 2014;45:677–82. https://doi.org/10.1161/STROKEAHA.113.002630.
15. Petersen NH, Ortega-Gutierrez S, Reccius A, Masurkar A, Huang A, Marshall RS. Comparison of non-invasive and invasive arterial blood pressure measurement for assessment of dynamic cerebral autoregulation. Neurocrit Care. 2014;20:60–8. https://doi.org/10.1007/s12028-013-9898-y.
16. Petersen NH, Ortega-Gutierrez S, Reccius A, Masurkar A, Huang A, Marshall RS. Dynamic cerebral autoregulation is transiently impaired for one week after large-vessel acute ischemic stroke. Cerebrovasc Dis. 2015;39:144–50. https://doi.org/10.1159/000368595.
17. Radolovich DK, Aries MJ, Castellani G, Corona A, Lavinio A, Smielewski P, Pickard JD, Czosnyka M. Pulsatile intracranial pressure and cerebral autoregulation after traumatic brain injury. Neurocrit Care. 2011;15:379–86. https://doi.org/10.1007/s12028-011-9553-4.
18. Reinhard M, Rutsch S, Lambeck J, Wihler C, Czosnyka M, Weiller C, Hetzel A. Dynamic cerebral autoregulation associates with infarct size and outcome after ischemic stroke. Acta Neurol Scand. 2012;125:156–62. https://doi.org/10.1111/j.1600-0404.2011.01515.x.
19. Solenski NJ, Haley EC Jr, Kassell NF, Kongable G, Germanson T, Truskowski L, Torner JC. Medical complications of aneurysmal subarachnoid hemorrhage: a report of the multicenter, cooperative aneurysm study. Participants of the Multicenter Cooperative Aneurysm Study. Crit Care Med. 1995;23:1007–17.
20. Suarez JI, Tarr RW, Selman WR. Aneurysmal subarachnoid hemorrhage. N Engl J Med. 2006;354:387–96. https://doi.org/10.1056/NEJMra052732.
21. Willie CK, Tzeng YC, Fisher JA, Ainslie PN. Integrative regulation of human brain blood flow. J Physiol. 2014;592:841–59. https://doi.org/10.1113/jphysiol.2013.268953.

Transcranial Doppler Ultrasound, Perfusion Computerized Tomography, and Cerebral Angiography Identify Different Pathological Entities and Supplement Each Other in the Diagnosis of Delayed Cerebral Ischemia

Caroline Dietrich, Jasper van Lieshout, Igor Fischer, Marcel A. Kamp, Jan F. Cornelius, Angelo Tortora, Hans Jakob Steiger, and Athanasios K. Petridis

Abstract *Introduction*: There is still controversial discussion of the value of transcranial Doppler (TCD) in predicting vasospasms in patients with aneurysmal SAH (aSAH). A newer method of predicting a delayed ischemic deficit (DCI) is CT perfusion (CTP), although it is not quite understood which kind of perfusion deficit is detected by this method since it seems to also identifying microcirculatory disturbances. We compared the TCD and CTP values with angiography and evaluated TCD and CTP changes before and after patients received intra-arterial spasmolytic therapy.

Material and Methods: Retrospective analysis of TCD, CTP, and angiographies of $N = 77$ patients treated from 2013 to 2016. In 38 patients intra-arterial spasmolysis had been performed, and in these cases TCD and CTP data were compared before and after lysis. Thirty-nine patients had a pathological CTP but no angiographically seen vasospasm.

Results: There was no correlation between the known thresholds of mean transit time (MTT) in CTP and vasospasm or with mean velocities in TCD and vasospasm. After spasmolysis in patients with vasospasms, only the MTT showed significant improvement, whereas TCD velocities and Lindegaard index remained unaffected.

Conclusion: TCD and CTP seem to identify different pathological entities of DCI and should be used supplementary in order to identify as many patients as possible with vasospasms after aSAH.

C. Dietrich
Institute of Radiology, University Hospital Duesseldorf, Heinrich Heine University Duesseldorf, Duesseldorf, Germany

J. van Lieshout · I. Fischer · M. A. Kamp · J. F. Cornelius
A. Tortora · H. J. Steiger
Department of Neurosurgery, University Hospital Duesseldorf, Heinrich Heine University Duesseldorf, Duesseldorf, Germany

A. K. Petridis (✉)
Department of Neurosurgery, Heinrich Heine University Duesseldorf, Duesseldorf, Germany

Keywords Aneurysmal subarachnoid hemorrhage · Perfusion computed tomography · Transcranial Doppler ultrasonography Angiography · Vasospasm

Introduction

Aneurysmal subarachnoid hemorrhage (aSAH) occurs in about 5% of all strokes and has still a mortality of 50% and a significant morbidity in survivors [1]. The second cause of disability after the initial hemorrhage is cerebral vasospasm and the delayed cerebral ischemia which occurs in 50–70% of patients [2]. These two pathological entities seem to have different pathophysiological etiologies and cannot be detected by the same techniques. Vasospasms of the vessels of the circle of Willis can be detected by transcranial Doppler ultrasonography (TCD), whereas microcirculation disturbances can be detected by perfusion imaging techniques. Digital subtraction angiography (DSA) remains until now the gold standard of imaging vasospasms, but it is invasive, and it is proven to be associated with the risk of mild neurological deficit as well as ischemic insults [3]. On the other side, DSA cannot display cerebral blood flow and is unsuitable to monitor changes in microcirculation [3]. TCD, which is still recommended for arterial vasospasm by the American Heart Association Management Guidelines for SAH, has a number of limitations like operator dependence and inter-observer variability, inadequate acoustic windows in 10% of patients, but, much more important, high variability of TCD vasospasm criteria in the literature as well as highly controversial results [4, 5]. However, in a number of cases TCD vasospasm could be identified and proven by DSA; therefore TCD should not be neglected from clinical routine [6].

The techniques used for identification of microcirculatory changes are xenon-enhanced CT scanning, positron emission tomography, single photon emission computed tomography, MRI perfusion imaging, and CT perfusion (CTP) with CTP being in advantage because of its low cost, rapid imaging, high spatial resolution, and ease of performance [3].

R. D. Martin et al. (eds.), *Subarachnoid Hemorrhage*, Acta Neurochirurgica Supplement 127,
https://doi.org/10.1007/978-3-030-04615-6_23,

Apart from imaging techniques, the clinical symptoms and the neurological examination of the patient play a crucial role. The disadvantage is that by the time cerebral vasospasms cause clinical symptoms, the ischemic event may have progressed too far, and the chance of a therapeutic intervention may have been missed [2]. Predictive factors of vasospasm occurrence and DCI have been named in a number of studies but remain inconsistent and controversial [2]. Such factors are age, sex, and SAH grade, to name a few.

Since vasospasm and DCI seem to be different pathologies, there is a possibility that TCD, DSA, and CTP are identifying different pathological entities and do not have to correlate but supplement each other. We aimed to study if there is any correlation between TCD, CTP, and DSA in the patient population as well as to evaluate if there is any change of the CTP and TCD values after intra-arterial spasmolytic therapy in patients with vasospasms on DSA.

Material and Methods

Patient Population

Seventy-seven patients with aneurysmal subarachnoid hemorrhage admitted to our department between January 2013 and September 2016 had a pathological CTP and received digital subtraction angiography. Patients in the present retrospective study were selected meeting the following criteria: (a) severe angiographic vasospasm followed by intra-arterial nimodipine (vasospasmolysis) as a rescue treatment, (b) transcranial Doppler (TCD) examination within 1 day before and after vasospasmolysis, and (c) perfusion computer tomography (CTP) within 1 day before and after vasospasmolysis. As a control cohort, patients with aSAH treated in our hospital during the same period, who did not receive i.a. vasospasmolysis but showed pathological TCD/CTP values, were analyzed ($n = 39$). Scientific use of the data was approved by the local ethics committee of the Medical Faculty of the Heinrich-Heine University Düsseldorf, Germany (study ID: 5276). The management of the patients in the presented cohorts was in accordance with current SAH guidelines [4].

Definitions

The indication of vasospasmolysis was severe vasospasm, defined in angiography as the radiographic narrowing of an intracranial vessel to 33% or less of its original diameter. For comparison, the initial angiographic imaging (DSA or CTA) upon admission was used. Vasospasmolysis consisted of 3.2 mg intra-arterial nimodipine, injected in the internal carotid artery of the pathological side.

The following TCD values were considered pathological: mean blood flow velocity of the middle cerebral artery (MCA) >120 cm/s and mean blood flow velocity of the anterior cerebral artery (ACA) >50 cm/s Lindegaard index >3. The Lindegaard index is the relation of MCA-mean velocity to ipsilateral mean velocity of the cervical internal carotid artery (ICA). TCD was performed by experienced neurosurgical residents in order to minimize inter-observer variability.

The CTP value indicating severe vasospasm was a mean transit time (MTT) > 3.98 s, based on a study by Mathys et al. [7]. CTP data were acquired with a Siemens scanner using singular-value decomposition with an acquisition time of 35 s. The automated image analysis integrated a 1 cm cortical layer with 180 overlapping regions of interests and corresponding values, using 360° cortical banding analysis. After the generation of perfusion maps, CTP data, such as MTT among others, were calculated using the STROKETOOL-CT software (Version 2.5, Digital Image Solutions, Frechen, Germany). MTT were pooled according to the cortical map, and mean values for each vessel territory (ACA, MCA, PCA) were calculated.

Statistical Analysis

For statistical analysis, CTP and TCD values were matched to the vessel territory showing angiographic vasospasm. For example, in case of severe angiographic vasospasm detected in the left MCA, mean MTT of the left MCA territory and ipsilateral mean MCA velocity and Lindegaard index of this patient were selected for further statistical analysis. If all cerebral vessels showed vasospasm, mean overall MTT and the higher mean MCA velocity and Lindegaard index were used.

To verify the value of TCD and CTP in predicting severe angiographic vasospasm, its sensitivity, specificity, and positive predictive value (PPV) were calculated using the Fisher's exact test. Furthermore, ICA mean velocity was correlated to MTT before and after vasospasmolysis using Pearson product moment correlation. In order to detect an effect of i.a. nimodipine after vasospasmolysis in TCD and CTP, first a Shapiro-Wilk normality test was performed to confirm normal distribution followed by a Student t-test. A level of $p \leq 0.05$ was considered significant. All statistical analysis was performed using the program R Core Team 2016, Version 3.3.0 (R: A language and environment for statistical computing. R Foundation for Statistical Computing, Vienna, Austria).

Results

Out of the 77 patients, 38 patients were treated with i.a. nimodipine (13 patients were treated twice, 2 patients 3 times, 1 patient 4 times, and 1 patient 6 times during their

hospital stay; the remaining 32 patients received spasmolysis once). Additionally, six patients got i.a. nimodipine without severe angiographic vasospasm, but they showed highly elevated MTT suggesting cerebral perfusion deficits. These patients were excluded in the present study. In nine cases exclusion from the study was necessary because of insufficient interventional documentation. Vasospasmolysis was performed between day 1 and 19 after ictus, averagely on day 8. Mean patient's age was 55.8 ± 11 years; 65% were female.

Transcranial Doppler Ultrasonography

Of the 38 vasospasmolysis cases, TCD was documented in 23 within 1 day before and in 20 cases within 1 day after the treatment. Only 14 cases had complete documentation of TCD before and after angiography. TCD values Lindegaard index and MCA and ACA velocity did not predict severe angiographic vasospasm ($p \geq 0.799$; PPV ≤ 0.231; sensitivity ≤ 0.167; specificity ≤ 0.955). Lindegaard index before spasmolysis was 2.29 ± 1.3 ($n = 18$), mean MCA velocity was 81.58 ± 37.2 cm/s ($n = 19$), and mean ACA velocity was 47.75 ± 8.8 cm/s ($n = 4$) according to the vasospasm territory. Intra-arterial nimodipine had no effect on Lindegaard index ($p = 0.95$), as TCD values did not differ significantly: Lindegaard 2.40 ± 1.2 ($n = 20$) and mean MCA velocity 89.2 ± 35.6 cm/s ($n = 20$) (Fig. 1). There was no mean ACA velocity documented after vasospasmolysis. We could not find a predictive cutoff for Lindegaard index and MFV as well as angiographically proven vasospasms.

Perfusion Computer Tomography

A CTP exam was performed in 77 cases within 1 day before and after vasospasmolysis. Mean MTT of the spastic vessel territory did not predict severe angiographic vasospasm ($p = 0.289$; PPV = 0.745; sensitivity = 0.673; specificity = 0.625). Thirty-nine patients had a pathological MTT in CTPs, but no angiographic vasospasm was detected. The mean MTT was 4.30 ± 1.0 s. In cases with intra-arterial nimodipine, the MTT went back to physiological values ($p < 0.001$; 3.71 ± 0.9 s; Fig. 2a). This effect was even more significant regarding only the vessel territory with vasospasm ($p < 0.0003$, MTT = 3.66 ± 0.9 s). The Tmax showed no statistical significant changes before and after spasmolysis (Fig. 2b).

Correlation of CTP, TCD, and Angiography

There was no correlation between mean MTT and ICA or MCA mean velocity before and/or after vasospasmolysis ($p = 0.37$, $n = 24$). There was no statistical correlation between angiographically proven vasospasm and CTP or TCD.

Discussion

We failed to show a congruence of TCD and angiography on the day of angiography although the number of cases with a TCD analysis before and after treatment was low. There was

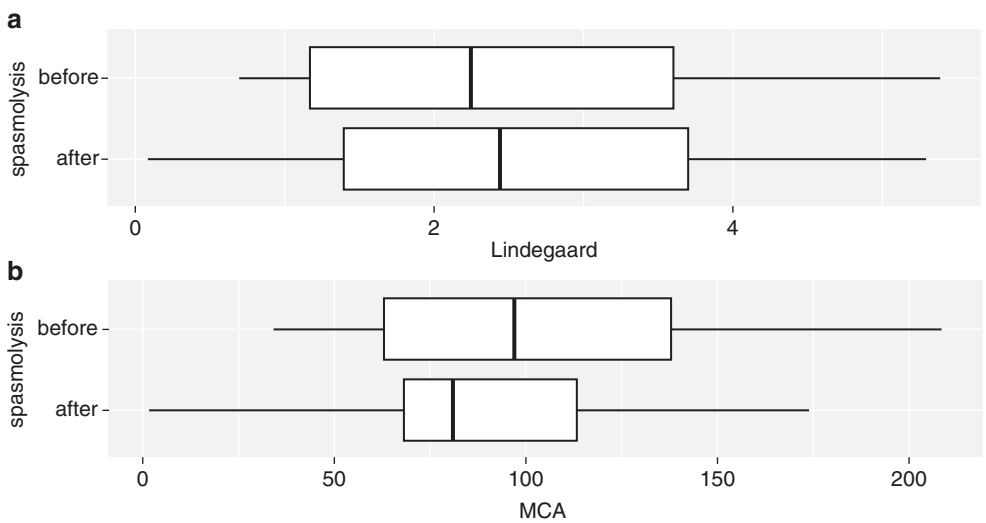

Fig. 1 (**a**) Lindegaard index in transcranial Doppler in CTP in patients with aSAH and severe angiographic vasospasm before (lower boxplot) and after (upper boxplot) the intra-arterial application of nimodipine. No significant changes could be seen. Even in patients with angiographically seen vasospasms, the Lindegaard index was physiological before and after spasmolysis. (**b**) The MCA velocity before and after spasmolysis was also insignificantly changed

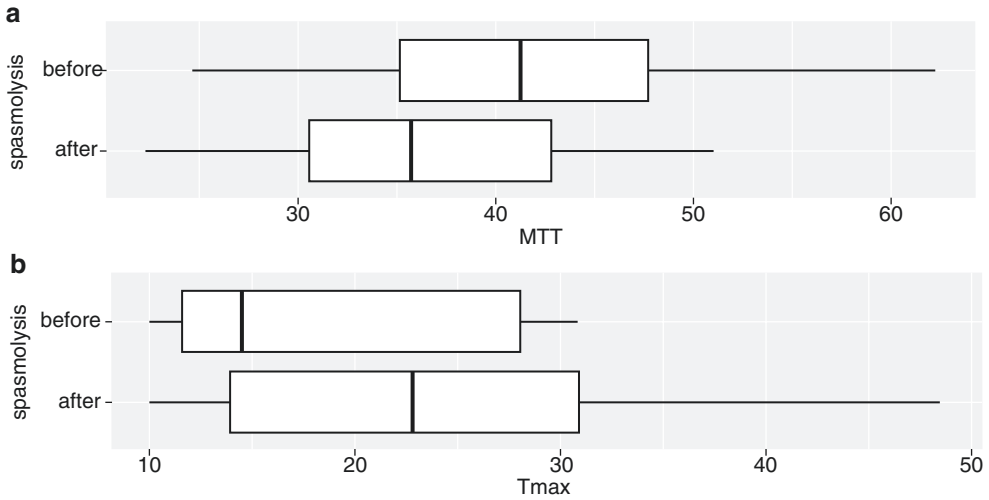

Fig. 2 (**a**) Overall mean transit time (MTT [s]) in CTP in patients with aSAH and severe angiographic vasospasm before (upper boxplot) and after (lower boxplot) intra-arterial application of nimodipine. (**b**) Tmax showed no statistical significance before and after spasmolysis

no significant change in the TCD mean velocity or the Lindegaard index before and after spasmolysis. The reason for this could be inter-observer variability and failure to monitor more distal vessels than around the circle of Willis. The failure of congruence between TCD and angiography could also be explained by microthrombotic incidents which were exclusively identified in CTP.

Since there would not be any chance to identify by TCD microthrombotic lesions which cause a DCI, CTP was performed every third day. Pathological TCD velocities and Lindegaard index as well as abnormal CTPs led to an early angiography in our patients.

TCD is easy to perform, and, in contrast to angiography where transport of the patient to the angio-suite is mandatory, the patient does not need to be transported anywhere for TCD. It needs about 20 min to complete the examination and is noninvasive. Therefore it is a recommended diagnostic tool in vasospasm detection of patients with aSAH [4, 8]. However, there are many inter-observer and intra-observer variabilities which lead to many controversies about the use of TCD as a routine, daily diagnostic tool. Additionally, the thresholds of mean velocity, Lindegaard index, etc. are not clearly defined, and TCD is unable to identify vasospasms of arteries other than the circle of Willis. In a prospective cohort series, patients with daily Doppler monitoring were compared to a group of aSAH patients without TCD monitoring, and there was no difference in mortality or outcome between the two patient groups [8]. No congruence between TCD and DSA could be seen in the study leading the authors to abandon TCD from their ICU routine in aSAH patients [8].

On the other side, TCD is the most used diagnostic tool in modern NICU. In a survey, 70% of US and 53% of non-US practitioners use TCD in aSAH patients because of lack of an alternative [9]. There are studies showing a good prediction of vasospasms by TCD, especially for the MCA like a mean flow velocity (MFV) of >175 cm/s and a Lindegaard index of >6 [1]. In general, a MFV of up to 120 cm/s is associated with a mild angiographic stenosis, between 120 and 200 with a moderate stenosis and > 200 with a severe stenosis although, as mentioned already, the cutpoints are open to debate [10–12]. For example, other studies show that only MFV of <120 cm/s or > 180 cm/s had a predictive value [12, 13]. Other studies emphasize that an absolute increase of MFV over days is predicting vasospasm [1, 14, 15]. Despite the questionable results of TCD, it did still influence the management of about 18% of aSAH patients in one study after detecting vasospasms (4). Even when angiographical vasospasms occur, they can be tolerated well and have no clinical significance owing to collateral flow, systemic flow, volume augmentation, metabolic activity, and other factors [1].

Awareness of the inter-observer failure led to the development of new-generation TCD which should minimize inter-observer variability [5].

After failure of improving clinical outcome of patients even after a satisfying treatment of vasospasms in the CONSCIOUS-1 study, the concept of DCI changed. DCI is not exclusively vasospasm dependent but seems to have a complex pathophysiology which is influenced by vasospasm of small distal vessels, microthromboses, and microcirculatory disturbances [12, 16]. Since TCD does not seem to reliably predict patients with vasospasms (at least only a small subgroup of patients is identified), clinical examination in comatose patients is not feasible, and angiography too invasive, we established a CTP monitoring protocol at days 3, 6, 9, and 12. Even when CTP values did fail to predict macrovasospasms (seen with TCD and angiography), it still identified DCI. On the other side, CTP values improved after spasmolytic therapy, showing a response to the spasmolysis in each individual patient with macrovasospasm.

There is an additional cause of CTP MTT prolongation except vasospasm, which we identify by our every 3 days CTP protocol. In one study of xenon-CT and CT perfusion in the acute phase of aSAH where vasospasms are absent, there was still a prolongation of MTT especially in territories that do not belong to one of the major arteries, indicating toward an increased small vessel resistance [17].

Unlike other studies we could not identify a cutoff value for MTT which would generally predict macrovasospasm [17, 18]. Differences between the hemispheres and between vascular territories led to angiography. In patients with vasospasm in angiography, CTP showed a significant improvement of MTT.

Mathys et al. [7] showed already that a MTT of >3.98 s was associated with a negative outcome. Hänggi et al. [19] could show an improved Tmax after i.a. spasmolytic therapy in $N = 24$ patients with angiographic vasospasm and a trend for improved MTT in CTP.

Despite the radiation, which is kept to a minimum, CTP in these critically ill patients is easier to perform than diffusion-perfusion MRI which takes longer (30 min), although a diffusion-perfusion mismatch has been demonstrated in the early stages of vasospasm too [20].

The mean transit time (MTT) in CTP has been proven to be the most reliable parameter of hypoperfusion. The MTT is related to cerebral blood flow and cerebral blood volume by the equation: MTT = CBV/CBF [21]. MTT could identify angiographic vasospasm in 15/15 patients even when CBV and CBF were minimally changed [22]. In comparison to the present study, the MTT threshold in the study of Wintermark et al. [22] was set much higher (6.4 s compared to 3.98 s), and this explains the higher rate of identifying vasospasms. By such a high MTT threshold though, there is a risk of missing patients with microcirculatory perfusion pathology not seen in angiography. In an experimental study with an aSAH rabbit model, the MTT on day 2 after SAH could predict the occurrence of later vasospasm [23]. This increase of MTT before the occurrence of vasospasms could be attributed to inflammatory cytokines and endothelial dysfunction of small vessels [23]. We also used the MTT in our study and decided to proceed to angiography when there were differences of MTT in different brain territories. However there was no significant correlation between these changes in CTP and angiographically proven vasospasms, which is similar to other studies showing only a weak correlation between CTP and CTA vasospasm [24].

Conclusion

Our study shows no correlation of TCD, angiographically proven vasospasms, and CTP. These results do not suggest that TCD or CTP should be abandoned but that every single diagnostic method seems to identify another patient group suffering a DCI. TCD is able to identify patients with macrovasospasms of basal arteries, whereas CTP identifies microcirculatory and macrocirculatory disturbances leading to neurologic deterioration without angiographically detected vasospasms. The fact that TCD values did not change after vasospasmolysis is complex and cannot be explained with this study. More patients and a prospective study would be needed. MTT on the other hand showed a significant response after vasospasmolysis. The weakness of the study is that the data was collected retrospectively, whereas its strength is the large number of patients and the frequency of CTP exams as well as the analysis of the response of TCD and CTP after spasmolysis which, to our knowledge, had not been studied until now.

Conflict of Interest All authors certify that they have no affiliations with or involvement in any organization or entity with any financial interest (such as honoraria; educational grants; participation in speakers' bureaus; membership, employment, consultancies, stock ownership, or other equity interest; and expert testimony or patent-licensing arrangements) or nonfinancial interest (such as personal or professional relationships, affiliations, knowledge, or beliefs) in the subject matter or materials discussed in this manuscript.

Funding: **No funding was received for this research.**

References

1. Malhotra K, Conners JJ, Lee VH, Prabhakaran S. Relative changes in transcranial Doppler velocities are inferior to absolute thresholds in prediction of symptomatic vasospasm after subarachnoid hemorrhage. J Stroke Cerebrovasc Dis. 2014;23:31–6.
2. Jabbarli R, Gläsker S, Weber J, Taschner C, Olschewski M, Velthoven VV. Predictors of severity of cerebral vasospasm caused by aneurysmal subarachnoid hemorrhage. J Stroke Cerebrovasc Dis. 2013;22:1332–9.
3. Zhang H, Zhang B, Li S, Liang C, Xu K, Li S. Whole brain CT perfusion combined with CT angiography in patients with subarachnoid haemorrhage and cerebral vasospasm. Clin Neurol Neurosurg. 2013;115:2496–501.
4. Connolly ES Jr, Rabinstein AA, Carhuapoma JR, Derdeyn CP, Dion J, Higashida RT, et al. Guidelines for the management of aneurysmal subarachnoid hemorrhage: a guideline for healthcare professionals from the American Heart Association/American Stroke Association. Stroke. 2012;43:1711–37.
5. Han SJ, Rutledge WC, Englot DJ, Winkler EA, Browne JL, Pflugrath L, Cronsier D, Abla AA, Kliot M, Lawton M. The Presto 1000: a novel automated transcranial Doppler ultrasound system. J Clin Neurosci. 2015;22:1771–5.
6. Deb S, Gogos AJ, Drummond KJ, Teddy PJ. The role of transcranial Doppler ultrasound monitoring in patients with aneurysmal subarachnoid haemorrhage. J Clin Neurosci. 2012;19:950–5.
7. Mathys C, Martens D, Reichelt DC, et al. Long-term impact of perfusion CT data after subarachnoid hemorrhage. Neuroradiology. 2013;55:1323.
8. Ehrlich G, Kirschning T, Wenz H, Hegewald AA, Groden C, Schmiedek P, Scharf J, Seiz-Rosenhagen M. Is there an influ-

ence of routine daily transcranial doppler examination on clinical outcome in patients after aneurysmal subarachnoid hemorrhage. World Neurosurg. 2016;88:214–21.
9. Holligworth M, Chen PR, Goddard AJP, Coulthard A, Söderman M, Bulsara KR. Results of an international survey on the investigation and endovascular management of cerebral vasospasm and delayed cerebral ischemia. World Neurosurg. 2015;83:1120–6.
10. Aaslid R, Huber P, Nornes H. Evaluation of cerebrovascular spasm with transcranial Doppler ultrasound. J Neurosurg. 1984;60:37–41.
11. Sloan MA. Detection of Vasospasm following subarachnoid haemorrhage. In: Babikian VL, Wechsler LR, editors. Transcranial Doppler sonography. St Louis: Mosby-Year Book; 1993. p. 105–27.
12. Vora YY, Suarez-Almazor M, Steinke DE, et al. Role of transcranial doppler monitoring in the diagnosis of cerebral vasospasm after subarachnoid haemorrhage. Neurosurgery. 1999;44:1237–47.
13. Suarez JI, Qureshi AI, Yahia AB, et al. Symptomatic vasospasm diagnosis after subarachnoid haemorrhage: evaluation of transcranial Doppler ultrasound and cerebral angiography as related to compromised vascular distribution. Crit Care Med. 2002;30:1348–55.
14. Grosset DG, Straiton J, McDonald I, et al. Angiographic and Doppler diagnosis of cerebral artery vasospasm following subarachnoid haemorrhage. J Neurosurg. 1993;7:291–8.
15. Seiler RW, Grolimund P, Aaslid R, et al. Cerebral vasospasm evaluated by transcranial ultrasound correlated with clinical grade and CT-visualized subarachnoid haemorrhage. J Neurosurg. 1986;64:594–600.
16. Ohta H, Ito Z. Cerebral infraction due to vasospasm, revealed by computed tomography (author's transl). Neurol Med Chir (Tokyo). 1981;21:365–72.
17. Honda M, Sase S, Yokota K, Ichibayashi R, et al. Early cerebral circulatory disturbance in patients suffering subarachnoid hemorrhage prior to the delayed cerebral vasospasm stage: xenon computed tomography and perfusion computed tomography study. Neurol Med Chir (Tokyo). 2012;52:488–94.
18. Dolatowski K, Malinova V, Fröhlich AMJ, Schramm P, et al. Volume perfusion CT (VPCT) for the differential diagnosis of patients with suspected vasospasm: qualitative and quantitative analysis of 3d parameter maps. Eur J Radiol. 2014;83:1881–9.
19. Hänggi D, Turowski B, Beseoglu K, et al. Intra-arterial nimodipine for severe cerebral vasospasm after aneurysmal subarachnoid hemorrhage: influence on clinical course and cerebral perfusion. Am J Neuroradiol. 2008;29:1053–60.
20. Ohtonari T, Kakinuma K, Kito T, Ezuka I, et al. Diffusion-perfusion mismatch in symptomatic vasospasm after subarachnoid hemorrhage. Neurol Med Chir (Tokyo). 2008;48:331–6.
21. Lee TY. Functional CT: physiological models. Trends Biotechnol. 2002;20:S3–S10.
22. Wintermark M, Ko NU, Smith WS, et al. Vasospasm after subarachnoid hemorrhage: utility of perfusion CT and CT angiography on diagnosis and management. Am J Neuroradiol. 2006;27:26–34.
23. Laslo AM, Eastwood JD, Pakkiri P, Chen F, Lee TY. CT perfusion-derived mean transit time predicts early mortality and delayed vasospasm after experimental subarachnoid hemorrhage. Am J Neuroradiol. 2008;29:79–85.
24. Dankbaar JW, Rijsdijk M, van der Schaaf IC, Velthuis BK, Wermer MJH, Rinkel GJE. Relationship between vasospasm, cerebral perfusion, and delayed cerebral ischemia after aneurysmal subarachnoid hemorrhage. Neuroradiology. 2009;51:813–9.

Role of Computational Fluid Dynamics for Predicting Delayed Cerebral Ischemia After Aneurysmal Subarachnoid Hemorrhage: Study Protocol for a Multicenter Prospective Study

Masato Shiba, Fujimaro Ishida, Fumitaka Miya, Tomohiro Araki, Mitsuhito Mase, Hiroki Kurita, Hidetoshi Kasuya, Takuji Yamamoto, Yoko Kato, Satoshi Iwabuchi, Hidenori Suzuki, and CFD³ Study Group

Abstract *Background*: Delayed cerebral ischemia (DCI) is a significant cause of morbidity and mortality after aneurysmal subarachnoid hemorrhage (SAH). Recently, we reported the possibility that computational fluid dynamics (CFD) could predict DCI in terms of the cross-sectional area and flow velocity of the ipsilateral extracranial internal carotid and distal parent arteries in a single-center retrospective study.

Methods: This is a multicenter, prospective, cohort study. Patients with aneurysmal SAH will undergo CFD analyses using preoperative three-dimensional computed tomography angiography, and we will investigate hemodynamic features of cerebral arteries in an acute stage of SAH. Primary outcome measures will be CFD features in patients with subsequent occurrence of DCI. Secondary outcome measures will be CFD features in patients with subsequent occurrence of cerebral vasospasm and cerebral infarction and the relationships with eventual modified Rankin scale score at 3 months.

Conclusions: The present protocol for a multicenter prospective study is expected to provide a novel diagnostic method to predict DCI before aneurysmal obliteration in an acute stage of SAH.

Keywords Subarachnoid hemorrhage · Delayed cerebral ischemia · Cerebral aneurysm · Computational fluid dynamics · Computed tomography angiography

CFD³ Study Group; Masato Shiba, Hidenori Suzuki, Ryuta Yasuda, Naoki Toma, Takeshi Okada, Hirofumi Nishikawa, Yoichi Miura (Mie University Graduate School of Medicine); Fujimaro Ishida (Mie Central Medical Center); Hiroshi Tanemura, Fumitaka Miya (Ise Red Cross Hospital); Yoshinari Nakatsuka, Tomohiro Araki (Suzuka Kaisei Hospital); Yusuke Nishikawa, Mitsuhito Mase (Nagoya City University Graduate School of Medicine); Yuichiro Kikkawa, Hiroki Kurita (Saitama Medical University International Medical Center); Hidenori Ohbuchi, Hidetoshi Kasuya (Tokyo Women's Medical University Medical Center East); Takuji Yamamoto (Juntendo University Shizuoka Hospital); Yoko Kato (Fujita Health University Banbuntane Hotokukai Hospital); and Satoshi Iwabuchi (Toho University Medical Center Ohashi Hospital).

Introduction

Delayed cerebral ischemia (DCI) remains a significant cause of morbidity and mortality after aneurysmal subarachnoid hemorrhage (SAH) [1–4]. Early brain injury, cerebral vasospasm, microcirculatory thrombosis and dysfunction, and cortical

M. Shiba (✉) · H. Suzuki
Department of Neurosurgery, Mie University Graduate School of Medicine, Tsu, Mie, Japan
e-mail: mshiba@clin.medic.mie-u.ac.jp

F. Ishida
Department of Neurosurgery, Mie Central Medical Center, Tsu, Mie, Japan

F. Miya
Department of Neurosurgery, Ise Red Cross Hospital, Ise, Japan

T. Araki
Department of Neurosurgery, Suzuka Kaisei Hospital, Suzuka, Japan

M. Mase
Department of Neurosurgery, Nagoya City University Graduate School of Medicine, Nagoya, Japan

H. Kurita
Department of Cerebrovascular Surgery, Saitama Medical University International Medical Center, Hidaka, Saitama, Japan

H. Kasuya
Department of Neurosurgery, Tokyo Women's Medical University Medical Center East, Tokyo, Japan

T. Yamamoto
Department of Neurosurgery, Juntendo University Shizuoka Hospital, Shizuoka, Japan

Y. Kato
Department of Neurosurgery, Fujita Health University Banbuntane Hotokukai Hospital, Nagoya, Japan

S. Iwabuchi
Department of Neurosurgery, Toho University Medical Center Ohashi Hospital, Tokyo, Japan

R. D. Martin et al. (eds.), *Subarachnoid Hemorrhage*, Acta Neurochirurgica Supplement 127,
https://doi.org/10.1007/978-3-030-04615-6_24,

spreading depolarization may contribute to the development of DCI [3, 5]. To improve outcomes of SAH patients, it is important to detect DCI in its earlier stage. However, for the purpose, transcranial Doppler, cerebral perfusion study, and cerebral angiography are not optimal because of its limited sensitivity or invasiveness. Recently, we retrospectively reported that the development of DCI was associated with the narrowing of extracranial internal carotid artery and distal parent artery and increased flow velocity of distal parent artery on computational fluid dynamics (CFD) using preoperative computed tomography angiography (CTA) in an acute stage of SAH [6]. Thus, the aim of this multicenter prospective study is to determine whether CFD is useful to predict the development of DCI after SAH.

Materials and Methods

This is a multicenter, prospective, cohort study and was approved by the ethical committee of Mie University Graduate School of Medicine and was performed in accordance with the institutional guidelines.

Participants

Neurosurgeons in charge will check all patients presenting with aneurysmal SAH for the study eligibility. Inclusion criteria are 20 or older years of age, modified Rankin scale 0–2 before onset, ruptured saccular aneurysms in the internal carotid artery (ICA) or middle cerebral artery (MCA) diagnosed with subtraction CTA within 72 h after onset, aneurysmal obliteration by surgical clipping or coil embolization within 72 h after onset, and written informed consent from patient's family members. Exclusion criteria are non-aneurysmal SAH, death within 14 days after onset, and rejection of participation (Fig. 1).

Patient Management

Timing of aneurysmal obliteration, selection of clipping or coiling, and other medical management or treatment will be decided by site investigators and not limited.

CFD Analysis

CFD analysis is performed as previously described (Fig. 2) [7]. Briefly, from preoperative three-dimensional CTA, the patient-specific geometries are generated as stereolithography (Mimics 16.0; Matelialise Japan, Yokohama, Japan). The computational meshes are generated with tetrahedral and prism elements (ANSYS ICEM CFD16.1; ANSYS, Inc., Canonsburg, PA, USA). A straight inlet extension is added to the cervical (C5) segment of the ICA to obtain fully developed laminar flow. Numeral modeling is performed using a commercially available CFD package (ANSYS CFX 16.1; ANSYS, Inc., Canonsburg, PA, USA). Blood is assumed to be an incompressible Newtonian fluid with a blood density of 1056 kg/m^3 and a blood dynamics viscosity of 0.0035 Pa s. Pulsatile boundary conditions are based on the superposition blood-flow waveforms of the common carotid artery as characterized by Doppler ultrasound in normal human subjects for CFD analysis.

The ipsilateral C1–3 segments and M1 segment are defined as the parent arteries of aneurysms at the ICA and MCA, respectively (Fig. 3).

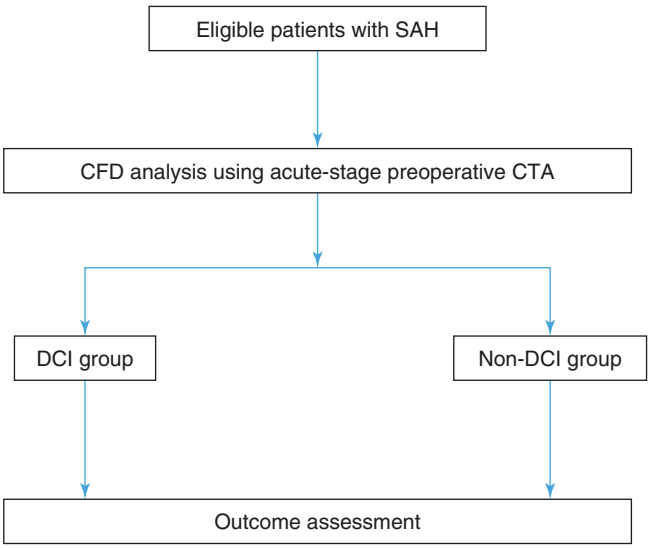

Fig. 1 Flow diagrams of this study. *SAH* subarachnoid hemorrhage; *CFD* computational fluid dynamics; *CTA* computed tomography angiography; *DCI* delayed cerebral ischemia

Outcome Measures

Primary outcome measures will be hemodynamic differences in cerebral arteries on CFD analyses between patients with and without subsequent development of DCI. DCI is defined as otherwise unexplained clinical deterioration (i.e., new focal neurological deficits [motor or speech deficits], decrease in Glasgow Coma Scale of ≥2 points, or both), which lasts for ≥1 h [1, 6]. Other potential causes of clinical deterioration, such as clipping- or coiling-related complications, rebleeding, hydrocephalus, electrolyte or metabolic disturbance,

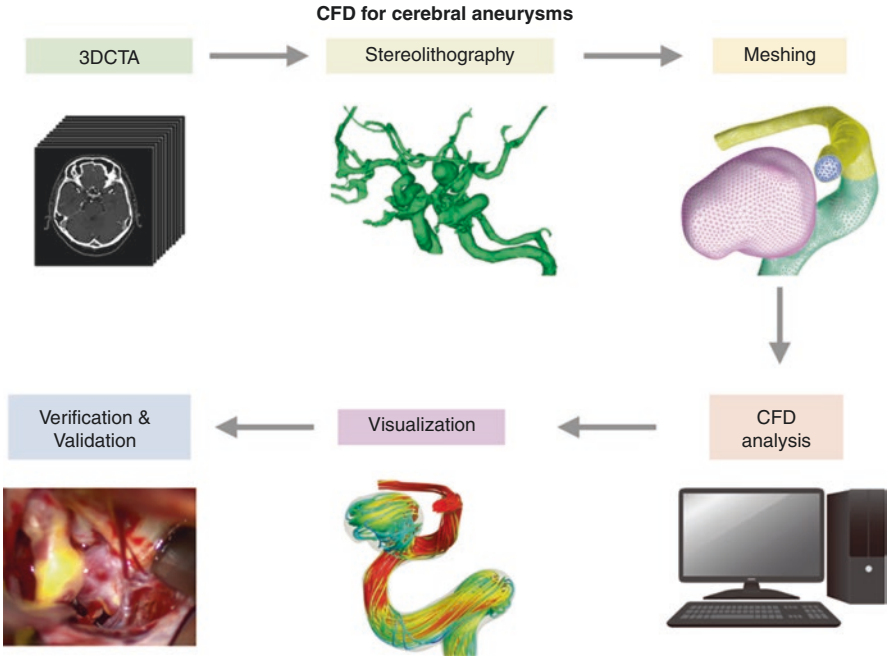

Fig. 2 Procedure for analysis of computational fluid dynamics. *CFD* computational fluid dynamics; *3DCTA* three-dimensional computed tomography angiography

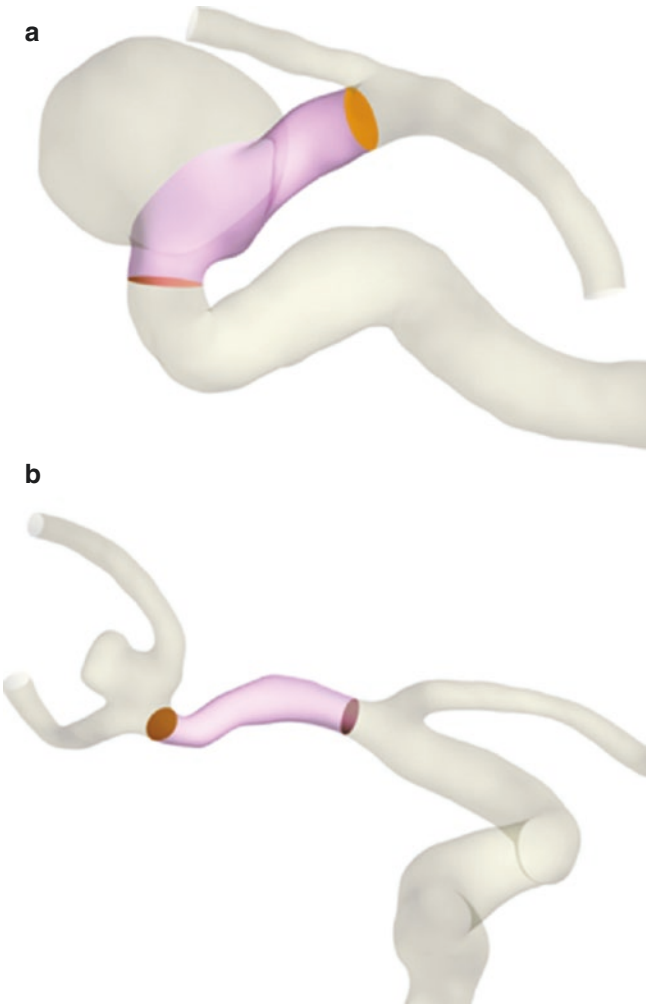

Fig. 3 Definition of parent arteries for aneurysms at the internal carotid artery (**a**) and middle cerebral artery (**b**). The C1–3 segments and M1 segment are defined as the parent arteries, respectively

infection, and seizures, will be rigorously excluded on clinical assessments, computed tomography (CT), magnetic resonance (MR) images, or laboratory studies.

Secondary outcome measures will be hemodynamic differences in cerebral arteries on CFD analyses in patients with subsequent occurrence of cerebral vasospasm and cerebral infarction and the relationships with eventual modified Rankin scale score at 3 months post-SAH. Cerebral vasospasm is defined as ≥50% arterial narrowing of the intracranial ICA, M1–2 segments, A1–2 segments of anterior cerebral artery, or P1–2 segments of posterior cerebral artery on CTA and/or digital subtraction angiography compared with the preoperative findings. Cerebral infarction is defined as newly developed cerebral infarction on CT or MR images that is not visible on admission or immediate postoperative or post-intervention scans or both.

Sample Size

Assuming that the incidence of DCI is 20%, a total of 200 patients will be required based on our preliminary study [6].

Statistical Analysis

Data will be expressed as mean ± standard error of the mean or median ± interquartile range. Comparisons between two groups will be made by unpaired *t*-tests or Mann-Whitney's *U* tests as appropriate. A value of $p < 0.05$ will be considered significant.

Discussion

The present study is intended to investigate whether CFD can predict DCI after SAH. Hemodynamic features obtained with CFD have shown the significant relationships with aneurysm initiation, growth, and rupture [8]. Recently, we reported that rupture status [7], rupture points [9], and hemostatic patterns [10] of cerebral aneurysms were characterized by hemodynamic parameters on CFD analyses.

Our previous study, which analyzed CFD with acute-stage preoperative CTA, showed that the cross-sectional area of ipsilateral extracranial ICA and distal parent artery tended to be smaller, and the flow velocity in the distal parent artery tended to be higher in patients who subsequently developed DCI after SAH [6]. In addition, we reported that CFD analyses using 3D-CTA could characterize ruptured cerebral aneurysms in poor-grade patients as a small diameter of parent artery, a large shape index, and a low wall shear stress [11]. The findings probably might reflect early vasospasm or early brain injury; however, the mechanisms have not yet been elucidated. Moreover, we did not investigate relationships between other hemodynamic parameters of cerebral arteries, such as wall shear stress, and the subsequent development of DCI in our preliminary study [6]. Thus, it would be meaningful to assess various hemodynamic parameters using CFD analyses in the present study. We believe that this multicenter prospective study will provide a novel useful diagnostic method to predict DCI before aneurysmal obliteration in an acute stage of SAH.

Study Status

The study is currently ongoing.

Acknowledgments This study is supported in part by a grant-in-aid for Scientific Research from Japan Society for the Promotion of Science to Drs. Shiba and Suzuki.

Conflict of Interest: **The authors declare that they have no conflict of interest.**

References

1. Nishikawa H, Nakatsuka Y, Shiba M, Kawakita F, Fujimoto M, Suzuki H, pSEED Group. Increased plasma galectin-3 preceding the development of delayed cerebral infarction and eventual poor outcome in non-severe aneurysmal subarachnoid hemorrhage. Transl Stroke Res. 2018;9(2):110–9. https://doi.org/10.1007/s12975-017-0564-0.
2. Okada T, Suzuki H. Toll-like receptor 4 as a possible therapeutic target for delayed brain injuries after aneurysmal subarachnoid hemorrhage. Neural Regen Res. 2017;12:193–6.
3. Suzuki H. What is early brain injury? Transl Stroke Res. 2015;6:1–3.
4. Suzuki H, Shiba M, Nakatsuka Y, Nakano F, Nishikawa H. Higher cerebrospinal fluid pH may contribute to the development of delayed cerebral ischemia after aneurysmal subarachnoid hemorrhage. Transl Stroke Res. 2017;8:165–73.
5. Suzuki H, Kawakita F. Tenascin-C in aneurysmal subarachnoid hemorrhage: deleterious or protective? Neural Regen Res. 2016;11:230–1.
6. Shiba M, Ishida F, Furukawa K, Tsuji M, Shimosaka S, Suzuki H. Conputational fluid dynamics for predicting delayed cerebral ischemia after subarachnoid hemorrhage. J Neurol Disord Stroke. 2017;5:1120.
7. Miura Y, Ishida F, Umeda Y, Tanemura H, Suzuki H, Matsushima S, Shimosaka S, Taki W. Low wall shear stress is independently associated with the rupture status of middle cerebral artery aneurysms. Stroke. 2013;44:519–21.
8. Meng H, Wang Z, Hoi Y, Gao L, Metaxa E, Swartx DD, Kolega J. Complex hemodynamics at the apex of an arterial bifurcation induces vascular remodeling resembling cerebral aneurysm initiation. Stroke. 2007;38:1924–31.
9. Fukazawa K, Ishida F, Umeda Y, Miura Y, Shimosaka S, Matsushima S, Taki W, Suzuki H. Using computational fluid dynamics analysis to characterize local hemodynamic features of middle cerebral artery aneurysm rupture points. World Neurosurg. 2015;83:80–6.
10. Tsuji M, Ishikawa T, Ishida F, Furukawa K, Miura Y, Shiba M, Sano T, Tanemura H, Umeda Y, Shimosaka S, Suzuki H. Stagnation and complex flow in ruptured cerebral aneurysms: a possible association with hemostatic pattern. J Neurosurg. 2016;3:1–7.
11. Shiba M, Ishida F, Furukawa K, Tanemura H, Tsuji M, Shimosaka S, Suzuki H. Relationships of morphologic parameters and hemodynamic parameters determined by computational fluid dynamics analysis with the severity of subarachnoid hemorrhage. J Neuroendovasc Ther. 2017;11:512–9.

Thromboelastometry as a Comprehensive Assessment of Hypercoagulation After Aneurysmal Subarachnoid Hemorrhage: A Case Report and Literature Review

Anastasia I. Baranich, Aleksandr A. Polupan, Aleksandr A. Sychev, Ivan A. Savin, Togrul F. Tabasaranskiy, Natalia V. Kurdumova, and Shalva Sh. Eliava

Abstract Subarachnoid hemorrhage after cerebral aneurysm rupture (aSAH) leads to delayed cerebral ischemia (DCI) in 25–35% of surviving patients. It is believed that DCI has a multifactorial etiology, including vasospasm. Furthermore, aSAH is associated with the development of hypercoagulation and microthrombosis; thus, its pharmacological correction may help to prevent DCI. We encountered a case where hypercoagulation was detected using rotational thromboelastometry (ROTEM), although the standard coagulation test results were within the normal ranges. Based on reviews of viscoelastic tests in cases of aSAH, ROTEM could be more sensitive to hypercoagulation after aSAH, compared to standard coagulation testing.

Keywords Subarachnoid hemorrhage · Microthrombosis Delayed cerebral ischemia · Secondary brain injury

Introduction

Aneurysmal subarachnoid hemorrhage (aSAH) is an acute cerebrovascular disease associated with high levels of mortality and disability [1]. Delayed cerebral ischemia (DCI) remains one of the main causes of poor neurological outcome after aSAH [2]. The mechanisms underlying the formation of DCI are incompletely understood. The historical assumption was that large-vessel cerebral vasospasm was the only cause of DCI. However, most of patients with aSAH develop angiographic vasospasm, but only ≥30% develop DCI [3]. Recent evidence indicates that other pathological mechanisms apart from vasospasm are involved [4]. For example, the coagulation system is activated early after the initial SAH, and these hypercoagulation changes lead to microthrombosis, which is considered one of the main pathophysiological mechanisms leading to DCI [5]. Adequate diagnosis of hypercoagulation and early initiation of prophylaxis and treatment may help prevent DCI (Fig. 1).

Case Report

A 52-year-old woman was admitted after rupture of an anterior communicating artery aneurysm, which led to intracerebral and intraventricular hemorrhages (Fisher IV) (Fig. 1). The patient was in stupor (Glasgow coma scale score, 10 points) with left-side hemiparesis, severe headache, and nuchal rigidity (Hunt-Hess 4 points). The patient was followed up in the neurocritical care department with a standard local protocol of care for acute period of aSAH, including early performed neurosurgery (aneurysm occlusion), intensive care with invasive hemodynamic monitoring, and management of intracranial complications. After aneurysm clipping, we evaluated hemostasis based on standard coagulation tests (Table 1) and rotation thromboelastometry (ROTEM) parameters (Table 2).

Blood samples were obtained via direct peripheral venipuncture after a tourniquet was placed for ≤30 s. Appropriate volumes were collected in vacuum tubes containing sodium citrate, and the first tube was not included in the coagulation testing. All coagulation tests were performed within 10 min after blood collection. ROTEM was performed using whole blood that was incubated at 37 °C in a heated cup. A pin in the cup was connected to an optical detector system, and the cup and pin were oscillated relative to each other. The forming clot impedes the pin's rotation, and the extrinsic coagulation pathway (EXTEM assay) and intrinsic coagulation cascade (INTEM assay) were evaluated. The influence of fibrinogen on clot firmness was estimated using the platelet-inactivating FIBTEM assay [6]. The following ROTEM parameters were

A. I. Baranich (✉) · A. A. Polupan · A. A. Sychev · I. A. Savin
T. F. Tabasaranskiy · N. V. Kurdumova · S. S. Eliava
Department of Neurocritical Care, N.N. Burdenko National Scientific and Practical Center for Neurosurgery, Moscow, Russia
e-mail: aarefeva@nsi.ru

R. D. Martin et al. (eds.), *Subarachnoid Hemorrhage*, Acta Neurochirurgica Supplement 127,
https://doi.org/10.1007/978-3-030-04615-6_25,

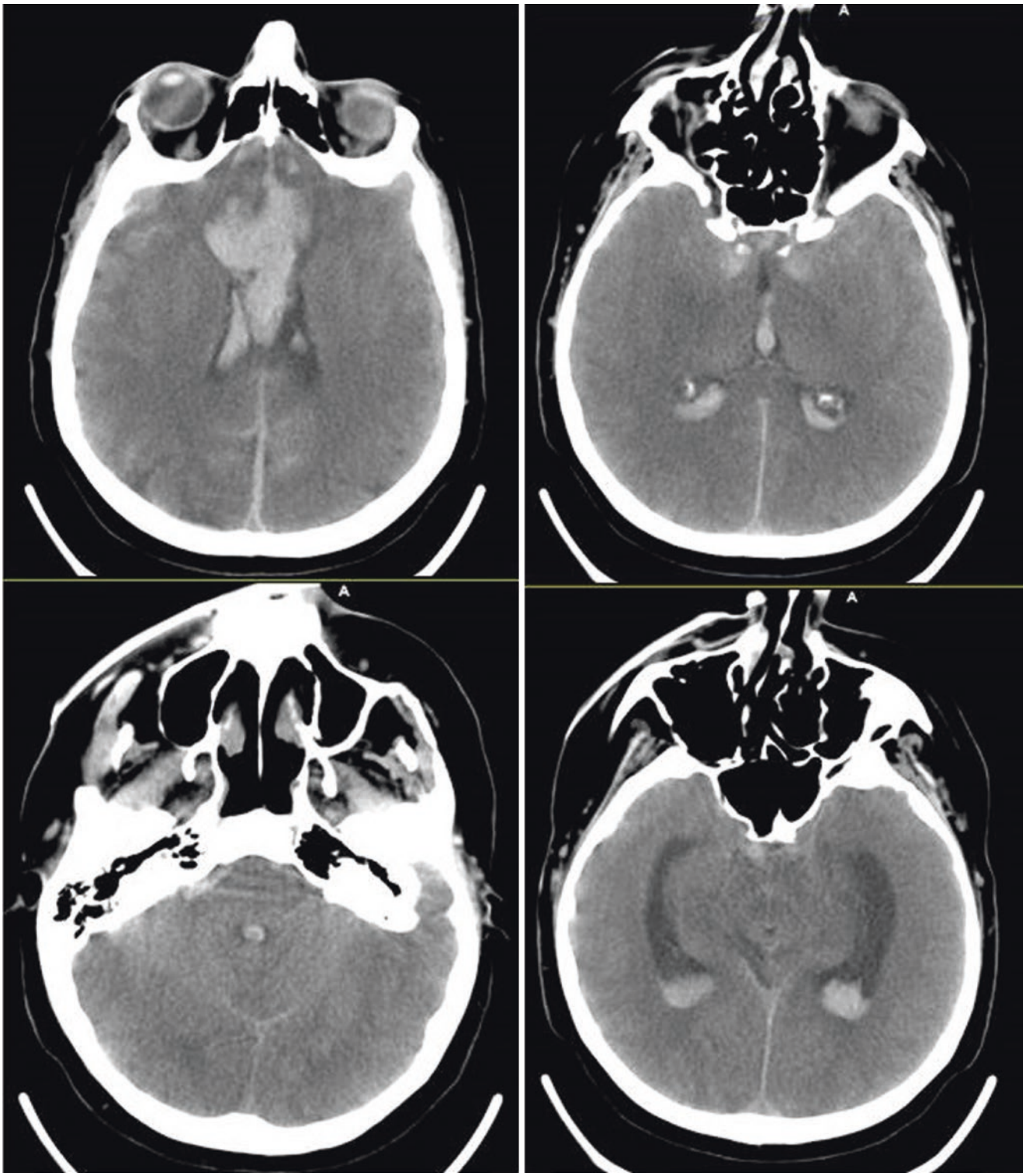

Fig. 1 Computed tomography scan upon admission

analyzed: (1) clotting times (CT, s), initiation of clotting, thrombin generation, and start of fibrinogen polymerization; (2) clot formation time (CFT, s) and α, estimation of clot growth kinetic by fibrin polymerization, platelets, and factor XIII; (3) clot strength based on oscillation amplitude at fixed times (A10–A20); and (4) maximum clot firmness (MCF). The standard coagulation tests included activated partial thromboplastin time (APTT), international normalized ratio (INR), fibrinogen level, and inhibition of factor X (anti-FXa assay). These tests were performed using ACL 9000 analyzer.

All standard coagulation test results were considered normal, although thromboelastometry revealed hypercoagula-

tion based on increased clot strength (elevated MCF values in the INTEM, EXTEM, and FIBTEM assays) on the second day after the aSAH. The patient also had clinical signs of hypercoagulability, such as preliminary thrombosis in the veins of the lower extremities. Infections of the central nervous system, blood, and urinary tract were excluded as causes of the hypercoagulation, as well as pneumonia and diabetes. Anticoagulation therapy was initiated with low-molecular-weight heparins (LMWH) and maintained within the prophylactic range using the anti-FXa assay (0.32). The next day, before the LMWH treatment, a dynamic evaluation of the hemostasis was performed using ROTEM, which revealed persistent hypercoagulability. Thus, a therapeutic LMWH dose was administered (0.6). The patient was discharged after 36 days, with clear consciousness and no signs of hypercoagulation (complete regression of venous thrombosis and the absence of ischemic foci on the brain CT scan).

Table 1 Serum lab values at serial time points after aSAH

	Normal range	PBD 1	PBD 2	PBD 3	PBD 4	PBD 5
APTT	25.4–36.9 s	27.0	25.5	26.4	26.2	25.7
INR	Below 1.1	0.96	1.10	1.00	1.00	0.98
Fibrinogen	1.7–4.4 mg/dL	3.5	4.0	3.3	3.6	3.8
D-dimer	Below 550 ng/mL	618	620	627	631	630
Platelet count	150–450 10^3/µL	243	237	226	240	200

PBD post bleed day; *APTT* activated partial thromboplastin time; *INR* international normalized ratio

Table 2 Parameters of ROTEM at serial time points after aSAH

	Normal range	PBD 1	PBD 2	PBD 3	PBD 4	PBD 5
EXTEM						
CT	38–79	53	68	77	72	57
CFT	34–159	57	70	85	73	99
α	63–83	79	76	73	76	71
A10	43–65	65	65	61	67	59
A20	50–71	70	76	72	71	66
MCF	50–72	71	76	74	71	68
INTEM						
CT	100–240	195	197	195	186	173
CFT	30–110	56	58	57	57	76
α	70–83	78	78	75	79	75
A10	44–66	64	65	60	67	56
A20	50–71	70	78	72	71	62
MCF	50–72	70	78	74	71	62
FIBTEM						
CT	38–62	54	59	62	62	51
α	N/A	79	78	75	72	73
A10	7–23	22	**27**	**24**	22	21
A20	8–24	23	**28**	**26**	22	22
MCF	9–25	23	**28**	**27**	23	22

Literature Review

Over the last years, vasospasm has been identified as the main pathophysiological mechanism contributing to DCI. However, recent studies suggest a multifactorial etiology of DCI, including microvascular dysfunction and microthrombi formation [4, 5, 7, 8].

Tissue factor (TF) is expressed by various cells within the vessel wall and surrounding blood vessels; thus, the endothelium physically separates this potent "activator" of hemostasis from the blood flow [9–12]. High levels of TF are detected in the brain, lungs, heart, kidneys, and placenta, while low levels are usually detected in the liver, spleen, skeletal muscle, and thymus [9]. High TF levels in the brain help to protect against intracranial hemorrhage, and damage to cerebral vessels can lead to hypercoagulation and thrombosis [4, 12].

The appearance of procoagulant activity precedes DCI [13], and Stein et al. [14] have reported that microthrombosis preceded DCI in various brain structures (e.g., cingulate, hippocampal, and insular areas) of 29 patients after fatal aSAH. For example, significantly more microthrombi were detected in patients with signs of DCI, compared to patients without ischemic lesions (10.0/cm^2 vs. 2.8/cm^2). Sehba et al. [15] also detected increased platelet aggregation in cerebral vessels within 10 min after rupture in animal models of aSAH. Juvela et al. [16] evaluated platelet aggregation and release of thromboxane B2 in 52 patients with aSAH and reported that increased platelet activity and thromboxane release were associated with DCI development. Furthermore, the highest values for thromboxane release were observed in patients with clinical and radiological signs of DCI. Another possible mechanism for hypercoagulation after aSAH involves the vasopressin receptor V1a, which is broadly dispersed throughout the brain (e.g., on the surface of endothelial cells) [17], as the interaction between vasopressin and the V1a receptor promotes platelet aggregation and vasoconstriction [18]. Thus, Liu et al. [19] studied the dynamics of vasopressin V1a receptor expression and its effect on platelet aggregation in experimental aSAH models and found that vasopressin levels rapidly increased during the first 6–24 h after hemorrhage. The peak expression of GPIIb/IIIa integrin responsible for platelet aggregation was located in the cortex and hippocampus, and was co-localized with vasopressin, which led the authors to conclude that high plasma levels of vasopressin were correlated with secondary brain damage after experimental aSAH [20]. Foreman et al. [21] have also reported that nosocomial infections were associated with DCI among 156 patients with aSAH, which they attributed to

a systematic inflammatory response leading to thrombosis and subsequently ischemia. Ettinger [22] reported that, among patients with aSAH, significantly elevated fibrinogen levels were associated with an increased risk of mortality. Other researchers [23] have also indicated that elevated levels of fibrinogen, D-dimers, and thrombin-antithrombin complex may be predictors of DCI after aSAH.

A search of the PubMed database using "thromboelastography" and "subarachnoid hemorrhage" only returns two studies that examined thromboelastography (TEG) in cases of aSAH. Ramchand et al. [24] evaluated 22 patients with moderate-to-severe SAH based on several TEG parameters, complete blood count, fibrinogen, C-reactive protein, and D-dimers at 1–10 days after hemorrhage and reported that TEG-detected hypercoagulation was associated with poor outcomes. Furthermore, they reported that the associations between several TEG parameters and the outcomes were stronger than the associations with traditional biomarkers. Frontera et al. [25] also analyzed platelet function in 106 patients with aSAH using TEG, as well as C-reactive protein dynamics. In that study, patients with severe early brain injury after aSAH (Hunt-Hess grade 4–5) had significantly increased levels of platelet activation and C-reactive protein compared to the control group, which were associated with poor 3-month functional outcomes.

Although aSAH is associated with the development of hypercoagulation and formation of microthrombosis, which may lead to DCI, the pathophysiological mechanisms underlying aSAH-related hypercoagulation are incompletely understood. Several studies have suggested that the relationship is driven by platelet hyperaggregability, while others have suggested that high brain levels of TF can predispose the patient to hypercoagulation.

Discussion

In the present case, we examined whole-blood samples using ROTEM, which revealed elevated clot strength (increased MCF during the INTEM, EXTEM, and FIBTEM assays), although normal results were observed during standard coagulation testing. This may because the most widely used screening tests (INR, APTT, and fibrinogen level) are performed using plasma, which may obscure information regarding interactions between coagulation factors and phospholipid surfaces, provide limited information regarding clot stability, and fail to detect minor shifts of hemostasis [12]. Thus, we believe that viscoelastic testing using whole blood is necessary during the acute period of aSAH. In this context, point-of-care viscoelastic testing using TEG and ROTEM provides more complete information regarding hemostasis by simultaneously measuring coagulation, platelet function, and fibrinolysis [6]. Moreover, the FIBTEM assay abolishes platelet function using cytochalasin D (an inhibitor of actin polymerization) and generates data specifically regarding fibrinogen. This crucial differentiation between the contributions of platelets and fibrin to clot strength can facilitate customized prophylaxis and microthrombosis treatment. Previous studies have suggested using the maximum amplitude from TEG, although this parameter does not distinguish fibrin and platelet bonding via GPIIb/IIIa and is strongly correlated with platelet function, which precludes a pathophysiological customized treatment. As our patient exhibited clinical and laboratory signs of hypercoagulation, early treatment was started using LMWH at only 15 h after surgery, although clinical signs of bleeding were absent. We believe that the success of this approach is related to specific dose assessments using the anti-FXa assay, as it is suited for monitoring patients who are receiving LMWH and provides the most accurate assessment of the anticoagulation effect. The anti-FXa assay should be ordered as a "peak" test at 3–4 h after the LMWH treatment, when the blood levels are expected to be highest. Our initial treatment targeted the prophylactic ranges (0.32), although the dose was subsequently increased to 0.6 because the lower dose was not effective. The patient subsequently experienced complete regression of venous thrombosis, had no ischemic foci on the brain CT scan, and was discharged with clear consciousness and no clinical or laboratory signs of hypercoagulation.

Conclusion

Hypercoagulability is common during the acute period of aSAH, and leads to microthrombosis and ischemic foci, although standard coagulation testing may not detect these changes. Thus, thromboelastometry may be effective for evaluating hemostasis using whole blood, as it is sensitive to even minor shifts in hemostasis. Furthermore, adequate prophylaxis and hypercoagulation therapy after aSAH may help to prevent DCI and improve neurological outcomes, although further studies are needed to evaluate this approach.

Conflict of Interest The authors declare no conflicts of interest.

References

1. Sehba FA, Hou J, Pluta RM, Zhang JH. The importance of early brain injury after subarachnoid hemorrhage. Prog Neurobiol. 2012;97(1):14–37. https://doi.org/10.1016/j.pneurobio.2012.02.003.

2. Francoeur CL, Mayer SA. Management of delayed cerebral ischemia after subarachnoid hemorrhage. Crit Care. 2016;20(1):277. https://doi.org/10.1186/s13054-016-1447-6.
3. Millikan CH. Cerebral vasospasm and ruptured intracranial aneurysm. Arch Neurol. 1975;32:433–49.
4. Rowland MJ, Hadjipavlou G, Kelly M, Westbrook J, Pattinson KT. Delayed cerebral ischaemia after subarachnoid haemorrhage: looking beyond vasospasm. Br J Anaesth. 2012;109(3):315–29. https://doi.org/10.1093/bja/aes26.
5. Terpolilli NA, Brem C, Bühler D, Plesnila N. Are we barking up the wrong vessels? Cerebral microcirculation after subarachnoid hemorrhage. Stroke. 2015;46(10):3014–9. https://doi.org/10.1161/STROKEAHA.115.006353.
6. Ranucci M. Point-of-care tests for severe hemorrhage. A manual for diagnosis and treatment. Cham: Springer; 2016.
7. Leonardo de Oliveira Manoel A, Goffi A, Marotta TR, Schweizer TA. The critical care management of poor-grade subarachnoid hemorrhage. Crit Care. 2016;20:21. https://doi.org/10.1186/s13054-016-1193-9.
8. Andereggen L, Neuschmelting V, Von Gunten M, Widmer HR. The role of microclot formation in an acute subarachnoid hemorrhage model in the rabbit. Biomed Res Int. 2014;2014:161702. https://doi.org/10.1155/2014/161702.
9. Mackman N. The role of tissue factor and factor VIIa in hemostasis. Anesth Analg. 2009;108(5):1447–52. https://doi.org/10.1213/ane.0b013e31819bceb1.
10. Berlot G. Hemocoagulative problems in the critically ill patient. Cham: Springer; 2012.
11. Monroe DM, Hoffman M. Theories of blood coagulation: basic concepts and recent updates. In: Hemostasis and thrombosis. Oxford: Wiley; 2014.
12. Lichtin A, Bartholomew J. The coagulation consult. A case-based guide. Cham: Springer; 2014.
13. Budohoski KP, Guilfoyle M, Helmy A, Huuskonen T, Czosnyka M. The pathophysiology and treatment of delayed cerebral ischaemia following subarachnoid haemorrhage. J Neurol Neurosurg Psychiatry. 2014;85(12):1343–53. https://doi.org/10.1136/jnnp-2014-307711.
14. Stein SC, Browne KD, Chen XH, Smith DH, Graham DI. Thromboembolism and delayed cerebral ischemia after subarachnoid hemorrhage: an autopsy study. Neurosurgery. 2006;59(4):781–7 . discussion 787-8. https://doi.org/10.1227/01.NEU.0000227519.27569.45.
15. Sehba FA, Mostafa G, Friedrich V Jr, Bederson JB. Acute microvascular platelet aggregation after subarachnoid hemorrhage. J Neurosurg. 2005;102(6):1094–100. https://doi.org/10.3171/jns.2005.102.6.1094.
16. Juvela S, Hillbom M, Kaste M. Platelet thromboxane release and delayed cerebral ischemia in patients with subarachnoid hemorrhage. J Neurosurg. 1991;74(3):386–92. https://doi.org/10.3171/jns.1991.74.3.0386.
17. Thomas ME, Osmani AH, Scrutton MC. Some properties of the human platelet vasopressin receptor. Thromb Res. 1983;32(6):557–66. https://doi.org/10.1016/0049-3848(83)90057-9.
18. Friedrich B, Müller F, Feiler S, Schöller K, Plesnila N. Experimental subarachnoid hemorrhage causes early and long-lasting microarterial constriction and microthrombosis: an in-vivo microscopy study. J Cereb Blood Flow Metab. 2012;32(3):447–55. https://doi.org/10.1038/jcbfm.2011.154.
19. Liu ZW, Gu H, Zhang BF, Zhao YH, Zhao JJ. Rapidly increased vasopressin promotes acute platelet aggregation and early brain injury after experimental subarachnoid hemorrhage in a rat model. Brain Res. 2016;1639:108–19. https://doi.org/10.1016/j.brainres.2016.02.038.
20. Hockel K, Schöller K, Trabold R, Nussberger J. Vasopressin V(1a) receptors mediate posthemorrhagic systemic hypertension thereby determining rebleeding rate and outcome after experimental subarachnoid hemorrhage. Stroke. 2012;43(1):227–32. https://doi.org/10.1161/STROKEAHA.111.626168.
21. Foreman PM, Chua M, Harrigan MR, Fisher WS 3rd., Vyas NA. Association of nosocomial infections with delayed cerebral ischemia in aneurysmal subarachnoid hemorrhage. J Neurosurg. 2016;125(6):1383–9. https://doi.org/10.3171/2015.10.JNS151959.
22. Gerlach R, Krause M, Seifert V. Hemostatic and hemorrhagic problems in neurosurgical patients. Acta Neurochir. 2009;151(8):873–900.discussion900.https://doi.org/10.1007/s00701-009-0409-z.
23. Hamilton MG, Golfios JG, Pineo GF. Handbook of bleeding and coagulation for neurosurgery. Stuttgart: Thieme; 2015.
24. Ramchand P, Nyirjesy S, Frangos S, Doerfler S, Nawalinski K. Thromboelastography parameter predicts outcome after subarachnoid hemorrhage: an exploratory analysis. World Neurosurg. 2016;96:215–21. https://doi.org/10.1016/j.wneu.2016.04.002.
25. Frontera JA, Provencio JJ, Sehba FA, McIntyre TM, Nowacki AS. The role of platelet activation and inflammation in early brain injury following subarachnoid hemorrhage. Neurocrit Care. 2017;26(1):48–57. https://doi.org/10.1007/s12028-016-0292-4.

The Treatment of a Ruptured Anterior Communicating Artery (ACoA) Aneurysm with Coiling and Flow Disruptor (WEB-Device) and Management of Symptomatic Post-Interventional Delayed Vasospasm: A Case Report

Michael Dobrzeniecki, Alex Trofimov, and Stefan Rath

Abstract The article reports a clinical case illustrating a favorable outcome of endovascular treatment of a patient with a ruptured wide range neck ACoA aneurysm by WEB-Device. The peculiar characteristics of the pre-procedural period and the procedure are described.

Keywords Cerebral aneurysm · ACoA aneurysm · WEB-Device · Perfusion CT

Introduction

The intrasaccular flow disruptor "WEB-Device" (Sequent Medical, Aliso Viejo, California) has been used successfully in the treatment of complex ruptured and unruptured wide range neck aneurysms with an adequate occlusion rate between 79.4 and 85% [1]. It was invented to provide flow disruption along the aneurysm neck and induce intrasaccular thrombosis [2].

Despite the safety of the WEB-Device with a periprocedure morbidity of 2% and mortality of 0%, respectively, and a 1-year morbidity 4% and mortality 2% [2], only a few post-procedure complications are described in the literature. Thromboembolic events up to 21% in ruptured and 5% in unruptured aneurysms [3] or incomplete occlusion with the need of re-intervention between 3.6 and 16.7% [4, 5] are found discussed in detail.

We present an illustrative case of a 45-year-old male with a history of SAH due to a ruptured anterior communicating artery (ACoA) aneurysm. The aneurysm was initially treated endovascular with coiling of the aneurysm tip and subsequently with WEB-Device. After insertion of the WEB-Device, the patient developed symptomatic delayed vasospasm.

Case

A 45-year-old male was transferred from a peripheral hospital to our department. The patient had a history of severe headache for 1 week before admission to the peripheral hospital. The headache initially improved during the week and then significantly worsened. In the peripheral hospital, a head CT with CT-angio was performed and showed a left wide range neck anterior communicating artery (ACoA) aneurysm.

The clinical status at admission in our department was Glasgow Coma Score 15, WFNS II, with positive meningism. The patient was very sensitive to light and noise with no neurological deficit.

The follow-up unenhanced computed tomography (CT) and CT angiography (CTA) done in our department showed no signs of hydrocephalus or vasospasm. The same day, an angiography was performed to estimate the configuration of the aneurysm and to establish the best treatment strategy. Therapy with nimodipine 6 × 60 mg over 24 h was initiated. Due to the complex configuration of the aneurysm (large ACoA aneurysm with multiple lobes and a wide neck), we considered our options to be surgery, stent-assisted coiling, or WEB-Device.

According to our hospital policy, we always attempt an endovascular approach to treating aneurysms.

Due to the age of the patient and the possible adverse effects of dual antiplatelet therapy, we took the WEB-Device into consideration. Unfortunately due to logistic reasons, we had to adjust our treatment strategy, and we decided to coil the aneurysm tip first, and in a subsequent procedure, we

M. Dobrzeniecki (✉) · S. Rath
Department of Neurosurgery, Spine Surgery and Interventional Neuroradiology DONAUISAR Klinikum Deggendorf, Deggendorf, Germany

A. Trofimov
Department of Neurosurgery, Nizhniy Novgorod State Hospital Named After NA Semashko, Nizhniy Novgorod, Russia

R. D. Martin et al. (eds.), *Subarachnoid Hemorrhage*, Acta Neurochirurgica Supplement 127,
https://doi.org/10.1007/978-3-030-04615-6_26,

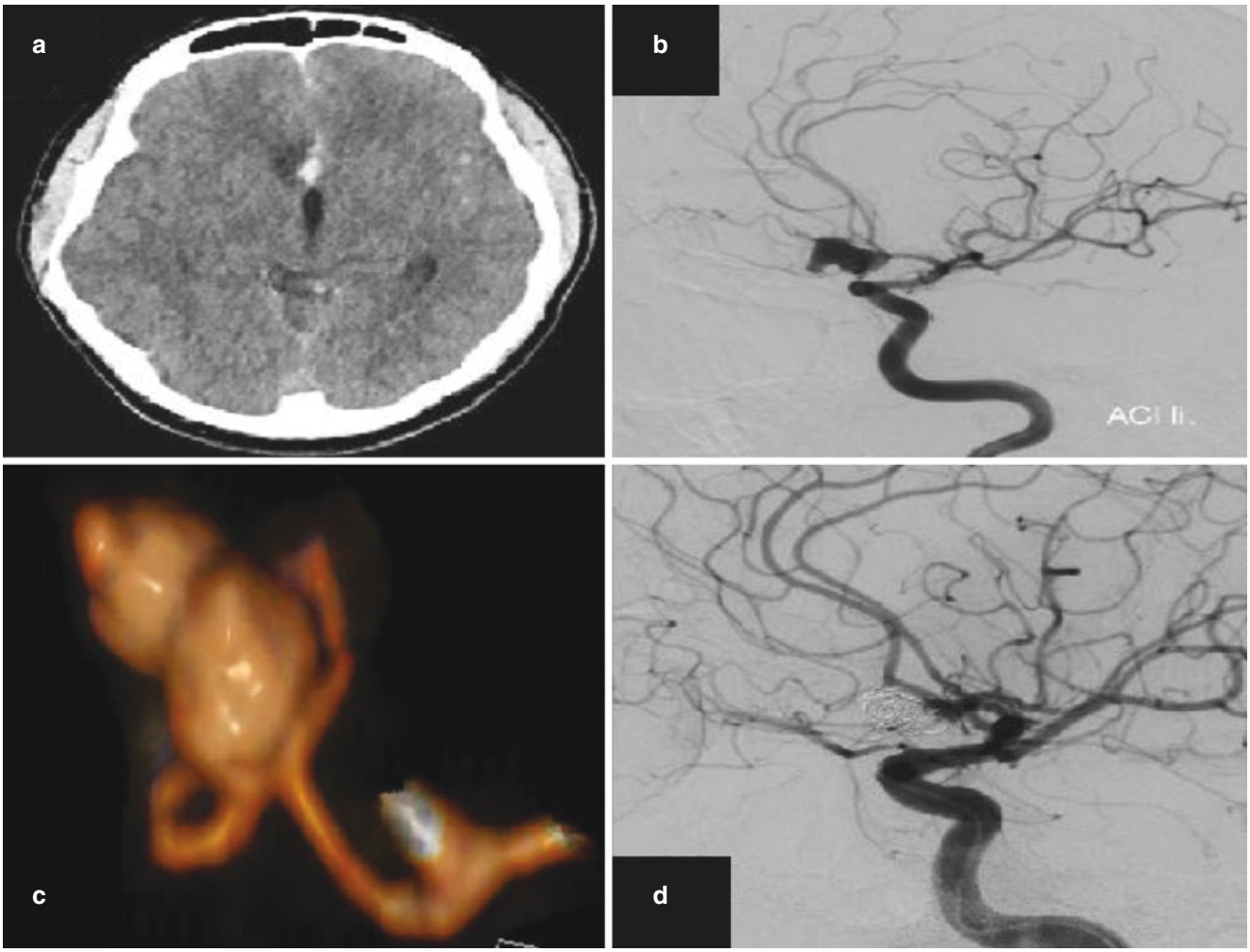

Fig. 1 CT and rotational digital angiography of the patient. L. ACoA aneurysm, no signs of hydrocephalus, no vasospasm (**a**), pre-interventional angiography (**b**), configuration of the ACoA aneurysm (**c**), implantation of WEB-Device post-coiling angiography (**d**)

performed the final closure of the aneurysm with the WEB-Device (Fig. 1).

Post-coiling, the patient was transferred to the ICU. Neurological status checks were performed hourly, and transcranial Doppler (TCD) was measured daily. On day 2 post admission, the patient developed non-symptomatic left middle cerebral artery (MCA) vasospasm detected by TCD. "Triple-H" therapy was initiated.

On day 17, no further vasospasm was detected through the TCD and CT perfusion. The "Triple-H" therapy was stopped. We continued daily TCD and waited 3 more days for the final procedure to complete the closure of the aneurysm.

On day 20 post admission, the final procedure with the WEB-Device (8 × 3 mm) was performed. No intra-procedural complications occurred.

A few hours after the procedure was completed, the patient developed a severe headache with right hemiparesis (BMC1–2/5) and right hemineglect. Vasospasm was detected of the left MCA in TCD. Urgent head CT with perfusion (PCT) was performed (Fig. 2) with no clear evidence of vasospasm. "Triple-H" therapy was initiated again and ASA 100 mg was given prophylactically.

During the next few hours, the neurological status of the patient deteriorated. He developed a right hemiplegia, disorientation, and persistent right hemineglect. Despite no clear evidence of vasospasm in the PCT, we decided to perform an urgent angiography with intra-arterial vasospasmolysis with nimodipine (2 mg over 30 min) of the left MCA based on the patient's deterioration in neurological status and TCD findings.

On day 22, the patient's neurological status decreased to GCS 7. He required intubation. A PCT with CTA was performed (Fig. 2).

Urgent angiography with intra-arterial vasospasmolysis (nimodipine 2 mg over 1 h) of the left ICA was performed. After the intervention the patient was extubated. The disorientation resolved. The hemiplegia and the hemineglect slowly resolved during the next few days.

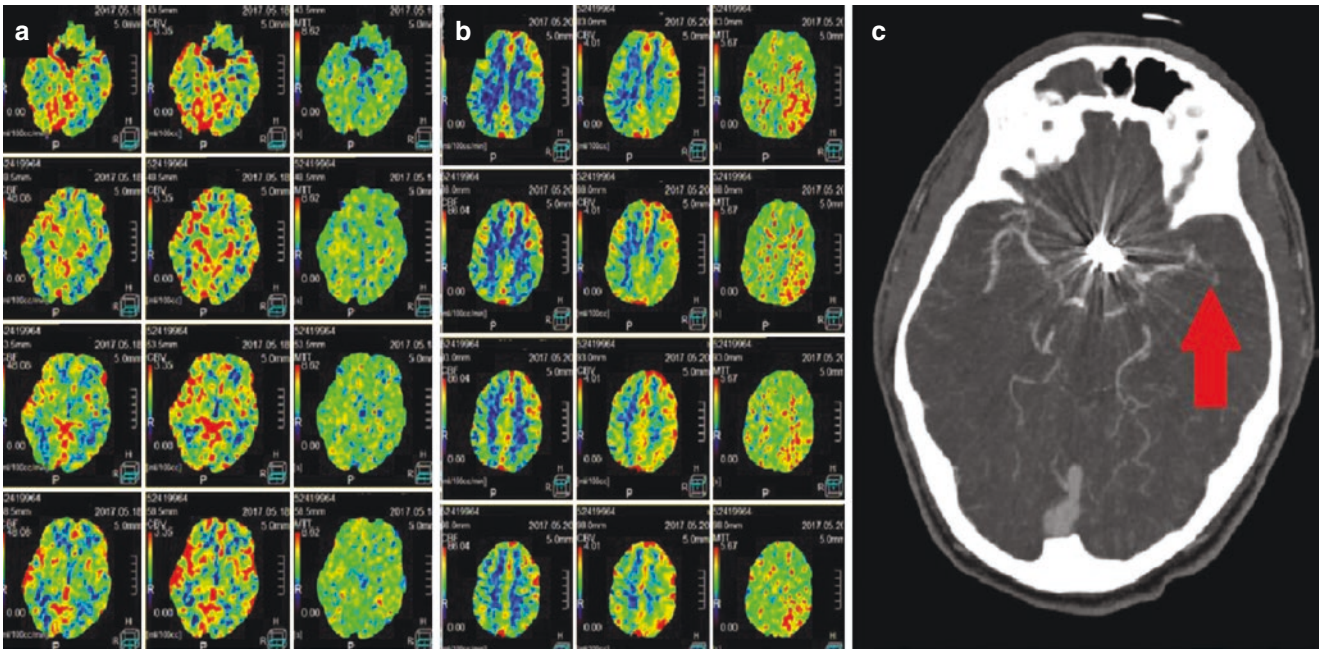

Fig. 2 CT perfusion with no signs of vasospasm or hydrocephalus (**a**), CT perfusion with signs of hypoperfusion in the left temporal lobe (**b**), CTA vasospasm of the left MCA (red arrow) (**c**)

Day 27 post admission, the TCD showed no cerebral vasospasm. One day later the "Triple-H" therapy was stopped. ASA 100 mg was continued.

On day 35 day post admission, the patient was discharged to rehab with GCS 15, mRS 0, no neurological deficit.

Discussion

Delayed symptomatic vasospasm after WEB-Device insertion is a very rare complication. In the literature only one report was found which describes two cases of post-interventional vasospasm [6] with no further detailed information about the onset, the severity, or their treatment strategy. In our department, we have used the WEB-Device since 2012. Since then, we treated 45 patients with the flow disruptor. As far as we know, this is the first described in detail case of post-interventional delayed symptomatic vasospasm after a WEB-Device based on our patient base and literature review. Reviewing this case raises the questions of whether vasospasm could be avoided or at least the severity reduced by performing only one procedure, by waiting longer until the final procedure with the WEB-Device was performed or if the vasospasm was induced because of intra-procedural manipulation.

Our case demonstrates that despite the sensitivity of only 58% [7], daily obtained TCD in experienced hands can be a useful tool in detecting peripheral vasospasm which is very difficult to detect even in CT perfusion.

Conclusion

Despite the complication, we believe that the WEB-Device is a very useful and safe device for the endovascular treatment of ruptured and unruptured wide neck aneurysms.

However, more studies with a larger patient numbers and longer follow-up as well as detailed descriptions of complications and their management are still needed.

Conflict of Interest *Disclosure*: Michael Dobrzeniecki Unrelated: Consultant Brainlab.

Funding: **None for this report.**

References

1. Lubicz B, Klisch J, Gauvrit JY. Short-term and mid-term follow-ups in patients with wide-neck bifurcation aneurysm treated with the WEB device: a retrospective European study. Am J Neuro Radiol. 2014;35:432–8.
2. Pierot L, Gubucz I, Buhk JH. Safety and efficacy of aneurysm treatment with the WEB: results of the WEBCAST 2 study. Am J Neuro Radiol. 2017;38(6):1151–15.
3. Asnafi S, Rouchaud A, Pierot L. Efficacy and safety of the Woven EndoBridge (WEB) device for the treatment of intracranial aneurysms: a systematic review and meta-analysis. Am J Neuro Radiol. 2016;37(12):2287–92.
4. Clajus C, Strasilla C, Fiebig T. Initial and mid-term results from 108 consecutive patients with cerebral aneurysm treated with WEB device. J Neurointerv Surg. 2017;9:411–7.

5. Pierot L, Spelle L, Molyneux A. Clinical and anatomical follow-up in patients with aneurysm treated with the WEB Device: 1-year follow-up report in the cumulated population of 2 prospective, multicenter series (WEBCAST and French Observatory). Neurosurgery. 2016;78(1):133–41.
6. Liebig T, Kabbasch C, Strasilla C. Intrasaccular flow disruption in acutely ruptured aneurysm: a multicenter retrospective review of the use of the WEB. Am J Neuro Radiol. 2015;36(9):1721–7.
7. Sloan MA, Haley EC Jr, Kassell NF. Sensitivity and specificity of transcranial Doppler ultrasonography in the diagnosis of vasospasm following subarachnoid hemorrhage. Neurology. 1989;39(11):1514–8.

Treating Patients with Frontal Neurocognitive Deficits After SAH and Stroke

Michael Gilewski

Abstract Five frontal systems circuits connect with the basal ganglia and other structures to control and regulate thinking and behavior. Subarachnoid hemorrhage and stroke following anterior circulation aneurysms typically disrupt these circuits, sometimes markedly affecting a patient's function. This article reviews the primary pathways and associated brain functions. The principles of cognitively and behaviorally rehabilitating these functions are also discussed by creating external structure and building on what the brain is still capable of doing.

Keywords Stroke · Subarachnoid hemorrhage · Frontal brain systems · Frontal lobes · Cognitive rehabilitation · Rehabilitation · Restoration of function

Many brain aneurysms involve the anterior cerebral artery (ACA) circulation, particularly the anterior communicating artery (AComm) [1]. Their rupture and resultant subarachnoid hemorrhage significantly impact a patient's frontal brain functions. The aim of this paper is to review the functional frontal systems and the nature of neuropsychological treatment for impairment.

Tekin and Cummings [2] among others have identified five primary frontal systems pathways involving areas of frontal cortex and subcortical connections in the basal ganglia and diencephalon. These include:

1. The *motor circuit* projects from neurons in the supplementary motor, premotor, motor, and somatosensory cortices to the putamen and then to other areas of the basal ganglia. This activates all motor functions, including thought-mediated executive functions.
2. The *oculomotor circuit* originates in the frontal eye field (Brodmann area 8) and posterior parietal cortex. The fibers project to the body of the caudate nucleus, dorsomedial globus pallidus, and ventrolateral substantia nigra and then to the mediodorsal thalamic nuclei and back to area 8. This provides attentional control of eye movement and awareness of and orientation to the environment.
3. The *dorsolateral prefrontal circuit* originates in Brodmann areas 9 and 10 on the lateral surface of the anterior frontal lobe and projects to the dorsolateral head of the caudate nucleus. Neurons project then to the globus pallidus and substantia nigra and then to the ventral anterior and mediodorsal thalamus. Feedback to the dorsolateral frontal cortex completes the circuit. This circuit involves all the typical cognitive thinking skills, such as complex attention, abstraction, reasoning, and analysis. Multiple white matter pathways to the parietal lobes integrate language and complex visual and contextual processes into the frontal thinking processes.
4. The *orbitofrontal circuits* originate in Brodmann areas 10 and 11 and send fibers to the ventromedial caudate nucleus. Neurons form this region of the caudate project to the mediodorsal globus pallidus and to the substantia nigra. Fibers connect to the ventral anterior and mediodorsal thalamus and project back to the orbitofrontal cortex from thalamus. This circuit is involved in integrating sensory information into behavior and emotional and behavior control.
5. The *anterior cingulate circuit* originates in the anterior cingulate cortex (Brodmann area 24) and projects to the ventral striatum onward to the ventral anterior nucleus of the thalamus and back to the anterior cingulate cortex. This area integrates memory into function and selectivity of response to environmental demands.

Although the middle cerebral artery circulation feeds most of the frontal cortex, all these circuits can get disrupted by ACA circulation as projections get disrupted between medial subcortical areas and feedback from the thalamus.

M. Gilewski (✉)
Department of Physical Medicine and Rehabilitation, Loma Linda University, Loma Linda, CA, USA
e-mail: mgilewski@llu.edu

R. D. Martin et al. (eds.), *Subarachnoid Hemorrhage*, Acta Neurochirurgica Supplement 127,
https://doi.org/10.1007/978-3-030-04615-6_27,

Functionally this can manifest in disruptions of frontal brain control of thinking and behavior.

One critical function of the frontal lobes is to *stop behavior.* This allows for persons to control and utilize attention in a willful way. Inhibition involves resisting the environment, such as pull-to-stimulus, in which the person reacts to an external stimulus in automatic fashion. This can manifest as picking up an object without thinking or purpose, interrupting a conversation by talking, or responding to someone without editing speech or behavior. Stopping allows for appropriate thinking and analysis, especially when a situation is complex. Impaired persons react in overly simplistic or self-centered ways without awareness of consequence. Stopping can also permit reflective thinking, dreaming, and sensory appreciation. Persons otherwise may stay in motion in a compulsive way, in purposeless activity or keep talking when they should otherwise be quiet. A final benefit of stopping is to become mindful, a skill essential for meditation and deep attentional concentration. Impaired persons cannot focus and remain constantly distracted internally or externally. They cannot remain on task, disrupting purposeful and efficient thinking and behavior.

A second basic function is to *initiate behavior*. Especially with impairment in the orbitofrontal circuit, such persons may be inert and vegetative. They may verbalize good intention but be unable to activate themselves to carry through on that intention. They may appear depressed but are not because they lack the necessary negativity of self, others, and the environment.

The first two functions then balance themselves to permit *control of behavior*. This involves shifting speech, thinking, and behavior to environmental demands or internal desire. Impaired persons often get stuck in a mental or behavioral set. They cannot inhibit impulsive actions, sustain their attention, adjust behavior as situations shift, or properly time reactions. Such individuals appear and are out of control, presenting problems for their own safety and demand constant efforts at control by others around them.

Growing out of these basic functions is the *capacity to think.* Internal symbolic analysis and external speech utilize the same functions, varying only in the relative shifts between the context of starting and stopping behavior. Manifested behavior often reflects the internal level of skill or impairment. Thinking can also take on a relational or contextual analysis that transcends language and sequential analysis. A simple response, "no," can be appropriate or inappropriate given the context of the situation. "No" in the context of a command from authority can reflect lack of cooperation. A pattern of "no" responses can infer an attitude of defiance and insubordination. In a situation of free choice, it may reflect one's desire or an attempt to defer decision to another. The loudness, directness, and emphasis of the "no" may also vary across situations. Persons impaired in this area remain out of sync with others and environmental demands. Thinking and behavior reflect poor analysis and result in disruptive behavior.

The pinnacles of these higher order frontal brain functions are *self-awareness* and *self-monitoring*. The more these develop in a patient's recovery, the greater the exercise of self-control and self-regulation. This will ease demands on family and others to provide structure and feedback.

Neuropsychological Treatment of Frontal Brain Impairment

Treating patients impaired by the cognitive effects of a ruptured aneurysm or subarachnoid hemorrhage affecting frontal thinking involves external or internal approaches (see Table 1). Both require treatment over time. *Externally*, the guiding principle is to externalize the impaired functions. Someone who is very impulsive, disorganized, and mentally incapacitated may require living in an institutional setting or need conservatorship of property or person. More commonly, family will assume the care of the patient. Others must do what the person cannot, assist the person in functional activities, and supervise the person's actions. Following an assessment, the neuropsychologist can educate the patient and family about the specific impairments and more efficiently guide the patient's assistance and supervision needs. The goal would be for the patient to assume more independent function as recovery from the hemorrhage progresses over months (and even years). The first rule for family and any caregiver is to care for oneself. Burnout and physical and psychological problems are major risks in caring for persons with frontal systems impairments. Because executive functions permeate every activity, family should prioritize interventions, focusing first on behaviors that impact everyone's safety. Family may not be able to modify every problem behavior or correct every impairment.

Table 1 Interventions for patients with frontal systems impairment

External interventions	Internal interventions
Guiding principle	
Externalize impaired functions	Utilize the functional organization of the brain
Types of interventions	
1. Caregiver supervision and assistance	1. Medication
2. Daily structure	2. Relaxation skills
3. Behavior management	3. Emotional self-control
4. Environmental control	4. Inhibition of sensory overstimulation
5. Compensatory mechanisms	5. Cognitive rehabilitation

A critical external intervention is to establish daily structure and routines. These not only helps the brain organize activity through the day, but routines can run automatically without the need for conscious use of frontal systems and memory. The foundation for any daily structure is sleep. In addition to patterning day and night, sleep is the primary source for internal healing and building of restorative energy. Family members also need their restorative sleep. The plan is to start with a time to rise each day and work backward to an appropriate sleep onset time. The hours before should wind down activity in preparation for sleep, much as a child learns a sleep routine. A brief power nap in the day (typically an hour or less) can be helpful rejuvenation if it does not disturb the longer night sleep. Meals and small snacks should be scheduled about the same time of day. This serves as the skeleton for daytime structure. Other activities such as exercise, chores, cognitive stimulation, community activity, downtime, and social activity are then built around this skeleton. Activities should balance energy demands and minimize stress. Such structure creates a sense of timing, which is an essential mechanism for the brain to function. The regular structure across the day and week also eases the need for frequent conscious moment-to-moment decisions that lead to distraction and loss of mental set. The structure then creates predictability and enhances problems with memory.

Another set of external interventions involves behavior management. These are behavioral interventions to increase desirable activity (initiation, remembering, organization, etc.) or decrease undesirable behavior (emotional dyscontrol, impulsiveness, inappropriate verbalization, etc.) The most problematic behaviors are the primary targets for intervention. It is very helpful to have a neuropsychologist, rehabilitation psychologist, or some other specialist in brain injury to help with the process. The aim is to avoid endless control battles between the person and caregiver and to help the patient develop better self-control. As an example of a positive behavior intervention to go for a walk at 10 a.m., the caregiver might start with an early reminder before the time, second reminder to get on walking shoes or other needs, and then at the time physically walk the person out the door. In time, this might be faded to one pre-reminder and then "Time to go!" at 10 a.m. This could progress to the patient having their own reminder system on a smart phone or computer calendar and waiting for the patient in another room. For reducing anger outbursts, the behavior plan might start with ceasing activity and walking away from the person. Then it might progress to incorporating a positive coping technique, such as a verbal or gestural cue to take a few relaxing breaths. Then perhaps progress to modeling the caregiver's own deep breath as a cue. The process of behavior management is very personalized and behavior focused and requires discovering and building on what works.

A third set of external interventions involves controlling the environment as feasible. Because the patient may not have the internal means of filtering environmental stimuli, there may need to be external control. Overstimulation by light, sound, or other sensory input or proximity to intense activity is a common trigger for anxiety, agitation, and behavioral problems. Understimulation can also be a problem if a patient is left alone without supervision and any graded activity. A sale at a large retail store may be enjoyable for a healthy adult hunting for good buys. For the patient with frontal brain impairment, the bright lighting, background noise, multitude of people, and inundation of visual products can be overwhelming. Monitor behavior in such situations. Persons with good insight need to learn to self-regulate environmental interaction with their capability to filter these sensory triggers.

For persons who have some awareness of deficits, a fourth set of external interventions involves the use of compensatory mechanisms. These can include calendars, lists, reminder systems, organizational notebooks, and other such devices. Current technology offers a host of programs and apps that might be useful. The guiding principle is to make any compensatory mechanism simple, straightforward in use, and personalized to the individual's needs. Even if one remembers an appointment, having it written in some way enhances encoding at the outset and serves as a backup if memory does fail. The external organization continues to facilitate the brain's internal organization. Reliance on such aids makes life easier, freeing energy for the tougher cognitive tasks. Reading larger print material, for instance, despite good vision frees up more brain energy for processing the content and enhancing memory.

Internal interventions include medication to help with symptom management and challenging the brain to function better. Medication will rarely alleviate impairments but can support better function. For medication, psychostimulants should be used cautiously in patients who are vegetative or under aroused. These typically activate the brain in a generalized fashion, which may be too much. Short-acting Ritalin (methylphenidate) could provide a trial for efficacy. There is a concern about the effect of stimulants on blood pressure, which is typically carefully controlled after a brain hemorrhage. The major frontal brain circuits all interact between frontal lobes and basal ganglia structures. As such, dopaminergic medication (e.g., amantadine or bromocriptine) can have an activating effect to enhance frontal brain systems. A trial with a short-acting agent can verify efficacy in a specific patient. BuSpar (buspirone) is a preferred anxiolytic because long-term use of benzodiazepines has the risk of dependence and adverse effects on physical balance and memory. The most common class of medications for mood and behavioral stability are the antidepressants. Mood stabilizers (anticonvulsants) can also help with more severe emotional and

behavioral control. One may already be taken for seizure control post hemorrhage. Novel antipsychotics (e.g., quetiapine and risperidone) can also be used to help with sleep, and some have a potential benefit on frontal brain cognition. Sleep agents may be necessary when structure and good sleep hygiene are insufficient. Psychiatrists are all aware of these classes of medications, but many may not be as knowledgeable about neurobehavior. Neuropsychologists may provide some guidance, but outside of a few states, psychologists cannot prescribe medication.

A guiding principle for neuropsychological treatment is the inherent functional organization of the brain (e.g., Luria [3]). Rehabilitation and any restoration of function move from the basic functions upward to the more complex. At the base are essential self-regulation functions woven into hormone production and control with the autonomic nervous system. Further upward is neurotransmitter production and control of arousal and emotions. Sensory reconstruction within the brain and integration across sensory domains take place in the posterior cortex and connections. The speech, motor, and thinking in frontal areas then generate responses to that stimulation. Thus, effective intervention starts with control of autonomic stress and emotional reactions, progresses to control of sensory input to the level one can process information effectively, and then builds frontal brain skills to expand cognitive capability.

To advance the patient beyond the need for external control via caregivers or environmental regulation, he or she is taught ways to breathe to regain self-control. Other relaxation methods can build the skill at calming and self-soothing. These methods serve as a means of emotional control as well. As the patient has insight and self-awareness, psychotherapy can be helpful to address depression, anger, and other emotional disorders with cognitive-behavioral techniques. For persons with less self-insight, techniques can train specific behavior responses or focus on management of triggers for emotional outbursts.

To deal with sensory overload, one treatment principle is guided inhibition. This involves gradual exposure to a sensory input that creates overstimulation and pairs it with relaxation, self-soothing, or self-talk until the level of stimulation is mastered. The exposure method helps rebuild lost neurological inhibition and sensory filtering. This is most effective when the overloading stimuli are limited in number or domain. For most patients, this becomes an additional tool along with external environmental control.

Frontal systems themselves can benefit from formal cognitive rehabilitation. This is often done in structured rehabilitation programs, by neuropsychologists that do treatment or speech or occupational therapists trained to work with persons with brain injuries. Evidence-based guidelines exist [4–6]. Sohlberg and Turkstra [7] provide a comprehensive method to address frontal brain and related impairments. Targets for intervention typically involve building speed and accuracy of response; improving the ability to initiate, sustain, and shift mental set; increasing attention capacity; enhancing visual attention in space; improving learning and retention skills; and challenging the brain with graded complexity of thinking and problem-solving. Some rehabilitation programs also focus on social cognition, building accurate self-awareness, and developing mindful self-control.

In summary, patients suffering subarachnoid hemorrhage and stroke that affect frontal systems thinking often have persistent cognitive and behavioral problems that challenge themselves and their families. Following a comprehensive assessment to identify the profile of impairment, treating neuropsychologists or rehabilitation psychologists can guide patients and families on effective means to maximize the patient's recovery of function and degree of self-control.

Conflict of Interest The author declares that there is no conflict of interest.

References

1. Nomura M, Mori K, Tamase A, Kamide T, Seki S, Iida Y, Nakano T, Kawabata Y, Kitabatake T, Nakajima T, Yasutake K, Egami K, Takahashi T, Takahashi M, Yanagimoto K. Pseudoaneurysm formation due to rupture of intracranial aneurysms: case series and literature review. Neuroradiol J. 2017;30:129–37. https://doi.org/10.1177/1971400916684667.
2. Tekin S, Cummings JL. Frontal-subcortical neuronal circuits and clinical neuropsychiatry: an update. J Psychosom Res. 2002;53:647–54.
3. Luria AR. The working brain: an introduction to neuropsychology. New York: Basic Books; 1973.
4. Cicerone KD, Dahlberg C, Kalmar K, Langenbahn DM, Malec JF, Berquist TF, Felicetti T, Giacino JT, Harley JP, Harrington DE, Herzog J, Kneipp S, Laatsch L, Morse PA. Evidence-based cognitive rehabilitation: recommendations for clinical practice. Arch Phys Med Rehabil. 2000;81:1596–615. https://doi.org/10.1053/apmr.2000.19240.
5. Cicerone KD, Dahlberg C, Malec JF, Langenbahn DM, Felicetti T, Kneipp S, Ellmo W, Kalmar K, Giacino JT, Harley JP, Laatsch L, Morse PA, Cantanese J. Evidence-based cognitive rehabilitation: updated review of the literature from 1998 through 2002. Arch Phys Med Rehabil. 2005;86:1681–92. https://doi.org/10.1016/j.apmr.2005.03.024.
6. Cicerone KD, Langenbahn DM, Braden C, Malec JF, Kalmar K, Fraas M, Felicetti T, Laatsch L, Harley JP, Berquist T, Azulay J, Cantor J, Ashman T. Evidence-based cognitive rehabilitation: updated review of the literature from 2003 through 2008. Arch Phys Med Rehabil. 2011;86:1681–92. https://doi.org/10.1016/j.apmr.2010.11.015.
7. Sohlberg MM, Turkstra LS. Optimizing cognitive rehabilitation: effective instructional methods. New York: Guilford Press; 2011.

Intra-arterial Administration of Verapamil for the Prevention and Treatment of Cerebral Angiospasm

K. G. Mikeladze, D. N. Okishev, O. B. Belousova, A. N. Konovalov, Yu. V. Pilipenko, I. S. Ageev, A. N. Kaftanov, O. D. Shekhtman, N. V. Kurdyumova, T. F. Tabasaransky, E. A. Okisheva, S. S. Eliava, and S. B. Yakovlev

Abstract From 2013 to 2017, at the Burdenko Institute of Neurosurgery, intra-arterial verapamil for treatment of cerebral vasospasm following intracranial hemorrhage after aneurysm rupture was administered to 35 patients (total 75 procedures). The age is from 8 to 77 years. All ruptured aneurysms were treated: in 26 cases with open approach—clipping—and in 9 cases with endovascular occlusion. The procedure was carried out from 0 to 11 days after the operation. Severity of spasm was assessed by angiography and TCDU. Efficacy of the administration was assessed by TCDU 1 h after the procedure and by clinical evaluation of the patient's condition. The dose of verapamil was 15–50 mg (on average 40 mg) per procedure/per carotid pool and depended on the data of TCDU and clinical and radiological picture. The procedure was performed repeatedly (1–5 times) according to the indications and depending on the patient's condition, with an interval of 24 h. The procedure was effective as a preventive measure for care of patients in the initial stage of cerebral ischemia and was ineffective with a formed focus of ischemia. Endovascular administration of verapamil for treatment of cerebral vasospasm is a safe technique which positively affects the overall recovery of such patients.

Keywords Intracranial aneurysm · Cerebral angiospasm Verapamil · Subarachnoid hemorrhage · Intra-arterial administration of verapamil

Introduction

One of the main complications after subarachnoid hemorrhage is a spasm of the cerebral vessels with subsequent delayed secondary ischemia of brain tissue, which significantly worsens the clinical outcome [1]. A large number of treatment options were introduced for this complication, but none of them has been very successful [2, 3]. Hence, the search for an effective method for the prevention and treatment of angiospasm still continues. In a number of clinics, intra-arterial administration of vasodilator drugs, in particular verapamil (IAV), has shown some promising results. It should be noted that there is no single protocol describing the exact time of initiation of therapy, frequency of administration, exact dosing, and other features of the procedure. However, the presence of sufficiently large series of patients for whom the positive effect of intra-arterial administration of vasodilators has been shown enabled this method to be included in the latest guidelines for the treatment of patients after SAH (class IIa, level of evidence B) [2]. In this article a retrospective series of 35 patients was analyzed, in which IAV was used.

Materials and Methods

During the past 6 years (2012–2017) at the Acad. N.N. Burdenko Institute of Neurosurgery, this method (IAV) has been implemented. This paper is a retrospective analysis of the results of treatment of 35 patients who underwent one or several procedures of IAV into cerebral vessels. The criteria for inclusion into analysis were the first (or only) IAV procedure within 2 weeks after the last SAH, total dose of verapamil per procedure ≥15 mg, and follow-up—not less than 3 months after discharge. Verapamil was intra-arterially administered at the concentration of 0.25 mg/mL at an average rate of 10 mL per minute. The dosage was selected empirically and depended on the severity of vasospasm. The drug was administered in a manual mode, based on hemodynamics and in some cases on intracranial pressure monitoring data. The condition of patients before the verapamil injection was analyzed according to the Hunt-Hess score at

K. G. Mikeladze (✉) · D. N. Okishev · O. B. Belousova
A. N. Konovalov · Y. V. Pilipenko · I. S. Ageev · A. N. Kaftanov
O. D. Shekhtman · N. V. Kurdyumova · T. F. Tabasaransky
E. A. Okisheva · S. S. Eliava · S. B. Yakovlev
Burdenko Institute of Neurosurgery, Moscow, Russia

R. D. Martin et al. (eds.), *Subarachnoid Hemorrhage*, Acta Neurochirurgica Supplement 127,
https://doi.org/10.1007/978-3-030-04615-6_28,

the time of admission, the severity of hemorrhage by Fisher's scale, the time (day) of the operation after SAH, the presence and nature of ischemic foci on CT, the patient's state according to the modified Rankin scale, the fact of the deterioration of the clinical state at the time of the procedure, and some other parameters. The following data concerning the IAV procedure were recorded: the day of the first procedure after SAH, the amount and doses administered, transcranial Doppler ultrasound (TCDU) data in dynamics, angiographic data in dynamics, and parameters of hemodynamics during treatment. "Angiographic spasm" of the vessel was calculated in percentage relative to the standard average size for the internal carotid artery on both sides, 4 mm; for the middle cerebral artery on both sides, 3.2 mm; for the larger anterior cerebral artery, 2.6 mm; and for the main artery, 3 mm [4, 5]. In accordance, mild (0–30%), moderate (30–60%), and severe (more than 60%) angiographic spasms were differentiated [6]. The outcomes of the treatment were evaluated based on the presence of new foci of ischemia after the completion of IAV. The patient's status was analyzed according to the modified Rankin scale at the time of discharge and more than 3 months after discharge.

Results

The average age in the analyzed group of 35 people was 46.7 ± 14.5 years (from 8 to 77 years), and gender was 13 males and 22 females. In 26 cases surgery was performed and—in 9 cases—endovascular intervention. All the patients analyzed in this study had an "angiographic spasm." The overwhelming majority, these were severe cases—77.2% of patients, had III or higher grade of Hunt-Hess scale. A massive SAH, whose degree according to the Fischer scale was classified as 3–4, was observed in 90.6% of patients (see Table 1). Each patient was operated within the first 2 weeks. The median day of the operation was the fourth; all patients were operated at the earliest possible time. In 12 cases, primary decompression was performed during the surgical intervention, and in three cases, delayed decompression according to vital indications was done. In 14 patients, external ventricular drainage was used for the first few days after the operation. Ischemic foci before the IAV were observed in eight patients; in seven of those patients, the foci were secondary to the developed angiospasm (not associated with intraoperative damage of any artery). Three patients had ischemic foci due to complete obstruction or stenosis of an arterial branch during surgery. Assessment of the clinical state of the patient by the time of the first IAV does not seem very informative, since most of the patients received some form of sedative therapy: 82.9% of patients were grade V of the modified Rankin scale. Nine patients were operated due to obvious clinical deterioration. The first IAV procedure was performed on different days within 2 weeks after SAH (on average 7.4 ± 3.2 days after SAH). The number of procedures ranged from one (minimum) to five (maximum). In some cases, if the condition improved after the first procedure, the next one was performed in 1 day or even later. The total dose of verapamil per course is—the average value—78.6 (15 to 220) mg and median 55 (32.5, 107.5) mg. In total, 75 IAV procedures were performed in all patients. The total dose of verapamil per procedure was 36.7 ± 9.7 (15 to 50) mg. In a number of cases, verapamil was administered only to the angiographically or clinically most spasmodic vascular bed, in other cases to all beds prophylactically. Administration to 1 bed was performed in 12 cases, to 2 in 48 cases, and to 3 in 15 cases. Quite often typical changes in hemodynamics in the form of lowering blood pressure and bradycardia were observed. The fall of systolic blood pressure by more than 11 mmHg and/or a decrease in heart rate by 5 beats per minute was observed in 43 cases (57.3%). A drop in the arterial blood pressure by more than 50 mmHg was observed in 8 cases (10.7%) and a decrease in heart rate by more than 20 beats/min in 8 cases (10.7%). Obviously, these reactions should be considered in view of the fact that many patients simultaneously received inotropic support. It should be noted that no complications directly related to hemodynamic fluctuations were observed. In eight cases, invasive ICP monitoring was performed. In one case, an uncontrolled rise in ICP was observed, requiring urgent decompressive craniotomy. In 20 cases an improvement in the neurological status was observed immediately after the IAV procedure. An analysis of angiographic spasm was possible for 30 patients, with moderate or pronounced narrowing of the lumen of the main vessels. The severity of spasm was evaluated at its worst state during the treatment period of the most affected vascular bed. Separately, the severity of spasm for MCI (M1 segment) was assessed. With repeated administration, the dynamics of angiographic spasm was evaluated in 16 cases. In 68.8% (11 cases), progression of spasm was noted, and only in 12.5% of cases (2 patients), its regression was noted as a result of procedures. At that in one of these two patients, the IAV course was started on day 10 and in the other on day 13; hence, the regress of spasm could

Table 1 Distribution of patients upon admission according to the clinical status per Hunt-Hess scale and the degree of hemorrhage per Fisher scale

Hunt-Hess			Fisher		
I	1	2.8%	II	3	9.4%
II	7	20%			
III	16	45.7%	III	8	25%
IV	8	22.9%	IV	21	65.6%
V	3	8.6%	No data	3	

Table 2 Immediate and long-term outcomes of treatment according to the modified Rankin scale

Modified Rankin scale	Short-term follow-up patients %			Long-term follow-up patients %		
1	1	2.9%		9	25.7%	74.3%
2	2	5.7%		8	229%	
3	7	20%	28.6%	9	25.7%	
4	14	40%	71.4%	2	5.7%	25.7%
5	7	20%		3	8.6%	
6	4	11.4%		4	11.4%	

be attributed to the natural course of the disease. In six cases, an angiographic control of the effectiveness of the IAV procedure was performed 30 min after the administration; in all the cases, an increase in the diameter of the vessels was recorded to varying degrees. The effect of enlarging the lumen of the vessels was more pronounced for the most spasmodic areas. TC USDG after the procedure (approximately an hour later) showed the decrease in LCA for CMA by 20–40% (on average by 27%) in all cases, with the difference disappearing the next day. Angiographic spasm of the peripheral bed was observed in 21 patients (70%). Treatment outcomes were analyzed for all 35 patients (see Table 2). At the time of discharge, only 28.6% (10 people) had favorable outcomes. In the long term (after the third month of observation), most patients were compensated, and favorable outcomes were noted in 74.3% of cases. New ischemic foci (delayed ischemia) after starting the IAV course occurred in 12 cases (34.3%). Of the four patients who died, only one died due to the progression of angiospasm, while the IAV course for him was started only after the appearance of an ischemic focus due to the progression of angiospasm. Causes of death of three other patients were postoperative ischemic changes, exacerbation of severe somatic pathology, and sepsis followed by detection of pathogens on the central catheter. When comparing outcomes with different parameters, a number of clinically relevant facts were identified. There was no correlation between the immediate and distant outcomes with the severity of the condition on the Hunt-Hess scale upon admission. It should be noted that none of the three patients with the Hunt-Hess score "5" die. Out of ten patients with a Hunt-Hess score of 4–5, in the long-term period, only two patients had adverse outcomes (mRs 4–6). Eight patients underwent the IAV after the appearance of secondary ischemic foci as a consequence of angiospasm. These were quite severe patients in the nearest postoperative period; the mRs score for each of them was at least 4, with the significant difference from the rest of the group ($p = 0.09$). In the long-term period, three of them were restored to grade III of mRs; nonetheless the outcomes in this group were significantly worse than in patients without secondary ischemia before IAV ($p < 0.05$). In six of these eight patients subsequently, occurrence of new secondary ischemic foci or expansion of the ischemic zone was observed, which also significantly distinguishes this group of patients from other patients ($p = 0.01$). Of the nine patients whose IAV was initiated due to the clinical worsening, only one patient had a satisfactory outcome (mRs 3). In this group of patients, there was also a significant difference in the immediate outcomes with respect to other patients ($p < 0.05$). Also, in four of these patients, secondary ischemic foci appeared after the procedure. In assessing the correlation of outcomes with angiographic data (angiographic spasm), a significantly worse outcome—by more than 70% ($p = 0.02$)—was observed in the nearest future in case of spasm of at least one vascular bed. All other attempts to detect a correlation have not yielded meaningful results. The progression of spasm in repeated angiography (11 patients) was not accompanied by a worse clinical outcome or a greater probability of secondary ischemia. We will only note here that among 8 patients with a moderate spasm only 1 had a secondary ischemic focus, while among 22 patients with a marked angiographic spasm, secondary foci appeared in 9 patients. Of the 20 cases in which we observed angiographic spasm of peripheral vessels, nine patients developed secondary ischemic foci after the initiation of the IAV course. Among patients without angiographic spasm of peripheral vessels, secondary ischemia did not occur in any case.

Discussion

The search for an effective method of treating angiospasm is one of the pressing problems medical science has yet to solve. To date, no conservative measures have been proposed that significantly affect the development and course of vascular spasm after SAH [2]. One of the effective methods of treating a local spasm is balloon angioplasty. However, this technique allows to eliminate only local spasms of large enough vessels and is ineffective in case of spasm of distal vessels and has a rather high percentage of complications—up to 7% [6–8]. Intra-arterial administration of drugs can provide an instantaneous maximum concentration of the drug in the area suffering from an arterial spasm, and in this connection, a number of studies assess the possibility of this particular method of treatment. For intra-arterial administration, various drugs have been used in various studies: papaverine, nimodipine, nicardipine, verapamil, milrinone, fasudil, and colforsin daropate [9]. The availability of verapamil, its low price, and its encouraging results of a number of studies with the minimum number of complications, all these factors led us to use this drug. Verapamil is an antiarrhythmic drug of class IV according to the Vaughan-Williams classification from the group of diphenylalkylamines. Verapamil also

reduces the tone of the smooth muscles of the coronary and peripheral arteries, as well as the general peripheral vascular resistance, and is the drug of choice for the treatment of vasospastic angina. Half-life with intravenous injection biphasic: early—about 4 min, terminal—2–5 h. After IV introduction, antiarrhythmic effect develops within 1–5 min and hemodynamic effects (vasodilation, decrease in blood pressure) within 3–5 min and maintained for 10–20 min [10, 11]]. Little is known about the dynamic and kinetic features after the intra-arterial administration. In animal experiments it has been shown that the effect of vasodilation occurs in 30 min [12, 13]. Due to temporary effect of vascular dilatation, a number of authors explain the positive effect after the administration of verapamil in SAH by its greater tropicity to resistive arterioles (prearterioles) [13, 14]. The intra-arterial administration of verapamil for the treatment of angiospasm was first used in cardiology for the treatment of coronary artery spasm in 1988 [15]. Later, cases of intracoronary administration of verapamil in patients with acute coronary syndrome were described, leading to a statistically significant improvement in coronary blood flow [16]. For the first time, the effect of the intra-arterial administration of verapamil on the cerebral blood flow was described by Joshi and co-authors in 1997 [17]. The first series of 29 patients who received the IAV course for cerebral angiospasm was published by Feng in 2002 [18]. Later five more original articles describing similar series of patients were published. In each of these studies, the authors spontaneously chose the dose of verapamil used. The recommended dose for intravenous administration is 5–10 mg [10]. In published studies on intra-arterial administration of verapamil, the dose varied from 3 to 360 mg per procedure for a different period of time. Depending on the effect of treatment and the severity of spasm, the authors would repeat the procedure multiple times; thus, according to Jun (2010), more than half of the patients underwent repeated injections [6]. Albanese and co-authors followed a different pathway, administering a solution of verapamil with heparin for many hours [19]. In the published works [20–22], the following evidence of the effectiveness of IAV for the prevention and treatment of spasm was presented: the dilatation of arteries (especially the most spasmodic) 20–30 min after IAV and the relatively good results of treatment of patients using IAV. We were unable to find any article containing discussion of comparable groups treated with and without IAV. After analyzing the available data from the literature, we came to the conclusion that verapamil bolus administration is safer at a dosage of up to 20 mg per carotid bed and up to 10 mg per vertebrobasilar bed. Due to the possibility of the thromboembolic complications from the prolonged administration of verapamil, it was decided to forgo it. Thus, the maximum dose of verapamil for the procedure in our cases was 50 mg. In the case of a moderate spasm, we adhered to smaller doses, especially at the initial stage. In all six cases of angiographic control, after 30 min, the dilatation of the arterial bed was recorded with a tendency to a greater effect on the spasmodic vessels, which is consistent with the results published in the literature. Reduction of the blood flow velocity according to the data of the TCDU was also recorded in all cases. However, both "angiographic" and "ultrasound" improvements in the vast majority of cases were not preserved the next day. Due to the obvious temporary effect of the procedure, we resorted to the repeated administration of verapamil in 60% of cases. To date, we believe that the daily IAV procedures are justified, which is at odds with the recommendations of Jun et al. [6] offering treatment every 3 days. We currently consider that the risks and technical difficulties during the IAV several times a day, as well as in the case of prolonged administration of the drug through a fixed catheter, exceed the possible benefits from such treatments. The series described by us included patients with rather severe conditions: grade III or more on the Hunt-Hess scale for 77.2% of patients and SAH 3–4 degrees on the Fisher scale in 90.6% of patients. In this regard, we believe that the results obtained (satisfactory outcomes in 28.6% of cases at discharge and in 74.3% of cases in the long-term period) indicate the effectiveness of the IAV technique. According to our data, the outcome of treatment is significantly influenced by the presence of secondary ischemic foci due to angiospasm prior to the initiation of intra-arterial administration of verapamil. This is due to both the irreversibility of brain necrosis in the field of ischemia and the limited "therapeutic power" of bolus intra-arterial administration of verapamil in the case of unfolded vasospasm. This also explains the worst results of treatment for patients who began intra-arterial treatment amid a worsening of the clinical condition. In this regard, in case of massive hemorrhage, we propose to perform the first intra-arterial administration of verapamil to all vascular beds already on day 3 or 4 after SAH to ensure a preventive effect. Subsequent administration, in case of a stable clinical status and in the absence of acceleration of blood flow according to USDG, is permissible every other day. The further scheme of treatment, dose, and catheterized vessels depend on the individual course of the disease. In the case of severe spasms, it is also acceptable to conduct IAV procedures daily. The duration of the IAV course can be up to 7–9 days. The change in the diameter of the main vessels by the time of repeated intra-arterial administration of verapamil is a conditional indicator of the effectiveness of treatment. The presence of spasm of peripheral vessels is often associated with an unfavorable outcome of the disease, which requires consideration of the possible expediency of super selective catheterization for the administration of verapamil. It should be noted that the presence of secondary ischemic foci is not a contraindication to IAV; endovasal treatment can stop the progression of the disease and favorably affect the penumbra zone. In our series, as in

the published literature, the minimal controlled effect of the intra-arterial administration of verapamil on systemic hemodynamics is shown. Cases of uncontrolled increase in intracranial pressure are rare; they are described in several publications [6, 19] and were also observed in our series. In this regard, with severe hemorrhages, we recommend IAV in conditions of external ventricular drainage or if a decompressive craniectomy was already performed.

Conclusion

The intra-arterial administration of verapamil to cerebral vessels is a simple and safe procedure. The effectiveness of this treatment, in our opinion, is obvious, but the degree of its effects is not the same for all patients. We recommend starting the IAV course as a preventive measure from 3 to 4 days after a massive hemorrhage. Further study and development of a protocol for the intra-arterial administration of verapamil—in view of the apparent infeasibility of conducting a randomized study—require comparison of large normalized retrospective series of patients with or without this treatment.

Conflict of Interest The authors declare that they have no conflict of interests.

References

1. Kassell NF, Torner JC, Haley EC, Jane JA, Adams HP. The International Cooperative Study on the Timing of Aneurysm Surgery. Part 1: Overall management results. J Neurosurg. 1990;73(1):18–36.
2. Connolly ES Jr, Rabinstein AA, Carhuapoma JR, Derdeyn CP, Dion J, Higashida RT, Hoh BL, Kirkness CJ, Naidech AM, Ogilvy CS, Patel AB, Thompson BG, Vespa P. Guidelines for the management of aneurysmal subarachnoid hemorrhage: a guideline for healthcare professionals from the American Heart Association/American Stroke Association. Stroke. 2012;43(6):1711–37.
3. Steiner T, Juvela S, Unterberg A. European Stroke Organization guidelines for the management of intracranial aneurysms and subarachnoid haemorrhage. Cerebrovasc Dis. 2013;35(2):93–112.
4. Muller HR, CHR B, Radü EW, Buser M. Sex and side differences of cerebral arterial caliber. Neuroradiology. 1991;33(3):212–6.
5. Smoker WRK, Price MJ, Keyes WD, Corbett JJ, Gentry LR. High-resolution computed tomography of the basilar artery: 1. Normal size and position. Am J Neuroradiol. 1986;7(1):55–60.
6. Jun P, Ko NU, English JD, Dowd CF, Halbach VV, Higashida RT, Lawton MT, Hetts SW. Endovascular treatment of medically refractory cerebral vasospasm following aneurysmal subarachnoid hemorrhage. Am J Neuroradiol. 2010;31(10):1911–6.
7. Eskridge JM, Song JK. A practical approach to the treatment of vasospasm. Am J Neuroradiol. 1997;18(9):1653–60.
8. Higashida RT, Halbach VV, Dowd CF, Dormandy B, Bell J, Hieshima GB. Intravascular balloon dilatation therapy for intracranial arterial vasospasm: patient selection, technique, and clinical results. Neurosurg Rev. 1992;15(2):89–95.
9. Sayama CM, Liu JK, Couldwell WT. Update on endovascular therapies for cerebral vasospasm induced by aneurysmal subarachnoid hemorrhage. Neurosurg Focus. 2006;21(3):E12.
10. Харкевич ДА. Фармакология - 10-е изд. Москва: ГЭОТАР-Медиа; 2010.
11. Dominic JA, Bourne DW, Tan TG, Kirsten EB, McAllister RG Jr. The pharmacology of verapamil. III. Pharmacokinetics in normal subjects after intravenous drug administration. J Cardiovasc Pharmacol. 1981;3(1):25–38.
12. Shimizu K, Ohta T, Toda N. Evidence for greater susceptibility of isolated dog cerebral arteries to Ca antagonists than peripheral arteries. Stroke. 1980;11(3):261–6.
13. Takayasu M, Bassett JE, Dacey RG Jr. Effects of calcium antagonists on intracerebral penetrating arterioles in rats. J Neurosurg. 1988;69(1):104–9.
14. Messing M, Essen H, van Smith TL, Smits JFM, Struyker-Boudierb HAJ. Microvascular actions of calcium channel antagonists. Eur J Pharmacol. 1991;198(2–3):189–95.
15. Babbitt DG, Perry JM, Forman MB. Intracoronary verapamil for reversal of refractory coronary vasospasm during percutaneous transluminal coronary angioplasty. J Am Coll Cardiol. 1988;12(5):1377–81.
16. Vijayalakshmi K, Whittaker VJ, Kunadian B, Graham J, Wright RA, Hall JA, Sutton A, de Belder MA. Prospective, randomised, controlled trial to study the effect of intracoronary injection of verapamil and adenosine on coronary blood flow during percutaneous coronary intervention in patients with acute coronary syndromes. Heart. 2006;92(9):1278–84.
17. Joshi S, Young WL, Pile-Spellman J, Duong DH, Hacein-Bey L, Vang MC, Marshall RS, Ostapkovich N, Jackson T. Manipulation of cerebrovascular resistance during internal carotid artery occlusion by intraarterial verapamil. Anesth Analg. 1997;85(4):753–9.
18. Feng L, Fitzsimmons B-F, Young WL, Berman MF, Lin E, Aagaard BDL, Duong H, Pile-Spellman J. Intraarterially administered verapamil as adjunct therapy for cerebral vasospasm: safety and 2-year experience. Am J Neuroradiol. 2002;23(8):1284–90.
19. Albanese E, Russo A, Quiroga M, Willis RN Jr, Mericle RA, Ulm AJ. Ultrahigh-dose intraarterial infusion of verapamil through an indwelling microcatheter for medically refractory severe vasospasm: initial experience. Clinical article. J Neurosurg. 2010;113(4):913–22.
20. Keuskamp J, Murali R, Chao KH. High-dose intraarterial verapamil in the treatment of cerebral vasospasm after aneurysmal subarachnoid hemorrhage. J Neurosurg. 2008;108(3):458–63.
21. Sehy JV, Holloway WE, Lin S-P, Cross DT, Derdeyn CP, Moran CJ. Improvement in angiographic cerebral vasospasm after intra-arterial verapamil administration. Am J Neuroradiol. 2010;31(10):1923–8.
22. Mazumdar A, Rivet DJ, Derdeyn CP, Cross DT, Moran CJ. Effect of intraarterial verapamil on the diameter of vasospastic intracranial arteries in patients with cerebral vasospasm. Neurosurg Focus. 2006;21(3):E15.

Cerebral Arterial Compliance in Polytraumazed Patients with Cerebral Vasospasm

Alex Trofimov, Michael Dobrzeniecki, and Denis E. Bragin

Abstract The purpose was to determine the status of the cerebral arterial compliance (cAC) in a concomitant head injury and cerebral vasospasm (CVS) with and without the development of intracranial hematomas (ICH). In Materials and Methods, we examined 80 polytrauma patients with severe TBI and CVS. During or immediately after dynamic helical computed tomography angiography (DHCTA), the monitoring of the transcranial Doppler of the MCA was recorded bilaterally with 2-MHz probes. The cerebral blood volumes were calculated from the DHCTA data with complex mathematical procedures using the "direct flow model" algorithm. In Results, CAC was significantly decreased ($p < 0.001$) in both the first and second group TBI and CVS (with or without ICH) in comparison with normal data ($p < 0.001$) and TBI without CVS. The cAC was significantly decreased on the side of the former hematoma with CVS than on the contralateral side with CVS ($p = 0.003$). In Conclusion, the cAC in TBI and CVS gets significantly lower as compared to the normal condition ($p < 0.001$). After removal of the ICH and development of CVS, the compliance in the perifocal zone remains much lower ($p = 0.003$) as compared to compliance of the other brain hemisphere.

Keywords Cerebral arterial compliance · Cerebral vasospasm · Intracranial hematomas · Traumatic brain injury

A. Trofimov (✉)
Department of Neurosurgery, Nizhny Novgorod State Medical Academy, Nizhny Novgorod, Russia

Department of Polytrauma, Regional Hospital Named After N.A. Semashko, Nizhny Novgorod, Russia

M. Dobrzeniecki
Department of Neurosurgery, Spine Surgery and Interventional Neuroradiology DONAUISAR Klinikum Deggendorf, Deggendorf, Germany

D. E. Bragin
Department of Neurosurgery, University of New Mexico School of Medicine, Albuquerque, NM, USA

Introduction

Cerebral vasospasm (CVS) after traumatic brain injury (TBI) may dramatically affect the neurological and functional recovery. Secondary insults in patients with TBI and CVS are greatly affected by changes in the compliance and stiffness of cerebral vessels. The walls of downstream vessels have no external elastic membrane; therefore, the cerebral capillary network becomes vulnerable to intracranial and intravascular pressure surges [1, 2].

One of the features characterizing flexibility of the vascular network and its resistance to the changes is cerebral arterial compliance (cAC) [3, 4].

The state of the cAC at TBI and CVS is of great importance for the brain microcirculation. Since the brain is located within an inextensible cranial cavity and is surrounded by an incompressible fluid [5], the compensation of intracranial pressure surges caused by the pulse wave passage through the brain blood vessels occurs also through the reciprocal changes in arterial lumens [2, 6, 7].

Thus, the higher is the cAC, the greater is the compliance of a vascular wall, and, respectively, the better is the capacity of a vessel to change its lumen (i.e., vasomotion phenomenon) and thereby to maintain the adequate capillary bed perfusion.

Information on the compliance and stiffness of the cerebral vascular bed in the damaged brain after CVS is currently rather inconsistent [4, 8], and the aspects of the cAC reaction to the intracranial hematoma (ICH) development and the disturbed cerebral blood flow (CBF) in the case of TBI and CVS are still under investigation [9].

The purpose of our work was to determine the status of the cerebral arterial compliance in a concomitant head injury and posttraumatic cerebral vasospasm with and without the development of intracranial hematomas.

R. D. Martin et al. (eds.), *Subarachnoid Hemorrhage*, Acta Neurochirurgica Supplement 127,
https://doi.org/10.1007/978-3-030-04615-6_29,

Materials and Methods

The study was approved by the Ethics Committee of the Nizhny Novgorod State Medical Academy and conformed to the standards of the Declaration of Helsinki. We examined 80 polytrauma patients with severe head injury and CVS who were treated at the Nizhny Novgorod Regional Trauma Center Level I in 2013–2015. The mean age of the patients with head injury was 35.5 ± 14.8 years (from 15 to 73 years, 38 women and 42 men). The criterion for the inclusion in the study was the CVS of the M1 and M2 segments of the middle cerebral artery revealed during the contrast-enhanced CT scanning of the brain.

All patients were divided into two groups. The first group included 41 polytraumazed patients with the CVS in the acute period head injury without the development of intracranial hematomas (ICH). The second included 39 polytraumazed patients with the developed CVS and the brain compression caused by epidural, subdural, or multiple hematomas (6, 29, and 4, respectively).

The average wakefulness level according to GCS (Glasgow Coma Score) was 9.7 ± 2.5 in the first group and 10.1 ± 2.5 in the second group. The severity of their state according to ISS (Injury Severity Score) was 34.3 ± 8.2 in the first group and 35.2 ± 9.3 in the second group. Clinical outcomes are summarized in Table 1.

Dynamic Helical Computed Tomography Angiography

All patients were subjected to dynamic helical computed tomography angiography (DHCTA) by 64-slice tomograph Philips Ingenuity CT (Philips Medical systems, Cleveland, USA). Tomography was performed 1–12 days after TBI (mean 4 ± 3 days) in the first group and 2–8 days (mean 4 ± 2 days) after surgical evacuation of the hematoma in the second group.

The perfusion examination report included an initial contrast-free CT of the brain. Extended scanning was further performed of 16 "areas of interest," 160 mm in thickness, within 60 s with a contrast agent ("Perfusion JOG" mode). The scanning parameters were 160 kVp, 160 mA, 70 mAs, 512 × 512. The contrast agent Ultravist 370 (Schering AG, Germany) was administered with an automatic syringe injector (Stellant, Medrad, Indianola, PA, USA) into a peripheral vein through a standard catheter (20 G) at a rate of 4–5 mL/s in a dose of 30–50 mL per one examination.

Table 1 Clinical outcome (Glasgow Outcome Score) of polytraumazed patients with CVS

	GOS 1 Good recovery	GOS 2 Moderate disability	GOS 3 Severe disability	GOS 4 Vegetative state	GOS 5 Death
Group 1	15	12	8	3	3
Group 2	16	9	8	3	3

After scanning, data were transferred to a PACS (JSC "KIR," Kazan, Russia) and a Philips Extended Brilliance Workspace workstation (Philips HealthCare Netherland B.V., Best, the Netherlands) and MATLAB 2013b (The MathWorks Inc., Natick, MA, USA). Artery and vein marks were automatically recorded, followed by the manual control of indices in the time-concentration diagram. The so-called region of interest (ROI) was established based on subcortical areas of middle cerebral artery.

The computed tomography angiography source image (CTASI) analysis enabled to visualize the main vessels of the brain and to assess the state of their lumen. In all patients the minimal intensive projection analysis identified the local luminal narrowing middle cerebral artery (MCA) more than 30% of the diameter as compared to adjacent sections of the same vascular segment; based thereon an "angiographic" CVS was diagnosed. Vasospasm according to its severity is usually classified into three grades: mild, the vessel still has 70% of luminal flow; moderate, more than 50% of reduction of the lumen; and severe, less than 30% of luminal flow on angiography.

Perfusion maps were derived from the tissue time-attenuation curve on the basis of the change in X-ray attenuation, which is linearly related to iodinated contrast concentration on aper-voxel basis with time. Errors introduced by delay and dispersion of the contrast bolus before arrival in the cerebral circulation were corrected by block-circulant deconvolution algorithm. Quantitative perfusion indices, including CBF, were calculated on a voxelwise basis and were used to generate color-coded maps. The voxels with CBF >100 mL/100 g/min or CBV >8 mL/100 g were assumed to contain vessels and removed from the ROI.

During or immediately after DHCTA, the transcranial Doppler (TCD) of the MCA was recorded bilaterally with 2-MHz probes within 10 min (Sonomed 300 M, Spectromed, Russia). Amplitude of arterial blood pressure (ABPamp) and ECG-gated duration of the systole (Tsys) and the diastole (Tdia) were measured noninvasively (IntelliView MP5, Philips Medizin Systeme, Germany). A complex of the neuromonitoring "Centaurus" was used during the study (Ver. 2.0, Nizhny Novgorod State Medical Academy, Russia).

The system view is shown in Fig. 1.

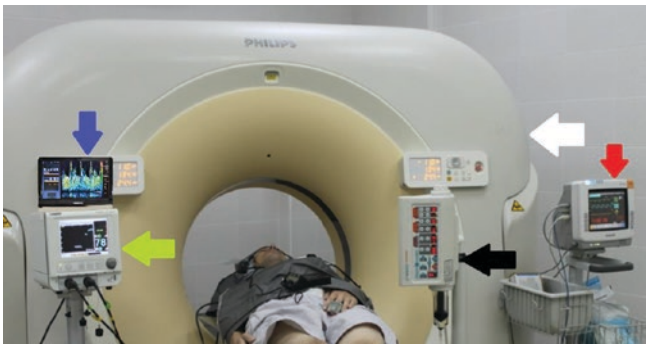

Fig. 1 The investigation system view. White arrow indicates a computer tomograph, blue arrow shows a TCD, red arrow shows ECG-ABP monitor, black arrow marks a syringe injector, and green arrow indicates cerebral oximeter

Statistical Analysis

CBF and cerebral blood volume (CBV) were calculated from DHCTA data by the "direct flow model" algorithm [10]. The systolic–diastolic values of the MCA diameters (Dsys and Ddia) were determined in DHCTA series in the proximal part of the M1 of both MCA. Amplitude of regional CBV oscillation (ΔCBV) was calculated as the difference between CBVs, which flowed through the MCA in systole (CBVsys) and diastole (CBVdia). We used Eqs. (1, 2, and 3) proposed by de Jong, Alexandrov, and Avezaat [11–13].

$$\Delta\mathrm{CBV} = \mathrm{CBVsys} - \mathrm{CBVdia} \tag{1}$$

$$\Delta\mathrm{CBV} = \frac{\pi}{4} \times \mathrm{Dsys}^2 \times \mathrm{CBFVsys} \times \mathrm{Tsys} - \frac{\pi}{4} \times \mathrm{Ddia}^2 \times \mathrm{CBFVdia} \times \mathrm{Tdia} \tag{2}$$

$$\mathrm{cAC} = \Delta\mathrm{CBV} \div \mathrm{ABPamp} \tag{3}$$

Reference range cAC was chosen according Ikdip K. as 0.105 ± 0.043 cm^3/mmHg [14].

The *t*-test for dependent samples was utilized to analyze differences in means of parameters between the ipsilateral and contralateral sides of the temporal lobes. Statistica 7.0 software (StatSoft Inc., USA) was used for the analysis. Data are presented as Mean ± SEM. Significance level was preset to $p < 0.05$.

Results

In the first group, the "angiographic" CVS was unilateral in 30 cases and bilateral in 11 cases, and in three cases it extended to segments of the anterior cerebral artery. In 15 cases the CVS was mild, in 21 cases it was moderate, and in 5 cases it was severe. The "angiographic" CVS coincided with the "dopplerographic" CVS in all patients with the severe CVS and in five patients with the moderate CVS. In the second group in 28 cases, the "angiographic" CVS was revealed on the side of the removed hematoma. In ten cases it was developed on the side opposite to the removed ICH, and in one case it was bilateral and included in addition to M1-2 also segments A1-2. In 13 cases the CVS was mild, in 16 cases it was moderate, and in 10 cases it was severe. The "angiographic" CVS coincided with the "dopplerographic" CVS in nine patients with the severe and moderate CVS.

Mean values of cAC were significantly decreased ($p < 0.001$) in both the first and second group of with TBI and CVS (with or without ICH) comparing to reference data ($p < 0.001$) and TBI without CVS.

The cAC was significantly decreased on the side of the former hematoma with CVS than on the contralateral side with CVS ($p = 0.003$). The acquired and analyzed data are summarized in Table 2.

Discussion

It has been proven that the constriction of cerebral arteries developing after traumatic subarachnoid hemorrhage (SAH) may result in reduction in CBF more distal than the spastic segment and depending on the state of the autoregulation may lead to brain ischemia and cerebral infarction [15, 16]. However, there are contradictory data on CVS as the cause of cerebral ischemia development after SAH. According to some reports, only in 20–30% of patients with the "angiographic" CVS some cerebral ischemia symptoms would develop [17]. Furthermore, the localization of the secondary ischemia in almost 25% of cases does not coincide with the territory of the spastic artery [10, 17, 18].

However, other researchers have reported high correlation between the "angiographic" CVS and secondary ischemia development. According to R. Crowley, only 3% of cerebral ischemia cases with SAH are either not followed by vasospasm, or it may be referred to a mild one [19].

Despite the fact that foregoing data mainly describe the dynamics of aneurysmal subarachnoid hemorrhages, they quite fully reflect total variety of cerebral microvascular reactions aimed at maintaining the adequate perfusion with available CVS, including a posttraumatic CVS [20–22].

It has been previously shown that cerebral microcirculation undergoes significant changes (especially in the compression of the brain by ICH), which remain even after hematoma's removal [23].

Table 2 Comparison of the analyzed parameters

		CBF (mL/100 g/min)	ABPamp (mmHg)	ΔCBV (cm^3)	CAC (cm^3/mmHg)
1	Group 1	33.1 ± 12.4	56.5 ± 15.6	2.3 ± 0.7	0.034 ± 0.029
2	Group 2 (ipsilateral sides with CVS)	28.3 ± 15.9	60.4 ± 21.6	2.1 ± 1.1	0.024 ± 0.027
3	Group 2 (ipsilateral sides without CVS)	37.4 ± 20.4	55.7 ± 29.2	2.4 ± 1.2	0.055 ± 0.049
4	Group 2 (contralateral sides with CVS)	29.6 ± 9.8	57.9 ± 17.9	2.2 ± 0.9	0.037 ± 0.029
	P (1–2)	0.183	0.563	0.510	0.097
	P (1–3)	0.312	0.892	0.764	0.172
	P (1–4)	0.215	0.892	0.351	0.34
	P (2–4)	0.695	0.616	0.282	0.003[a]

CVS cerebral vasospasm, *CBF* cerebral blood flow, *ABPamp* amplitude of arterial blood pressure, *ΔCBV* amplitude of regional cerebral blood volume oscillation, *cAC* cerebral arterial compliance

[a]Significant difference ($p < 0.01$)

At the same time, it is known that enveloped hematoma and the concomitant injury are factors that provoke posttraumatic CVS development [3, 4, 24].

Thus, the study of the cerebral arterial compliance state during the CVS formation in the acute period of head injury is obviously important for its prevention and timely diagnosis [25].

This study has shown that with developing CVS in the acute period (on the 2nd–third day after the accident) of a concomitant craniocerebral injury, the cAC significantly decreases as compared to the "normal" (reference) data.

One of the common causes of decreasing cAC is the development of a cytotoxic and vasogenic cerebral edema causing the compression of pial vessels [5, 26].

The indirect proof for this hypothesis is the identification of CT signs of cerebral edema in all 80 patients. However, as we have not carried out the blood-brain barrier breakdown study, we could not distinguish zones of ischemic injury and vasogenic edema.

Because of this limitation in our study, we have not been able to investigate the correlation between the change in cAC, the CVS development, and the secondary ischemia.

Another reason for the decreasing cAC may be a regional microvascular CVS due to the formation of a large amount of blood degradation products fallen into the subarachnoid cisterns. This effect is realized through the auto-oxidation of hemoglobin to methemoglobin with release of iron ions, which in turn cause the formation of superoxide radicals. Superoxide is supposed to cause change in the nitric oxide concentration and peroxide damage to the endothelium of pial vessels, thus causing the microvascular CVS development [27–29].

We have not used laser Doppler flowmetry (another limitation of the work); therefore, we could not directly examine the state of microvessels. However, taking into account that the "dopplerographic" CVS have coincided with the "angiographic" CVS in the most severe patients of the both groups, we assume that in this forth part of the patients (24% in first group, 23% in second group), the symptomatic character of a spasm took place, which was typical for its microvascular CVS [30].

Another possible reason for microvascular bed compression may be astrocytic endfeet swelling. Such swelling evolving in the first hours after injury may persist for a week thereafter [31, 32].

Finally, the compression of pial vessels both in a brain injury and in a vasospasm is associated with the dysfunction of pericytes—cells located in the basal pericapillary membrane. It was shown that the narrowing of arterioles and capillaries occurs because of the disturbance in the expression of endothelin-1 and pericytial receptors, types A and B, as well as the migration of over 40% of pericytes from the basal membrane [33–36].

All these factors as it has been shown above may result in the reduction of the total capillary bed lumen and accordingly to the decrease of cAC [37, 38]. It should be noted that the CVS formation after elimination of the brain compression by enveloped ICH changes even more the cAC value [39, 40].

It results in the sudden reduction of the number of functioning capillaries and in the decreasing cAC on the side of the vascular spasm and compression [4, 8]. The findings of our investigation may have the practical significance for optimizing the selection of individual regimens for brain edema therapy and vascular treatment with CVS available, which would prevent the development of cerebral perfusion disorders in patients with concomitant craniocerebral injury. Further studies are required to delineate the role of cAC in CVS.

Conclusion

The peripheral resistance of brain vessels in the cerebral vasospasm development in the acute period of a concomitant craniocerebral injury significantly increases as compared to

the norm. The CVS formation in the perifocal zone after the removal of an enveloped hematoma is followed by a significant decrease of the cAC as compared to the symmetric area of the opposite hemisphere.

Acknowledgments D.B. was supported by NIH P20GM109089, DOD DM160142 and RSF No. 17-15-01263.

Conflict of Interest: **We declare that we have no conflicts of interest.**

References

1. Loret JE, Zemmoura I, Daumas-Duport B, Buffenoir K, Paulus J. Delayed post traumatic vasospasm leading to ischemia in a patient with mild traumatic brain injury. J Neurol Disord Stroke. 2013;1(2):10–4.
2. Pluta RM, Hansen-Schwartz J, Dreier J. Cerebral vasospasm following subarachnoid hemorrhage: time for a new world of thought. Neurol Res. 2009;31(2):151–8.
3. Oertel M, Boscardin WJ, Obrist WD, Glenn TC, McArthur DL, Gravori T. Posttraumatic vasospasm: the epidemiology, severity, and time course of an underestimated phenomenon: a prospective study performed in 299 patients. J Neurosurg. 2005;103:812–24.
4. Shahlaie K, Keachie K, Hutchins IM, Rudisill N, Madden LK, Smith KA. Risk factors for posttraumatic vasospasm. J Neurosurg. 2011;115:602–11.
5. Cernak I, Vink R, Zapple D. The pathobiology of moderate diffuse traumatic brain injury as identified using a new experimental model of injury in rats. Neurobiol Dis. 2004;17:29–43. https://doi.org/10.1016/j.nbd.2004.05.011.
6. Herz DA, Baez S, Shulman K. Pial microcirculation in subarachnoid hemorrhage. Stroke. 1975;6:417–24.
7. Ohkuma H, Itoh K, Shibata S. Morphological changes of intraparenchymal arterioles after experimental subarachnoid hemorrhage in dogs. Neurosurgery. 1997;41:230–5.
8. Yundt KD, Grubb RL Jr, Diringer MN. Autoregulatory vasodilation of parenchymal vessels is impaired during cerebral vasospasm. J Cereb Blood Flow Metab. 1998;18:419–24.
9. Hart MN. Morphometry of brain parenchymal vessels following subarachnoid hemorrhage. Stroke. 1980;11:653–35.
10. Brown RJ, Kumar A, Ilodigwe D. The relationship between delayed infarcts and angiographic vasospasm after aneurysmal subarachnoid hemorrhage. Neurosurgery. 2013;72:702–8.
11. Alexandrov AV. Neurovascular examination: the rapid evaluation of stroke patients using ultrasound waveform interpretation. Oxford: Blackwell Publishing Ltd; 2013.
12. Avezaat CJJ. Cerebrospinal fluid pulse pressure and craniospatial dynamics. A theoretical, clinical and experimental study. Rotterdam: Erasmus University; 1984.
13. de Jong S. Quantifying cerebral blood flow of both the micro- and macrovascular system using perfusion computed tomography. Twente: The Netherlands; 2015.
14. Ikdip K. Exploring differences in vascular aging and cerebrovascular hemodynamics between older adults of White Caucasian and South Asian origin. Waterloo: Ontario; 2014.
15. Fitch W, Ferguson GG, Sengupta D. Autoregulation of cerebral blood flow during controlled hypotension in baboons. J Neurol Neurosurg Psychiatry. 1976;39:1014–22.
16. Rasmussen G, Hauerberg J, Waldemar G. Cerebral blood flow autoregulation in experimental subarachnoid haemorrhage in rat. Acta Neurochir. 1992;119:128–33.
17. Hattingen E, Blasel S, Dettmann E. Perfusion-weighted MRI to evaluate cerebral autoregulation in aneurysmal subarachnoid haemorrhage. Neuroradiology. 2008;50:929–38.
18. Weidauer S, Lanfermann H, Raabe A. Impairment of cerebral perfusion and infarct patterns attributable to vasospasm after aneurysmal subarachnoid hemorrhage: a prospective MRI and DSA study. Stroke. 2007;38:1831–6.
19. Crowley RW, Medel R, Dumont AS. Angiographic vasospasm is strongly correlated with cerebral infarction after subarachnoid hemorrhage. Stroke. 2011;42:919–23.
20. Martin NA, Doberstein C, Zane C, Caron MJ, Thomas K, Becker DP. Posttraumatic cerebral arterial spasm: transcranial Doppler ultrasound, cerebral blood flow, and angiographic findings. J Neurosurg. 1992;77:575–83.
21. Weber M, Grolimund P, Seiler RW. Evaluation of posttraumatic cerebral blood flow velocities by transcranial Doppler ultrasonography. Neurosurgery. 1990;27:106–12.
22. Westermaier T, Pham M, Stetter C. Value of transcranial Doppler, perfusion-CT and neurological evaluation to forecast secondary ischemia after aneurysmal SAH. Neurocrit Care. 2014;20(3):406–12. https://doi.org/10.1007/s12028-013-9896-0.
23. Furuya Y, Hlatky R, Valadka A. Comparison of cerebral blood flow in computed tomographic hypodense areas of the brain in head-injured patients. Neurosurgery. 2003;52:340–6. https://doi.org/10.1227/01.neu.0000043931.83041.aa.
24. Zubkov AY, Lewis AI, Raila FA, Zhang J, Parent AD. Risk factors for the development of post-traumatic cerebral vasospasm. Surg Neurol. 2000;53:126–30.
25. Marmarou A. A review of progress in understanding the pathophysiology and treatment of brain edema. Neurosurg Focus. 2007;22(5):E1. https://doi.org/10.3171/foc.2007.22.5.2.
26. Glushakova OY, Johnson D, Hayes RL. Delayed increases in microvascular pathology after experimental traumatic brain injury are associated with prolonged inflammation, blood-brain barrier disruption, and progressive white matter damage. J Neurotrauma. 2014;31:1180–93.
27. Dhar R, Diringer MN. Relationship between angiographic vasospasm, cerebral blood flow, and cerebral infarction after subarachnoid hemorrhage. Acta Neurochir Suppl. 2015;120:161–5. https://doi.org/10.1007/978-3-319-04981-6_27.
28. Østergaard L, Engedal T, Aamand R. Capillary transit time heterogeneity and flow-metabolism coupling after traumatic brain injury. J Cereb Blood Flow Metab. 2014;34:1585–98. https://doi.org/10.1038/jcbfm.2014.131.
29. Rey F, Li X, Carretero O. Perivascular superoxide anion contributes to impairment of endothelium-dependent relaxation: role of gp91(phox). Circulation. 2002;106(19):2497–502. https://doi.org/10.1161/01.cir.0000038108.71560.70.
30. Armin SS, Colohan AR, Zhang JH. Vasospasm in traumatic brain injury. Acta Neurochir Suppl. 2008;104:421–5.
31. Armulik A, Genove G, Mae M. Pericytes regulate the blood-brain barrier. Nature. 2010;468:557–61. https://doi.org/10.1038/nature09522.
32. Bullock R, Maxwell W, Graham D. Glial swelling following human cerebral contusion: an ultrastructural study. J Neurol Neurosurg Psychiatry. 1991;54:427–34. https://doi.org/10.1136/jnnp.54.5.427.
33. Dore-Duffy P, Wang S, Mehedi A. Pericyte-mediated vasoconstriction underlies TBI-induced hypoperfusion. Neurol Res. 2011;33:176–86. https://doi.org/10.1179/016164111x12881719352372.
34. Hall C, Reynell C, Gesslein B. Capillary pericytes regulate cerebral blood flow in health and disease. Nature. 2014;508:55–60. https://doi.org/10.1038/nature13165.
35. Kreipke C, Schafer PC, Rossi NF. Differential effects of endothelin receptor A and B antagonism on cerebral hypoperfusion following

traumatic brain injury. Neurol Res. 2010;32:209–14. https://doi.org/10.1179/174313209x414515.
36. Yemisci M, Gursoy-Ozdemir Y, Vural A. Pericyte contraction induced by oxidative-nitrative stress impairs capillary reflow despite successful opening of an occluded cerebral artery. Nat Med. 2009;15:1031–7. https://doi.org/10.1038/nm.2022.
37. Ursino M, Lodi C. A simple mathematical model of the interaction between intracranial pressure and cerebral hemodynamics. J Appl Physiol. 1997;82:1256–69. https://doi.org/10.1007/bf02368459.
38. Vollmar B, Westermann S, Menger M. Microvascular response to compartment syndrome-like external pressure elevation: an in vivo fluorescence microscopic study in the hamster striated muscle. J Trauma. 1999;46:91–6. https://doi.org/10.1097/00005373-199901000-00015.
39. Bragin D, Bush R, Muller W. High intracranial pressure effects on cerebral cortical microvascular flow in rats. J Neurotrauma. 2011;28:775–85. https://doi.org/10.1089/neu.2010.1692.
40. Rhee C, Fraser C, Kibler K, Easley B. Ontogeny of cerebrovascular critical closing pressure. Pediatr Res. 2015:1–5. https://doi.org/10.1038/pr.2015.6.

The Cerebrovascular Time Constant in Patients with Head Injury and Posttraumatic Cerebral Vasospasm

Anatoly Sheludyakov, Dmitry Martynov, Michael Yuryev, Artem Kopylov, and Alex Trofimov

Abstract The aim of the study was to assess the time constant of cerebral arterial bed in TBI patients with cerebral vasospasm (CVS) with and without intracranial hematomas (ICH).

We examined 84 patients with severe TBI (mean 35 ± 15 years, 53 men and 31 women). The first group included 41 patients without ICH and the second group included 43 patients with epidural (7) and subdural (36) hematomas.

Perfusion computed tomography (PCT) was performed in 1–12 days after TBI in the first group and in 2–8 days after craniotomy in the second group. Arteriovenous amplitude of regional cerebral blood volume oscillation was calculated as the difference of arterial and venous blood volume in the "region of interest." Mean arterial pressure was measured and the flow rate of middle cerebral artery was recorded with Transcranial Doppler after PCT. Time constant was calculated by the formula modificated by M. Kasprowicz.

Results and Conclusion: The τ was shorter ($p < 0.005$) in both first and second group in comparison with normal values. The τ in the second group on ipsilateral side former hematoma with CVS was shorter than in the first group and in the second group on contralateral side former hematoma without CVS ($p = 0.024$).

A. Sheludyakov
Department of Neurosurgery, Privolzhsky Research Medical University, Nizhny Novgorod, Russia

D. Martynov
Nizhny Novgorod State Technical University Named After R.E. Alexeev, Nizhny Novgorod, Russia

M. Yuryev · A. Kopylov
Department of Polytrauma, Regional Hospital Named After N.A. Semashko, Nizhny Novgorod, Russia

A. Trofimov (✉)
Department of Neurosurgery, Privolzhsky Research Medical University, Nizhny Novgorod, Russia

Department of Polytrauma, Regional Hospital Named After N.A. Semashko, Nizhny Novgorod, Russia

Keywords Head injury · Cerebrovascular time constant · Cerebral vasospasm

Introduction

Initial management of traumatic brain injury (TBI) after polytrauma focuses on patient stabilization and treatment of elevated intracranial pressure (ICP). Surgical treatment of TBI can decrease mass effect and brain edema, thus mitigating progressive neurologic decline.

The basic principle of the brain damage therapy is to maintain adequate perfusion and oxygenation, which is impossible without the evaluation of these parameters and the timely correction of detected disorders [1].

It is believed that neuromonitoring should not be limited to monitoring of single parameters of homeostasis but should tend to determine and monitor the state of various organs and systems based on the integral analysis with the calculation of "surrogate" indices and values, which reflect the state of various parts of homeostasis for further correction of any detected disorders [2].

This approach enables us to determine the functional state of those structures, the direct study thereof is either impossible at all or only accessible experimentally, such as the microvasculature [2].

However, in clinical practice, the determination of these values has had until recently some significant technical constraints associated with the necessity of the lifetime assessment of pulse changes in the area of the main vessel under study during one cardiac cycle [3, 4].

There are no such constraints when determining τ—cerebrovascular time constant, which characterizes the time for complete filling with blood of the cerebral pial bed during one cardiac cycle [5].

Hence, cerebrovascular time constant can be evaluated, by analogy with an electrical RC circuit, as a product of

R. D. Martin et al. (eds.), *Subarachnoid Hemorrhage*, Acta Neurochirurgica Supplement 127, https://doi.org/10.1007/978-3-030-04615-6_30, © Springer Nature Switzerland AG 2020

compliance of the cerebral arterial bed [6] and cerebrovascular resistance [5].

This index is independent of the pulse difference of the blood transfer vessel area [7].

Although the term "time constant" is used, the values of the time constants vary widely with different cerebral pathology, such as subarachnoid hemorrhage, carotid stenosis, and traumatic brain injury [8–10].

In a broad sense, τ changes reflect the brain ability to maintain the continuous perfusion of the cerebral microcirculation under conditions of spontaneous variations of intracranial pressure [11, 12]. However, τ peculiarities at TBI and CVS remain poorly studied.

The aim of the study was to assess the time constant of cerebral arterial bed in severe traumatic brain injury patients (TBI) with CVS with and without intracranial hematoma (ICH).

Materials and Methods

The study was approved by the Ethics Committee of the Nizhny Novgorod Regional Hospital n.a. Semashko.

We examined 84 polytrauma patients with severe head injury who were treated at the Nizhny Novgorod Regional Trauma Center Level I in 2012–2017.

The mean age of the patients with head injury was 35 ± 15 years (from 15 to 79 years). They were 31 women and 53 men.

The first group included 41 patients with CVS without intracranial hematoma, and the second group included 43 patients with CVS and with epidural (7) and subdural (36) hematomas.

The wakefulness level according to Glasgow Coma Score (GCS) in first group averaged 11.2 ± 1.4, in the second group −10.1 ± 3.4.

Perfusion Computed Tomography

All patients were subjected to the perfusion computed tomography (PCT) by 64-slice tomograph Toshiba Aquilion TSX-101A (Toshiba Medical Systems, Europe BV, Netherland).

PCT was performed in 2–12 days after TBI in the first group and in 2–8 days after surgical evacuation of the hematoma in the second group. The computed tomography angiography source image (CTASI) analysis enabled us to visualize the main vessels of the brain and to assess the state of their diameter. In all patients included in this study, the minimal intensive projection data analysis identified the focal narrowing MCA more than 30% of the diameter as compared to adjacent sections of the same vascular segment, based thereon an "angiographic" CVS was diagnosed.

The perfusion examination report included an initial contrast-free CT of the brain [13]. The so-called area of interest was established based on areas of middle cerebral artery.

There were further performed four extended scanning of such "area of interest," 32 mm in thickness, within 55 s with a contrast agent administered (the Brain Perfusion mode). The scanning parameters were 120 kVp, 70 mA, 70 mAs, and 1000 ms. The contrast agent Ultravist (Schering AG, Germany) was administered with an automatic syringe injector (Stellant, One Medrad, Indianola, PA) into a peripheral vein through a standard catheter (20 G) at a rate of 4–5 mL/s in a dose of 50 mL per 1 examination.

After scanning the data volume was transferred to work station Vitrea 2 (Vital Imaging, Inc., ver 4.1.8.0). Artery and vein were marks automatically recorded followed by the manual control of indices in the Time-Concentration Diagram.

The so-called area of interest was established based on subcortical areas of middle cerebral artery.

Arteriovenous amplitude of regional cerebral blood volume oscillation (delta Cerebral Blood Volume—ΔCBV) was calculated as the difference of arterial and venous blood volume in the "region of interest" of 1 cm^3 [11].

Cerebral blood flow velocity of middle cerebral artery was recorded bilaterally using Transcranial Doppler ultrasound with 2-MHz probes attached with a headband (Sonomed 300M, Spectromed, Russia). Arterial blood pressure and amplitude of arterial blood pressure (ABPamp) were measured noninvasively (MAP-03, Cardex, Russia) after PCT.

Statistical Analysis

Used for the calculation of the time constant formula proposed M. Kasprowicz [11] amended Czosnyka [14]:

$$\tau = \text{ampCaBV} \times \text{MAP} / \text{Vmean} \times \text{ampABP}$$

- ampCaBV—arteriovenous amplitude of cerebral blood volume.
- MAP—mean arterial pressure.
- Vmean—mean flow velocity rate of middle cerebral artery.
- ampABP—amplitude arterial blood pressure.
- Reference range τ was chosen according Kasprowicz M. [7] 0.22 ± 0.06 sec.

The *t*-test for dependent samples was utilized to analyze differences in means of parameters between the ipsilateral and contralateral sides of the temporal lobes. The program

Statistica 7.0 (StatSoft Inc., USA, 2004) was used for the said analysis. The significance level of less than 0.05 was determined.

Results

Mean values and standard deviations of the data were summarized in Table 1.

The time constant was shorter ($p < 0.005$) in both first and second group in comparison with normal data [7].

The time constant in the second group on ipsilateral side former hematoma with CVS was shorter than in the first group.

Item τ in the second group on ipsilateral side former hematoma with CVS was shorter than in the second group on contralateral side former hematoma without CVS ($p = 0.024$).

No significant effects of sufferers' age on the τ value have been found ($p > 0.05$).

Discussion

Microcirculatory disorders play a key role in the development of hypoperfusion and secondary brain ischemia at posttraumatic CVS [14, 15].

One of the factors, which enables to estimate simultaneously both the capacitive and resistive characteristics of the cerebral pial bed, is cerebrovascular time constant, which is calculated as the product of cerebrovascular arterial compliance and cerebrovascular resistance [10].

In our opinion, there may be a few reasons for τ reduction but all of them seem to be associated with the brain edema.

First, development of the combined (vasogenic and cytotoxic) edema due to fall of arterial compliance [6, 16].

Second, brain edema may cause the pial compression and reduce the total volume of capacitive vessels, thus changing the value of resistivity [17].

The changes in vascular lumen (e.g., in CVS) still change τ. We have shown that there is a shortening of τ on the side of posttraumatic CVS. In addition, τ decreased even more in the perihematomic area. Perhaps this can be explained by the fact that CVS changes the total volume of the vascular bed and increases the cerebrovascular resistance.

The time constant shortening by hematoma on the side of the eliminated cortical compression may be explained by the vasodilation of vessels resulting from the vascular wall tone dysautoregulation [17].

It is indirectly confirmed by the fact of remaining τ variations even after the compression factor elimination. The failure of microcirculatory autoregulation may result in the disturbed venous blood outflow from the channel and in the long stagnation of a part of blood in resistive vessels, whereby the pial bed may be filled much faster [18].

Limitation of the Study

We suppose that it is impossible to carry out the dynamic assessment of τ without a repeated PCT.

We have to admit that we have failed to completely eliminate a mathematical error associated with the measurement of the "area of interest" space.

We believe that the results of our study shall provide conditions for a differentiated approach to solving the question on timing of orthopedic correction of extracranial injuries in polytraumatized patients with CVS—during the period of microcirculatory normalization and the minimal risk of the secondary brain injury. Further research is needed for the understanding of these phenomena.

Table 1 Comparison of the analyzed parameters

		MAP (mmHg)	ampABP (mmHg)	Vmean (cm/s)	ΔCBV (cm^3)	τ (s)
1	Group 1 (without hematoma with CVS)	98.3 ± 11.7	56.5 ± 15.6	44.4 ± 10.5	2.3 ± 0.7	0.09 ± 0.05
2	Group 2 (ipsilateral side former hematoma with CVS)	97.5 ± 15.2	60.4 ± 21.6	48.4 ± 19.3	2.1 ± 1.1	0.07 ± 0.04
3	Group 2 (ipsilateral side former hematoma without CVS)	97.5 ± 15.2	55.7 ± 29.2	42.0 ± 10.4	2.4 ± 1.2	0.10 ± 0.06
4	Group 2 (contralateral side former hematoma without CVS)	97.5 ± 15.2	57.9 ± 17.9	41.1 ± 12.7	2.2 ± 0.9	0.09 ± 0.06
	P (1–2)	0.756	0.563	0.172	0.510	0.0004[a]
	P (1–3)	0.756	0.892	0.897	0.764	0.379
	P (1–4)	0.756	0.892	0.379	0.351	0.437
	P (2–4)	1	0.616	0.045[a]	0.282	0.024[a]

[a]Difference is statistically significant

Conclusion

The cerebrovascular time constant was shorter ($p < 0.005$) in both first and second group in comparison with normal values. The time constant in the second group on ipsilateral side former hematoma with CVS was shorter than in the first group and in the second group on contralateral side former hematoma without CVS ($p = 0.024$).

The results indicate severe dysregulation of cerebral blood flow in severe TBI, which increases in the patients with polytrauma and traumatic hematomas.

Conflict of Interest We declare that we have no conflicts of interest.

References

1. Lewis P, Rosenfeld J. Monitoring of the association between cerebral blood flow velocity and intracranial pressure. Acta Neurochir. 2012;114:147–52.
2. Varsos GV, Richards H, Kasprowicz M. Critical closing pressure determined with a model of cerebrovascular impedance. J Cereb Blood Flow Metab. 2013;33:235–43.
3. Carrera E, Kim D, Castellani G. Cerebral arterial compliance in patients with internal carotid artery disease. Eur J Neurol. 2010;18:711–8.
4. Riva N, Budohoski K, Smielewski P. Transcranial Doppler pulsatility index: what it is and what it isn't. Neurocrit Care. 2012;17:58–66.
5. Dewey R, Pierer H, Hunt WE. Experimental cerebral hemodynamics-vasomotor tone, critical closing pressure, and vascular bed resistance. J Neurosurg. 1974;41:597–606.
6. Avezaat CJ, Eijndhoven JH. Cerebrospinal fluid pulse pressure and craniospatial dynamics. A theoretical, clinical and experimental study. Rotterdam: Erasmus University; 1984.
7. Kasprowicz M, Diedler J, Reinhard M. Time constant of the cerebral arterial bed. Acta Neurochir Suppl. 2012;114:17–21.
8. Howlett J, Northington F. Cerebrovascular autoregulation and neurologic injury in neonatal hypoxic-ischemic encephalopathy. Pediatr Res. 2013;74(5):525–35.
9. Kasprowicz M. Badania hemodynamiki mózgowej na podstawie analizy pulsacji ciśnienia wewnątrzczaszkowego, ciśnienia tętniczego i przepływu krwi mózgowej. Wrocław: Oficyna Wydawnicza Politechniki Wrocławskiej; 2012.
10. Trofimov A, Kalentiev G, Gribkov A, Voennov O, Grigoryeva V. Cerebrovascular time constant in patients with head injury. Acta Neurochir Suppl. 2016;121:295–7. https://doi.org/10.1007/978-3-319-18497-5_51.
11. Kasprowicz M, Diedler J, Reinhard M. Time constant of the cerebral arterial bed in normal subjects. Ultrasound Med Biol. 2012;38:1129–37.
12. Ursino M, Lodi C. A simple mathematical model of the interaction between intracranial pressure and cerebral hemodynamics. J Appl Physiol. 1997;82:1256–69.
13. Shin BJ, Anumula N. Does the location of the arterial input function affect quantitative CTP in patients with vasospasm? Am J Neuroradiol. 2014;35:49–54.
14. Czosnyka M, Richards H, Reinhard M. Cerebrovascular time constant: dependence on cerebral perfusion pressure and end-tidal carbon dioxide concentration. Neurol Res. 2012;34:17–24.
15. ter Laan M. Neuromodulation of cerebral blood flow. Groningen: Groningen University; 2014.
16. Avezaat CJ, van Eijndhoven JH. Clinical observations on the relationship between cerebrospinal fluid pulse pressure and intracranial pressure. Acta Neurochir. 1986;79:13–29.
17. Marmarou A. A review of progress in understanding the pathophysiology and treatment of brain edema. Neurosurg Focus. 2007;15.22(5):E1.
18. Lassen NA. Autoregulation of cerebral blood flow. Circ Res. 1964;15:201–4.

Current Open Surgical Indications for Revascularization in Cerebral Ischemia

Marc Timothy Eastin, Vikram Badhri Chakravarthy, Fransua Sharafeddin, Daniel Hoss, and Miguel Angel Lopez-Gonzalez

Abstract Cerebral revascularization was pioneered half a century ago. Gradual improvements in microsurgical instrumentation and training in microsurgical techniques have allowed significant changes that improved outcomes in neurosurgery, extrapolating this knowledge to other neurosurgical diseases (brain tumor, aneurysms, and skull base tumor surgery). But the popularity of cerebral bypass procedures was followed by their decline, given the lack of clear benefit of bypass surgery in chronic cerebrovascular ischemia after the EC-IC bypass studies. Over the last couple of decades, the formidable advance of neuro-endovascular techniques for revascularization has lessened the need for application of open cerebral revascularization procedures, either for flow augmentation or flow replacement. However, there is still a select group of patients with chronic cerebral ischemia, for whom open cerebral revascularization with flow augmentation is the only treatment option available, and this will be the objective of our current review.

Keywords Cerebral bypass · Cerebral ischemia Revascularization · Flow augmentation · Flow replacement · Vertebrobasilar insufficiency · Microsurgery

M. T. Eastin · M. A. Lopez-Gonzalez (✉)
Neurosurgery Department, School of Medicine, Loma Linda University, Loma Linda, CA, USA
e-mail: mlopezgonzalez@llu.edu

V. B. Chakravarthy
Neurosurgery Department, Cleveland Clinic Foundation, Cleveland, OH, USA

F. Sharafeddin
Center for Neuroscience Research, School of Medicine, Loma Linda University, Loma Linda, CA, USA

D. Hoss
Interventional Neuroradiology Department, School of Medicine, Loma Linda University, Loma Linda, CA, USA

Introduction

More than a century was required to refine the surgical techniques in cerebrovascular anastomosis. Alexis Carrel was awarded the Nobel Prize for Medicine and Physiology in 1912 for pioneering vascular suturing techniques [1]. Microsurgical magnification was introduced in neurosurgery by Theodore Kurze in 1957 at University of Southern California. In 1965, Yasargil joined Donaghy and Suarez at their laboratory in Vermont where they worked together on experimental microvascular anastomosis techniques, though it was not until 1972 that Yasargil performed the first successful STA-MCA bypass for Moyamoya disease [2], which remains one of the most precise microsurgical procedures performed until date.

At the same time, other cerebral revascularization options emerged with the use of saphenous graft by Lougheed in 1971 [3], radial artery graft by Ausman in 1978 [4], as well as posterior circulation revascularization procedures for vertebrobasilar insufficiency and unclippable aneurysms by Sundt [5].

This very productive period saw a worldwide decline in cerebral revascularization after the International Cooperative Study of Extracranial/Intracranial Arterial Anastomosis (EC/IC Bypass Study) in 1985 [6]. This study included 1377 patients with MCA or ICA stenosis or occlusion, or a recent (within 3 months) TIA or stroke in the same territory. Patients were randomized for medical treatment with aspirin and blood pressure control or medical treatment and STA-MCA bypass. The patency of the graft was above 96%, but it did not prevent stroke compared with medical treatment, and presence of nonfatal and fatal stroke increased in the surgical group. The dissemination of these results led to a worldwide decrease in the use of these techniques and lack of training in microvascular anastomosis techniques at residency programs. Later, in 1987 Sundt questioned the results of the EC/IC Bypass Study regarding the inadequate identification of population at higher risk for stroke [7].

R. D. Martin et al. (eds.), *Subarachnoid Hemorrhage*, Acta Neurochirurgica Supplement 127,
https://doi.org/10.1007/978-3-030-04615-6_31,

The COSS trial (Carotid Occlusion Surgery Study) is a randomized trial conducted from 2002 to 2010, where the best medical therapy was compared against STA-MCA bypass and best medical therapy [8]. In this study, 195 patients with symptomatic internal carotid artery occlusion and ischemia identified by ipsilateral increased oxygen extraction fraction measured by positron-emission tomography (PET) were selected, of whom 97 were randomized to receive surgery and 98 for medical therapy. The main outcome measures were stroke in initial 30 days after surgery or randomization and ipsilateral stroke within 2 years of randomization. The results showed that 30-day rates of stroke were 14.4% (14/97) in the surgical group and 2.0% (2/98) in the nonsurgical group, whereas the 2-year rates did not differ significantly, with 21.0% for the surgical group and 22.7% for the nonsurgical group. Much criticism emerged, due to the fact that early surgical morbidity could be the result of lack of uniformity and experience among centers performing the bypass.

More recently, the ELANA technique was introduced as an option for extracranial to intracranial anastomosis with the potential benefit of avoiding temporary occlusion. This technique mainly targets flow replacement rather than flow augmentation. Additionally, it cannot be used in donor sites smaller than 2.6 mm in diameter [9].

Acute ischemic stroke treatment has changed radically since 2015 with the publication of multiple randomized controlled trials evaluating the endovascular therapies where stent retrievers have become the standard of care, significantly improving outcomes, with such therapies being coupled with improvement in multimodal imaging, multidisciplinary approach with workflow improvement, and creation of comprehensive stroke centers [10].

Functional Neuroimaging for Chronic Cerebral Ischemic Disease

Functional neuroimaging aids in determining cerebrovascular reserve (CVR) and may therefore help predict which patients could benefit from endovascular or surgical revascularization [11]. In the face of decreased cerebral perfusion pressure (CPP), both hemodynamic and metabolic responses occur to maintain adequate cerebral rate of oxygen metabolism (CMRO2) [12].

Hemodynamically, cerebrovascular dilatation downstream from stenosis or occlusion seeks to maintain cerebral blood flow (CBF)—the amount of blood passing through a portion of the brain per unit time [12]. Dynamic CT and MR perfusion imaging allows for assessment of flow dynamics of a bolusperfusion, imaging passing through a portion of the brain [13, 14]. Specifically, the mean transit time (MTT)—the amount of time a bolus takes to travel through a region of the brain—has been demonstrated to correlate with CVR [15]. Acetazolamide, an indirect cerebral vasodilator, can be used to further evaluate CVR for a patient [16, 17]. Dynamic CT or MR perfusion imaging is performed both prior to and following a dose of acetazolamide, with calculation of percent change in perfusion parameters between the two exams. In particular, the percent change in CBF (pcCBF) has been shown to correlate strongly with CVR [18, 19].

As CPP falls, the metabolic response is to increase oxygen extraction fraction (OEF) from blood to maintain CMRO2 [12]. The gold standard for imaging OEF is 15O-PET, during which a patient inhales 15O-labeled oxygen, and then subsequently has cerebral PET imaging. While increased OEF assessed with 15O-PET has been associated with a sixfold increased stroke risk for a given degree of stenosis [20], the 123 second half-life of 15O requires an on-site cyclotron and significantly limits availability. Due to these limitations, research is ongoing to find additional methods for evaluating OEF with MRI. Many methods have been proposed or attempted [21, 22], but quantitative susceptibility mapping (QSM) shows perhaps the greatest promise, with its ability to quantitatively evaluate venous deoxygenated hemoglobin [23].

Moyamoya Disease

It was in 1972 that Yasargil performed the first successful STA-MCA bypass for Moyamoya disease [2]. Since then, the EC-IC bypass procedure for Moyamoya disease has been in and out of favor with surgeons for revascularization of cerebral ischemia based on landmark studies like the EC/IC Bypass Study in 1985 [6] and the COSS trial in 2011 [8]. Current literature leaves surgeons in need of finding ways to lower their complication rate, achieve a high level of surgical safety, select patients based on preoperative measurements, and monitor flow intraoperatively to ensure that the benefits of bypass significantly exceed the risks associated with this procedure [24].

EC-IC bypass for symptomatic Moyamoya disease can be categorized as direct, indirect, or a combination of the two. The direct method involves taking an external carotid (EC) artery branch and anastomosing it to either the temporal M4 branch or to the anterior cerebral artery (ACA) branch. Classically, the EC branch is the superior temporal artery (STA) because of its location, length, and lack of collaterals with the ophthalmic artery. The M4 branch of the middle cerebral artery (MCA) is normally chosen, to avoid ischemia in the frontal branches during occlusion and because of good collaterals with the posterior cerebral artery (PCA). This causes immediate revascularization of the ischemic brain [25].

The indirect method involves multiple techniques, including encephalo-myo-synangiosis (EMS), encephalo-duro-myo-arterio-pericranial-synangiosis (EDMAPS), encephalo-arterio-duro-myo-synangiosis (EDAMS), and encephalo-duro-arterio-synangiosis (EDAS) for bypass. EDAS and EDAMS are the most commonly used indirect theses to these methods, which involve taking the EC branch, as in EDAS, and both the EC branches with a portion of the temporalis muscle in the case of EDAMS, and laying them over the dura in the hope that with time new capillary collaterals will develop and revascularize the ischemic brain. If the indirect technique is to be used, the surgeon must be sure that immediate revascularization is not needed, since it takes time for the collaterals to develop. The indirect method is a low-flow method and can be used when the brain is unable to accommodate a high flow rate [25].

The combined method pairs the direct/indirect techniques to take advantage of the strengths of each method, namely, the early flow restoration of the direct (STA/MCA) and the durable long-term revascularization of the indirect method (EDAMS). Although the combined direct and indirect anastomosis in patients with Moyamoya disease is in itself a more complex surgical procedure than each of these methods singly, it is associated with an immediate increase in cerebral blood flow and has been shown to be an excellent option when one faces the challenge of treating this condition [26]. However, the decision as to which technique to use should ultimately be made on a patient-to-patient basis and the operating neurosurgeon's familiarity with the procedure.

Unilateral or Bilateral Carotid Steno-Occlusive Disease

Carotid artery occlusion (CAO) is associated with high morbidity and mortality rates. Fifteen percent of stroke patients and those who present with transient ischemic attack in the carotid artery territory present with carotid artery occlusion [27]. The reasons for cerebral ischemia may include embolic occlusion distal to the arterial stenosis or reduced perfusion in the territory of the occluded artery [28]. One of the treatment strategies of patients with hemodynamically notable carotid artery stenosis is carotid endarterectomy (CE), which has supported the prevention of stroke and shown good clinical recovery after CAO [27, 29].

The main benefit of CE is that it allows the removal of potential source of emboli and increases the diameter of the occluded vessel by eradicating the stenosis itself. However, patients undergoing carotid endarterectomy still have increased risk of recurrent stroke, which represents a clinical dilemma and brings to light the necessity for advancement of existing management strategies [30].

In patients with uni- or bilateral chronic carotid occlusion with failure of maximal medical treatment, the surgical strategy consists of cerebral revascularization by extracranial-intracranial (EC-IC) arterial bypass. The decision of EC-IC bypass is made based on different imaging modalities, including xenon-enhanced computed tomography (CT), xenon single-photon emission CT, and PET scanning [31, 32]. The principal intention of EC-IC bypass is raising the blood flow to the cerebral hemisphere, where due to occlusion of the CA there is significant hemodynamic insufficiency with subsequent metabolic disturbances [33].

Despite results of EC-IC bypass study and COSS trial, in patients with unilateral or bilateral carotid occlusion with persistent symptoms after failure of medical treatment and documented hypoperfusion, open cerebral revascularization with flow augmentation is still performed at experienced cerebrovascular centers.

Vertebrobasilar Insufficiency

Less common, and more complex, are cases of vertebrobasilar insufficiency where flow augmentation procedures have been performed.

Vertebrobasilar insufficiency (VBI) describes the lack of blood flow to the posterior circulation due to embolism, large vessel atherosclerosis, and arterial dissection. Patients present with ischemic symptoms stemming from the occipital or temporal lobes, cerebellum, pons, and brain stem with associated cranial nerves (posterior circulation supply). Hemodynamic ischemia occurs due to progressive atherosclerotic plaque narrowing of the vasculature. Evaluation for VBI includes a noninvasive computed tomography with angiography (CTA) or a magnetic resonance angiography (MRA), followed by a diagnostic cerebral angiogram. Treatment options largely center around risk factor modification and the use of antiplatelet medication like aspirin, which has been shown to decrease the incidence of brain stem strokes [34]. In those patients that fail maximal medical therapy and have evidence of progressive, symptomatic vertebrobasilar stenosis with flow-related pathology, surgical revascularization with bypass surgery may be indicated.

Extracranial-intracranial bypass has been utilized to help revascularize the posterior circulation in the setting of VBI. It has been demonstrated to have low complication rates, improved symptoms, and augmented regional blood flow along with a reduction of future strokes [35, 36]. The first EC-IC bypass for VBI was performed by Khodad et al. in 1976, via an occipital artery to posterior inferior cerebellar artery (OA-PICA) anastomosis [37]. A follow-up angiogram at 2 weeks demonstrated patency of the bypass, with partial improvement of symptoms. Low-flow vascular bypass routes

include the superficial temporal artery to superior cerebellar artery (STA-SCA), superficial temporal artery to posterior cerebral artery (STA-PCA), and OA-PICA [36, 38, 39]. High-flow bypasses include the radial artery and saphenous vein grafting with revascularization routes from the carotid artery to the posterior cerebral artery (PCA) [40, 41]. The goal of bypass is to choose an arterial pedicle that can be anastomosed to a vessel distal to the site of occlusion. Known complications of bypass include restenosis, graft occlusion, surgical hematomas, infection, and postoperative stroke.

Ausman et al. published in 1990 their series on 83 patients who underwent EC-IC bypass to the posterior circulation for VBI [42]. Using the aforementioned techniques, 69% had complete resolution of their symptoms, with an 8.4% mortality rate and a 13.3% morbidity rate. OA-PICA demonstrated a 73% patency with 53% of patients demonstrating complete relief of symptoms, as compared to the OA-AICA group which had 94% patency with 70% of patients experiencing complete resolution of symptoms. At long-term follow-up, 83% of patients were improving, and 48% were achieving normal function after bypass. Upon conclusion of their series, it was felt that STA-SCA anastomosis was well tolerated and less technically demanding compared to the other techniques. Patients with stable VBI tolerated the bypass procedure better than those presenting with crescendo transient ischemic attack (TIA) or evolving strokes.

Other options for revascularization include the use of an interposition graft, derived from either the saphenous vein or radial artery. Britz et al. [40] published on their case series of three patients the use of radial artery graft for revascularization, augmenting flow from the common carotid artery (CCA) to the posterior cerebral artery (P2 segment). Sixty-seven percent of patients had complete resolution of symptoms. In contrast, Sundt et al. utilized saphenous vein grafts in their series of 13 (1 additional for treatment of aneurysm) patients, augmenting flow from the external carotid artery to the PCA (34). This series yielded a 67% graft patency rate, with 50% of patients demonstrating complete resolution of their symptoms. Although small sample sizes, both studies demonstrate the utility of interposition grafts in augmenting flow to the posterior circulation.

Multiple studies have attempted to argue for an increased role of EC-IC bypass for VBI. Since the first bypass for VBI in 1976 by Khodad et al., thanks to medical and technological advances surgical intervention has fallen by the wayside, with arguments surrounding morbidity and mortality of the surgical approach. Authors have argued the use of transposition grafting as compared to direct anastomosis, analyzing high-flow versus low-flow bypasses. However, there is understanding that this approach is not without its technical challenges. Based on a multitude of case series in the literature, there is a role for EC-IC bypass for VBI in carefully selected patients.

Conclusions

With all the progress in the field of stroke management, and despite the controversial viewpoints related to extracranial to intracranial bypass in numerous publications, this procedure remains one of the principal elements of treatment of chronic cerebrovascular occlusion with refractory hypoperfusion. Adequate identification of a subset group of patients with chronic and progressive ischemic conditions not amenable to endovascular techniques and refractory to maximal medical treatment, such as Moyamoya disease, unilateral or bilateral carotid steno-occlusive disease, and vertebrobasilar insufficiency, is crucial to ensure benefit from open revascularization interventions at experienced cerebrovascular surgery centers.

Conflict of Interest The authors declare that they have no conflict of interest.

References

1. Dente CJ, Feliciano DV. Alexis Carrel (1873-1944) Nobel Laureate, 1912. Arch Surg. 2005;140:609–10.
2. Yasargil MG, Y Y. Results of microsurgical extra-intracranial arterial bypass in the treatment of cerebral ischemia. Neurosurgery. 1977;1:22–4.
3. Lougheed WM, Marshall BM, Hunter M, Michel ER, Sandwith-Smyth H. Common carotid to intracranial carotid bypass venous graft: technical note. J Neurosurg. 1971;34(1):114–8.
4. Ausman JI, Nicoloff DM, Chou SN. Posterior fossa revascularization: anastomosis of vertebral artery to PICA with interposed radial artery graft. Surg Neurol. 1978;9(5):281–6.
5. Sundt TM Jr, Piepgras DG, Marsh WR, Fode NC. Saphenous vein bypass grafts for giant aneurysms and intracranial occlusive disease. J Neurosurg. 1986;65:439–50.
6. The EC/IC Bypass Study Group. Failure of extracranial-intracranial arterial bypass to reduce the risk of ischemic stroke. Results of an international randomized trial. N Engl J Med. 1985;313:1191–200.
7. Sundt TM Jr. Was the International randomized trial of extracranial-intracranial arterial bypass representative of the population at risk? N Engl J Med. 1987;316:814–6.
8. Powers WJ, Clarke WR, Grubb RL Jr, Videen TO, Adams HP Jr, Derdeyn CP, COSS Investigators. Extracranial-intracranial bypass surgery for stroke prevention in hemodynamic cerebral ischemia: the Carotid Occlusion Surgery Study randomized trial. JAMA. 2011;306:1983–92.
9. Langer DJ, D V. Excimer laser-assisted nonocclusive anastomosis. Neurosurg Focus. 2008;24:1–11.
10. Appireddy R, Zerna C, Menon BK, Goyal M. Endovascular interventions in acute ischemic stroke: recent evidence, current challenges, and future prospects. Curr Atheroscler Rep. 2016;18(7):40.
11. Sheth SA, Liebeskind DS. Imaging evaluation of collaterals in the brain: physiology and clinical translation. Curr Radiol Rep. 2014;2(1):29.
12. Derdeyn CP, Videen TO, Yundt KD, Fritsch SM, Carpenter DA, Grubb RL, Powers WJ. Variability of cerebral blood volume and oxygen extraction: stages of cerebral haemodynamic impairment revisited. Brain. 2002;125:595–607.

13. Lythgoe DJ, Ostergaard L, William SC, Cluckie A, Buxton-Thomas M, Simmons A, Markus HS. Quantitative perfusion imaging in carotid artery stenosis using dynamic susceptibility contrast-enhanced magnetic resonance imaging. Magn Reson Imaging. 2000;18(1):1–11.
14. Wintermark M, Sesay M, Barbier E, Borbely K, Dillon WP, Eastwood JD, Glenn TC, Grandin CB, Pedraza S, Soustiel JF, Narial T, Zaharchuk G, Caille JM, Dousset V, Yonas H. Comparative overview of brain perfusion imaging techniques. Stroke. 2005;36(9):e83–99.
15. Kaneko K, Kuwabara Y, Mihara F, Yoshiura T, Nakagawa M, Tanaka A, Sasaki M, Koga H, Hayashi K, Honda H. Validation of the CBF, CBV, and MTT values by perfusion MRI in chronic occlusive cerebrovascular disease: a comparison with 15O-PET1. Acad Radiol. 2004;11(5):489–97.
16. Chen A, Shyr MH, Chen TY, Lai HY, Lin CC, Yen PS. Dynamic CT perfusion imaging with acetazolamide challenge for evaluation of patients with unilateral cerebrovascular steno-occlusive disease. Am J Neuroradiol. 2006;27(9):1876–81.
17. Vagal AS, Leach JL, Fernandez-Ulloa M, Zuccarello M. The acetazolamide challenge: techniques and applications in the evaluation of chronic cerebral ischemia. Am J Neuroradiol. 2009;30(5):876–84.
18. Kang KH, Kim HS, Kim SY. Quantitative cerebrovascular reserve measured by acetazolamide-challenged dynamic CT perfusion in ischemic adult Moyamoya disease: initial experience with angiographic correlation. Am J Neuroradiol. 2008;29(8):1487–93.
19. Rim NJ, Kim HS, Shin YS, Kim SY. Which CT perfusion parameter best reflects cerebrovascular reserve? Correlation of acetazolamide-challenged CT perfusion with single-photon emission CT in Moyamoya patients. Am J Neuroradiol. 2008;29(9):1658–63.
20. Gupta A, Baradaran H, Schweitzer AD, Kamel H, Pandya A, Delgado D, Wright D, Hurtado-Rua S, Wang Y, Sanelli PC. Oxygen extraction fraction and stroke risk in patients with carotid stenosis or occlusion: a systematic review and meta-analysis. Am J Neuroradiol. 2014;35(2):250–5.
21. Lu H, Ge Y. Quantitative evaluation of oxygenation in venous vessels using T2-relaxation-under-spin-tagging MRI. Magn Reson Med. 2008;60:357–63.
22. Xu F, Ge Y, Lu H. Noninvasive quantification of whole-brain cerebral metabolic rate of oxygen (CMRO2) by MRI. Magn Reson Med. 2009;62:141–8.
23. Kudo K, Liu T, Murakami T, Goodwin J, Uwano I, Yamashita F, Higuchi S, Wang Y, Ogasawara K, Ogawa A, Sasaki M. Oxygen extraction fraction measurement using quantitative susceptibility mapping: comparison with positron emission tomography. J Cereb Blood Flow Metab. 2016;36(8):1424–33.
24. Nakaji P. The necessity of technical excellence and safety in EC-IC bypass surgery. World Neurosurg. 2014;82(5):577–8. https://doi.org/10.1016/j.wneu.2013.08.038.
25. Giovani A, Brehar F, Gorgan RM. Cerebral revascularization: direct versus indirect bypass. Case presentation and review. Rom Neurosurg. 2014;21:459–69. https://doi.org/10.2478/romneu-2014-0062.
26. Kazumata K, Ito M, Tokairin K, Ito Y, Houkin K, Nakayama N, Kuroda S, Ishikawa T, Kamiyama H. The frequency of postoperative stroke in moyamoya disease following combined revascularization: a single-university series and systematic review. J Neurosurg. 2014;121(2):432–40. https://doi.org/10.3171/2014.1.JNS13946.
27. Executive Committee for the Asymptomatic Carotid Atherosclerosis Study. Endarterectomy for asymptomatic carotid artery stenosis. JAMA. 1995;273:1421–8.
28. Tummala RP, Chu RM, Nussbaum ES. Extracranial-intracranial bypass for symptomatic occlusive cerebrovascular disease not amenable to carotid endarterectomy. Neurosurg Focus. 2003;14(3):e8.
29. North American Symptomatic Carotid Endarterectomy Trial Collaborators. Beneficial effect of carotid endarterectomy in symptomatic patients with high-grade carotid stenosis. N Engl J Med. 1991;325:445–53.
30. Lopes DK, Mericle RA, Lanzino G, Wakhloo AK, Guterman LR, Hopkins LN. Stent placement for the treatment of occlusive atherosclerotic carotid artery disease in patients with concomitant coronary artery disease. J Neurosurg. 2002;96(3):490–6.
31. Klijn CJM, Kappelle J, Tulleken CAF, van Gijn J. Symptomatic carotid artery occlusion. A reappraisal of hemodynamic factors. Stroke. 1997;28:2084–93.
32. Ogasawara K, Ogawa A, Yoshimoto T. Cerebrovascular reactivity to acetazolamide and outcome in patients with symptomatic internal carotid or middle cerebral artery occlusion: a xenon-133 single-photon emission computed tomography study. Stroke. 2002;33:1857–62.
33. Miyamoto S. Japan Adult Moyamoya Trial Group: study design for a prospective randomized trial of extracranial-intracranial bypass surgery for adults with moyamoya disease and hemorrhagic onset—the Japan Adult Moyamoya Trial Group. Neurol Med Chir. 2004;44:218–9.
34. Merwick A, Werring D. Posterior circulation ischaemic stroke. BMJ. 2014;348:g3175.
35. Grubb RL Jr. Extracranial-intracranial arterial bypass for treatment of occlusion of the internal carotid artery. Curr Neurol Neurosci Rep. 2004;4:23–30.
36. Spetzler RF, Hadley MN, Martin NA, Hopkins LN, Carter LP, Budny J. Vertebrobasilar insufficiency. Part 1: microsurgical treatment of extracranial vertebrobasilar disease. J Neurosurg. 1987;66:648–61.
37. Khodadad G. Occipital artery-posterior inferior cerebellar artery anastomosis. Surg Neurol. 1976;5:225–7.
38. Coert BA, Chang SD, Marks MP, Steinberg GK. Revascularization of the posterior circulation. Skull Base. 2005;15:43–62.
39. Hopkins LN, Martin NA, Hadley MN, Spetzler RF, Budny J, Carter LP. Vertebrobasilar insufficiency. Part 2. Microsurgical treatment of intracranial vertebrobasilar disease. J Neurosurg. 1987;66:662–74.
40. Britz GW, Agarwal V, Mihlon F, Ramanathan D, Agrawal A, Nimjee SM, Kaylie D. Radial artery bypass for intractable vertebrobasilar insufficiency: case series and review of the literature. World Neurosurg. 2016;85:106–13.
41. Sundt TM Jr, Piepgras DG, Houser OW, Campbell JK. Interposition saphenous vein grafts for advanced occlusive disease and large aneurysms in the posterior circulation. J Neurosurg. 1982;56:205–15.
42. Ausman JI, Diaz FG, Vacca DF, Sadasivan B. Superficial temporal and occipital artery bypass pedicles to superior, anterior inferior, and posterior inferior cerebellar arteries for vertebrobasilar insufficiency. J Neurosurg. 1990;72:554–8.

The Role of Transcranial Doppler in Cerebral Vasospasm: A Literature Review

Sayesha Sharma, Reggie Jayson Lubrica, Minwoo Song, Rashmi Vandse, Warren Boling, and Promod Pillai

Abstract Transcranial Doppler ultrasonography (TCD) is a noninvasive technique used to detect vasospasms following a subarachnoid hemorrhage. While the gold standard to evaluate vasospasms is angiography, this technique is invasive and poses additional risks as compared to TCD. TCD is performed by insonating circle of Willis arteries to measure cerebral flow velocity. TCD allows dynamic monitoring of CBF-V and vessel pulsatility, with a high temporal resolution. It is relatively inexpensive, repeatable, and portable; however, the performance of TCD is highly operator dependent and can be difficult, especially with inadequate acoustic windows. This review summarizes the use of transcranial Doppler ultrasonography (TCD) for the assessment of cerebral vasospasm.

Keywords Transcranial Doppler ultrasonography · Cerebral vasospasm · Subarachnoid hemorrhage · Angiography · Prevention

Abbreviations

aSAH	Aneurysmal subarachnoid hemorrhage
BA	Basilar artery
CBF	Cerebral blood flow
CT	Computed tomography
CTA	Computed tomography angiography
DCI	Delayed cerebral ischemia
DSA	Digital subtraction angiography
ICA	Internal carotid artery
LR	Lindegaard ratio
MCA	Middle cerebral artery
mFV	Mean flow velocity
MRA	Magnetic resonance angiogram
MRI	Magnetic resonance imaging
SAH	Subarachnoid hemorrhage
SR	Sviri ratio
TCD	Transcranial Doppler ultrasonography

S. Sharma · R. J. Lubrica · M. Song · R. Vandse · W. Boling
P. Pillai (✉)
Loma Linda University, Loma Linda, CA, USA
e-mail: rpromodkumar@llu.edu

Introduction

Transcranial Doppler ultrasonography (TCD) is a simple, noninvasive, nonradioactive, portable technique that indirectly estimates cerebral blood flow (CBF) by measuring the CBF velocity [1]. TCD has been used increasingly as a diagnostic tool for detecting intracranial vasospasm following aneurysmal subarachnoid hemorrhage (aSAH). The purpose of this review is to provide an understanding of the techniques and clinical application of TCD, TCD's role in monitoring cerebral vasospasm, and to summarize the CBF thresholds that can be used to indicate vasospasms in various cerebral arteries. Cerebral vasospasm after aneurysmal subarachnoid hemorrhage (aSAH) is defined as the narrowing of the large- and medium-sized intracranial arteries that leads to impaired perfusion of the brain [1]. Delayed cerebral ischemia (DCI) stemming from the cerebral vasospasm is associated with significant morbidity and mortality; hence much interest has been focused on developing effective preventive, diagnostic, and therapeutic measures for vasospasm [2]. The evolution of vasospasms is usually initiated between the third and seventh day after initial hemorrhage, with a typical increase on the fourth day after SAH and a gradual decrease following the 14th day [3, 4]. This phenomenon is primarily located adjacent to the initial hemorrhage, or it can be diffuse and affect blood vessels distal to the bleed [1]. While the exact mechanisms behind these phenomena have not been fully elucidated, it is hypothesized that extravasated blood from the initial hemorrhage triggers complex cellular mechanisms which culminate in vascular smooth muscle contraction [1, 5–7].

R. D. Martin et al. (eds.), *Subarachnoid Hemorrhage*, Acta Neurochirurgica Supplement 127,
https://doi.org/10.1007/978-3-030-04615-6_32,

Currently, the gold standard for diagnosing vasospasms is cerebral digital subtraction angiography (DSA) or computed tomography angiography (CTA); however these diagnostic measures are not as feasible as bedside assessments [8]. Conversely, bedside clinical assessments are only able to detect symptoms once the vasospasms have already manifested their deleterious effects on cerebral function [8]. The use of TCD, a noninvasive tool, allows for bedside monitoring and can recognize cerebral vasospasm in its earlier stages before it becomes clinically apparent and can be used pre-, intra-, and postoperatively.

Principles of Transcranial Doppler (TCD)

Transcranial Doppler ultrasonography (TCD), which is based on the theory of the "Doppler effect," was originally introduced by Christian Andreas Doppler in 1842; in 1981, Aaslid and colleagues developed a 2.00 MHz Doppler which allowed for better skull penetration [9].The Doppler effect is based on the principle that the velocity of blood flow in a given artery is inversely proportional to the respective cross-sectional area of the artery [9]. TCD ultrasonography involves the use of a low-frequency (≤2.00 MHz) transducer to insonate the basal cerebral arteries through a relatively thin bone windows to measure the cerebral blood flow velocity (CBFV) [9]. The TCD probe emits an ultrasonic beam at a particular frequency (f_1) and speed (c), which after crossing the skull gets reflected back by the moving erythrocytes at an altered frequency f_2 [9]. This difference in frequency is known as the "Doppler shift"($f_d = f_2 - f_1$) which is directly proportional to the velocity (V) of the reflector [9]. The following equation derived from this principle is the basis for calculating CBF velocity (CBF-V) via TCD:

$$\text{CBF} \quad V = \left(cf_d\right) / \left(2 \cdot f_1 \cdot \cos\theta\right)$$

where θ is the angle between the direction of the ultrasonic beam and the direction of blood flow [9]. In order to determine a particular vessel's depth, the time interval from emission of f_1 frequency and reflection of f_2 frequency is calculated to derive the Doppler frequency shift [9]. Since individual erythrocytes move at different speeds, the Doppler signal is a mixture of different frequency components displayed as a Doppler signal graph where peak velocities, mean velocities, and pulsatility indexes are calculated [1, 9]. Mean flow velocity (FVm) is a central parameter in TCD calculated as: (FVm) = (systolic velocity − diastolic velocity/3) + diastolic velocity. Each vessel has a normal mean flow velocity. The middle cerebral artery (MCA) and anterior cerebral artery (ACA) have the highest velocities and the posterior cerebral artery (PCA) and basilar artery (BA) have lower velocities. It is important to note what the normal velocities for each vessel highly dependent on the patients age. Velocities that fall out of the normal range may be indicators of disease. The use of color TCD has further improved this technique by giving color-coding flow information to denote the directionality of the blood flow. This technology is called power M-mode TCD [1].

Technique

TCD is a noninvasive monitoring tool for cerebral vasospasm in SAH patients [10]. In this technique, the first effort is to establish the location or "windows" where ultrasound beams can penetrate the skull to assess the intracranial arteries [10, 11]. To evaluate cerebral arteries, the ultrasound beams pass through the transtemporal window, which is located between the eye and pinna [10], the transorbital window is used to evaluate the ophthalmic artery [10], and the transforaminal window (which crosses the foramen magnum) is used to evaluate vertebral arteries [10]. Through each "window," blood flow characteristics of the vessels and resultant waveforms are evaluated [10]. Using the transtemporal window, the middle cerebral artery (MCA), bifurcation of MCA, and the internal carotid artery (ICA) and the anterior carotid artery (ACA) are evaluated. The MCA is often insonated at a depth of 30–60 mm from the skull surface while ACA, at 65–80 mm depth with the probe in an anterosuperior position and ICA, at 55–70 mm depth, with the probe in a posteroinferior position [10].

While there are useful alternatives available for diagnosing cerebral vasospasms, including CTA and cerebral DSA, these techniques have additional risks, are invasive, and require radiation exposure [10, 12]. As a result, these techniques are less practical surveillance tools, making transcranial Doppler ultrasonography the clear choice. With the development of new technology including power motion Doppler, better visualization of posterior circulation vessels is achievable, even in patients with thick temporal bone [10]. In addition, the power motion Doppler's window finding tool allows the visualization of flow intensity, giving it an overall advantage to other conventional methods like conventional catheter angiography, as vasospasms are dynamic in nature and constantly reconfigure [10]. Doppler ultrasonography is able to detect other physiologic outcomes of SAH, including increased intracranial pressure via analyzing the trends in both pulsatility and changes in waveforms [10]. Conclusively, Transcranial Doppler surveillance provides a reliable and accurate means for continued monitoring and management of SAH.

Diagnostic Criteria for Transcranial Doppler Evidence of Cerebral Vasospasm

Evidence from as recent as 2015 is in strong support of the use of TCD in patients status post-SAH to diagnose MCA vasospasm [13, 14], whereas the use of TCD to detect basilar artery (BA) [15] and other arteries in the circle of Willis is not as strongly supported [13, 16–18]. In addition to FVm, additional diagnostic measures include Lindegaard ratio (LR) for MCA vasospasm and the Sviri ratio (SR) for BA vasospasm. Both the LR and SV are indexed measures that account for diffuse systemic changes in FVm. Their use has applications in an array of diseases that make vasospasm and other hyperdynamic circulatory states more likely, including SAH and others (anemia, fever, etc.). Kumar et al. have demonstrated that the calculation of the LR entails dividing the FVm of the MCA by the FVm of the proximal ipsilateral internal carotid artery (ICA). The FVm of the ICA is to be measured via a 2.00 MHz pulsed wave transducer. The SV is calculated similarly by dividing the FVm of the BA the by the time averaged maximum average of the FVm of the bilateral vertebral arteries. The raw FVm values of the vertebral arteries are to be measured via 2.00 MHz transducer (pulsed wave) below the tip of the mastoid process at a depth of 40–50 mm [12]. FVm values of the vertebral arteries are difficult to obtain due to their proximity to both the occipital arteries and ICA. To discern these vessels from one another: first, adequate probe pressure must be applied to obliterate the occipital artery, next, the probe is to be moved in the anterior direction until both the ICA and vertebral artery are identified, ensuring that the ICA is anterior to the vertebral artery will allow for accurate selection of the vertebral artery to be made.

$$\text{Lindegaard Ratio}(\text{LR}) = \frac{\text{FVm}_{\text{MCA}}}{\text{FVm}_{\text{ipsilateralICA}}} \qquad (1)$$

Although the LR and SR should in theory allow for accurate distinction between hyperdynamic flow and vasospasm, their utility does not surpass that of cerebral DSA when it comes to determining the occurrence of vasospasm or in predicting delayed neurologic deficits resulting from cerebral ischemia [4].

The Use of TCD in Predicting MCA Vasospasm

Symptomatic vasospasm frequently occurs following SAH, typically occurring four to 17 days after initial hemorrhage. Predictors of MCA vasospasm and its severity are mean flow velocity (FVm) in the MCA and angiographic lumenal diameter of the vessel. Sloan et al. [19] have delineated a significant correlation between MCA FVm and angiographic lumen diameter of MCA, while Lindegaard et al. [20] have shown that the two measures exhibit an indirect relationship to each other, as lumen diameter decreases, MCA FVm increases.

Further studies suggest a correlation between MCA FVm and vasospasm severity with FVm ranges from <120 cm s^{-1}, ≥120 cm s^{-1} to <200 cm s^{-1} and > 200 cm s^{-1} corresponding to varying degrees of arterial stenosis and vasospasm severity of mild, moderate, and severe, respectively [21–23]. Such spikes in FVm can be used to indirectly indicate the occurrence of a vasospasm and can be detected via TCD up to 2 days prior to symptom onset with high sensitivity and specificity [4, 19, 21, 24, 25] as well as a high positive predictive value of 0.97 [26].

A cohort study conducted by McGirt showed that vasospasm preceded over half (64%) of SAH cases where delayed neurological deficits were seen [27]. Thresholds indicative of possible development of vasospasm include both relative (increase of 20–50 cm s^{-1}) [19, 28, 29] and absolute (>120 cm s^{-1}) [11] FVm values. Maschia et al. [24] provided strong support for the use of daily TCD when they showed that an absolute threshold FVm of ≥160 cm s^{-1} could be used to distinguish between those with and without MCA vasospasm with a sensitivity and specificity of 1.00. However, when considering the results of 26 independent studies, a more inclusive absolute FVm of >120 cm s^{-1} found via TCD identified patients with MCA vasospasm of greater than 25% stenosis with a sensitivity and specificity of 0.99 and 0.67, respectively, when compared to the findings of a cerebral DSA as the gold standard [30]. In a retrospective study conducted by Vora et al., an FVm of >120 cm s^{-1} was found to have sensitivity and specificity of 0.72 and 0.88, respectively (compared to cerebral DSA), in identifying MCA vasospasm with ≥33% stenosis [4]. In the same study, an FVm of <120 cm s^{-1} corresponded with a negative predictive value of 0.94 [4].

The Use of TCD in Predicting BA Vasospasm

Analogous FVm thresholds for BA vasospasms have also been explicated in previous studies, but these require the adjunct of an SR threshold. It has been delineated that an FVm > 85 cm s^{-1} and SR > 3 could predict BA vasospasms of greater than 50% occlusion with a sensitivity of 0.92 and specificity of 0.97 [15]. A similar study suggests that FVm > 95 cm s^{-1} corresponds with a sensitivity of 1.00 [22]. Interestingly, there exists a strong correlation between SR and BA diameter, which may provide insight as to why the SR is used over others as a concomitant measure with FVm

over others for predicting BA vasospasm [15]. Sousitel and colleagues found that an SR > 3 indicated 50% BA stenosis for all patients in their study.

TCD in Practice

All patients at risk of vasospasm receive preemptive care (prophylaxis includes nimodipine and management of sodium balance) in attempt to establish a euvolemic state. Physical exams and TCD daily are performed to establish baseline FVm. Should any abnormalities, obscurities, or difficulties be seen in physical exam or TCD, even at a low threshold, we proceed with either MRI perfusion, MRA, CTA, or cerebral DSA to confirm or rule out vasospasm. Treatment if required includes more frequent physical examination, increased application of positive sodium protocols, hemodynamic augmentation, and endovascular intervention.

Limitations of the TCD

Although there are obvious advantages to the use of TCD in intensive care patients status post-SAH, there are limitations nonetheless. The following are the three limitations of the TCD. First, the accuracy and reliability of the study is highly dependent upon the one conducting the TCD. Therefore, only the most adept TCD technicians should be tasked. Secondly, certain populations, typically women and the elderly, lack sufficient bone windows for proper ultrasound beam penetration and may lead to false-negative results [19]. The final limitation results from the fact that not all studies on the TCD are in agreement. Indeed, the relationship between a positive TCD and delayed neurologic deficit following SAH has been questioned [11]. One prospective study showed that among SAH patients who exhibited delayed neurologic deficits, only 84% showed evidence of vasospasm in cerebral DSA [31].

Conclusion

The use of TCD and concomitant LR as tools in the early detection of cerebral vasospasm following aSAH has been studied for several decades and entails several advantages including that the procedure is noninvasive, is easily available at the bedside, is radiation free, and can help prevent delayed neurologic deficits. In line with this, current recommendations included in the American Heart Association's evidence-based national guidelines for the management of SAH indicate the use of transcranial Doppler ultrasonography to be a reasonable tool for vasospasm monitoring [32].

Conflict of Interest The authors declare that they have no conflict of interest.

References

1. Rigamonti A, Ackery A, Baker AJ. Can J Anesth. 2008;55:112.
2. Vergouwen MD, Vermeulen M, van Gijn J, Rinkel GJ, Wijdicks EF, Muizelaar JP, et al. Definition of delayed cerebral ischemia after aneurysmal subarachnoid hemorrhage as an outcome event in clinical trials and observational studies: proposal of a multidisciplinary research group. Stroke. 2010;10:2391–5.
3. Dorsch NW, King MT. A review of cerebral vasospasm in aneurismal subarachnoid hemorrhage. Part I: incidence and effects. J Clin Neurosci. 1994;1:19–26.
4. Vora YY, Suarez-Almazor M, Steinke DE, Martin ML, Findlay JM. Role of transcranial Doppler monitoring in the diagnosis of cerebral vasospasm after subarachnoid hemorrhage. Neurosurgery. 1999;44(6):1237–48.
5. Sobey CG, Faraci FM. Subarachnoid hemorrhage: what happens to the cerebral arteries? Clin Exp Pharmacol Physiol. 1998;25:867–76.
6. Tani E, Matsumoto T. Continuous elevation of intracellular Ca2+ is essential for the development of cerebral vasospasm. Curr Vasc Pharmacol. 2004;2:13–21.
7. Woszczyk A, Deinsberger W, Boker DK. Nitric oxide metabolites in cisternal CSF correlate with cerebral vasospasms in patient with subarachnoid haemorrhage. Acta Neurochir. 2003;145:257–64.
8. Naqvi J, Yap KH, Ahmad G, Ghosh J. Transcranial Doppler ultrasound: a review of the physical principles and major applications in critical care. Int J Vasc Med. 2013;2013:629378.
9. Aaslid R, Markwalder TM, Nornes H. Noninvasive transcranial Doppler ultrasound recording of flow velocity in basal cerebral arteries. J Neurosurg. 1982;57:769–74.
10. Sarkar S, Ghosh S, Ghosh SK, Collier A. Role of transcranial Doppler ultrasonography in stroke. Postgrad Med J. 2007;83(985):683–9.
11. Ekelund A, Saveland H, Romner B, Brandt L. Is transcranial Doppler sonography useful in detecting late cerebral ischaemia after aneurysmal subarachnoid hemorrhage? Br J Neurosurg. 1996;10:19–25.
12. Kumar G, Alexandrov AV. Vasospasm surveillance with transcranial doppler sonography in subarachnoid hemorrhage. J Ultrasound Med. 2015;34:1345–50.
13. Alexandrov AV. Cerebrovascular ultrasound in stroke prevention and treatment. Elmsford, NY: Blackwell; 2004.
14. Lindegaard KF, Nornes H, Bakke SJ, Sorteberg W, Nakstad P. Cerebral vasospasm diagnosis by means of angiography and blood velocity measurements. Acta Neurochir. 1989;100:12–24.
15. Sviri GE, Ghodke B, Britz GW, et al. Transcranial Doppler grading criteria for basilar artery vasospasm. Neurosurgery. 2006;59(2):360–6.
16. Burch CM, Wozniak MA, Sloan MA, et al. Detection of intracranial internal carotid artery and middle cerebral artery vasospasm following subarachnoid hemorrhage. J Neuroimaging. 1996;6:8–15.
17. Sharma D, Prabhakar H. Transcranial Doppler ultrasonography. In: Neuromonitoring techniques. New Delhi: Academic; 2018. p. 113–45.
18. Wozniak MA, Sloan MA, Rothman MI, et al. Detection of vasospasm by transcranial Doppler sonography: the challenges of

the anterior and posterior cerebral arteries. J Neuroimaging. 1996;6:87–93.
19. Sloan MA, Haley EC Jr, Kassell NF, et al. Sensitivity and specificity of transcranial Doppler ultrasonography in the diagnosis of vasospasm following subarachnoid hemorrhage. Neurology. 1989;39:1514–8.
20. Lindegaard KF, Nornes H, Bakke SJ, Sorteberg W, Nakstad P. Cerebral vasospasm after subarachnoid haemorrhage investigated by means of transcranial Doppler ultrasound. Acta Neurochir Suppl (Wien). 1988;42:81–4.
21. Aaslid R, Huber P, Nornes H. Evaluation of cerebrovascular spasm with transcranial Doppler ultrasound. J Neurosurg. 1984;60: 37–41.
22. Sloan MA, Burch CM, Wozniak MA, et al. Transcranial Doppler detection of vertebrobasilar vasospasm following subarachnoid hemorrhage. Stroke. 1994;25(11):2187–97.
23. Sloan MA. Detection of vasospasm following subarachnoid hemorrhage. In: Babikian VL, editor. Transcranial Doppler ultrasonography. St. Louis: Mosby—Year Book; 1993. p. 105–27.
24. Mascia L, Fedorko L, terBrugge K, et al. The accuracy of transcranial Doppler to detect vasospasm in patients with aneurysmal subarachnoid hemorrhage. Intensive Care Med. 2003;29: 1088–94.
25. Proust F, Callonec F, Clavier E, et al. Usefulness of transcranial color-coded sonography in the diagnosis of cerebral vasospasm. Stroke. 1999;30:1091–8. 16.
26. Lysakowski C, Walder B, Costanza M, Tramer M. Transcranial Doppler versus angiography in patients with vasospasm due to a ruptured cerebral aneurysm: a systematic review. Stroke. 2001;32:2292–8.
27. McGirt MJ, Blessing RP, Goldstein LB. Transcranial Doppler monitoring and clinical decision- making after subarachnoid hemorrhage. J Stroke Cerebrovasc Dis. 2003;12:88–92.
28. Aaslid A, Huber P, Nornes H. A transcranial Doppler method in the evaluation of cerebrovascular spasm. Neuroradiology. 1986;28:11–6.
29. Groslimund P. Transmission of ultrasound through the temporal bone. In: Aaslid R, editor. Transcranial Doppler sonography. Vienna: Springer; 1986.
30. Lysakowski C, Walder B, Costanza MC, Tramèr MR. Transcranial Doppler versus angiography in patients with vasospasm due to a ruptured cerebral aneurysm: a systematic review. Stroke. 2001;32(10):2292–8.
31. Frontera JA, Fernandez A, Schmidt JM, et al. Defining vasospasm after subarachnoid hemorrhage: what is the most clinically relevant definition? Stroke. 2009;40(6):1963–8.
32. Connolly ES Jr, Rabinstein AA, Carhuapoma JR, et al. Guidelines for the management of aneurysmal subarachnoid hemorrhage: a guideline for healthcare professionals from the American Heart Association/American Stroke Association. Stroke. 2012;43:1711–37.

Author Index

R. D. Martin et al. (eds.), *Subarachnoid Hemorrhage*, Acta Neurochirurgica Supplement 127,
https://doi.org/10.1007/978-3-030-04615-6, © Springer Nature Switzerland AG 2020

G

I

L

N

Subject Index

R. D. Martin et al. (eds.), *Subarachnoid Hemorrhage*, Acta Neurochirurgica Supplement 127, https://doi.org/10.1007/978-3-030-04615-6, © Springer Nature Switzerland AG 2020